NOVEMBER · 1953

Proceedings of the I·R·E

A Journal of Communications and Electronic Engineering

JUNCTION TRANSISTOR

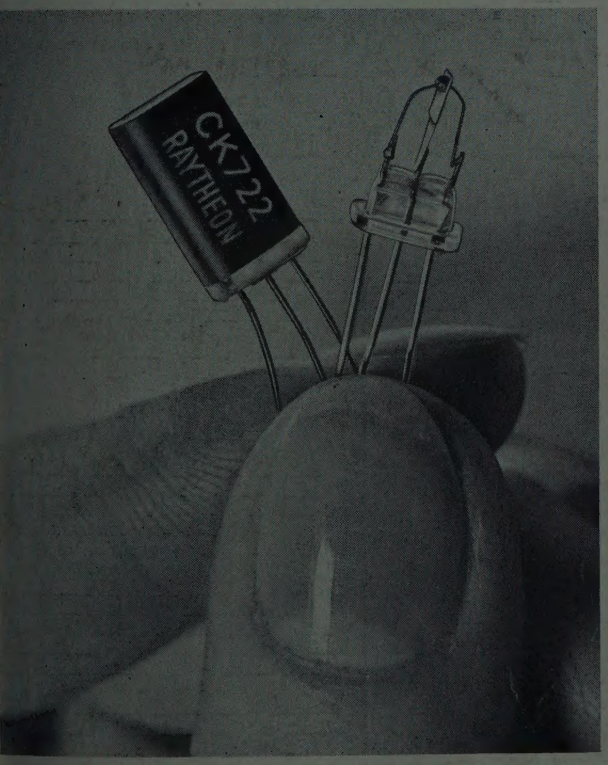

Raytheon Mfg. Co.

A junction transistor made by the diffusion of indium into germanium is shown encapsulated (left) and exposed to view (right).

Volume 41 Number 11

IN THIS ISSUE

Problems in Aviation Electronics
Variable Time Delay
Design of a High-Power Klystron
Backward-Wave Tubes
Quartz Crystal Resonators
Optimum DC Design of Flip-Flops
Helix Impedance of Traveling-Wave Tube
Traveling-Wave Slot Antennas
Magnetron Frequency Characteristics
Hyperbolic Transmission Line
Conformal Mappings for Transfer Function Synthesis
Permeability of Spherical Particles
Alignment of Band-Pass Amplifiers
Beamwidths of Tschebyscheff Arrays
Abstracts and References

TABLE OF CONTENTS INDICATED BY BLACK-AND-WHITE MARGIN, FOLLOWS PAGE 80A

The Institute of Radio Engineers

ULTRA COMPACT UNITS...OUNCER UNITS

HIGH FIDELITY.... SMALL SIZE.... FROM STOCK

UTC Ultra compact audio units are small and light in weight, ideally suited to remote amplifier and similar compact equipment. High fidelity is obtainable in all individual units, the frequency response being ± 2 DB from 30 to 20,000 cycles.

True hum balancing coil structure combined with a high conductivity die cast outer case, effects good inductive shielding.

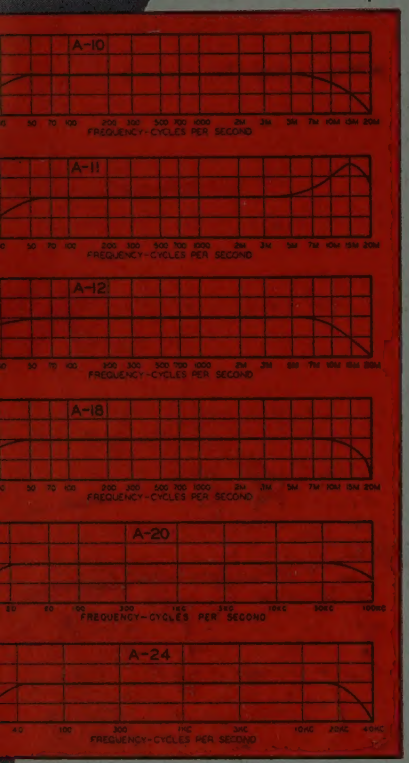

Type No.	Application	Primary Impedance	Secondary Impedance	List Price
A-10	Low impedance mike, pickup, or multiple line to grid	50, 125/150, 200/250, 333, 500/600 ohms	50 ohms	$16.00
A-11	Low impedance mike pickup, or line to 1 or 2 grids (multiple alloy shields for low hum pickup)	50, 200, 500	50,000 ohms	18.00
A-12	Low impedance mike pickup, or multiple line to grids	50, 125/150, 200/250, 333, 500/600 ohms	80,000 ohms overall, in two sections	16.00
A-14	Dynamic microphone to one or two grids	30 ohms	50,000 ohms overall, in two sections	17.00
A-20	Mixing, mike, pickup, or multiple line to line	50, 125/150, 200/250, 333, 500/600 ohms	50, 125/150, 200/250, 333, 500/600 ohms	16.00
A-21	Mixing, low impedance mike, pickup, or line to line (multiple alloy shields for low hum pickup)	50, 200/250, 500/600	200/250, 500/600	18.00
A-16	Single plate to single grid	15,000 ohms	60,000 ohms, 2:1 ratio	15.00
A-17	Single plate to single grid 8 MA unbalanced D.C.	As above	As above	17.00
A-18	Single plate to two grids. Split primary.	15,000 ohms	80,000 ohms overall, 2.3:1 turn ratio	16.00
A-19	Single plate to two grids. 8 MA unbalanced D.C.	15,000 ohms	80,000 ohms overall, 2.3:1 turn ratio	19.00
A-24	Single plate to multiple line	15,000 ohms	50, 125/150, 200/250, 333, 500/600 ohms	16.00
A-25	Single plate to multiple line 8 MA unbalanced D.C.	15,000 ohms	50, 125/150, 200/250, 333, 500/600 ohms	17.00
A-26	Push pull low level plates to multiple line	30,000 ohms plate to plate	50, 125/150, 200/250, 333, 500/600 ohms	16.00
A-27	Crystal microphone to multiple line	100,000 ohms	50, 125/150, 200/250, 333, 500/600 ohms	16.00
A-30	Audio choke, 250 henrys @ 5 MA 6000 ohms D.C., 65 henrys @ 10 MA 1500 ohms D.C.			12.00
A-32	Filter choke 60 henrys @ 15 MA 2000 ohms D.C., 15 henrys @ 30 MA 500 ohms D.C.			10.00

TYPE A CASE
1½" x 1½" x 2" high

UTC OUNCER components represent the acme in compact quality transformers. These units, which weigh one ounce, are fully impregnated and sealed in a drawn aluminum housing ⅞" diameter... mounting opposite terminal board. High fidelity characteristics are provided, uniform from 40 to 15,000 cycles, except for 0-14, 0-15, and units carrying DC which are intended for voice frequencies from 150 to 4,000 cycles. Maximum level 0 DB.

OUNCER CASE
⅞" Dia. x 1⅛" high

Type No.	Application	Pri. Imp.	Sec. Imp.	List Price
0-1	Mike, pickup or line to 1 grid	50, 200/250 500/600	50,000	$14.00
0-2	Mike, pickup or line to 2 grids	50, 200/250 500/600	50,000	14.00
0-3	Dynamic mike to 1 grid	7.5/30	50,000	13.00
0-4	Single plate to 1 grid	15,000	60,000	11.00
0-5	Plate to grid, D.C. in Pri.	15,000	60,000	11.00
0-6	Single plate to 2 grids	15,000	95,000	13.00
0-7	Plate to 2 grids, D.C. in Pri.	15,000	95,000	13.00
0-8	Single plate to line	15,000	50, 200/250, 500/600	14.00
0-9	Plate to line, D.C. in Pri.	15,000	50, 200/250, 500/600	14.00
0-10	Push pull plates to line	30,000 ohms plate to plate	50, 200/250, 500/600	14.00
0-11	Crystal mike to line	50,000	50, 200/250, 500/600	14.00
0-12	Mixing and matching	50, 200/250	50, 200/250, 500/600	13.00
0-13	Reactor, 300 Hys.—no D.C.; 50 Hys.—3 MA. D.C.,		6000 ohms	10.00
0-14	50:1 mike or line to grid	200	½ megohm	14.00
0-15	10:1 single plate to grid	15,000	1 megohm	14.00

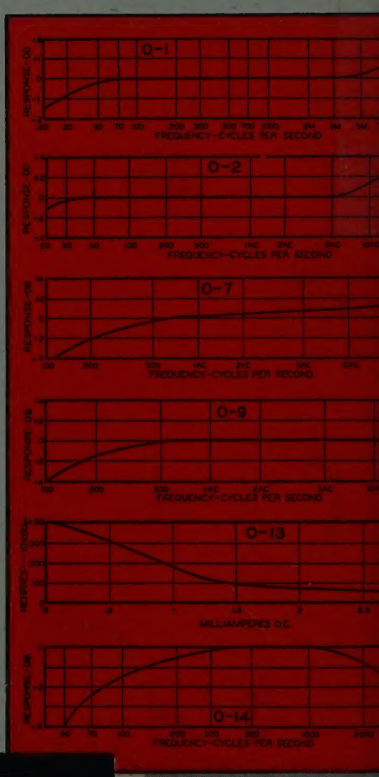

United Transformer Co.
150 VARICK STREET • NEW YORK 13, N. Y.
EXPORT DIVISION: 13 EAST 40th STREET, NEW YORK 16, N. Y., CABLES: "ARLAB"

AM-FM-TV manufacturers—

Here are 2 NEW Ways to NEW PROFITS with

New Centralab Plug-in Components

Again Centralab is first in developing NEW components for NEW advancements in etched or printed chassis

Centralab is the only source for all three new components: (1) Capacitors (disc, tubular or plate) (2) PEC* plates (3) Controls

1. *Faster assembly*

Look at the photo at right and you'll see what we mean! These special, new "Plug-in" Components are *still another example* of how Centralab is moving ahead with more firsts — so you can gain maximum savings in electronic assembly time. To gain *greatest advantages,* make sure you specify Centralab — it's the industry's *only* source of *all three* components.

2. *Eliminates costly conventional wiring and soldering*

Note that all components are designed with short leads for fast automatic or dip soldering. All solder tabs meet RTMA standards in length, thickness and mounting characteristics. You merely follow two simple steps: (1) plug-in, and (2) solder. That's all there's to it! By saving extra work, new Centralab "Plug-ins" bring extra profits wherever applied.

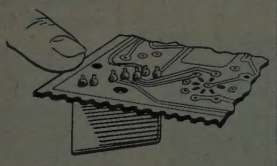

You'll want all the facts on these Centralab pioneered "firsts" so you can properly evaluate their many potential savings for you. Complete technical information and *manufacturer's samples* are available on request. Use handy coupon, or write for details.

Centralab

A Division of Globe-Union Inc.
In Canada: 804 Mt. Pleasant Road, Toronto 12, Ontario

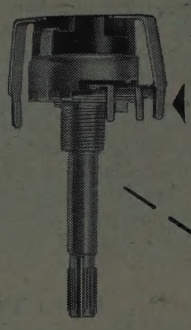

NEW CONTROLS plug directly into any etched, printed or plated chassis. Reverse-bend tabs are 1.16" wide with a standard length of 1/8" from mounting surface on .679" radius. Available in any standard taper and resistance value.

This feature is another Centralab exclusive! SPST or DPST switch eliminates all conventional wiring in printed or etched paths. Switch solder lugs can be plugged directly into the chassis. One lug is automatically grounded to one control terminal, taking the place of the jumper wire which would otherwise be required. Eliminates two extra steps!

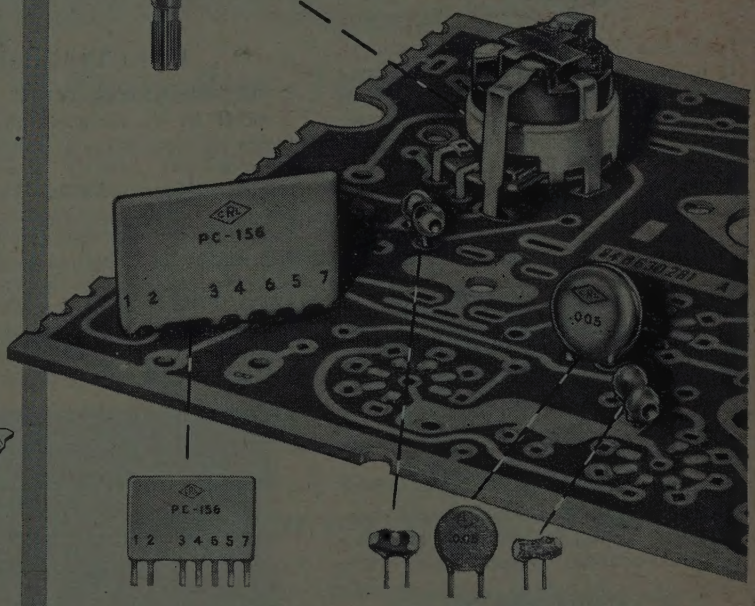

AUDIO DETECTOR COUPLATE®
7 leads — eliminate 8 parts and 9 extra connections. Technical data and *samples* available.

DISC AND TUBULAR CAPACITORS — for by-pass, coupling, general use and TC requirements. **Tubulars** have special length, special spaced wire leads. **Ceramic Flat Plate** HI-KAP Capacitors are available in standard units. Technical data and *samples* available.

PEC's are available in any standard Printed Electronic Circuit offered by Centralab. The same goes for Disc and Tubular Capacitors and Plate Capacitors.

*Trademark — Printed Electronic Circuits

CENTRALAB, A Division of Globe-Union Inc.
920-K E. Keefe Ave., Milwaukee 1, Wisconsin

Please send technical data on NEW Centralab Plug-in style components for: ☐ Controls ☐ Disc Capacitors ☐ Plate Capacitors ☐ Printed Electronic Circuit Plates ☐ Tubular Capacitors.

Name.....

Address.....

City.....State.....

NEWS and NEW PRODUCTS

November 1953

Miniature Pulse Forming Network

National Capacitor Co., 585 Washington St., Quincy, Mass., announces development and production of the NC-34 series, miniature pulse-forming networks. The NC-34-644-9 (which is illustrated actual size), designed from customer's specifications, is one-fifth the size of the original unit. Dimensions of this unit are:

$1\frac{1}{16}$ inches high ($1\frac{3}{4}$ inches over bushings), $1\frac{1}{2}$ inches long, and $\frac{3}{4}$ inch wide. It has a pulse width of 0.5 microsecond at 70 per cent, a rise time of 0.12 μs and a pulse repetition rate of 1,000/second. The unit is rated at 3 kv dc, 0.005 μf, 50 ohms impedance, up to 90°C maximum ambient temperature. Average life is 30,000 hours. This miniaturization is due to careful coil winding and construction of the integral capacitor. The network is especially constructed to eliminate breakdown and pulse irregularities due to expansion of components or to vibration. The complete unit is hermetically sealed and has molded ceramic bushings.

DC Power Supply

Sorenson & Co., 375 Fairfield Ave., Stamford, Conn., designers and manufacturers of electronic voltage and power regulation equipment, now has available an important new addition to its line of Nobatron-Rangers (wide-range-variable DC sources).

These manufacturers have invited PROCEEDINGS readers to write for literature and further technical information. Please mention your I.R.E. affiliation.

Designated as the model SR2 Nobatron-RANGER, the newly designed instrument converts nominal 115 ac line to regulated dc of 100–300 volts at 1–10 amperes. Output regulation accuracy is ± 0.25 per cent at any voltage setting; ripple is 1 per cent RMS maximum.

It is expected that this instrument will be particularly valuable to designers working in computers or in electronic, nucleonic, and related fields, since it provides wide-range voltage at comparatively heavy current. Meters and controls are conveniently arranged on a compact panel. The instrument is self contained, easily rolled or transported from one location to another, connects into any standard ac outlet.

For information write directly to the manufacturer.

Gyro Test Set

TLG Electric Corp., 31 W. 27 St., New York 1, N. Y., designers and manufacturers of electrical and electronic components, has recently announced the release of their new Model TAV Gyro Test Set. When employed with gyro testing fixtures, this electronic instrument materially reduces the time required to properly adjust gyro rotor bearings that are lubricated by oil; and it reveals certain faults of gyro rotor assembly components (due to material or workmanship) which cannot be detected by other means.

The Model TAV has three functions: (1) to measure gyro rotor speeds from 300 to 1,000 rpm on the low scale and 5,000 to 20,000 rpm on the high scale; (2) to measure gyro rotor deceleration directly in coast time from 8 to 16 minutes; (3) to give an audible and visual indication produced by gyro rotors at different speeds through the use of a speaker and neon indicating lamp.

The unit is encased in a wood cabinet, and is $20\frac{1}{2}''$ long $\times 12''$ high $\times 13''$ deep. It weighs 62 lbs. exclusive of the constant voltage transformer and connecting cables that are furnished as standard equipment.

For complete details, write directly to TLG Electric Corp.

Phasemeter

Deltron, Inc., P.O. Box 492, Glenside, Pa., has designed a new Model 100A phasemeter, which indicates directly on a $4\frac{1}{2}$ inch meter the phase angle between two alternating signals. After the balancing operation, the phase angle between the voltages is indicated on the panel meter. The sense of the angle is determined by depressing a polarity button. Phase angle measurements are determined in a matter of a few seconds.

The specifications are: 0° to 180° lead or lag in 90° expanded scale ranges; Frequency Range is 2 cps to 200 kc; Error is less than 4° from 20 cps to 20 kc, above 20 kc and below 20 cps increasing gradually to 8°; input impedance is approximately 20 megohms shunted by 10 μf; Input voltage is 1 to 50 volts sine wave, to 500 volts with Model 10A accessory input dividers at $8.50 per set; Power requirements are 115 volts, 50/60 cps, 35 watts.

TV Voltage Regulator

A tv voltage regulator has recently been placed on the market by **Perma-Power Co.,** 4727 North Damen Ave., Chicago 25, Ill.

This voltage regulator has been engineered and designed to insure maximum performance of any television set by returning full height and width of picture when low line voltage distorts picture.

Features include reduction of tube failures, increasing of set sensitivity, and elimination of intermittent sync and oscillator drift caused by low line voltage. It has 300 watt rating, is automatically operated, and has a selector switch which permits boosting or lowering of voltage. Illustrated literature may be obtained from the Company.

(Continued on page 24A)

RADAR · TELEMETERING · COMMUNICATIONS · NAVIGATIONAL AIDS · ELECTRONIC MINIATURIZATION

for the World of Electronics

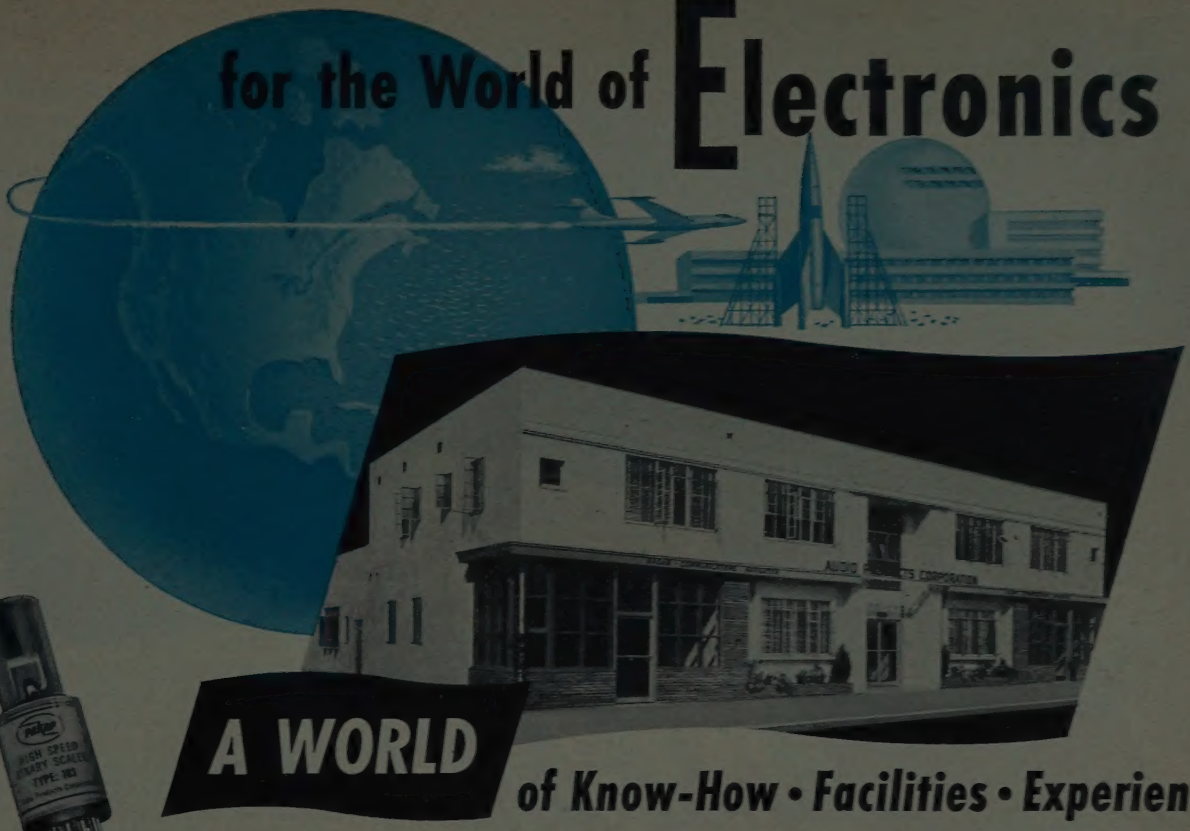

A WORLD of Know-How • Facilities • Experience

MINIATURIZED PACKAGED CIRCUITS

Plug-in circuitry in a compact unit. Custom-engineered to individual specifications based on circuit requirements or performance needs.

THE MODULAR SYSTEM

A basic electronic tool of great flexibility to aid in the design and use of pulse methods for information transmission, storage and computation.

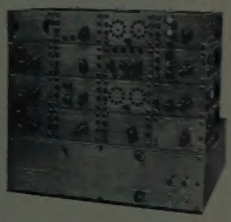

Do you have an application in the fields of radar, telemetry, communications, navigational aids or electronic miniaturization? If so, it will pay you to consult AUDIO PRODUCTS CORPORATION.

Here you'll find 35,000 square feet of modern production facilities and a staff of engineers accustomed to working in the more advanced phases of electronic development. From basic design to prototype, to final engineering tests—their knowledge, experience and facilities are applied to deliver a finished product to meet the highest standards of performance and reliability. A host of successful electronic units for military agencies and commercial organizations the world over is your proof. That is why we say—

For the Best in Electronic Design, Development and Manufacture, Consult

AUDIO PRODUCTS CORPORATION

2265 WESTWOOD BOULEVARD, LOS ANGELES 64, CALIFORNIA

The emphasis is on telemetry, radar relays, modulars and packaged circuitry

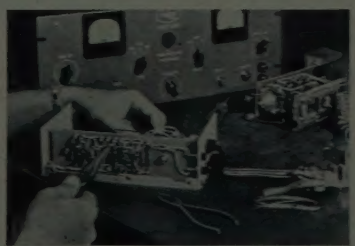

Highly skilled Audio Products technicians work with advanced production test facilities

Ever-expanding plant facilities provide more than 35,000 square feet of production space

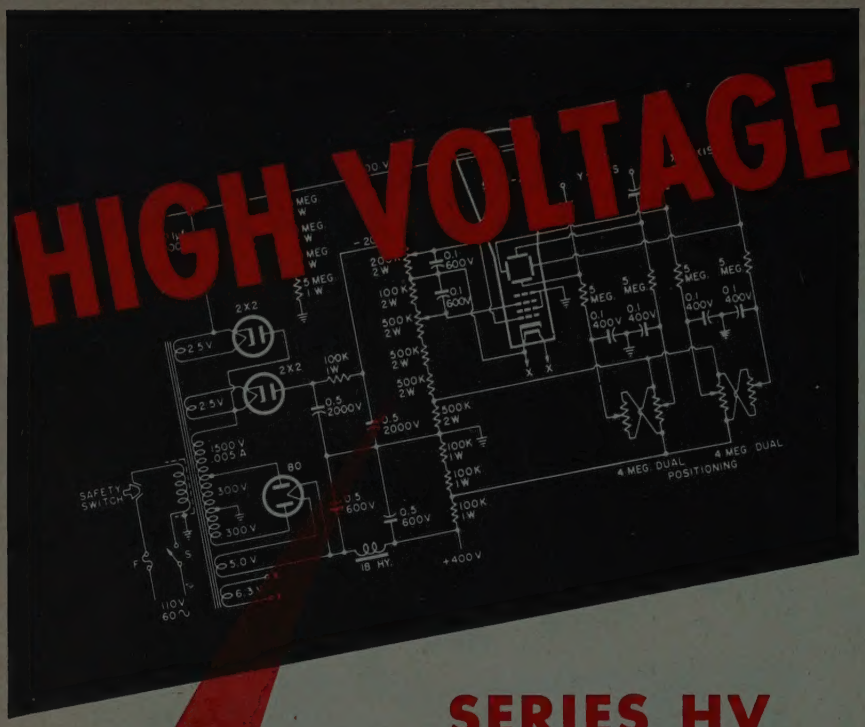

SERIES HV

Hi-Q® ceramic

*capacitors**

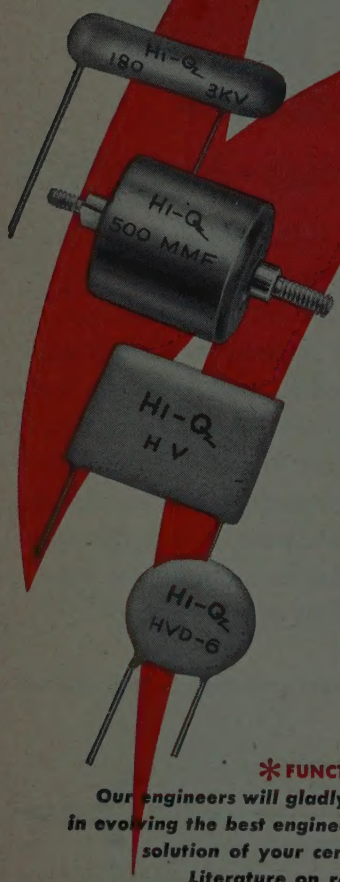

Tiny, yet so mighty, in guarding against voltage breakdowns. Yes, special dielectric materials developed by ceramic pioneer-specialists do safeguard your circuitry, associated components, operational conditions, reputation.

The Hi-Q Series HV line includes extra-severe-service *slug type* ceramic capacitors in ratings up to 20,000 V. D. C. W.; *disks* up to 6,800; *tubulars* to 7,000; and high-voltage plates where cubical configuration permits greater space utilization.

*FUNCTION-FITTED:
Our engineers will gladly work with you in evolving the best engineering and economical solution of your ceramic-capacitor problem. Literature on request.

Hi-Q® DIVISION

AEROVOX CORPORATION

Hi-Q® CERAMICS—WILKOR RESISTORS OLEAN, N. Y.

AEROVOX CORPORATION
NEW BEDFORD, MASS.

ACME ELECTRONICS INC.
PASADENA 4, CALIF.

In Canada: AEROVOX CANADA LTD., Hamilton, Ont. JOBBER ADDRESS: 740 Belleville Ave., New Bedford, Mass.
Export: 41 E. 42nd St., New York 17, N. Y. • Cable: AEROCAP, N. Y. •

News—New Products

These manufacturers have invited PROCEEDINGS readers to write for literature and further technical information. Please mention your I.R.E. affiliation.

(Continued from page 20A)

Filters

Ortho Filter Corp., 196 Albion Ave., Paterson, N. J., announces a new series of Type DE filters for eliminating distortion from signal sources. These filters will eliminate harmonic frequencies from the second to the eighth by a minimum of 60 db. The filters are so designed that a drift of ±3

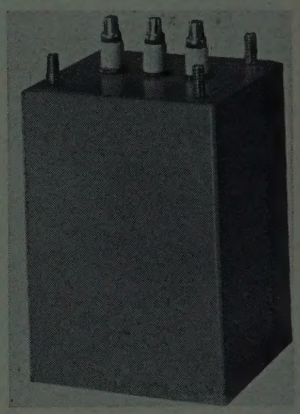

per cent in frequency of the signal source will not effect the filtering action. These units are available in variety of impedances and can be made for any frequency from 20 cps to 20 kc. The type DE can be made for use in balanced or unbalanced circuits, and will find application in production test setups making it possible to make low distortion measurements using any available signal generator.

For complete information, write direct to technical department.

DC Power Supplies

Kalbfell Laboratories, Inc., P.O. Box 1578, 1090 Morena Blvd., San Diego 10, Calif., now has a new absolute dc power supply.

These KAY-LAB absolute dc power supplies utilize automatic comparison of the output voltage against a standard cell which assures long time stability and absolute calibration of the output voltage independent of line and load variations. They have good output impedance and very low hum and noise characteristics. They are designed so that a number of complex circuits may be operated from them without cross-coupling. Interaction of ac signals in circuits under operation or test is kept at a minimum by the low ac output impedance. High gain amplifiers afford immunity to line voltage and load current variations.

(Continued on page 25A)

News—New Products

These manufacturers have invited PROCEEDINGS readers to write for literature and further technical information. Please mention your I.R.E. affiliation.

(Continued from page 24A)

Transistor Analyzer

A new Transistor Current Gain Meter and Curve Tracer is announced by **Polyphase Instrument Co.**, 705 Haverford Road, Bryn Mawr, Pa.

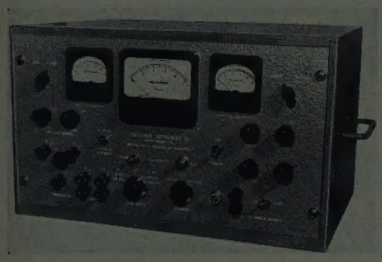

The Model TA-1 Transistor Analyzer measures the emitter-to-collector current gain of both N-type and P-type point contact transistors and the base-to-collector current gain of pnp and npn type transistors directly on a panel meter.

When used with an oscilloscope the TA-1 will produce curves of emitter-to-collector current gain against emitter current and base-to-collector current gain against base current.

Constant collector voltage is obtained from a regulated power supply the output of which is available for external use.

The instrument is housed in an oak cabinet and incorporates a front panel suitable for relay rack mounting.

50 OHM Coaxial Cable

Prodelin Inc., 307 Bergen Ave., Kearny, N. J., announces the availability of 50 ohm vhf teflon coaxial line. The New Series 600 is manufactured in accordance with the latest industry standard, RTMA-134.

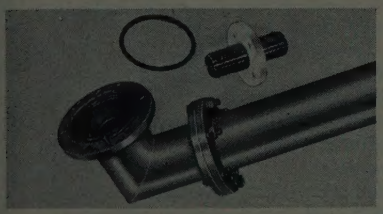

The new line is pin type insulated, similar in construction to the previously developed microwave coaxial lines. The "New Series" 600 vhf line incorporated RTMA anchor insulated connectors for better positioning of the inner conductors with other features that provide better positioning of the inner conductors with other features that provide better VSWR and attenuation characteristics than 51.5 ohm lines (according to the manufacturer).

The new 50 ohm line is made by Product Development Company, Inc., of Kearny, N. J., and is sold through Prodelin Inc., its sales and service organization.

Chart ES-3001, covering attenuation and power handling data, is available together with prices, on request.

(Continued on page 43A)

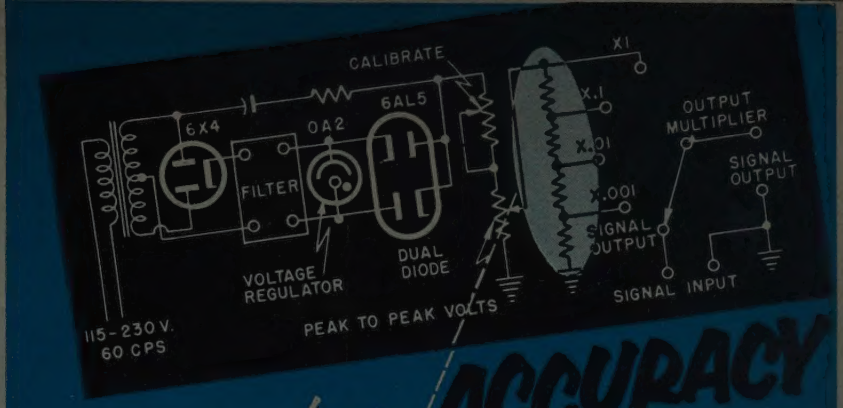

where ACCURACY counts...

Carbofilm precision resistors

Guaranteed tolerance of ±1%. Excellent stability re. temperature and voltage coefficients, overload, ageing, noise, etc. Carbofilm (deposited-carbon) resistors, made under Western Electric patents, provide the dependability of wire-wounds with compactness of carbons. In two types:

Coated (special resin film) units for economy as well as accuracy and stability.

Hermetically-sealed (metal-case glass-to-metal sealed) units. *Extraordinarily protected*—mechanically, electrically, climatically.

Both types come in ½, 1 and 2 watt sizes.

✻ FUNCTION-FITTED *to your precision resistance needs. Available in standard numbers and in special units made to order. Let us quote. Literature on request.*

Hi-Q® DIVISION

AEROVOX CORPORATION

Hi-Q® CERAMICS—WILKOR RESISTORS OLEAN, N. Y.

AEROVOX CORPORATION NEW BEDFORD, MASS.

ACME ELECTRONICS INC. PASADENA 4, CALIF.

In Canada: AEROVOX CANADA LTD., Hamilton, Ont. JOBBER ADDRESS: 740 Belleville Ave., New Bedford, Mass.

Export: 41 E. 42nd St., New York 17, N. Y. • Cable: AEROCAP, N. Y. •

25% LESS WEIGHT!

castohm®

FIXED WIREWOUND POWER RESISTORS

. . . new homogeneous core and coating

✓ REDUCES SIZE AND WEIGHT

✓ ELIMINATES SHORTED TURNS

- **350°C hot spot operation**
- **Higher power dissipation with less weight, smaller diameters**
- **Higher maximum resistances**
- **Closer tolerances—to 1% (5% standard)**
- **Better heat conductivity**
- **Exceptional resistance to thermal shock**

By eliminating the heavy ceramic core with the wire-bunching and shorted turns characteristic of vitreous enamel types, Shallcross has developed a radically new wirewound resistor that outperforms *all other* types of high temperature fixed power resistors. Through a unique process, the windings are imbedded in a special ceramic which forms an integral coating and core. Designed to MIL-R-10566 specifications, Castohms are destined to leave MIL-R-26A types far behind.

Find out how Castohms can reduce size and weight in your equipment - improve efficiency and reliability as well. Write, wire, or phone for details. Ask for Engineering Bulletin L-29.

SHALLCROSS MANUFACTURING CO.,
524 Pusey Avenue, Collingdale, Pa.

Shallcross

Designed to
MIL-R-10566
Specifications

R-30— 8 watts
R-33— 28 watts
R-37—125 watts
R-46—225 watts

News—New Products

These manufacturers have invited PROCEEDINGS readers to write for literature and further technical information. Please mention your I.R.E. affiliation.

(Continued from page 25A)

Transistor Characteristic Plotter

A new piece of transistor test equipment, the DEA Model 2 Transistor Characteristic Plotter, which automatically displays any one of 4 different families of static characteristic curves on the face of an auxiliary oscilloscope, had been designed by **Dunn Engineering Associates,** 11 Windsor St., Cambridge, Mass.

The sets of curves presented are the transfer characteristic and the collector characteristic, for both grounded-emitter and grounded-base connections. The rapid repetition rate of the displays obviates flicker and thermal effects. n-p-n and p-n-p junction transistors, as well as point-contact transistors are accommodated. Input-current step increments are adjustable from 5 to 1,000 ma, and collector voltage is adjustable up to 50 volts peak-to-peak. The curves permit immediate recognition of mediocre or defective transistors, and allow the determination of all the small-signal transistor parameters, including the current gain, Alpha. Calibration of display axes is accomplished by internal calibration signals. The unit is intended for production line as well as laboratory use. A descriptive bulletin is available from the manufacturer.

New Jobber Catalog

Newark Electric Co., 223 W. Madison St., Chicago 6, Ill., has just published a comprehensive parts catalog No. 56. Originally scheduled for early September release, its publication was held up in order to incorporate the many price and model changes made throughout the electronics industry during September.

This 196 page book, known as "The Complete Electronics Reference Book," contains thousands of items for industry laboratories, high-fidelity radio and television. Whole sections are devoted to test equipment, industrial equipment and supplies, high-fidelity systems and components, television chassis, accessories and antennas; including the latest uhf antennas and converters, tape and disc recorders; phonographs and chargers, P.A. and intercommunication systems books, tools and amateur equipment. Wherever possible, the complete lines of nationally-known manufacturers are listed.

(Continued on page 45A)

518,400 MILES
36,000 HOURS

"Simpson Model 303 is t
rugged to break!"

Carroll W. Hoshour
Director of Sales Engineering
and Service Raytheon Television and
Radio Corporation

"Nine Raytheon television se
ice representatives are constan
on the road covering 65 distribu
territories. Not only must their equipment rema
accurate, but it also must be built to withstand t
rigors of constant travel by car, train, bus a
plane."

"The only test instrument our Raytheon te
vision service representatives carry is the Simps
Model 303 Vacuum Tube Volt-Ohmmeter. We a
enthusiastic about this instrument because not o
303 has ever failed to operate or perform
inaccurately. The Model 303's in service
Raytheon television representatives have go
through, at a rough estimate, 518,400 miles a
36,000 hours of rigorous handling. We thi
Simpson Model 303 is too rugged to brea

C.W. Hoshou

Simpson Model 303 Vacuum Tube Volt-Ohmme
dealer's net . . $68
HV Probe $8
RF Probe $5

Ask your jobber for full information or write:
Simpson Electric Company
5200 West Kinzie Street
Chicago 44, Illinois ES 9-1
In Canada: Bach-Simpson, Ltd., London,

Another reason why

Simpson *is the world's larg*
manufacturer of test equipm

BURTON BROWNE ADVERTISING

Behind the radar curtain that guards our shores

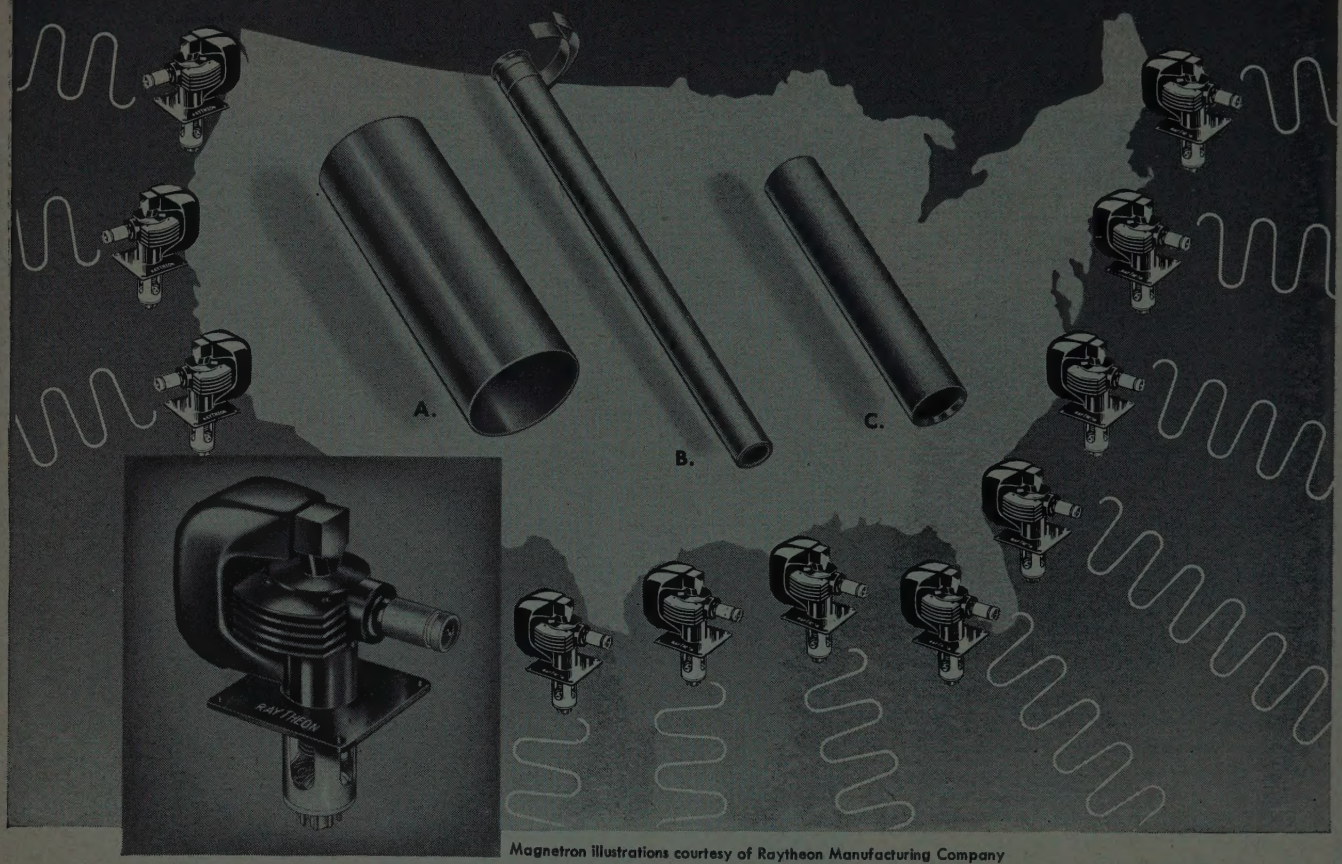

Magnetron illustrations courtesy of Raytheon Manufacturing Company

Source of UHF waves that make possible the radar screen guarding our continental perimeter is the magnetron.

Essential elements of the magnetron, and the anodes and cathodes of the companion direct-reading oscilloscope are produced by Superior Tube Company. For example, in the Raytheon magnetron above, Superior furnishes: A. The cathode (heart of the magnetron); B. The anode; C. The sleeve on the wave trap (or choke) assembly.

All of these parts are made from Superior seamless nickel tubing. As a matter of fact, there is Superior tubing *in every one* of the 400 different types of Raytheon magnetrons—a record possible only because of great satisfaction with Superior alloys, fabrication, deliveries and service. Put *your* chief dependence upon Superior. Superior Tube Company, 2506 Germantown Ave., Norristown, Pa.

Superior
THE BIG NAME IN SMALL TUBING

All analyses .010" to 5/8" OD.
Certain analyses in Light Walls up to 2 1/16" OD.

Seamless Nickel Cathode. Oval, double bead, .025" x .048" x .003" Wall. 12mm long.

Lockseam* Nickel Cathode Round, vertical emboss, .045" OD x .0021" Wall. 26.5 mm long.

Disc Cathode* .121" OD, .312" long.

No. 2 Grid Cup, 305 Stainless Steel, Rolled edge. .499" OD x .010" Wall x .262" long.

Many other types of nickel cathodes—such as Lockseam*, made from nickel strip, disc cathodes, and a wide variety of stainless anodes, grid cups and other tubular fabricated parts are available from Superior. For information and free literature on these products as well as Cathaloy A-30, A-31**, our latest Cathode Alloys, address Superior Tube Company, Electronics Division, 2500 Germantown Avenue, Norristown, Pa.

*Manufactured under U.S Patents
**U.S Trademark applied for

News—New Products

These manufacturers have invited PROCEEDINGS readers to write for literature and further technical information. Please mention your I.R.E. affiliation.

(Continued from page 43A)

Sub-Miniature Hermetically Sealed Relay

Polytron Engineering Co., 32 W. Biddle St., Baltimore 1, Md., has designed a new model PE5A relay for applications where size and sensitivity are a major factor; and where extreme shock and vibration are prevalent. This unit although 1 9/32 inches

long and ¾ inch in diameter, will withstand 100 G's shock and vibration. Built to meet standard military specifictions this unit is sealed in a metal can and uses a standard 7 pin miniature plug in base. It has an operating voltage of 24–28 volts dc and uses Palladium silver contacts which are rated up to 2 amperes inductive load. Available coil resistances range from 400 to 1,000 ohms which will meet a wide variety of application requirements.

Tube Shielding for Printed Circuits

The Staver Company, Inc., 41–51 North Saxon Ave., Bay Shore, L. I., N. Y., manufacturers of electronic specialties, announces a new series of "Mini-Shields" especially designed for shielding miniature tubes in printed circuits.

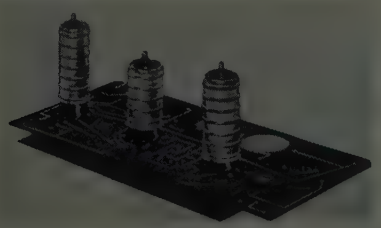

Principal design change is a flared bottom which allows the shield to pass over the ground lug of the printed socket easily. This holds the shield firmly in place and assures contact between shield and ground.

Called the "400 Series," these miniature shields, like the standard "Mini-Shields," are designed to minimize vibration, and provide cooler operation. For complete details and specifications, write to the Staver Company, Inc.

(Continued on page 141A)

BEST ALL-AROUND TESTER ON THE MARKET

USE IT FOR

- TV SETS
- RADIOS
- TRANSMITTERS
- BROADCASTING EQUIPMENT
- HOME APPLIANCES
- TWO-WAY RADIO COMMUNICATIONS SYSTEMS
- PHONE LINES
- AIR CONDITIONING SYSTEMS
- STARTER CONTROLS
- AUTO IGNITIONS, GENERATORS, BATTERIES
- MOVIE EQUIPMENT
- PANEL INSTRUMENTS
- TV CAMERAS
- AUTO LIGHTING SYSTEMS
- GENERATORS
- VOLTAGE SOURCES
- "HAM" RADIO EQUIPMENT
- CABLES
- CONNECTORS
- AUDIO FREQUENCY SOUND CURRENTS

and write for your complimentary copy of "1001 Uses for the Simpson Model 260" 50 pages of uses

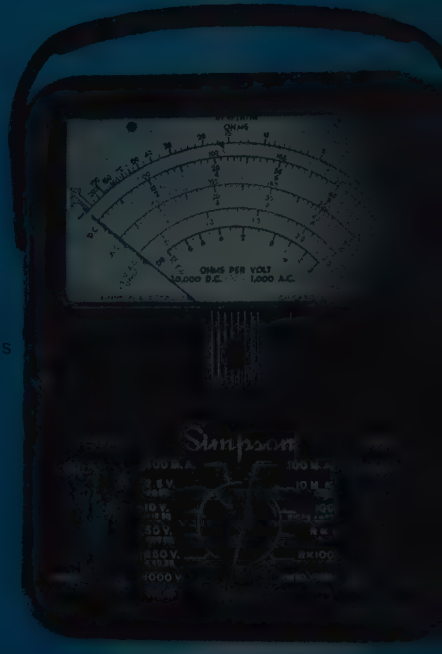

RANGES:
20,000 OHMS PER VOLT DC
1,000 OHMS PER VOLT AC
VOLTS, AC AND DC: 2.5, 10, 50, 250, 1,000, 5,000
OUTPUT: 2.5, 10, 50, 250, 1,000
MILLIAMPERES, DC: 10, 100, 500
MICROAMPERES, DC: 100
AMPERES, DC: 10
DECIBELS (5 RANGES): −12 TO +55 DB
OHMS: 0-2000 (32 OHMS CENTER), 0-200,000 (1,700 OHMS CENTER), 0-20 MEGOHMS (120,000 OHMS CENTER)

Simpson
Model 260
VOLT-OHM-MILLIAMMETER

$38.95 Dealer's net.

SIMPSON ELECTRIC COMPANY
5200 W. Kinzie St., Chicago 44 • ESTebrook 9-1121

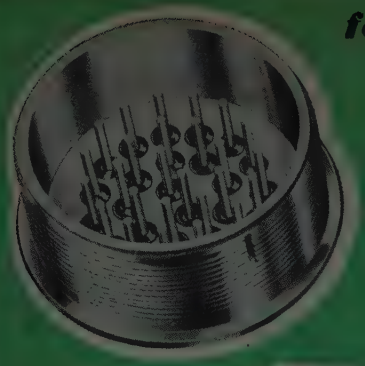

for rugged, moisture-proof

AN TYPE MULTI-PIN CONNECTOR PLUGS

Constantin

These quality-engineered high compression glass-to-metal vacuum sealed connecting plugs are ideal for generator filters, position indicators, tachometers, direction finding equipment, or almost any equipment which must be sealed against moisture or pressure changes. Construction is of glass and metal fused together to make a sturdy vacuum tight seal.

Available in a wide variety of pin configurations, these connectors may be furnished in many plating finishes for ease of soldering, appearance, and corrosion tests such as salt spray and humidity. Truly fine connectors—specified by leading manufacturers.

Also manufacturers of
MULTI-PIN HEADERS
TERMINALS
END SEALS
TRANSISTOR MOUNTS
CRYSTAL HOLDERS
VACUUM COATING EQUIPMENT

L. L. Constantin & Co.

MANUFACTURING ENGINEERS

Rt. 46 and Franklin Ave., Lodi, N. J.

SEALS AVAILABLE IN EITHER HIGH COMPRESSION OR HARD GLASS TO KOVAR TYPES.

Watch **TENSOLITE** *for progress in ELECTRONIC WIRING!*

For High Dielectric Strength, specify–

TENSOLON
TEFLON-INSULATED WIRE & CABLE

- **THIN WALL**
- **14 COLORS**
- **FREE STRIPPING**
- **EXTRA FLEXIBILITY**
- **TOUGH TEFLON INSULATION**
- **TEMPERATURE RATING: —90° to +250°C**

For an extra margin of dependability at maximum operating temperatures, specify these rugged Teflon insulated hook-up wires. Available in stranded sizes from 20 to 30 AWG with shields and teflon jackets or lacquered braids. Constructed to meet highest government and commercial standards, Tensolon Wires feature the new Tensulated-Teflon covering that eliminates pin holes and other imperfections.

ASSORTED TENSOLON HIGH-TEMP WIRES IN LABORATORY AND TEST QUANTITIES

An economical sample kit for designers, engineers, testing departments and development laboratories. Prices on request.

WRITE FOR CATALOG TODAY

TENSOLITE INSULATED WIRE CO., INC., TARRYTOWN, NEW YORK

WAVEGUIDE *Components*

TO SPECIFICATIONS SINCE 1943

Tees	Bends
Mixers	Ratraces
Duplexers	Cavities
Rotating Joints	Pads
Filters	Phasers
Attenuators	Flanges

Electronic Assemblies
Special Purpose Components

For the complete story on *Premier's* fully integrated engineering, production and testing facilities, write Dept. IRE today for our new brochure.

PREMIER INSTRUMENT CORP.

52 West Houston Street
New York 12, N. Y.

BOARD OF DIRECTORS, 1953

J. W. McRae
President

S. R. Kantebet
Vice-President

W. R. G. Baker
Treasurer

Haraden Pratt
Secretary

Alfred N. Goldsmith
Editor

I. S. Coggeshall
Senior Past President

D. B. Sinclair
Junior Past President

1953

R. D. Bennett
G. H. Browning (R1)
W. H. Doherty
A. W. Graf (R5)
W. R. Hewlett
A. V. Loughren
R. L. Sink (R7)
G. R. Town
Irving Wolff (R3)

1953–1954

J. T. Henderson (R8)
C. A. Priest (R4)
J. R. Ragazzini (R2)
J. D. Ryder
A. W. Straiton (R6)
Ernst Weber

1953–1955

S. L Bailey
B. E. Shackelford

●

Harold R. Zeamans
General Counsel

●

George W. Bailey
Executive Secretary

Laurence G. Cumming
Technical Secretary

●

Changes of address (with advance notice of fifteen days) and communications regarding subscriptions and payments should be mailed to the Secretary of the Institute, at 450 Ahnaip St., Menasha, Wisconsin, or 1 East 79 Street, New York 21, N. Y.

All rights of publication, including translation into foreign languages, are reserved by the Institute. Abstracts of papers with mention of their source may be printed. Requests for republication privileges should be addressed to The Institute of Radio Engineers.

PROCEEDINGS OF THE I.R.E.®

Published Monthly by

The Institute of Radio Engineers, Inc.

VOLUME 41 — *November, 1953* — NUMBER 11

PROCEEDINGS OF THE I.R.E.

Benjamin E. Shackelford, Director, 1953 1570
The Technical Institute ..... Albert Preisman 1571
4743. Aviation Electronics ..... Arthur Van Dyck 1572
4744. The Development of a Variable Time Delay ... Kenneth W. Goff 1578
4745. Design and Performance of a High-Power Pulsed Klystron ..... M. Chodorow, E. L. Ginzton, I. R. Neilsen, and S. Sonkins 1584
4746. Backward-Wave Tubes ..... R. Kompfner and N. T. Williams 1602
4747. Underearth Quartz Crystal Resonators ... Thomas A. Pendleton 1612
4748. The Optimum DC Design of Flip-Flops ..... D. K. Ritchie 1614
4749. Traveling-Wave Tube Helix Impedance ..... Ping King Tien 1617
4750. Traveling-Wave Slot Antennas ..... J. N. Hines, V. H. Rumsey and C. H. Walter 1624
4751. Prediction of Traveling Wave Magnetron Frequency Characteristics: Frequency Pushing and Voltage Tuning .. H. William Welch 1631
4752. The Hyperbolic Transmission Line as a Matching Section ..... Herbert J. Scott 1654
4753. Conformal Mappings for Filter Transfer Function Synthesis .... George L. Matthaei 1658
4754. Complex Magnetic Permeability of Spherical Particles ..... James R. Wait 1664
4755. Correction to: "RLC Lattice Networks" ..... Louis Weinberg 1667
4756. A Method of Band-Pass Amplifier Alignment ..... J. J. Hupert and A. M. Reslock 1668
4757. Excitation Coefficients and Beamwidths of Tschebyscheff Arrays ..... Robert J. Stegen 1671
Contributors to PROCEEDINGS OF THE I.R.E. 1674

INSTITUTE NEWS AND RADIO NOTES SECTION

W. L. Everitt Receives IRE Medal of Honor 1677
1953 Student Branch Awards 1677
Professional Group News 1678
Meteorological Factors in Radio-Wave Propagation 1678
IRE People 1679
Books:
4758. "The Science of Color" by the Committee on Colorimetry of the Optical Society of America ..... Reviewed by Pierre Mertz 1680
4759. "Synchros Self-Synchronous Devices and Electrical Servo Mechanisms" by Leonard R. Crow ..... Reviewed by W. C. Tinus 1680
Professional Groups 1680
Sections 1681
4760. Abstracts and References 1683
Meetings with Exhibits 2A
News—New Products 20A
Industrial Engineering Notes .. 84A
Professional Group Meetings .. 114A
Section Meetings 120A
Membership 124A
Positions Open 132A
Positions Wanted 138A
Advertising Index 166A

Copyright 1953, by The Institute of Radio Engineers, Inc.

EDITORIAL DEPARTMENT

Alfred N. Goldsmith
Editor

E. K. Gannett
Administrative Editor

Marita D. Sands
Assistant Editor

●

ADVERTISING DEPARTMENT

William C. Copp
Advertising Manager

Lillian Petranek
Assistant Advertising Manager

●

BOARD OF EDITORS

Alfred N. Goldsmith
Chairman

PAPERS REVIEW COMMITTEE

George F. Metcalf
Chairman

ADMINISTRATIVE COMMITTEE OF THE BOARD OF EDITORS

Alfred N. Goldsmith
Chairman

Reg. U. S. Pat. Off.

Responsibility for the contents of papers published in the PROCEEDINGS OF THE I.R.E. rests upon the authors. Statements made in papers are not binding on the Institute or its members.

MEMBER AUDIT BUREAU OF CIRCULATIONS

Benjamin E. Shackelford

DIRECTOR, 1953

Benjamin E. Shackelford was born on August 12, 1891, in Richmond, Missouri. He received the A.B. degree in 1912 and the A.M. degree in 1913, both from the University of Missouri. In 1916, he received his Ph.D. from the University of Chicago.

From 1912 to 1914, Dr. Shackelford assisted in the physics department of the University of Missouri, and in the summer of 1915 he was the first Brush Research Fellow at the Nela Research Laboratory. The following year he joined the staff of Westinghouse Lamp Company, where his activities included work in illumination and incandescent lamp physics. His direct connection with radio began in 1918 when he undertook the engineering development of radio tubes for the company. He became manager of the radio engineering department in 1925, and his work with Westinghouse continued for approximately five years thereafter.

He became a member of the manufacturing department, Radiotron Division, of the Radio Corporation of America at Harrison, N. J., in 1930, and in 1934 was appointed manager of the patent department, the activities of which included the operation of foreign technical agreements. After serving as manager of the company's foreign licensee service, Dr. Shackelford transferred to New York where he became assistant to the director of research and later to the chief engineer. In 1942, he was appointed engineer-in-charge of RCA's Frequency Bureau. In 1944, he was made assistant to the Vice President in charge of RCA Laboratories, and in 1945, Director of the License Department of the RCA International Division.

Dr. Shackelford is a Fellow of the Institute of Radio Engineers, the American Institute of Electrical Engineers and the American Association for the Advancement of Science, and a member of the American Physical Society, the Franklin Institute, Sigma Xi, Gamma Alpha and Alpha Chi Sigma.

Dr. Shackelford was President of the Institute during the year 1948, a member of the Board of Directors, 1945–1950, and was recently elected member of the Board of Directors 1953–1955.

The Technical Institute

ALBERT PREISMAN

The technical institutes are training schools for advanced technicians. Despite their intense and large-scale activities, and the notable accomplishments of certain of these schools, they are relatively little known and perhaps not fully appreciated.

It is therefore helpful to the readers of these PROCEEDINGS to consider the following guest editorial dealing with the aims and methods of these schools, prepared by a Fellow of the Institute, who is Vice President in charge of engineering of the Capitol Radio Engineering Institute, in Washington.—*The Editor.*

In the last twenty years or so the technical institute has made its presence acutely felt in engineering circles, and this is therefore a propitious time to ask, "What is a technical institute, and what does it accomplish?"

In entrance requirements and range of engineering subjects, it is similar to the degree-granting engineering school. In either case, the requirements are high-school graduation with emphasis on physics and mathematics, and both cover about the same engineering subjects, often over a similar period of actual instruction time.

It is, however, in the viewpoint and intent of the course that the two differ. The technical institute is intensely pragmatic in its approach: it teaches English in the guise of technical report writing; the principles of psychology, as an aid to getting along with people and to obtain promotion. It is not hostile to cultural subjects; it is simply indifferent to them as such. Similar considerations apply to mathematics: it seeks to show the application of the formulas to practical problems, rather than how the formulas are derived.

A technical institute is terminal in its nature. It fits its graduates specifically for engineering work whether this be the operation or maintenance of broadcast, television, or aeronautical equipment, or the building, testing, and even elementary design of such equipment. It does not pretend to train a man for research or development work, yet actually many of its graduates have achieved renown in such fields, and hold many significant patents. Furthermore, its terminal nature does not preclude its graduates from subsequently attending an engineering college to become full-fledged engineers; conversely, many engineering graduates have attended a technical institute to acquire proficiency in a particular phase of their profession.

In spite of the important contributions made to engineering education by the technical institute, recognition has been tardy and niggardly. Although the publication of the Spahr-Wickenden report twenty years ago spotlighted the need for accreditation, it was not until 1943 that E. H. Rietzke, a pioneer in this field, almost singlehandedly organized the National Council of Technical Schools for this purpose.

In 1944 Dean H. P. Hammond, chairman of the Sub-Committee on Technical Institutes of the Engineer's Council for Professional Development, invited Mr. Rietzke to join in the formation of this group, and in 1945 the accreditation of technical institutes was initiated. Since that time sixty-seven curricula of twenty-three schools, including one correspondence course, have been accredited.

Some other highlights are as follows: The American Society for Engineering Education has recognized the technical institute as an integral part of engineering education, and since 1947 has had special technical institute programs as part of its annual meetings. The U. S. Office of Education has listed about forty such schools in the higher education section of its Education Directory. Our institute now admits students of technical institutes to student membership, and is evincing a growing interest and concern for the status and welfare of the graduates of this type of school.

In view of the fact that industry requires about five technicians for every engineer, it is encouraging—not only to the technical institutes, but to the country as a whole—that such recognition is being evoked to an ever-increasing extent.

Aviation Electronics*

ARTHUR VAN DYCK†, FELLOW, IRE

Summary—**This paper concerns the present well-known problems of complexity and unreliability in aviation electronics. It points out that the situation is unique in radio engineering and does not exist in other branches of engineering. It explains how this came about, points out that the demands for greater complexity will continue, and states that correction requires more than attention to such things as more reliable tubes and components. Suggestions are given for improvement, with particular emphasis on the need for more realistic requirement specifications by planning agencies, and for more intimate relations among electronic engineers, aircraft engineers, and field operations.**

IT WAS A POTENT coincidence that the decade or so following 1938 saw unusually rapid advance in both electronics and aviation. Radically new possibilities in electronics came from timing and pulsing techniques and microwave systems. Radically new possibilities in aviation came from aerodynamic improvements and new engines, particularly jets. The simultaneous occurrence of powerful new possibilities in the two fields was mutually stimulating and mutually beneficial. However, the added stimulus of a world war resulted in overly rapid growth and some growing pains.

The symptoms accompanying these growing pains are high complexity of apparatus, lack of standardization of parts and elements, difficulty of maintenance, criticality of operation, and insufficient reliability in service. Recently, some of these problems have received much attention. Many papers dealing with them have been published, and various agencies vitally concerned with the situation have set up special committees and organizations to study them.

It may be helpful in the solution of these problems to understand clearly just how they came about, and how they reached such magnitude. No other branch of engineering than electronic has such a situation. Civil engineers do not have a reliability problem in bridges and buildings; mechanical and chemical engineers build complex devices, large and small, from atomic plants to wristwatches, without undue difficulty; and electrical engineers make many delicate instruments and systems, including many for aviation, with high reliability.

I have been in this business for over forty years, in research, manufacture, and operation, and, having seen it grow from infancy to its present size and complexity, I have noticed the entry of some factors which have not had much recognition, although they have been of great influence in creating the present conditions. I believe that an appreciation of these factors will assist materially in the determination of corrective measures. Much more is required than the present emphasis on improvements in vacuum tubes, resistors, capacitors, and transformers.

The Present Situation

It may be well to outline the present situation, for the sake of clarity and definiteness.

First, the electronic functions to be performed in a large, modern transport plane include, among others, various operations before and during take-off, particularly communications with and control of engines; in-flight communication; use of automatic pilot; radar for navigation and detection; compasses and other navigation instruments and computers. Military planes also will include numerous addition devices, especially those needed for gunfire and bomb control. Some of these planes will have electronic equipment utilizing more than 2,000 tubes, and some will have so much electronic equipment that the cost will approach that of half that of the entire aircraft.

A bomber mission of thirty modern airplanes, lasting 15 hours, requires 60,000 tubes to burn throughout the mission, or about one million tube-hours.

Former Assistant Secretary of the Navy for Air Floberg said recently: "I hope we have not created such complex machines that we are in danger of contributing to our own ultimate destruction, for we are becoming so dependent upon the automatic electronic brains for the conduct of modern warfare that their failure during combat could very well mean the difference between victory and defeat in an engagement."

Captain F. R. Furth, United States Navy, said recently:[1] "Electronic equipment is no longer a novelty to the Armed Forces, but is an absolute military necessity. We have become so reliant upon electronic brains in the conduct of modern warfare that the outcome of an engagement with enemy forces, and even of a total war, could well be determined by their performances. Many of the functions performed by electronic devices are desirable and can be performed more rapidly and more accurately by these devices than by man, but only when they operate at their rated performances. Most of these electronic devices, however, are so complex and difficult to adjust, that when placed in the hands of average operators and maintenance men, they seldom are operated at, or even close to, their required performances. All too frequently they are inoperative! Like the creator of Frankenstein, we have produced devices which, in the hands of the operating forces, are so unreliable that they could lead to our ultimate destruction.

* Decimal classification: R520. Original manuscript received by the Institute April 27, 1953. Read April 7, 1953 before the joint meeting of the New York Section of the Institute of Aeronautical Sciences and the New York Section of I.R.E.

† Staff Assistant to the Vice President and Technical Director, Radio Corporation of America.

[1] Address, Armed Forces Communication Association, Philadelphia, Pa.; February 10, 1953.

I can assure you that the situation has become so critical that we must divert a sizeable portion of our engineering efforts from the creation of new wonders, to the 'reliabilizing' of current types. Our operating forces must be provided with equipment that will function as intended at all times when needed."

Mr. E. H. Heineman, Chief Engineer of El Segundo Division of Douglas Aircraft, recently said: "There is a great deal of concern in top echelon industry and government circles about this problem. Most top level personnel are not sufficiently acquainted with detail design problems to know how to integrate the many complicating requirements and how to take corrective action. Education originating from the experienced engineers is essential."

A survey of Navy electronic equipment failures made recently by the Bell Telephone Laboratories revealed that 50 per cent were caused by poor quality of components, 25 per cent by previous failure of other components, and 25 per cent by inadequate design.

That is the present situation. How did it come to pass? How could a branch of engineering which has provided methods and devices of such miraculous precision and ingenious nature, permit such an unsatisfactory and even dangerous condition to develop in practical operation? I think that the answer can be found in the history of electronic engineering.

The Growth of Electronic Engineering

Prior to World War I, radio engineering was a small profession, and its field was limited to equipment for wireless communication between ships and shore, and across the oceans. Up to that time, practically every radio equipment designer had had operating experience. He knew what it was to have to "get messages off the hook" before a deadline, whether the static was bad or not. He had had to maintain equipment himself, and he had a full appreciation of equipment efficiency, convenience, and reliability.

With the advent of sound broadcasting in 1920, the radio field began a large and rapid growth, and the radio engineering profession expanded enormously in a very short time. The entry of radio into the home brought into radio design emphasis on new factors such as appearance, merchandizing, and cost. It lessened emphasis on ruggedness of apparatus, because conditions in the home are considerably less severe than they are on a ship at sea, or in an airplane at 50,000 feet.

Between 1920 and 1940 the techniques of the art expanded very rapidly. Most of the engineers in the profession were occupied with applications for the home, and designers were increasingly insulated from the realities in more rugged fields.

Radio engineering in the early days gave much attention to practical operating requirements. But even then, there were occasions when not enough was given. An incident occurred in World War I which shows how easy it is to overlook basic requirements.

There is a lesson in this for us now. The United States Navy had been a leader in radio development prior to that war, and, when we entered the war in 1917, was equipped with the latest and best radio apparatus which the state of the art knew. The transmitters were of the spark type, to be sure, but they were very efficient, and they even included provision for wave-changing, whereby the transmitter wavelength could be shifted instantly to any one of about ten wavelengths. That was considered to be the height of operational requirements. It was thought nothing could be superior to that for efficient communication. Likewise, the receivers were tops in selectivity, sensitivity, operating convenience, and ruggedness.

In spite of all this, when our first warships went to Europe to join the British Fleet, the first thing they had to do was to go into British Naval Yards and have their beautiful radio equipments ripped out and British gear installed. The British gear was not the latest which the art knew, in scientific aspects, and in fact was rather crude, but it did meet operational needs very well.

Our designs had overlooked two operational requirements—first, that in war time, under battle conditions, it is necessary to be able to read radio signals when guns are firing nearby. Second, it is necessary to operate two communication circuits simultaneously on each ship without interference of one with the other. Our ships had several transmitters, but when any one was working, reception on the ship was impossible.

The British radio equipment was installed in radio rooms which were beautifully sound-proofed and vibration-proofed. Simultaneous operation of two circuits had been secured by the development of highly selective "acceptor-rejector" circuits, and by the use of about three megacycles for one channel, an extraordinarily high frequency for that time. For practical use of radio in sea operations, it was necessary to revise completely the plans for radio installations in U. S. Naval vessels. It was true, of course, that World War I was the first war in which radio was used, except for the very limited use in the short Russo-Japanese conflict, and therefore there was no background experience with radio in war. Nevertheless, it seems incredible that our designers overlooked the simple, practical operational requirement for sound-proofed radio rooms on warships.

The lesson from this is that operational practicalities should come first, over technical characteristics or scientific niceties. Only when a technical innovation is so radical that it introduces new operational possibilities, is it worthy of rapid introduction, with the resultant penalties to convenience and reliability.

It is interesting to note that the radio technical situation in World War I and immediately thereafter, was quite similar to that of World War II and after. The introduction of the vacuum tube and radio telephony in the middle of World War I, caused the same kind of complex and urgent activity as did the appearance of radar and related devices in World War II.

Ruggedness of vacuum-tube equipment is not a new problem. The first tube equipments in World War I, involving quite different kinds of components from those used in previous rugged radio equipment, suffered badly for a time. It was found quickly that there was a definite relationship between the caliber of guns aboard ship and the number of components which could be found in the bottom of equipment enclosures, after the firing of one or two salvos.

The Entry of Aviation and Radar

Between World War I and World War II, aviation had its rapid expansion period, and electronic equipment in military and civil aviation had opportunity to to gain service experience. The equipment in use by 1938 had reached a fairly high degree of reliability, and the new situation was in a fair way to be met adequately, when suddenly the heavens opened, and radar fell out. Practically simultaneously, the World War II adventure began. The service which radar could deliver in military applications was so valuable that it was permissible, even mandatory, to produce it without going through the ordinary stages of development and design which are usual with an entirely new service, and it was rushed into production and service use, without opportunity for adequate attention to details.

Radar quickly proved to be so effective that, under the urgencies of war, not only it, but all related electronic devices, came to be handled with short-cut procedures, and with the same minimum attention to reliability and practical details in general. This became regular procedure, and apparatus finally was being chosen almost entirely on scientific merit, with minor attention to operational evaluation of such factors as reliability, complexity, suitability to personnel and training, etc.

Of course, routine attention was given to various standard specifications aimed at reliability, and many were the temperature tests and shock tests, but the chief results were to make the devices even more complex. Often the showings of such tests were disregarded, in the interests of getting equipment quickly. The atmosphere was such that the ideals of technical performance—more sensitivity, selectivity, range, or intriguing new functions—always won out over the prosaic demands of simplicity, ruggedness, and reliability. There were cases where electronic equipment was installed in planes and carried around but never used, because time was not available to train the crews in its operation and maintenance.

Before the days of radar common sense was a familiar ingredient in radio design, but the initial radar equipments did such marvelous things that we became dazzled by the possibilities which beckoned us on to greater and greater miracles, until finally we reached the point where the addition of a new bit of electronic equipment to a naval vessel required the removal of an equivalent weight of something else, and aircraft designers said, with almost as much truth as humor, that every airplane needed a glider in tow to carry the electronic equipment.

It sometimes occurs that our judgments and attitudes toward the conflicting factors of design become distorted and we put too much emphasis on one factor or another. To illustrate—suppose that the time is December 1941 or thereafter, and radar has not been invented or even thought of by anyone. Suddenly a man appears at the Navy Department with a big black box which he calls radar, and which he says will direct accurate fire on enemy ships eight miles away in inky darkness. The box is 6 feet cubic and weighs six tons. By some miraculous dispensation he obtains immediate opportunity to demonstrate his gadget, and proceeds to make good his claims completely. Would the Navy Department accept his device and install it, even if they had to remove a gun or some other six-ton equivalent? They would have done so without hesitation, and radar would have started in the Navy on the basis of doing a marvelous job with an instrument weighing six tons.

But what actually happened was that radar appeared in the category of radio equipment, and therefore there was immediate pressure to make it similar to radio communication equipment. It could be made small, as all these modern electronic gadgets can, and the designers responded to these pressures. But one of the costs of this process has been in reliability. The movement toward reduction in size and weight has proceeded too rapidly to maintain a proper balance with reliability. Smallness and lightness are desirable objectives, of course, and maximum efforts should be expended to obtain them, but the efforts can be overdone. If you put more pressure on designers for small size than for reliability, you will get small size at the expense of reliability. This situation is aggravated by the fact that designers of service equipment are remote from the point of use, are unfamiliar with the conditions of use, are not intimately aware of the vital importance of reliability. Consequently, they will take chances with reliability, without realizing it, in order to meet the high pressure demands for reduction in size and weight.

Reliability of Equipment

The radio engineer formerly put reliability at the top of his list of requirements, but it began to go downward on his list when broadcasting came in, and dropped still further when radar and its very complex relatives came in. The designer no longer has either the responsibility or the "feel" of the operating end, but he does have terrific pressure to get size and weight down. The commercial or military requirements dominate, and it is likely that the manufacturer whose design is lighter and smaller gets the job. Size and weight can be measured readily—reliability, unfortunately, can not.

Difficulties are enchanced considerably by the fact that there is little attempt to maintain continuity of basic designs in newer equipments. Each new equipment

usually is planned new from top to bottom without regard to the older equipment it replaces. In most products, including electronic products for the home, new models utilize as much as possible of the previous ones, with consequent benefit to cost, operation, and maintenance. But in aviation electronic products any similarity to previous models is purely coincidental.

Electronic equipment design can obtain much benefit from use of more mechanical engineering talent. Until recently electronic equipments were designed almost wholly by electrical engineers. The mechanical arts which are common practice in typewriters, cameras, adding machines, clocks, and such, have been almost completely absent in electronic apparatus. As a result, as electronic apparatus grew from three tubes in a wooden box, to the superheterodyne receiver, to the television receiver, to the radar fire-control equipment, the apparatus became, first, a rat's nest of parts and wires, and finally a serviceman's nightmare. Electronic equipment can be vastly improved merely by adopting some of the techniques which enable calculating machines, Leica cameras, wrist-watches, and telephone exchanges to keep on working for years, with little maintenance difficulty.

Every effort should be made to provide opportunity for field testing new equipments before final production runs. I recall that during World War II, the British Royal Air Force finally set up a separate and complete air base solely for aviation electronic testing, manned by British Royal Air Force personnel with recent combat experience. All new electronic devices were sent first to this operational air base, where they received rugged testing by people with fresh operational viewpoints. This unit had authority to make any design changes necessary to secure reliability or operational efficiency. I understand that the United States Air Force also has set up this kind of operational field testing facility.

Some such procedure saves time, trouble, and expense in the long run. Exceptions may occur, in those cases where the new device is revolutionary, and so powerful that introduction to service is worth while even if accompanied with unreliability and some defects. However, we have reached the point where such revolutionary devices are rare, and in most cases, it would pay to take the time, first, to give field experience to the design engineers, and, second, to give thorough field testing to early production units before full production is executed.

Reliability of electronic equipment in service depends upon the designs of many details, of course. For a high degree of reliability, it is essential that the design engineer have intimate knowledge of the service conditions, and of service experience with similar previous equipments. Contact of the electronic designer with the field has been far from intimate, and in many cases is negligibly small. This has resulted from the enormous expansion of the electronic field in aviation, and from the high degree of compartmentalization in operating organizations. The situation might be illuminated by comparison with another branch of electronic production, namely, broadcasting. In broadcasting-receiver production, there is little chance of a serious defect appearing in a new model on a large scale, because of past experience with very similar equipments. Even where a defect does creep in, the organization for reports of trouble in the field is so clear and direct, that corrective changes are made within a very short time after initial production. In contrast, military-equipment production contracts are often completed before any reports from the field are available. Laboratory testing of a few pre-production or early production samples, while of some benefit, does not catch many things which show up in actual service, and which often are sufficiently serious to create the reliability problem that so concerns us now.

The Future

So far, we have looked at the past and the present, and we now should attempt to see what is indicated by them for the future. There are distinct lessons, warnings, and guide posts. Before attempting to remark on them, it may be interesting to note ways in which the Soviet Union attacks the problem of modern complex equipment. Their policies on design are as different from our as are their political methods. While there is no good in the latter, there may be something useful to us in the former.

A recent article on Soviet ordnance,[2] by Jarrett of the Army Aberdeen Proving Ground, states the case clearly. He says:

"It is indeed time that both official and nonofficial circles understand why and how the Communists devised their tools of war.

"Accustomed as we are to glistening automobiles, polished machinery, and beautiful design, the realization that the Soviet weapons, crude in appearance, rough in finish, and functional in design are capable of sufficient performance that they can have a high pay-off, comes as something of a shock.

"The Soviets believe that there is no sense in building into an appliance any 'fancy' features or giving a finish to the parts which makes for beauty. They build nothing into an item that does not aid its intended purpose. In addition to this, they strive for great simplicity, both in manufacture and maintenance. They try to make an item simple enough so as not to require the services of a specialist for its everyday maintenance.

"The point simply is that so much of what we design and build in this country is 'Pullman-car' comfort, while most of that made by the Soviets is cattle-car quality. Surely somewhere in between lies a suitable compromise—a coach-type accommodation.

[2] Col. G. B. Jarrett, "Soviet ordnance," *Ordnance;* March–April issue, 1953.

"An interesting point lies in the recent remark of an ordnance technician writing from Korea: 'The shame of it all is these Maxims always seem to work when often our own do not.' So often a degree of perfection is sought by our own designers which, while desirable, is unnecessary.

"All Soviet equipment is characterized by the following:

1. Simplicity of design for ease of manufacture, operation, and maintenance. It is designed to be made by workers who in many cases have little or no training. . . . Further, the piece can be maintained and operated in the field by the soldier who doesn't have even the mechanical qualifications of the factory worker.
2. Economy of strategic or natural materials and assembly time.
3. Lightness in weight for shipping and handling.

"Perhaps it would be prudent to weigh carefully the presumed advantages of added features in modern fighting equipment that we may not produce items which are over-costly from a manpower-resources viewpoint. Theorists frequently confuse the basic values, trying to design an improvement when the unimproved device is already adequate.

"It will be folly to forget that any future war will consume such vast amounts of materiel that we will be forced to economize in order to keep pace with the replacement demands. *One way to do this today is to differentiate between quality and refinement.*"

Now, what of the future? What can we do to meet the grave practical problems in aviation electronics? Something must be done because, troublesome as the present situation is, the end of growth toward more and more complexity is not yet in sight. There is need for electronic, automatic jet-engine control to improve engine efficiency, and need for various automatic systems to remove some of the burdens on the pilot. There is need for better means for rendezvous and traffic control of planes under all weather conditions. Automatic blind landing devices are needed. Refinement of equipment from radar to computer, to auto pilot, to plane control, is needed. Better information to planes from ground radar and computers is needed. Better identification equipment is needed. Civil aviation must do something about radar for avoidance of collision and weather turbulence, and for traffic control. The great possibilities of television for simplification of communication and traffic control by visual means should be exploited. Even all these items do not make a complete list.

The limited responses of the human being in the face of requirements for more and faster reactions, brought on by high-speed jet operation, make automatic control of various elements mandatory. Getting the big, expensive, atom-bomb-carrying bomber or the large civil transport plane through to destination is important. Getting it back again is important also! Longer missions, smaller crews, more fatigue, all require more automatic operation, more electronic equipment, more complexity.

All this means that the pressure for more complexity will be heavy and continuous. But somehow we must get the whole matter under control, or we will have flying machines which are test laboratories, rather than instruments for military defense and civil transport.

Operational Requirements

There are at least a few things which can be done to meet the problems. First, and most effective of all, is to minimize operating requirements. This may seem to be a drastic and undesirable thing to do, but there are many cases where it is feasible and desirable, simply because there has been and still is a natural tendency to set operating requirements unnecessarily high. In every stated requirement there should be a really careful, thorough weighing of each of the many possible compromises between performance on the one hand, and cost, simplicity, reliability, and ease of operation and maintenance on the other. That compromise which accepts the lowest practicable performance will pay big returns all along the line.

The Navy is meeting this situation by reviewing military characteristics to eliminate all but the essential functions required to perform primary missions. In his address to the Armed Forces Communication Association on February 10th, 1953, Captain F. R. Furth, United States Navy, described several examples of good results already obtained by this review. In the case of one transmitter, parts eliminated were 35 tubes, 60 relays, 80 switches. The weight saving was 168 pounds and the estimated "down time" will be 80 per cent less. In another case, that of a search radar, dozens of parts were eliminated, the original 22 controls were reduced to 10, and the cost of the device was reduced 40 per cent.

Integration

The second possibility for better future design results is that practice which has come to be called "integration." In the past, every electronic device added to the airplane has been complete in itself. If it required a gyroscope, it included one, even if there were a half dozen gyroscopes in other instruments already on the airplane. If a new radio transmitter required a plate supply source, it was built in, although another transmitter already on board had a power source equally good. The two transmitters probably came from two different manufacturers, with no co-ordination between them.

Treatment of the aircraft as a whole, from the system viewpoint, is an obvious "must" for the future, and integration of devices aboard aircraft clearly should be the next major step. Since every pound eliminated from equipment weight means from five to eight pounds less gross weight of the airplane, the tremendous value of integration is clearly evident. Many elements are susceptible to integration benefits. Some of these are power

supply, cooling, navigation aids, communication, fire control, gyroscopes, kinescopes, electronic computers.

Extraordinary co-operation between the electronic designer and the air frame designer will be required to obtain maximum benefits of integration. Obviously, the co-operative effort must begin very early in the design of the airplane, and must deal intimately with every detail of the electronic equipment. It will be a difficult process, requiring considerable reorganization of the processes of procurement and supply, but the results which can be achieved will be worth the effort.

An encouraging step toward integration is reported from the recent Montreal Conference of the International Civil Aviation Organization, at which recommendations were made on integration of bad-weather landing aids, such as approach lighting systems, electronic landing systems, and radar systems.

One difficulty in applying integration on a large scale is that new developments come very frequently. The temptation to introduce them quickly is great, but should be resisted, if reliability and maintenance are to have adequate consideration. In all but rare cases, new developments had better be held for inclusion in the next integrated design.

Unit Construction

The third item on the list of things which can improve future conditions is the use of unitized construction, with a high degree of utilization of "plug-in" of the units. This may involve some sacrifice in performance, in some cases, but in probably all of these, the sacrifice will be small in comparison with the gains. Not only is manufacture improved, and greater use of standard units in different equipments made possible, but maintenance is very greatly simplified. Unitized construction probably offers the only solution to the problem of maintenance of new complex devices with the necessarily insufficiently-trained maintenance personnel. Unitized construction can not only improve maintenance, but it can save manpower by lessening the training requirements for maintenance, and the personnel required.

An additional advantage of unitized construction is that it makes feasible the inclusion in equipment of means for simple testing of the units. Such provisions permit the establishment of simple procedures for preventive maintenance and protection against failure, and such procedures are necessary in any complex apparatus if it is to have operational readiness consistently and reliably. No one would think of undertaking a long trip in a plane, automobile, or motor boat, without inspection of parts, cleaning, lubrication, changing of spark plugs, etc. Similarly, no complex electronic equipment should have to go into the air without an inspection. If the examination is to be both effective and practicable, means must be designed into the equipment to make it so, and test instruments, designed for the purpose, must be part of the equipment.

Procurement Policy

Procurement agency policy often has large but hidden effect on integration and quality of product. Usually the planning of a new airplane carries the development of the air frame and engine well along before electronic equipment is considered at all. When the completion date for the airframe is pretty well known, consideration of electronics begins, and the prospective electronics suppliers find themselves under pressure to meet the airframe completion date. This was permissible when the electronic equipment was relatively simple, but, now that it is such a large and vital part of the airplane, it is not good practice. This situation has often occurred, however, and the contract often goes to that electronic supplier who will meet the airframe date, even if he does not have time to develop his designs to the degree of reliability and maintenance quality that he could if given more time. If procurement agencies will give more weight to reliability in the early stages of planning, that is, allow time for it, there will be less later difficulty with reliability in service.

I happen to know of one aircraft communication equipment which is entering production, and in which time has been afforded for extensive consideration of the reliability question. It uses unitized construction to considerable degree, includes provision for simple test procedures, and should be a highly satisfactory equipment. However, over 130 man-years were required for its engineering design. We will have more reliability in electronic equipment when design time is applied in proper proportion to the complexity of the equipment.

Detail Design

There are several matters of detail-design character which will give aid in solving the practical problems now facing us. The "reliabilizing" of all components is one of these. Another is the substitution of the transistor or the magnetic amplifier for the vacuum tube wherever practicable, with consequent benefit in the several directions of more ruggedness, less heat generation, fewer component parts. Another is standardization of units wherever possible. There is no good reason why the audio amplifier in a new equipment should be completely different from every audio amplifier ever built previously. Still another is automatic factory production of parts and sub-assemblies, which can increase the uniformity and reliability of equipment.

At this point, I would like to make a suggestion, a rather radical one, which I think could have much effect in improving equipment from the maintenance and operating viewpoints. It is that whenever an important new design job is undertaken by an engineering department, those engineers of the department who will have the responsibility of detail-design decisions—there will be some junior and some senior engineers in the group—be required, as their first step, to spend about one month's time on the repair bench of a large aviation electronic maintenance shop. I am sure that the time

thus spent will be returned later many times over in the lessened requirements on hundreds of maintenance and aircrew men who will handle the equipments in service.

The problem is not *too* difficult. I understand that the B-29 central fire control system, which was far from a simple system, made the record in World War II of better than 95 per cent operational over target. This was accomplished by good design, and well-trained maintenance personnel equipped with good test equipment.

Conclusion

At the present moment, we are in a very special and transitional period in electronic design. World War II and the immediately subsequent years saw the introduction into service of many new, complex equipments, designed, built, and rushed into service with all possible speed. They had good basic ideas, but time was not afforded to make the designs adequate for good maintenance and reliability. Recently, we have begun the process of turning out complex equipment with better designs. I think that within a year or two the reliability problem will be much less serious than it is now. However, and here I think a word of caution is justified, this desirable condition will come about only if we do not go off half-cocked in response to demands for the still newer, fancier equipments which the laboratories will continue to produce.

Planning agencies must strike a better balance between the natural desire to have the latest gadget, and the cold, hard, high-inertia factors of logistics, personnel training, maintenance, repair, and operational readiness generally. We have now reached the point where new designs need to be reviewed very carefully, to determine whether the advantages which they well may have, outweigh the disadvantages which their introduction necessarily brings about in the field. A new radar should be introduced quickly when you don't have *any* radar, but when you do have a pretty good radar, working well and all forces familiar with it, a new one must have a large degree of improvement over the old to justify its introduction. Even then, the introduction must be orderly, if the new device is to be a positive contribution to over-all operational effectiveness.

We want progress, we must not delay progress, but we should make sure that hoped-for progress is real and useful up there in the air, where there is such a place as a point-of-no-return.

The Development of a Variable Time Delay*

KENNETH W. GOFF†, STUDENT, IRE

The following paper is published through the courtesy and with the approval of the IRE Professional Group on Audio.—*The Editor.*

Summary—**This paper describes the design, construction, and performance of a magnetic-recording drum time-delay system. The device, which has been developed for use in such acoustic studies as noise localization, reverberation analysis and others amenable to correlation techniques, utilizes conventional proportional recording. Two channels yield a relative time delay between their outputs which may be varied from minus 15 milliseconds to plus 190 milliseconds with an accuracy of ±0.2 per cent using the instrument dial.**

Principal attention in the paper will be paid to the following: (1) Obtaining a uniform layer of magnetic material by spraying with a dispersion of iron oxide; (2) analyzing the effect of spacing between the magnetic material and the head upon the processes of recording and reproducing; (3) developing a mechanical driving system as free from flutter as possible.

Introduction

THERE ARE MANY applications in acoustics and allied fields for a variable time delay of the type described in this paper. Probably foremost among these applications is the use of a precision variable time delay as a component in analog electronic correlators for use in acoustical measurements. A time delay can also be used as an auxiliary to a sampling analog correlator to speed up the computation of correlation functions for large values of τ. The original work of Haas and Meyer[1] and later work of Bolt and Doak[2] and Parkin[3] show that the use of time delays can help to preserve realism in speech reinforcement systems. The applications of time delays also include sound ranging, speech scrambling and producing artificial reverberation.

Methods of delaying audio frequency electrical signals might be listed in three general categories: (1) purely electrical, (2) electro-acoustical, and (3) electro-mechanical. Real and artificial transmission lines make up the

* Decimal classification: R143.4/R365.35. Original manuscript received by the Institute, April 2, 1953. Report supported by Office of Naval Research under contract no. N5 ori 07869.

† Acoustics Laboratory, Massachusetts Institute of Technology, Cambridge, Mass.

[1] H. Haas, "The influence of a single echo on the audibility of speech." (A dissertation for a doctor's degree under the supervision of Prof. E. Meyer, University of Göttingen.)

[2] P. E. Doak and R. H. Bolt, "A tentative criterion for the short-term transient response of auditoriums," *Jour. Acous. Soc.*, vol. 22, no. 4, p. 507; 1950.

[3] P. H. Parkin and W. E. Scholes, "Recent developments in speech reinforcement in St. Paul's Cathedral," *Wireless World*; February, 1951. P. H. Parkin and J. H. Taylor, "Speech reinforcement in St. Paul's Cathedral," *Wireless World*, pp. 54–57, February, 1952; pp. 109–111, March, 1952.

first category and are generally useful only for delays of less than a few microseconds. The transmission of sound between transducers separated by solid, liquid, or gaseous media characterizes the electro-acoustical methods. These methods afford longer delays but their performance is frequently limited by the transducers, and the attenuation and frequency response are functions of the magnitude of the delay.

The development of magnetic recording during recent years has made possible the use of a magnetic material as the medium in the electromechanical type of delay. The magnetic material is commonly in the form of a continuous loop of recording tape or a disc or drum plated or coated with a magnetic material.

The system described in this paper is of the electromechanical type utilizing a drum coated with magnetic material as the moving medium. A drum was chosen instead of a loop of tape to avoid the dimensional instability of the tape.

The applications listed earlier require that the delay system have a uniform frequency response throughout most of the audio spectrum and that the relative time delay between its output signals be adjustable from zero to a few tenths of a second.

Outline of the System Employed

The processes of recording, reproducing and erasing employed in this system are similar to those of a conventional tape recorder. In the case of a drum, however, the length of a magnetic track is the drum's circumference, and with continuous erasing and recording no part of the signal remains recorded for less than the period of rotation of the drum. By the end of one period of rotation the signal has been recorded, reproduced, and erased.

In order to obtain a relative time delay, τ, which can go through zero, the system uses two tracks around the periphery of the drum, and the operations of recording, reproducing, and erasing go on simultaneously on both tracks. Fig. 1 shows cross sections of the tracks and a block diagram of the remainder of the system. The input $f(t)$ is recorded on both tracks which rotate with the angular velocity ω of the drum. The outputs from channels 1 and 2 are $f(t-\alpha/\omega)$ and $f(t-\beta/\omega)$ where α and β represent the angular separations of the respective record and reproduce heads. If only relative delays are of interest, let $t'=t-\alpha/\omega$. Then the output of channel 1 becomes $f(t')$ and the output of channel 2 becomes $f(t'-\tau)$ where $\tau=(\beta-\alpha)/\omega$. If α and ω are held constant and β is varied from β_1 to β_2 by rotating either the record head or reproduce head of channel 2 around the periphery of the drum, τ will vary from $(\beta_1-\alpha)/\omega$ to $(\beta_2-\alpha)/\omega$.

It can be seen from the relations given above that the accuracy with which τ can be adjusted for a given mechanical accuracy of the system depends upon the magnitude of ω. In order to permit adjustments of short time delays without requiring unreasonable mechanical accuracy, a movement of one mil (0.001 inch) along the surface of the drum was made to represent a change in τ of 10 microseconds. This set the surface velocity at 100 inches per second. The diameter chosen for the drum was 8 inches, and therefore the angular velocity was required to be approximately 8π radians per second.

The recording, reproducing, and erasing heads were spaced from the surface of the drum to prevent wear. Spacing the heads from the surface of the drum also reduced the mechanical load on the drum drive to that of bearing friction alone, which made it possible to design a mechanical coupling system more effective in reducing fluctuations in the relative time delay.

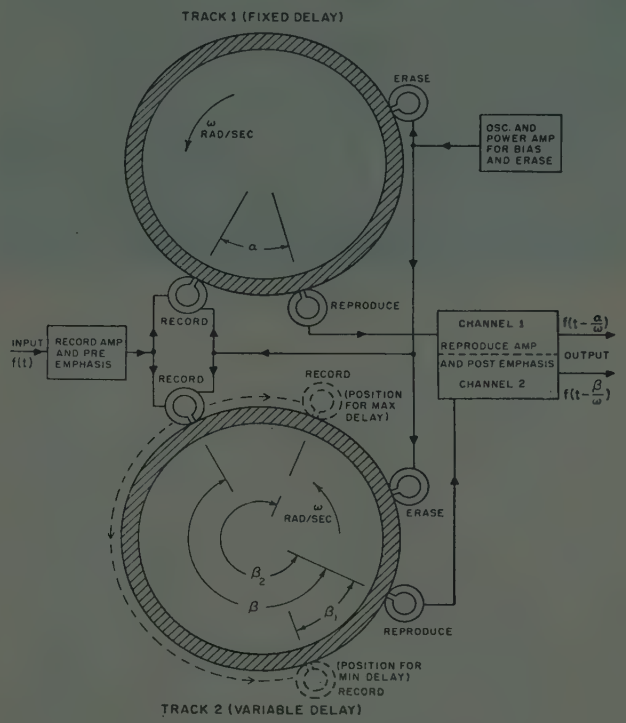

Fig. 1—Block diagram of the system.

The Mechanical System

The Drum and Magnetic Surface

Fig. 2 shows the drum and its supports. The drum was made 6 inches wide to allow for the addition of other recording tracks in the future. The bearings were placed at one end so that the inside surface of the drum could also be used. A pair of precision, pre-loaded bearings were located directly under the left-hand edge of the drum proper. A single precision bearing was located at the extreme left-hand end of the assembly inside the flywheel, which, as will be explained later, is on a separate bearing. The entire drum was machined from 17 ST aluminum alloy, and the 8-inch diameter outer surface has a runout of less than ± 0.1 mil. This accuracy is required in order to reduce variation in the head-to-medium spacing and the attendant amplitude modulation of the output signals.

A coating of magnetic material consisting of a dispersion of iron oxide was sprayed onto the surface of the drum. The oxide coating has good magnetic properties

Fig. 2—The drum and its supports.

for recording and it can be readily applied and removed without dismounting the drum.

The spraying process is similar to that used by the Harvard Computation Laboratory for coating drums used to store digital data by pulse recording. The ring supporting the heads was removed and the remainder of the drum assembly was placed on the table of a milling machine. A small spray gun was clamped to the frame of the milling machine and was fed a very dilute dispersion of the iron oxide held in suspension by the constant stirring of a small electric motor. The drum was then rotated by its normal drive and moved back and forth in front of the spray gun until the desired number of coats was obtained. A few coats of an adhesive were applied to the drum before and after the dispersion to seal the aluminum surface and protect the final surface.

Standard commercial dispersions of black iron oxide and red iron oxide were obtained. Each dispersion was tested by applying 40 coats to the drum resulting in layers approximately 0.4 mil thick. The information thus obtained indicates that although there is little difference in either the output versus frequency or the output versus bias characteristics for the two media, the black oxide, because of its higher coercivity, requires approximately twice as much erase power as the red oxide to decrease the recorded signal by a given number of decibels. Since the higher velocity of the medium and the spacing between erase head and medium make adequate erasing difficult, the lower coercivity of the red oxide was sufficient reason for its choice.

These coatings were sufficiently uniform to produce no measured change in the drum runout. It was found, however, that a larger signal-to-noise ratio was obtained

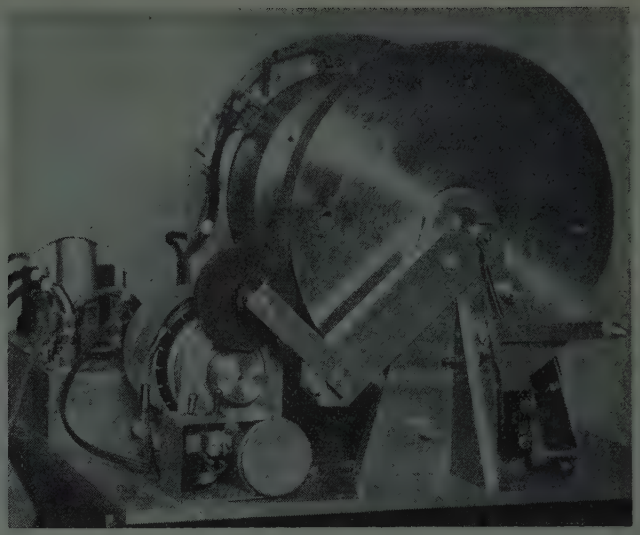

Fig. 3—View of drum showing driving system.

by applying approximately the same thickness of coating in more layers. The coating now in use on the drum is approximately 0.5 mil thick and resulted from 225 passes under the spray gun.

The Mechanical Drive System

In order to eliminate fluctuations in τ, the velocity of the drum should be constant. Both belts and idler wheels were tried as coupling devices between the motor and the drum in an effort to reduce variations in the drum velocity. The idler wheel showed two distinct advantages over the belt: (1) The idler wheel can be operated so that increased load pulls it into tighter contact with the capstan and driven surface, thus making it partially self adjusting. (2) The idler wheel can be operated so that speed fluctuations introduced by its irregularities are of much higher frequency than those introduced by a belt. These high-frequency fluctuations are more highly attenuated by the low-pass, inertia-controlled system. This smoothing or filtering action can be enhanced further by increasing the compliance of the drum-idler wheel coupling. The driving system shown in Figs. 2 and 3 provides one way of increasing this compliance while also adding inertia to the system in the form of a flywheel. The flywheel runs on an independent bearing concentric with the drum and is rim driven by the idler wheel as shown in Fig. 3. The idler wheel is disengaged from the flywheel and capstan when the motor is turned off, in order to prevent any plastic deformation that might result from prolonged contact. Fig. 2 shows the spring coupling between the flywheel and the drum. Stop pins prevent excessive stretching of the springs as the drum is accelerated to full speed.

Fig. 4 shows an electrical circuit analogous to the mechanical driving system. Current is analogous to torque and voltage is analogous to angular velocity. The motor-to-idler-wheel and idler-wheel-to-flywheel speed-ratios have been used to refer all velocities, torques, and component values to the drum side of the system.

The synchronous drive motor shown in Fig. 3 is of the hysteresis type and has an almost constant torque characteristic during starting. This enables it to accelerate the system to synchronous speed without stalling or causing excessive slipping of the idler wheel. After the system reaches the steady state the motor can be considered as the constant velocity source ω_0 which is shown in Fig. 4.

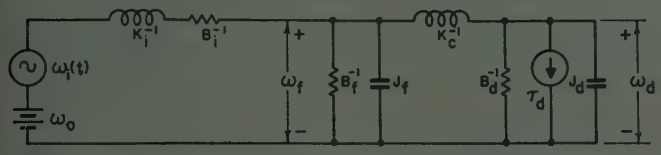

Fig. 4—Analogous electrical circuit of the mechanical driving system.

The fluctuations in speed caused by irregularities in the idler wheel are represented by the velocity source $\omega_i(t)$. The rotational compliance K_i^{-1} and rotational resistance B_i represent the compliance of the idler wheel and motor suspension and the slippage of the idler wheel; B_f and J_f represent the viscous bearing friction and moment of inertia of the flywheel, the rotational compliance K_c^{-1} represents the coupling springs between the flywheel and the drum, and J_d represents the moment of inertia of the drum. The drum bearings are pre-loaded to such a pressure that their behavior is more nearly that of rolling friction than that of viscous friction. The quantity τ_d in Fig. 4 is a torque, constant in magnitude and always opposing the motion so as to represent the rolling friction of the drum bearings. The viscous bearing friction is represented by B_d. The complex, natural angular frequencies of the analog circuit of Fig. 4 are approximately $-2\pm j0$ and $-0.22\pm j7.5$. These values indicate an underdamped resonance of frequency 1.2 cps with a decay time of 4.5 seconds.

The period of rotation of the idler wheel is approximately 1/14 second and thus the lowest frequency component of $\omega_i(t)$ is approximately 14 cps. To evaluate the usefulness of placing the compliant coupling K_c^{-1} between the flywheel and the drum, the ratio of the ac component of the drum velocity ω_d to ω_i was calculated for both the normal coupling springs and for rigid coupling between the drum and flywheel ($K_c^{-1}\rightarrow 0$). These calculations show that the compliant coupling gives a 43-db reduction in the 14-cps component of ω_d as compared to rigid coupling.

Variations in the velocity of the drum such as those just discussed have two effects upon the operation of the system:

1. The frequencies of the reproduced signals are modulated.

2. The magnitude of the relative time delay is modulated.

The first effect is a function only of the ratio of the instantaneous velocity of the drum as a given point passes under a recording head to the velocity when it passes under the reproducing head of the same channel. The magnitude of this frequency modulation is given directly by information such as that shown in Fig. 5 which is a plot of the instantaneous frequency of the reproduced signal versus time for a 4-kc input signal.[4] These curves show the effectiveness of adding the coupling springs. The conditions for both curves were the same except that for curve (a) the flywheel was rigidly coupled to the drum and for curve (b) the normal coupling was employed. The predominant component remaining in (b) is a 4-cps fluctuation corresponding to the period of rotation of the drum.

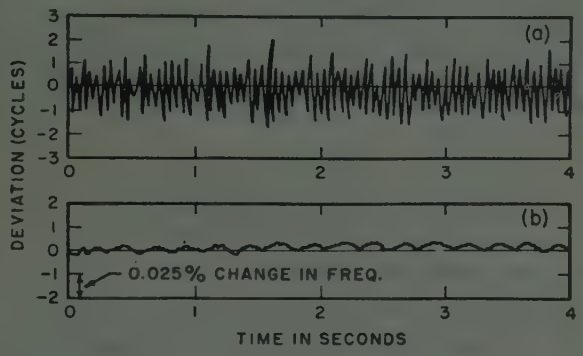

Fig. 5—Frequency modulation of the output for 4-kc input signal: (a) rigid coupling and (b) normal compliant coupling between the flywheel and drum.

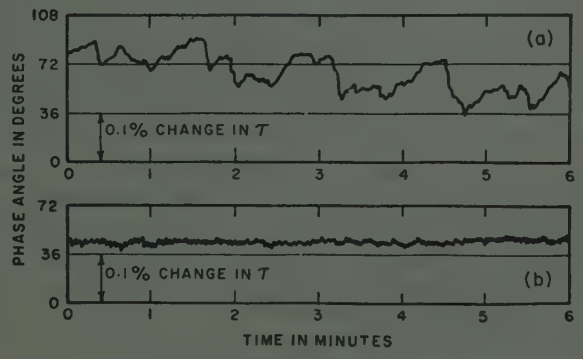

Fig. 6—Modulation of the relative time delay, τ: (a) 60-cps power line and (b) constant 60-cps source used to operate drive motor.

The modulation in τ is dependent upon the variations in drum velocity between the time the signal is reproduced from channel 1 and the time it is reproduced from channel 2. Fig. 6 is a plot of the phase angle between the two outputs of the system for a relative delay of 100 milliseconds and a frequency of 1 kc, and thus gives a measure of the modulation of τ. Curve (a) shows that variations in line frequency result in a slow drift of approximately ± 0.1 per cent in τ. Curve (b) shows that by operating the drum drive motor from a steady source of 60 cps, the variations in τ are reduced to ± 0.02

[4] The frequency deviations shown in Fig. 5 were measured by the axis-crossing interval meter (ACIM) developed in the M.I.T. Acoustic Laboratory and described in the *Acous. Lab. Quar. Prog Report*, pp. 32–34; July–September, 1951.

per cent. This remaining fluctuation is composed of random variations plus 4-cps and 1.2-cps components. The random variations are caused by changes in idler wheel slippage (changes in B_i of Fig. 4). The 4-cps and 1.2-cps components correspond respectively to the frequency of rotation of the drum and the underdamped natural frequency of the mechanical filter.

The mechanism for rotating the record head of channel 2 around the drum is shown in Fig. 2. The gearing is such that the mechanical revolution counter indicates τ directly in tenths of milliseconds. The record head was chosen rather than the reproduce head to be moved around the periphery of the drum to vary the magnitude of the time delay. This choice was made because the mechanism for rotating the head causes small variations in its spacing from the medium, and, as will be shown, the performance of the recording process can be made almost independent of small variations in head to medium spacing.

The Recording, Reproducing, and Erasing System

Choice and Mounting of Heads

The heads used for the operations of recording, reproducing, and erasing are all modified versions of a half-track erase head. These heads are 0.125 inch wide and originally had front and back gaps of approximately 5 mils. The surfaces along the pole pieces where the tape would normally run were ground flat for about 50 mils on either side of the gap. This permits a more uniform area of relative contact with the magnetic medium and assures that these surfaces are exactly perpendicular to the side of the head used for mounting. The heads were mounted around the periphery of the drum from a ring support as shown in Fig. 2. A fine-thread set-screw and spring are used to permit adjustment of the head-to-drum spacing. The heads have been operated with spacings of approximately 1 mil for several months without requiring adjustment.

The Recording Process

In order to investigate the effect upon the recording process of spacing between the record head and the magnetic material, data for Fig. 7 were taken on a red oxide coating. The wavelength, λ, of the recorded signal is given by $\lambda = v/f$ and is in mils if v, the velocity of the medium, is in inches per second, and f, the recorded frequency, is in kc. For wavelengths long compared to l, the width of the gap, and d, the spacing, the principal effect of the spacing is a division of flux between the paths l and l' of Fig. 7. For this approximation the division is dependent primarily upon the reluctance of the two paths, and the magnitude of flux going through the recording medium (path l') is a function of the ratio of d to l.

Variations in the record head to medium spacing cause corresponding changes in both the signal and bias intensities in the medium. In order to separate the effects of the changes in bias and signal fields, data for the dashed curves of Fig. 7 were taken with the bias readjusted for maximum output for each value of spacing. It can be seen that the effect of increasing the spacing is the same on the 100- and 1,000-cps signals ($\lambda = 0.1$ and 0.01 inch respectively).

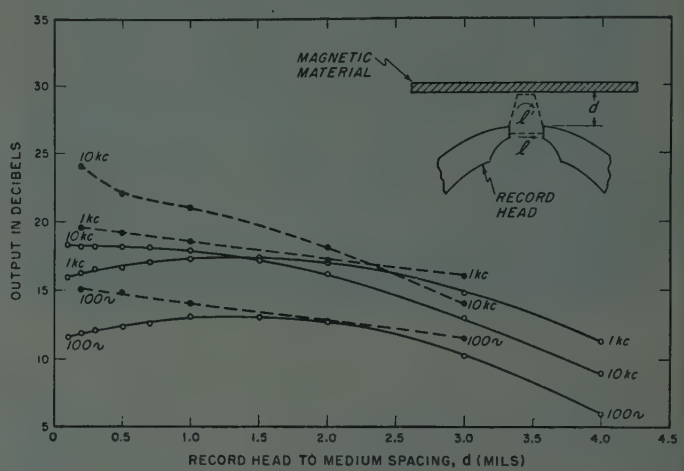

Fig. 7—Output versus spacing of the recording head. Bias set at one value for solid curves. Bias adjusted for maximum output at each value of spacing for broken curves.

For shorter wavelengths, this simple approximation must be revised to include the effect of broadening the magnetic field with increasing spacing. The graphical analysis of the field of the recording head given by Begun[5] is applicable to this refinement. While Begun's analysis was made for the flux distribution within powdered iron oxide in contact with the record head, it would not be appreciably different for air since the permeability of the iron oxide was only 3. This analysis shows that the field is much less sharply defined even at a relatively short distance from the record head. Begun then shows by a graphical analysis of the recording process employing ac bias that this broadening of the field causes a loss in high-frequency response. In the present case, therefore, there is a departure from the frequency independence discussed earlier. The broken curves of Fig. 7 illustrate this effect in that the curve for 10 kc ($\lambda = 10$ mils) has a steeper slope than the curves for 100 and 1,000 cps.

It should be noted that the reduction in the signal field illustrated by the broken curves of Fig. 7 is only a part of the total effect of spacing upon the recording process. For a constant bias mmf applied to the record gap, the bias field as well as the signal field in the magnetic medium decreases as the spacing increases. The effect of an ac bias upon the recording process is covered from several points of view in the literature.[6–8] In general, the process of linearly superimposing the signal on

[5] S. J. Begun, "Magnetic field distribution of ring recording head," *Audio Eng.*, vol. 32, pp. 11–13; December, 1948.
[6] S. J. Begun, "Magnetic Recording," p. 57, Murray Hill Books, New York, N. Y.; 1949.
[7] R. E. Zenner, "Magnetic recording with ac bias," Proc. I.R.E., vol. 39, pp. 141–146; February, 1951.
[8] W. O. Muckenhirn, "Recording demagnetization in magnetic recording," Proc. I.R.E., vol. 39, p. 891; August, 1951.

a high-frequency bias of several times the signal amplitude makes it possible to obtain a remanent induction in the magnetic material that is very nearly proportional to the instantaneous intensity of the signal field at the trailing edge of the record-head gap. As a compromise between high output and low distortion it is frequently recommended that the bias be adjusted to a value 20 to 30 per cent greater than the value yielding maximum output for medium wavelengths.[9] Since the output versus bias-mmf curves have a negative slope in this region, the decrease in bias intensity in the recording medium caused by an increase in the record head to medium spacing tends to produce an increase in output. The solid curves of Fig. 7, taken for a fixed bias level at the record head, show that this effect tends to cancel the effect owing to division of flux discussed earlier giving approximately zero slope for values of spacing in the vicinity of 1 mil.

When the zero-slope spacing is used, this method appears to give the same freedom from signal amplitude fluctuations owing to variations in record head-to-medium spacing that would be given by boundary-displacement recording[10] without the necessity for maintaining a saturated medium with the accompanying high noise level.

The Reproducing Process

A sinusoidal signal recorded in a longitudinal manner on a magnetic material can be thought of as a series of half wavelength magnets end to end along the direction of motion as shown in Fig. 8. As stated before, the recorded wavelength is given by $\lambda = v/f$. Thus, as the frequency increases, the length of these half-wavelength magnets decreases and their field decays more rapidly with distance from the surface. The head-to-medium spacing for the reproducing process is therefore more effectively expressed in terms of wavelengths (d/λ in Fig. 8).

The curve shown in Fig. 8 agrees quite well with the theoretical and experimental values given in the literature.[11,12] The function has an almost constant slope of -56 db per unit of d/λ, or $(56f/v)$ db/mil of spacing in the units used above. It can thus be seen that the amplitude modulations of the signal produced by variations in the reproduce head-to-medium spacing will increase directly with frequency. For the drum run-out of approximately ± 0.1 mil, $v = 100$ inches per second as given before, and $f = 10$ kc, the amplitude modulations of the signal owing to the reproducing process would be approximately ± 0.5 db. If the bias and record head-to-medium spacing are adjusted for cancellation of the amplitude modulation in the recording process,

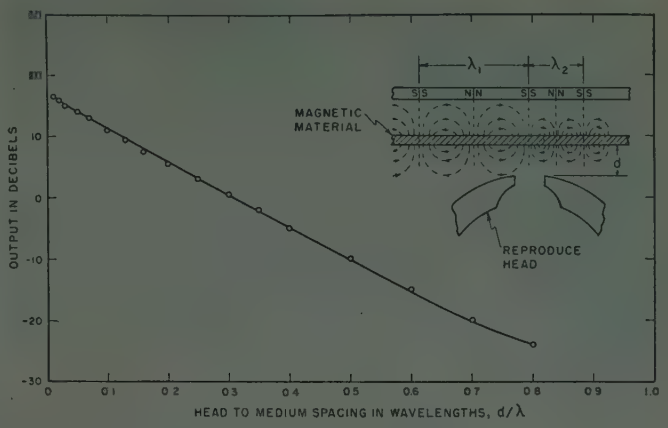

Fig. 8—Output versus spacing of the reproducing head in wavelengths. Insert in a cross section of the reproduce head together with flux distribution in magnetic material on which two frequencies have been longitudinally recorded.[13]

the total amplitude modulation of a 10 kc signal is ± 0.5 db. This is illustrated in Fig. 9 which shows the over-all frequency response of the system. The amplitude modulations appear to begin suddenly at 8 kc because the graphic level recorder used to plot the curve could not respond to changes of less than 0.5 db.

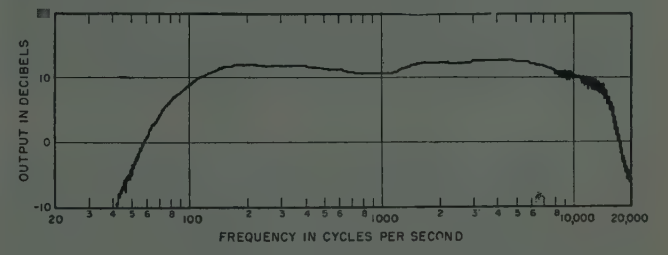

Fig. 9—Over-all frequency response of the system.

The length of relative contact between the reproduce heads and the medium is approximately 0.1 inch. Thus, below about 200 cps ($\lambda = 0.5$ inch) only the leakage flux from the magnetized medium passes through the reproduce head and the unequalized reponse changes from a 6-db per octave to a 12-db per octave slope.[14] The low-frequency limit of the system was set at 100 cps because the post-emphasis necessary to equalize the response for lower frequencies would cause a prohibitive increase in the hum and noise level.

Many of the factors that affect the amplitude-frequency response of the system produce no corresponding phase-frequency characteristic. Thus, when the over-all amplitude response is equalized by a minimum phase network the phase-frequency characteristic is not flat. This phenomenon is characteristic of magnetic recorders utilizing the high-frequency region of their response and restricts the application of the system to operations not requiring waveform preservation. This is not detrimental to the performance of the delay as a component of a correlator because in this application

[9] S. J. Begun, "Magnetic Recording," p. 212, Murray Hill Books, New York, N. Y.; 1949.
[10] H. L. Daniels, "Boundary-displacement magnetic recording," *Electronics*, vol. 25, p. 116; April, 1952.
[11] "Effects of tape contact on frequency response," *Sound Talk*, (Minnesota Mining and Manufacturing Company, St. Paul, Minn.), no. 6; January 10, 1949.
[12] R. L. Wallace, Jr., "Reproduction of magnetically recorded signals," *Bell Sys. Tech. Jour.*, vol. 30, part II, p. 1145; October, 1951.
[13] S. J. Begun, "Magnetic Recording," p. 74, Murray Hill Books, New York, N. Y.; 1949.
[14] O. Kornei, "Frequency response of magnetic recording," *Electronics*, vol. 20, pp. 124–128; August, 1947.

only the relative phase shift between the two channels is of importance. Departure of this relative phase shift from that of a pure time delay can be minimized by careful circuit symmetry in the two channels.

The Erasing Process

The front gaps of the erase heads were increased to 23 mils in order to obtain a sufficiently broad spatial field distribution to give adequate erasing action. The same source of 40 kc ac was used for both bias and erase to eliminate the possibility of audio frequency beats between the two.

The Electronic Circuits

The electronic circuits are quite conventional with several high-Q traps inserted at strategic points to reduce the 40-kc signal resulting from erase and bias leakage to approximately the level of the hum and noise. The record current is constant with frequency to 1 kc and rises to a maximum pre-emphasis of 7 db at 10 kc.

Summary of Performance Characteristics

The mechanical filter in the driving system makes it possible to hold the peaks of the flutter in τ to approximately 0.02 per cent of τ or less for all values of τ. The rejection of the flutter components due to irregularities in the idler wheel is so high that the performance is relatively independent of the condition of the idler wheel.

The relative time delay between channels 1 and 2 is continuously variable from -15 milliseconds to 190 milliseconds. The mechanical revolution counter shown in Fig. 2 indicates the value of τ directly in tenths of a milliseconds. As mentioned before, variations in line frequency cause a drift of approximately ± 0.1 per cent in τ. The over-all fluctuation in τ can be reduced to approximately ± 0.02 per cent by using a more stable 60-cps source. The factors mentioned above, together with inaccuracies in the gears used to rotate the record head, limit the calibration of the revolution counter in absolute values of τ to approximately ± 0.2 per cent.

The over-all frequency response of the system is shown in Fig. 9. It is within ± 2 db from 100 cps to 10 kc and drops rapidly below 70 cps. Noises owing to nonuniformity of the magnetic material, hum pickup in the reproduce heads, circuit noise and bias leakage are all at about the same level. The total noise measured with a Ballantine 300 VTVM is 50 db below the reproduced signal corresponding to the recording level causing over-all system distortion of 3 per cent at 400 cps. The relative phase shift between channels for zero τ is less than 1 degree for frequencies from 500 cps to 5 kc, and gradually increases to approximately 4 degrees at 100 cps and 10 kc.

Applications of the System

The performance characteristics of this system appear to be satisfactory for a wide range of laboratory applications. This system has been used in conjunction with a sampling analog correlator to compute the autocorrelation functions of various types of music, and to compute the crosscorrelation function between stimulus and brain waves. It has also been used briefly in psychoacoustical studies. Upon completion of the remaining components of an analog correlator it is hoped that this time delay system can be used in applying correlation techniques to some of the problems in room acoustics.

Acknowledgment

The author would like to express his appreciation to Professor Jordan J. Baruch who supervised the development of this time-delay system.

Design and Performance of a High-Power Pulsed Klystron*

M. CHODOROW†, senior member, ire, E. L. GINZTON†, fellow, ire, I. R. NEILSEN‡, associate, ire, and S. SONKIN§, member, ire

Summary—**This paper describes the design, theory, construction, and operation of multi-megawatt pulsed klystrons.**

* Decimal classification: R355.912.3×R351. Original manuscript received by the Institute, March 15, 1953. The research reported in this document was conducted at the Microwave Laboratory, Stanford University, and sponsored by contracts with the Office of Naval Research, which were supported by the U. S. Navy (ONR), the Atomic Energy Commission, the U. S. Army Signal Corps, and the U. S. Air Force.

† Stanford University, Stanford, Calif.
‡ Pacific Union College, Angwin, Calif.
§ The City College of New York, New York, N. Y. Stanford University 1948–50 on leave from The City College of New York.

I. Introduction

THE PURPOSE of this paper is to describe the generation of high pulsed power by means of klystrons, and the design and general behavior of such tubes. The problems involved in designing and building megawatt klystrons were first attacked and successfully solved at Stanford University, and an account of this work is given here. Specifically discussed will be the design and operating characteristics of pulsed klystrons, operating at 3,000 mc in the voltage range of 100–400 kv and delivering power output in the

vicinity of 20 megw. These tubes were the first pulsed klystrons ever to deliver more than 20 to 30 kw of power at this frequency, and, as far as is known, have delivered higher pulsed power, at any frequency, than any other tube now in existence.

As an original investigation in the field of such unusually high power and voltage, many new and basic problems were encountered which had to be solved before a successful design could be established. Among the most important were:

1. The extension of basic klystron theory into the range of relativistic velocities. In spite of the fact that a considerable body of theory and empirical data exists upon which a design of the klystron can be based, much of this information is not applicable on account of the relativistic effects.
2. The analysis of the magnetic focusing of a cylindrical beam. Subsequent to the completion of this work on the problem, equivalent theoretical analyses by other workers have been published.
3. The general question of cathode emission from oxide cathodes at voltages of 400 kv.
4. The voltage breakdown limits in the various parts of the structure, including the rf interaction gaps. In a successful design, the gradients had to approach the dc field-emission limits. It was not certain that dc experience could be applied to microwave frequencies.
5. Methods of generation of short pulses, at about 100 kv and 1,000 amps had to be developed, together with the requisite gap switches.
6. Pulse-transformers, stepping up the modulator voltage to the desired range of 400 kv, had to be developed.
7. Dielectric strength of various materials had to be measured at short pulse-lengths, so that proper design of pulse-transformer, cathode bushings, and so forth, could be established.

In most of these matters there was little and often no previous experience for guidance. As it turned out, however, none of these problems proved to be very difficult, and the first tube designed on paper operated successfully in March, 1949. Since then, something like 30 tubes have been built, and as many as 15 have been operated simultaneously at power levels of the order of 10 megw each. The tubes, as they are now being built, except for minor modifications in construction technique are essentially the same as the original design, and aside from certain minor differences in fabrication, and so on, are identical to the first model.

We shall describe here in some detail the fundamental problems involved in the design of a tube to run at these power levels, explain why this particular type of tube was selected for our purpose, and also give some of the operating characteristics of the tubes which have been built and tested.

The successful operation of the first design is taken as evidence that the theoretical predictions are correct, and that there are no major practical difficulties. The fact that operating voltages are high does not appear to be a serious practical matter. By providing a single oil bath for the cathode bushing and the pulse transformer, the problems of handling such high voltages are immediately reduced to those of standard practice.

It is hoped that the experimental material in this paper will be regarded as representative of the new art, and not as any limitation of what can be expected by way of performance from the pulsed klystron tube. It is believed that the theoretical results here presented, together with experimental data, will allow many other designs to be arrived at, with good assurance of success.

II. Basic Design Considerations

A. Design Objectives

While the principal purpose of this work had to do with the desire to demonstrate the feasibility of generating high pulsed power by means of the klystron, the specific laboratory work was profoundly affected by another project at Stanford, the development of the billion-volt linear electron accelerator. In fact, the choice of operating parameters for the first model, and subsequent construction of additional models, was determined as a consequence of accelerator development. For a period, during 1948–1950, the klystron work was supported by funds provided for accelerator work. It might not be inappropriate to review the reasons for the specific requirements which were established for the first model.

In 1947 a linear electron accelerator, driven by a single magnetron delivering 0.7 to 0.8 megw, was successfully operated at Stanford University, and its operation confirmed all the theoretical analyses of the performance of such a machine. On the basis of this performance and the theory, it seemed entirely feasible to build a linear electron accelerator to produce electrons of a billion volts or higher. In order to do this, however, it would be necessary to provide 400 megw of pulsed rf power, preferably around 3,000 mc.

If this power was produced by multiple sources, all of them would have to be synchronized in phase in a suitable manner. One could produce this amount of power by using a sufficiently large number of lock pulsed oscillators, presumably magnetrons. This seemed completely out of the question as a practical solution, since it would require something like 600–700 magnetrons. The problems of maintenance of synchronization seemed too complex to make this at all practical.

It was suggested by Gintzon in 1944 that it might not be difficult to build klystron amplifiers, each delivering 15–30 megw of pulsed power, and since they would be driven as amplifiers from a single master oscillator, the problem of phase synchronization would be relatively simple. Although the previous best figure for pulsed klystrons had been about 30 kw,[1] there are

[1] As developed by Electric and Musical Instruments, Ltd., in England in their CV150, about 1944. L. F. Broadway, C. J. Milner, D. R. Petrie, W. J. Scott, G. P. Wright, "Velocity-modulation valves," *Jour. I.E.E.*, vol. 93, Part IIIA, no. 5, p. 855; 1946.

some elementary reasons which indicated that much higher powers could be obtained. Most simply stated, the advantage of klystrons over other tubes in producing high pulses (or cw) power, is a matter of geometry.

If one refers to the schematic drawing in Fig. 1, it can be seen that the regions of beam formation, rf interaction, and beam collection are separate.

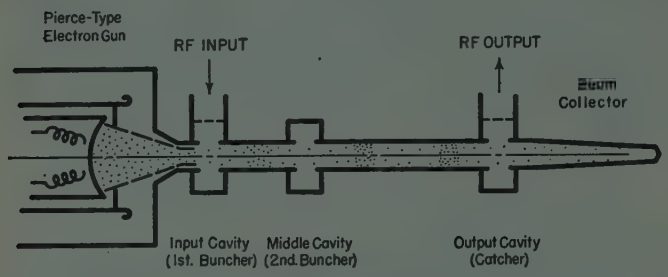

Fig. 1—Schematic representation of a typical three-cavity cascade amplifier klystron. Magnetic focusing is not shown.

The design of each region can be made almost independently of the others and optimized to give best performance of its particular function. One can design the cathode-anode region with sufficiently large cathode area and sufficient inter-electrode spacings so that emission density and voltage gradients are not excessive. By care in beam focusing one can minimize the interception of beam by the rf region so that heat dissipation is not excessive. Since in the klystron the collector has just one function of dissipating heat, it can be designed to be of any arbitrary size and shape to handle the average or peak beam power. In other tube types these functions, i.e., emission, rf interaction, and collection occur in the same region whose dimensions have to be an uneasy compromise between rf and heat dissipation requirements.

The actual choice of operating frequency for the first model, as determined by accelerator requirements, is not critical. For various reasons, it seemed that an operating frequency of around 3,000 mc would be a good choice. For a billion-volt electron accelerator, the total power required at 3,000 mc would then be of the order of 400 megw, preferably delivered by about 20 tubes, with a pulse length of 2 μsec and a pulse repetition frequency of 60 cps. These requirements determined the specifications for our first klystron, and were used as the basis for the design. These specifications will be justified in some detail later.

Wavelength	10.5 cm
Maximum beam voltage	400 kv
Maximum peak vurrent	250 amp
Power input	100 megw
Power output	20–40 megw
Pulse duration	2 μsec
Power gain	30 db

The last specification would permit one to drive all of the tubes, namely 20, at 20 megw output, using a master oscillator which delivered about $\frac{1}{2}$ megw, or allowing for padding, and so forth, perhaps 1 megw. This was within the range of available magnetrons. If necessary, a klystron oscillator similar to the amplifiers could be used.

In order to meet the gain requirement, it was necessary that the klystron be a three-cavity cascade amplifier, such as shown in Fig. 1.

Following are the detailed considerations which entered into the selection of some of these specifications and what is involved in meeting them.

B. Electron Beam Design

For operation at the required output power level, it was necessary to analyze in some detail the relativistic effects on the operation of a klystron amplifier.[2] The details of this analysis will be reported in a separate paper, and only some of the results will be quoted here as needed.

For a power output of 20–30 megw, assuming efficiencies between 30 and 40 per cent, something like 60–100 megw of beam power input are required. Such efficiencies are based on experience with low-power klystrons. As will be discussed later, calculations indicate that the efficiency would not be decreased until the voltages approached extremely relativistic values.

With the requirement of 100 megw of beam power, one still has a range of choices of beam voltage and current. At higher beam voltages and, therefore, lower current, space charge effects would be decreased and focusing problems would be simplified. However, there are adverse relativistic effects which put a limit on the feasible voltage. As the electron velocity approaches the velocity of light, (at 510 kv, velocity of electrons is 86 per cent of velocity of light) changes in the electron energy produced by the modulating gap voltage appear essentially as changes in electron mass rather than velocity. It is the velocity modulation that is, of course, required for klystron bunching action. Even at 400 kv, where the beam velocity is 0.8 c, the per cent of velocity modulation, as produced by a given ratio of modulating voltage to accelerating voltage, is only 0.4 of the value for nonrelativistic velocities. In addition, there are obvious problems connected with the modulator which become more difficult at the higher voltages.

If one goes in the direction of higher current and lower voltage, space charge effects, both dc and rf, would tend to become greater. Klystron operation at conventional power levels indicates that performance deteriorates somewhat as one tries to exceed perveances of unity. As an example of voltage reduction which might be feasible, consider a cathode of perveance of two at which, presumably, the space charge effects would not be appreciably worse than at perveance of unity. One hundred megw input would require about 300 kv at

[2] M. Chodorow and E. L. Ginzton, "High Power Pulsed Klystron Project N6onr-251, Task Order IX," Microwave Laboratory Quarterly Report No. 1; September, 1947.

330 amp, so that the reduction in voltage obtained is not too significant compared to 400 kv and 250 amp at the more conservative perveance of unity.

The question arises as to the influence of relativistic voltages on the various space charge effects. Theoretical calculations were carried out to study several phenomena, including transverse spreading of a beam under the action of its own space charge, and the longitudinal debunching of a velocity modulated beam. In all these cases the effect of relativistic voltage was merely to modify the debunching parameter h, sometimes called plasma wave number,[3] by a factor $(2/R+1)^{3/4}$, where $R=1/(1-\beta^2)=v/c$. This means that space charge effects will be slightly reduced as one goes to higher voltages, but this is a negligible improvement, as even at 400 kv this factor is only about 0.75 as compared to unity at the very low voltages.

The gun to produce a beam of the required kind was chosen to be of the Pierce type. This cathode is conventional in every way, except size. It is designed by standard procedures, and as it is used presently, is a modification of one originally designed for us at Sperry Gyroscope Company. It was decided to attempt to use an oxide-coated cathode. Dimensions of the cathode as finally used are such that the cathode area is about 55 sq. cm, and the maximum current density will not be greater than 5 amp per sq cm. This can be taken as a conservative number in terms of tests made on diodes elsewhere. Therefore, there seemed to be no objections to the use of an oxide cathode because of current density limitations. Similarly, the gradients at the cathode were also well within previously determined safe limits.

The only factor which could not be anticipated (because of lack of previous experience) was the effect of ion bombardment at these high voltages. However, calculations of the probability of ion formation by a 300 or 400 kv beam at the usual pressures indicate that the rate of ion formation is very low and, therefore, the number of ions available would be relatively small. Further, most of these would be formed in the drift tube where there are no dc fields to accelerate the ions toward the cathode. The drift velocities are not great enough to bring them to the cathode-anode region during the pulse. The performance of the tube has born out these predictions, and apparently oxide cathodes at these voltages are practical.

One more factor which must be considered is the effect of relativity on the Child-Langmuir Law. These calculations were made by us[4] in 1947 and have been quoted and recalculated recently in various publications (in one case incorrectly). The result of the relativistic voltages can be simply represented by a formula for the relativistic perveance

$$K_{\text{rel}} = K\left(1 - \frac{3}{28}\frac{eV_0}{mc^2}\right),$$

where K is nonrelativistic perveance, V_0 is beam voltage. This indicates a lowering of the perveance of about 2 per cent at 100 kv, and 8 per cent at 400 kv. This is not large enough to affect the design seriously.

Cathodes that were actually used are shown schematically in Fig. 2 and in a photograph, Fig. 3.

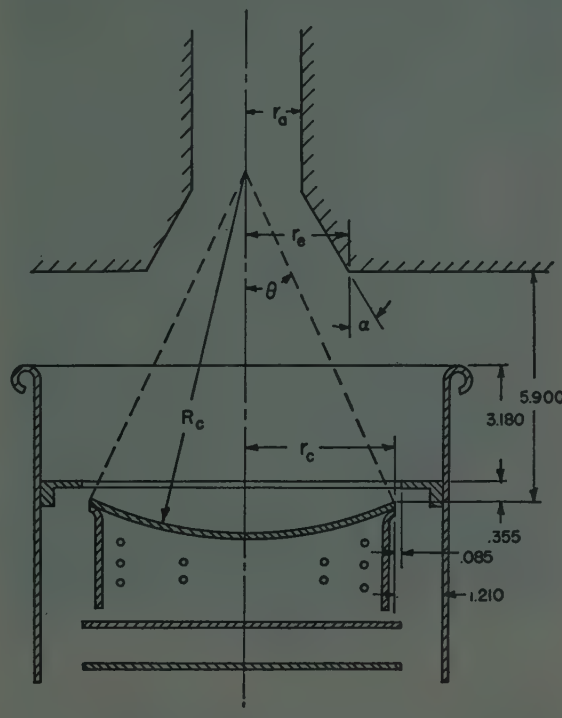

Fig. 2—Cathode-anode design for 400 kv, 250 amp gun. All dimensions are in cm. $\alpha=30°$; $\theta=25°$.

C. Beam Focusing

The length of the rf portion of the klystron is determined by the fact that one must have sufficient transit time between cavities to get the required gain. In a cascade amplifier such as is being considered, to get the gain required it turns out that distances of about a 4-inch drift space between cavities 1 and 3, and 8 inches between cavities 2 and 3, are required. The diameter is also determined by rf considerations of adequate coupling between the beam and the gap, and was chosen to be about 1.25 in. These values will be justified in appropriate later sections of this paper.

For the present considerations one need point out only that with these values of length and diameter of drift tube, it would not be possible to transmit the beam through the drift tube without the use of magnetic focusing. There exist calculations of the optimum transmission of an electro-statically focused beam through a cylindrical drift tube. One can obtain an optimum ratio of length to diameter for a given perveance. As previ-

[3] The plasma wave number is more convenient to use in discussing space charge effects than the plasma frequency since the former is a constant independent of voltage for a constant perveance cathode. $h=0.03K^{1/2}/r_0$ where r_0 is beam radius and K is perveance.

[4] M. Chodorow and E. L. Ginzton, "High Power Pulsed Klystron Project N6onr-251, Task Order IX," Microwave Laboratory Quarterly Report No. 2; January, 1948.

ously stated, relativistic effects tend to improve this slightly, but not sufficiently to permit the transmission of a beam of perveance unity through a drift tube of the length and diameter required here. The net conclusion is that some means of magnetic focusing must be used.

Fig. 3—Cathode, heater, and support assembly. (See Fig. 6 for an assembly drawing.) Cathode is a conventional oxide type.

According to previously published information, the standard practice in magnetically focusing a beam had been to immerse the tube in a strong axial magnetic field. The electrons then start in a region of a strong field. The elementary theory then shows that if a field is strong enough, any transverse motion of the electrons produced by their own space charge will cause the electrons to spiral tightly around the magnetic field lines and "follow the field lines." Although this method would seem simple to apply, it is essentially a brute force method and requires unnecessarily strong fields.

For practical application, such strong fields are difficult to obtain. It was felt that a more detailed analysis of magnetic focusing should be undertaken, and the general treatment of magnetic focusing in an axially symmetric field with an arbitrary distribution of field was worked out.[5,6] This included the case in which the field has the same value at the cathode as in the beam proper, as well as the case where the cathode is completely magnetically shielded. For the *general case* of an arbitrary amount of flux going through the cathode, with some other value of flux in the drift tube, and without restriction to the case of a uniform field along the axis, one can write for the radial motion of an electron at radius r

$$\frac{d^2r}{dt^2} = \frac{e}{m}\frac{I_0}{V_0^{1/2}}\frac{3\times 10^4}{r} - \frac{e^2}{8\pi^2 m^2}\frac{\partial}{\partial r}\left(\frac{\phi-\phi_c}{r}\right),$$

where I_0 is the current and V_0 the voltage corresponding to the average axial velocity of the beam, ϕ is the total flux linked by the circle of radius r where r is the radial position of the electron, and ϕ_c is the total flux inside the circle defined by the radial position of the electron at the cathode.

It is to be noticed that the effective inward force on the electrons depends on the difference between the total flux linked by the beam at the cathode and at the point under consideration. Thus, any configuration of field in which this difference is large uses the flux in an economic fashion as opposed to the brute force or "infinite" field method. The special case of no flux through the cathode can thus be considered as a special and limiting case of the entire range of field configurations covered by our theory. For any configuration, if one knows the field distribution one can calculate, either numerically or otherwise, the electron trajectories in detail.

For the actual choice of a suitable magnetic focusing field two designs were considered. The first was to locate the cathode outside the magnetic field by using an iron pole piece to shield the cathode anode region. The second was to use a field configuration without iron, such that the field flared out in the right manner to make the field perpendicular to the cathode at the cathode surface. If the flux density increases sufficiently rapidly as one enters the drift tube, a very large, effective amount of focusing field is obtained.

Shielding the cathode completely leads to the special limiting case mentioned above and to the type of electron flow which has come to be known as *Brillouin flow.* Although the basic equations used in calculating this motion were first worked out by Brillouin[7] in 1945, and detailed trajectory equations have been subsequently given by Samuels[8] and Wang,[9] as far as is known the tube under discussion here has been the first one to use anything other than a so-called infinite field.

For the case of Brillouin flow, it is necessary to introduce the flux at the point of minimum diameter of the beam in such a way that the beam is maintained at a constant diameter thereafter. While theoretically this is elegant, practically it is not always simple,[10] and it is

[5] M. Chodorow and E. L. Ginzton, "High Power Pulsed Klystron Project N6onr-251, Task Order IX," Microwave Laboratory Quarterly Report No. 3; April, 1948.

[6] K. L. Brown, "Focusing of the Electron Beam in a High Power Pulsed Klystron," Master's Thesis, Stanford University; March, 1949.

[7] L. Brillouin, "A theorem of larmor and its importance for electrons in magnetic fields," *Phys. Rev.*, vol. 67, pp. 260–266; April, 1945.

[8] A. L. Samuels, "On the theory of axially symmetric electron beams in an axial field," PROC. I.R.E., vol. 37, p. 1252; Nov., 1949.

[9] C. C. Wang, "Electron beams in axially symmetrical electric and magnetic fields," PROC. I.R.E., vol. 38, p. 135; Feb., 1950.

[10] Unpublished work by workers at Bell Telephone Laboratories has considered this injection problem in great detail.

doubtful whether accurate Brillouin flow has ever been achieved except by accident. In addition, and much more important, in any power tube the field for Brillouin flow under dc conditions is not the optimum field configuration for a beam spreading under the action of rf space charge effects at the output end. Because of the uncertainty in the flux distribution with iron, and the probability that pure Brillouin flow was by no means the ideal solution for a tube operating with large signals, a focusing system without iron, and with the flux lines at the cathode being perpendicular to the cathode, was chosen.

This meant that the electrons initially, and until they get up to fairly high velocities, are unaffected by the field. Beyond this, knowing the field configurations exactly, it was possible by numerical methods to calculate trajectories and to find how variations in flux distribution along the beam would affect the motion. These calculations were carried out in great detail for various coil and field combinations and for a range of values of the initial slope of the beam at the anode. A certain amount of unreliability in this initial slope[11] also makes an attempt to get pure Brillouin flow somewhat academic. The absence of iron permitted quite accuate calculation of the dc trajectories, including the effect of different exciting currents in solenoid of several coils. This flexibility was considered to be useful since it would enable one to vary the field along the trajectories of the electron to take care of any rf spreading produced by large signal behavior. These are usually not calculable, but one can always adjust the field to produce optimum power.

It was found in practice that a nonuniform excitation was required for optimum adjustment. As an extra adjustment, it is possible also to wind a small coil approximately in the plane of the cathode, which produces an opposing field to the remaining coils. By this means one can control the flux distribution at the cathode quite closely. It was found in practice that this also had some value in getting better power.

D. Electron Dynamics of Pulsed Klystrons

For the high voltages mentioned, it is necessary to consider the relativistic effects on velocity modulation and the bunching process. Results of the detailed calculations can be briefly summarized. First, for a simple gridded gap and a very small gap transit angle, the velocity v of an electron after it leaves the gap will be given by

$$v = v_0\left(1+\left(\frac{2}{R(R+1)}\right)\frac{\alpha}{2}\sin\omega t\right)$$

where v_0 is the dc velocity, $\alpha = V_1/V_0$, the ratio of rf gap voltage to beam voltage and $R = 1/\sqrt{1-\beta^2}$. Comparison with the standard nonrelativistic results shows that the only difference is the presence of the factor $2/R(R+1)$ (at low velocities this reduces to unity). As previously mentioned, at 400 kv this is equal to 0.4 and is considerably smaller at 500 kv. The only consequence of this in the operation of a tube at extremely high voltages is that a larger gap voltage is necessary to obtain a desired velocity modulation.

For a finite gap transit angle, and no grids, one has to modify this equation by the beam-coupling coefficient. The beam-coupling coefficient is a product of two factors, one which depends on the gap spacing, and one which is a function of the radial position of the electron, since electrons at different radial positions undergo different amounts of velocity modulation.

The beam-coupling coefficient which depends on the gap is unchanged by relativistic considerations, and is still given by $\sin(D/2)/(D/2)$ where D is the transit angle across the gap in radians. The radial dependency is conventionally written for nonrelativistic velocities as

$$\frac{J_0(jk'r)}{J_0(jk'a)}$$

where a is gap radius, r the radial position of the electron, and $k' = 2\pi/\lambda\beta$. This always tacitly assumes that $k' = 2\pi/\lambda\beta$ is much greater than $k = 2\pi/\lambda$. In the relativistic case this is not true and the relativistic radial coefficient becomes

$$\frac{J_0(jr\sqrt{k'^2-k^2})}{J_0(ja\sqrt{k'^2-k^2})}.$$

At 400 kv the effect is not negligible and is favorable.

At the time the tube was originally designed, approximate calculations were made on the rf space charge effects, usually called longitudinal and transverse debunching, to determine in some simple fashion the probable effect of relativity.

Specifically, it was found that for a beam of infinite cross section the longitudinal debunching could be expressed by changing the factor $h = \omega_p/u_0$ by the factor $(2/R+1)^{3/4}$. Similar results were obtained for transverse spreading of a cylindrical beam, calculated in a very simple fashion. Detailed calculations for correct geometry which have been done subsequently[12,13] have verified that the non-relativistic calculations merely have to be modified by this factor, and in addition, by replacing k' by $\sqrt{k'^2-k^2}$, as in the beam coupling coefficient.

The effect of the space charge debunching is to limit the length of drift tube that can be used, since if one goes to values larger than the optimum value, the space

[11] One conventionally uses a focal-length formula to describe the effect of the aperture in the anode. This holds strictly for a small aperture and does not allow for aberrations which are undoubtedly produced by the large aperture and the effect of the hole at the cathode. It is probable that the entrance slope obtained this way, while accurate, is not accurate enough to permit exact evaluation of the minimum beam position.

[12] L. Zitelli, "Space Charge Effects in Gridless Klystrons," Microwave Laboratory Technical Report 149; September, 1951.

[13] M. Chodorow and L. Zitelli, "Space Charge Waves in Magnetically Focused Beams," Address at U.R.S.I. Meeting, Washington; April, 1952.

charge forces start to spread the bunches apart and reduce the available current. There exist detailed calculations by Feenberg[14] which determine these optimum lengths for various beam geometries for nonrelativistic conditions. On the basis of the relativistic calculation made for special cases mentioned, it was felt that it is possible to use Feenberg's results for determining the optimum length with the relativistic correction obtained for these special cases.

Feenberg's theory included the case of cylindrical beams with zero magnetic field (positive ion focusing) and infinite magnetic field so that, strictly speaking, even in the nonrelativistic limit his calculations did not apply to this case.

However, for all types of fields the optimum lengths are not far different (usually in the range (hl) opt = 3–5) even though the detailed behavior of the beam and the mathematics may vary markedly, depending on the actual magnetic fields. The rf space charge effects for a finite focusing field, specifically with zero flux through the cathode, were treated subsequently to tube design and do not disagree with this conclusion.[15,16]

The optimum drift tube lengths, then, are determined by these rf space charge effects. Actually, these were used to determine the drift tube length between cavities *two* and *three*. It is desirable to maximize the gain for this section so as to minimize the voltage in cavity *two*. Even under these optimum conditions the rf voltage required at the *second* cavity to produce optimum current at the *third* is quite large, of the order of 0.50 of the beam voltage.

To get optimum gain between cavities *one* and *two* the same length should be used, but actually this would have given much more gain than was required. The voltage gain between two such cavities is of the order of $\pi N(R/R_0)$, where R is cavity impedance, N is the transit angle between cavities in cycles and R_0 is the beam impedance I_0/V_0. This is not quite accurate, but even with appropriate corrections, at the optimum length, the voltage gain is about 50–60.

In order to simplify the problem of magnetic focusing, it was decided to make the drift tube between cavities *one* and *two* only long enough to give required gain and no more. This is the reason, then, for the fact that the distance between *one* and *two* is less than between *two* and *three*. (No attempt was made to increase the *efficiency* by the expedient of making distances *one–two* equal to *two–three* for a number of reasons, although it was known that this could be done.)

E. Cavity Design

The cavities had to be designed to have: a) proper interaction between the beam and the cavity; b) adequate cavity impedance; c) proper coupling irises for the input and output cavities so that the tube would look approximately matched at the input to the driver and would be properly loaded by a matched output line; d) to permit a certain amount of tuning; and e) a tuning mechanism suitable for a cavity with large rf voltages.

The question of adequate beam coupling depends on a suitable choice of gap spacing and gap diameter. Roughly speaking, the gap spacing must correspond to a transit angle of less than a half-cycle. The beam coupling coefficient previously mentioned will approach unity as one approaches zero gap spacing, but it is fairly close to unity even at a quarter-cycle transit angle. Too close a spacing will reduce the impedance of the cavity, but more important, if the spacing is too close there is a possibility of the so-called multipactor phenomena occurring.[17,18] This is an electronic loading, produced by a cascade process of secondary emission in the gap, in which secondary electrons released from one surface get across the gap in a half cycle under the action of the rf fields. Because the rf voltage will be comparable to beam voltage, in order to prevent multipactor, the actual gap spacing should be equal to or greater than a quarter cycle transit angle.

For beam transmission, the gap diameter should be as large as possible, but there is a limit imposed by the need to get uniformity of coupling to the beam. The determining factor is the variation in beam coupling, as given by the factor

$$\frac{J_0(jr\sqrt{k'^2 - k^2})}{J_0(ja\sqrt{k'^2 - k^2})}.$$

For $a\sqrt{k'^2-k^2}$ equal to unity or less, the variation in beam coupling across the cross-section is less than 10 per cent and is certainly tolerable. For the beam voltages contemplated for this tube, this requirement was more than adequately met by a gap diameter of 1.125 in.

The second item listed above was adequate cavity impedance. If one uses the gap diameters and spacings dictated by coupling considerations, then for almost any resonator built around such gaps it is found that the unloaded impedance will be nearly equal to one million ohms. The exact number is not very relevant since it turns out that in the range of operation the cavity impedance is a completely negligible factor in determining the rf losses. This is because the cavity is heavily loaded by electronic beam loading, due to finite transit time across the gap.

This transit-time loading has been calculated previously by various authors, with the results expressed as a beam loading admittance or impedance. These were again recalculated to find out the effects at relativistic voltages. The results of the relativistic calculations can be expressed by multiplying the nonrelativistic beam-loading admittance by the factor $2/R(R+1)$. The values

[14] E. Feenberg, "Notes on Velocity Modulation," Report 5221-1043, Sperry Gyroscope Company; September, 1945.
[15] Zitelli, *op. cit.*
[16] Chodorow and Zitelli, *op. cit.*
[17] P. T. Farnsworth, "Television by electron image scanning," *Jour. Frank. Inst.*, vol. 218, p. 411; 1934.
[18] W. G. Abraham, "Interactions of Electrons and Fields in Cavity Resonators," Ph.D. Thesis, Stanford University; 1950.

of these beam loading admittances are proportional to the dc beam admittance defined by $I_0/V_0=G_0=1/R_0$, and the ratio is of the order of 0.05–0.1.

For the beam admittance in this tube, namely 250 amp at 400,000 v, i.e., 1,600 ohms, the beam loading resistance is about 15,000 to 30,000 ohms. It is difficult to say more precisely what this value is. The beam-loading calculations have been made on the assumption of *either* no axial magnetic field, or an infinite magnetic field.

In the first case, radial motion of the electrons is permitted in passing through the gap, which makes a contribution to the beam loading. In the second case, there is no radial motion due to the rf field, and no contribution from this motion. Since a finite focusing field was used, neither of these calculations applies exactly, and all one can say is that the magnitude of the impedance must be within this range. Whatever the number is, it is obvious that this is a much smaller value than the cavity impedance itself. Therefore, all the impedance properties of the cavity are determined entirely by the electronic loading rather than by the cold cavity impedance.[19] This is particularly relevant in choosing the coupling iris for the input cavity.

The final cavity design is shown in Fig. 4. The rectangular cross section was used merely because of the ease of fabrication. The input cavity iris is so chosen that when the tube is in operation, the standing-wave ratio looking into the cavity is close to unity. Q-external of this iris should therefore equal the loaded Q of the cavity, and, as it has already been pointed out, this will be almost entirely determined by the beam loading. Due to the uncertainty in this beam loading, Q_{ext} of about 300 was taken as appropriate. At worst this would give a swr of about 2. This assumes the loaded impedance of the cavity $R_{SH}=30{,}000$ and $R_{SH}/Q=100$.

For the output cavity, the coupling condition is determined by the requirement that the tube shall deliver maximum power into a matched guide. Here, the impedance one wishes to present across the output gap is a little uncertain because of the absence of an exact large-signal theory.[20] However, the calculations for gridded gaps, which then existed and which we have since extended to gridless gaps,[21] all indicated that optimum power is to be expected from the electrons when the rf voltage across the gap is approximately equal to the accelerating voltage, with the impedance across the gap about equal to the beam impedance.

It should be pointed out that this is a condition which applies only for a case where the beam impedance is sufficiently small, i.e., when there is sufficient current. Under these circumstances, the equivalent load impedance is much smaller than the cavity plus beam loading impedance, and the circuit efficiency is quite high. For a low beam current, even with optimum bunching, the rf voltage across the cavity may be considerably smaller than the beam voltage. If there is no question of turning back electrons, then the condition for optimum power delivered to the load is to have the load impedance just equal to the cavity impedance. This is the condition one gets for a constant current generator with a fixed internal impedance. This is a true representation of the current at the output cavity for small rf voltages, in which case the circuit efficiency is 50 per cent. If the rf voltage under these conditions turns out to be much larger than the beam voltage, then this reasoning no longer applies and the statements previously made do.

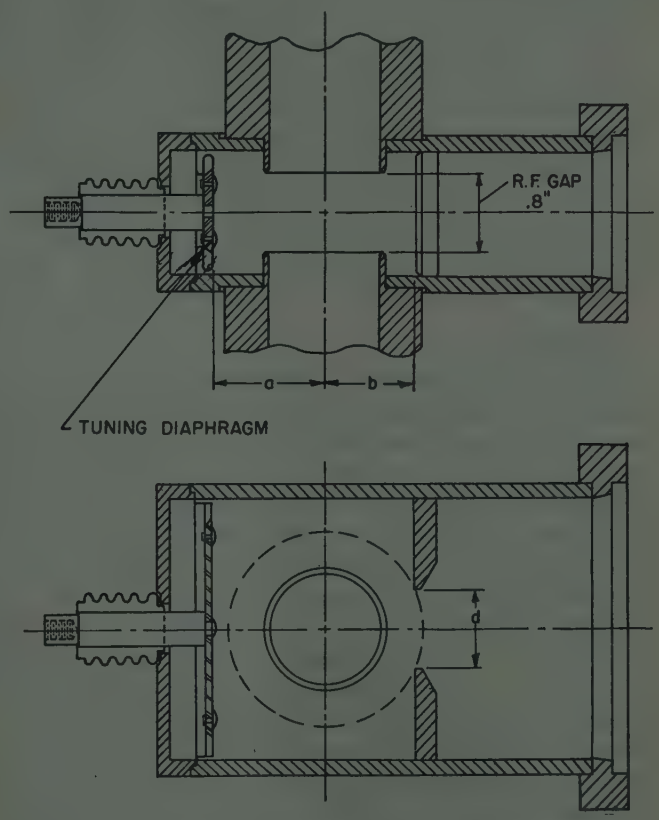

Fig. 4—Cavity resonator as used in the 20-megw klystron; (a) is the profile, and (b) is the top view of the cavity.

For this tube, these latter conditions are certainly well fulfilled since the beam impedance, as previously stated, is of the order of 1,500 to 2,000 ohms, and to reduce the rf voltage to beam voltage the total gap impedance must be of this order. Since the cavity impedances (including beam loading) is perhaps 30,000 ohms, essentially all the impedance that the beam sees will be due to the external load. Calculations indicate a Q_{ext} of about 20 or 30 would result in an impedance across the gap of about 2,000 ohms, with a matched load in the line. These are the numbers that were actually chosen and result in a wide coupling aperture.

The tuning mechanism was chosen as a matter of

[19] This result will be true for almost any pulsed klystron using reasonable perveances. The beam impedance V_0/I_0 decreases with voltage as $1/KV_0^{1/2}$ where K is the perveance, and for voltages in the range of 50°kv up, V_0/I_0 has values of about 3,000–2,000 ohms, the beam loading impedance is roughly 10–20 times as great and this will usually be a much smaller number than the impedances of the cavities used at these voltages.

[20] Feenberg, *op. cit.*

[21] J. H. Tillotson, "Large Signal Behavior of Gridless Klystrons," Ph.D. Thesis, Stanford University, Stanford, Calif.; July, 1950.

convenience, though there were certain special restrictions because of the existence of large rf voltages in the cavity. As shown here, it is a flexible diaphragm which is folded back, and free at the ends. These ends can be free, since the current flow in the cavity is parallel to these edges of the diaphragm. The diaphragm is moved by means of a bellows and post behind the diaphragm, and one can distort it appreciably without being concerned about small cracks developing since the whole mechanism is in vacuum.

Since the cavities for this tube operate in a range of rf voltages, which were to be larger than in any previous tube at this frequency, it was felt that tests should be made to examine whether any discharge effects would occur. A series of tests were run on a cold cavity driven by a pulsed magnetron.[22] Because the cold-cavity impedances are high, it was possible to develop rf voltages of the order of 400–500 kv. It was found that in the absence of an axial magnetic field the cavities behaved in a perfectly normal fashion. With an axial magnetic field there was evidence of cavity loading of some sort and evolution of gas and x-rays. However, these disorders were found to disappear after a few hours of operation. Subsequently, it was found that by care in the processing of the cavities and maintaining the surfaces very clean, these phenomena would not occur and the cavities can stand the rf voltages required in operation.

F. Collector

The remaining problem in the design of this tube involves the beam collector. As has been previously pointed out, its only function is to collect the beam, and therefore it can be made any size or shape which is desirable for the power dissipation, as required. This is one of the most important reasons why one can go to such extremes of pulsed powers (and presumably average powers) with a klystron.

For our application, the average power input is only of the order of 12 kw, and with a cylindrical bucket of the correct size and adequate cooling, there is no difficulty in dissipating this much average power. There is, however, a special problem which has to do with peak power. If a high-intensity pulse of sufficiently short duration impinges on a flat surface, then the thermal constants of metal are such that the heat generated does not penetrate into the surface an appreciable amount during the time of the pulse. The surface will be heated between the beginning and end of the pulse by an amount which is independent of the cooling applied as long as the thickness of the metal is greater than some thermal skin depth.[23] (Of the order of 0.1 cm. for Cu.)

For example, for the beam intensity such as exists in this tube, calculations indicate that if the beam *were not spread in any way*, but was incident normally on a flat copper surface equal to the area the size of the beam, the temperature rise between the beginning and end of the pulse would be of the order of 9,000°C. Therefore, it is necessary to build the collector in such a way that the beam be dissipated over a sufficiently large area to reduce the peak power density to a safe limit. This was done in the collector by tapering it so that the beam, as it spreads, distributes itself along a large area which reduces the peak power density to a tolerable value. The collector is shown in Fig. 5.

The estimates of required areas for power dissipation are slightly pessimistic since they assume that all the power is dissipated directly at the surface. Actually, the high-voltage electrons penetrate a considerable distance into the copper and distribute their energy over some finite thickness. For 400-kv electrons, for example, the range in copper is about 0.01 cm. A calculation on the basis that the energy of the electrons is uniformly distributed through this thickness would indicate the temperature rise at the end of the pulse to be only 1,100°C instead of 9,000°C as above. This is still greater than tolerable and requires that the area be quite large.

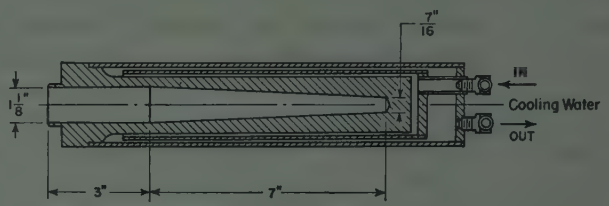

Fig. 5—Design of the beam collector and water-cooling jacket.

III. General Design and Mechanical Construction

Having considered the various basic questions pertaining to the design of the individual components of the klystron, the problem of complete design and construction will be considered next. For the sake of completeness, the design values are collected below.

Pulse length	1–2 μsec
Beam voltage	400 kv
Beam current	250 amp
Cathode current density	4.7 amp/cm²
Perveance	1.25×10^{-6} amp/volts$^{3/2}$
Drift-tube diameter	1.25 in
Drift-tube lengths	
first to second cavity	3.94 in
second to third cavity	7.875 in
Cavity gap spacing	0.800 in
Q_0 for all cavities	6,000 (approx.)
R/Q for all cavities	100–120 (approx.)
Q_L (input)	400 (approx.)
Q_L (output)	30 (approx.)
Cathode	oxide, indirectly heated
Heater power	800 w, max.
Fil. Voltage	22.2 v
Fil. Current	36 amp
Cooling water	2½ gals/min.

[22] These tests were made by A. Harrison and A. Eldredge. "High Power Pulsed Klystron Project N6onr-251, Task Order IX," Microwave Laboratory Quarterly Report No. 2; January, 1948.

[23] A. M. Clogston, "Microwave Magnetrons," M.I.T. Radiation Laboratory Series, McGraw-Hill Book Co., Inc., New York, N. Y., vol. VI, pp. 520–523; 1948.

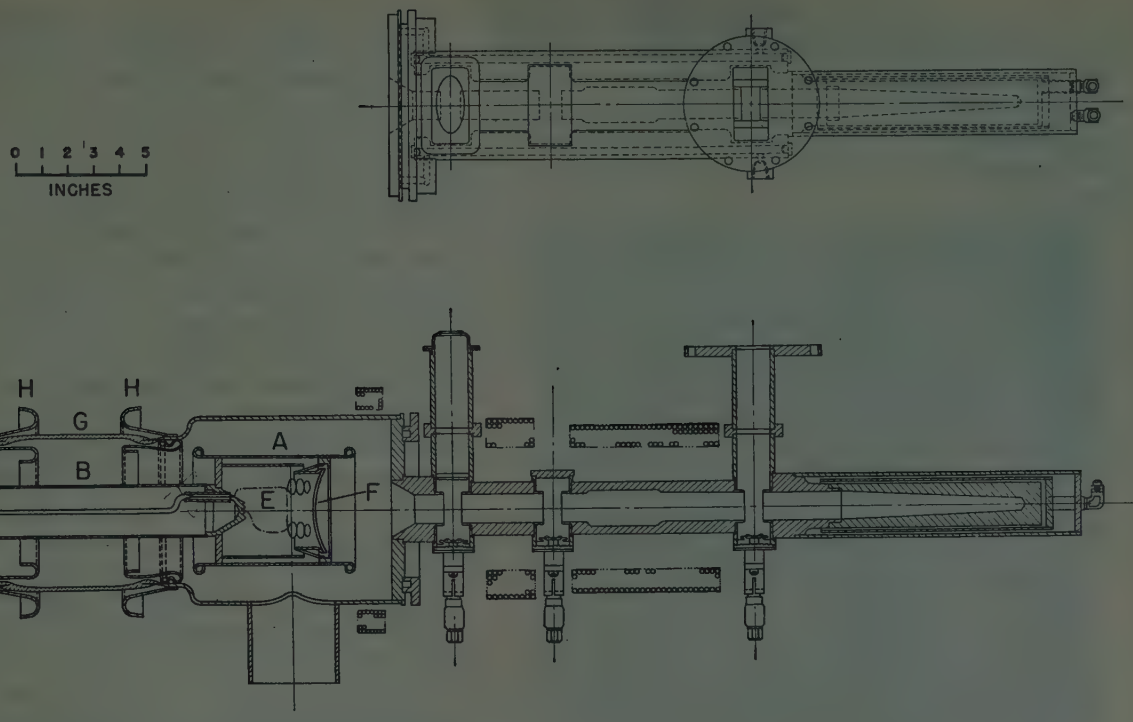

Fig. 6—Simplified assembly drawing of the pulsed klystron amplifier.

Magnetic field	1,000 gauss, approx.
Magnetic-field coil current	30 amp, max.

A. Tube Construction

To insure long-life of the klystron in normal operation, the tube was built so it could be thoroughly outgassed by baking. It was also felt best to follow normal tube manufacturing practice wherever practicable, and to avoid anything that would preclude the tubes being sealed-off, if desired or necessary. Because of these reasons, hard brazing was used exclusively. Having access to sufficiently large hydrogen brazing furnaces, it was decided to build this klystron principally of oxygen-free copper (OFHC), using gold-copper and silver-copper brazing alloys exclusively. It was further felt necessary to provide a simple method of repairing or replacing the cathodes. Because of the above requirements, ordinary gaskets in such joints were avoided.

A simplified assembly drawing of the klystron is shown in Fig. 6. The cathode assembly *A* is supported by means of a stainless-steel tube *B* from the base-plate *C*. The material of the tube *B* and its dimensions have been chosen with some regard to heat-loss through such a support. The support is electro-polished to reduce electrical gradients near the glass insulator *G*, and is vacuum-fired prior to final assembly. The filaments *E* are heated by means of ac current, with the voltage being supplied through lead *D* at the base *C*. The glass insulation *G* is nonex glass, feather-edge, sealed to copper. The glass is sand-blasted inside, with the feather-edges being protected by "corona-shields" *H*. The last two features have been added as precautionary measures; it is not known if they are really required. Photographs of the cathode assembly *A* and its support *B* are shown in Fig. 3.

The cathode surface is made of $\frac{1}{16}$ in. pure nickel, covered by nickel mesh (0.005 in wire, 80 by 80 wires per in.). The mesh is spot-welded to the nickel surface at about $\frac{1}{8}$ in. intervals. The spot-welding is done under alcohol to prevent oxidation. The cathode paint is ordinary oxide material, RCA 144 mix. It is applied with a brush, in several layers, and dried under a lamp. Total coat thickness is about 0.010 in.

The physical relationship of the cathode assembly to the remaining parts can be best understood by comparing Figs. 3, 6, 7, the latter being a composite view of several of the sub-assemblies.

As can be seen from Fig. 7, both the cathode assembly and the klystron are equipped with thin flanges. These are made of nickel and mate when assembled, as shown in Fig. 6. The final vacuum joint is made on the klystron by heliarc-welding of the two flanges together. Replacement of the cathode is then possible by cutting off the heliarc weld (losing in this process about $\frac{1}{16}$ of an inch (radially) each time; the nickel flanges are long enough to allow about ten cathode replacements).

The pump-out tube is located near the cathode and had to be large to maintain adequate pumping speed during activation of the large cathode. The diameter of the tube was $3\frac{1}{2}$ in.—probably larger than necessary.

The cavity resonators are fabricated from home-made electroformed waveguide because of a) special dimensions, and b) unavailability of OFHC rectangular tubing. Electroforming produces excellent OFHC copper about 50 per cent of the time (if and only if the operator

is known to be diligent, careful, patient, and of good moral character). The tuning diaphragms are of 0.003 in. monel for the sake of flexibility, plated with 0.001 in. of copper. The bellows through which the motion is transmitted to the diaphragms is also of monel. The construction of the cavities should be self-evident from Fig. 4.

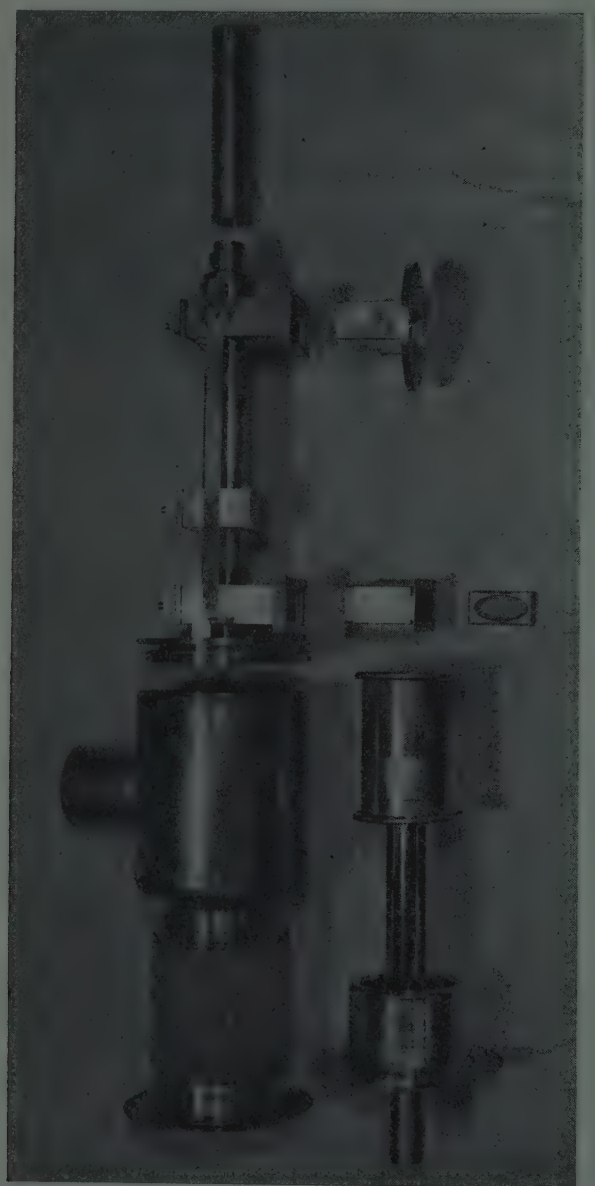

Fig. 7—Photograph showing the relation between the various klystron sub-assembly units.

The assembly of the klystron is carried out in an obvious fashion. The "rf section" is stacked together, with brazing material imbedded wherever required, and the brazing operation of the cavities, drift-tubes, reinforcing ribs, water-cooling jackets, and so on, is made in one operation in the hydrogen furnace. In the next major operation, the cathode glass-seal, the collector, and the window assemblies are silver-brazed to the rf section. This is done by immersing the glass seal into a tube of water, and stacking the various parts on top, wiring them in place with wire wherever necessary. The tub is filled with hydrogen, and oxygen-acetylene hand torches are used to heat the required area. Heliarc-welding is used to attach the input window frame (Kovar) to the completed assembly.

B. Focusing Coils

The focusing coils are wound around the klystron on water-cooled forms, the latter being bolted directly to the klystron support. The coils are wound with copper wire, insulated with a woven glass sleeve. The reason for winding the coils as a permanent part of the klystron is a matter of convenience only. The baking of the glass-covered wire causes some oxidation of the wire, but no significant changes in its resistance have been observed. The glass insulated wire is custom-made only to the extent that the usual binder in the insulation is avoided, as the latter carbonizes in baking, causing partial short-circuits.

C. Completed Assembly

Two klystrons are shown in Fig. 8. One at the left is shown just before the focusing coils are wound, while the one at the right has the focusing coil, the water-jacket on the collector, the outer corona shields around

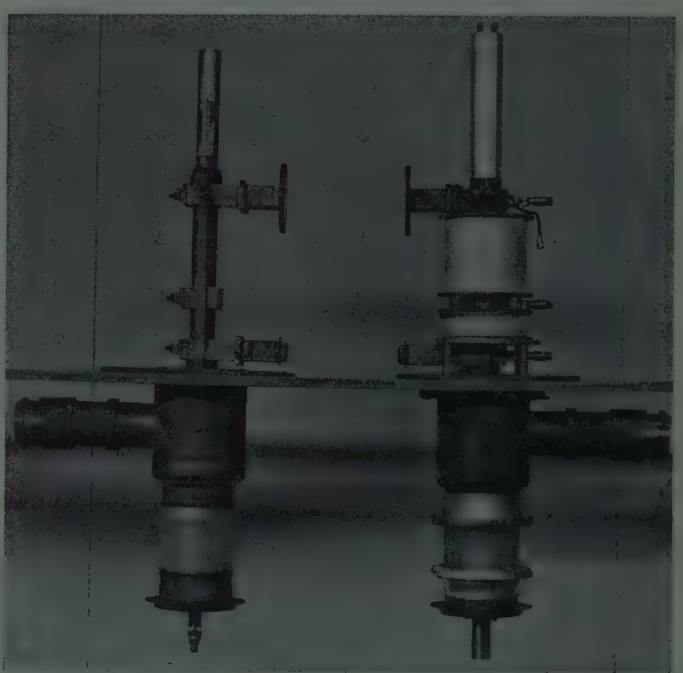

Fig. 8—Two completed klystrons: one at left less its focusing coils; at right with coils and cooling jackets in place.

the cathode bushing, and the tuning micrometers attached to the cavity below. In this condition, the klystron is ready to be placed on the pumping table, to be coupled to the vacuum system, and processed. The processing operation and performance will be described later.

IV. Auxiliary Equipment

A. X-ray Shielding

Unfortunately, a klystron operating at 400-kv level is a very strong source of penetrating X-rays. These need to be shielded in order to make the device safe for personnel in its immediate proximity.

From Bureau of Standards data,[24] one can deduce that a klystron, operating at 400 kv and 30 ma average current, will produce about 1,100 roentgens per hour. To reduce this to the desired standard tolerance rate of 7.5 mr/hr, for a man working in the vicinity of the tube 40 hours a week, would require an attenuation factor of about 1.5×10^5. Using information in available tables,[25] it is found that 2.8 cm of lead is required.

Actually, there are two considerations which will modify the above conclusions. The tables predict the x-ray intensity on the basis of monochromatic radiation. In practice, a continuous X-ray spectrum is produced, and most of the radiation is less penetrating than those that correspond to the limiting 400-kv energy. The second omission has to do with the fact that an oscillating klystron has groups of electrons accelerated to voltages approaching twice the beam voltage, i.e., to 800 kv. This would produce greater X-ray intensity, with greater penetrating powers. These considerations complicated the problem, as the velocity and space distribution of electrons in an oscillating klystron cannot be predicted with any degree of precision in the region beyond the third cavity. It is thus best to use the calculated thickness of lead as a guide, and to determine the safe radiation protection by suitable experiments with an operating tube.

This was done, and Fig. 9 shows the distribution of lead as is used in the laboratory. This amount of shielding is deemed adequate if no personnel is allowed within six feet of the tube for prolonged periods of time. Even with this amount of protection, there are regions in space in which the radiation is excessive. These are the area below the cathode end, above the collector, and in direction of the output waveguide.

In our case, these areas were of no consequence, but point to the problems of making a high-voltage, high-power klystron a really safe device. The reader should note that the efficiency of generation of X-rays and their penetrating power vary rapidly with voltage. A tube designed for a lower voltage would have much less radiation danger.

B. High-Voltage Pulser Design

When the project was started, it was not at all plain that 400-kv pulses could be generated with pulse-lengths of the order of one μsec duration. It was feared that in order to provide adequate insulation for the various cathode parts, the resultant capacity would be so high that it would be impossible to obtain the required rise time. Fortunately, these fears proved unfounded, and the problem of generating the pulsed power at high voltages does not seem to be greatly different from the usual practice at levels previously explored, such as at 50 kv.

[24] "Medical X-ray Protection up to Two Million Volts," U. S. Department of Commerce, National Bureau of Standards, Handbook 41; Superintendent of Documents, Washington 25, D. C.

[25] X-ray mass absorption-coefficients compiled by S. J. M. Allen are tabulated in the *Handbook of Physics and Chemistry*. Chemical Rubber Publishing Co., Cleveland, Ohio; 1949.

As a preliminary to the construction of the pulser, tests had to be made on the voltage breakdown properties of various insulators that might have to be used.[26] The high voltages were obtained by charging a 700-foot open wire line to 650 kv by means of a 60-cps transformer set and discharging the line every half cycle through a water load by means of point to sphere gaps. The voltage across the load was used to test various insulators.

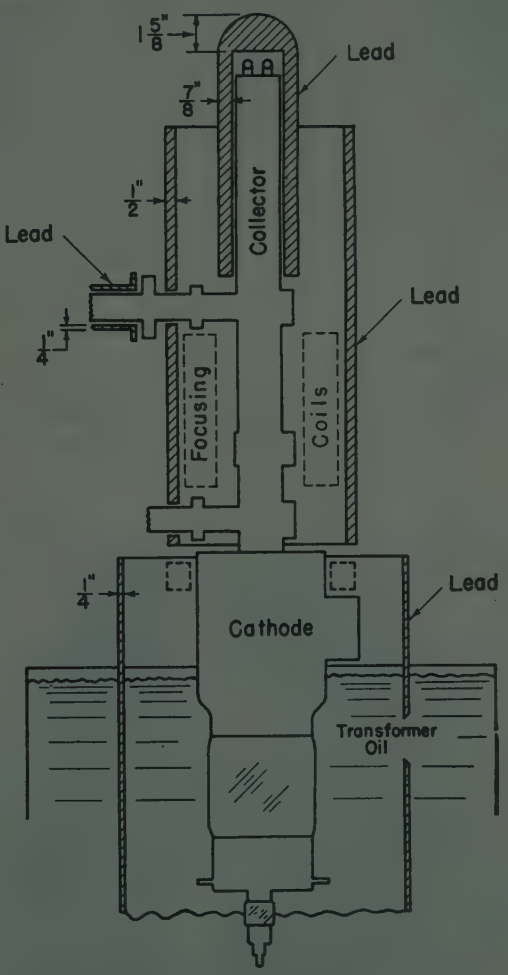

Fig. 9—X-ray shielding of the klystron, showing location and thickness of lead required to establish relatively safe protection.

While outside the interest of this paper, the results proved to be most encouraging. Oil, for example, could stand about 330 kv per in. and the presence of substantial amounts of water did not change its dielectric strength. It appeared that for most things tested, one μsec was too short a time to establish electrical breakdown, and resultant dielectric strengths were most gratifying. Breakdown occurred in "Special Marcol" (a transformer oil), at 330 kv/inch; polystyrene in oil at 260 kv/inch; porcelain stanfoff insulator in oil, less than 35 kv/inch; Nonex 772 Glass tube (oil filled), in oil, 300 kv/inch.

On the basis of these tests, it was decided that the glass bushing of the klystron would be located in the

[26] This equipment was built and the tests made by C. Jones of Stanford Microwave Laboratory.

same bath of oil in which the 400-kv voltages were generated. If, for example, a suitable pulse-transformer could be developed, then only moderately high voltages would have to be handled in air by the remaining components, and the whole problem of generation of the required pulsed power would approximate the usual practice.

With this in mind, pulse transformers of various kinds were studied. Without giving the details of the work, we will merely state that the problem did not turn out to be very difficult. Several types of transformers were built, mostly successfully.[27]

a) A self-supporting winding made of $\frac{1}{4}$-in. copper tubing, with a design value of about 6 kv per turn.
b) A ribbon-type, patterned after a University of California Radiation Laboratory design, resembling paper condenser winding, with about 1 kv per turn.
c) A wire-wound polystyrene supported winding; to be described more fully below.

All of these were wound around a 0.002 in. hipersil strip, built up to about 4×4 in. cross section, with window size of about 6×13 in. The transformer presently being used is shown in Fig. 10. It consists of two pri-

Fig. 10—Photograph showing a 400-kv pulse transformer with a 6:1 step-up ratio. This model, one of the latest models, uses about 1 kv per turn.

maries in parallel, one wound on each leg of the core and two secondary coils in series, also wound on each leg. The ground connection to the secondary is through a meter shunted by a capacity, which provides a reading of the average klystron current.

Embodying these common features, many types of pulsers were considered, and several were built and tested successfully. As it is hoped to publish a separate paper on this work, only a brief description will be given of one satisfactory model.

The essential features of the line-type pulser are shown in Fig. 11. The inductors L and the capacitors C make up the artificial transmission line, or pulse-forming-network. This pulse-line is charged by the method commonly referred to as ac-resonant-charging, and is discharged once per cycle of the ac supply. The charging choke is selected to have an inductance so that in combination with the leakage inductance of the high-voltage transformer it forms a series resonant circuit with the *transformed* capacitance nC of the pulse-line (where n is the number of sections in the pulse-forming-network). This series resonance can be made to occur at the supply frequency, and results in the transient build-up of voltage across the pulse-line, which is characteristic of ac-resonant-charging. The pulse-line is switched to the load by means of a triggered gap, as indicated in the diagram, and a pulse of length $\tau = 2n(LC)^{1/2}$ flows into the load.

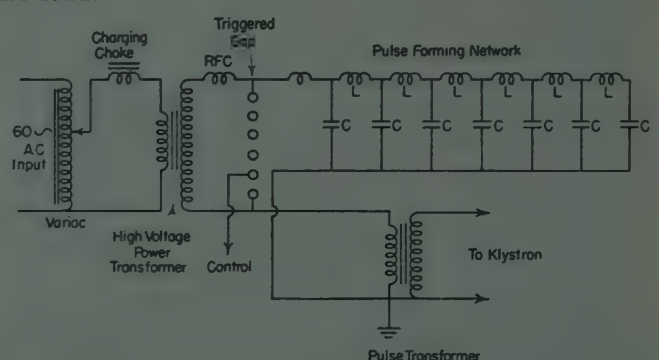

Fig. 11—One type of 100 kv, 1,000 amp, 2 μsec modulator. An important feature of this ac-resonance-charging modulator is the novel triggered gap. See text for further details. The pulse transformer steps the voltage up to a maximum of 400 kv.

Early model pulsers used a rotary gap for the switching, but this was mechanically awkward, had a large jitter time, and operated over only a relatively small voltage range without physical adjustment of the gap. Suitable electrically-triggered gaps have been developed[28] which operate satisfactorily over a wide voltage range (10 to 1 or so) without mechanical adjustment. The jitter time is of the order of hundredths of a μsec, so that the pulse of the klystron can be synchronized accurately with other operations.

There is one difficulty that sometimes occurs in connection with ac-resonant-charging and the use of the triggered gaps mentioned. If for any reason (intentional or otherwise) the gap does not fire, then during succeeding cycles there is a continuing resonant build-up of pulse-line voltage. This higher-than-normal voltage

[27] This work will be reported elsewhere. It was done principally by R. Neal, P. Pearson, and M. St. Clair of the Microwave Laboratory. We were helped in our first design by R. Gillette who was then employed by the Sperry Gyroscope Co.

[28] P. A. Pearson, "Pulsers for the Stanford Linear Accelerator," Ph.D. dissertation, Stanford University, Stanford, Calif.; 1952.

may cause the gap to fire (even if it is not triggered) thereby giving the klystron a higher pulse voltage than normal, and even sometimes one of the wrong polarity.

It should also be noted that the klystron beam-impedance varies inversely as the square root of the beam voltage. Hence, the characteristic impedance of the pulse-line can match its klystron load at only one voltage. At other voltages a mismatch occurs and with it, reflections. In general, it has been found that these reflections can be tolerated, and that klystrons can be operated at differing voltage levels without doing anything at all about the impedance mismatches. The requisite voltage variation is accomplished through change of the voltage applied to the primary of the high-voltage transformer by means of the variac, as shown in Fig. 11.

The operation and design of such pulsers is well understood, and has been adequately described in the literature,[29] but only for voltages relatively low compared to the ones of interest here. Fortunately, it has been possible to extend the design to high-voltage levels without undue difficulty.

Some thought was given to the direct production of 400-kv pulses. When the pulse-line works into a matched load, the pulse voltage is one-half that to which the line is charged. For the production of 400-kv pulses, this would then require the line to be charged to 800 kv. It appeared more practical to produce the pulses at some lower voltage and build a suitable pulse transformer for the required voltage step-up. Blumlein, Marx, and other circuits have also been tried, but shall not be described.

C. High-Power Waveguide Components

For the sake of simplicity, and on account of special requirements imposed by linear accelerator systems, it was decided to evacuate the output waveguide system. In other applications, pressurization would have been more sensible, and is no doubt possible, although we have had but limited (although successful) experience. Many special problems were encountered with the design of evacuated waveguide components, but these do not seem to be of sufficient general interest to be described here.[30]

One of these components, however, may be of interest. An artificial load is required to test the klystron, the requirements being:

1. Capable of handling 2×10^7 w or more of peak power.
2. Electrically matched to standard $1\frac{1}{2}\times3$ in. waveguide.
3. Suitable for high-vacuum operation.

Unfortunately, most "vacuum-clean" materials do not provide enough attenuation per unit length to make a termination of reasonable physical size without doing something special. Iron was tried but the surface quickly oxidized and the resulting iron oxide caused vacuum troubles. Various other unsuccessful expedients were tried.

A final design was made which has been completely satisfactory, consisting of a low-impedance ridged waveguide, such as shown in Fig. 12. It is fabricated of 410 stainless steel, made in two matching halves and welded in an argon atmosphere. The load is 54 in. long and in a length of 24 in. tapers from standard $1\frac{1}{2}\times3$ in. waveguide to a ridge spacing of 0.35 in. In the last 30 in. the ridge spacing is kept constant but the width of the guide is decreased so that its cut-off frequency increases. This results in an increasing attenuation per unit length as one goes down the load and provides a more uniform distribution of power dissipation than a constant attenuation structure.

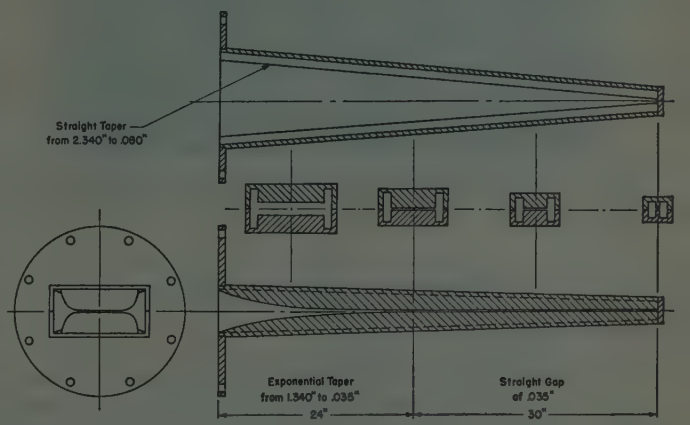

Fig. 12—Details of a high-power termination, capable of handling more than 10 megw when evacuated. It is a tapered ridged waveguide.

D. Vacuum System

In the original tests of the high-power klystron it was found that the production of an adequate vacuum presented some difficulties. A great deal of gas was given off during baking, cathode conversion, and during the early stages of tube operation. Various factors, to be discussed later, contribute to better vacuum conditions in current operation. As a result of experience, a satisfactory vacuum system which is now a part of a standard klystron "package unit" was arrived at.

The photograph of such a package unit is shown in Fig. 13. Visible in the photograph are the Welch $33\frac{1}{3}$ liter per minute mechanical forepump, the Litton diffusion pump, and the liquid nitrogen trap. The latter was considered to be preferable to a charcoal trap since it was found that the charcoal trap did not prevent oil from getting to the cathode. The mechanical pump is spring-mounted so that its vibration is not transmitted to the tube. On the left of the cold trap, the ionization gauge for continuously monitoring the vacuum can be seen. On the panel are switches for the pumps and an automatic control unit for the ionization gauge.

[29] G. N. Glasoe and J. V. Lebacqz, "Pulse Generators," M.I.T. Radiation Laboratory Series, McGraw-Hill Book Company, Inc., New York, N. Y., vol. V; 1948.

[30] I. T. Neilsen, "Design and Performance of a High Power Pulsed Klystron," Ph.D. dissertation, Stanford University, Stanford, Calif.; 1952.

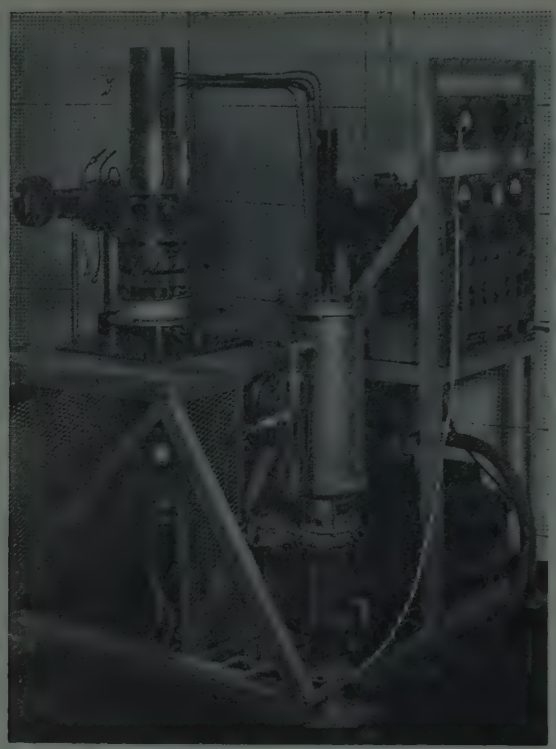

Fig. 13—Klystron mounted on a vacuum table. These klystrons are continuously pumped, and the entire system is called a "package unit."

V. Operating Characteristics

A. Processing of the Klystron

The last step in the assembly of the klystron is insertion of the cathode and the heliarc welding of the nickel eyelet, as previously described. If it is found to be vacuum tight, it is placed on a special rotating table and the glass-insulated focusing coils are wound in place. Electrically-heated ovens are then placed over the tube, and the tube is baked from four to six hours at a temperature between 400° and 425°C. The temperature is raised slowly so that the vacuum is not allowed to get worse than 10^{-4} mm of Hg at any time. The tube is baked until the pressure goes down to about 2×10^{-6} mm with the tube at baking temperature. Approximately 25 w is run into the cathode heaters during the bake-out.

Cathode conversion is accomplished in approximately three hours. The time required depends somewhat on the thickness of the cathode coating. During the conversion period the heater power is raised as rapidly as possible while keeping the vacuum always better than 10^{-4} mm of Hg. There are three distinct steps which can be observed in this process. First, as the heater power is raised, there is an immediate gassing from the heaters and heater supports. Second, there is gassing associated with the breakdown of cathode-coating binder at about 300 w heater power. Third, the major source of gas is the chemical breakdown of the coating material itself. As the heater power gets up around 800 w, it is observed that the vacuum in the klystron starts to improve and continues to improve even though the heater power is advanced to 1,000 w. This is an indication that the conversion process is complete. At this time cathode emission is checked with low voltage dc—40 milliamperes at 1,000 v being a representative value. After the tube pumps down to about 2×10^{-6} mm of Hg (with the cathode still hot) it is ready for pulsing.

The tube is first operated as a diode on μsec pulses. 100 kv is a convenient voltage at which to begin pulsing, and this voltage is gradually increased until the tube stands full voltage without gassing. As usual, it is found desirable to go to a voltage somewhat higher than it is planned to use for steady operation in order to get stable performance at a lower voltage.

As the pulse voltage is gradually raised, there are usually gas bursts in the tube which make it necessary to turn off the pulser, and in many cases go to a lower voltage again before operation can be resumed. There is a gradual clean-up of some sort, however, and the voltage at which break-down occurs gets higher and higher until finally stable operation is possible at the desired voltage.

After operation as a diode at the desired beam voltage becomes steady, the klystron is operated as an rf amplifier. In the first tests a great deal of further outgassing was necessary as high rf levels were attained. This effect was so pronounced that it was actually possible to tune the klystron cavities by watching the ion gauge meter. Fortunately, this rf gassing is no longer typical of high-power klystron operation. This is probably due in part to better general technique in tube manufacture, but it is thought very likely that effective trapping of the diffusion pump (through the use of a liquid-nitrogen cold trap) so that pump oil vapor is kept out of the tube is a very important factor. The present fairly typical behavior is to process a tube for 10 megw operation in an eight-hour day, including tuning up, and so forth.

In testing the first high-power klystrons, various difficulties, some of them quite serious, were encountered in connection with processing and early phases of operation. The process described above as requiring possibly a few hours, at first required weeks. Even the conversion of the cathode was very slow. So much gas was given out that the pumps were kept near the stalling point for from 10 to 15 hours. The great improvement in this particular situation was accomplished by a number of expedients.

The first few trials were ruined in a short time by electrical puncturing of the glass-seal. This puncturing occurred most frequently near the copper feather-edges of the housekeeper-type seals. A number of tubes were ruined in this way, and for a while it appeared to be a very serious problem. The difficulty has been eliminated by means of the following changes, and failure due to puncturing of glass seals is now a rare event.

1. Corona shields around the copper feather-edges. (See Fig. 14.)
2. Thickening of the glass over the feather-edges.
3. Sand-blasting the inner surface of the glass.
4. Incorporation of an electronic switch which shuts off the pulser in a single cycle if the gas pressure in the tube rises above some pre-set value.

The relative importance to be assigned to each of the above is not known. However, it appears that some device such as is mentioned in item 4 may be essential to the successful processing of these tubes. With such an arrangement in operation a gas burst may be produced in the tube by a given pulse, but the tube will not be pulsed again until the vacuum pumps have reduced the gas pressure to a safe operating value. The first arrangement of this sort which was tried made use of a mechanical relay which was operated by the ionization gauge. This device required a number of cycles for operation and was not fast enough to prevent puncturing.

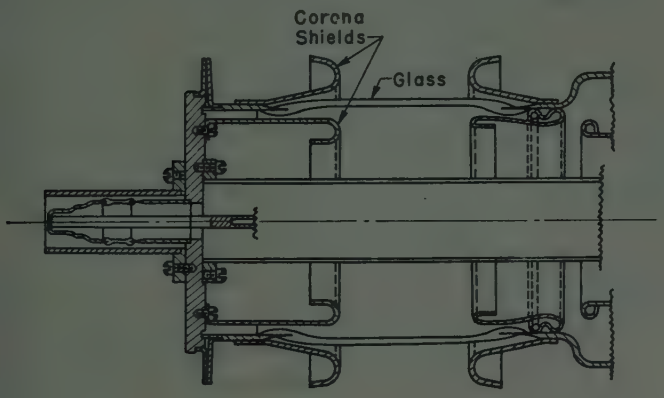

Fig. 14—Corona shields around the edges of the cathode bushing.

Two electronic circuits have since been developed—both of which operated satisfactorily. Both circuits operate from a signal delivered by a standard ionization gauge. This gause is located sufficiently near the tube and with a large enough tubulation into the gauge so that significant changes in the gas pressure within the klystron are reported by the ionization gauge in a time that is short compared to 1/60 sec., i.e., in less than the time between pulses.

B. Observed Performance

The high-power klystrons have been operated as diodes at voltages exceeding 400 kv. Fig. 15 shows beam current versus beam voltage on a logarithmic plot. The straight line with the 3/2 slope indicates space charge limited operation over the entire range from 1 kv to 400 kv. As was mentioned, it is the practice to check the cathode emission of newly converted cathodes at 1 kv on a dc basis. The higher points on the plot were obtained on a pulsed basis. As mentioned in section C, there is an 8 per cent decrease in perveance at 400 kv due to relativity effects. As there is some uncertainty in the measurement of instantaneous pulse voltage, the 8

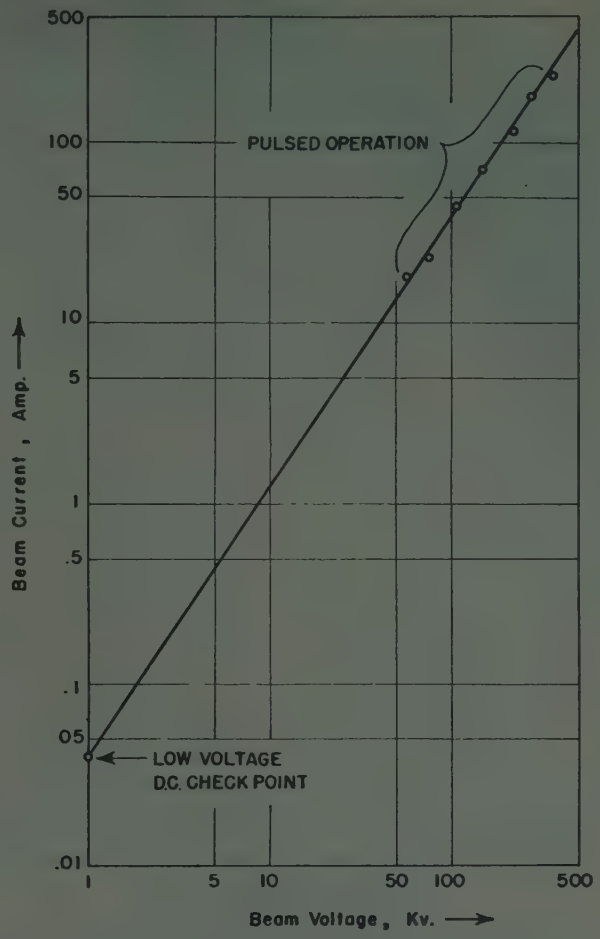

Fig. 15—Diode characteristics of the cathode gun.

per cent is within the experimental error and is not in evidence. In some cases of partially poisoned cathodes, a droop in this emission curve is observed, indicating partial temperature limitation. Normal cathodes exhibit space-charge limited operation up to the highest voltages tried.

There is no reason to assume that the voltages and currents shown represent maximum values for this tube. The only difficulties so far appearing to limit higher-level operation have been of an obviously nonfundamental

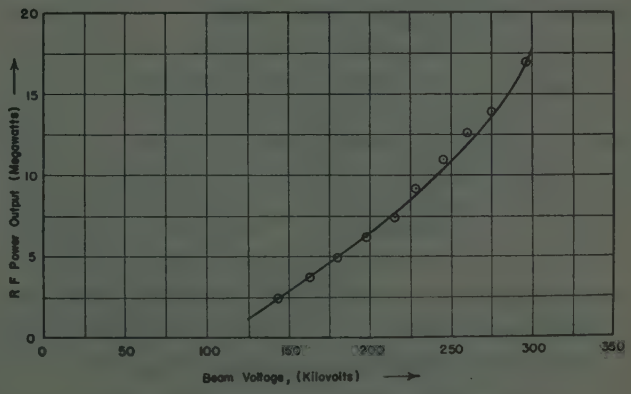

Fig. 16—Power output vs. beam voltage.

type. The rf output as a function of beam voltage is shown in Fig. 16. The rf input, magnetic focusing field, and output cavity loading were optimized at each level. This particular curve shows power outputs up to 17 megw; later measurements carried this up to 21 megw.

A plot of efficiency versus power output is shown in Fig. 17. These data indicate that the efficiency is practically constant in the range from about 16 to 20 megw. Later measurements seem to suggest that the efficiency curve reaches its maximum around 15 to 17 megw.

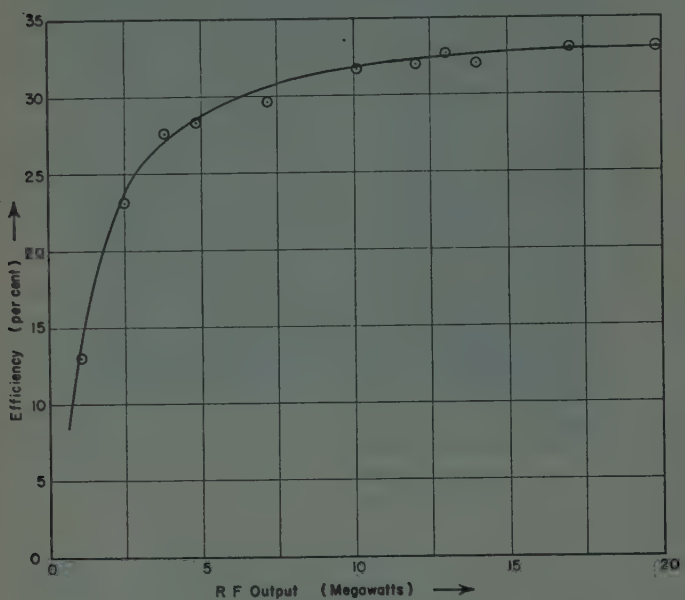

Fig. 17—Dependence of efficiency upon rf level.

Fig. 18 shows the dependence of output on output impedance. The data for Fig. 18 were obtained by setting the pulser for a given voltage, thereby establishing a certain value for the beam current as indicated on each curve of the family shown. The voltages corresponding to the currents indicated can be found by reference to Fig. 16. The rf drive, magnetic focusing field,

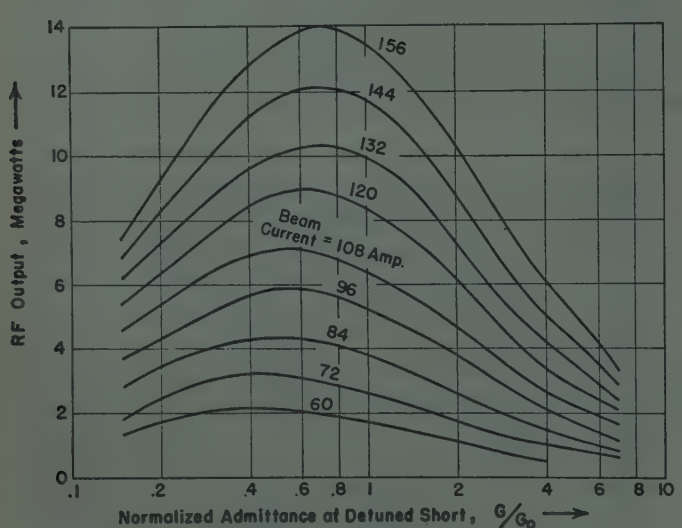

Fig. 18—RF output vs. output cavity loading.

and cavity tuning were optimized for maximum output for each measurement. The curves show rf output as a function of the admittance at the detuned short (normalized relative to the characteristic admittance of the output waveguide, Y_0).

Actually, the admittances chosen were pure conductances. A reactive component would be just equivalent to a detuning of the output cavity. Comparative data are available only for outputs up to 14 megw. It is clear from the curves that optimum loading is heavier at the higher power levels. Isolated measurements, in the region of 20 megw seem to be in accordance with the more complete data shown at lower levels. It seems probable that a matched waveguide is close to optimum load for power outputs of about 25 megw.

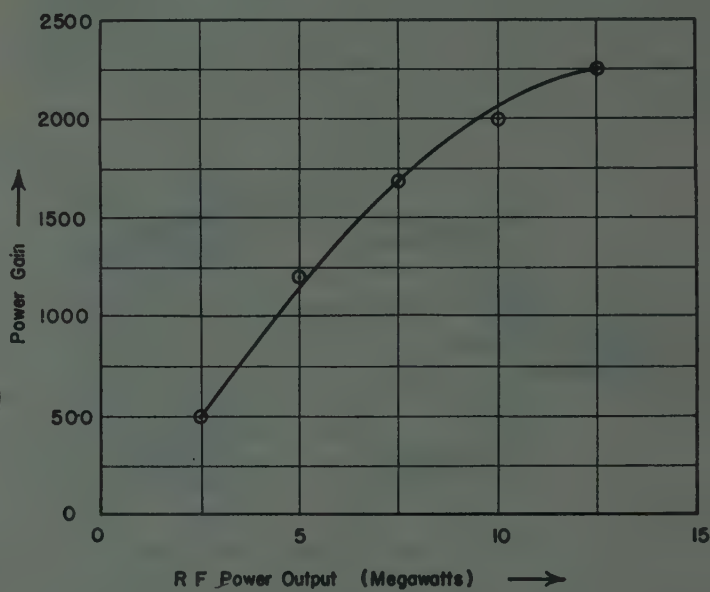

Fig. 19—Power gain as a function of power output.

Fig. 19 is a plot of power gain as a function of output loading. Cavity tuning, and input rf drive power were all optimized for maximum obtainable output at each beam power level. The power gain is found to depend quite critically on the tuning of the high Q middle cavity.

Some of the calculations in regard to beam focusing suggested that part of the beam was being intercepted by the anode face. This seemed to be confirmed by experiments performed with a beam tester. It appeared that a slight modification of the geometry of the anode hole would increase the percentage of the beam transmitted down the drift tube. This change was made in two tubes, and the expected improvement in beam transmission was apparently realized.

In testing these two modified tubes, a new phenomenon was observed. What appeared to be fairly large amounts of rf power was radiated from both the output and the input windows. This power was observed even in the absence of rf drive power. Further investigation

disclosed that this radiated power had a free-space wavelength of about 5.2 cm. This was not second-harmonic output. Tuning the klystron cavities caused the frequency of this spurious rf to change and proved it to be a multi-cavity oscillation of some sort. Cold tests made on klystron cavities disclosed a higher mode resonance at just the frequency observed in the oscillating tubes.

Exploration of the field pattern of this unwanted mode indicated that a relatively simple change in the geometry of the middle cavity (second buncher) would shift its resonance enough to suppress the spurious oscillations. This change could be done in such a way as not to appreciably affect the normal 10.5-cm resonance. Plans to make such a change on a test klystron have been worked out, but the actual tests have not yet been done. Apparently the modified anode geometry altered the beam shape so as to somehow couple more effectively to this unwanted mode. The feedback mechanism is not understood at present.

This same effect has since been observed in tubes with unmodified anode geometry on occasion, but has not proved to be a serious problem. It has, in some cases, complicated the problem of getting adequate performance data. In any case, it is thought that it can probably be completely eliminated by the simple expedient mentioned.

It seems likely that, with the unwanted oscillations suppressed by some scheme such as that mentioned, slight modification of the anode-throat geometry may substantially increase efficiency over that in Fig. 17.

C. Life

Only limited experience in regard to life, and then of a specialized kind, is available at this time. Thirty klystrons have been built to date for operation with Stanford electron accelerators. No significant changes were made from the original design. Processing and operation are now routine.

These salient facts may be of interest:

1. Although the klystrons were continuously pumped, some units lived for a period of over one year.
2. The greatest accumulated life tests are:
   a. At 17 megw output—200 hours.
   b. At 8 megw output—greater than 460 hours.

Until recently the bulk of the experience was not nearly this good, principally on account of failure of output windows.

On the subject of windows and window failures we could say a great deal. If the elements of frustration and despair were omitted, the record of our experience could, no doubt, be confined to a report the length of this paper. Suffice it to say, that the failure problem has been solved. Using Coors AI-200 circular disks in round waveguide, and *hiding* the window from electrons and x-rays, the failures have disappeared.

There has not yet been the opportunity to collect enough life data on klystrons equipped with the new off-set windows to be completely meaningful. But it can be said that over a six-month period those klystrons (five in number) that could sport the off-set windows did not fail. We have reason to believe that the life of pulsed klystrons, operating in 300-kv region can be greater than 1,000 hours.

It should once more be appropriate to point out that the cathodes in the tubes are replaceable. The first tube built by us has led the usual life of a guinea-pig, has seen (successfully) about 19 cathode-replacement operations and is still useable.

D. Summary of Typical Performance

A summary of operating characteristics at the 20-megw output level is:

Operating frequency	2,857 mc
Tuning range	100 mc
Heater power	800 w
Beam voltage	325 kv
Beam current	185 amp
Power gain	35 db
Efficiency[31]	33 per cent
Power output[31]	20 megw

These results are taken to infer that the design and operation of high power klystron amplifiers in the megawatt power range is practical and straightforward.

VI. Acknowledgments

This paper could not be closed without paying deep appreciation to a number of individuals and organizations, without whose interest, support, and devotion this work could not have been completed (nor started).

First, this project would have been needless, on one hand and hopeless on the other, had it not been for the constant encouragement of our friend and colleague, the late Professor W. W. Hansen. It has been of some solace to know that W. W. Hansen lived long enough to witness the first successful tests.

Next, E. Piore, of the Office of Naval Research, had the courage to support us in a program intended to extrapolate the power output of a klystron by a factor of about 1,000 times at a time when such a project, superficially at least, seemed quite foolhardy. To him and to ONR we are deeply grateful.

Also the advice of C. Litton was sought on a number of crucial matters, including the over-all design of the tube. The fact that after 4 years of effort and over 30 models it is found unnecessary to change the design is a tribute to C. Litton.

Roger Gillette and several others from the Sperry Gyroscope Company assisted in the design the pulse transformer, the cathode, and the filaments.

Credit should be given to a large number of graduate

[31] Since this paper has been written a power output of 30 megw has been attained, at an efficiency of 43 per cent.

students who worked with us and without whose initiative, interest, and ingenuity the development could not have been done at Stanford. A. Eldredge, P. Pearson, R. Neal, C. B. Jones, J. Soderstrom, N. Hiestand, J. Jasberg, need special mention. It is hoped that they will write papers on their special contributions.

Lastly, it should be mentioned that R. Messimer built the first tube, and as the foreman of the Tube Shop, supervised the construction of the remaining 30 models. J. Pope electroformed the waveguides and other components. To members or the various shops go our thanks for diligence and intense interest.

Backward-Wave Tubes*

R. KOMPFNER†, FELLOW, IRE AND N. T. WILLIAMS‡

Summary—**It has been surmised for some time that a traveling-wave tube in which backward-traveling field components can be excited—such as for instance the "Millman" tube—may oscillate in a backward mode, the RF power emerging at the gun-end of the tube and its frequency depending only on the beam voltage. Experiments with the "Millman" tube show this to be so and oscillations have been observed in the first and second backward spatial-harmonic modes. The latter is excited between 600 and 900 volts, the tube oscillating between 5.9 and 6.4 mm. The former more powerful mode is excited between 1600 and 4000 volts, the tube tuning continuously between 6.0 and 7.5 mm, thus covering a frequency band of 10,000 mc. Power output of about 10 mw has been measured at 6.4 mm.**

The tube has also been studied as an amplifier and more than 20 db stable backward gain has been obtained.

A simple theory of backward gain and of oscillation starting conditions is given.

Introduction

AN OSCILLATOR THAT can be tuned electronically over a wide frequency range is a very desirable thing. The reflex klystron for example, is tunable over a wide range *mechanically* by varying one or the other dimension of the resonant circuit associated with it; alternatively, it can be tuned *electronically* by varying the reflector voltage, although only over a frequency range of at most a few per cent. To be able to tune over a much wider range electronically would not merely be a matter of convenience, or elegance; it is a matter of fundamental importance in a number of branches of the fast-growing microwave art.

Accordingly, attention had early been given to the problem of how the traveling-wave tube (abbreviated T.W.T.) might be adapted to operate as an electronically tuned oscillator, since one of the apparent essential requirements, namely ability to provide gain over a very wide frequency band, is eminently well fulfilled in the T.W.T.

As shown further on, there exists indeed a type of T.W.T. which operates as an electronically tunable oscillator; it makes use of a circuit capable of supporting a wave which has components traveling in opposite directions and has therefore been called the "backward-wave oscillator" (abbreviated B.W.O.). It may be interesting to reproduce the chain of reasoning that led from the T.W.T. to the B.W.O.

Electronic-tuning Circuits

A conventional T.W.T. provided with an external feedback path (the internal feedback path along the helix is usually deliberately suppressed by a heavy concentration of attenuation somewhere near the middle of the tube) will start to oscillate at a frequency near which the lowest value of the net gain exceeds the loss around the complete loop consisting of tube and feedback path provided there is a whole number of wavelengths around the complete loop. Such a circuit is ordinarily not tunable electronically to any great extent, and is likely to oscillate in many modes all at once. If a narrow band-pass filter is included in the feedback path, it is possible to ensure oscillation in one mode only, while a limited amount of electronic tuning can be had because the phase shift through the tube varies with the beam voltage.

Quite a different method of electronic tuning relies on the dispersive properties of the circuit, such as the helical conductor in the ordinary T.W.T. The helix has positive dispersion, that is to say, the phase velocity of the slow wave on it increases with increasing wavelength, although over an extremely wide band of frequencies the dispersion is negligibly small. (This accounts for the extreme bandwidth of the T.W.T. as an amplifier.) When the circumference of the helix is much smaller than the wavelength of the slow wave along the helix, the helix is rather strongly dispersive, and use has been made of this fact to restrict the bandwidth over which the tube amplifies. Strong dispersion enables one to use such a tube as an electronically tunable amplifier, where the frequency band over which the tube amplifies is determined by the beam voltage only.

How can such an electronically tunable amplifier be turned into an electronically tunable oscillator? If the output of the tube is connected to the input via an external feedback path, oscillations will be obtained whenever there is a whole number of wavelengths around the loop: tube plus feedback path. Thus as we vary the beam voltage we will have distinct "modes" where there

* Decimal classification: R339.2. Original manuscript received by the Institute, May 15, 1953.

† Bell Telephone Laboratories, Murray Hill, N. J.

‡ Formerly with Bell Telephone Laboratories, Murray Hill, N. J.; now with Edison Laboratory, T. A. Edison, Inc., West Orange, N. J.

are n, $n+1$, $n+2$, $n+3$, $\cdots$ wavelengths around the loop, and although—because of the inherent phase shift versus beam voltage "bandwidth"—there will be a certain amount of electronic tuning in each mode, there will be jumps, or discontinuity between modes, which make this arrangement unsuitable for many purposes for which a true electronically tuned oscillator is required. By making n very small (in normal tubes its value lies between 30 and 50), one can indeed increase the amount of electronic tuning within one mode, but such a tube is only a little better than the reflex klystron in respect of tuning range, and rather complex.

If the number of wavelengths around the loop could be kept constant and whole at all frequencies, the solution would then be known.

One way of carrying this out consists in using an electron beam as a feedback path, as depicted in Fig. 1. The number of wavelengths along a given length of electron beam can be varied at will over an extremely wide range merely by varying the beam voltage V_2. Thus a circuit can be constructed consisting of a dispersive T.W.T. providing gain and electronic tuning in conjunction with a separate electron beam as part of the feedback mechanism, the latter's beam voltage being varied so as to make the total number of wavelengths around the loop always constant and whole.

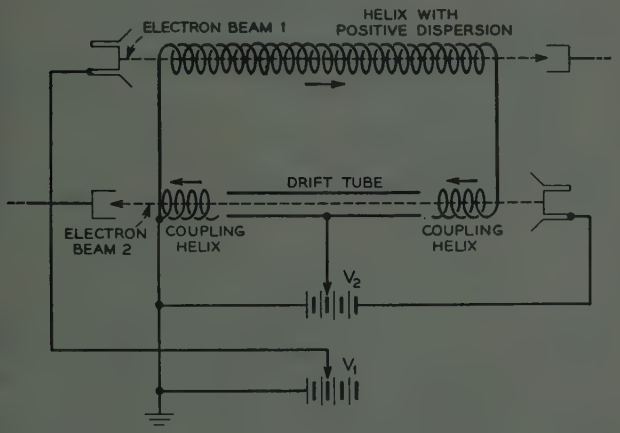

Fig. 1—Electronically-tunable oscillator circuit using a separate electron beam as feedback path. Variation of the velocity of beam 1 varies the frequency of maximum gain of the dispersive T.W.T.; variation of the potential of the drift tube varies the delay along the feedback path in such a way as to maintain the total number of wavelengths around the loop constant and integer.

It is clear that the number of wavelengths in a circuit of fixed length will, even without dispersion, grow with frequency; if the circuit has positive dispersion it will grow at an even faster rate. Therefore the number of wavelengths (bunches) in the feedback beam has to *decrease* with frequency, that is to say, the velocity has to *increase* with frequency at a corresponding rate; thus the beam is made to have "negative dispersion." The proper rate of increase of the feedback beam voltage (which governs the beam velocity) with frequency can be calculated from the geometrical lengths of circuit and beam and from the amount of dispersion in the circuit. Although not very elegant, such a purely electronically tunable oscillator circuit is feasible.

Another way of realizing such a circuit might be thought of as a combination of a circuit element having none or positive dispersion with circuit elements having compensating negative dispersion. Let us examine this proposal in more detail as shown in Fig. 2. Suppose the

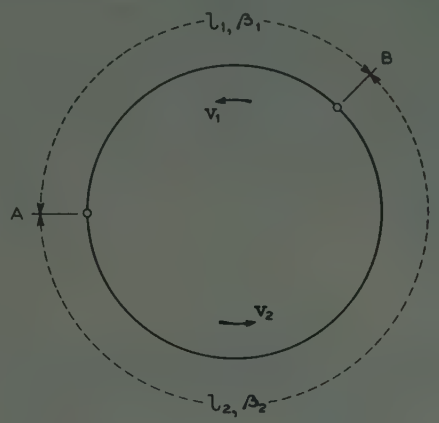

Fig. 2—Symbolic representation of two circuit elements having compensating dispersions. l_1, v_1 and β_1 and l_2, v_2 and β_2 are lengths, phase velocities and phase constants of the two respective circuit elements.

geometric length of one element is l_1, supporting a wave having a phase velocity v_1, and let it be n_1 wavelengths long at an angular frequency ω. Suppose the geometric length of the other element is l_2, supporting a wave with a phase velocity v_2, and let it contain n_2 wavelengths at the frequency ω. We then postulate, as before, constancy of number of wavelengths around the loop:

$$n_1 + n_2 = \text{integral} = N \tag{1}$$

where

$$n_1 = \frac{\omega l_1}{2\pi v_1} = \frac{1}{2\pi}\beta_1 l_1, \qquad n_2 = \frac{\omega l_2}{2\pi v_2} = \frac{1}{2\pi}\beta_2 l_2. \tag{2}$$

β_1 and β_2 are the respective phase constants of the circuits. If the frequency be varied by a small amount $\partial\omega$, while the total number of wavelengths is kept constant and equal to N, a relation between the group velocities v_{g1} and v_{g2} of the two circuits is obtained as follows:

$$l_1 \frac{\partial\beta_1}{\partial\omega} + l_2 \frac{\partial\beta_2}{\partial\omega} = 0 \tag{3}$$

$$v_{g1} = -\frac{l_2}{l_1} \cdot v_{g2} \tag{4}$$

since

$$v_g = \left(\frac{\partial\beta}{\partial\omega}\right)^{-1}. \tag{5}$$

Consideration of Fig. 2 will show that this implies, for instance, that energy enters the circuit at A and leaves

it at B, or vice versa, and that there is *no circulation of energy around the circuit. If v_{g1} is positive*, i.e., in the same direction as v_1, then v_{g2} *must be negative*, i.e., in a direction opposite to v_2. The number of wavelengths around the loop may well be made to be constant, but it is not a loop in the sense that energy can circulate around it, and thus it is useless for the purpose of making an electronically-tuned oscillator.

The next step in our argument is to consider a loop consisting of a periodic element type of circuit which supports forward and backward wave components plus an electron beam, as shown in Fig. 3. If β is the phase

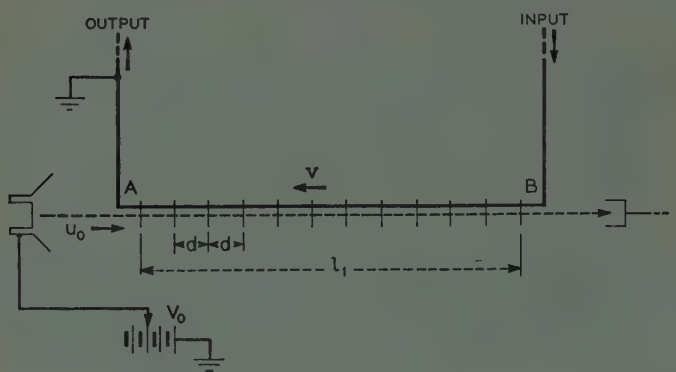

Fig. 3—Symbolic representation of periodic element type of circuit in conjunction with an electron beam. A wave traveling backwards with a phase velocity v is supposed to interact with the forward traveling beam at points spaced apart at regular intervals d.

constant of the fundamental component on the circuit, the phase constant of the nth spatial-harmonic component is given by

$$ {}_s\beta_{(n)} = \beta + \frac{2n\pi}{d} \tag{6} $$

where d is the distance between the periodic elements of the circuit, and $n = \pm 1, \pm 2, \cdots$ etc., the order of the spatial-harmonic. Specifically, the first backward spatial-harmonic component has a phase constant

$$ {}_s\beta_{(-1)} = \beta - \frac{2\pi}{d} \tag{7} $$

which can be a negative quantity; we note that its associated group velocity is the same as that of all the other spatial-harmonics, namely

$$ {}_sv_{g(-1)} = \left(\frac{\partial\beta}{\partial\omega}\right)^{-1} = v_g. \tag{8} $$

Suppose we inject a signal at the input B; at the frequency ω it will cause a wave to be propagated from right to left with a fundamental phase velocity v. Because of the periodicity d of the circuit there will be an infinite number of spatial-harmonic components associated with this wave. Let us direct our attention particularly to the first backward spatial-harmonic component, which, in the case considered, will travel from left to right with a velocity

$$ {}_sv_{(-1)} = \frac{\omega}{{}_s\beta_{(-1)}} = \frac{\omega}{\beta - \dfrac{2\pi}{d}}. \tag{9} $$

Suppose we project an electron beam through the circuit with exactly the same velocity,

$$ u_0 = {}_sv_{(-1)}. \tag{10} $$

This electron beam now forms our feedback path analogous to circuit 2 in Fig. 2.

On the assumption that there is interaction between the beam and the circuit, varying with distance with a periodicity d, the beam will become bunched, i.e., there will be a wave on the beam traveling from left to right with a velocity u_0 and with a phase constant $\beta_e = \omega/u_0$. As the frequency is varied, *the beam velocity should be varied so that it is always equal to the velocity of the first backward spatial-harmonic;* this is done by suitably varying the beam voltage V_0. Thus the electron beam behaves like a circuit with rather peculiar properties:

1. It has a positive phase constant β_e.
2. It has a "group velocity" defined by

$$ {}_sv_g = \frac{(\partial\beta_e)^{-1}}{d\omega} = -\left(\frac{\partial_s\beta_{(-1)}}{d\omega}\right)^{-1} $$

   which is negative, since it is in a direction opposite to ${}_sv_{g(-1)}$.
3. *No energy is transmitted in a backward direction.*

The physical length of the electron beam equals that of the circuit, hence

$$ l_1 = l_2, $$

and so we have all the conditions fulfilled which are necessary if a closed loop consisting of two circuits with different propagation characteristics is to have a constant number of wavelengths over a wide band of frequencies, namely $v_{g1} = -(l_2/l_1)\cdot v_{g2}$. If, in addition, the number of wavelengths around the loop is integral the circuit will exhibit the phenomenon of *positive* feedback. A signal injected at B—provided interaction with the electron beam causes it to grow as it travels along the circuit—will emerge at B amplified to a greater extent than if there had been no feedback. (It has to be realized feedback is an inseparable ingredient in this type of circuit, and cannot be "thought away.")

It is not difficult to imagine that an increase, for instance, of the beam current, will cause the gain around the circuit to increase to such an extent that oscillation sets in. This is, in fact, what happens. The frequency of oscillation is then determined by the beam voltage only; maximum gain and oscillations will occur at a frequency such that the phase velocity of the strongest backward-traveling spatial-harmonic component is about equal to velocity of electrons in the beam.

Thus the backward-wave oscillator can be explained as a loop of which one part is a material circuit, while the other part is an electron beam—the beam being now not only the source of energy but also of the feedback path.

Theory of Backward Gain and Oscillation

In order to arrive at a simple theory of the interaction between an electron beam and a circuit in which phase and group velocities are reversed we go back to an approximate theory of the T.W.T.[1] in which the assumption is made that the final wave on the circuit is composed of an infinite series of waves: first, the initial or primary wave; then a secondary wave induced in the circuit by the bunching in the beam due to the primary wave; this is followed by a tertiary wave induced in the circuit by the bunching in the beam due to the secondary wave . . . and so forth. Use of this theory can be made because it can be shown that only the first two terms of the series are needed.

Following Pierce[2] in Chapter XI on Backward Waves of his book on T.W.T.'s, it should be noted that interaction with a backward wave is taken into account merely by reversing the sign of the impedance of the circuit (sometimes denoted by K and sometimes by $[E^2/\beta^2 P]$).

The amplitude of the final wave on the circuit can be written as the sum of the amplitudes of the partial waves

$$\Sigma V = V\left[1 + j\frac{(\beta lC)^3}{3!} = j^2\frac{(\beta lC)^6}{6!} + \cdots\right], \quad (11)$$

where

V = amplitude of initial voltage
β = phase constant of circuit and beam—$\omega/v = \omega/u_0$ (synchronous velocities)
l = active length of circuit
C = Pierce's gain parameter defined by

$$C^3 = \frac{I_0 K}{4V_0} \quad (12)$$

where

I_0 = beam current
K = circuit impedance
V_0 = beam voltage.

When βlC is small enough, the series can be stopped at the second term. Under these conditions it is possible to write down the voltage on the circuit when beam and wave have different velocities, and when the circuit is not lossless; the resulting relations have been found useful in deriving the conditions under which the traveling-wave tube presents an infinite attenuation to an incident signal.[3]

Following C. F. Quate's suggestion, use shall now be made of similar relations in order to derive conditions under which a backward-wave tube presents infinite gain to an incident signal. To simplify matters it may be assumed, to start with, that the circuit is lossless.

Let the primary wave be described by

$$V_1 = V\cos(\omega t - \beta z). \quad (13)$$

This corresponds to the first term of the series.

If the electron speed u_0 differs from the phase velocity v of the wave, one can define a hypothetical phase shift between beam and wave in the absence of the beam over the distance z

$$\theta = \beta z\left(\frac{v}{u_0} - 1\right) \quad (14)$$

(in Pierce's notation $\theta = -\beta z C b$).

As shown in the above mentioned paper the second term in the series, that is to say, the secondary voltage wave on the circuit can then be written

$$V_2 = \frac{1}{2}V(\beta zC)^3\frac{v^2}{u_0^2}\frac{\dfrac{\sin\theta/2}{\theta/2} - \cos\theta/2}{(\theta/2)^2} \cdot \sin[\omega t - \beta z - \theta/2]. \quad (15)$$

The voltage at the end of the tube ($z = l$) is

$$V_l = V_1 + V_2 \quad (16)$$

where z has been replaced by l everywhere. The essential difference between the present and the previous case is that $V_1 + V_2$ now represent the amplitude of the input voltage, V_1 now the output. Hence the gain is

$$G = \frac{|V_1|}{|V_1 + V_2|}. \quad (17)$$

We are primarily interested in the conditions under which we get oscillations, that is to say, when the gain goes to infinity. This requires

$$V_1 + V_2 = 0 \quad (18)$$

which gives one set of phase conditions and one amplitude condition, namely,

$$\theta = -\pi, -3\pi, -5\pi, \text{ etc.} \quad (19)$$

and

$$\frac{1}{2}(\beta lC)^3\frac{v^2}{u_0^2}\frac{\dfrac{\sin\theta/2}{\theta/2} - \cos\theta/2}{(\theta/2)^2} = +1 \quad (20)$$

since with K now negative, C^3 is also negative.

With the first phase condition $\theta = -\pi$, and defining a new symbol C' by

[1] J. R. Pierce, "Traveling Wave Tables," Van Nostrand & Co., New York, N. Y.; 1950.
[2] R. Kompfner, "T.W.T.," *Wireless Engineer*, vol. 24, p. 255; 1947.
[3] R. Kompfner, "Operation of T.W.T. at low level," *Jour. Brit. IRE*, vol. 10, p. 283; 1950.

$$C^3 \frac{v^2}{u_0^2} = (C')^3 \tag{21}$$

and putting

$$\beta l = 2\pi N \tag{22}$$

(where N is the number of wavelengths on the circuit) into the amplitude conditions, the trigonometrical term becomes $8/\pi^3$ and *we must have*

$$C'N = 2^{-5/3} = 0.315 \tag{23}$$

for oscillations to start. C' differs from C only in that the actual beam voltage U_0 is taken instead of the synchronous voltage V_0.

The starting current for oscillations is obtained by substitution:

$$I_0' = \frac{U_0}{8KN^3} \text{ ampere.} \tag{24}$$

The phase condition $\theta = -\pi$ indicates that the beam has to be faster than the wave by a fraction $1/2N$. The phase conditions $\theta = -3\pi$, -5π, etc. correspond to higher "modes" of oscillations requiring substantially higher starting currents and will not be considered here.

Finally, it remains to be shown that higher-order wave components can be neglected. Since $(\beta lC)^3$ equals $\pi^3/4$, the ratio of the amplitude of the tertiary wave to the amplitude of the secondary wave must be

$$\frac{3!}{6!} \cdot \frac{\pi^3}{4} = 0.0645.$$

It is obvious that the error committed cannot be large.

Intuitive Description of B.W.T. Type Interaction

The essential point about this type of interaction is that the electron beam acts not only as the energy source, as in the ordinary T.W.T., but now also as a feedback path. If one so desires, he can trace a great number of complete loops through any pair of interaction gaps along the filter type circuit and back through the electron beam, and count the number of complete wavelengths or cycles around such a loop. He will find (apart from a phase shift of $\pi/2$ inherent in the mechanism of bunching) that every such loop is an integral number of cycles long when the beam voltage equals the phase velocity of the backward spatial-harmonic wave. Thus the feedback is essentially positive, and in common with all positive feedback circuits, oscillations must begin, once the gain around the loop exceeds the loss. The frequency of oscillation is determined by the geometry of the circuit, i.e., the phase velocity of the wave as function of frequency and the distance between gaps, on the one hand and by the beam velocity on the other. The former parameters being constant, the latter parameter—represented by the beam voltage—is the independent variable, the frequency of oscillation becoming the dependent variable. Thus the tube "tunes with beam voltage."

Experimental Results

All the experiments to be described were done with Millman tubes in the 6-mm band. The Millman tube is a traveling-wave amplifier tube utilizing the first forward spatial-harmonic component of the wave propagated on the circuit, and has been described in the literature.[4,5] See Fig. 4. The circuit is essentially a ridged waveguide with about 100 transverse nearly-resonant slots spaced 0.021 inch apart. The phase characteristic of the circuit has been designed so as to give a relatively broad band over which the tube amplifies, at a beam voltage of about 1200 volts. Longitudinal slots milled along the whole length of the waveguide ridge allow for better penetration of the RF fields by the electron beam, of which, usually, a few milliamperes reach the collector. A uniform magnetic field of about 1600 gauss is required to maintain straight electron flow.

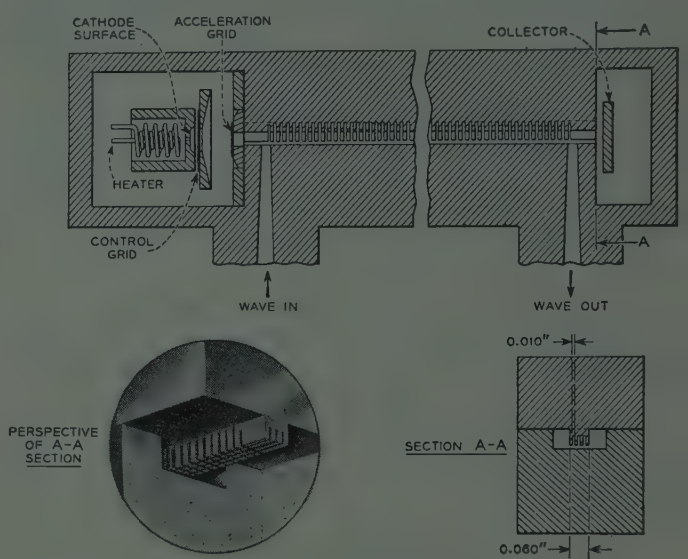

Fig. 4—The Millman tube, a spatial harmonic type of traveling-wave amplifier. Longitudinal and cross section and perspective view of interaction circuit.

The tube is capable of giving between 20 and 30 db net gain over a frequency band between 6.00 and 6.40 mm wavelength with a power output in excess of 10 milliwatts.

Thus, it has been demonstrated that traveling-wave type interaction can be obtained by means of forward spatial-harmonic wave components. It is not difficult to envisage interaction of a beam with backward spatial-harmonics. Millman indeed reports observing oscillations which he, correctly, ascribes to interaction with such components.

Oscillations in the Low-Voltage Mode

The first experiments were carried out with a Millman tube F7-18, which operates normally as an amplifier with gains around 25 db. This tube had no control grid

[4] S. Millman, "A spatial harmonic traveling-wave amplifier for six millimeters wavelength," Proc. I.R.E., vol. 39, pp. 1035–1043, Sept., 1951.

[5] S. Millman, "Spacial harmonic traveling—wave amplifier," *Bell Lab. Record*, vol. 30, p. 413; 1952.

and out of a total current of 40 milliamperes 5 milliamperes go to the collector at a beam voltage of 1200 volts and a magnetic focusing field of 1600 gauss. The cold loss of the tube varies between 30 db at 6.0 mm and 10 db at 6.4 mm.

Practically all experiments were carried out with the beam voltage swept sinusoidally at 60 cycles with a suitable amplitude. The arrangement is shown in Fig. 5. When the tube oscillated, output was normally obtained, from output *A* (at the gun-end of the tube). This was detected with a crystal detector, amplified and displayed on the *y*-axis of a C.R.O., the *x*-deflection being swept sinusoidally at 60 cycles. Thus the pattern seen on the C.R.O. corresponds to detected oscillator power versus beam voltage. The frequency of the oscillation was determined by observing the dip due to the wavemeter absorption.

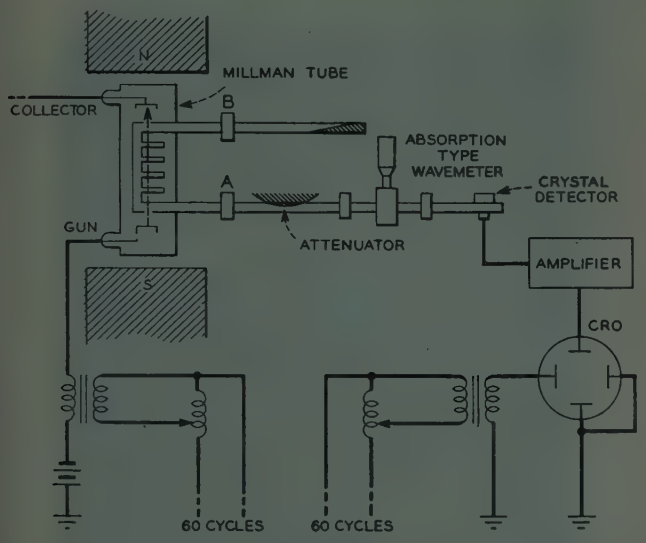

Fig. 5—Experimental arrangement used in observing backward-wave oscillations.

Oscillations were detected at first near a beam voltage of 700 volts, and it was realized that this must be the second backward space harmonic mode, that is to say, when $n=-2$ in (1). Oscillations were obtained over most of the range between 5.91 mm and 6.54 mm, and Fig. 6 is a plot of frequency versus beam voltage as measured with the wavemeter. Also shown is a plot of similar relations derived on the basis of Millman's filter-circuit analogy of the tube and it will be seen that the curve $n=-2$ is not too bad a fit.

Fig. 7 is an oscillograph trace of power output versus beam voltage at two different values of focusing field. It will be noted that there are gaps in which the tube does not oscillate, though it is possible to influence the depth of one or the other of the gaps by a slight variation of focusing field or of the alignment of the tube in the field. The gaps are explained by the presence of strong oscillations occurring at frequencies below the cut-off of the waveguide but which disturb the electron flow sufficiently to prevent oscillations in second backward space harmonic which is only a very feeble mode.

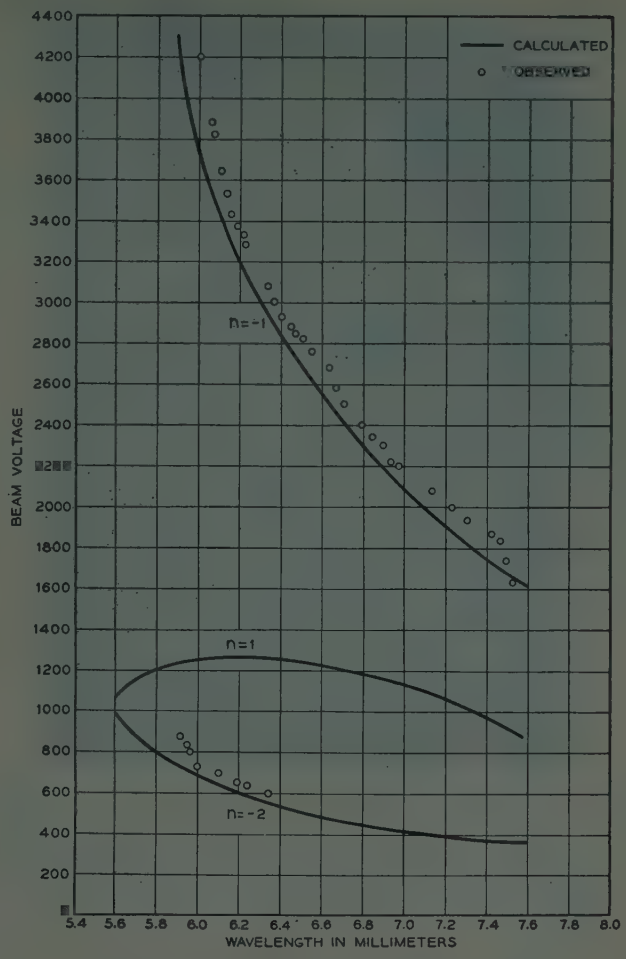

Fig. 6—Frequency of oscillation as function of beam voltage, experimental and as calculated from an approximate theory of the circuit of the "Millman" tube.

Strong oscillations were detected at voltages above 2000 volts. Because of the absence of a control grid in this tube it was very difficult to keep the dissipation at a safe level at these voltages, and only exploratory measurements were made. These showed, however, that oscillations were then occurring in the *first* backward space harmonic mode and were at a milliwatt level. Fig. 8 shows a small portion of the high-voltage mode oscillations together with the low-voltage ones on the left-hand side of the trace (see page 1608).

Oscillations in the High-Voltage Mode

In order to be able to control the current better at the high voltages a tube with a control grid was used and experiments were next made with Millman tube #F7-14 which gives, in the normal forward amplifying mode, 6-db gain with 2-milliampere beam current at 1240 volts. This tube had previously been rejected as an amplifier because of its low gain. Oscillations were readily obtained at voltages between 1600 and 4000 volts, and at beam currents of the order of 2 milliamperes. Fig. 9 shows a plot of power output versus beam voltage, with the wavelengths noted on the curve. *Continuous* oscillations are obtained from $\lambda_0=6.00$ to $\lambda_0=7.5$ mm. This

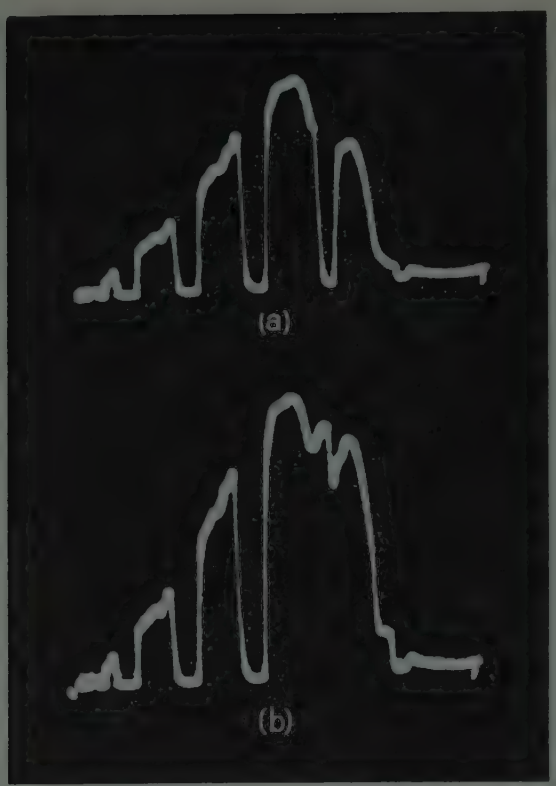

Fig. 7 (a and b)—Oscillograph traces of oscillator power versus beam voltage at two different values of magnetic focusing field in the low-voltage mode. Gaps are due to oscillations in the high-voltage mode occurring at frequencies below the cut-off of the waveguide; these oscillations perturb the electron flow sufficiently so that the relatively weaker low-voltage mode oscillations are inhibited.

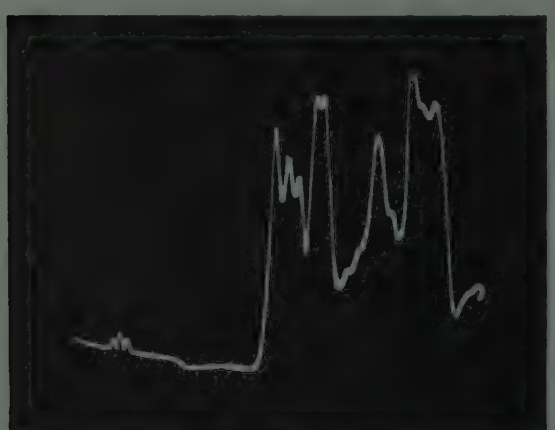

Fig. 8—Oscillograph trace of oscillator power versus beam voltage covering both high and low-voltage modes. (The low-voltage mode is the small squiggle on the left.) (Note the difference in amplitude.)

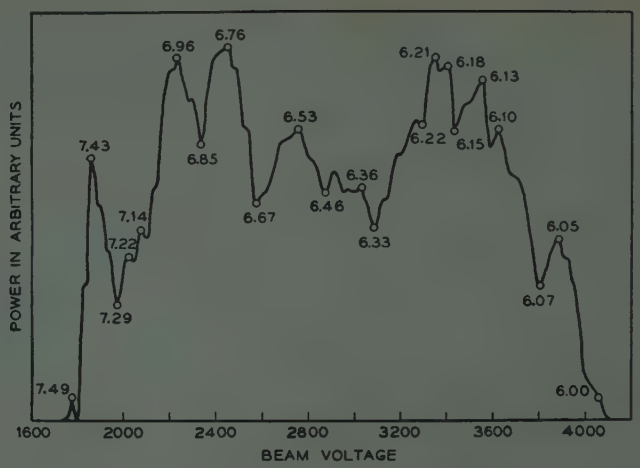

Fig. 9—Plot of oscillator power versus beam voltage, with the wavelength in millimeters of oscillation noted on the curve.

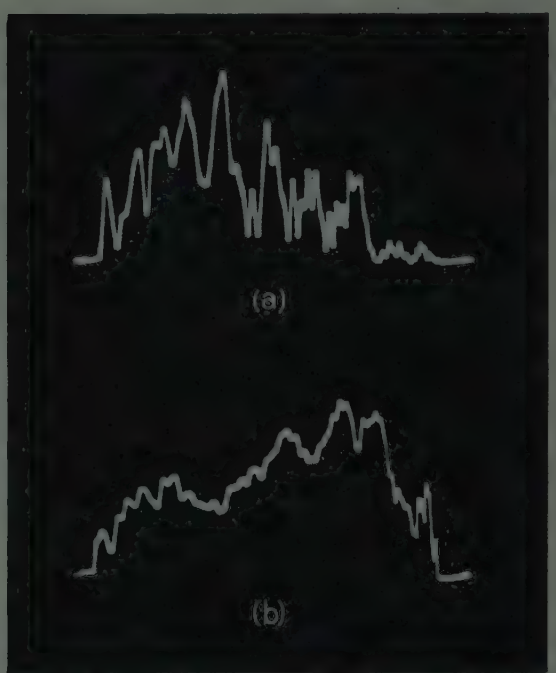

Fig. 10—(a) Oscillogram of power output from the collector end versus beam voltage; (b) oscillograph of power output from the gun-end versus beam voltage. (Note correspondence between peaks and valleys of one curve and valleys and peaks of the other curve.)

corresponds to a frequency interval of 10,000 megacycles, or 22 per cent of the mid-frequency. The power was measured at $\lambda_0 = 6.4$ mm with a thermistor bolometer kindly lent us by W. M. Sharpless and was in the neighborhood of 10 milliwatts. The over-all shape of the power output curve is very sensitive to the tuning of the crystal detector mount. The "fine-structure" of humps, peaks, and valleys is undoubtedly produced by reflections at the numerous discontinuities both inside and outside the tube. As partial proof of this statement, consider Fig. 10 where the power obtained from either outputs can be compared; there is considerable correspondence of peaks in one output with valleys in the other, and vice versa. Fig. 11 shows the power obtained at the gun-end when the collector end is connected to a mismatch, in this case, a crystal mount without interposed padding.

A plot of frequency versus beam voltage for the high-voltage mode is also given in Fig. 6; the agreement with a curve based on Millman's equivalent lumped filter circuit is good.

An instructive modification was made with tube #F7-20, which incorporates an attempt to produce a

broad-band internal nonreflecting match near the collector end of the retarded-wave structure. A piece of ceramic rod was ground like a wedge and coated with aquadag of about 500 ohm/square resistance. The wedge was inserted into the space on one side of the slotted ridge guide, producing an increase of insertion loss of about 25 db, when cold-tested. Looking into the gun-end of the tube (by means of another Millman tube used as a swept-oscillator), no change in reflected power could be observed on moving the wedge longitudinally over several wavelengths.

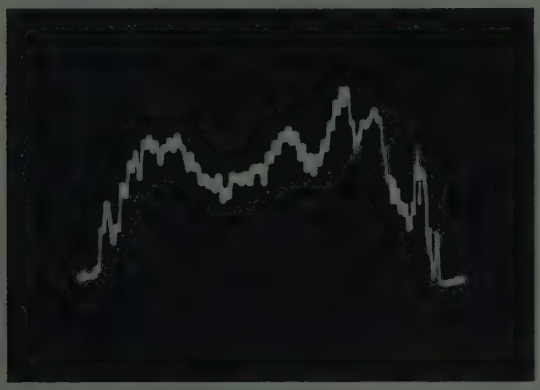

Fig. 11—Oscillogram of power output from the gun-end when collector end is deliberately mismatched.

The tube was evacuated and processed in the normal way, which does not, however, include outgassing the aquadag-covered wedge which is in a position where it intercepts part of the beam. Consequently it has not been possible to run this tube at beam voltages in excess of 1000 volts, and nothing is known about the behavior of the tube in the first backward spatial-harmonic mode. In the second backward spatial-harmonic mode, however, centered around 750 volts, the tube oscillates readily between 5.90 and 6.30 mm with a starting current of 0.70 milliampere.

A notable feature is absence of gaps in oscillation spectrum, which were inevitably present when non-modified Millman tubes were operated in this mode.

Backward Gain

Equation (17) in the section on the theory of backward gain can be transformed to represent the voltage gain as a function of the beam current I_0:

$$G = \frac{1}{1 - \frac{I_0}{I_0'}} .$$

I_0', the starting-current for oscillation, as is shown there, given by

$$I_0' = \frac{U_0}{8KN^3}$$

where U_0 is beam voltage for maximum gain, K the circuit impedance in the space harmonic mode and N the number of wavelengths of space harmonic wave.

Thus, in principle, any amount of gain should be expected, depending only on how close to the starting current one might be able to approach.

This is, in fact, what happens.

Backward gain was measured with Millman tube #F7-12 both in the low-voltage and in the high-voltage mode. In both cases gains well above unity were observed, increasing rapidly as the beam current approaches the starting current. Gain above 30 db was rather unstable on account of fluctuations in the power supplies. Experiments also showed that the product of gain times bandwidth did *not* stay constant, as might have been expected, *but increased with gain.* Some experiments were carried out in which great care was taken to avoid overloading in any of the amplifiers; the corresponding readings of gain versus collector current for the high-voltage mode are plotted on Fig. 12. In the absence of a quantitative theory we may surmise that this phenomenon is connected with the fact that the feedback is now carried by the electron beam, and not as is usual, by a passive element.

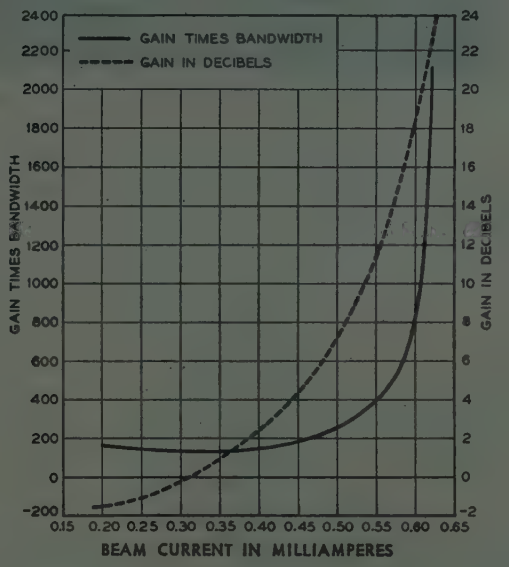

Fig. 12—Observed gain and gain-times-bandwidth product against beam current in milliamperes. In the product, gain is taken as its numerical value and bandwidth in megacycles.

It will be noted that the starting current is in the region of 0.60 milliampere. The beam voltage was then 2900 volts and the free space wavelength 6.50 mm. This corresponds to $N = 76$ wavelengths of the space harmonic, on the assumption that the active length of the circuit was 2.100 inches. On the assumption that the effective impedance of the circuit is 0.90 ohm (as calculated by Millman), we should have a starting current of 0.92 milliampere.

The fact that we actually observe a lower starting current can be explained partly by the fact that the real active current must always exceed the collector current and partly by the unavoidable presence of reflections which can cause an increase in effective impedance.

In an experiment in which controlled amounts of ex-

ternal feedback could be provided, large variations in starting currents were observed, depending on whether the feedback was in phase or out of phase. Such feedback can increase the power of the oscillations considerably, by a factor of an order of magnitude; however the feature of smooth continuous tuning is lost thereby and the tube frequency jumps from one mode to the next as the beam voltage is varied.

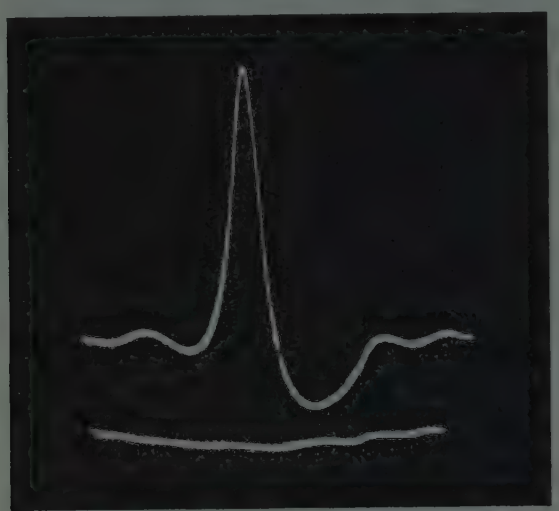

Fig. 13—Oscillogram of "backward-gain" versus beam voltage.

On Fig. 13 is shown a cathode-ray tube trace of backward gain versus beam voltage."[6] Compare with Fig. 14, where a curve of power gain versus beam velocity is drawn based on the theory outlined in section 3,

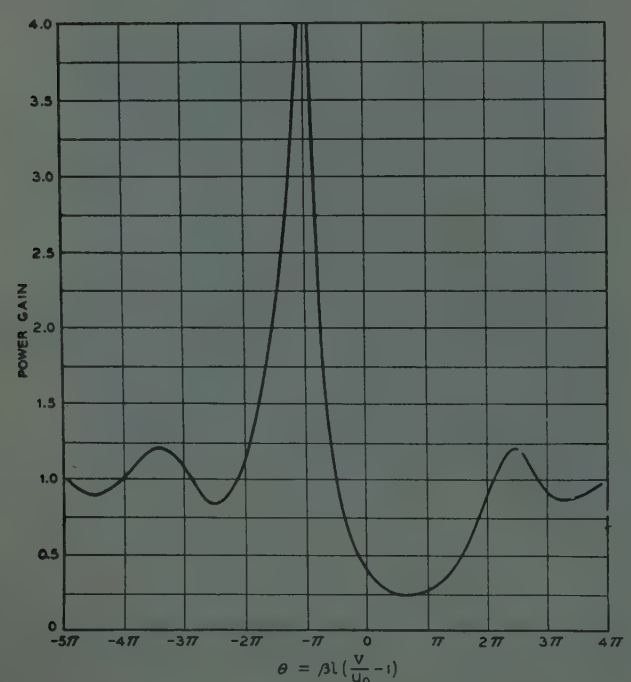

Fig. 14—Theoretical curve of power gain of the backward-wave amplifier versus difference between beam and spatial harmonic phase velocity. (Note agreement with oscillogram on Fig. 13.)

[6] C. F. Quate has pointed out the close relation between this curve and the inverse of the corresponding curve of gain versus voltage obtained with a forward wave T.W.T. run at "zero-gain" current.

and it appears that the main features of the experiments, namely, value of starting current and variation of gain with beam velocity, are well reproduced.

Oscillator Power as Function of Beam Current

A representative plot of oscillator power versus collector current is shown in Fig. 15. It will be noted that this curve commences with practically zero power at the starting current; no "breaking into oscillations" with a finite amplitude as observed with some other types of oscillators has been observed. At higher values of beam currents it seems as if the power output could be described by a function of the type

$$W = A \cdot I - B.$$

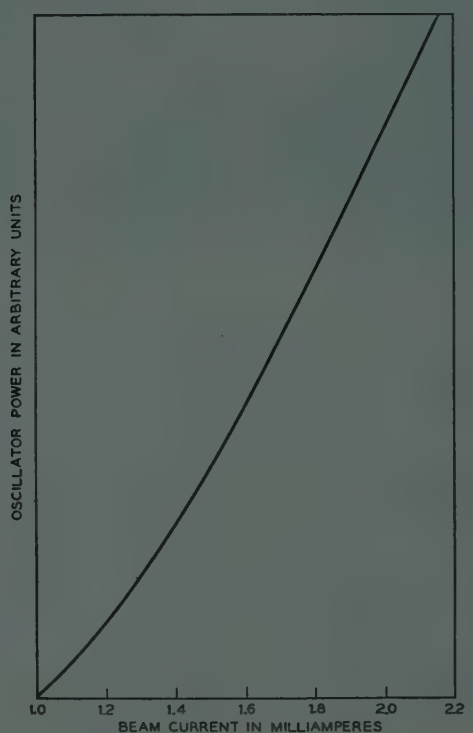

Fig. 15—Oscillator power versus beam current.

Amplification in the Presence of Oscillations

On Fig. 16 are shown C.R.O. traces obtained when a signal was being backward-wave-amplified while the tube (#F7-12) was oscillating simultaneously. As usual, the beam voltage and the C.R.O. X-deflection are swept at 60 cycles. It will be seen that nothing very drastic happens to the amplification process when oscillations set in; if anything, the gain is somewhat increased. However, on one or the other side, or even on both sides, of the gain peak there occur now regions of loss, that is to say, of negative gain.

Frequency-pushing

The term "frequency-pushing" describes the fact that the frequency of oscillation of the backward wave oscil-

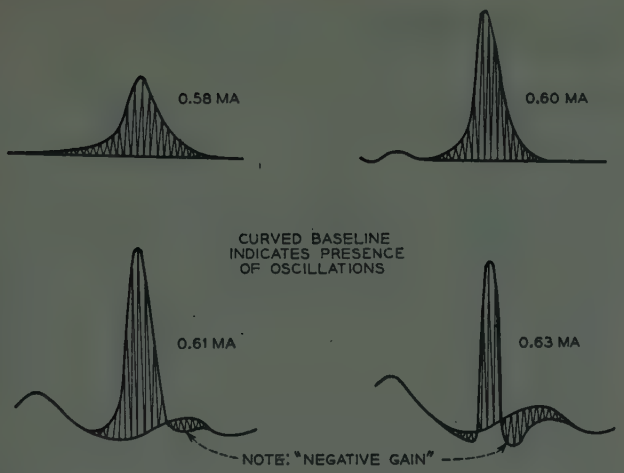

Fig. 16—Oscillograph traces of backward-wave gain in the presence of backward-wave oscillation. The abscissae are beam voltage, the ordinates signal power and oscillator power.

lator increases as the beam *current* is increased, while the voltage is held rigidly constant. This experiment was performed with the tube both in the low-voltage and in the high-voltage mode. Fig. 17 gives result.

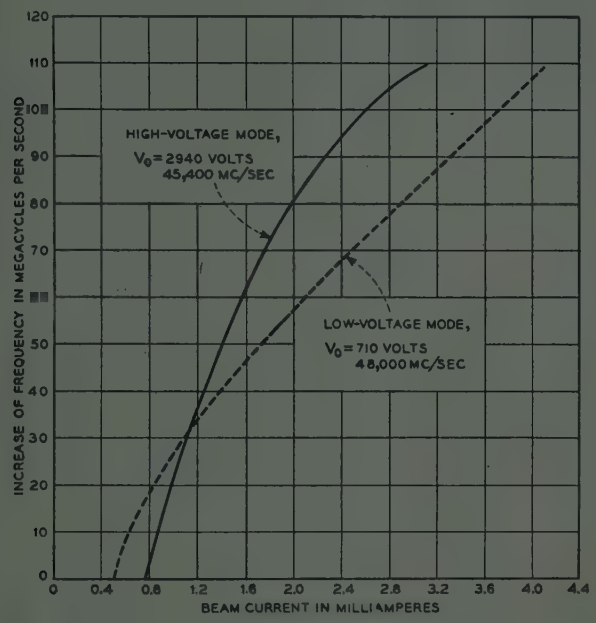

Fig. 17—Observed increase in oscillator frequency as function of beam current; beam voltage held constant.

The corresponding experiment of "frequency pulling," namely, observing the oscillator frequency as the impedance into which the output is looking is changed, has not been performed yet. This is a difficult experiment and will be undertaken as soon as good tubes with near-perfect internal termination are available.

Conclusion

Experiments with the Millman tube, a spatial harmonic type of traveling-wave amplifier tube, have shown that amplification and oscillations utilizing backward traveling spatial harmonic components of an electromagnetic wave can be obtained. The most important feature is the fact that both oscillations and amplification can be tuned over a very wide range purely electronically, merely by varying the beam voltage. A simple theory of backward-wave gain, from which the starting current for backward-wave oscillation can be calculated, is given and shown to agree quite well with experiment. A number of experiments on amplification and oscillations under various circumstances are described, though quantitative comparisons with a more complete theory are still lacking at this relatively early stage of the investigation. It is to be hoped that future work, both experimental and theoretical, will bring to light many new interesting and useful facts about this novel kind of tube.

List of Symbols

β, β_1, β_2	phase constants of circuits, given by ω/v, ω/v_1, ω/v_2 respectively
β_e	phase constant of electron beam
${}_s\beta_n$	phase constant of n-th spatial-harmonic wave component
${}_s\beta_{(-1)}$	phase constant of first backward spatial harmonic wave component
C	Pierce's T.W.T. gain parameter, given by $C^3=I_0K/4V_0$
C'	modified gain parameter, in which the nonsynchronous beam voltage U_0 takes the place of V_0.
d	geometric length of periodic element of circuit
G	voltage gain
I_0	dc beam current
I_0'	starting current
K	circuit impedance for the purpose of calculating interaction with an electron beam
l, l_1, l_2	geometric lengths of circuit
n, n_1, n_2, N	numbers of wavelengths in circuit
n	order of spatial-harmonic wave component
ω	angular frequency of signal
v, v_1, v_2	phase velocities of waves
V, V_1, V_2, V_i	RF voltages on circuit
V_0	synchronous electron beam voltage
u_0	electron beam velocity
U_0	non-synchronous electron beam voltage
${}_sv_n$	phase velocity of n-th spatial-harmonic wave component
${}_sv_{(-1)}$	phase velocity of first backward spatial-harmonic wave component
v_g, v_{g1}, v_{g2}	group velocities
z	distance
$\theta=\beta z[v/u_0-1]$	phase shift between beam and wave in a distance z (in Pierce's notation $\theta=-\beta zCb$).

Underearth Quartz Crystal Resonators*

THOMAS A. PENDLETON†, ASSOCIATE, IRE

Summary—**Advantages of using precision quartz resonators in conjunction with frequency standard oscillators are explained. Advantages of locating the precision-resonators underearth are also described. A method of measuring resonator drift rate with sensitivity of the order of 2 parts in 10^{10} by means of a direct voltage instead of a high-stability variable oscillator is explained.**

PRIMARY STANDARDS of frequency and time[1,2] employ piezo-oscillators in conjunction with dividers, clocks, counters and other associated equipment. Precision quartz-resonator units find practical application in checking such piezo-oscillators.

A precision quartz-crystal unit may be operated under more favorable conditions as a resonator than in an oscillator; low crystal-current may be easily obtained and the value of reactances associated with the circuit arrangement may be readily predetermined. Also, one of the primary advantages lies in the fact that a stable crystal unit may be put to practical use with a minimum of associated equipment and without a dependence upon oscillator power supplies. For instance, if due to an extended power failure all oscillators in a group stop, a good resonator can be used in resetting the oscillators on correct frequency when they are put into operation again.

However, a resonator in an electrically heated oven is also affected by a power failure. For example, on return to operating temperature the values of frequency and drift rate may not return. In order to make the resonator temperature and frequency independent of external power, advantage may be taken of the relatively constant earth-crust temperature by placing the resonator unit underearth. Also the resonator is well isolated from mechanical shock when buried, except of course in earthquake belts.

The time lag and exponential attenuation of the cyclic surface temperature variations[3,4] by the earth's crust depends upon the depth, thermal diffusivity of the soil, and the existence of underground inhomogeneities and water streams. Measurements taken at a depth of 40 feet in clay soil at Beltsville, Maryland, indicate maximum and minimum temperatures of 14.55°C and 14.15°C for the year 1951. Calculations[3] for a depth of 60 feet, where an experimental resonator unit is mounted, predict an amplitude of temperature variation of approximately 0.004°C for damp soil (diffusivity $=0.005$ cgs units). However, the actual value of the amplitude may be somewhat different from the calculated value due to unknown soil conditions.

With temperature variations of not more than a few thousandths of a degree Centigrade, changes of crystal frequency with time are believed to be due to the aging of the quartz-crystal unit in the case of low-temperature co-efficient GT units. The small variations of earth temperature at depths of 50 or 60 feet are not a disadvantage, since they are not of such a magnitude to thermally shock the crystal unit and may be accurately determined. The influence of temperature changes may then be accurately computed to determine the normal drift rate caused by aging of the resonator.

Resonator frequency measurements are usually accomplished by adjusting a precision oscillator to the resonance frequency of the crystal, using some form of an impedance bridge, and the frequency of the oscillator is then measured. However, the oscillator required for this method of measurement must be capable of a short time stability of about 1 part in 10^{10} in measuring modern high stability resonators. When it is desired to test the long time stability and drift rate of a particular crystal unit, its absolute resonance frequency is not important, and a high stability adjustable oscillator and high-precision frequency measuring equipment are not required. However, a standard frequency oscillator is needed. Two techniques are available when it is used: 1) an adjustable reactor may be placed in series with the resonator and its absolute value used to determine the resonator changes, or 2) an adjustable direct voltage may be placed across the electrodes of the GT quartz-crystal unit and its absolute value used to determine frequency changes in the resonator.[5] For simplicity of operation and accuracy of results, each of these methods requires that the resonator's resonance frequency be within a few parts in 10^6 of the standard frequency.

The method of resonator drift rate measurement which employs a direct-voltage source instead of an adjustable-frequency oscillator or adjustable reactor was chosen. In some types of quartz-crystal units an applied direct voltage of one polarity causes a noticeable increase of crystal resonance frequency, whereas a voltage of opposite polarity causes a decrease in crystal-unit resonance frequency. This is caused by the converse piezoelectric effect, i.e., dimensional changes in crystalline quartz with properly oriented applied fields.

The direct voltage is adjusted to bring the crystal unit to resonance at the applied standard frequency. Typical 100 kc GT-cut units have a direct voltage coefficient of frequency of approximately ± 1 part in 10^8 per volt. In the application here described, random

* Decimal classification: R214.2. Original manuscript received by the Institute, November 11, 1952; revised manuscript received June 11, 1953.

† National Bureau of Standards, Washington, D. C.

[1] J. M. Shaull, "Adjustment of high-precision frequency and time standards," PROC. I.R.E., vol. 38, pp. 6–15; 1950.

[2] W. A. Morrison, "The evolution of the quartz crystal clock," *Bell Sys. Tech. Jour.*, vol. 27, pp. 510–588; 1948.

[3] B. Gutenberg, "Internal Constitution of the Earth," Dover Publications, Inc., New York; 1951.

[4] Ingersoll and Zobel, "Heat Conduction," McGraw-Hill; 1948.

[5] L. Myers, "Investigation of the official effects in electrically stressed quartz," *The Marconi Rev.*, part I, pp. 16–25, January /February, 1935; part II, pp. 9–18, March/April, 1935.

variations in polarizing voltage should be limited to less than 0.01 volt. This degree of stability (1 part in 10^4) for a power supply of 100 volts or less is believed more easily attained than a stability of 1 part in 10^{10} for an adjustable oscillator or 1 part in 10^4 for an adjustable reactor.

It is recommended that voltages not in excess of 100 or so be used since increased difficulties with the higher voltage instability will cause a broad indication of resonance. Although not investigated, it is possible that the voltage co-efficient of frequency may be noticeably non-linear above 300 volts.

If the resonance frequency of a particular resonator is far removed from the standard frequency so that more than approximately 100 volts are required for balance, a stable fixed reactance of known temperature co-efficient may be inserted at the bridge to provide most of the correction. The value of this reactance may be checked periodically in a standards laboratory. A small voltage of the correct polarity may then be applied to the crystal unit to bring its apparent resonance frequency into exact equality with that of the standard frequency.

At the time of writing, preliminary measurements have been taken of the frequency changes (sensitivity between 1 and 2 parts in 10^{10}) and resistance of an unloaded high Q (3.5×10^6), 100 kc, GT-cut, quartz-crystal unit mounted at the bottom of a 60-foot well where the initial temperature was approximately 13°C.

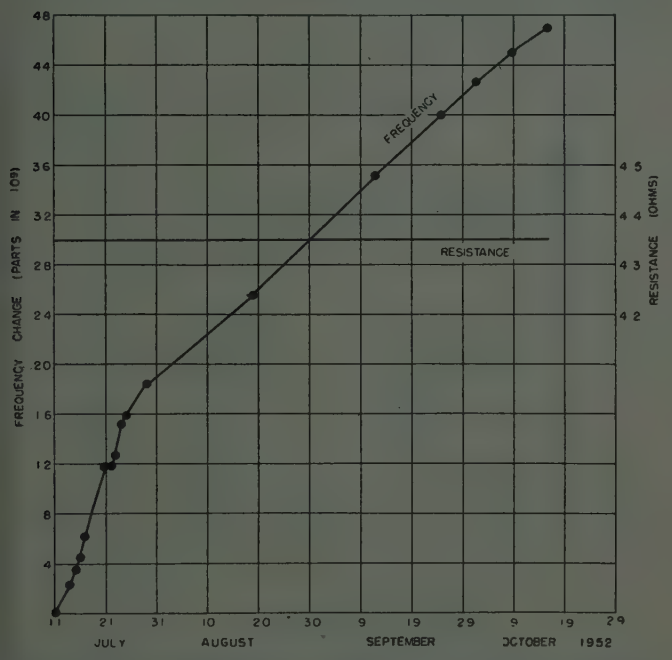

Fig. 1—Results of initial measurements on a high-precision 100 kc quartz-crystal unit, RF current 20 microamperes, direct polarizing potential 67.52 to 69.67 volts.

The well, of diameter $2\frac{1}{2}$ inches, was lined with thin-walled pipe, through which a coaxial cable (RG-9/U) connected the crystal unit. The crystal unit was installed on July 3. A graph of over-all performance for the period July 11 to October 16, 1952 is shown in Fig. 1. In a more permanent installation thermally conducting washers may be placed between the outer conductor of the cable and the periphery of the well to reduce the effects on the crystal unit of changes of temperature at the upper end of the cable. Furthermore, the washers would reduce convection air currents between the top and bottom of the well. Also, it is planned to use a periodically recalibrated platinum resistance-thermometer to determine the small temperature changes at the crystal unit and to correct for their effects on frequency drift rate.

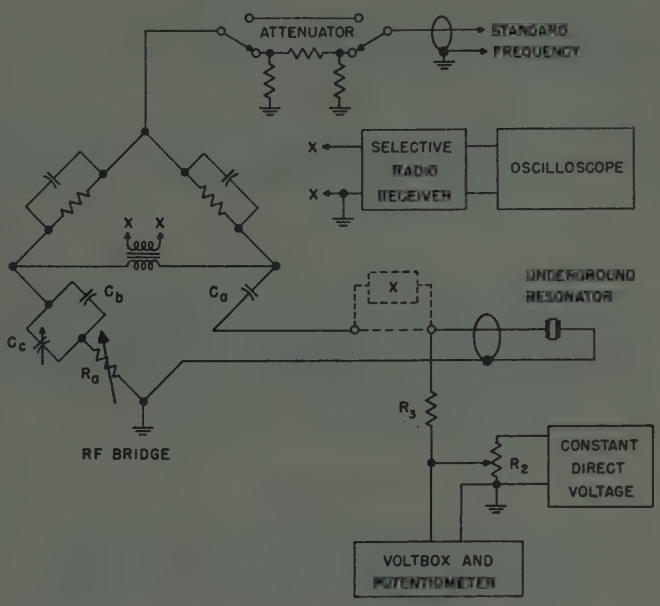

Fig. 2—Circuit arrangement for frequency change and resistance measurements on a high precision 100 kc quartz-crystal unit.

An arrangement of the measuring equipment is shown in Fig. 2. The bridge circuit is a typical RF impedance bridge, with the exception of capacitors C_a and C_b. Capacitor C_a not only prevents direct current through the bridge, but also allows C_c to be adjusted for initial balance. Capacitor C_b is approximately equal to C_a in order to maintain an equal-arm bridge. Resistor R_3 is of sufficiently high value to cause negligible shunting of the resonator. Reactance X may be inserted if the resonator's frequency is far removed from the standard frequency.

The bridge is adjusted for initial balance with the unknown terminals shorted and R_a set to zero. The attenuator may be shorted out to increase the bridge sensitivity. After initial balance is achieved, the attenuator is switched in to limit the crystal current, and the short is removed from the crystal. Resistors R_a and R_2 are then adjusted for bridge balance (crystal unit plus line unity power factor), and the voltage read from the potentiometer while the resistance of the crystal with connecting coaxial line is read from the dial of R_a.

Under the assumptions that the crystal unit has low, constant resistance and a resonance frequency close enough to the standard frequency so that no series reactance is required, the change in crystal unit resonance frequency is given by:

$$\Delta f_r = \Delta f + K\Delta V,$$

where Δf_r, Δf, and ΔV are the changes in resonance frequency, standard frequency and dc voltage respectively. The constant K is the voltage coefficient of frequency for the particular crystal unit used. Its value may be found by switching the bridge between two standards of known frequency difference ($\Delta f'$) and recording the difference of the direct voltages ($\Delta V'$) required for balance in each case

$$K = -\frac{\Delta f'}{\Delta V'}.$$

In obtaining the frequency values shown in Fig. 1, consecutive measurements were made against each of two standard oscillators. The results agreed precisely (within 2 parts in 10^{10}) with the adopted values of the two standard oscillators.

The Optimum DC Design of Flip-Flops*

D. K. RITCHIE†

Summary—**A method for the design of flip-flops has been described which includes component and voltage tolerances. The method may also be applied to the design of other similar switching circuits. The advantage of such methods is that designs meeting desired specifications may be obtained by a direct process rather than by one of trial and error.**

Introduction

THIS PAPER is concerned with the dc design of simple Eccles-Jordan flip-flops[1] such as that shown in Fig. 1. Since the original circuit was published, much work has been done to increase the maximum switching rate and improve the reliability.[2–8]

Well designed flip-flops should be stable in either quiescent state, have reliable triggering characteristics, and have a maximum switching or counting rate well above that required in service. When speed of operation is important, tubes should be selected with high transconductance and low input capacitance; stray capacitances should be minimized and operating voltages and load resistances should be chosen so that the tube may be operated in a high transconductance region of its characteristics. This method may be used with any type of tube suitable for use in flip-flops. A criterion is developed which shows quickly whether or not the flip-flop corresponding to a given set of design specifications is realizable.

An optimum dc design is defined here as one which meets certain design specifications described below with the lowest possible value of load resistance. Usually such a design will result in the maximum switching speed for a flip-flop using a given tube and subject to the conditions to be discussed.

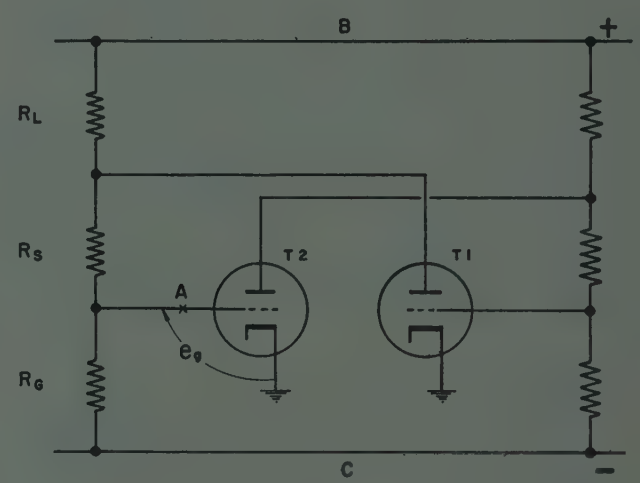

Fig. 1—DC circuit of simple flip-flop.

Design Specifications

The circuit shown in Fig. 1 may be considered as a two-stage amplifier with positive feedback. Stability of such an amplifier may be obtained only if the loop gain is less than unity. This is usually achieved by causing one tube to operate at approximately zero bias, while the other tube is biased beyond cut-off. These two modes of tube operation will be referred to as the conducting and non-conducting states respectively.

* Decimal classification: 621.375.2. Original manuscript received by the Institute, January 14, 1953; revised manuscript received June 12, 1953.

† Research Department, Ferranti Electric Ltd., Toronto, Canada.

[1] W. H. Eccles, F. W. Jordan, "A Trigger Relay Utilizing 3 Electrode Thermionic Vacuum Tubes," *Radio Rev.*, vol. 1, p. 143; 1919.
[2] E. C. Stevenson, I. A. Getting, "A Vacuum Tube Circuit for Scaling Down Counting Rates," *Rev. Sci. Inst.*, p. 414; 1937.
[3] H. Lifschutz, J. L. Lawson, "A Triode Vacuum Tube Scale-of-two Circuit," *Rev. Sci. Inst.*, p. 83; 1938.
[4] H. J. Reich, "New Vacuum Tube Counting Circuits," *Rev. Sci. Inst.*, p. 222; 1938.
[5] W. A. Higinbotham, J. Gallagher, M. Sands, "The Model 200 Pulse Counter," *Rev. Sci. Inst.*, p. 706; 1947.
[6] Val Fitch, "A High Resolution Scale-of-four," *Rev. Sci. Inst.*, p. 942; 1949.
[7] W. B. Lewis, "Electrical Counting," Cambridge University Press, Ch. VIII; 1942.
[8] B. Chance, V. Hughes, E. F. MacNichol, D. Sayre, F. C. Williams, "Waveforms," vol. 19, M.I.T. Radiation Lab. Series, McGraw-Hill Book Co., Inc., New York, pp. 174–179, pp. 604–611; 1949.

It is necessary to include in the design procedure, the voltage and component tolerances, a specification of the limits of the tube characteristics and finally, the minimum excursion of the grid voltage e_g occurring when the flip-flop changes state. First the resistance and voltage tolerances must be defined:

(a) The supply voltage tolerance, expressed as a fraction of the nominal value is $\pm x$ where x is a positive number;

(b) The resistance tolerance, expressed as a fraction of the nominal value is $\pm y$.

Tube characteristic specifications may be stated as:

(c) The plate voltage of the conducting tube must always be less than or equal to a specified value E_p;

(d) When the plate voltage of the conducting tube is E_p, the plate current must never be less than a specified value I_p.

When T_1, Fig. 1, is non-conducting, the voltage e_g must be sufficiently positive so that T_2 is conducting. Suppose, if the connection at the point A were broken, that e_g would be greater than or equal to some specified positive voltage e_1; then with the normal connection, conduction of T_2 would be assured. Therefore, the next condition is:

(e) When T_1 is non-conducting, $e_g \geqq e_1$.

Similarly when T_1 is conducting, e_g must be sufficiently negative to ensure cut-off in T_2. In this case e_g usually is chosen to be several times larger than the nominal cut-off voltage. If the least negative value of e_g that is desired under these conditions is e_2, then the next requirement is:

(f) When T_1 is conducting, $e_g \leqq e_2$.

The final condition is;

(g) The lowest value of load resistance shall be used that will permit (a) to (b) to be met.

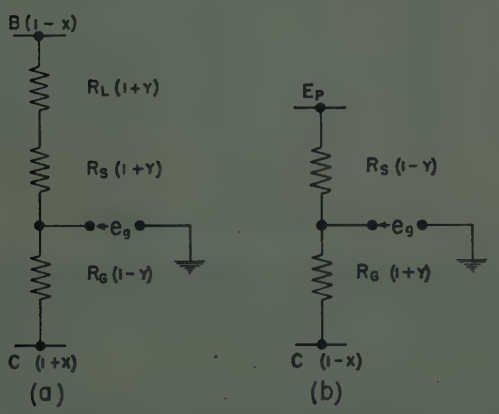

Fig. 2—Extreme conditions: (a) T_1 non-conducting. (b) T_1 conducting.

The Resistance Ratios

In order to meet the design specifications, it is necessary to consider the most extreme combinations of voltage and resistance values. These are shown in Fig. 2 (a) and (b). In Fig. 2 (a) each voltage and resistance considered separately tends to reduce e_g below that value which would be obtained with the corresponding nominal voltage or resistance. In Fig. 2 (b) the reverse is true. Thus these two configurations represent the two worst possible conditions under which specifications (a) to (c) may be met.

Requirements (e) and (f) may be applied to the circuits of Fig. 2 (a) and (b) respectively to obtain the inequalities

With T_1 non-conducting,

$$e_g = \frac{(1-y)(1-x)BR_G+(1+y)(1+x)C(R_L+R_S)}{(1-y)R_G+(1+y)(R_L+R_S)} \geqq e_1,$$

hence

$$\begin{aligned}[(1-y)(1-x)B-(1-y)e_1]R_G \\ +[(1+y)(1+x)C-(1+y)e_1]R_S \\ +[(1+y)(1+x)C-(1+y)e_1]R_L \\ \geqq 0.\end{aligned}$$

This may be written in the form

$$L_1 = a_1\frac{R_G}{R_L} + b_1\frac{R_S}{R_L} + b_1 \geqq 0. \tag{1}$$

Similarly, with T_1 conducting

$$e_g = \frac{(1+y)E_pR_G + (1-y)(1-x)CR_S}{(1+y)R_G + (1-y)R_S} \leqq e_2.$$

This may be put in the form

$$L_2 = a_2\frac{R_G}{R_L} + b_2\frac{R_S}{R_L} \leqq 0. \tag{2}$$

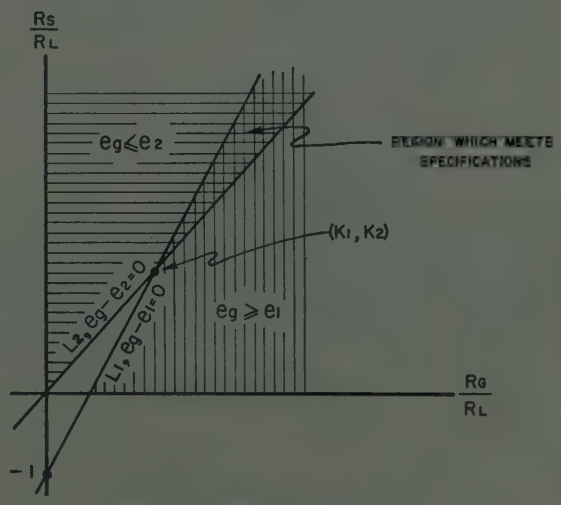

Fig. 3—Tolerance requirements.

Equations (1) and (2) specify regions in the $(R_G/R_L, R_S/R_L)$ plane. If a solution is to be obtained, the regions must overlap. Fig. 3 illustrates these regions which are bounded by $L_1=0$ and $L_2=0$, as well as the positive

reference axes. Any point within the overlapping region may be used to select ratios R_G/R_L and R_S/R_L which will meet all specifications except (g). To meet (g) the point of intersection of $L_1=0$ and $L_2=0$ must be chosen, as will be seen. The co-ordinates of this point are

$$K_1 = \frac{R_G}{R_L} = -\frac{b_2/a_2}{\frac{a_1b_2}{a_2b_1} - 1}$$

$$K_2 = \frac{R_S}{R_L} = \frac{1}{\frac{a_1b_2}{a_2b_1} - 1}.$$

Criterion for Realizability

Since both K_1 and K_2 must be positive, the slope of L_2 must be less than that of L_1. Hence a solution may be found only if

$$\frac{a_1b_2}{a_2b_1} > 1.$$

This criterion is both necessary and sufficient.

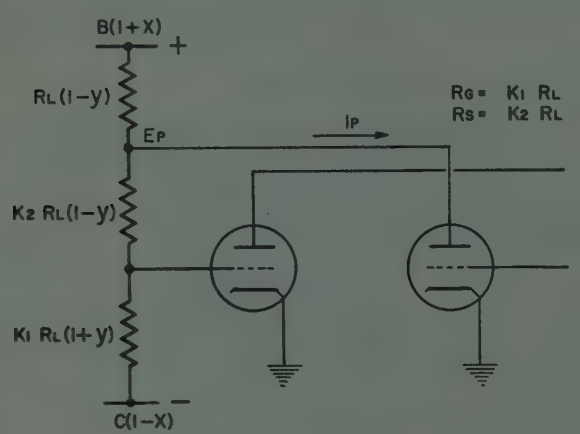

Fig. 4—Determination of R_L.

Determination of R_L

To determine the absolute value of R_L, use may be made of the extreme case illustrated by Fig. 4. Here the equivalent plate supply voltage B' and the equivalent load resistance R_L' must be determined. These are given by

$$B' = \alpha(B - C + x(B + C)) + C(1 - x)$$

$$R_L' = (1 - y)\alpha R_L$$

where

$$\alpha = \frac{K_1 + K_2 + y(K_1 - K_2)}{K_1 + K_2 + y(K_1 - K_2) + (1 - y)}.$$

Here, the tube characteristics (d) must be introduced. If the plate current in the conducting state is I_p when the plate voltage is E_p, then

$$R_L' = \frac{B' - E_p}{I_p}.$$

Note that the smallest value of R_L' is obtained with the smallest value of B' and thus with the smallest value of R_α. That is, both K_1 and K_2 must be as small as possible. Therefore, the point (K_1, K_2), Fig. 3 represents the optimum choice of resistance ratios.

Design Formulas

To design a flip-flop by this method, it is necessary to list the requirements and carry out the computations indicated below. It should be noted that C and e_2 are negative quantities.

Requirements: B, C, E_p, I_p, e_1, e_2, x, y.
Formulas:

$$a_1 = (1 - y)(1 - x)B - (1 - y)e_1$$

$$b_1 = (1 + y)(1 + x)C - (1 + y)e_1$$

$$a_2 = (1 + y)(E_p - e_2)$$

$$b_2 = (1 - y)(1 - x)C - (1 - y)e_2$$

$$K_1 = \frac{-b_2/a_2}{\frac{a_1b_2}{a_2b_1} - 1}, \qquad K_2 = \frac{1}{\frac{a_1b_2}{a_2b_1} - 1}$$

If $\frac{a_1b_2}{a_2b_1} \leq 1$ the design is not realizable.

$$\alpha = \frac{K_1 + K_2 + y(K_1 - K_2)}{K_1 + K_2 + y(K_1 - K_2) + (1 - y)}$$

$$B' = \alpha(B - C + x(B + C)) + C(1 - x)$$

$$R_L' = \frac{B' - E_p}{I_p}$$

$$R_L = R_L'/(1 - y)\alpha$$

$$R_G = K_1R_L$$

$$R_S = K_2R_L$$

Example

A typical set of requirements is listed here:

$B=+300$ v	When the calculations are carried
$C=-150$ v	out, the values of R_L, R_S and R_G
$E_p=$ 100 v	obtained are:
$I_p=$ 5.9 ma	$R_L=37.4$k
$e_1=$ 0 v	$R_S=277$k
$e_2=-25$ v	$R_G=212$k
$x=$ 0.05	
$y=$ 0.1	

Usually the nominal resistance values may not be obtained as standard or preferred values. A compromise solution is to use the preferred values most nearly approximating the nominal ones and which keeps the re-

sistance ratios R_G/R_L and R_S/R_L within the overlapping region of Fig. 3. For the present example the set of values $R_L=39$k, $R_S=300$k and $R_G=225$k is quite suitable.

ACKNOWLEDGMENT

The author is indebted to J. F. C. Harben for his valuable assistance in the writing of this paper.

Traveling-Wave Tube Helix Impedance*

PING KING TIEN†, ASSOCIATE MEMBER, IRE

Summary—**The impedance parameter[1] of a circular helix, from which the gain of a helix-type traveling wave amplifier is computed, is investigated for a "Tape-Helix" model.[2] Results obtained in this paper indicate that the impedance has a smaller value than for the "Sheath-Helix" model,[1,2] and is considerably reduced at larger values of *ka*, the ratio of the helix circumference to the free space wavelength.**

A tape helix surrounded by a dielectric medium is analyzed. It is shown that the results obtained from the theory can be used to evaluate the helix impedance for usual types of traveling wave tubes. They have been found to be in agreement with measurements on many tube designs.

INTRODUCTION

HELIX TYPE TRAVELING wave tubes were investigated by Pierce,[1] Kompfner,[3] and Rydbeck.[4] The relation[1] between gain and helix impedance is:

$$G = (A + BCN)db \tag{1}$$

with

$$C^3 = K\frac{I_0}{4V_0}f \tag{2}$$

where G is the amplification in db. "A" is the initial loss of the increasing wave; "N", the number of active wavelength; "C", the gain parameter; and "B", a parameter depending on space charage and circuit attenuation. V_0/I_0 is the electron beam impedance; f is a factor depending on the ratio of the beam and helix diameters. "K", defined by:

$$K = \frac{E_z^2(0)}{2\beta^2 P} \tag{3}$$

is known as the *Helix Impedance*. $E_z(0)$ is the maximum value (both in time and in Z) of the axial electric field on the axis of a helix carrying an electromagnetic wave of power P and with a phase constant β. K has the dimensions of (Voltage)^2/Power i.e., impedance. It is the ratio of the square of the line integral of the effective axial E field to the power carried by the helix circuit and is generally considered as the parameter that measures the effectiveness of the helix.

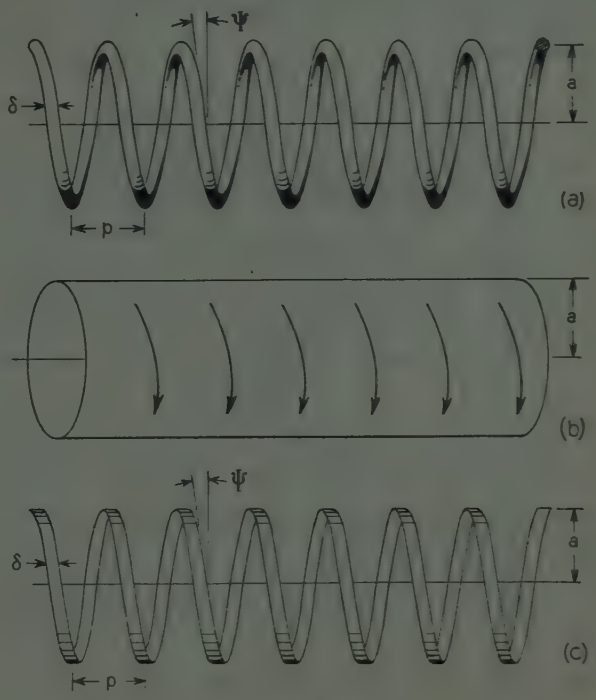

Fig. 1—(a) The actual helix;
(b) The *SHEATH HELIX* model;
(c) The *TAPE HELIX* model.

Helix impedance was computed previously by Pierce[1] from an approximation which assumed the helix to be an ideal cylinder with conduction only in the wire direction (Fig. 1b). The name "Sheath Model" is given to the helix studied under this assumption. The impedance[1,2] of a sheath helix is:

$$K = (\pi\beta^3 a^3 \omega\varepsilon a g_0)^{-1};$$

$$g_0 = \frac{1}{\eta^2}\left(\left(1+\frac{I_0K_1}{I_1K_0}\right)(I_1^2 - I_0I_2) + \frac{I_0^2}{K_0^2}\left(1+\frac{I_1K_0}{I_0K_1}\right)(K_0K_2 - K_1^2)\right) \tag{4}$$

* Decimal classification: R339.2×R145.3. Original manuscript received by the Institute, July 21, 1952; revised manuscript received June 9, 1953.

† Bell Telephone Labs., Inc., Murray Hill, N. J.

[1] J. R. Pierce, "Traveling Wave Tubes," Van Nostrand; 1950.

[2] Samuel Sensiper, "Electromagnetic wave propagation on helical conductors" (thesis), *Mass. Inst. Tech.*; 1951.

[3] R. Kompfner, "Traveling wave tube as amplifier at microwaves," PROC. I.R.E., vol. 35, p. 124; 1947.

[4] O. E. H. Rydbeck, "Theory of the traveling wave tube," *Ericsson Tech.*, vol. 46, p. 3; 1948.

where

$$\eta = (\beta^2 a^2 - k^2 a^2)^{1/2} \tag{5}$$

$$k^2 = \omega^2 \mu \epsilon \tag{6}$$

ω is the angular frequency of the signal, a, the radius of the helical cylinder and μ, and ϵ, the permeability and dielectric constant respectively of the medium. I_0, I_1, I_2 and K_0, K_1, K_2 are respectively modified Bessel functions of the zeroth, first, and second order of the first and the second kinds. All the Bessel functions have the argument η. The factor $1/g_0$ of the sheath impedance is plotted in Fig. 2. Because of difficulties in experimental techniques, expression (4) has never been verified by direct measurements, although we may calculate a value of impedance from (1) and (2) by measurements based on tube performances. This was done by Cutler[5] and he found that a reduction factor of about 0.5 is necessary to account for the differences between the experimental value and that computed from (4).

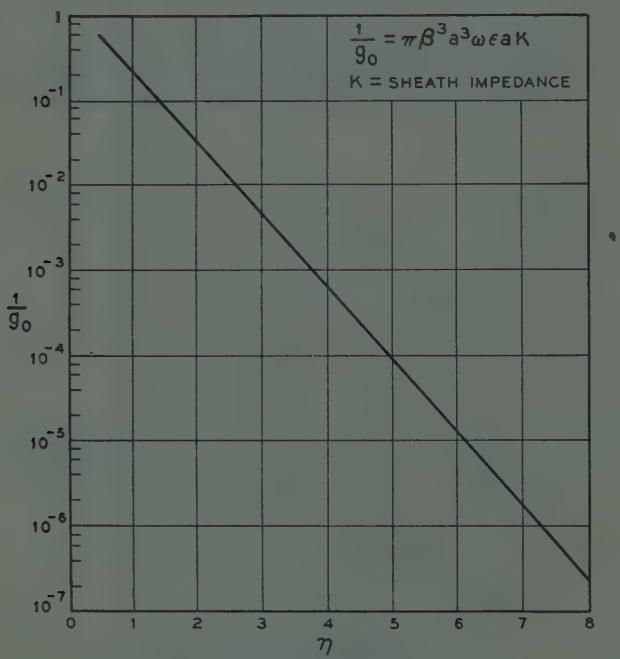

Fig. 2—The factor $1/g_0$ of the sheath impedance computed by (4).

It is the purpose of this paper to compute the helix impedance by means of a more accurate analysis. The best method available seems to be to use the tape-helix model studied by Sensiper.[2] In his analysis the helix is assumed to be wound of infinitely thin conducting tape (Fig. 1c). A tape helix with pitch p and width δ will therefore be assumed.

Theory of a Tape Helix Surrounded by a Dielectric Medium

Field expressions for a tape helix in free space were derived by Sensiper.[2] However we are here concerned with a more complicated case in which the tape helix is surrounded by a dielectric medium (Fig. 3). M.K.S. units and cylindrical co-ordinates r, θ, Z are used. The helix possesses one kind of symmetry, it coincides with itself by a proper translation and rotation. Because of

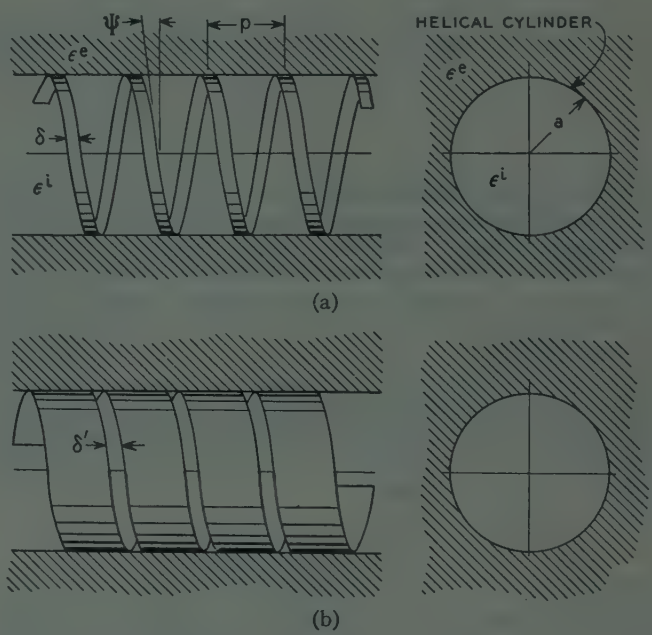

Fig. 3—*TAPE HELIX* surrounded by a dielectric medium; (a) narrow tape helix; (b) narrow gap helix.

this periodic property, Floquet's theorem[6] can be applied[2] for both axial and angular co-ordinates. One thus obtains, for the solution of the scalar wave equation:

$$E_{zm}{}^e = (-\beta_m{}^2 + k_e{}^2) A_m{}^e K_m\left(\eta_m{}^e \frac{r}{a}\right) \tag{7}$$

$$H_{zm}{}^e = (-\beta_m{}^2 + k_e{}^2) B_m{}^e K_m\left(\eta_m{}^e \frac{r}{a}\right) \tag{8}$$

$$E_{rm}{}^e = -j\beta_m \frac{\eta_m{}^e}{a} A_m{}^e K_m{}'\left(\eta_m{}^e \frac{r}{a}\right) + \frac{m\omega\mu}{r} B_m{}^e K_m\left(\eta_m{}^e \frac{r}{a}\right) \tag{9}$$

$$E_{\theta m}{}^e = \frac{m\beta_m}{r} A_m{}^e K_m\left(\eta_m{}^e \frac{r}{a}\right) + j\omega\mu \frac{\eta_m{}^e}{a} B_m{}^e K_m{}'\left(\eta_m{}^e \frac{r}{a}\right) \tag{10}$$

$$H_{rm}{}^e = -\frac{m\omega\epsilon^e}{r} A_m{}^e K_m\left(\eta_m{}^e \frac{r}{a}\right) - j\beta_m \left(\frac{\eta_m{}^e}{a}\right) B_m{}^e K_m{}'\left(\eta_m{}^e \frac{r}{a}\right) \tag{11}$$

[5] C. C. Cutler, "Traveling-wave tube gain," PROC. I.R.E., vol. 39, p. 8; 1951.

[6] J. C. Slater, "Microwave Electronics," Van Nostrand; 1950.

$$H_{\theta m}^{e} = -j\omega\epsilon^{e}\frac{\eta_m^{e}}{a}A_m^{e}K_m'\left(\eta_m^{e}\frac{r}{a}\right) + \frac{m\beta_m}{r}B_m^{e}K_m^{e}\left(\eta_m^{e}\frac{r}{a}\right) \quad (12)$$

$$E_{zm}^{i} = (-\beta_m^{2} + k_i^{2})A_m^{i}I_m\left(\eta_m^{i}\frac{r}{a}\right) \quad (13)$$

$$H_{zm}^{i} = (-\beta_m^{2} + k_i^{2})B_m^{i}I_m\left(\eta_m^{i}\frac{r}{a}\right) \quad (14)$$

$$E_{rm}^{i} = -j\beta_m\frac{\eta_m^{i}}{a}A_m^{i}I_m'\left(\eta_m^{i}\frac{r}{a}\right) + \frac{m\omega\mu}{r}B_m^{i}I_m\left(\eta_m^{i}\frac{r}{a}\right) \quad (15)$$

$$E_{\theta m}^{i} = \frac{m\beta_m}{r}A_m^{i}I_m\left(\eta_m^{i}\frac{r}{a}\right) + j\omega\mu\frac{\eta_m^{i}}{a}B_m^{i}I_m'\left(\eta_m^{i}\frac{r}{a}\right) \quad (16)$$

$$H_{rm}^{i} = -\frac{m\omega\epsilon^{i}}{r}A_m^{i}I_m\left(\eta_m^{i}\frac{r}{a}\right) - j\beta_m\frac{\eta_m^{i}}{a}B_m^{i}I_m'\left(\eta_m^{i}\frac{r}{a}\right) \quad (17)$$

$$H_{\theta m}^{i} = -j\omega\epsilon^{i}\frac{\eta_m^{i}}{a}A_m^{i}I_m'\left(\eta_m^{i}\frac{r}{a}\right) + \frac{m\beta_m}{r}B_m^{i}I_m\left(\eta_m^{i}\frac{r}{a}\right) \quad (18)$$

with

$$\eta_m^{e} = [(\beta_m^{2} - k_e^{2})a^{2}]^{1/2};\quad \eta_m^{i} = [(\beta_m^{2} - k_i^{2})a^{2}]^{1/2} \quad (19)$$

$$\beta_m = \beta_0 + m\frac{2\pi}{p} \quad (20)$$

$$k_e^{2} = \omega^{2}\mu\epsilon^{e};\qquad k_i^{2} = \omega^{2}\mu\epsilon^{i}. \quad (21)$$

where $E_{rm,\,\theta m,\,zm}$ and $H_{rm,\,\theta m,\,zm}$ are Fourier components of electric and magnetic fields, that is:

$$E_{r,\theta,Z}^{i,e} = \sum_m E_{rm,\theta m,Zm}^{i,e}$$
$$H_{r,\theta,Z}^{i,e} = \sum_m H_{rm,\theta m,Zm}^{i,e} \quad (22)$$

Fields with subscript $m=0$ are denoted in this paper as fundamental fields and those with $m\neq 0$, as space harmonic fields. m may be any integer including zero. Superscripts i and e denote, respectively, quantities inside and outside the helical cylinder. I_m, K_m are modified Bessel functions of mth order of the first and the second kinds respectively. I_m' and K_m' are their derivatives with respect to the argument. p is the pitch and a is the radius of the helical cylinder. The common factor $e^{j\omega t}e^{-jm[(2\pi/p)Z-\theta]}$ is omitted in all the expressions. j is $\sqrt{-1}$.

It is seen from (7) to (18), that the field expressions involve the following quantities. k_i and k_e, as given in (21), depend upon the operating frequency and the dielectric constants of the media. β_m is the phase constant associated with the mth component of the fields and can be calculated from (20), if β_0 is known. β_0 is the phase constant of the fundamental component of he fields and will be discussed later in Section 4. η_m^{e} and η_m^{i} can be calculated by means of (19) from the "β_m's" and "ka's." "A_m's" and "B_m's" are constants associated with the solutions and will be determined by the boundary conditions and the current distribution assumed over the helical tape as given later in (28) to (31).

Let κ be the total current density over the tape conductor. We have:

$$\kappa_{11} = e^{-j\beta Z}\sum_m \kappa_{11m}e^{-jm((2\pi/p)Z-\theta)}$$
$$\kappa_{\perp} = e^{-j\beta Z}\sum_m \kappa_{\perp m}e^{-jm((2\pi/p)Z-\theta)}. \quad (23)$$

With:

$$\kappa_{11m} = \kappa_{Zm}\sin\Psi + \kappa_{\theta m}\cos\Psi$$
$$\kappa_{\perp m} = \kappa_{Zm}\cos\Psi - \kappa_{\theta m}\sin\Psi. \quad (24)$$

Where Ψ is the angle between the direction of helical conductor and the circumference of the helical cylinder. Subscripts 11 and $\perp$ denote the directions parallel to and normal to the helical wire, respectively. In the case of the sheath model, the current density is evenly distributed over the helical cylinder and therefore all the "κ_{11m}'s" except "κ_0's" are zero.

Considering first the case that the tape is narrow as compared to the pitch, i.e., $\delta/p \ll 1$, we may assume, according to Sensiper[2], that: (a) current flow normal to the direction of the helical tape is zero; (b) the magnitude of the current flowing in the direction of helical tape is constant over the conducting tape; and (c) the constant phase contour of the current is at the constant Z-plane. From the assumptions, we have:[2]

$$\kappa_{\perp m} = 0 \quad (25)$$

$$|\kappa_{11m}| = \left|\frac{\sin m\frac{\pi\delta}{p}}{m\frac{\pi\delta}{p}}\kappa_{110}\right|. \quad (26)$$

At the boundary $r=a$, the tangential electric fields must be continuous and the tangential magnetic fields must be matched to the current flow. That is:

$$E_{z,\theta}^{i} = E_{z,\theta}^{e}$$
$$\kappa_\theta = H_z^{i} - H_z^{e} \quad \text{at } r = a \quad (27)$$
$$\kappa_z = H_\theta^{e} - H_\theta^{i}.$$

By these boundary conditions and the assumptions about the current distribution of (25) and (26), the "A_m's" and "B_m's" of (7) to (18) can be determined:

$$\frac{jA_m^i}{\omega\mu a} = \frac{a^2\kappa_{11m}\sin\Psi}{I_m(\eta_m)} M_m;$$

$$M_m \cong \frac{\eta_m^2 - m\beta_m a\cot\Psi}{\eta_m^3\left[k_i^2a^2\dfrac{I_m'(\eta_m)}{I_m(\eta_m)} - k_e^2a^2\cdot\dfrac{K_m'(\eta_m)}{K_m(\eta_m)}\right]} \tag{28}$$

$$\frac{jA_m^e}{\omega\mu a} = \frac{a^2\kappa_{11m}\sin\Psi}{K_m(\eta_m)} N_m; \qquad N_m \cong M_m \tag{29}$$

$$B_m^i = \frac{a^2\kappa_{11m}\sin\Psi}{I_m(\eta_m)} Q_m;$$

$$Q_m \cong \frac{1}{\eta_m} I_m(\eta_m)K_m'(\eta_m)\cot\Psi \tag{30}$$

$$B_m^e = \frac{a^2\kappa_{11m}\sin\Psi}{K_m(\eta_m)} S_m;$$

$$S_m \cong \frac{1}{\eta_m} I_m'(\eta_m)K_m(\eta_m)\cot\Psi. \tag{31}$$

Here an approximation $\eta_m^i \cong \eta_m^e \cong \eta_m$ has been made. The approximation is good when $k_i a \ll \beta_m a$, which is generally true.

From (28) to (31), and the field expressions (9) to (12) and (15) to (18), the power associated with the mth component of the fields can be computed using Poynting's theorem:

$$P_m = P_m^i + P_m^e$$

$$P_m^i = Re\left[\frac{1}{2}\int_0^{2\pi} d\theta \int_0^a (E_{rm}^i\tilde{H}_{\theta m}^i - E_{\theta m}^i\tilde{H}_{rm}^i) r dr \tag{32}$$

$$P_m^e = Re\left[\frac{1}{2}\int_0^{2\pi} d\vartheta \int_a^\infty (E_{rm}^e\tilde{H}_{\theta m}^e - E_{rm}^e\tilde{H}_{rm}^e) r dr, \tag{33}$$

where $\sim$ denotes the conjugate value and "Re" means the real component.

For $m \neq 0$, we have:

$$P_m^i = \pi a^2\omega\mu a \sin^2\Psi T_m^i;$$

$$T_m^i = |\kappa_{11m}|^2\Bigg(\beta_m a[k_i^2a^2M_m^2 + Q_m^2]$$
$$\cdot\left[\eta_m^i\frac{I_m'(\eta_m^i)}{I_m(\eta_m^i)} + \frac{\eta_m^{i2}}{2}\frac{I_m'^2(\eta_m^i)}{I_m^2(\eta_m^i)} - \frac{1}{2}(\eta_m^{i2}+m^2)\right]$$
$$- mM_mQ_m(\beta_m^2a^2 + k_i^2a^2)\Bigg) \tag{34}$$

$$P_m^e = \pi a^2\omega\mu a \sin^2\Psi T_m^e;$$

$$T_m^e = |\kappa_{11m}|^2 = \Bigg(\beta_m a[k_e^2a^2N_m^2 + S_m^2]$$
$$\cdot\left[-\eta_m^e\frac{K_m'(\eta_m^e)}{K_m(\eta_m^e)} - \frac{\eta_m^{e2}}{2}\frac{K_m'^2(\eta_m^e)}{K_m^2(\eta_m^e)} + \frac{1}{2}(\eta_m^{e2}+m^2)\right]$$
$$+ mN_mS_m(\beta_m^2a^2 + k_e^2a^2)\Bigg) \tag{35}$$

and for $m=0$, the fundamental component,

$$P_0^i = \pi a^2\omega\mu a \sin^2\Psi T_0^i;$$

$$T_0^i = |\kappa_{110}|^2\beta a[k_i^2a^2M_0^2 + Q_0^2]$$
$$\cdot\left(\frac{\eta_0^{i2}}{2}[I_1^2(\eta_0^i) - I_2^2(\eta_0^i)] - \eta_0^iI_1(\eta_0^i)I_2(\eta_0^i)\right)$$
$$\cdot\frac{1}{I_0^2(\eta_0^i)} \tag{36}$$

$$P_0^e = \pi a^2\omega\mu a \sin^2\Psi T_0^e;$$

$$T_0^e = |\kappa_{110}|^2\beta a[k_e^2a^2N_0^2 + S_0^2]$$
$$\cdot\left(\frac{\eta_0^{e2}}{2}[K_2^2(\eta_0^e) - K_1^2(\eta_0^e)] - \eta_0^eK_1(\eta_0^e)K_2(\eta_0^e)\right)$$
$$\cdot\frac{1}{K_0^2(\eta_0^e)}, \tag{37}$$

where M_m, N_m, Q_m and S_m are defined in (28) to (31).

We may also express (36) and (37) in terms of $E_z(0)$, this giving:

$$P_0^i = \tfrac{1}{2}a^2\pi\beta a\omega\epsilon^i aU_0^iE_z^2(0)$$

$$U_0^i = \left[\frac{1}{\eta_0^{i2}} + \frac{I_0^2(\eta_0^i)}{\cot^2\Psi k_i^2a^2I_0'^2(\eta_0^i)}\right]$$
$$\cdot[I_1^2(\eta_0^i) - I_0(\eta_0^i)I_2(\eta_0^i)] \tag{38}$$

$$P_0^e = \tfrac{1}{2}a^2\pi\beta a\omega\epsilon^i aU_0^eE_z^2(0)$$

$$U_0^e = \frac{\epsilon^e}{\epsilon^i}\left[\frac{1}{\eta_0^{e2}} + \frac{K_0^2(\eta_0^e)}{\cot^2\Psi k_e^2a^2K_0'^2(\eta_0^e)}\right]$$
$$\cdot[K_2(\eta_0^e)K_0(\eta_0^e) - K_1^2(\eta_0^e)]\frac{I_0^2(\eta_0^i)}{K_0^2(\eta_0^e)}. \tag{39}$$

Helix Impedance

In the above theory, the field distribution as well as the current distribution over the helical tape, is expanded in an infinite number of Fourier components. All of these components are orthogonal functions. They are solutions of the wave equation and may thus be considered as component waves. As may be seen from (20), all the components related to a common mode must have a common group velocity but different phase velocities and some of them may have negative phase velocities. According to traveling wave tube theory, the interaction between waves for amplification only occurs when the electron stream and the fields have nearly the same velocity. In usual traveling wave amplifiers, the electron velocity is adjusted to be nearly in synchronism with the phase velocity of the fundamental fields, and therefore, the only component of fields useful for amplification is the fundamental component. The presence of the space harmonic fields does not increase the amplification of the tube, but to the contrary increases the factor P in the impedance expression (3), and therefore lowers the value of the helix impedance. In the sheath helix theory, all the space harmonic fields are neglected, and the calculated impedance is higher than for a real helix.

Taking $E_z(0)$ and β of (3), the axial electric field and

the phase constant of the fundamental fields, and P, the total power of the fundamental and the space harmonics carried by the circuit, we have from (34) to (39), for the impedance of a narrow tape helix surrounded by a dielectric medium:

$$K = \frac{E_z^2(0)}{2\beta_0^2 \sum_{m=-\infty}^{+\infty} P_m} = \frac{E_z^2(0)}{2\beta_0 P_0} \frac{P_0}{\sum_{m=-\infty}^{+\infty} P_m}$$

$$= \frac{1}{\pi\beta_0^3 a^3 \omega\epsilon^i a(U_0^i + U_0^e)} \frac{T_0^i + T_0^e}{\sum_{m=-\infty}^{+\infty} (T_m^i + T_m^e)}. \quad (40)$$

Phase Velocity

Before calculating the impedance based on (40), the phase constant, β_0, which is the ratio of the angular signal frequency to the phase velocity of the fundamental fields must be first determined. The exact determination of this quantity is quite involved.[2] Since we are only concerned here with one particular propagating mode (the h_{t0} mode in Sensiper's analysis[2]), it is much simpler to compute β_0 from the sheath model. We thus have:[7]

$$\frac{\eta_0^i}{\eta_0^e}\left\{\frac{1 - \frac{k_i^2 a^2}{\eta_0^{i2}} \frac{I_1^2(\eta_0^i)}{I_0^2(\eta_0^i)} \cot^2\Psi}{\frac{I_1(\eta_0^i)}{I_0(\eta_0^i)}}\right\}$$

$$= -\frac{K_0(\eta_0^e)}{K_1(\eta_0^e)} + \frac{k_e^2 a^2}{\eta_0^{e2}} \cot^2\Psi \frac{K_1(\eta_0^e)}{K_0(\eta_0^e)} \quad (41)$$

$$\eta_0^{i2} = (\beta_0^2 - k_i^2)a^2$$

$$\eta_0^{e2} = (\beta_0^2 - k_e^2)a^2.$$

For the helix in free space, $\eta_0^i = \eta_0^e = \eta$, expression (41) is reduced to the familiar equation given by Pierce:[1,2]

$$\frac{I_1(\eta)K_1(\eta)}{I_0(\eta)K_0(\eta)} = \frac{\eta^2}{k^2 a^2 \cot^2\Psi}. \quad (42)$$

As experimentally verified by Cutler,[8] expression (42) appears to be a very good approximation in the usual operating ranges of the traveling wave tube. (41) should hold to the same degree of accuracy for a very thin tape-helix.

Results computed from (41) and (42) indicate that the phase velocity is reduced as the dielectric constant of the surrounding medium is increased.

The Impedance Reduction Factor

In order to show the reduction in impedance due to the presence of the dielectric and the space harmonics, we will compare the impedance of an actual helix with dielectric surroundings, to that of an idealized sheath helix in free space. Equations (19) to (21) show that two helices of equal radii and with equal phase velocities have equal values of $k_i a$, β_m and η_m^i, and have approximately the same values of η_m^e since $k_e \ll \beta_m$. They thus have similar field distributions and should be comparable. The impedance reduction factor, F, is therefore defined as the ratio of the impedance of an actual helix with dielectric to that of a sheath helix in free space of equal radius and with equal phase constant β_0. From (4) and (40) we have:

$$F = \frac{g_0}{U_0^i + U_0^e} \frac{T_0^i + T_0^e}{\sum_{m=-\infty}^{+\infty} (T_m^i + T_m^e)}. \quad (43)$$

It has been mentioned in the last section that the phase velocity is also reduced because of the dielectric. In order that a helix with dielectric and a sheath helix in free space, of equal radii, have the same phase constant β_0, the sheath helix must have a larger value of cot Ψ. The ratio of their values of cot Ψ indicates the reduction in phase velocity due to the presence of the dielectric and is defined here as the dielectric loading factor. Stated more specifically, the dielectric loading factor is the ratio of the value of cot Ψ of an actual helix with dielectric to that of a sheath helix in free space, of equal radius and with equal phase constant β_0. For a tape helix surrounded by a dielectric medium, the dielectric loading factor can be computed from (41) and (42).

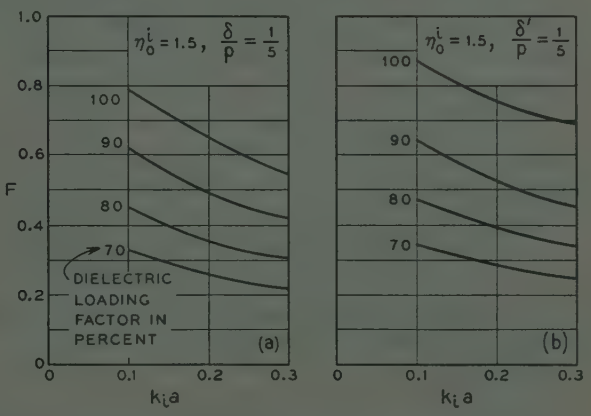

Fig. 4—The impedance reduction factor F of the tape helix;
(a) narrow tape helix, $\eta_0^i = 1.5$, $\delta/p = \frac{1}{5}$;
(b) narrow gap helix, $\eta_0^i = 1.5$, $\delta'/p = \frac{1}{5}$.

In Fig. 4a, the impedance reduction factor of the narrow tape helix with $\eta_0^i = 1.5$, $\delta/p = \frac{1}{5}$, is plotted versus $k_i a$, using the dielectric loading factor as a parameter. It is seen that the impedance decreases, with increasing $k_i a$ or with decreasing dielectric loading factor.

The impedance reduction factor of the narrow gap helix (Fig. 3b) is also calculated following Sensiper's[2] narrow gap helix theory, and is plotted in Fig. 4b for comparison. It may be seen that the narrow gap helix has slightly higher impedance reduction factors com-

[7] L. A. Harris, H. R. Johnson, A. Karp and L. D. Smullin, "Some measurements of phase velocity along a helix with dielectric supports," *Mass. Inst. Tech. R. L. E. report no. 93*; January, 1949.

[8] C. C. Cutler, "Experimental determination of helical wave properties, Proc. I.R.E., vol. 36, p. 2; Feb. 1948.

pared to the narrow tape helix for $\delta/p=\delta'/p$, where δ' is the width of the gap between helical conductors. We will confine our discussions in the rest of this paper to the narrow tape helix which is generally used in traveling wave tubes.

We may further express the impedance reduction factor F, defined above, in the form:

$$F=\frac{\text{Tape impedance with dielectric}}{\text{Sheath impedance in free space}}=F_1\times F_2;$$

$$F_1=\frac{\text{Tape impedance in free space}}{\text{Sheath impedance in free space}};$$

$$F_2=\frac{\text{Tape impedance with dielectric}}{\text{Tape impedance in free space}}. \qquad (44)$$

F_1 is seen to be the impedance reduction factor of the free space tape helix as that given by the first curve (curve marked with D.L.F.=1) in Fig. 4a. It may be considered as the impedance reduction due to the space harmonic fields only. F_2 is considered as the impedance reduction due to the dielectric surroundings, and may be computed from Fig. 4a by dividing F by F_1. It is plotted in Fig. 5a.

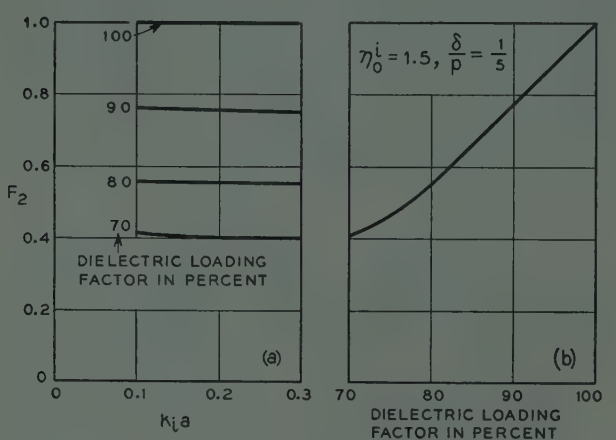

Fig. 5—The impedance reduction factor F_2 of the narrow tape helix $\eta_0^i=1.5$, $\delta/p=\frac{1}{5}$;
(a) F_2 vs. $k_i a$;
(b) F_2 vs. D.L.F.

F_1 and F_2 have been computed for the cases: $k_i a=0.1$, 0.2, 0.3, $\eta_0^i=1$, 1.5, 2, 2.5 and $\delta/p=0.2$, 0.3, 0.4, 0.5. In all those cases, F_2 varies very little with values of $k_i a$ and varies only a few per cent with values of η_0^i and δ/p; F_1 varies slightly with values of η_0^i, but considerably with values of $k_i a$ and δ/p. It is thus only necessary for us to choose some standard values for F_2 and to plot F_1 with different values of $k_i a$ and δ/p in order to have a complete picture of the impedance reduction over usual operating ranges of traveling wave amplifiers. For practical purposes, the values of F_2 may be taken as those given in Fig. 5(b) with reasonable accuracy. There will be more in the next section about F_1.

Current Distribution

When the tape width becomes wider, that is the ratio δ/p approaches $\frac{1}{2}$, the assumptions for current distribution, used in the narrow tape helix computation, may not hold true. No method of determining the actual current distribution over the helical tape is available.[2] We may, however, base helix impedance calculations upon different assumptions concerning the current and compare the results. This is done in Fig. 6. The different assumptions used are:

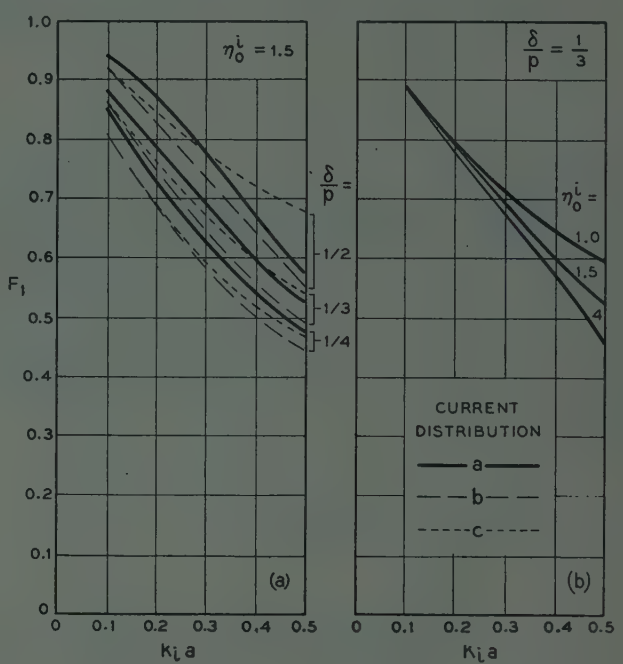

Fig. 6—(a) A comparison of the calculated impedance reduction factors F_1 with different current distributions, $\eta_0^i=1.5$; (b) F_2 computed by means of current distribution (a), $\eta_0^i=1$, 1.5, 4.

(a) The magnitude of the current density is taken as becoming infinitely large in an inverse square root manner as the tape edges are approached and is zero in the gap between helical conductors. The constant phase contour of the current is normal to the edge of the helical tape. In this case:

$$|\kappa_{11m}|\cong\left|\frac{J_0\left(\frac{\beta_m\delta}{2}\right)}{J_0\left(\frac{\beta_0\delta}{2}\right)}\kappa_{110}\right|; \qquad (45)$$

(b) The magnitude of the current density is taken constant over the conducting tape and is zero in the gap. The constant phase contour of the current is normal to the edge of the helical tape. In this case:

$$|\kappa_{11m}|\cong\left|\frac{\beta_0}{\beta_m}\frac{\sin\frac{\beta_m\delta}{2}}{\sin\frac{\beta_0\delta}{2}}\kappa_{110}\right|; \qquad (46)$$

(c) The magnitude of the current density is constant over the conducting tape and is zero in the gap. The constant phase contour of the current is at the constant

$-Z$ plane. (This is the assumption used in the above narrow tape helix theory.)

In all cases, $\kappa_\perp$ is assumed to be zero. All these assumptions have been suggested by Sensiper.[2]

It may be seen in Fig. 6 that when $k_i a$ or δ/p is small, assumptions (b) and (c) give nearly the same impedance reduction factors. In case $k_i a$ or δ/p is larger, assumption (a) is preferred as it approximates the current distribution of an isolated narrow thin tape.

Traveling Wave Tubes of Different Dielectric Structures

In the usual types of traveling wave tube, the helix is either supported by a concentric glass tube or by several dielectric rods. Strictly speaking, the helix impedance computations should be based upon the actual dimensions and shape of the dielectric supporting structure, but this is practically impossible. It has keen found, however, in section 5, that F_1 and F_2 depend primarily on the values of $k_i a$, δ/p, and the dielectric loading factor. We may thus expect to evaluate the helix impedance with reasonable accuracy, using those values. The following procedures are suggested.

(1) Measure the phase velocity of the fundamental fields either by measuring the standing wave pattern along the helix with a sliding probe, or by sliding a metallic reflector along the inside of the helix and observing the standing wave pattern at the input end.[7]

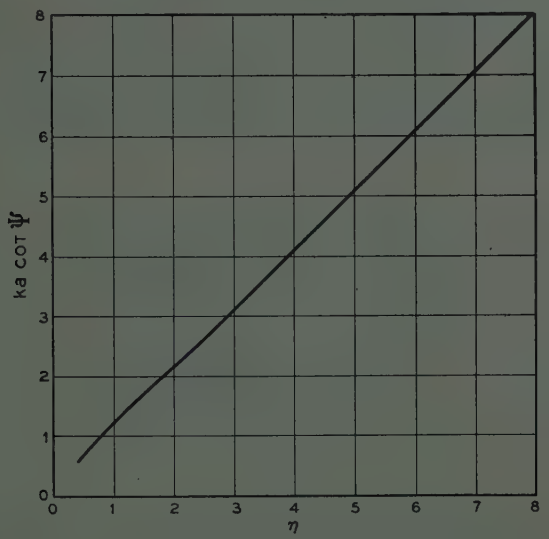

Fig. 7—ka cot Ψ versus η of the sheath helix (computed by 42).

Based upon the measured value of phase velocity, compute η_0^i. Using this value of η_0^i and the value of $k_i a$, calculate from Fig. 7 the value of cot Ψ of the idealized sheath helix. The ratio of the value of cot Ψ of the actual helix to that calculated from Fig. 7 is the dielectric loading factor.

(2) Using the value of the dielectric loading factor, find F_2 from Fig. 5(b); using values of $k_i a$ and δ/p, find F_1 from Fig. 6. In Fig. 6, the curves computed from the assumption (a) concerning the current is preferred.

(3) The total reduction factor F is the product of F_1 and F_2. The actual helix impedance is obtained by multiplying F by the impedance of the sheath helix. This can be found by means of Fig. 2, using the value of η_0^i found in (1) as η.

Most tubes are designed with $k_i a$ about 0.1, η_0^i about 1.5 and dielectric loading factor about 0.8. It is observed from Fig. 4(a) that with these values, F is approximately equal to 0.5 which agrees with the factor found by Cutler[5] and based upon measurements on tube performance. The results of measurements on different tube designs have been analyzed in Table I and it is found that in general the agreement with theory is good.

Table I

Data Supplied by	$k_i a$	η_0^i	D.L.F.	δ/p	Calculated* F	Measured F
Mr. C. C. Cutler Bell Labs.	.069	1.76	.93	.5	.81	.79
Mr. C. F. Quate Bell Labs.	.232	2.82	.87	.4	.546	.50
Mr. J. S. Cook Bell Labs.	.096	1.54	.78	.5	.489	.45
Mr. H. Poulter Stanford Univ.	.15	1.2	.75	.4	.41	.46

* Calculations are based upon values found in Fig. 5(b) and the current distribution (a).

Conclusions

This analysis indicates two ways to improve the helix design for the use in traveling wave tubes: (1) to raise the dielectric loading factor and (2) to reduce the space harmonic component fields. The dielectric loading factor can be raised by supporting the helix by small dielectric tubes or by wedge-shaped dielectric supports so that most of dielectric material is away from the helical surface. The space harmonic component fields can be reduced either by using a ratio of $\delta/p \cong 1/2$ or a smaller value of $k_i a$. A further improvement might be obtained by using a properly arranged multi-wire helix.

It is also found in this paper that the impedance is reduced more at larger values of $k_i a$. This imposes a basic limitation on the design of traveling wave tubes. In particular, in high power tubes and millimeter wave tubes, a relatively large value of $k_i a$ is necessary in order to have a helix large enough to allow the passage of the electron beam for amplification.

Acknowledgment

This paper was started at the Electronic Research Laboratory, Stanford University, and completed at Bell Telephone Laboratories. The work in Stanford was made possible through support jointly by the Naval Department (Office of Naval Research), the U. S. Army (Signal Corps) and the U. S. Air Force under ONR Contract N6-ONR-251 Consolidated Task No. 7.

Most of the numerical work was done by Miss J. A. Aichele and Mrs. C. A. Lambert, some was done with I.B.M. equipment under the direction of Dr. R. W. Hamming, all of the Bell Laboratories.

Traveling-Wave Slot Antennas*

J. N. HINES†, ASSOCIATE, IRE, V. H. RUMSEY†, SENIOR MEMBER, IRE, AND C. H. WALTER†, ASSOCIATE, IRE

Summary—The traveling-wave slot antenna is similar to a traveling-wave wire antenna, but it is far more versatile because the phase velocity and rate of radiation of the fields in the antenna can be controlled. Four types of traveling-wave slot antennas have been identified. These are: (a) the conventional transverse electric, TE (no tangential E field parallel to the slot length); (b) transverse magnetic, TM (no tangential H field parallel to the slot length); (c) a hybrid with negligible transverse E, and (d) a hybrid with negligible normal H. Only the hybrid types are capable of producing maximum radiation in the direction of the slot axis (i.e., end-fire radiation).

The complex propagation constant which is characteristic of uniform traveling-wave slots has been measured for a variety of waveguide geometries and is presented in the form of graphs.

The radiation pattern of a traveling-wave slot can be controlled to give low side lobe or "cosecant squared" type patterns by appropriate variation of slot width with distance z along the axis. An approximate formula for the variation of attenuation α with z required to give a specified pattern can be derived. This in turn gives the required variation of slot width with z.

An examination of the principle of superposition shows that the conventional technique of array design is an approximation which has proved inadequate in the design of certain slot arrays. A more elaborate technique is described which has the merit that the array pattern can be predicted exactly from measurements made by exciting individual elements of the array.

Introduction

THE APPLICATIONS of half-wave slot antennas are well-known.[1–3] A traveling-wave slot antenna may be considered as a slot, many wavelengths long, which is energized at one end so that the field distribution in the slot consists of a traveling wave, in a manner analogous to traveling-wave wire antennas. It therefore performs like an array of half-wave slot antennas, but it is often much easier to design and construct than such an array. One side of a traveling-wave slot antenna is usually enclosed by a waveguide. In this form it is more versatile than the traveling-wave wire antenna because the phase velocity and rate of radiation can be controlled by the waveguide dimensions.

Various forms of traveling-wave slot antennas have been considered by different authors.[4–10] The basic features can be illustrated by considering the form suggested by Booker.[4] In a conventional rectangular waveguide operating in the lowest order TE mode, as in Fig. 1, the magnetic field components H_y and H_z are zero on the central plane represented by a dashed line in Fig. 1.

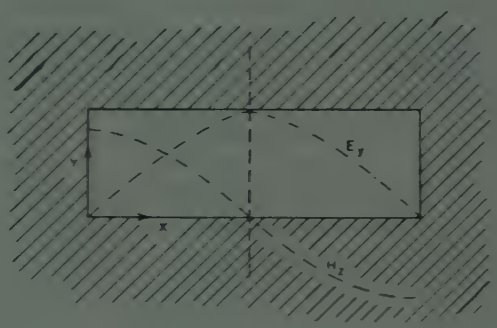

Fig. 1

It follows that this central plane can be replaced by a sheet of infinite impedance, i.e., a perfect magnetic conductor, without disturbing the field, (Fig. 2.)

The equivalent of a magnetic conductor is obtained approximately when the opening in the half-guide is

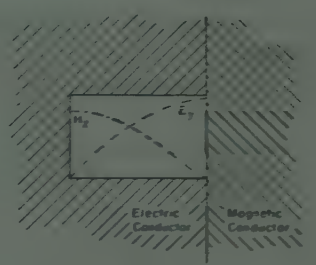

Fig. 2

* Decimal classification: R326.81. Original manuscript received by the Institute, November 10, 1952; revised manuscript received May 28, 1953. The work reported in this paper was done at the Antenna Laboratory under sponsorship of the Air Research and Development Command, Wright Air Development Center, Wright-Patterson Air Force Base, Dayton, Ohio.

† The Antenna Laboratory, Department of Electrical Engineering, The Ohio State University Research Foundation, Columbus, Ohio.

[1] H. G. Booker, "Slot aerials and their relation to complementary wire aerials (Babinet's principle)," *Jour. IEE* (London), vol. 93, part III-A, pp. 620–626; 1946.

[2] W. H. Watson, "The Physical Principles of Wave Guide Transmission and Antenna Systems," Oxford University Press, Oxford, England; 1947.

[3] "Very High-Frequency Techniques," Radio Research Laboratory Staff, Harvard University, vol. I, McGraw-Hill Book Co., Inc.; New York, N. Y.; 1947.

[4] H. G. Booker, "Girders and trenches as end-fire aerials," Report N 30, *TRE Jour.*, Swanage, England; 1941.

[5] W. W. Hansen, "Radiating Electromagnetic Waveguide," U. S. Patent No. 2402622.

[6] W. W. Hansen, S. Seeley, and E. E. Pollard, "Notes on Microwaves," vol. 3, Radiation Laboratory, M.I.T., Cambridge, Mass., Chapter 22; pp. 24–33.

[7] Interim Engineering Report 301-9, Antenna Laboratory, The Ohio State University Research Foundation; prepared under Contract W 33-038 ac 16520 (17380), with Wright Air Development Center, Wright-Patterson Air Force Base, Dayton, Ohio; August 1, 1948.

[8] A. L. Cullen, "On the channel section waveguide raditor," *Phil. Mag.*, vol. 40, pp. 417–428; April, 1949.

[9] W. Rotman, "The Channel Guide Antenna," Air Force Cambridge Research Laboratories, Cambridge, Mass.; January, 1950.

[10] D. R. Rhodes, "Theory of axially slitted circular and elliptic cylinder antennas," *Jour. Appl. Phys.*, vol. 21, pp. 1181–1188; November, 1950.

fitted onto an infinite slot in a ground plane as in Fig. 3, provided the width of the slot, W, is a small fraction of a wavelength. Such an arrangement, therefore, sets up a wave in an infinite slot which travels with a phase velocity very nearly the same as would be obtained in the complete waveguide.

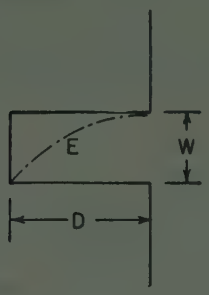

Fig. 3

As the wave travels along the slot its strength is gradually dissipated by radiation. Assuming, for greater generality, that the waveguide is filled with dielectric, we can picture the radiation as due to a wave incident at angle ϕ on the slot, part of which is refracted at angle θ, and the remainder reflected at angle ϕ (Fig. 4).

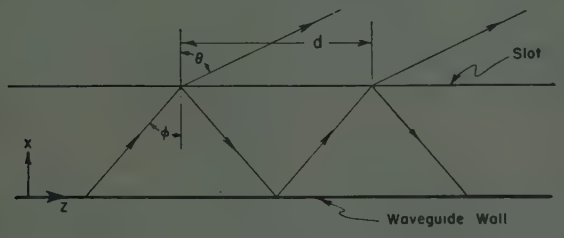

Fig. 4

The refracted wave is radiated in a radiation pattern which has its main beam in the direction θ. In waveguide terminology the rate of radiation is a maximum at the cut-off frequency ($\phi=\theta=0$) and diminishes to a very small value when $\theta=90°$. (A literal interpretation of this model shows that the rate of radiation is zero when $\theta=90°$, and for all ϕ greater than the value which gives $\theta=90°$. This result is incorrect because the actual field is not exactly the same as the unperturbed waveguide field.)

Polarization Properties

In a conventional slot antenna the electric field in the slot is transverse to the length because such slots are usually too narrow to support any other field configuration. If the slot is half a wavelength or more wide, this restriction disappears and it is possible to set up an arbitrary polarization in the slot.

When energy radiates from a slot (or hole of any shape) in some metal surface, the radiation field is the same as would be obtained if the slot were covered with metal and an array of magnetic currents K set up in place of the slot, where

$$K = E \times n. \tag{1}$$

E is the electric field of the slot and n is a unit outward vector normal to the metal surface. (This follows from Schelkunoff's equivalence principle.) When the metal surface is an infinite plane, the field is the same as the field of an array of magnetic currents $2K$ radiating in free space.

To illustrate this point let a set of axes be chosen as in Fig. 5. The x-axis is normal to the plane, and the z-axis is parallel to the length of the slot. Then the distribution of magnetic currents can be divided into currents flowing parallel to the z-axis, which are determined from E_y in the slot, and currents flowing parallel to the y-axis, which arise from E_z.

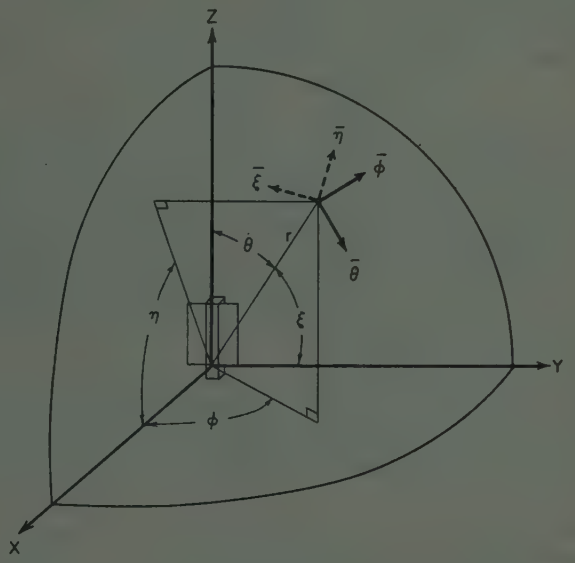

Fig. 5—A co-ordinate system showing the direction of the unit vectors, θ, ϕ, and ξ, η. The ground plane of the antenna is located in the yz-plane.

The electric field radiated by an individual magnetic current element lies parallel to the circles of latitude about the axis of the current element. Thus in the spherical co-ordinates (r, θ, ϕ) (Fig. 5), a magnetic current element K_z flowing parallel to the z-axis radiates an electric field which has an E_ϕ component only. Similarly, a magnetic current element K_y radiates an electric field which has an E_η component only, where spherical co-ordinates (r, ξ, η) are defined in Fig. 5 also.

If a receiving dipole is oriented to pick up E_θ, the signal it receives must be due to only those magnetic currents which flow parallel to the y-axis. A measurement of the E_θ radiation pattern over a complete hemisphere, therefore, gives all the information about E_z in the slot required to predict the radiation field. In the same way a measurement of the E_ξ radiation pattern can be analyzed to give the E_y distribution in the slot. The strength of E_y in the slot, relative to E_z in the slot, is given by polarization measurements in the radiation field as explained below.

When the field configuration in the slot is traveling at a constant phase velocity, the analysis of these measurements is straightforward. In this way it is possible to determine tangential E in the slot without having to set up probing apparatus in the slot (which is difficult to arrange without upsetting the field to be measured).

Assume that the tangential electric field in the slot can be represented approximately by

$$E_x = A \cos \frac{\pi y}{W} e^{-\gamma z}, \tag{2}$$

$$E_y = C \sin \frac{\pi y}{W} e^{-\gamma z}. \tag{3}$$

Then it can be shown that[11]

$$\frac{C}{A} = j \frac{\lambda}{2W} \left[\frac{E_\phi / E_\theta}{\tan \phi} + \cos \theta \right], \tag{4}$$

where θ and ϕ are the co-ordinates of the point of observation and E_ϕ/E_θ is the relative magnitude and phase of the conventional far field components. The complex number E_ϕ/E_θ is obtained from the measured polarization "dumbbell." (A convenient method is described in an I.R.E. article on transmission between elliptically polarized antennas.[12])

From such polarization measurements it has been found that there are four typical field configurations associated with traveling-wave slot antennas which are excited by a uniform waveguide whose axis is parallel to the length of the slot. These are: (*a*) the conventional transverse electric (no tangential E parallel to slot length);[13] (*b*) transverse magnetic (no tangential H parallel to slot length); (*c*) a hybrid with a negligible E_y component; and (*d*) a hybrid with a negligible H_x component.

Any of these configurations can be excited by proper positioning of a long slot in the wall of a uniform waveguide of rectangular cross section. To obtain the transverse electric excitation a narrow slot must be placed where the current in the wall of the waveguide is perpendicular to the slot. The transverse magnetic excitation is obtained from an air-filled waveguide having a wide slot (about $\lambda/2$) positioned so that the current flow is parallel to the slot length. The hybrid excitation (*c*) is obtained under the same conditions as the TM excitation, except that the waveguide is filled with dielectric having a dielectric constant of 2.0 or greater. The hybrid excitation (*d*) is obtained from a waveguide partly filled with dielectric (such as paraffin) which is excited in the lowest order (hybrid) waveguide mode.

The polarization patterns show that the far field is essentially linearly polarized for $0.4 \leqq W/\lambda \leqq 0.9$, $1 \leqq \epsilon_r \leqq 2.5$ and $0.4 \leqq \lambda/\lambda_g \leqq 1.0$. In some instances slight elliptical polarization was observed. This, however, was attributed to the presence of another wave, relatively small in magnitude, traveling at a velocity close to the dominant wave. The spurious wave was presumably caused by imperfections in the antenna model used for the experiment.

The Propagation Constant

If the field in the slot consists of a traveling wave, the performance of the antenna can be represented by a propagation constant $\gamma = \alpha + j\beta_z$, where α and β_z are real. The problem is then essentially two dimensional in exactly the same sense that a conventional waveguide problem is two dimensional. If the region in which the field exists is homogeneous, the transverse propagation constant κ (which is related to the "free space" propagation constant β and to γ by $\kappa^2 = \beta^2 + \gamma^2$) is independent of frequency, and is determined uniquely by the shape of the boundary. Thus for the cross section of Fig. 3, κ is a function of the dimensions W and D. From dimensional analysis the relation can be written in terms of two dimensionless products, as

$$\kappa W = f\left(\frac{W}{D}\right). \tag{5}$$

This kind of relation is an identifying property of traveling-wave fields and can be used as a check on experimental results. The validity of this assumption has been tested by probing the field variation along the length of the slot and by measurement of the radiation pattern. It has been found that the representation by means of a single propagation constant is valid for phase velocities greater than the velocity of light.

Exploration of the field along the axis of the waveguide gives values of the attenuation constant α with good accuracy except for very small values of α. The radiation pattern from a finite length of slot usually consists of two well-defined beams corresponding to the outgoing and reflected traveling waves, as illustrated by Fig. 6. The angle between these beams gives the phase constant β_z, and the ratio of their amplitudes gives the attenuation constant α, with good accuracy provided α is not too large.

Combining these techniques we have obtained experimental curves for β_z and α which have an estimated accuracy of about 5 per cent. The results are shown in Figs. 7–14. β_z is related to the velocity ratio c/v by

$$\beta_z = \frac{2\pi}{\lambda} \frac{c}{v},$$

where c/v is the ratio of the velocity of propagation in

[11] Final Engineering Report 400-11, Antenna Laboratory, The Ohio State University Research Foundation; prepared under Contract AF 33(038)-9236, with Wright Air Development Center, Wright-Patterson Air Force Base, Dayton, Ohio; December 15, 1951.

[12] V. H. Rumsey, "Transmission between elliptically polarized antennas," Proc. I.R.E., vol. 39, pp. 535–540; May, 1951.

[13] The relation for C/A does not apply to the TE configuration. In this case the slot field can be expressed as $E_y = Be^{-\gamma z}$, where B is a constant.

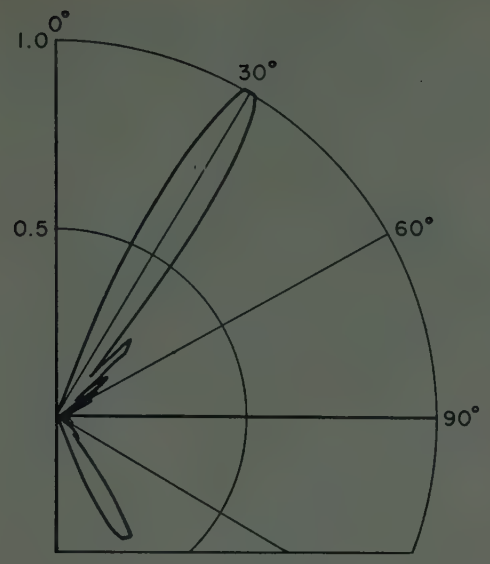

Fig. 6—Measured radiation pattern of a TE traveling-wave slot antenna.

free space to the phase velocity along the slot. Some comparisons with theoretical results[14,15] are given.

Pattern Control

Ideally, the pattern of a traveling-wave line source (along the z-axis) is obtained from source distribution function, $e^{-\gamma z}$, multiplied by a sinusoidal factor which depends on the polarization of the source. This idealized pattern is a satisfactory approximation for practical traveling-wave slots, provided the slot is relatively narrow and an absorber is placed at the end of the slot to absorb the reflected wave. However, there are some patterns which look like the superposition of the idealized pattern and the pattern due to point sources at the ends of the slot. It has been found experimentally that this effect, when it occurs, can be greatly improved for air-filled slots by tapering the slot at the ends. The "discontinuity effect" appears to be rather unpredictable; sometimes it is insignificant in cases where on the basis of the geometrical discontinuity, one might expect it to be strongest. The indications are that it can be minimized by feeding the slot so that the mode in the feed section is as close as possible to the field configuration in the vicinity of the radiating portion.

In practice the kind of pattern control required is, for example, an approximation to a "cosecant squared" or a pattern with good directivity and low side lobes. Such patterns can be obtained to a good approximation from traveling-wave line sources if the amplitude of source strength varies with distance along the line source in the appropriate manner. For instance, an exponential variation of amplitude gives a good approximation to a "cosecant square" pattern,[16,17] and a symmetrical Gaussian (e^{-z^2}) distribution of amplitude gives good side lobe suppression.[18,19]

A traveling-wave slot antenna can be designed to give a desired amplitude distribution by using a slot whose width W varies with distance z along the slot. This implies that both α and β_z are functions of z, but the variation of the phase constant β_z can be made insignificant compared with the variation of α. See Figs. 7–14.

The radiation pattern is due to an array of sources where the strength of an individual source is proportional to the current moment M of the equivalent dipole. In order to produce a desired pattern the first step is to determine the distribution of M which gives the best approximation to the pattern, subject to the restriction that the phase variation of M is that of a traveling wave. The next step is to determine how the attenuation parameter α must vary in order to produce the desired amplitude distribution of M.

The power radiated from a source of given current moment M is proportional to M^2 if the source is radiating by itself. In the actual problem a given source radiates in the presence of the rest. Consequently, the power radiated from a given source is proportional to M^2 provided that the variation of source strength with position is gradual, and that contributions to the field at the source from distant sources is insignificant. These restrictions appear to be approximated in practice except for the case when the phase velocity equals c where the latter condition would not be justifiable, *a priori*. Under conditions where these two provisions are satisfied it is possible to write

$$\frac{dP}{dz} \sim A^2,$$

where P is the power flowing down the guide in the z-direction, and A represents the amplitude distribution of current moment. Therefore,

$$2\alpha = -\frac{1}{P}\frac{dP}{dz} = -\frac{A^2}{\int A^2 dz}. \qquad (6)$$

[14] R. F. Harrington, "Propagation along a slotted cylinder," *Jour. Appl. Phys.*, vol. 24, pp. 1366–1371; Nov., 1953.

[15] V. H. Rumsey, "Theory of traveling-wave slot antennas," vol. 24, pp. 1358–1365; Nov., 1953.

[16] Interim Engineering Reports 301-14, Section 4; February 1, 1949, and 301-19, Section 8; October 1, 1949, Antenna Laboratory, The Ohio State University Research Foundation; prepared under Contract W 33-038 ac 16520 (17380) with Wright Air Development Center, Wright-Patterson Air Force Base, Dayton, Ohio.

[17] A. S. Dunbar, "Uniform Progressive Phase Antennas Having Asymmetric Amplitude Distributions," Technical Report No. 13, Stanford Research Institute; prepared under Contract No. AF 19(122)78; September, 1950.

[18] Interim Engineering Report 301–15, Section 4, Antenna Laboratory, The Ohio State University Research Foundation, prepared under Contract W 33-038 ac 16520 (17380) with Wright Air Development Center, Wright-Patterson Air Force Base, Dayton, Ohio; May 1, 1949.

[19] Interim Engineering Report 301-16, Section 4, Antenna Laboratory, The Ohio State University Research Foundation; prepared under Contract W 33-038 ac 16520 (17380) with Wright Air Development Center, Wright-Patterson Air Force Base, Dayton, Ohio; August 1, 1949.

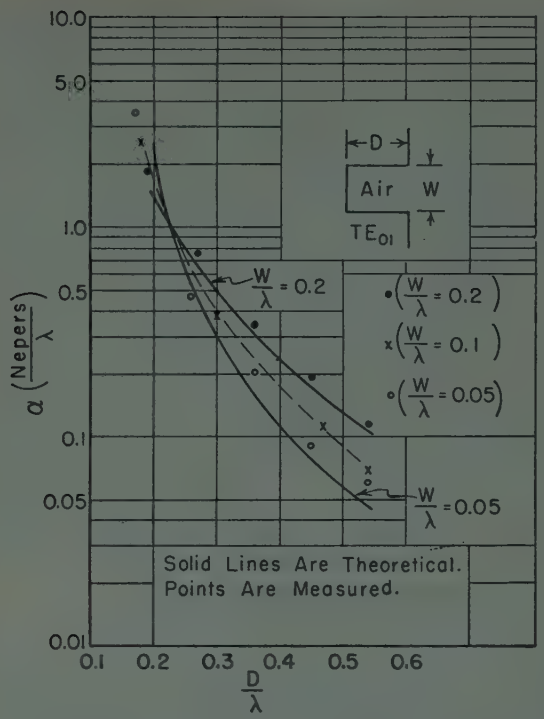

Fig. 7—Attenuation constants of an air-filled TE traveling-wave slot antenna.

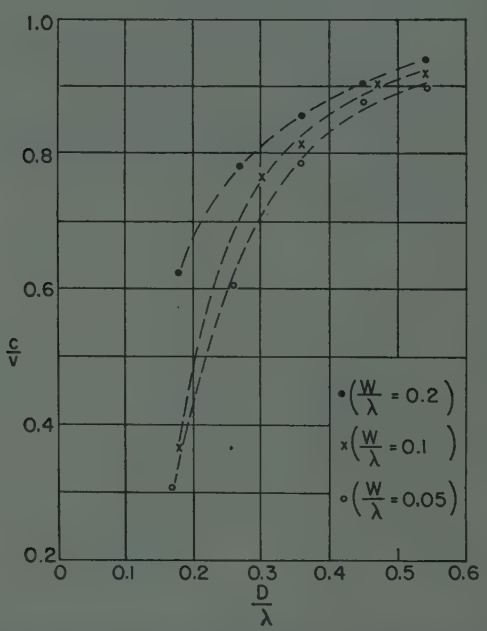

Fig. 8—Measured velocity ratios, c/v, of an air-filled TE traveling-wave slot antenna.

Given the amplitude distribution A, (6) determines α as a function of z, but it does not give $\alpha(z)$ uniquely because the limits on the integral are unspecified. If the slot extends from $z=0$ to $z=L$, the input power, $P(0)$, is related to the power left over, $P(L)$, by

$$P(0) - P(L) \sim \int_0^L A^2 dz. \tag{7}$$

Then (6) can be expressed in the form

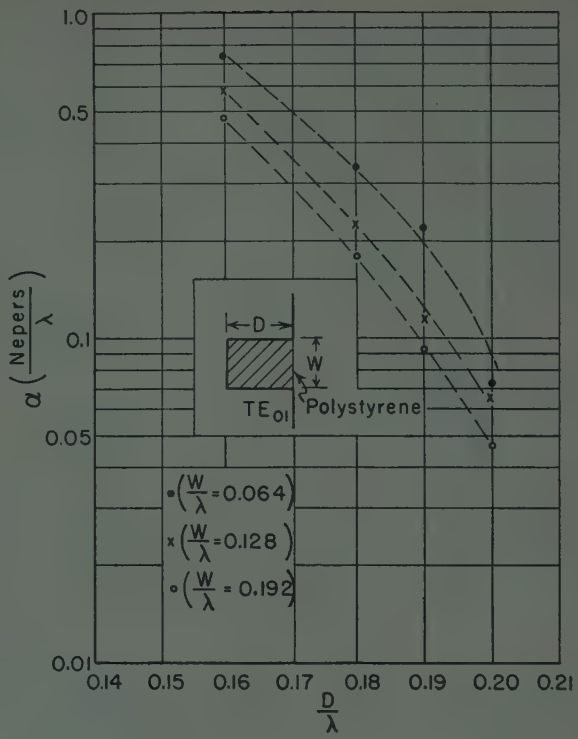

Fig. 9—Measured attenuation constants of a polystyrene-filled TE traveling-wave slot antenna.

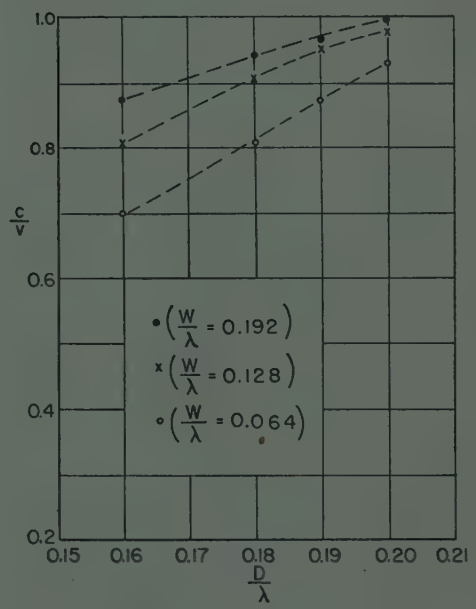

Fig. 10—Measured velocity ratios, c/v, of a polystyrene-filled TE traveling-wave slot antenna.

$$2\alpha(z) = \frac{A^2}{\int_0^L A^2 dz + \dfrac{P(L)}{P(0) - P(L)} \int_0^L A^2 dz}. \tag{8}$$

Equation (8) shows that $\alpha(z)$ is determined not only by the amplitude distribution A, but also by the fraction of incident power which is radiated. If practically all of the power is radiated, α rises to a very high value

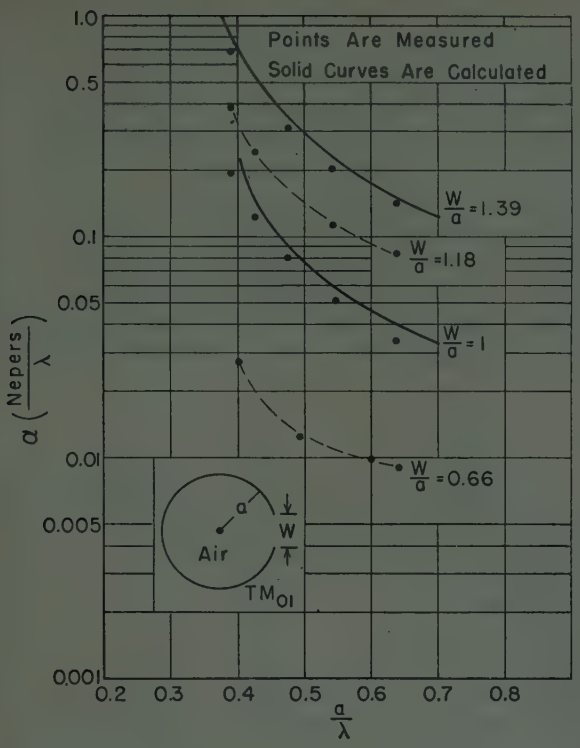

Fig. 11—Attenuation constants of an air-filled TM_{01} excited traveling-wave slot antenna of circular cross section.

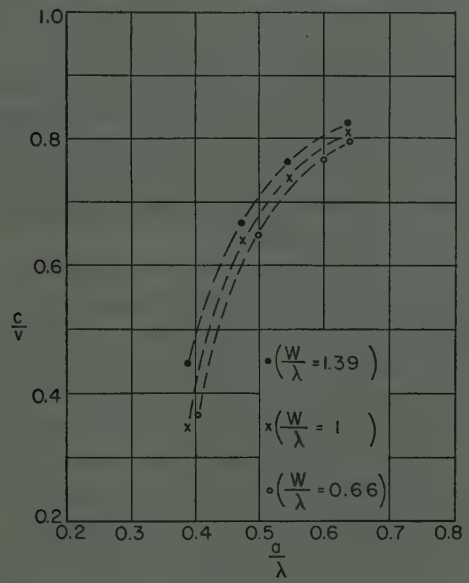

Fig. 12—Measured velocity ratios, c/v, of an air-filled TM_{01} excited traveling-wave slot antenna of circular cross section.

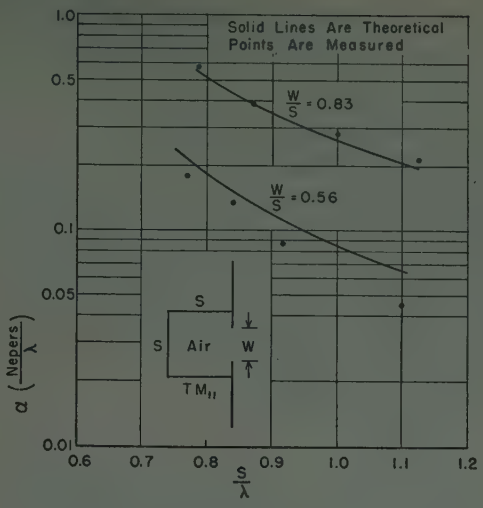

Fig. 13—Attenuation constants of an air-filled TM traveling-wave slot antenna of square cross section with TM_{11} excitation.

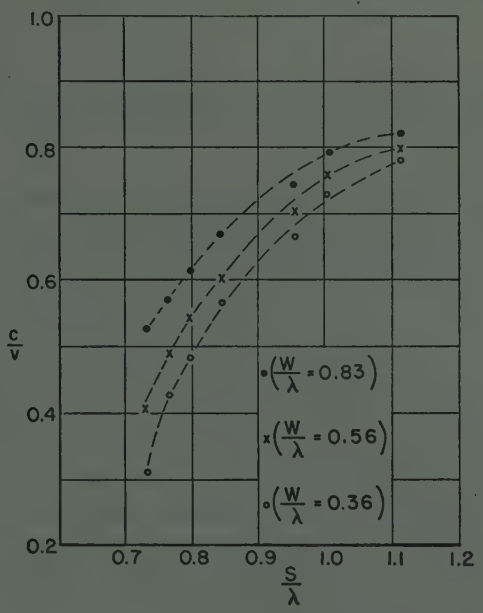

Fig. 14—Measured velocity ratios, c/v, of an air-filled TM traveling-wave slot antenna of square cross section with TM_{11} excitation.

near the end, $z=L$. In practice one would set the radiated power one or two decibels down from the incident power and then apply (8) to determine $\alpha(z)$.

Pattern control for TM or hybrid slots is usually simpler than for TE slots because the variation of W required for a given variation of α is much smaller for TM or hybrid operation than for TE operation. Despite this, excellent control can be obtained even with TE excitation. A Gaussian distribution was approximated without excessive phase change by placing an iris of variable width W over a TE-excited guide Fig. 15.

Good side-lobe suppression was obtained over 2:1 frequency range, the side lobes being insignificant over a substantial part of the range.[18] Typical radiation patterns are shown in Fig. 16.

The attenuation α can be alternatively controlled by means of a horn fitted onto the slot so that the horn acts as a transformer between the slot aperture and free space. In this way successful side-lobe suppression can be obtained by varying the length of horn to produce the desired amplitude distribution.[20]

[20] Interim Engineering Report 301-19, Section 8, Antenna Laboratory, The Ohio State University Research Foundation; prepared under Contract W 33-038 ac 16520 (17380) with Wright Air Development Center, Wright-Patterson Air Force Base, Dayton, Ohio; October 1, 1949.

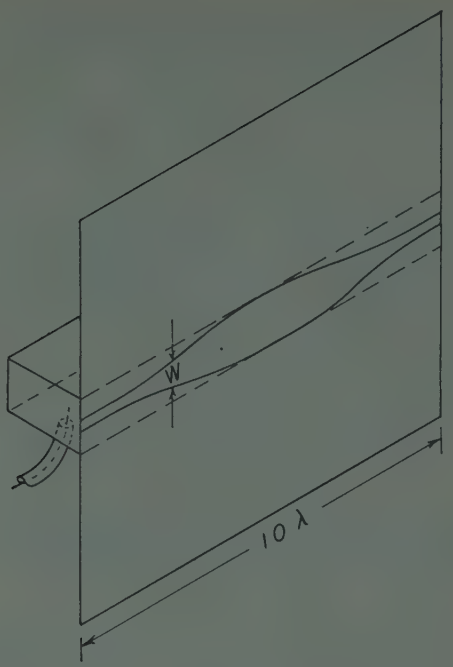

Fig. 15—Sketch of a TE traveling-wave slot antenna showing the iris used to obtain a Gaussian amplitude distribution.

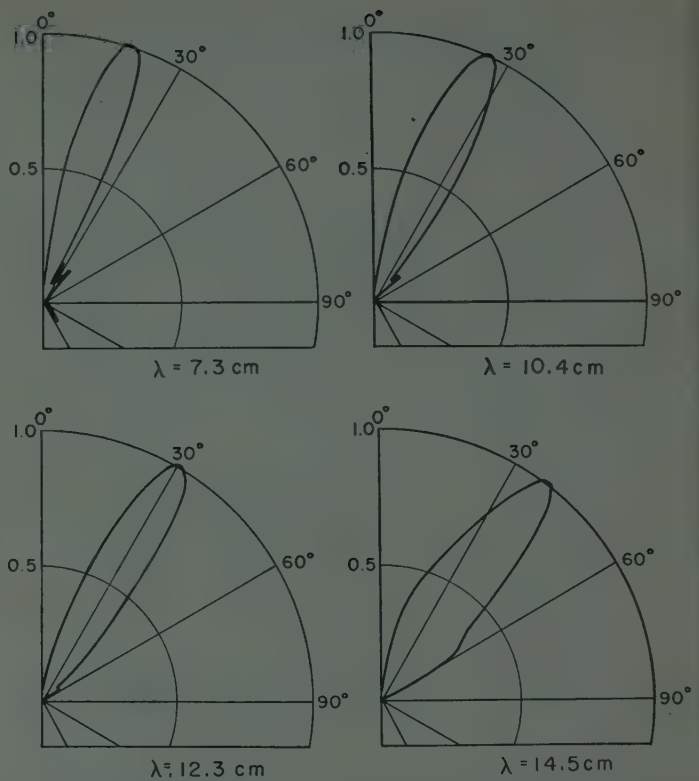

Fig. 16—Measured radiation patterns of a TE traveling-wave slot with an amplitude distribution approximately that of a Gaussian error curve.

Arrays of Traveling-Wave Slots

The problem of designing a flush-mounted directional antenna to fit in a given area is a typical application for a traveling-wave slot array. The conventional array problem is to design a suitable element (or primary radiator) of the array and then to design a feed system for energizing an appropriate array of these elements to give the desired pattern. The pattern of the array is obtained by superimposing the individual radiation fields of the elements of the array. In the familiar case of an array of half-wave dipoles it happens that the individual radiation field of a dipole (called the primary pattern for simplicity) is practically the same whether the dipole radiates in free space or in the presence of the other dipoles, provided they are open-circuited. The preoccupation with arrays of half-wave dipoles has made this fact so familiar that one is apt to assume (erroneously) that the primary pattern is, in general, the pattern of an element of the array radiating by itself.

In order to apply the principle of superposition correctly the first step is to choose the location of the "input terminals" of each element of the array. For this purpose "input terminals" can be defined as some accessible point in the feed system where the field consists of a single mode. Then the primary pattern F_i of an individual radiator can be defined as the field due to unit input current to its terminals in the presence of all the other radiators when their input terminals are open-circuited. Then the pattern of the array, when the input currents are $I_1, I_2, \cdots$, is given by $\sum_i I_i F_i$.

Alternatively, the primary pattern G_i may be defined as the field due to unit input voltage to the i^{th} radiator when the others are short-circuited, in which case the array pattern due to input voltages $V_1, V_2, \cdots$ is given by $\sum_i V_i G_i$. Note that the "primary pattern" F_i or G_i may be interpreted as a vector, having components E_θ and E_ϕ, where E_θ and E_ϕ are themselves represented by complex numbers representing the radiated signal in phase and amplitude relative to the input signal I_i in the case of F_i or V_i in the case of G_i.

Having determined the primary patterns F_i (or G_i), the problem is to find the distribution of I_i (or V_i) which gives the best approximation to the desired pattern. This problem is greatly simplified if the mutual impedance between radiators (with respect to the chosen set of input terminals) is insignificant. Then the problem of designing the feed system reduces to the problem of feeding a known set of loads with specified currents or voltages.

This technique of array design is much more involved than the conventional method but it is absolutely accurate, and it has been found from experience on traveling-wave slot arrays designed for low side lobes, that the conventional technique is inadequate.

The mutual impedance between traveling-wave slot antennas may be analyzed by picturing the traveling-wave slot as a directional coupler. When two such slots are placed along parallel lines, the field induced in one due to energization of the other will consist primarily of a wave traveling in the same direction as the wave in the slot which is energized directly. This wave will be reflected at the end of the parasitic slot and will travel back to its input terminals. However, it is attenuated by ra-

diation as it travels along the slot so that the amount available at the input terminals of the parasitic slot is very small. If the slots are long enough to be good directional antennas, the coupling between adjacent input terminals is very small. In practice it has proved to be negligible.

The magnitude of the mutual impedance is quite different for the TE, TM, or hybrid slots. For example the equivalent magnetic dipoles associated with parallel slots are broadside-to-broadside for TE operation, whereas they are end-to-end for the hybrid operation (*c*) (no transverse *E*). Consequently the mutual impedance effects associated with hybrid operation (*c*) are much less than with TE operation.

Acknowledgment

This work was performed under Contract AF 33(038)-9236 between Wright-Patterson Air Force Base and The Ohio State University Research Foundation. It is a pleasure to acknowledge the help given by R. W. Masters, O. Click, R. Krausz, B. J. Stephenson and other members of the Ohio State University Antenna Laboratory Staff.

Prediction of Traveling Wave Magnetron Frequency Characteristics: Frequency Pushing and Voltage Tuning*

H. W. WELCH, Jr.†, SENIOR MEMBER, IRE

Summary—**An approximate method has been developed for determining the shape and density of the spokes of electronic space charge when large RF potentials exist in the magnetron. With the estimation of space-charge configuration which this method makes possible, induced current theory and knowledge of the magnetron electrode geometry and external circuit can be applied to the calculation of frequency characteristics. These characteristics relate frequency to operating anode potential and anode current and are defined as frequency pushing or voltage tuning characteristics. Relatively simple equations for these characteristics are presented. Calculated characteristics for typical values of the variables of magnetron design are presented. The correspondence of the results of the theory with experimental data is discussed very briefly.**

Introduction

THIS PAPER PRESENTS an analysis which leads to the understanding of two cw magnetron characteristics which are important in the use of magnetrons for radio communication; namely, frequency pushing and voltage tuning. These terms require definition and part of the purpose of the following discussion will be to provide a basis for explicit definition. Definitions acceptable to those who are well acquainted with cw magnetron behavior are the following:

Frequency pushing is defined as the variation of the frequency which is generated by an oscillating magnetron and which is associated with the change in dc anode current as the anode voltage is raised with the resonator temperature held constant. A *frequency-pushing characteristic* would therefore be a plot of generated frequency versus dc anode current for the conditions mentioned. Actually, to be complete, a three-dimensional plot including anode voltage, current and frequency, should be used.

A typical frequency-pushing characteristic is shown in Fig. 1a.

Voltage tuning is defined as the variation in frequency which is generated by an oscillating magnetron and which is associated with the change in dc anode voltage when dc anode current, load impedance, magnetic field, and resonator temperature are held constant. In order for dc anode current to be held constant, the cathode emission must be limited in some way, such as by operation at a reduced temperature. Otherwise, an increase in anode voltage will increase the anode current. A voltage-tuning characteristic is therefore a plot of generated frequency versus anode voltage for the conditions mentioned.

A typical voltage-tuning characteristic is shown in Fig. 1b.

Examination of a number of typical sets of data on cw magnetrons shows that, in normal operation (when frequency pushing is observed), the frequency is relatively insensitive to the voltage change which is required to increase anode current compared to the large frequency shifts obtained under the conditions required for voltage-tuning operation. For example, in the figures shown, a change of 100 volts produces a frequency pushing of 10 megacycles, while a change of 12.2 volts produces a voltage tuning of the same amount. Typical voltage tuning characteristics show a change of from 0.1 to 2 megacycles per volt.

* Decimal classification: R355.912.1×R139. Original manuscript received by the Institute, February 2, 1953; revised manuscript received, June 8, 1953. (This paper is based on work done for the Signal Corps, U. S. Army, Contract No. DA-36-039 sc-5423. It is a condensed part of a thesis submitted by the author in partial fulfillment of the requirements for the Ph.D. degree at the University of Michigan. "Dynamic frequency characteristics of the magnetron space charge; frequency pushing and voltage tuning," also issued as *Tech. Report* No. 12, Electron Tube Lab., Dept. Elec. Eng., University of Michigan; November, 1951.

† University of Michigan, Ann Arbor, Mich.

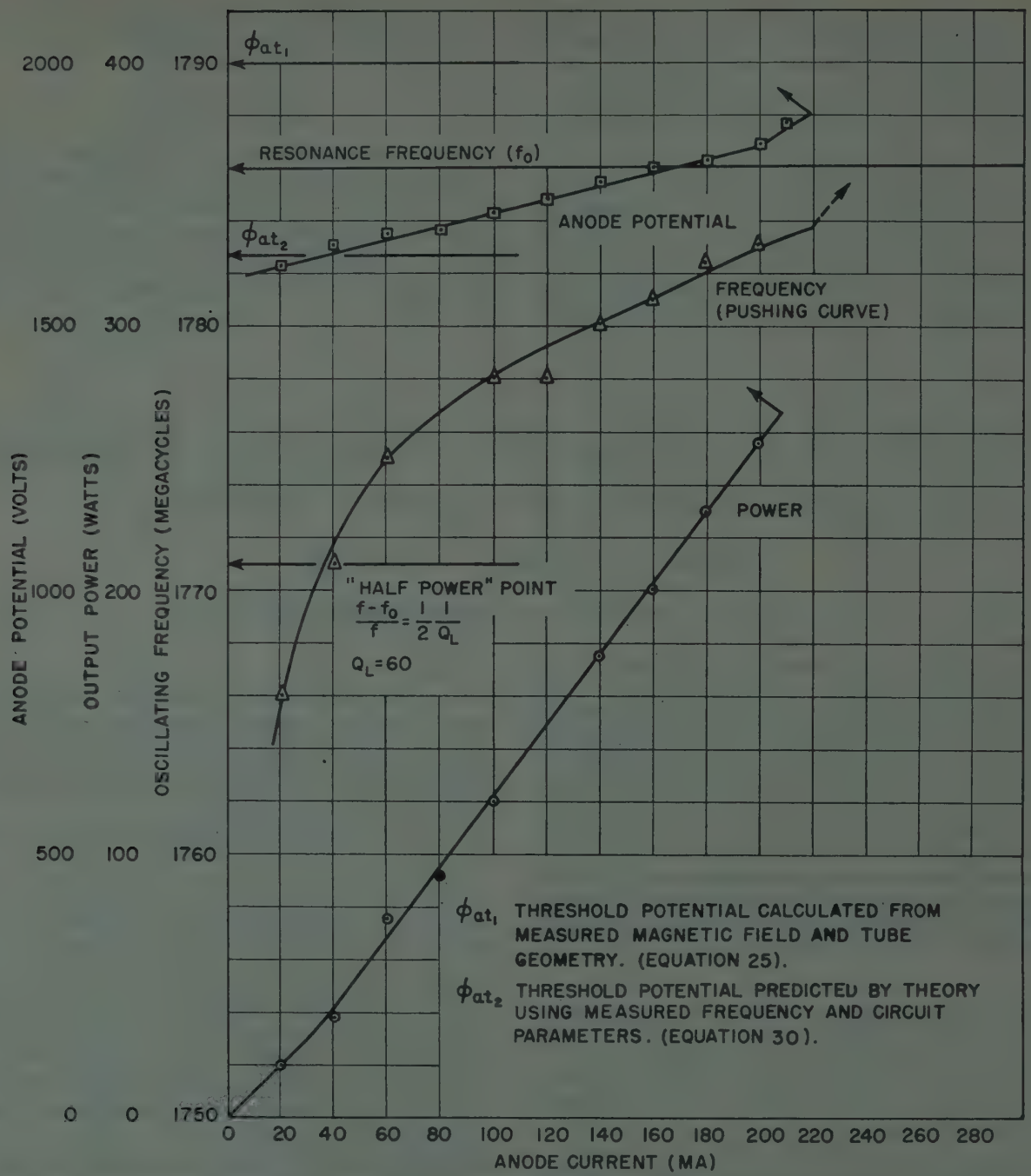

Fig. 1(a)—Experimental pushing characteristics on magnetron constructed at the University of Michigan. (model 3, no. 8) B = 1820 gauss.

Since frequency pushing is obtained coincident with amplitude modulation, there seems to be little possibility of use in the conventional FM communication system. There is, however, a possibility of minimizing it for use in AM systems and the possibility of development of new types of systems in which it would be usable.

In Fig. 2 the spectra resulting from plate modulation of an S band magnetron (Raytheon QK59) are shown. In Fig. 2a, 2 megacycle modulation frequency is used. It is observed that the resulting spectra appear as conventional FM spectra but one sided because of the amplitude modulation associated with the frequency pushing. A constant modulation voltage was applied; modulation frequency was varied. Note that the spectrum width remains substantially constant, independent of modulating frequency.

The present major objectives in studies of voltage tuning are for more power output, higher frequencies, and less noise in the voltage-tunable signal. Tubes operable at low power levels (of the order of milliwatts) and very wide tuning ranges have application as local oscillators in search receivers, spectrum analyzers and signal generators. For higher power levels (of the order of hundreds of watts), and relatively narrow tuning range, they have application as the transmitter tube in frequency-modulation systems. At the present time the

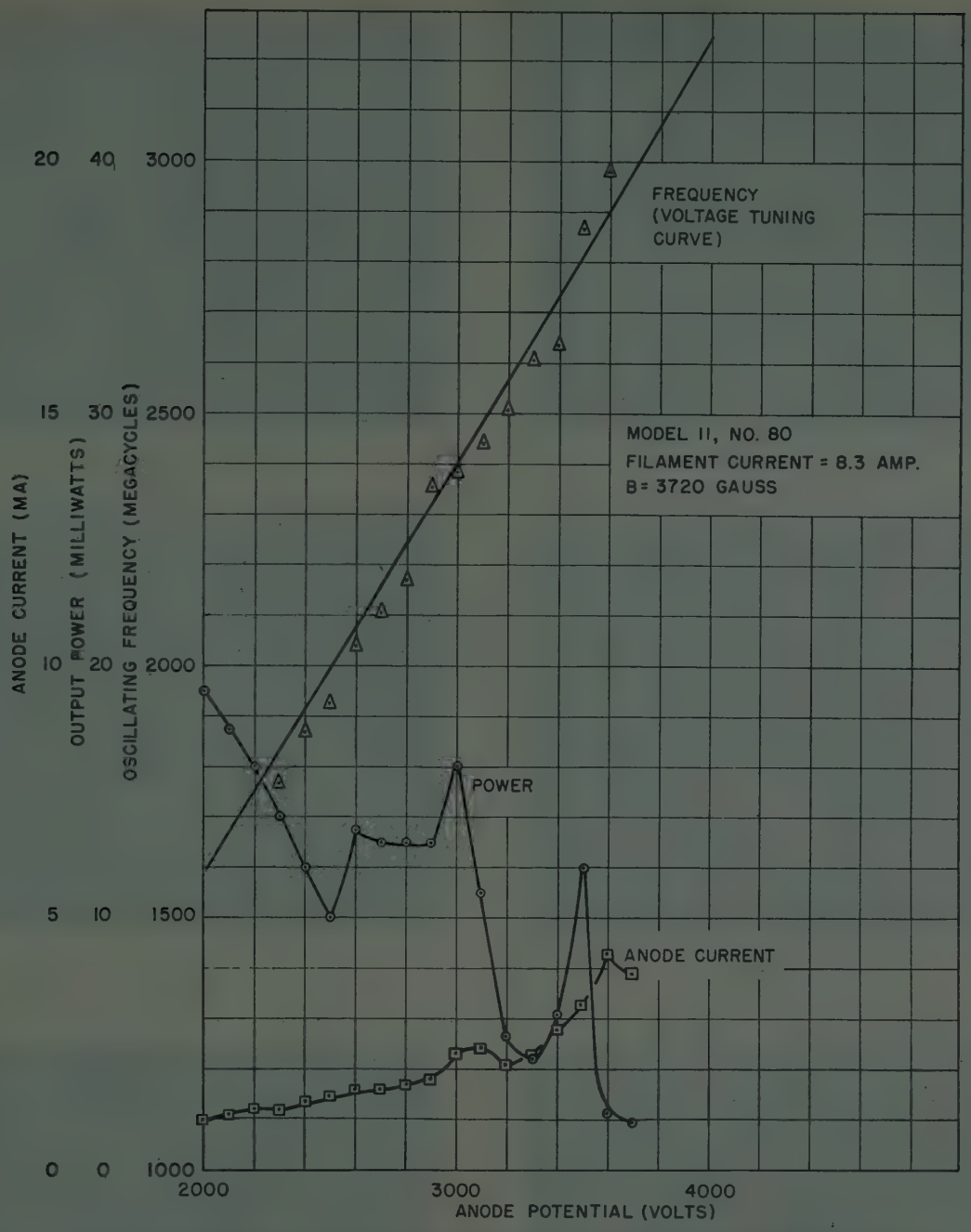

Fig. 1(b)—Typical voltage tuning characteristics on magnetron constructed at the University of Michigan. (Courtesy of J. A. Boyd.)

ow-power level tube development is reasonably successful.[1]

Heretofore published treatments have demonstrated that phase-focusing of the electrons favorable to energy transfer from the electrons to the circuit will occur in the magnetron.[2] This has resulted in the well-known concept of spokes in the magnetron space charge (Fig. 3).

[1] Messrs. Boyd and Needle, Electron Tube Lab., Dept. Elec. Eng., University of Michigan, have promising results in the 1000–4000 mc range. (See J. S. Needle, "The insertion magnetron," *Tech. Report* No. 11, Doctoral thesis; and J. A. Boyd, Doctoral thesis in preparation to be issued as *Tech. Report* No. 15.)

Wilbur and Peters, General Elec. Co., are working with tubes for application below 1000 mc.

[2] K. Posthumus, "Oscillations in a split-anode magnetron, mechanism of generation," *Wireless Eng.*, vol. 12, pp. 126–132; 1935.

L. R. Walker, "The interaction of the electrons and the electromagnetic field," G. B. Collins, Editor, "Microwave Magnetrons," McGraw-Hill Book Co., New York, N. Y. chap 6; 1948. (*M.I.T. Radiation Lab. Series*, vol. 6, pp. 253–288.)

F. Lüdi, "Zur Theorie Des Magnetfeldgenerators für Mikrowellen," *Helv. Phys. Acta*, vol. 19, pp. 3–20; 1946.

O. Doehler, "Les oscillations de résonance dans le tube à champ magnétique constant," *Ann. Radioélect.*, vol. 3, pp. 169–183; July, 1948.

J. G. Fisk, H. D. Hagstrum and P. L. Hartman, "The magnetron as a generator of centimeter waves," *Bell Sys. Tech. Jour.*, vol. 25; April, 1946.

W. E. Willshaw, L. Rushforth, A. G. Stainsby, R. Latham, A. W. Balls and A. H. King—"The high power pulsed magnetron; development and design for radar applications," *Jour. IEE (London)*, vol. 93, pp. 985–1005; 1946.—"Discussion," vol. 95, pp. 130–134; May, 1948.

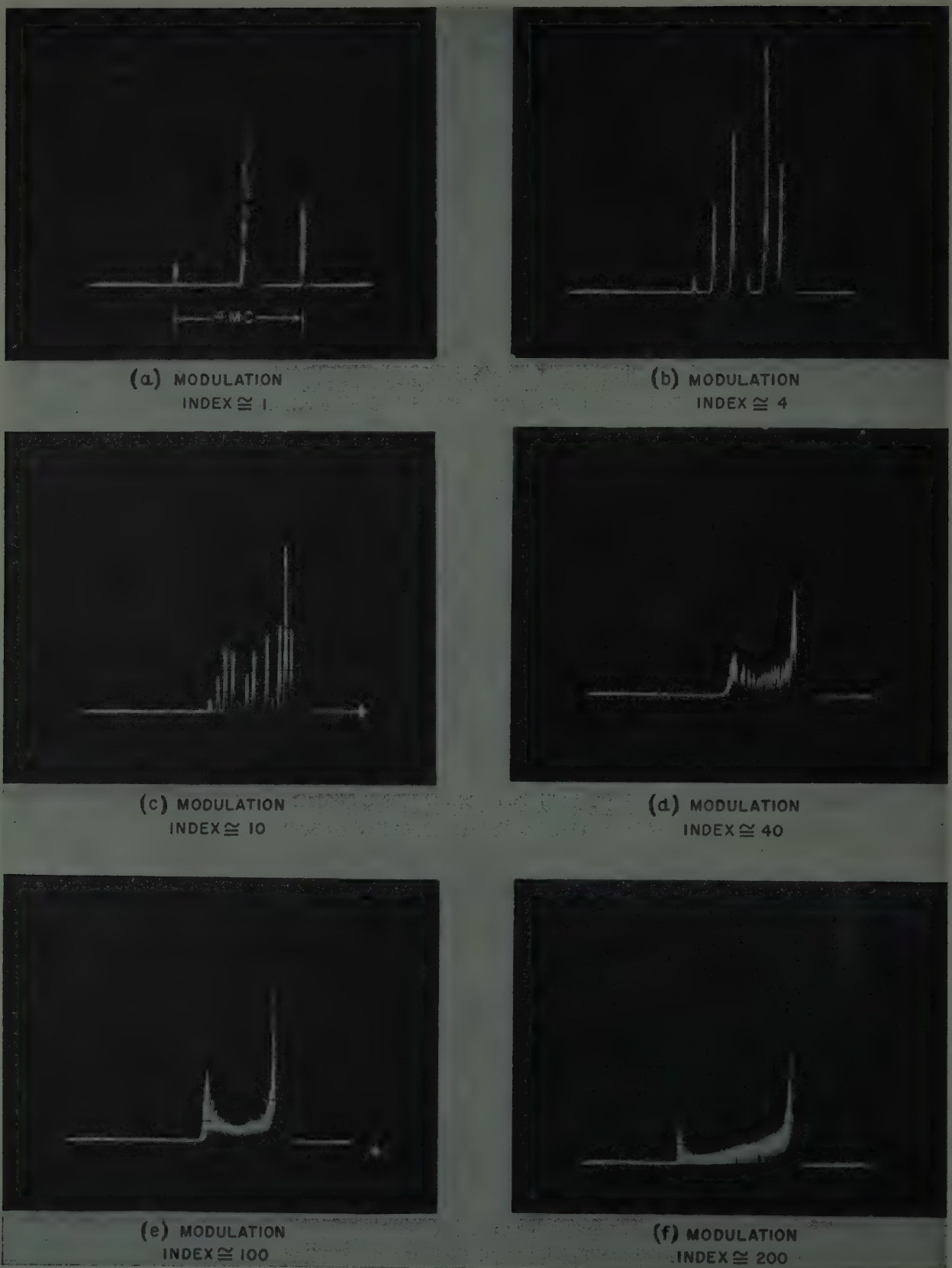
2 MC
(a) MODULATION INDEX ≅ 1
(b) MODULATION INDEX ≅ 4
(c) MODULATION INDEX ≅ 10
(d) MODULATION INDEX ≅ 40
(e) MODULATION INDEX ≅ 100
(f) MODULATION INDEX ≅ 200

Fig. 2—Response of the spectrum analyzer to sine wave modulation of the QK59 magnetron for various values of the modulation index. $Q_L \cong 200$.

The present analysis will have, as shown, the following new results:

a. A method for calculating the approximate phase position of the spokes of space charge relative to the radio frequency potential maximum in a traveling reference frame;

b. An estimate of the space charge density in the spokes;

c. Application of induced current theory, making use of the first two results, to compute the current induced in external circuit of the magnetron;

d. Demonstration that frequency pushing can be explained by a change in phase position of the spokes;

e. Theoretical explanation of voltage tuning.

The subject matter divides conveniently into two independent parts: the large-signal theory of phase-focusing describing the action of the electric and magnetic fields on the electrons in the magnetron interaction space when a large RF potential is superimposed upon the static anode potential; and the calculation of the current and RF potential induced in the external circuit. By combination of the two results, the relationships between power, frequency and anode voltage are derivable. The predicted characteristics compare favorably with experimental results.

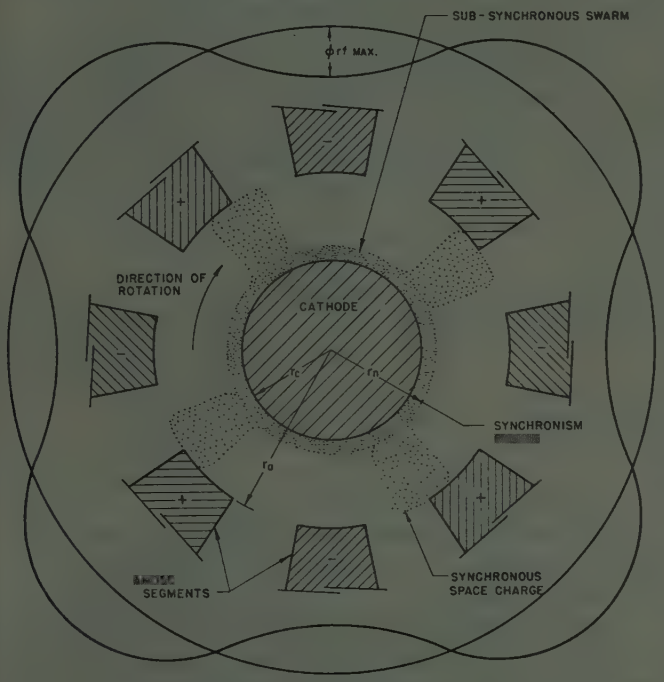

Fig. 3—Basic physical picture of the magnetron space charge with large signal RF potential on the anode.

The approximate phase position of the spoke relative to the traveling RF potential wave can be derived from the basic assumptions leading to the well-known Hartree equation for the threshold potential. The result is expressed in terms of the actual anode potential, the RF potential between anode segments and the threshold potential. The threshold potential is conventionally considered to be the approximate anode potential which will support oscillations of infinitesimal amplitude. In the following discussion it will be given a broader meaning which includes this definition. The basic assumptions which support this concept will be discussed briefly since they are important to the understanding of phase focusing. Algebraic details are omitted in the interest of conserving space. (See standard sources in literature on magnetrons for derivation, which arrive at the same answer with differences in method only.)

In addition to the threshold potential, understanding of the phase-focusing action depends upon the concepts of synchronism and conditions favorable to a drift of electrons through the spokes toward the anode. These will be discussed in the next two sections. Once the phase position of the spoke is approximately established, the approximate phase angle of the current induced in the external circuit can be calculated, and thus frequency characteristics can be determined.

Synchronous Energy and Synchronism Potential

There are several basic assumptions which are standard and justifiable in the discussion of the magnetron. For a complete discussion and justification of certain of these assumptions the reader is referred to the treatment by Walker in the book on magnetrons of the M.I.T. Radiation Laboratory series.[3]

It will be assumed that the effect of initial velocities of the electrons may be neglected. In normal high power operation this is justifiable on the basis that the mean thermal energy is small compared to the energy obtained by the electrons from the field. However, it is not clearly justified when the effects at extremely low anode currents or the noise problem are under consideration. Electron-electron interaction effects will also be neglected.

The assumption usually made which is not justified in this discussion is that the behavior at the cathode is space-charge limited. Space-charge-limited conditions imply zero gradient at the cathode. Under temperature-limited conditions a gradient will exist at the cathode and consequently the electron behavior in the interaction space must be entirely different for the same boundary conditions at the anode. In order to compare the two cases approximately the space-charge-limited behavior of the electron will be compared to the space-charge-free behavior. The procedure of neglecting, in analysis, temperature-limited operation in favor of space-charge-limited operation is more based on habit than scientific judgment and in many cases should be discarded in the detailed analysis of high frequency power tubes. Experimental evidence in the case of magnetron very forcefully indicates that the conditions at the cathode can completely alter the details of operational behavior.[4]

In this treatment the problem will be approached by, first, presenting relationships for the energy of the electron as a function of position in the interaction space with various assumed boundary conditions and, second, determining the direction of drift motion of the electrons as a function of position. The resulting conditions eliminate certain portions of the volume as inaccessible to electrons. The case of the plane magnetron will be emphasized because it is considerably simpler and a reasonably good approximation to the large cathode magnetron. The co-ordinate arrangement is shown in Fig. 4.

[3] Walker, *loc. cit.*, pp. 209–253; particularly pp. 243–253.

[4] Dr. S. R. Tibbs and F. I. Wright, "Temperature and space-charge-limited emission in magnetrons," *C.V.D. Report*, May, 1938.

The effect of the RF field which exists in between the anode segments in the oscillating magnetron is superimposed on the effect of the dc field. The potential distribution shown in Fig. 3 is usually referred to as the π mode and is so named because of a phase difference between the voltages on adjacent segments of π radians or 180°. This distribution, which is a stationary wave in space, can be represented as the Fourier sum of a number of traveling waves which proceed in opposite directions around the interaction space. The fundamental wave of this sum moves around the cathode with a velocity such that the maximum of the wave proceeds from one anode segment to the next in one-half cycle. For a given frequency, f, and a given number of anodes, $2n$, the time of one-half cycle is $1/2f$, and the angular distance between adjacent anodes is $2\pi/2n$, thus the angular velocity corresponding to the fundamental wave is

$$\omega_n = \frac{2\pi f}{n}. \tag{1}$$

For a plane magnetron the corresponding equation is:

$$v_n = x_n f, \tag{2}$$

where $x_n/2$ is the distance between centers of adjacent anode segments and v_n is the synchronism linear velocity in the X direction.

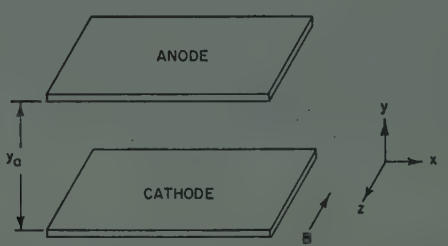

Fig. 4(a)—Co-ordinate arrangement used in the discussion of the plane magnetron.

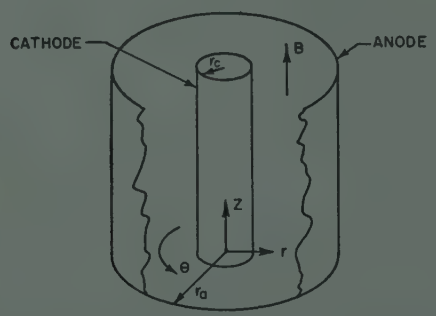

Fig. 4(b)—Co-ordinate arrangement used in the discussion of the cylindrical magnetron. (B = magnetic field.)

In general, the scalar potential in the interaction space of the magnetron is a function of time as well as position. However, electron interaction is predominantly with the fundamental traveling-wave component of potential which moves in the direction of electron drift motion parallel to the cathode surface.[5]

[5] Other modes of interaction will not be considered in this article.

A suitable choice of moving coordinate system will cause the effects of this traveling-potential wave to appear stationary. The effects of other wave components can be neglected in the first approximation since, in the moving system, they are rapidly varying compared to the stationary fundamental, and the total effect of interaction with the electron during transit, therefore, is small in comparison.

Thus with the following definitions:

v_x' = x-component of velocity in planar-moving coordinate system,

v_n = constant velocity of moving-planar-coordinate system in positive x-direction,

ω' = angular velocity in rotating cylindrical coordinate system,

ω_n = constant angular velocity of rotation of cylindrical coordinate system in positive θ-direction,

the component force equations can be written:

$$\frac{d}{dt}\left(\tfrac{1}{2}mv_y^2\right) = e\frac{\partial\phi}{\partial y}\frac{dy}{dt} - Be(v_x' + v_n)\frac{dy}{dt}, \tag{3}$$

$$\frac{dv_x'}{dt} = \frac{e}{m}\frac{\partial\phi}{\partial x} + \frac{Be}{m}\frac{dy}{dt}, \tag{4}$$

in the planar system,[6] and:

$$\frac{d}{dt}\left(\tfrac{1}{2}mv_r^2\right) = e\frac{\partial\phi}{\partial r}\frac{dr}{dt} - \left[Be(\omega' + \omega_n)r - m(\omega' + \omega_n)^2 r\right]\frac{dr}{dt}, \tag{5}$$

$$\frac{d(\omega' + \omega_n)r}{dt} = \frac{e}{m}\frac{\partial\phi}{r\partial\theta} + \left[\frac{Be}{m} - (\omega' + \omega_n)\right]\frac{dr}{dt}, \tag{6}$$

in the cylindrical system.[7]

This particular form for the component force equations is chosen for convenience in application to the following discussion.

The variables v_x' and ω' are still, in general, functions of t. The potential ϕ, however, is stationary. It is only necessary therefore to be able to express v_x' and ω' as functions of x and r, respectively, to make (3) and (5) integrable. Complete calculation of this functional relationship involves computation of trajectories of all electrons, which depend on the phase of emission from the cathode and on the spatial potential distribution. This has been done for special cases by the method of self-consistent field calculations.[8] *The express purpose of the development presented here is to make an estimate of the gross space-charge behavior on the basis of an approximate choice of values for v_x' and ω'.*

It is assumed that the potential wave with which electrons interact moves with a phase velocity characteristic of the magnetron anode structure, given by v_n or ω_n. This phase velocity depends on the frequency and the geometry of the structure. The combined action of crossed electric and magnetic fields in the interaction

[6] B is arbitrarily assumed to be in the negative z-direction.

[7] B is arbitrarily assumed to be in the positive z-direction.

[8] Walker review of Stoner, Tibbs, and Wright work, *op. cit.*, p. 270, Fig. 6.15.

space will bring electrons from zero velocity in the stationary reference frame to zero velocity in the moving reference frame. Such electrons are said to be in "synchronism" with the traveling wave. The relationships between anode potential, magnetic-field intensity, electron swarm extent, and electron energy at the edge of the swarm have been computed for electron velocity just synchronous with the velocity characteristic of the anode structure. All anodes are assumed to be at the same potential so that potential gradients in the X and θ directions are zero. Initial velocities are assumed zero in the stationary reference frame. The results are:

Case I—Planar Magnetron. The velocity of the electron as a function of distance from the cathode is obtained by solution of (4):

$$v_x' + v_n = \frac{Be}{m} y. \tag{7}$$

Thus the tangential electron velocity in stationary coordinates is linearly related to the distance from the cathode. The distance y_n will be defined such that the electron moves with synchronism velocity (v_n) in the stationary reference frame (i.e., $v_x'=0$, the electron is stationary in the moving reference frame).

$$y_n = \frac{m}{e}\frac{v_n}{B}. \tag{8}$$

If the value from (7) is substituted into (3), the energy equation becomes integrable. The result is:

$$e\phi = \tfrac{1}{2}mv_y^2 + \frac{B^2e^2}{2m} y^2. \tag{9}$$

The second term on the right can be written:

$$\tfrac{1}{2}m\left(\frac{Be}{m} y\right) = \tfrac{1}{2}mv_x^2.$$

This shows that (9) is simply a statement of the conservation of energy. If it is assumed that the swarm is bounded between cathode and anode, the y-directed velocity must be zero at the boundary. For electrons to be synchronous at this boundary they must have acquired a certain "synchronism energy" given by:

$$e\phi_n = \tfrac{1}{2}mv_n^2. \tag{10}$$

If the y-directed velocities are zero throughout the swarm of electrons, the potential energy of the electrons will be decreased by:

$$e\phi = \frac{B^2e^2}{2m} y^2, \tag{11}$$

in moving from $y=0$ to y. All of this energy, in this case, will appear as kinetic energy of the electron. This is usually called the "cutoff energy parabola."

If there is an ample supply of electrons at the cathode and initial velocities are neglected, the space charge in the swarm within y_n will build up until the gradient at the cathode is zero. The potential within the swarm may exceed that given by (11) if electrons are streaming inward and outward through the swarm because of the energy of y-directed velocities. At the boundary (11) must give the electron energy since it is assumed that the electrons do not cross the boundary. It has been shown by Slater[9] that for the case of zero electric-field gradient at the cathode the actual potential distribution curve is tangent to the cutoff parabola at the swarm boundary. Thus the gradient at the swarm boundary is known and the anode potential required to establish the swarm can be calculated. For a swarm boundary $y_n(v_x'=0)$:

$$\phi_{an} = Bv_ny_a - \frac{1}{2}\frac{m}{e} v_n^2. \tag{12}$$

This potential, which will be called the "synchronism potential" for the anode, must be exceeded before any electrons exist in the interaction space which are moving fast enough to deliver energy to the traveling wave. Above this potential, if such a wave exists and if there is a mechanism for collecting the electrons which have expended energy, a net energy can be transferred from the dc field to the wave through the medium of the space charge.

Case II—Cylindrical Magnetron. The discussion of the planar magnetron case presents a physical picture of the meaning of synchronism energy and synchronism potential. The mathematics of the cylindrical case is slightly more involved because of the presence of the centrifugal force term and because of the linear dependence of the tangential velocity on radius for a constant angular velocity. The resulting relationship will, nevertheless, have similar significance.

In this case the angular velocity as a function of radial distance from the cathode is obtained by solution of (6). The result is:

$$\omega' + \omega_n = \frac{Be}{2m}\left(1 - \frac{r_c^2}{r_n^2}\right). \tag{13}$$

If ω' is set equal to zero the synchronism radius is determined.

$$\frac{r_n}{r_c} = \sqrt{\frac{Be/2m}{\frac{Be}{2m} - \omega_n}}. \tag{14}$$

At the value r_n/r_c given by this relationship the electron is stationary in the moving reference frame.

The energy (5) becomes integrable upon substitution of the angular velocity from (13). The result of the integration is:

$$e\phi = \tfrac{1}{2}mv_r^2 + \frac{B^2e^2}{8m} r^2\left(1 - \frac{r_c^2}{r^2}\right)^2, \tag{15}$$

again the second term on the right can be shown to represent energy of motion parallel to the cathode surface. If the swarm is bounded at the synchronism radius the electron must have the synchronism energy.

$$e\phi_n = \tfrac{1}{2}m\omega_n^2 r_n^2. \tag{16}$$

[9] J. C. Slater, "Microwave Electrons," D. Van Nostrand Co., New York, N. Y., chap. 13, p. 340; 1950.

The cutoff energy parabola is:

$$e\phi = \frac{B^2e^2}{8m} r^2\left(1 - \frac{r_c^2}{r^2}\right). \tag{17}$$

The derivation of the synchronism anode potential for which electrons just reach the synchronism boundary is based on the same assumptions used in the planar case resulting in the synchronism anode potential.[10]

$$\phi_{an} = \frac{r_c^2}{r_a^2} \frac{1}{1 - \frac{2m}{Be}\omega_n}\left[B\omega_n r_a^2\left(1 - \frac{m}{Be}\omega_n\right)\right.$$

$$\left.\cdot \ln\left(\frac{r_a}{r_c}\sqrt{1 - \frac{2m}{Be}\cdot\omega_n}\right) + \frac{1}{2}\frac{m}{e}\omega_n^2 r_a^2\right]. \tag{18}$$

The important differences from the planar case are that the synchronism energy is no longer constant but increases with the square of the radius and the potential distribution in charge-free space is now logarithmic rather than linear. The fact that electrons in synchronism at the anode have more energy than electrons just reaching the synchronism boundary in the case of the cylindrical magnetron, and the same energy in the planar magnetron, is significant, and will be discussed further.

Drift Velocity and Threshold Energy Conditions

In this section it will be assumed that an RF voltage exists between the anode segments so that the field due to the fundamental traveling-wave component is actually present. This potential is superimposed on the dc potential which is still applied between anode and cathode. The field component parallel to the cathode surface is now non-vanishing. The presence of this component makes possible the drift of electrons from the cathode toward the anode at potentials lower than the static-cutoff anode potential which is given by substitution of the anode-cathode distance in (11) and (17). The region of the interaction space which is accessible to the electrons will be determined by an approximate method. This method involves estimation of the minimum energy required for an electron to reach the anode and the boundaries of the region through which electrons drift toward the anode.

A semi-graphical illustration of the traveling-wave potential and field distributions along the anode surface is shown in Fig. 5. The lower potential graph is in the moving reference frame so that the electrode system and upper potential graph are moving toward the left with the synchronism velocity. The illustration is made for the instant that the maximum potential difference exists between anode segments. The following symbols are defined with reference to this picture.

$\phi_{rf\ max}$ = maximum value of RF potential difference between anode segments,

ϕ_f = maximum value of fundamental traveling-wave component of anode RF potential, and

ϕ_a = average dc anode potential.

The relationship between ϕ_f and ϕ_{rf} can only be determined as a result of analysis of the particular electrode system.

The synchronism anode potential derived in the last section was sufficient to bring electrons to the synchronism boundary. In typical practical cases calculations show that this boundary is very close to the cathode. Variation in the potential distribution due to the RF field becomes relatively small very rapidly with increasing distance from the anode in conventional anode structures. It is, therefore, reasonable to assume that the velocity distribution within the subsynchronous swarm is the same as was obtained for the static case.

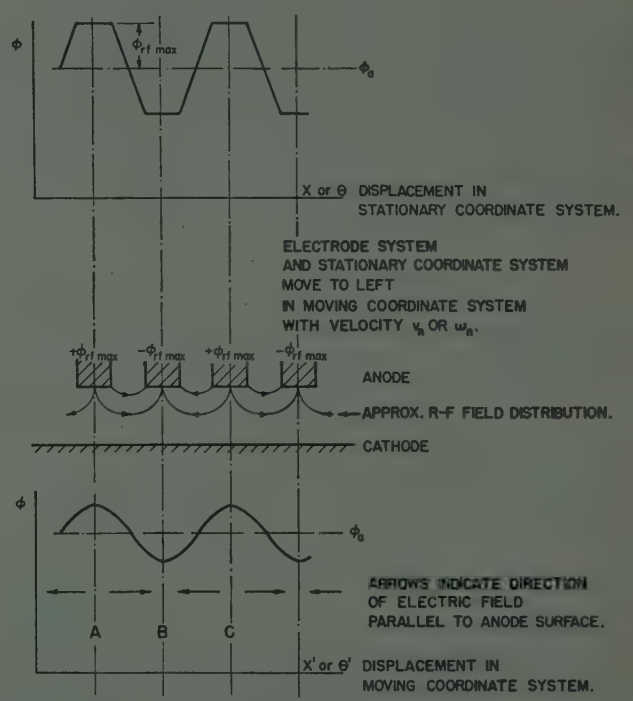

Fig. 5—Fundamental traveling wave component of anode potential and approximate RF field distribution in the magnetron interaction space at the instant for maximum potential between anode segments.

Electrons which have reached the synchronism boundary are stationary in the moving reference frame so that the action of the tangential field, however small, will begin to be significant as this boundary is exceeded. Behavior in the synchronism region can be discussed with reference to Fig. 5.

Case I—Planar Magnetron. If it is assumed that v_x' is expressed as a function of y, (3) can be written in integrated form:

$$\int e\,d\phi = \int Bev_n\,dy + \int Bev_x'\,dy + \int d(\tfrac{1}{2}mv_y^2). \tag{19}$$

For the purpose of this discussion, (4) is conveniently rewritten:

$$v_y = \frac{E_x}{B} + \frac{m}{Be}\frac{dv_x'}{dt}, \tag{4a}$$

[10] This equation has been derived by H. W. Welch, Jr. and W. G. Dow, in "Analysis of synchronous conditions in the cylindrical magnetron space charge," *Jour. Appl. Phys.*, vol. 22, pp. 433–438; April, 1951. The assumption discussed by Slater (*loc. cit.*) was not clearly stated in this article.

where

$$E_x = -\frac{d\phi}{dx}.$$

Let us assume that the dc voltage ϕ_a is greater than the synchronism potential ϕ_{an}. Without the presence of the RF potential v_x' would have a positive value. With the RF present E_x may be positive or negative. In Fig. 5 this sign is indicated by the arrows in the lower diagram. Let us examine the behavior of an electron in the region A–B and then in the region B–C.

In the region A–B, E_x has a positive direction. The force on the electron is opposite to the direction of the field so that the electron will be forced to the left, or be decelerated, making v_x' smaller and dv_x'/dt negative. A reduction of the velocity v_x' will cause a reduction in the term $Be\,v_x'$ in (19) which represents a force on the electron directed toward the cathode. The force due to the y-component of electric field is still the same so that the electron tends to move toward the anode giving v_y a positive value. In the region A–B, therefore:

$$v_y = \frac{E_x}{B} + \frac{m}{Be}\frac{dv_x'}{dt} > 0,$$

and since:

$$\frac{E_x}{B} \text{ is positive,}$$

$$\frac{m}{Be}\frac{dv_x'}{dt} \text{ is negative,}$$

we have:

$$\left|\frac{E_x}{B}\right| > \left|\frac{m}{Be}\frac{dv_x'}{dt}\right|.$$

As long as v_x' is positive the electron is moving to the right in the moving reference frame. While dv_x'/dt is negative v_x' is becoming smaller, the electron is drifting outward, and the maximum of E_x is becoming larger. Since v_y is positive the force due to v_y ($Be\,v_y$) is tending to balance the force due to the tangential field component (eE_x).

In the region B–C, E_x has a negative direction. The electron will be accelerated making v_x' larger and dv_x'/dt positive. The term $Be\,v_x'$ is increased, tending to force the electron toward the cathode. In the region B–C, therefore:

$$v_y = \frac{E_x}{B} + \frac{m}{Be}\frac{dv_x'}{dt} < 0,$$

$$\frac{E_x}{B} \text{ is negative,}$$

$$\frac{m}{Be}\frac{dv_x'}{dt} \text{ is positive,}$$

therefore:

$$\left|\frac{E_x}{B}\right| > \left|\frac{m}{Be}\frac{dv_x'}{dt}\right|.$$

Here the tendency for v_x' to become larger is balanced by the fact that the electron is drifting inward where the maximum of E_x is becoming smaller; also, the electron is drifting toward the region A–B where it will drift outward.

The conclusions to be derived from these arguments are:

a. In the region A–B where a decelerating tangential field exists, v_y is directed toward the anode.
b. In the region B–C where an accelerating field exists, v_y is directed toward the cathode.
c. The term E_x/B dominates over the term $(m/Be)(dv_x'/dt)$ in (4a).
d. The motion of the electron is always such that v_x' tends toward zero.

Actually, more elaborate calculations would show show that the electron executes a cycloidal-like motion around a path of drift which tends to follow constant potential contours.[11] The term E_x/B is recognized as the translation velocity of the rolling circle which generates a cycloid in the case of uniform crossed electric and magnetic fields.

The preceding discussion makes reasonable the following choice of v_x' in integrating (19) to obtain the anode potential which must be approximated if electrons are to reach the anode.

In the subsynchronous region:

$$v_x' = \frac{Be}{m}y - v_n,$$

the value which it has in the static magnetron.

In the synchronous region:

$$v_x' = 0.$$

Integrating and making use of (8), the result is:

$$e\phi_a = \tfrac{1}{2}mv_y^2\big|_{y=y_a} + Bev_n y_a - \tfrac{1}{2}mv_n^2. \qquad (20)$$

The *threshold anode potential* ϕ_{at} will be defined as the anode potential given by (20) for which the y-component of velocity is just zero. The term $\frac{1}{2}mv_y^2$ represents kinetic energy in excess of the minimum energy which the electron must accept from the dc field in order to exist at the anode.

$$e\phi_{at} = Bev_n y_a - \tfrac{1}{2}mv_n^2. \qquad (21)$$

It is interesting to note that this anode potential is the same as the synchronism anode potential defined in the last section. This is a consequence of the fact that no kinetic energy, in addition to the synchronism energy, is retained by the electron in its passage from the synchronism boundary to the anode. Work is done on the electron by the radial field, represented by the term:

$$\int_{y_n}^{y_a} Bev_n dy. \qquad (22)$$

However, this energy is immediately transferred from the electron to the RF field, in order that the electron reaches the anode, retaining only the kinetic energy

[11] Slater, *op. cit.*, p. 307.

represented by:

$$\int_0^{y_n} \frac{B^2e^2}{m} y dy, \qquad (23)$$
$$= \tfrac{1}{2}mv_n^2.$$

The two terms of (22) and (23) have an interesting interpretation. They represent the work done on an element of current in moving it from 0 to y_a through the magnetic field B. This element of current is that due to a single charge moving with a velocity given by $(Be/m)y$ between 0 and y_n and a velocity v_n between y_n and y_a.

This problem is typical of many physical problems where the energy required to perform an operation can be determined from a force-distance integral but the disposition of the energy can only be determined by more detailed examination of the physical system. In this particular case, the energy given by (23) is dissipated into heat in the anode. It is concluded that the rest of the energy must be transferred to the RF field. Some of this energy is, in turn, transmitted to the cathode in back-bombardment power by the electrons which have negative y-directed velocities.

Case II—Cylindrical Magnetron. The discussion of the cylindrical magnetron proceeds with exactly the same basic assumptions which were used in the treatment of the planar magnetron problem. The angular velocity of the electron is assumed to have the following distribution:

In the subsynchronous region:

$$\omega' = \frac{Be}{2m}\left(1 - \frac{r_c^2}{r^2}\right) - \omega_n. \qquad (13)$$

In the synchronous region:

$$\omega' = 0.$$

After integrating (5) with these substitutions and simplifying algebraically the following results:

$$e\phi_a = \tfrac{1}{2}mv_r^2\big|_{r=r_a} + \tfrac{1}{2}Be\omega_n(r_a^2 - r_c^2) - \tfrac{1}{2}m\omega_n^2 r_a^2. \qquad (24)$$

Thus the threshold anode potential in the cylindrical system is:[12]

$$e\phi_{at} = \tfrac{1}{2}Be\omega_n(r_a^2 - r_c^2) - \tfrac{1}{2}m\omega_n^2 r_a^2. \qquad (25)$$

This is the well known Hartree equation.

Comparison of this result with the synchronism anode potential of (18) will show that the threshold anode potential is greater. This difference results from the additional energy which must be given to the electron to maintain the angular velocity synchronism as the radial distance to the position of the electron is increased. We must conclude that, if the gradient at the cathode is still zero, the total space charge in the interaction space must be greater than it was at the synchronism anode potential. In a previous publication it has been shown that this space charge density corresponding to the threshold potential is a constant independent of radius, given by:

$$\rho_0 = -2\epsilon_0 \frac{m}{e}\omega_n\left(\frac{Be}{m} - \omega_n\right). \qquad (26)$$

This value will be used later in calculation of induced currents in the magnetron.

Phase Focusing; Formation of Space-Charge Spokes

The threshold energy and drift velocity conditions present approximate physical limitations on the space-charge distribution, which will be used as a basis for the prediction of large-signal phase focusing in the magnetron. This fact is represented graphically, in the moving reference frame, in Fig. 6.

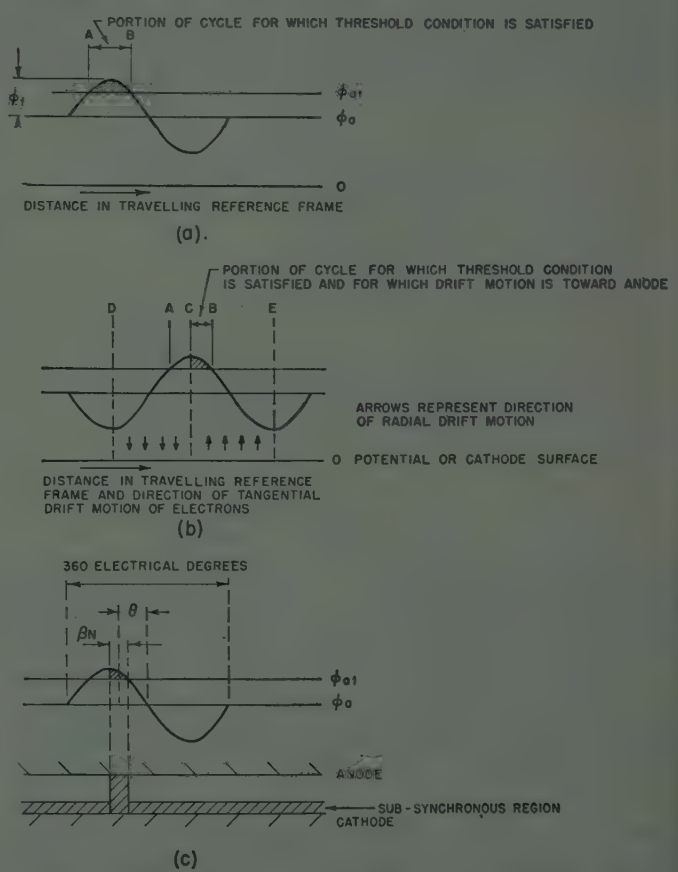

Fig. 6—Illustration of graphical method for determining spoke width and phase angle.

The threshold energy level is represented by the line labeled ϕ_{at}, the actual anode voltage by the line ϕ_a. An RF potential is represented with peak amplitude ϕ_f. This is the peak value of the fundamental traveling-wave component which appears stationary in the moving reference frame. Fig. 6a illustrates the possibility, even though the threshold potential is not exceeded by ϕ_a, that the threshold may be exceeded during part of the cycle designated by the interval AB if an RF potential exists. In Fig. 6b the effect of the drift-velocity condi-

[12] Welch and Dow, *op. cit.*, p. 436.

tion is illustrated. The drift motion of the electrons is toward the anode in the region CE and away from the anode in the region DC. Therefore, although the threshold energy is exceeded in the entire region AB, electrons can only drift toward the anode in half of this region bounded by CB. In the region AC electrons can only exist if they come from the anode and the assumption is that all electrons are emitted from the cathode. The final picture to be derived from this line of argument is shown in Fig. 6c. Here the potential distribution is plotted over a diagram of the interaction region. The width of the spoke and its phase angle relative to the RF potential are approximately determined. These quantities are defined by the following symbols which will be used when the current induced into the circuit is to be calculated.

θ = phase angle between center of spoke and zero of RF potential in electrical degrees, negative as shown.

βN = width of spoke in electrical degrees.

β = half the actual space angle width of the spoke.

N = number of anodes.

There are $N/2$ full wavelengths (each 360 electrical degrees) around the cylindrical magnetron structure. The width of a spoke in electrical degrees, therefore, is:

$$\frac{N}{2} \cdot 2\beta = \beta N.$$

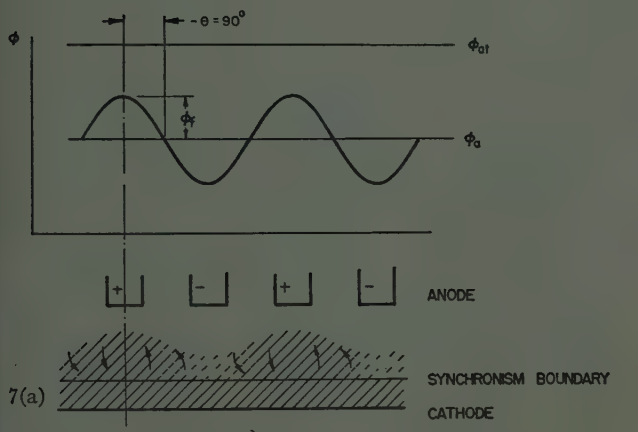

7(a)

Phase focusing diagram. To be studied with related illustration of Figs. 7(b), (c), (d), (e) and Figs. 8(b), (c), (d) and (e) on page 1642.

θ represents the phase angle between the current induced in the circuit by the motion of the spoke parallel to the anode surface and the RF potential which is developed between the anode sets.[13] The way in which θ depends upon dc anode voltage is illustrated by the development of the graphs in Fig. 7 and Fig. 8. In these graphs the RF potential and the frequency are assumed constant, thus placing a special requirement on the circuit operating parameters.

[13] The RF currents due to radial motion, although not a first order effect, may be significant in magnetrons operating at large anode currents. This effect is neglected in the analysis presented here.

In Fig. 7a, a case is illustrated which cannot occur in the oscillating magnetron, but is observable experimentally if an external source of RF is imposd on the magnetron circuit. If the anode potential is above the synchronism potential but below the threshold potential and an RF potential superimposed, the electrons will tend to drift toward the anode, but, because the threshold energy is not exceeded, will be forced to drift back again toward the cathode. However, the bunching effect of the radial component of the RF will take effect to the extent that a greater density of electrons will circulate under a positive potential maximum than under a negative potential maximum symmetrically disposed about the positive maximum. The induced current into the circuit due to the motion of the electrons parallel to the cathode will go through zero from negative to positive as the spoke passes under the anode segment at the same instant the anode segment reaches its maximum positive value. This is illustrated in Fig. 8a. The maximum current into the circuit lags the RF potential maximum by 90°. This is equivalent to a current into the electron swarm which leads by 90° or to the addition of a capacitance between the anode segments in the interaction space. This capacitance is entirely due to the synchronous bunching of the electrons and not related to the capacitance effect which can be introduced by an evenly distributed swarm of electrons. Experimental evidence of this effect was presented in a previous paper by the author.[14]

In Fig. 7b the anode potential has been increased to the point where the RF exceeds the threshold potential

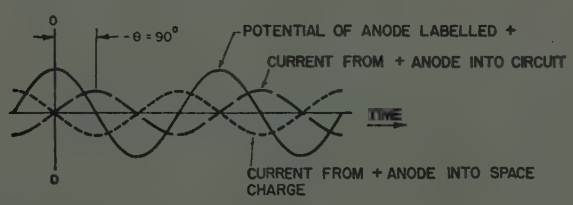

8(a) ELECTRONS CAPACITIVE

To be studied with related illustrations of Figs. 7(b), (c), (d), (e), and Figs. 8(b), (c), (d) and (e), on page 1642.

during part of the cycle. Electrons in the spoke now drift toward the anode and are collected so that power can be delivered to the system. There is now an in-phase component of current as illustrated in Fig. 8b. The zero of the current slightly precedes the RF potential maximum in time. The space-charge swarm as an induced-current generator is delivering energy into a highly inductive load. Oscillations can be supported if they have been initiated. At the potential, ϕ_a, however, an infinitesimal RF potential would not exceed the threshold potential. One must assume that the threshold potential has been exceeded by ϕ_a in order to

[14] H. W. Welch, "Effects of space charge on frequency characteristics of magnetrons," Proc. I.R.E., vol. 38, pp. 1434–1449; December, 1950. (Fig. 10.)

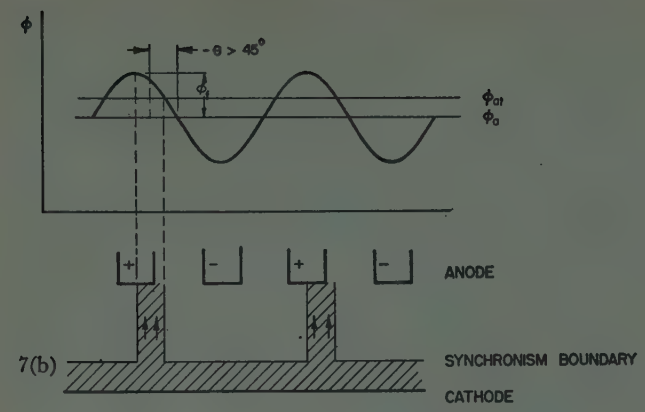

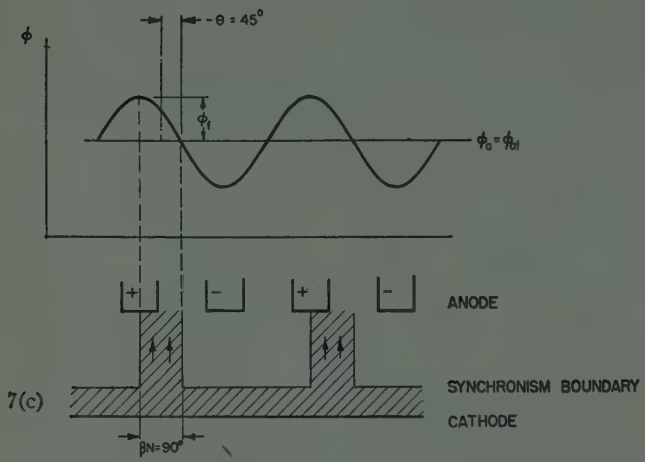

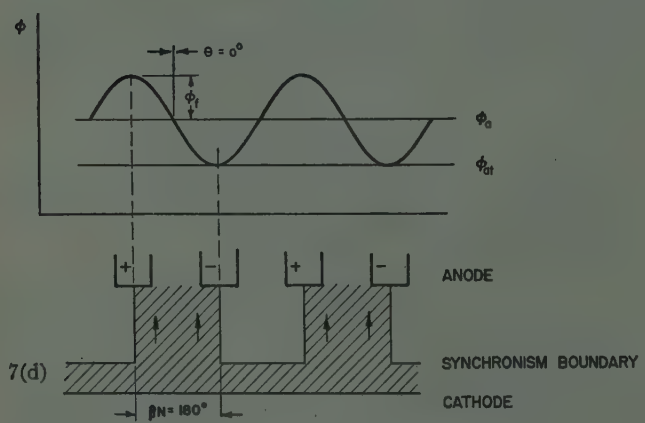

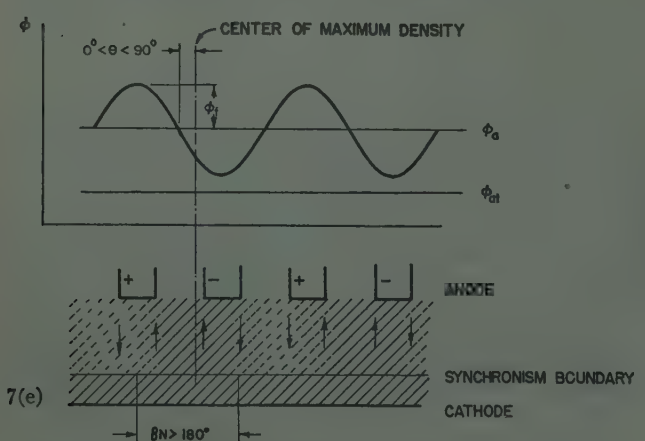

Fig. 7—Phase focusing diagram. Graphical development of relationship between phase angle θ and anode potential. Constant RF potential and frequency are assumed. Arrows indicate direction of electron drift between anode and cathode.

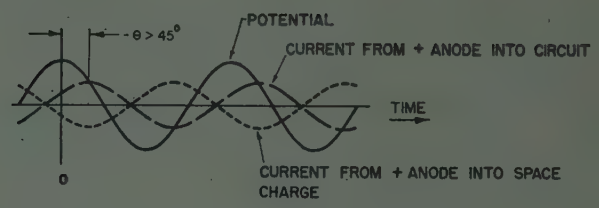

8(b) CIRCUIT INDUCTIVE

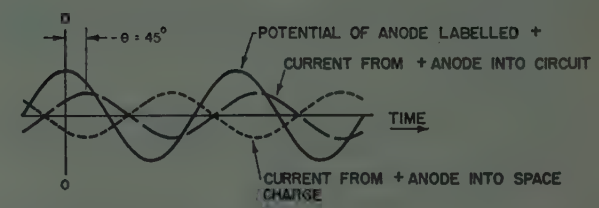

8(c) CIRCUIT INDUCTIVE AT HALF POWER POINT

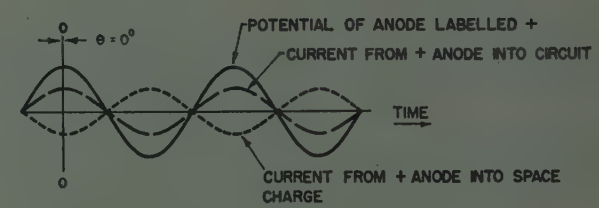

8(d) CIRCUIT RESISTIVE ON RESONANCE

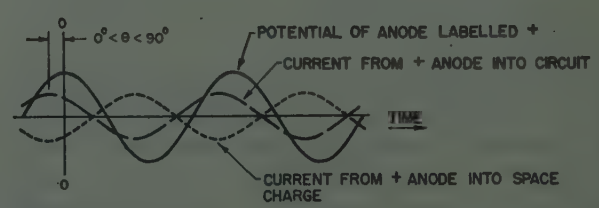

8(e) CIRCUIT CAPACITIVE

Fig. 8—Current induced by spoke into circuit on time scale. Time 0–0 marks the instant observed in illustration labeled by the same letter in Fig. 7. (Fig. 7 should be studied with Fig. 8.)

initiate the oscillation and that ϕ_a subsequently dropped (i.e, by power supply regulation), or that a pulse of noise or external RF source set the tube into oscillation.

In Fig. 7c the case for ϕ_a exactly equal to the threshold potential, ϕ_{at}, is illustrated. The phase angle is $-45°$ so that, for operation into a resonant circuit, the frequency would be such that the point of operation would be at the "half-power points."

Fig. 7d represents a case of particular importance. The anode potential is raised above the threshold potential so that the condition:

$$\phi_a = \phi_{at} + \phi_f, \tag{27}$$

is just satisfied. The entire region in which drift velocity is toward the anode is filled. The spokes have reached a width just half filling the interaction space. The phase angle θ is zero degrees so that the circuit must be on resonance to present a real admittance to the induced current. At a higher anode potential, represented by Fig. 7e, the threshold potential is exceeded everywhere and the only focussing mechanism left is that due to the tangential component of the RF field. The electrons are, therefore, not in well defined bunches but continuously distributed with periodic condensations and rarefactions. Moreover, as the circuit passes through resonance, the admittance of the circuit goes through a minimum; raising the anode potential will result, in general, in greater power input; a smaller RF potential (therefore smaller power output) will tend to be the result of the induced current; and the focussing forces will tend to be reduced. These factors result in inconsistency which leads one to expect that the magnetron will cease oscillating or oscillate in another mode. The conclusion is that (27) represents a critical condition defining an upper-mode boundary on magnetron oscillation.

In Fig. 9 a series of phase-focusing diagrams illustrates the behavior to be expected over the range of a typical volt-ampere characteristic when the magnetron is operating into a resonant load. The characteristic corresponding to the diagrams is shown in Fig. 10. When the anode potential reaches a threshold potential ϕ_{at}, characteristic of a frequency for which the circuit presents an impedance sufficient to start the phase focusing, the magnetron will start oscillating. This potential may, in general, be as much as 10 or 20 per cent below the threshold potential which is characteristic of the resonance frequency. This condition is represented by the diagram of Fig. 9a. The RF potential is very small and the synchronism velocity is not definitely determined; bunching is weak so that noisy operation may be expected. As the anode potential is raised further to a value ϕ_{a2}, the frequency increases substantially to a value two or three per cent off resonance. The characteristic threshold potential ϕ_{at2} is proportionally higher than ϕ_{at}. The RF is now strong enough to produce a well-focused spoke. As the anode potential is increased further, the threshold potential remains substantially constant since the frequency is a very slowly varying

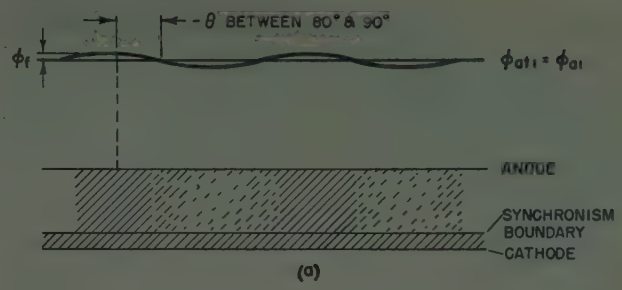

Fig. 9(a)—Magnetron just starting. ϕ_f is very small. Frequency is 5 or 10% off resonance. Bunching not complete, possibly noisy operation.

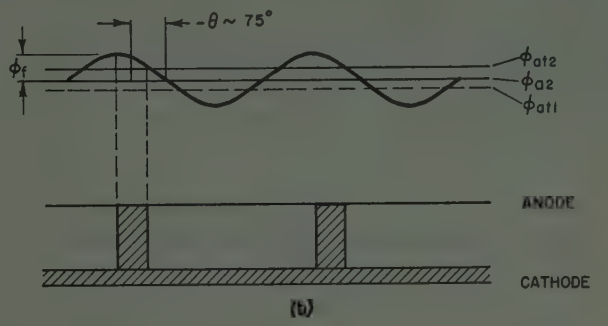

Fig. 9(b)—Magnetron is oscillating strongly. ϕ_f is greater than 10% of ϕ_a. Frequency is 1 to 3% off resonance. Bunching is complete but bunches and induced current are much less than maximum.

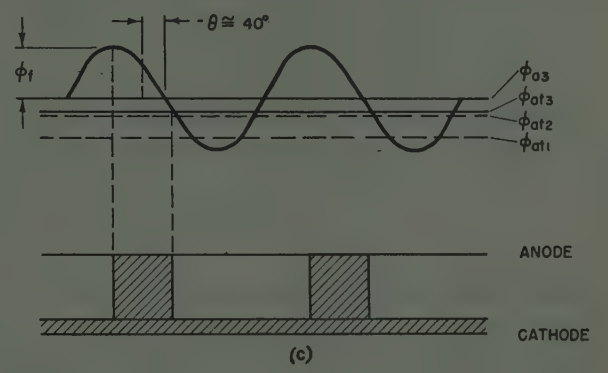

Fig. 9(c)—Magnetron is oscillating at a medium power level. ϕ_f is 30 or 40% of ϕ_a. Frequency is less than 1% off resonance. Bunch has increased in size and induced current is greater than in last picture.

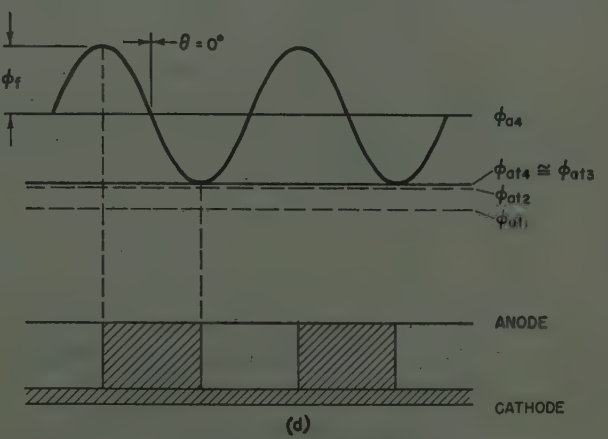

Fig. 9(d)—Magnetron is oscillating at highest possible level. ϕ_f is of the order of half ϕ_a. Frequency is on resonance. Bunches occupy half of the space. Induced current is maximum.

Fig. 9—Phase focusing diagrams for a typical magnetron volt-ampere characteristic.

function of phase angle near resonance. The separation between ϕ_a and ϕ_{at} increases with the increased power input and the RF amplitude builds up, because of the decreasing total circuit admittance, until finally the critical condition of (27) is reached and oscillation ceases.

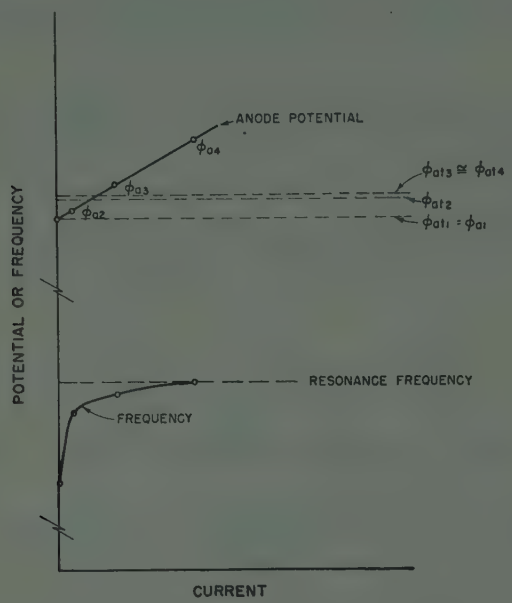

Fig. 10—Typical volt-ampere characteristic used in making phase-focusing diagrams of Fig. 9.

The quantity $\phi_a - \phi_{at}$ can be analytically related to βN by use of the phase-focusing diagram. Referring to Fig. 6c:

$$\frac{\phi_a - \phi_{at}}{\phi_f} = -\cos \beta N. \tag{28}$$

The phase angle θ is given by:

$$\pi + 2\theta = \beta N. \tag{29}$$

Note, in normal operation, the current lags the voltage and θ, therefore, is negative as conventionally defined for an admittance. Thus, βN is less than π. Therefore:

$$-\cos \beta N = \cos 2\theta = \frac{\phi_a - \phi_{at}}{\phi_f}. \tag{30}$$[15]

ϕ_f, the peak value of the fundamental traveling-wave, is related to the actual peak RF potential between anode segments by a constant which depends only on the electrode geometry:

$$\phi_f = K\phi_{\text{RF max}}, \tag{31}$$

where $K < 1$.

The final condition on ϕ_{RF} is that it be produced as the result of the flow of the induced current through the external circuit, i.e.:

$$\phi_{\text{RF max}} \left| Y_T \right| \angle\theta = I_1 \tag{32}$$

$\left| Y_T \right|$ = absolute value of the circuit admittance.

I_1 = amplitude of the fundamental component of the current induced in the circuit by the rotation of the space-charge spokes in the interaction space. It is given by (43) below.

θ = the phase angle determined by the circuit. θ must be equal to the value determined by (30) and defined in Fig. 6.

This discussion of the phase-focusing diagram shows that the circuit phase characteristic, as well as the induced current due to the particular spoke configuration involved, must be known in order to predict magnetron frequency characteristics. In order to calculate the induced current, it will be necessary to estimate the space-charge density in the spokes. This problem is discussed in the following section.

Estimation of Space-Charge Density in the Interaction Region

The space-charge density given by (26), a constant independent of radius, applies only to the condition $\phi = \phi_{at}$ or $\theta = -45°$.

It will be desirable to calculate the induced current over the range of operation indicated as feasible in the discussion of the phase-focusing diagrams from $\theta = -90°$ to $\theta = 0°$. It is therefore necessary to estimate the space-charge density in the spokes over this range. Actual calculations of the space-charge-density distribution is prohibitively laborious and only possible by a self-consistent field calculation. For the purposes of this treatment, therefore, it will be assumed that the average space-charge density is a constant independent of radius at all anode potentials within the range of interest as it is at the threshold potential. This means that, whether the anode potential is below or above the threshold potential, a potential distribution of the following form is assumed to exist.

$$\phi = ar^2 + b. \tag{33}$$

Application of Poisson's equation to (33) yields:

$$\rho = -4\epsilon_0 a. \tag{34}$$

After evaluating the constant a using the boundary conditions on ϕ with (33), the constant average space-charge density is expressed by:

$$\rho = -4\epsilon_0 \frac{\phi_a - \phi_n}{r_a^2 - r_n^2}. \tag{35}$$

If $\frac{1}{2}mv_r^2$ is negligible it can be shown that:

$$\frac{1}{2}\frac{m}{e}\omega_n^2 r_n^2 = \phi_n = \phi_{at} - \frac{\omega_n}{2}\frac{m}{e}\left(\frac{Be}{m} - \omega_n\right)(r_a^2 - r_n^2). \tag{36}$$[16]

Substituting into (35) yields:

$$\rho = -\left[2\epsilon_0 \frac{m}{e}\omega_n\left(\frac{Be}{m} - \omega_n\right) + 4\epsilon_0 \frac{\phi_a - \phi_{at}}{r_a^2 - r_n^2}\right]. \tag{37}$$

[15] In the author's opinion, this equation is the most important single result of the analysis presented here.

[16] This is a preliminary form of (24).

The first term of this expression is identical with the value given by (26). If we define:

$$R_n = \frac{r_n}{r_c}, \quad (14)$$

$$R_a = \frac{r_a}{r_c},$$

(37) may be written:

$$\rho = \rho_0\left(1 + \frac{4\epsilon_0}{\rho_0 r_c^2}\,\frac{\phi_a - \phi_{at}}{R_a^2 - R_n^2}\right). \quad (38)$$

The effect of deviation of the anode potential from the threshold potential is now contained in the second term. Equation (38) is plotted in Fig. 11. The theory of phase focusing presented here applies only to large-signal analysis and large-signal operation is seldom observed at ϕ_a less than 90 per cent of ϕ_{at}. ϕ_n is usually of the order of 10 per cent or less of ϕ_{at}. ϕ_a is seldom more than 20 or 30 per cent greater than ϕ_{at}. This range is indicated on the graph.

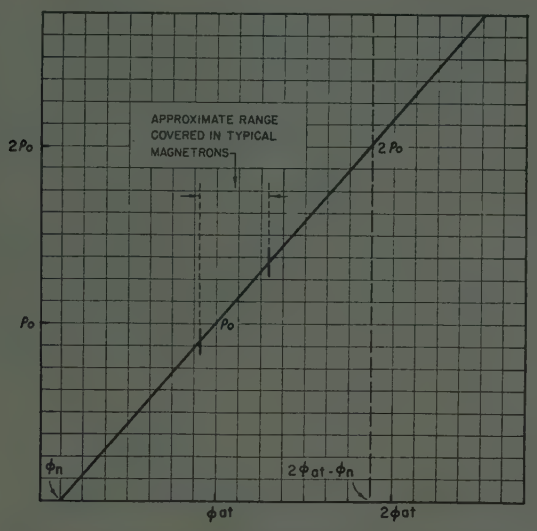

Fig. 11—Average space-charge density as a function of anode potential.

Electron Behavior in the Space-Charge-Free Magnetron. Temperature-Limited Operation

In all of the material which has just been presented, it has been assumed that zero field gradient existed at the cathode, or that the magnetron was operating under space-charge-limited conditions. This is not realistic in the analysis of many experimental results since, because of necessity for compromise in design, cathodes for cw magnetrons are frequently marginal in their emission capabilities. The enhanced emission which provides the very large currents in pulsed magnetrons does not exist when tungsten or other pure metal cathodes are used in cw tubes. It can easily be shown[17] that the subsynchronous space-charge swarm does not act as a reservoir as has sometimes been proposed. Experimental evidence of the fact that cathode emission, and cathode properties other than straightforward emission-density capabilities, may have strange effects on oscillatory behavior is plentiful, and, for the most part, uninterpreted. Attempts to derive complete relationship for field gradient at the cathode and energy distribution in the swarm, for various emission currents, result in discouragingly complex relationships even for the planar static magnetron. For the cylindrical static magnetron the information to be derived from the analytical solution assuming zero gradient at the cathode is questionably commensurate with the difficulty involved. The problem with a gradient at the cathode has received attention for the non-magnetic diode as recently as October, 1950,[18] although earlier papers[19] give fairly comprehensive treatments. If the solution for the static magnetron did exist, there is no known method of extending the ideas to calculation of dc current in the oscillating magnetron.

In order to get some idea of the effect of a positive field gradient at the cathode on the behavior of the oscillating magnetron, the various results involving anode potential and synchronism conditions which have been discussed will be compared with similar results of the analysis of the completely space-charge-free magnetron. The initial differential equations of (3), (4), (5) and (6) are the same. The problem, however, becomes simpler, since not only are the boundary conditions known, but the complete potential distribution within the interaction space is known. On paper, at least, it becomes conceivable to calculate the position and velocity of an electron at every instant. It is discouraging to discover that even this relatively simple physical problem leads to nonlinear differential equations which have not been solved except for very simplified boundary conditions in the large-signal, traveling-reference-frame problem.[20] The important difference from the preceding analysis will be found in the anode potential required for synchronism and in the division between energy due to motion directed perpendicular to the anode and energy due to motion directed parallel to the anode.

Case I—Planar Magnetron. The solution for the x-component of velocity in the static planar magnetron is, regardless of the field gradient at the cathode, the result given in (7) and the electron reaches the synchronism velocity at the same distance from the cathode given by (8). However, since it is assumed that the space charge is having a negligible effect on the field and potential distribution, the minimum anode

[17] H. W. Welch, Jr., S. Ruthberg, H. W. Batten and W. Peterson, "Analysis of dynamic characteristics of the magnetron space charge—preliminary results," *Tech. Report No. 5*, University of Michigan, Dept. Elec. Eng., Electron Tube Lab.; January, 1951.

[18] P. L. Copeland and D. N. Eggenberger, "The electric field at a thermionic cathode as a function of space current," *Phys. Rev.*, vol. 80, p. 298; October 15, 1950.

[19] C. E. Fay, A. L. Samuel, and W. Shockley, "On the theory of space charge between parallel plane electrodes," *Bell Sys. Tech. Jour.*, vol. 17, p. 49; 1948.
H. F. Ivey, "Cathode field in diodes under partial space-charge conditions," *Phys. Rev.*, vol. 76, pp. 554–558; August 15, 1949.
L. Page and N. I. Adams, Jr., "Diode space charge for any initial velocity and current," *Phys. Rev.*, vol. 76, pp. 381–388; August 1, 1949.

[20] F. Lüdi, "Zur Theorie der geschlitzten Magnetfeldröhre," *Helv. Phys. Acta*, vol. 16, p. 64; 1943.

potential required to bring electrons to this boundary is now changed. The potential of a given point in the interaction space will be linearly related to the distance from the cathode. With these facts we can show that the synchronism anode potential is given by:

$$\phi_{an} = \tfrac{1}{2}Bv_n y_a \text{ (for space-charge-free case).} \quad (39)$$

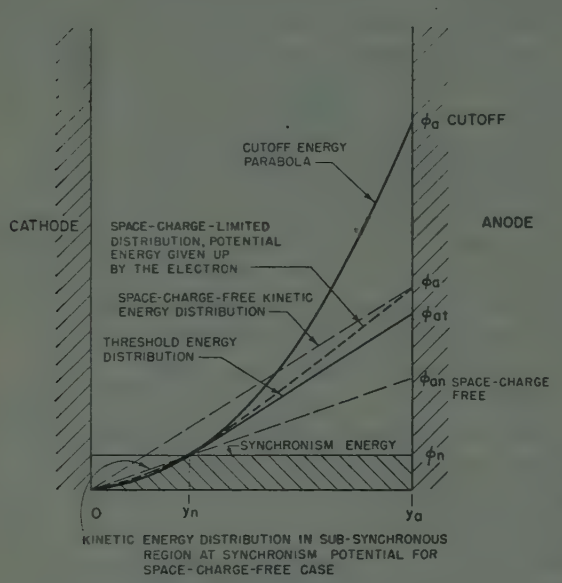

Fig. 12—Energy distributions in the plane magnetron (in relative electron volts).

For large B this is approximately one-half the synchronism anode potential for the space-charge-limited case (12). There is nothing in the space-charge-free problem which gives reason to change the choice of v_x' used in the integration of the energy equation which leads to the threshold anode potential and the cutoff anode potential. The various energy distributions are plotted for comparison in Fig. 12. The curve for the space-charge-limited energy distribution displays a slight upward flexion in the synchronism region due to the presence of space charge in the spokes. If, for the same anode potential, the emission current were reduced gradually to zero, the flexion would gradually disappear and the energy distribution gradually approach the straight line of the space-charge-free energy distribution. The difference between the actual energy distribution curve and the threshold-energy curve is the energy of y-directed motion. The energy of the x-directed motion is represented by the shaded area under the synchronism-energy level outside the synchronism boundary and the cutoff energy parabola inside the synchronism boundary. The remaining energy must be delivered to the RF field.

In Fig. 13 the phase-focusing diagram is placed beside a potential diagram to illustrate behavior of the magnetron under temperature-limited conditions. Two conditions are shown, indicated by 1 and 2. In condition 1 the anode current is sufficiently small that the operation is space-charge-limited. The anode potential, ϕ_{a1}, is equal to the threshold potential, ϕ_{at1}, corresponding to the frequency, f_1. The phase angle, θ_1, is represented as almost 90° since the space-charge swarm is assumed to be very weakly bunched. As the anode potential is raised a relatively small amount, the anode current rises rapidly to the saturation value. The reduction of space-charge density inside the magnetron causes a positive gradient to exist at the cathode and the potential required to produce synchronous electrons approaches the

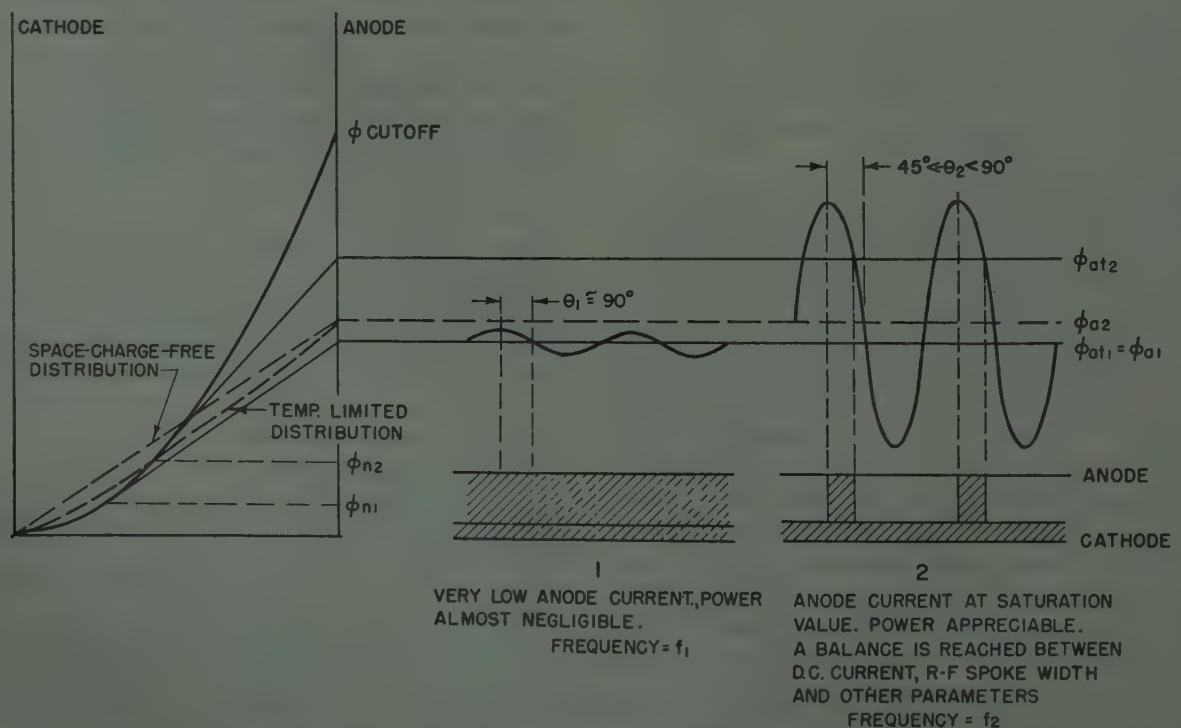

Fig. 13—Phase-focusing diagram and energy-distribution diagram for temperature-limited operation.

value given by (39). For a given anode potential, ϕ_{a2}, the synchronism velocity might be higher than in the space-charge-limited case as represented in condition 2. (Under these conditions, velocities directed toward the anode may become significant.) The frequency is directly proportional to the synchronism velocity since $v_n = x_n f$ (2) and $y_n \approx \sqrt{\phi_n}$. We have, therefore:

$$\frac{f_2}{f_1} = \frac{v_{n2}}{v_{n1}} = \frac{\sqrt{\phi_{n2}}}{\sqrt{\phi_{n1}}}. \tag{40}$$

For the case illustrated it is implied that the difference between f_2 and f_1 is rather substantial, but that the phase angle, θ_2, is still large and not greatly different from θ_1. A change in any parameter would result in a different frequency, or phase angle, a new requirement for circuit impedance and a change in the RF potential or spoke width. It is reasonable to assume that the dc collection current is proportional to the spoke width. must increase in the same proportion as the anode potential. This is illustrated by the phase-focusing diagrams of Fig. 14. The unique balance between all of the parameters at the saturation current level is approximately maintained if the whole phase-focusing diagram is raised with the anode potential. The frequency is therefore determined by the anode potential under these particular conditions.

An important assumption underlying these remarks is that the gross behavior of the space charge in response to given imposed voltages and boundary conditions is not a critical function of frequency. This is certainly true[21] and is an extremely important characteristic of magnetron behavior. The ability of the magnetron to operate over a wide range of voltages and magnetic fields and relatively large tuning ranges is a direct consequence of this property.

We have shown that the spoke configuration is determined by the RF potential caused by the flow of current

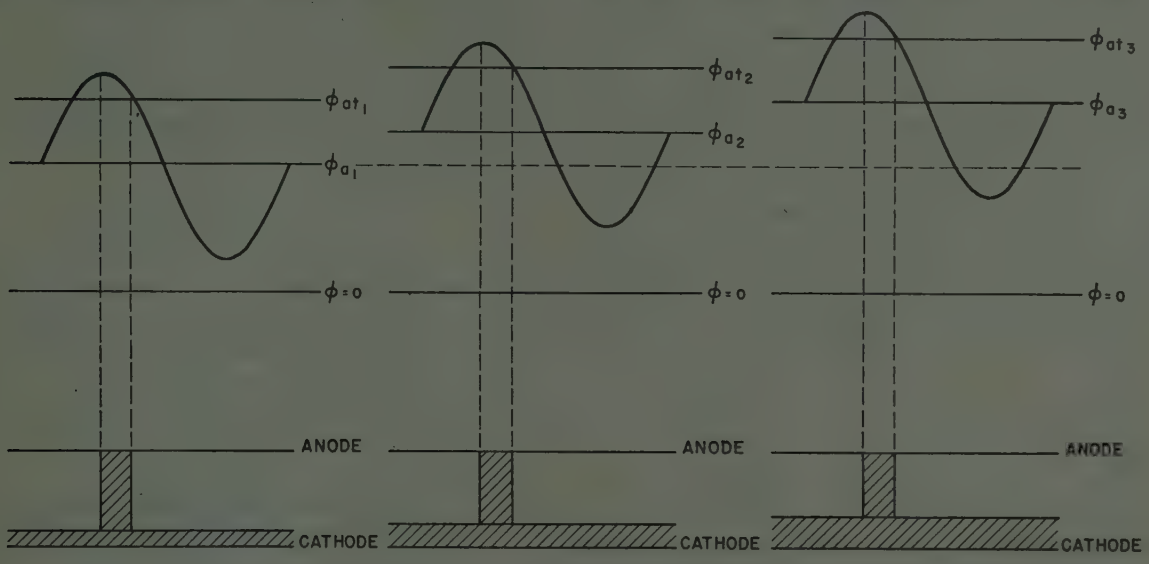

Fig. 14—Phase-focusing diagrams for various anode potentials. Magnetic field, circuit impedance and anode current maintained constant.

(Observed dc currents, in the oscillating magnetron, are always a fraction of the known diode current capabilities.) Thus, if the particular operating anode potential and current are assumed constant, it becomes difficult to argue a change in any of the other parameters in the phase-focusing diagram without a change in the circuit. It is concluded that the operating conditions as specified by diagram 2 are unique.

Suppose the anode potential is now raised above the value, ϕ_{a2}, and that, in addition to keeping the dc current constant at the saturation level, the circuit impedance is kept constant. Since the dc current is limited by saturation, any change in spoke width which would produce a change in induced current would tend to be suppressed. Since the circuit impedance has been maintained constant, the phase angle and RF voltage remain the same and we are led to the conclusion that the threshold potential and, consequently the frequency, induced in the circuit by the spoke motion. Therefore, certain specific circuit properties must be achieved in order to produce particular types of behavior in the phase-focusing diagrams illustrated by the examples in the last two sections. The results of considerations of induced current and circuit problems are presented in the concluding section with particular reference to the final definition of frequency pushing and voltage tuning. It is evident that the conditions just described are those required for voltage tuning and that the conditions described in connection with Figs. 9 and 10 are those required for frequency pushing. The present analysis will be completed by a brief discussion of the space-charge-free energy distribution of the cylindrical magnetron.

[21] G. B. Collins, Editor, "Microwave Magnetrons," McGraw-Hill Book Co., New York, N. Y.; 1948. (*M.I.T. Radiation Lab. Series*, vol. 6, p. 217; excepting frequencies near $Be/2\pi m$.)

Case II—Cylindrical Magnetron. The equation for the synchronism anode potential in the space-charge-free cylindrical magnetron is based on the assumption of a logarithmic potential distribution between anode and cathode. Assuming initial velocities equal to zero:

$$\phi_{an} = \frac{r_c^2}{r_a^2} \frac{\frac{1}{2}\frac{m}{e}\omega_n^2 r_a^2}{1 - \frac{2m}{Be}\omega_n} \cdot \frac{\ln \frac{r_a}{r_c}}{\ln \sqrt{\frac{1}{1 - \frac{2m}{Be}\omega_n}}}. \quad (41)$$

Typical energy distribution curves are plotted in Fig. 15. The major physical difference from the planar magnetron results from the fact that the energy of the electron corresponding to its position must increase as the square of the radius in order to maintain synchronism. In order for the average potential throughout the space to be as great as the potential corresponding to synchronism energy, it is necessary for the anode to exceed the synchronism anode potential. The potential must be raised still further to meet the threshold condition. As a consequence, there will be a relatively large proportion of the electrons traveling at super-synchronous velocities just before the threshold is reached and the magnetron takes off. Immediately after the takeoff the distribution inside is altered completely, particularly so under temperature-limited conditions. An appreciable space-charge density must exist in the spokes so that the induced current and the consequent RF potential immediately assume appreciable values.

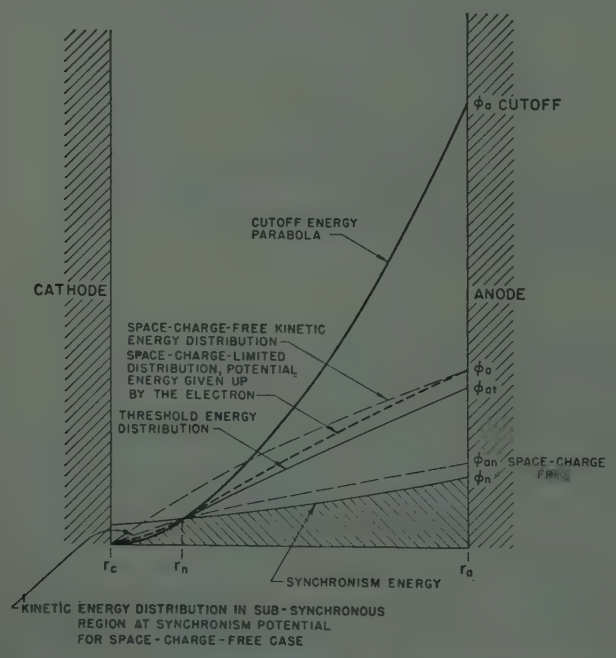

Fig. 15—Energy distributions in the cylindrical magnetron (in relative electron volts).

The over-all conclusion is that the cylindrical magnetron will be expected to jump into oscillation, whereas the planar magnetron may go through quite a smooth transition.

This conclusion can be extended to say that a magnetron with relatively large ratio of anode-to-cathode radius, say greater than 1.5 to 1, will be expected to jump into oscillation at finite anode current, whereas a magnetron which physically approaches the planar case, say, r_a/r_c less than 1.5 to 1, will experience a smooth transition with oscillation at very low anode currents.

Once the magnetron has started oscillating, the remarks relating to the phase-focusing diagrams of Fig. 14 still apply. The description of starting given in connection with Fig. 13 is, however, no longer accurate.

Calculation of Current Induced in the External Circuit[22]

If the space charge distribution is known, the theory of induced currents permits an exact calculation of the effect of the electrons on the circuit. Therefore any errors in the following results should arise from the assumptions made about the space charge. These assumptions are based on the preceding discussion. The approximate method which is offered permits reasonably quantitative estimates of frequency characteristics of the oscillating magnetron. Such an estimate is not readily made, perhaps not humanly possible, by use of the more accurate self-consistent field method.

The basic equation for induced current calculation used in obtaining the following results is:

$$i_k = \int_{S_k} (\rho v)_n dS_k + \frac{\partial}{\partial t}\int_V \psi_k \rho dV, \quad (42)$$

where i_k is the current to the kth electrode in an arbitrary system of electrodes due to a distribution of charge density ρ. S_k is the surface of the k'th electrode, $(\rho v)_n$ the normal component of current *at* this surface and V the volume occupied by the space charge density. ψ_k is defined as follows:

ψ_k = unity on S_k
= 0 on all other electrodes and satisfies the Laplace equation throughout the interaction region. It is not an electrical potential.[23]

This equation has been applied to the space charge distribution and geometry shown in Fig. 16. Since the magnetron is considered operating in the π mode there are half as many spokes of charge as anodes and the picture repeats at every other anode.[24] Therefore, ψ_k was assigned the value unity on one set of alternate anodes and 0 on the other set. The term ρv_n was neglected. The fundamental component of the current induced in the admittance Y_T with these assumptions is the following:

[22] More detail available in H. W. Welch, "Dynamic frequency characteristics of the magnetron space charge; frequency pushing and voltage tuning" (Doctoral Thesis), *Tech. Report* No. 12, Electron Tube Lab., Dept. Elec. Eng., University of Michigan; November, 1951.

[23] D. Gabor, "Energy conversion in electronic devices," *Jour. IEE*, vol. 91, pp. 128–145; June, 1944.
S. Ramo, "Currents induced by electron motion," Proc. I.R.E., vol. 27, pp. 584–585; September, 1939.
W. Shockley, "Currents induced by a moving charge," *Jour. Appl. Phys.*, vol. 9, pp. 635–636; 1938.
C. K. Jen, "On the induced current and energy balance in electronics," Proc. I.R.E., vol. 29, pp. 345–348; June, 1941.

[24] Number of spokes = n; number of anodes = N; other modes than π mode deserve discussion but are left out here in order to simplify presentation.

$$I_1 = 8Lr_c^2 f\rho_s \sin\frac{N}{2}\beta F(\alpha N R_a R_n), \tag{43}$$

where:

$$F(\alpha N R_a R_n) = \frac{\sin\frac{N}{2}\alpha'}{\frac{N}{2}\alpha}\,\frac{1}{R_a^{N/2} - R_a^{-N/2}}$$

$$\cdot\left[\frac{R_a^{2+(N/2)}}{2+\frac{N}{2}} - \frac{R_a^{2-(N/2)}}{2-\frac{N}{2}} - \frac{R_n^{2+(N/2)}}{2+\frac{N}{2}} - \frac{R_n^{2-(N/2)}}{2-\frac{N}{2}}\right]$$

and L = axial length of anodes.

$\alpha = \frac{1}{2}$ the angular width of the gap between anode segments.

In this expression the effect of the space-charge density distribution and the effect of the electrode geometry are essentially separable. The space-charge distribution appears in the factor:

$$\rho_s \sin\frac{N}{2}\beta$$

and the terms involving R_n in the remainder of the expression.

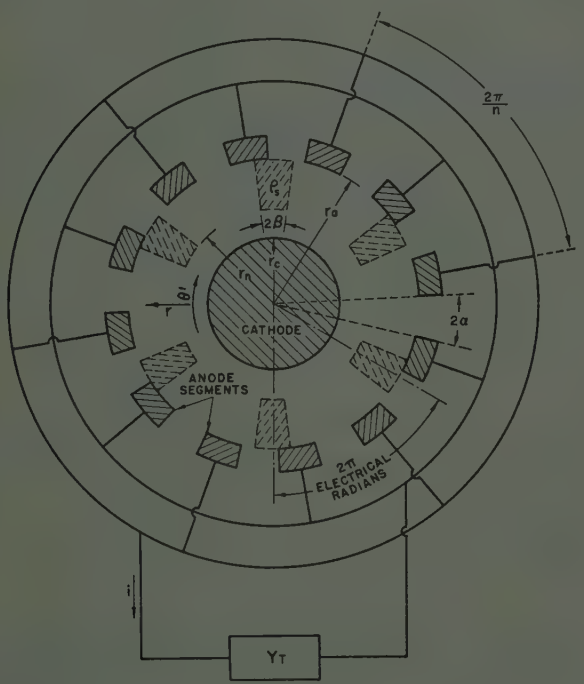

Fig. 16—Space-charge spoke configuration, electrode geometry and circuit assumed in calculation of induced current.
N = number of anode segments,
$n = N/2$.

There is little question as to the validity of the use of R_n as an inner boundary in the integration. Moreover, R_n is substantially constant for the ranges of frequencies generally encountered at constant magnetic field. On the other hand, the terms including ρ_s and β change substantially over a typical volt-ampere characteristic and bear further discussion. *It is the variation in these terms which causes the characteristics of the magnetron space charge as an induced-current generator to differ from the characteristics of a constant-current generator.*

Substituting for ρ_s from (38):

$$\rho_s \sin\frac{N}{2}\beta = \pi\rho_o\left[1 + \frac{4\epsilon_o r_c^2}{\rho_o}\,\frac{\phi_a - \phi_{at}}{R_a^2 - R_n^2}\right]\frac{\sin\frac{N}{2}\beta}{\frac{N}{2}\beta}, \tag{44}$$

but:

$$\frac{\sin\frac{\beta N}{2}}{\frac{\beta N}{2}} = \frac{\cos\theta}{\frac{\pi}{2}+\theta}, \qquad \text{[from (29)]}$$

and the rms current generated by the magnetron can be written:

$$I_g = \frac{I_1}{\sqrt{2}} = K_1\left(1 + \frac{\phi_a - \phi_{at}}{\sqrt{2}\,K K_2}\right)\frac{\cos\theta}{\frac{\pi}{2}+\theta} \tag{45}$$

$$K_1 = \frac{8}{\sqrt{2}}\pi L r_c^2 f\rho_o F(\alpha, N, R_a, R_n) \text{ amperes} \tag{46}$$

$$K_2 = \frac{\rho_o r_c^2(R_a^2 - R_n^2)}{4\sqrt{2}\,K\epsilon_o} \text{ volts.} \tag{47}$$

A convenient form for ρ_o is:

$$\rho_o = -\,8\pi\epsilon_o\frac{m}{e}\,\frac{f}{N}\left(\frac{Be}{m} - \frac{4\pi f}{N}\right). \tag{48}$$

R_n is given by (14).

$$K = \frac{\phi_f}{\phi_{RF\,max}}.$$

ϕ_f = the peak value of the fundamental traveling wave. By substituting ϕ_f/ϕ_{RFmax} for K, using:

$$\phi_{RF} = \frac{I_g}{|Y_T|} \text{ (rms)}$$

and (30), and solving for I_g we have:

$$I_g = \frac{K_1}{\frac{\frac{\pi}{2}+\theta}{\cos\theta} - \frac{K_1}{K_2}\,\frac{\cos 2\theta}{|Y_T|}}. \tag{49}$$

Frequency Pushing

If a simple parallel resonant circuit is assumed (Fig. 17) as follows:

$$|Y_T| = \frac{Y_{oc}}{Q_L}\,\frac{1}{\cos\theta},$$

where:

$$Y_{oc} = \sqrt{\frac{C}{L}}$$

and Q_L is the loaded Q of the circuit then:

$$\frac{I_g}{K_1} \cong \frac{1}{\dfrac{\dfrac{\pi}{2}+\theta}{\cos\theta} - A\cos\theta\cos 2\theta} \qquad (50)^{25}$$

$$A = \frac{K_1}{K_2}\frac{Q_L}{Y_{oc}}.$$

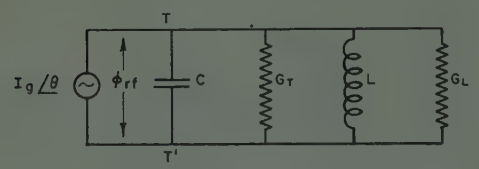

Fig. 17—Equivalent circuit for oscillating magnetron.

This relationship is plotted in Fig. 18 for various values of A against δQ_L [i.e., against frequency $\delta = (f-f_o/f_o)$]. The auxiliary equation, applicable to a simple parallel resonant circuit,

$$2\delta Q_L \cong \tan\theta \qquad (51)$$

is used.

For conventional cw magnetrons the ratio K_2/K_1 has a value of the order of 500 to 1500 ohms.

Equations for the power and anode potential can be written:

$$\frac{P_L}{G_L K_2^2} \cong A^2\cos^2\theta\left(\frac{I_g}{K_1}\right)^2, \qquad (52)$$

and

$$\frac{\phi_a - \phi_{at}}{\sqrt{2}\,KK_2} \cong A\frac{I_g}{K_1}\cos\theta\cos 2\theta. \qquad (53)$$

These equations are plotted for various conditions in Figs. 19, 20 and 21, again using (51). If it is assumed that a direct proportionality exists between power and dc anode current (as is usually the case) these curves give the expected form of the frequency pushing and volt ampere characteristics. (Compare Fig. 1a.)

Voltage Tuning

When temperature-limited conditions prevail at the cathode the total dc current cannot increase beyond a specified value as the anode potential is raised. Assuming that the dc current has reached this value, a particular phase-focusing diagram will apply (Fig. 13-2). The current generated will be given by (43).

$$I_g = \frac{I_1}{\sqrt{2}} = 8Lr_c^2 f\rho_s \sin\frac{N}{2}\beta F(\alpha, N, R_a, R_n), \qquad (54)$$

where ρ_s is undetermined. The current density through the spoke to the anode will be proportional to the temperature-limited dc anode current:

$$(\rho_s v)_n = C_1 I_T, \qquad (55)$$

I_T = temperature-limited current
C_1 = a constant
$(\rho_s v)_n$ = arrival current at the anode.

The total amount of charge collected per second is limited to I_T. An increase in anode potential, then, must increase the arrival velocity of the electrons. We may expect, therefore, that:

$$v = C_2\phi_a. \qquad (56)$$

Combining this relationship with (55), we have:

$$\rho_s = \frac{C_1}{C_2}\frac{I_T}{\phi_a}. \qquad (57)$$

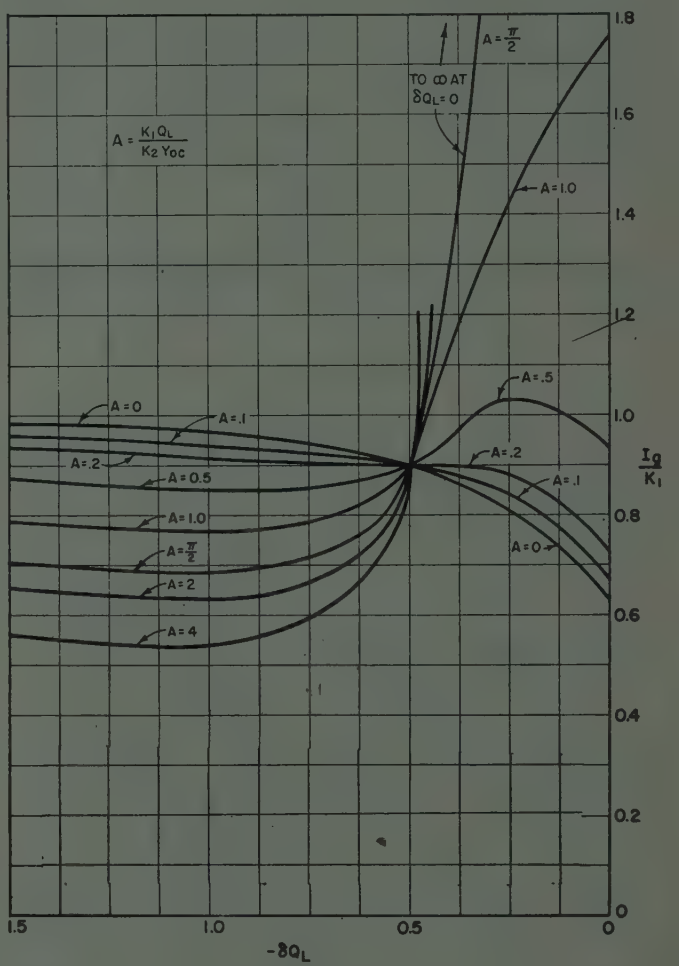

Fig. 18—Theoretically predicted current generated as a function of δQ_L from (50) and (51).

We are assuming, a priori, that the circuit conditions are such as to encourage voltage-tunable operation. We may write:

$$f \cong C_3\phi_a. \qquad (58)$$

Combining these conditions into (54) we have finally:

$$I_g = 8Lr_c^2\frac{C_3\cdot C_1}{C_2}I_T\sin\frac{N}{2}\beta F[A, N, R_a, R_n). \qquad (59)$$

[25] It is reminded that θ is conventionally negative when it represents a lagging phase angle so that $[(\pi/2)+\theta] < (\pi/2)$.

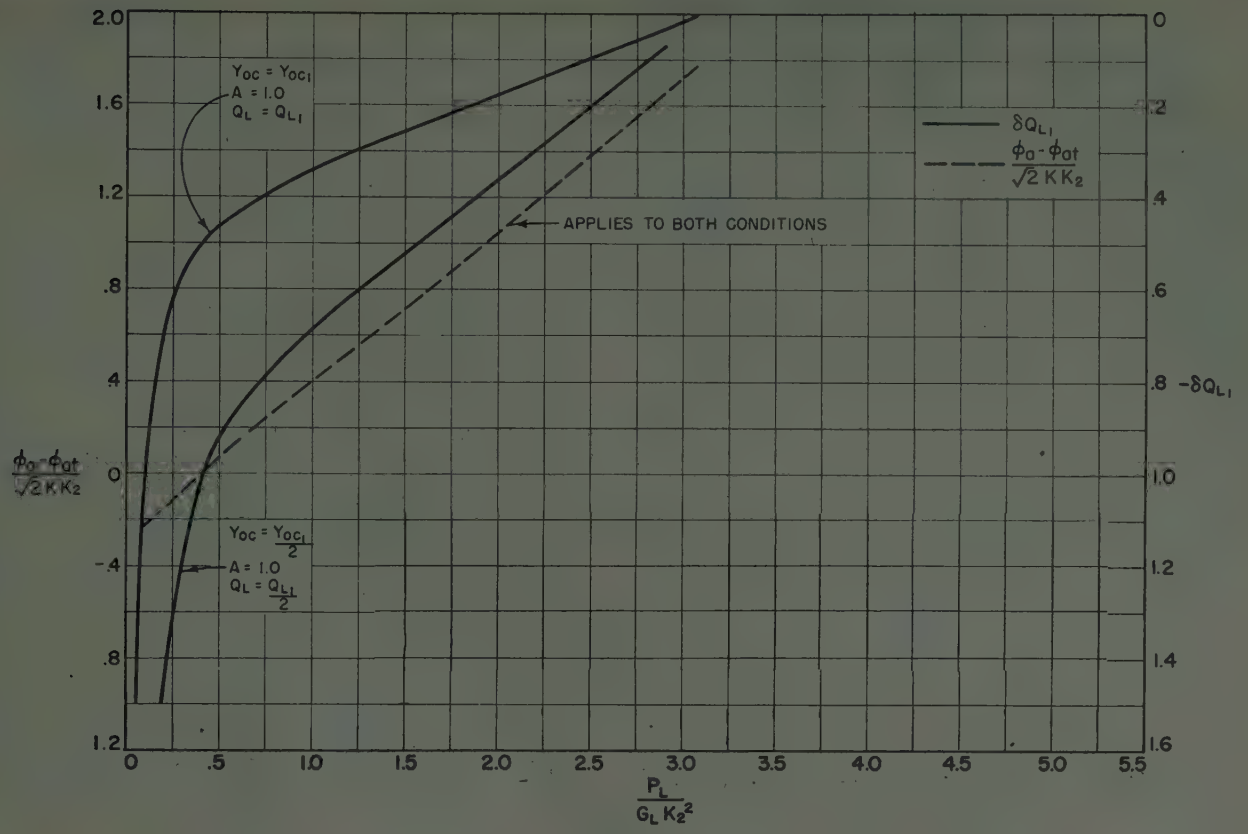

Fig. 19—Theoretically predicted form of frequency pushing curves and volt-power characteristics.

G_L = constant $Q_L = Q_{L_1}$ and $\frac{Q_{L_1}}{2}$.

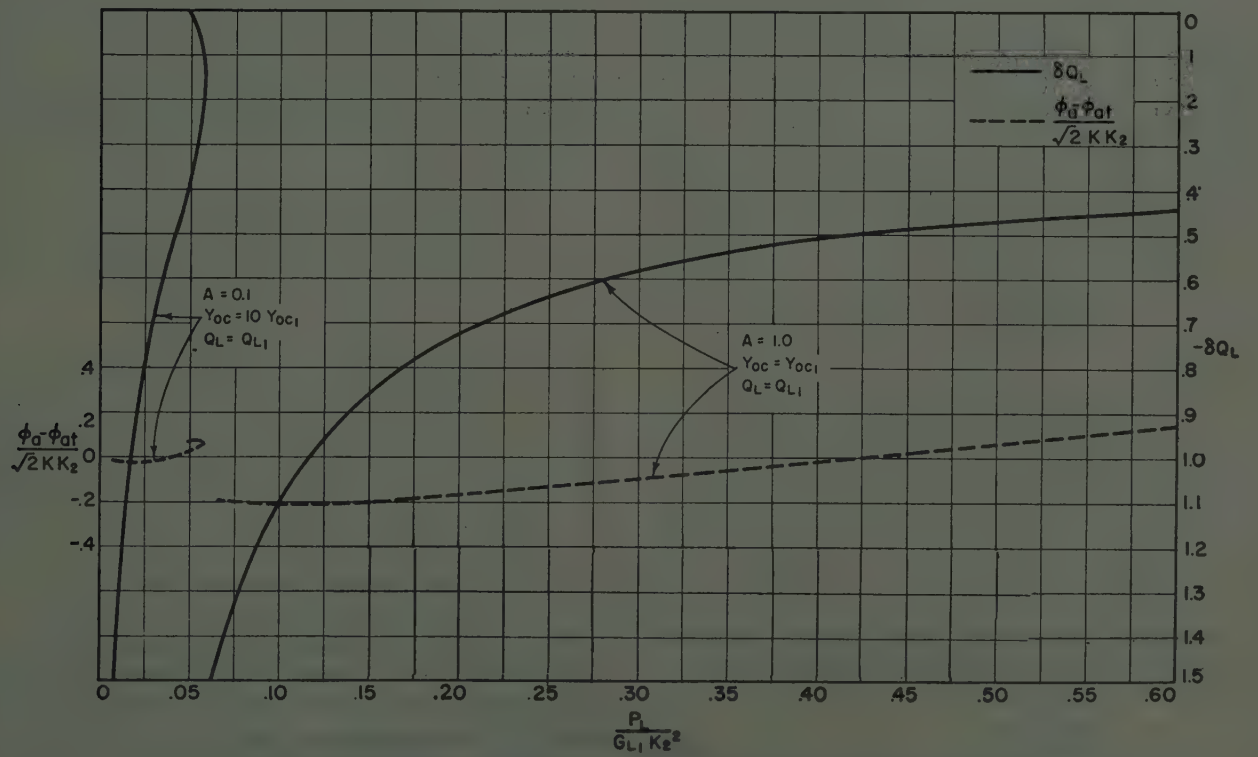

Fig. 20—Theoretically predicted form of frequency pushing curves and volt-power characteristics.

Q_L = constant $G_L = G_{L_1}$ and $10\ G_{L_1}$

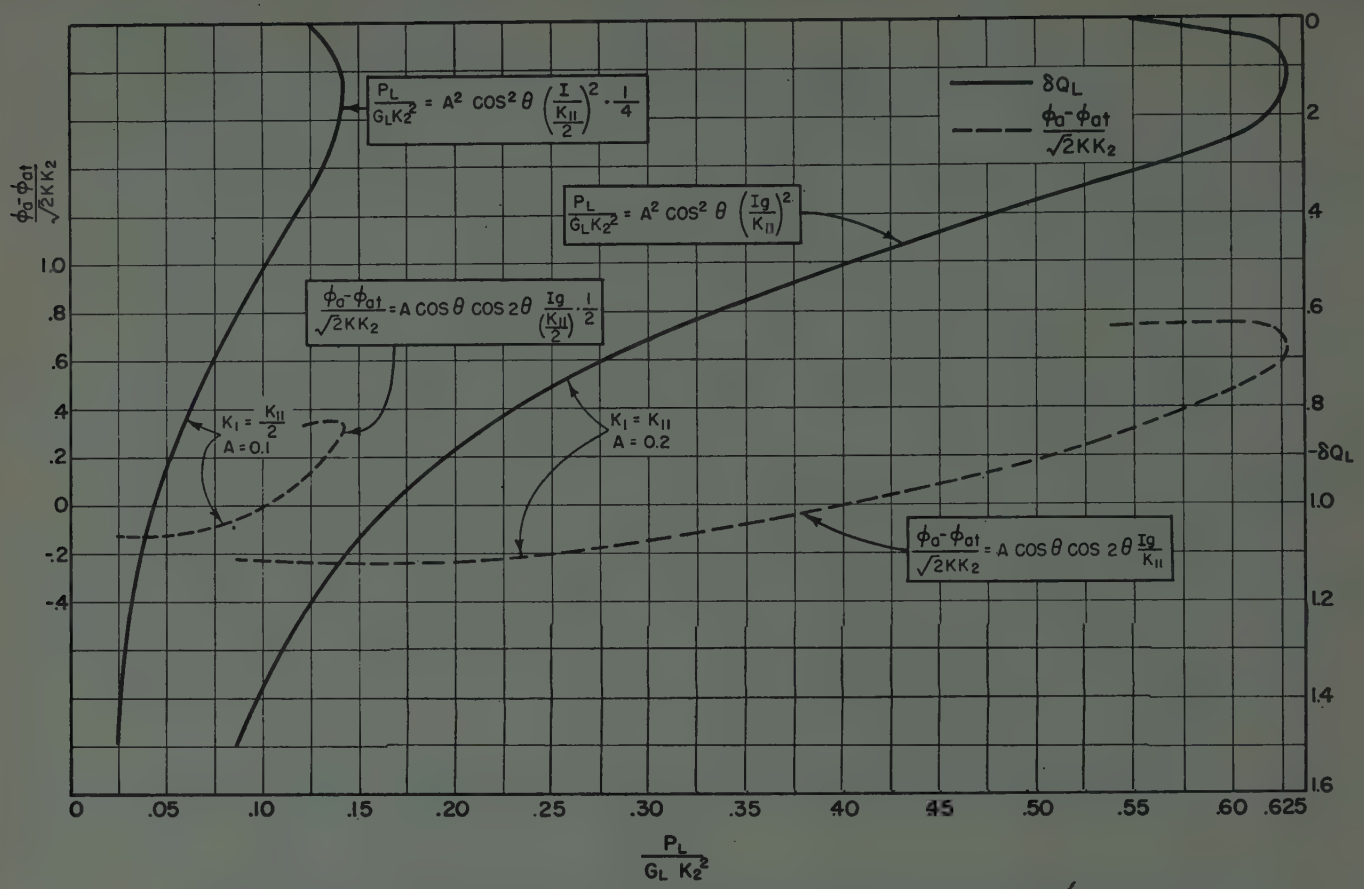
$\frac{P_L}{G_L K_2^2} = A^2 \cos^2\theta \left(\frac{I}{\frac{K_{II}}{2}}\right)^2 \cdot \frac{1}{4}$
$\frac{P_L}{G_L K_2^2} = A^2 \cos^2\theta \left(\frac{I_g}{K_{II}}\right)^2$
$\frac{\phi_a - \phi_{at}}{\sqrt{2}KK_2} = A \cos\theta \cos 2\theta \frac{I_g}{\left(\frac{K_{II}}{2}\right)} \cdot \frac{1}{2}$
$\frac{\phi_a - \phi_{at}}{\sqrt{2}KK_2} = A \cos\theta \cos 2\theta \frac{I_g}{K_{II}}$
$K_1 = \frac{K_{II}}{2}$ A = 0.1
$K_1 = K_{II}$ A = 0.2
δQ_L
$\frac{\phi_a - \phi_{at}}{\sqrt{2}KK_2}$
$\frac{\phi_a - \phi_{at}}{\sqrt{2}KK_2}$
$-\delta Q_L$
0 .05 .10 .15 .20 .25 .30 .35 40 45 .50 .55 .60 .625
$\frac{P_L}{G_L K_2^2}$

Fig. 21—Theoretically predicted form of frequency pushing curves and volt-power characteristics.

G_L=constant Q_L=constant $K_1 = K_{II}$ and $\frac{K_{II}}{2}$.

The resulting current depends on frequency through the variation of R_n in the function $F(\alpha, N, R_a, R_n)$. F varies extremely slowly with frequency. Note also that I_g is directly proportional to I_T.

The constant, C_3C_1/C_2, has not been evaluated. However, if the circuit characteristics are known, prediction of the shape of the power vs. frequency curve can be based on the fact that a constant current generator results. The general relationships:

$$P_L = \frac{I_g^2}{|Y_T|}\cos\theta, \qquad \phi_{RF} = \frac{I_g}{|Y_T|} \tag{60}$$

can be used.

The voltage-tuning curve can be predicted using the definition of the synchronism velocity (1), the threshold potential (25) and the expression relating anode potential to the threshold potential:

$$\frac{\phi_a - \phi_{at}}{\sqrt{2}\,K\phi_{RF}} = \cos 2\theta \qquad \text{[from (30) and (31)]}.$$

The resulting relationship is:

$$\phi_a = \sqrt{2}\,K\cos 2\theta\,\frac{I_g}{|Y_T|} + \frac{\pi B}{n} r_c^2 f(R_a^2 - 1) - 2\pi^2 \frac{m}{e}\frac{r_c^2}{n^2} R_a^2 f^2. \tag{61}$$

Equation (61) presents a strictly linear relationship between anode potential and frequency only for the conditions that:

(1) I_g, θ, $|Y_T|$ are not frequency dependent; and
(2) the f^2 term is negligible, i.e., for relatively large magnetic fields.

The first condition also makes the power, given by (60) a constant. These ideal conditions are illustrated in Fig. 22.

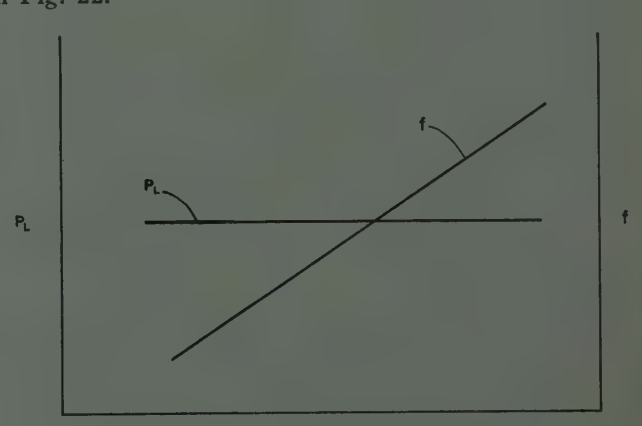

Fig. 22—Ideal voltage tuning characteristics.

Equation (61) is general if (24) is used rather than (25) for the threshold potential, thus including the energy of radial velocities.

A lagging phase angle of the order of $-20°$ to $-50°$, and a high input impedance, are desirable to achieve good phase focusing. A circuit which has these characteristics, as well as a constant admittance over a wide fre-

quency range, is difficult to achieve, since the magnetron anodes present a capacitance (a leading phase angle to the interaction space). It is necessary, therefore, to add inductance in parallel and work well below resonance. This is under investigation at the University of Michigan Laboratories by Mr. J. A. Boyd and Dr. J. S. Needle.

Conclusions

Frequency pushing and voltage tuning can be distinguished by the general statements: Frequency pushing is a relatively small variation in frequency associated with a large change in phase-position of the space charge spoke. It may be expected when the phase angle of the circuit external to the magnetron varies rapidly with frequency (in a resonant circuit). Voltage tuning is a large variation in frequency associated with little or no change in phase position of the space charge spokes. It may be expected when the phase angle of the circuit does not vary, or varies slowly with frequency (in a nonresonant circuit). Frequency pushing is characteristic of space-charge-limited operation; the radio-frequency current induced in the external circuit varies (generally increases) as power output and frequency are increased. Voltage tuning is characteristic of operation with limited dc current (generally temperature limited); the current induced in the external circuit is essentially constant, i.e., the magnetron acts as a constant current generator.

The author has studied pushing characteristics on numerous cw magnetrons constructed by Litton Industires and Raytheon Manufacturing Company and in the University of Michigan Laboratory. Voltage tuning characteristics have been available from the General Electric Research Laboratories and from the author's associates, Mr. J. A. Boyd and Dr. J. S. Needle. The complete check of the theory presented here against experiment requires complete and accurate information on the admittance characteristics of the magnetron circuit and accurate knowledge of the magnetic field intensity during the experiment. The latter knowledge is particularly important in the checking of (30),

$$\phi_a = \phi_f \cos 2\theta + \phi_{at} \tag{30}$$

since ϕ_{at} is linearly related to the magnetic field B and $(\phi_a - \phi_{at})/\phi_{at}$ is of the same order as $\Delta B/B$ where ΔB is the expected deviation in magnetic field from a precalibrated value of B for a given magnet current due to hysteresis. The threshold for Hartree potential is frequently observed not to coincide with predicted value.[26] The term $\phi_f \cos 2\theta$ in (30) above predicts the difference between operating anode potential and the threshold (or Hartree) potential ϕ_{at}. Very large errors in correspondence of measured and predicted θ are thus introduced using an incorrect value of the threshold potential.

Where sufficiently complete data were available comparisons of theory and experiment have been made. Detailed discussion of experimental results is beyond the scope of this paper. The points of theory which have been confirmed by experimental results are the following:

a. The magnetron oscillates at frequencies below resonance.[27]

b. At approximately one-tenth of the maximum, power generated the magnetron will operate between $(2/Q_L)f_o$ and $(1/2Q_L)f_o$ megacycles below resonance. The range of operation is from this point to between $f_o/2Q_L$ below resonance and f_o.[27]

c. The form of the pushing curve predicted by the theory is a good approximation of the observed form. This is significant since the form predicted, assuming a constant current generator, is not a good approximation. The characteristics of the current generator which are predicted, therefore, alter the resulting pushing curve in the right direction.[27]

d. The criteria favorable to voltage tuning are correctly predicted. The voltage tuning frequency characteristic itself is predicted by (61).[28] Condition (1) described in connection with this equation is not so readily obtained. The power characteristic depends on the determination of the constants C_1, C_2, and C_3 in (59). This remains to be accomplished.

Experimental checks of the power levels predicted by the theory of pushing are in question since the approximations made in considering particular magnetron circuits are questionable. After consideration of the theoretical approach the conclusion is that the weakest point is in the calculation of the space-charge density. The shape of the curves for I_a/K_1 in Fig. 18 is also sensitive to the variation of space-charge density with anode potential and should be considered subject to this limitation in the comparison with experimental results.

The general conclusion is that the theory offers a reasonably accurate approach to the prediction of frequency characteristics of magnetrons and that the theory is partially confirmed experimentally if a relative power scale is used rather than an absolute power scale. The very critical relationship between the quantity $\phi_a - \phi_{at}$ and magnetic field makes difficult the experimental confirmation of the relationship between anode potential and frequency. However, as in the case of the power-frequency characteristic, the form of the curve, i.e., the change in voltage expected between two given frequencies, can be determined.

Acknowledgments

The author is indebted to many people for their interest and assistance in the development of the concepts presented here, in particular to the following: Professor W. G. Dow, Dr. J. S. Needle and Mr. Gunnar Hok of the University of Michigan; Mr. J. F. Hull of Evans Signal Laboratory; Dr. D. A. Wilbur and Mr. P. H. Peters of General Electric Research Laboratories; Mr. W. C. Brown and Mr. E. C. Dench of Raytheon Manufacturing Co.; and Dr. J. S. Donal of RCA Laboratories.

[26] O. Doehler, *loc. cit.*, pp. 173–174. Note discrepancy in Fig. 1a.

[27] Compare Figs. 1a, 2 and 18 through 21.

[28] The straight line through the experimental points in Fig. 1b is plotted from this equation. The first term is negligible. $R_a = 5/3$, $r_c = 1.9$ mm, $n = 6$. In some cases the effects of radial velocities may become appreciable.

The Hyperbolic Transmission Line as a Matching Section*

HERBERT J. SCOTT†, SENIOR MEMBER, IRE

Summary—**A concentric matching section in which the characteristic impedance of the section varies along the section as a hyperbolic function provides a matching section which is relatively insensitive to frequency change. The performance of the line is described in terms of its reflection coefficient. Two lines are considered, one of which has a characteristic impedance which varies as a hyperbolic tangent along the section, the other line has postulated a reflection per unit length of the form of a hyperbolic secant squared.**

Introduction

IN ANY TRANSMISSION LINE the voltage and current along the line are described by the differential equations:

$$dV/dx = -ZI \tag{1}$$

$$dI/dx = -YV, \tag{2}$$

where:

V = the voltage across the line
I = the current in the line
Z = the series impedance per unit length of line
Y = the shunt admittance per unit length of line

all of these being functions of position on the line.

Separation of variables in (1) and (2) results in the well known voltage equation

$$\frac{d^2V}{dx^2} - \frac{1}{Z}\cdot\frac{dZ}{dx}\cdot\frac{dV}{dx} - ZYV = 0, \tag{3}$$

which may also be written:

$$\frac{d^2V}{dx^2} - \frac{d(\ln Z)}{dx}\cdot\frac{dV}{dx} - ZYV = 0. \tag{4}$$

Similarly, the current equation is:

$$\frac{d^2I}{dx^2} - \frac{d(\ln Y)}{dx}\cdot\frac{dI}{dx} - ZYI = 0. \tag{5}$$

Equations (4) and (5) readily lend themselves to solution when Z and Y are constant along the line, the solutions being the standard transmission line equations for voltage and current. When Z and Y are not constant, but instead are functions of position along the line, the second order differential equations for voltage and current are no longer linear. Under these conditions, except for some special cases as the exponential line[1] and Bessel line,[2] (4) and (5) do not yield to solution.

Transformation to First Order Non-Linear Differential Equation

It is possible, however, to transform (4) or (5) into a first order non-linear differential equation involving the reflection coefficient. In carrying out this transformation let the following quantities be defined:

$$Z_0 = \sqrt{Z/Y} \tag{6}$$

$$\gamma = \sqrt{ZY} \tag{7}$$

$$\rho = \frac{\frac{V}{I} - Z_0}{\frac{V}{I} + Z_0}, \tag{8}$$

where:

Z_0 = nominal characteristic impedance
γ = nominal propagation factor
ρ = voltage reflection coefficient

all of these in general being functions of position on the line.

By proper substitution of these quantities into (1) and (2) there is obtained, after some manipulation:[3]

$$\frac{d\rho}{dx} - 2\gamma\rho + \frac{(1-\rho^2)}{2}\,\frac{d(\ln Z_0)}{dx} = 0. \tag{9}$$

It is to be noted that this expression is exact and no restrictions of any kind have been imposed upon it.

Reduction to First Order Linear Differential Equation

In any *practical* matching section, one of the requirements which must be met if the matching section is to satisfy the purpose for which it is designed, is that the

* Decimal classification: R117.12. Original manuscript received by the Institute, September 29, 1952; revised manuscript received January 13, 1953.

† University of California, Berkeley, Calif.

[1] C. R. Burrows, "The exponential transmission line," *Bell Sys. Tech. Jour.*, vol. 17, pp. 555–573; October, 1938.
Harold A. Wheeler, "Transmission lines with exponential taper," PROC. I.R.E., vol. 27, pp. 65–71; January, 1939.

[2] A. T. Starr, "The non-uniform transmission line," PROC. I.R.E., vol. 20, pp. 1052–1063; June, 1932.

[3] L. R. Walker and N. Wax, "Non-uniform transmission lines and reflection coefficients," *Jour. Applied Physics*, vol. 17, pp. 1043–1045; December, 1946.
Folke Bolinder, "Fourier transforms in the theory of inhomogeneous transmission lines," PROC. I.R.E., vol. 38, p. 1354, November 1950; also Kungl. Tekn. Högsk. Handl. Stockholm, no. 48; 1951.

reflections due to any mismatch shall be small. Insofar then, as the assumption that $\rho^2 \ll 1$ is acceptable, (9) reduces to:

$$\frac{d\rho}{dx} - 2\gamma\rho + \frac{1}{2}\frac{d(\ln Z_0)}{dx} \doteq 0. \qquad (10)$$

As is customary in dealing with radio-frequency transmission line problems, it will be assumed that the line is loss-free and that the nominal propagation factor is a pure imaginary and is independent of position, i.e., $\gamma = j\beta$. Equation (10) then becomes:

$$\frac{d\rho}{dx} - j2\beta\rho + \frac{1}{2}\frac{d(\ln Z_0)}{dx} = 0. \qquad (11)$$

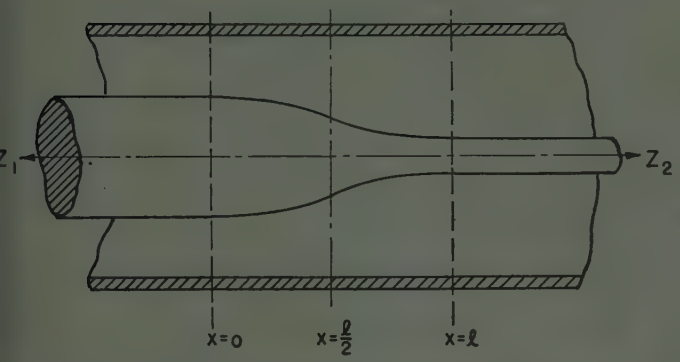

Fig. 1—Concentric matching section extending from $x=0$ to $x=l$ and terminated in impedances Z_1 and Z_2.

Application to a Line with a Given Variation of Characteristic Impedance

Consider now a non-uniform line as a matching section inserted between two transmission lines of impedances Z_1 and Z_2 respectively as indicated in Fig. 1 and presume for convenience that these terminating lines are indefinite in extent. A wave progressing from the sending end towards the receiving end of the section undergoes continuous reflection as it progresses outwards along the section. These reflections come about as a result of the continuously varying section parameters and are directed towards the sending end. When the wave arrives at the receiving end it meets an impedance match and so, without any further reflection, it passes into the uniform line beyond. As the wave travels down the uniform line, its history and performance beyond the end of the matching section are of no interest except for the realization that when $x \geqq l$ the reflections per unit length of line,

$$R(x) = \frac{1}{2}\frac{d(\ln Z_0)}{dx},$$

are zero. Under these conditions then, (11)[4] gives for the reflection coefficient at $x=0$, i.e., the sending end of the matching section:

$$\rho = \int_0^l \frac{1}{2}\frac{d(\ln Z_0)}{dx} \cdot e^{-j2\beta x} dx. \qquad (12)$$

Consider now a concentric matching section extending from $x=0$ to $x=l$, in which the impedance at the sending end is that of the connecting line Z_1 and the impedance at the receiving end is that of the connecting line Z_2 as indicated in Fig. 1. Let the nominal characteristic impedance vary as the hyperbolic tangent along the section so that

$$Z_0 = \frac{Z_2 + Z_1}{2} + \frac{Z_2 - Z_1}{2} \tanh a\left(\frac{x}{l} - \frac{1}{2}\right). \qquad (13)$$

This variation of Z_0 with x/l is shown in Fig. 2 when $Z_1 = 50$ ohms, $Z_2 = 150$ ohms, and the taper constant[5] $a = 6$.

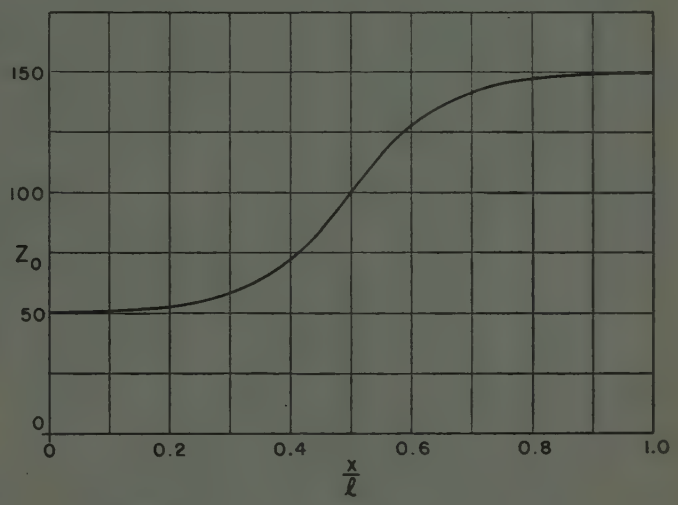

Fig. 2—Variation of

$$Z_0 = \frac{Z_2 + Z_1}{2} + \frac{Z_2 - Z_1}{2} \tanh a\left(\frac{x}{l} - \frac{1}{2}\right)$$

along the section when $Z_1 = 50$ ohms, $Z_2 = 150$ ohms, and taper constant $a = 6$.

With the variation of Z_0 as indicated in (13) there is obtained:

$$\frac{1}{2}\frac{d(\ln Z_0)}{dx} = \frac{a}{2l}\cdot\frac{Z_2 - Z_1}{Z_2 + Z_1} \cdot \frac{\operatorname{sech}^2 a\left(\frac{x}{l} - \frac{1}{2}\right)}{1 + \frac{Z_2 - Z_1}{Z_2 + Z_1}\tanh a\left(\frac{x}{l} - \frac{1}{2}\right)} = R(x), \qquad (14)$$

which upon substitution into (12) gives for ρ:

[4] Bolinder (loc. cit.) obtains the solution of (11) in terms of a Fourier integral; Walker and Wax (loc. cit.) by the substitution $\rho = e^{j\theta}$ obtain a solution for θ which is used in determining the resonant wavelengths of tapered lines.

[5] The taper constant a is chosen such that at the junction of the matching section and the line the value of the hyperbolic tangent i.e., $\tanh(a/2)$, should be essentially unity. Actually for $a=6$ it differs from unity by approximately 0.5%.

$$\rho = \frac{a}{2l}\cdot\frac{Z_2 - Z_1}{Z_2 + Z_1}\int_0^l \frac{\operatorname{sech}^2 a\left(\frac{x}{l} - \frac{1}{2}\right)}{1 + \frac{Z_2 - Z_1}{Z_2 + Z_1}\tanh a\left(\frac{x}{l} - \frac{1}{2}\right)} \cdot e^{-j2\beta l(x/l - 1/2)}dx. \quad (15)$$

This integral cannot be evaluated in simple analytic form. A plot of the variable part of (14) which appears as a factor in the integrand was made and is shown in Fig. 3 as a function of

$$a\left(\frac{x}{l} - \frac{1}{2}\right).$$

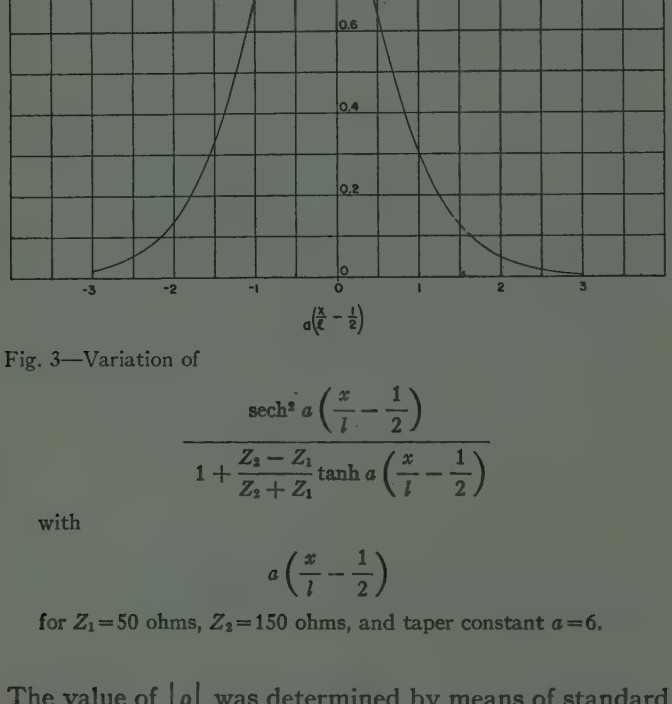

Fig. 3—Variation of

$$\frac{\operatorname{sech}^2 a\left(\frac{x}{l} - \frac{1}{2}\right)}{1 + \frac{Z_2 - Z_1}{Z_2 + Z_1}\tanh a\left(\frac{x}{l} - \frac{1}{2}\right)}$$

with

$$a\left(\frac{x}{l} - \frac{1}{2}\right)$$

for $Z_1 = 50$ ohms, $Z_2 = 150$ ohms, and taper constant $a = 6$.

The value of $|\rho|$ was determined by means of standard graphical methods. The value of $|\rho|$ thus obtained was normalized[6] and appears as a function of l/λ, the length of the matching section expressed in wavelengths and is indicated as curve (a) in Fig. 4.

Application to Line with a Given Variation in Unit Reflection

When the nominal characteristic impedance is defined as in (13) observe that the variable part of

$$\frac{1}{2}\frac{d(\ln Z_0)}{dx}$$

[6] Normalization is with respect to the value $|\rho|$ would have if the lines were directly connected with no matching section in between them.

inherently becomes skewed with respect to

$$a\left(\frac{x}{l} - \frac{1}{2}\right) = 0$$

(i.e., $x = l/2$). Suppose then that a different approach to the problem is made by starting with a symmetrical form for

$$\frac{1}{2}\frac{d(\ln Z_0)}{dx}$$

instead of with an assumed form for Z_0 and let this symmetrical form be not greatly different from the form of (14). Specifically let this be:

$$\frac{1}{2}\frac{d(\ln Z_0)}{dx} = k\operatorname{sech}^2 a\left(\frac{x}{l} - \frac{1}{2}\right). \quad (16)$$

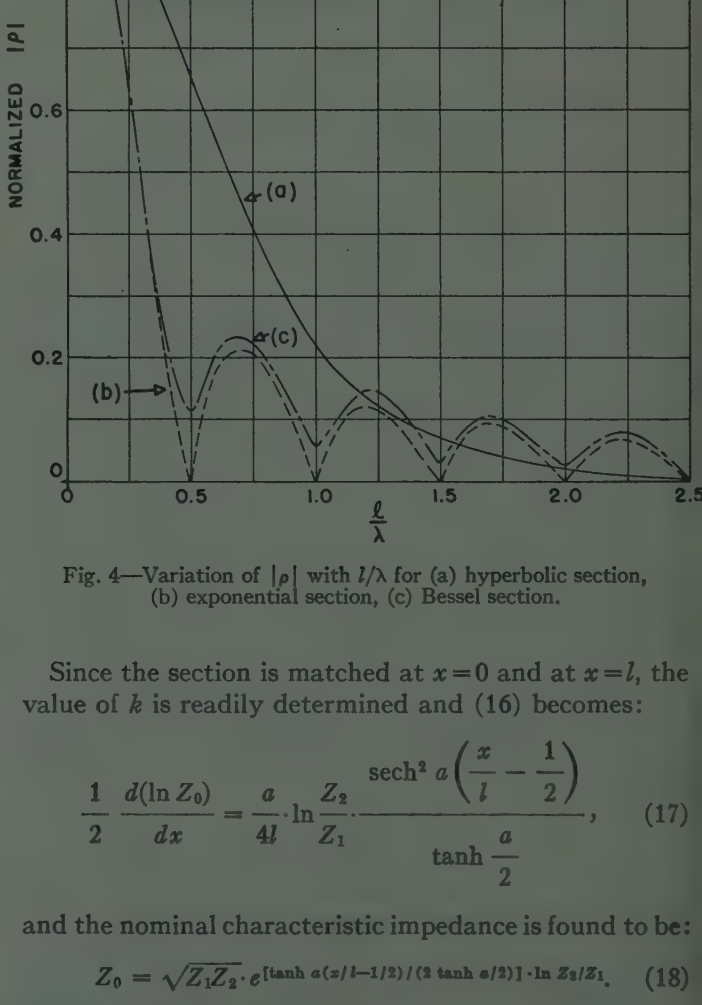

Fig. 4—Variation of $|\rho|$ with l/λ for (a) hyperbolic section, (b) exponential section, (c) Bessel section.

Since the section is matched at $x = 0$ and at $x = l$, the value of k is readily determined and (16) becomes:

$$\frac{1}{2}\frac{d(\ln Z_0)}{dx} = \frac{a}{4l}\cdot\ln\frac{Z_2}{Z_1}\cdot\frac{\operatorname{sech}^2 a\left(\frac{x}{l} - \frac{1}{2}\right)}{\tanh\frac{a}{2}}, \quad (17)$$

and the nominal characteristic impedance is found to be:

$$Z_0 = \sqrt{Z_1 Z_2}\cdot e^{[\tanh a(x/l - 1/2)/(2\tanh a/2)]\cdot\ln Z_2/Z_1}. \quad (18)$$

The variable part of (17) is shown in Fig. 5 and the resulting nominal characteristic impedance in Fig. 6. These may be compared with Figs. 3 and 2 respectively.

The resulting expression for the reflection coefficient becomes:

$$\rho = \frac{a \ln \frac{Z_2}{Z_1}}{4l \tanh \frac{a}{2}} \int_0^l \operatorname{sech}^2 a\left(\frac{x}{l} - \frac{1}{2}\right) \cdot e^{-j2\beta l(x/l - 1/2)} dx. \tag{19}$$

The normalized value of $|\rho|$ from this expression, obtained in the same manner as that for (15), is shown as curve (a) in Fig. 4.[7]

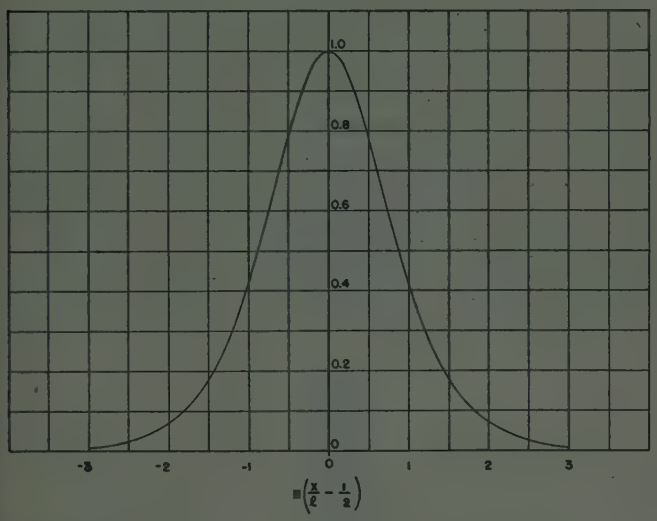

Fig. 5—Variation of

$$\operatorname{sech}^2 a\left(\frac{x}{l} - \frac{1}{2}\right)$$

with

$$a\left(\frac{x}{l} - \frac{1}{2}\right)$$

for $a = 6$.

Comparison of Reflection Coefficients

For purposes of comparison, the normalized values of $|\rho|$ for an exponential matching section and for a Bessel line are shown in Fig. 4 as curves (b) and (c) respectively. It will be noted that the undulations in $|\rho|$ present in the latter two lines are absent in the hyperbolic line. For a given length of matching section, the hyperbolic line is less frequency sensitive than either the exponential or the Bessel line. These in turn are far less frequency sensitive than a matching section composed of a length of uniform transmission line. This would indicate that the hyperbolic line is relatively broad band in its operation.

Once $|\rho|$ has been determined the voltage standing wave ratio may be evaluated from

$$VSWR = \frac{1 + |\rho|}{1 - |\rho|}. \tag{20}$$

[7] The values of $|\rho|$ obtained from (15) and (19) are so nearly the same they cannot be shown as two separate curves in this illustration.

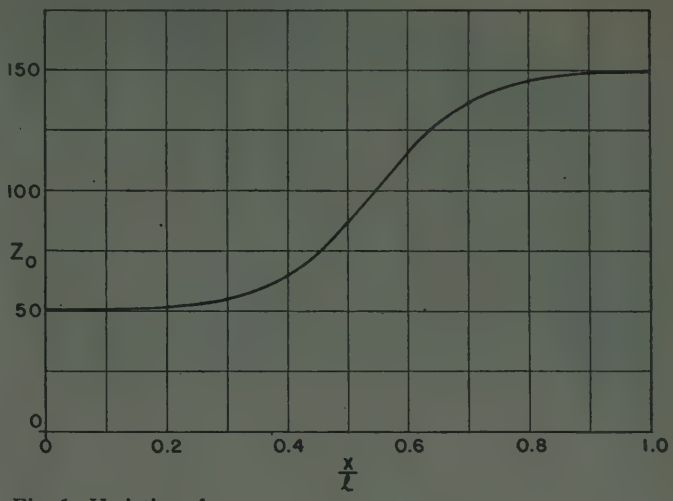

Fig. 6—Variation of

$$Z_0 = \sqrt{Z_1 Z_2} \cdot e^{[\tanh a(x/l - 1/2)]/(2 \tanh a/2) \cdot \ln Z_1/Z_2}$$

along the section when $Z_1 = 50$ ohms, $Z_2 = 150$ ohms, and $a = 6$.

Design of Matching Section

In the design of the matching section, once Z_0 is known, the conductor contour may readily be determined from:

$$Z_0 = 138 \log_{10} \frac{b}{a}, \tag{21}$$

where:

b = inner radius of the outer conductor
a = outer radius of the inner conductor.

The conductor contour for the cases considered are shown in Fig. 7. The contour for the line of (13) appears in Fig. 7a and that for the line of (18) appears in Fig. 7b.

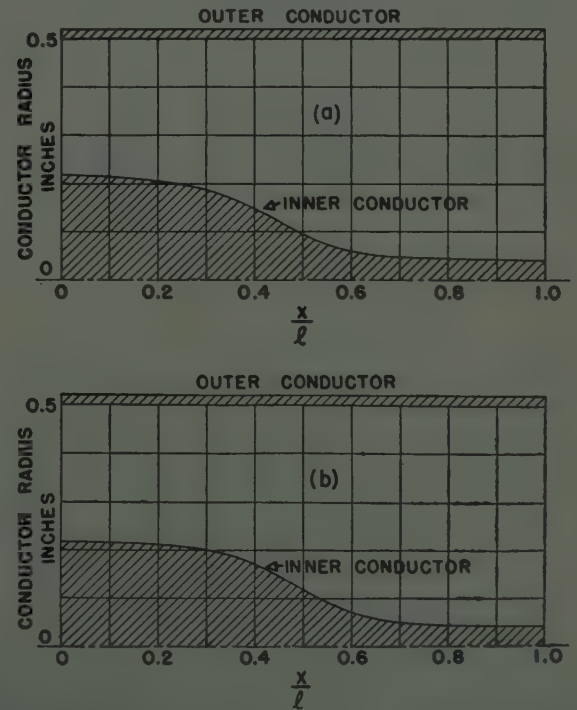

Fig. 7—Conductor contour, radius of inner and outer conductors as functions of x/l for (a) line of Fig. 2, and (b) line of Fig. 6.

Conformal Mappings for Filter Transfer Function Synthesis*

GEORGE L. MATTHAEI†, ASSOCIATE MEMBER, IRE

Summary—**In a previous paper the author outlined a general method for synthesis of filter and amplifier transfer functions by setting up fictitious electrostatic problems. This paper shows that techniques utilizing conformal mappings provide practical ways for solving these electrostatic problems. Analysis in the mapped plane also yields convenient methods for predetermining the number of poles and zeros required to meet given design specifications.**

Introduction

THIS IS ESSENTIALLY a sequel to the author's paper "Filter Transfer Function Synthesis."[1] There, the fundamental principles were presented for a method of synthesis of system transfer functions with bands approximating various constant amplitudes in an equal-ripple manner. The method made use of the electrostatic potential analogy and involved computation of flux distributions at the surfaces of fictitious charged conducting plates. The purpose of this paper is to show how the technical difficulties of determining these flux distributions may be overcome.

As we shall see, the use of a conformal mapping enables us in most cases to solve the flux distribution problem quite readily. The mapping is used to remold the original potential field in a new plane where the problem will have symmetries which make it easy to solve. After the problem is solved in the new plane, the solution is mapped back to the original plane to give the desired results.

The Elliptic-Tangent Mapping

An excellent mapping for use in solving many low-pass and high-pass filter or amplifier problems is the elliptic-tangent function mapping:

$$p = A \operatorname{tn}(w, k) = \frac{A \operatorname{sn}(w, k)}{\operatorname{cn}(w, k)}. \qquad (1)$$

Here we shall designate p as the complex frequency variable $p=\sigma+j\omega$ while $w=u+jv$ is the corresponding variable in the new plane. The functions tn (w, k); sn (w, k); and cn (w, k) are respectively the elliptic tangent, elliptic sine, and elliptic cosine functions (Jacobian elliptic functions). The parameter k is called the modulus of the elliptic function, and it will in this case be fixed by ω_1/ω_2, the ratio between the frequencies at the edges of the pass and stop band. The parameter A is merely a scale factor.[2-5]

Now let us note what this mapping does. Fig. 1 shows the potential problem for the low-pass LC filter,[1] while Fig. 2 shows this same problem after being mapped to the w-plane. We may consider the mapping process as having split the $j\omega$ axis from $j\infty$ to $j\omega_1$ and from $-j\infty$ to $-j\omega_1$ (thus slicing the stop-band plates in half); then having opened the splits by double right-angle bends at $j\omega_2$, $j\omega_1$, $-j\omega_1$, and $-j\omega_2$. In this manner the four quadrants of the infinite p-plane are mapped onto a finite rectangle of width $2K$ and height $2K'$. Herein this rectangle will be referred to as a "quasi-cell."[4] Note that each quadrant of the p-plane comprises one-quarter of this rectangle and the point at infinity has been split to appear on both the left and right side of the quasi-cell.

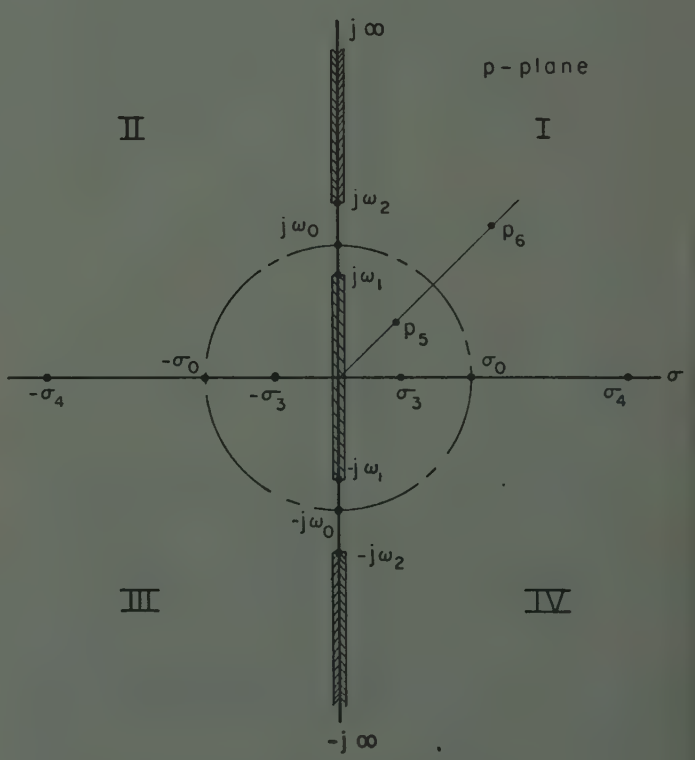

Fig. 1—The p-plane potential problem.

* Decimal classification: R143.2. Original manuscript received by the Institute, March 11, 1953.

† Elec. Eng. Div., University of California, Berkeley, Calif.

[1] G. L. Matthaei, "Filter transfer function synthesis," Proc. I.R.E., vol. 41, pp. 377–382; March, 1953.

[2] P. Franklin, "Methods of Advanced Calculus," McGraw-Hill Book Co., N. Y., chap. VII; 1944.

[3] K. Knopp, "Theory of Functions," Dover Publications, N. Y., part II; 1947.

[4] E. T. Whittaker and G. N. Watson, "Modern Analysis," Cambridge University Press; 1950. (For definition of mathematical term "cell," see p. 430.)

[5] E. Jahnke and F. Emde, "Tables of Functions," Dover Publications, N. Y.; 1945.

It is a property of conformal mappings that they only distort a surface; they do not tear it. Let us call this the "continuity property." Due to this property the quasi-cell in Fig. 2 will not exist by itself, but is surrounded by similar quasi-cells oriented in various ways so as to provide continuity of the mapping. Fig. 3 suggests how they fit together. To see how continuity is provided note that when crossing the $j\omega$ axis in the p-plane from quadrant I we must arrive at quadrant II.

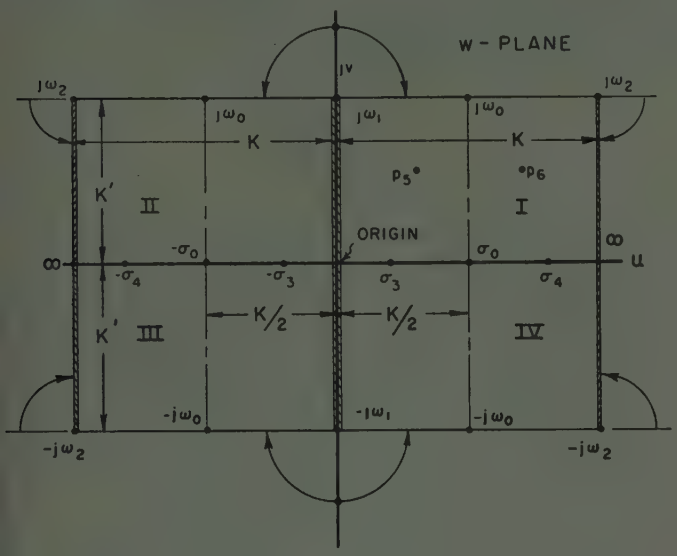

Fig. 2—The p-plane mapped to a w-plane quasi-cell.

In Fig. 3 the reader will observe that when crossing a mapping of the $j\omega$ axis from a mapping of quadrant I, we shall always arrive at a mapping of quadrant II. Because of the repetitive nature of this mapping it is known as a doubly-periodic mapping.

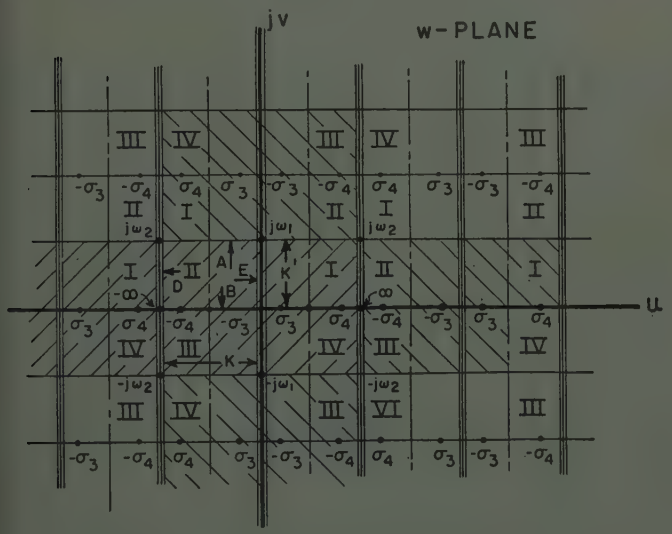

Fig. 3—A portion of the w-plane potential problem.

Perhaps we should note that technically each quasi-cell of the w-plane should be considered as mapping to a sheet which covers the entire p-plane. These sheets are joined together along the $j\omega$ axis by branch cuts. Thus the p-plane has a continuous Riemann surface composed of an infinite number of sheets.[6] However, since all sheets and quasi-cells are alike in our problem, we need study only one sheet of the p-plane and one quasi-cell of the w-plane.

To analyze the mapping quantitatively we may begin by defining the scale factor:

$$A = \omega_1. \tag{2}$$

Next let us introduce the parameter k' which is known as the comodulus. The modulus k and comodulus k' are related by the equation:

$$k^2 + k'^2 = 1. \tag{3}$$

Now the parameters:

$$k,\ k',\ K, \text{ and } K' \tag{4}$$

are all uniquely defined if any one of them is defined. (As shown in Fig. 2, K and K' are respectively the width and height of one quadrant of the quasi-cell.) For example if k' is known, k can be found by (3), and then K and K' can be found from a table of elliptic functions.[5,7,8] Most elliptic functions are not tabulated with respect to the modulus k directly but instead are referred to a modular angle defined as:

$$\theta = \sin^{-1} k. \tag{5}$$

Now the parameter k' may be defined as:

$$k' = \omega_1/\omega_2. \tag{6}$$

Thus the bandwidth ratio ω_1/ω_2 determines the parameters (4) which in turn establish the proportions of the quasi-cell rectangle. Knowing the parameters (4) and the scale factor (2) any point in the p-plane may be identified with its corresponding points in the w-plane by the relation:

$$\begin{aligned} p = \sigma + j\omega &= A \text{ tn } (u + jv,\ k) \\ &= A\left[\frac{(DB - DC^2B) + j(B^2C + D^2C)}{B^2 + D^2C^2}\right], \end{aligned} \tag{7}$$

where

$$A = \omega_1, \quad B = \text{cn } (u,\ k) \text{ cn } (v,\ k'),$$

$$C = \text{sn } (v,\ k') \text{ dn } (u,\ k), \quad \text{and}$$

$$D = \text{sn } (u,\ k) \text{ dn } (v,\ k').$$

(The function $dn\ (w, k)$ is another Jacobian elliptic function.) Along w-plane contours which are mappings of the p-plane σ and $j\omega$ axes, (7) simplifies considerably. In Fig. 2, the line defined by $jv = 0$ maps the p-plane by the relations:

[6] R. V. Churchill, "Introduction to Complex Variables and Applications," McGraw-Hill Book Co., N. Y., chap. 12; 1948.

[7] L. M. Milne-Thomson, "Jacobian Elliptic Function Tables," Dover Publications, N. Y.; 1950.

[8] G. W. Spenceley, and R. M. Spenceley, "Smithsonian Elliptic Functions Tables," Smithsonian Inst., Washington, D. C.; Nov. 1, 1947.

$$\sigma = \frac{A \text{ sn } (u, k)}{\text{cn } (u, k)}; \qquad j\omega = 0. \tag{8}$$

Similarly the line where $u=0$ maps to:

$$\sigma = 0; \qquad j\omega = jA \text{ sn } (v, k'); \tag{9}$$

the line $jv=jK'$ maps to the line:

$$\sigma = 0; \qquad j\omega = \frac{jA}{\text{dn } (u, k)}; \tag{10}$$

the line $jv=-jK'$ maps to:

$$\sigma = 0; \qquad j\omega = \frac{-jA}{\text{dn } (u, k)}; \tag{11}$$

and the lines defined by $u=\pm K$ map to:

$$\sigma = 0; \qquad j\omega = \frac{jA}{k' \text{ sn } (v, k')}. \tag{12}$$

Some Helpful Symmetries

When using the elliptic-tangent mapping a considerable amount of labor can be avoided by utilizing some symmetry properties which the mapping possesses. If a circle of radius:

$$\omega_0 = \sqrt{\omega_1\omega_2}, \tag{13}$$

is drawn in the p-plane (Fig. 1), then this circle will map to straight lines down the centers of the w-plane quasi-cell quadrants as is shown in Fig. 2. Now suppose that the points σ_3 and σ_4 are arranged so as to have geometric symmetry with respect to the p-plane circle, i.e., they are arranged so:

$$\sigma_3\sigma_4 = \sigma_0^2, \tag{14}$$

then these points will map to the quasi-cell so as to have arithmetic or mirror symmetry about the centerline through the quadrants. Consider points p_5 and p_6 on the radial line from the origin in Fig. 1. We shall regard these points as being arranged with geometric symmetry with respect to the circle if:

$$|p_5||p_6| = \omega_0^2. \tag{15}$$

Note that in Fig. 2 these points have mapped so as to have mirror symmetry about the quadrant centerline. In general we may state: *Any points in the p-plane arranged so as to have geometric symmetry with respect to the circle of radius* $\omega_0=\sqrt{\omega_1\omega_2}$ *about the origin will map to the w-plane quasi-cells so as to have mirror symmetry about the straight lines which are the mappings of the circle.*

If we have a rational function $F(p)$ with poles and zeros arranged with even mirror symmetry about a line (i.e., for every zero on one side of the line there is another at the image point on the other side, and likewise for the poles) then by reasoning from the electrostatic potential analogy it can be shown that if p_1 and p_2 are symmetrical points about the line of symmetry,

$$F(p_1) = \overline{F(p_2)}e^{j\psi}. \tag{16}$$

Here $\overline{F(p_2)}$ denotes the conjugate of $F(p_2)$, and ψ is a constant angle (usually zero in practical cases) which depends on the nature of the constant multiplier of the rational function. Similarly if the poles and zeros of $F(p)$ are arranged so as to have odd mirror symmetry about a line (i.e., for every zero on one side of the line of symmetry there is a pole at the symmetrical point on the other side), then it can be shown that if p_1 and p_2 are symmetrical points and if p_0 is any point on the the line of symmetry,

$$F(p_1) = \frac{|F(p_0)|^2}{\overline{F(p_2)}}. \tag{17}$$

The elliptic-tangent function mapping shows that any function having even or odd geometric symmetry with respect to a circle can be mapped to a plane where it will appear with even or odd mirror symmetry with respect to straight lines. Thus we see that (16) and (17) will also apply for functions having even or odd geometric symmetry with respect to a circle of radius $|p_0|$ about the origin. In this case, p_1 and p_2 will be points having geometric symmetry with respect to the circle and p_0 is any point on the circle.

The upshot of the preceding phenomena is that if a function has either mirror or geometric symmetry and if the function is defined on one side of a contour of symmetry, it is defined implicitly on the other side also. Because of this, when synthesizing the $H(p)$ functions[1] after finding the locations of the poles and zeros which lie within a quarter-circle, the rest can be located by use of the symmetry properties.

The LC Filter Potential Problem

Let us consider Fig. 1 as representing the LC filter potential problem.[1] The conducting plate in the pass band carries eight units of negative charge while each of the two stop band plates carries four units of positive charge. To be mathematically correct we should consider this potential problem as being set up on each sheet of the p-plane Riemann surface. Then each sheet of the p-plane maps to one quasi-cell of the w-plane as shown in Fig. 3. The plates from the infinite number of p-plane sheets are mapped together in the w-plane so as to form an infinite number of parallel plates which are infinitely long. Each quasi-cell has eight units of positive and negative charge associated with it, and due to the symmetrical arrangement of the plates, this charge is evenly distributed giving a uniform flux variation at the surfaces of the plates. Using the double-charge quantization procedure described elsewhere in the literature,[9] the quantized filaments or poles and zero in the w-plane will appear as in Fig. 4.

[9] G. L. Matthaei, "Filter transfer function synthesis," Proc. I.R.E., vol. 41, p. 380 (Fig. 8); March, 1953.

Observe that the array of poles and zeros in Fig. 4 has a continuous repetition of odd mirror symmetry in the horizontal direction and even mirror symmetry in the vertical direction. This will cause the corresponding p-plane function to have odd geometric symmetry with respect to the circle of radius ω_0 and even mirror symmetry with respect to the real and imaginary axes. Thus by mapping the w-plane double-zeros which occur at $w=jv=jv(1/4)K'$ and $w=jv=j(3/4)K'$ to the p-plane by use of (9), the entire $H(p)$ function is quickly found by virtue of the symmetries. Having found the $H(p)$ function the remainder of the transfer function synthesis proceeds as described.[1]

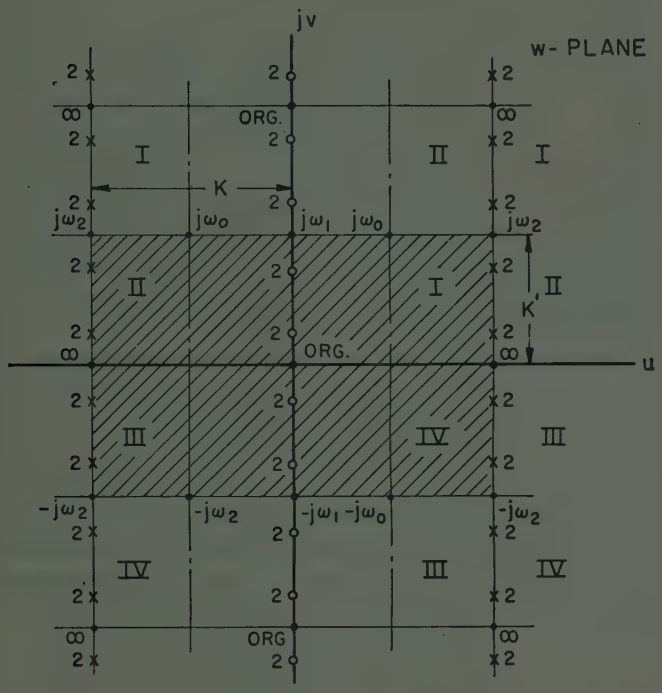

Fig. 4—Part of the infinite array of poles and zeros of the function $H'(w)$ for an LC filter example.

Solution of RC Filter Potential Problem

This time let us discuss the solution of the RC filter potential problem.[9] There is a small degree of freedom available to us in the locating of real-axis poles and zeros. They must be located so as to yield a maximum number of saddle points on the real axis, and if in addition they are located with odd geometric symmetry with respect to the circle of radius $\sigma_0=\omega_0=\sqrt{\omega_1\omega_2}$, a great deal of labor can be saved. Let us imagine that in Fig. 1 of this paper there are unit filaments of positive charge at $\pm\sigma_3$ and unit filaments of negative charge at $\pm\sigma_4$, where $\sqrt{\sigma_3\sigma_4}=\sigma_0$. If the pass-band plate has four units of negative charge and the two stop-band plates each have two units of positive charge, this will be the RC filter potential problem.[1]

When our RC filter potential problem is mapped to the w-plane, the pass- and stop-band plates will once again map into an infinite set of parallel plates. However, this time there will be positive filaments between the plates at the points which are mappings of $\pm\sigma_3$ and negative filaments at the points which are mappings of $\pm\sigma_4$. It appears that this problem is most easily solved in two steps: First, all of the plates are grounded and the flux distribution at the surfaces of the plates due to induced charge is determined; second, the induced flux distribution caused by the presence of the charged filaments having been accounted for, the remaining part of the flux at the surface of the plates will be distributed like the flux field between charged plates without filaments, and this flux is easily determined. Due to the repetitive symmetries of the potential problem in Fig. 3, it will suffice to solve the quantization problem in one quadrant of one quasi-cell.

To solve the grounded-plate problem we shall use a "simulating function" which will imitate the effects of the boundary conditions and filaments associated with one quadrant of a quasi-cell. Note that in Fig. 3 the boundaries of the quadrant II marked by arrows A and B are lines of even symmetry, and hence will be lines of constant flux. The boundaries marked by arrows D and E are contours of constant potential (grounded plates), and hence can be simulated by a line of odd symmetry since a line of odd symmetry will be a line of constant potential. This potential field can therefore be represented by the logarithm of the array of poles and zeros in Fig. 5. For the representation to be exact this array of poles and zeros should continue on symmetrically out to infinity. Such an array can be achieved by use of elliptic functions; however, excellent results can be obtained by use of only a few chains of poles and zeros constructed from trigonometric functions.[10] The function:

$$g(w)=\frac{\sin\left[(\pi/K)(w-s)\right]\sin\left[(\pi/K)(w-s-j2K')\right]}{\sin\left[(\pi/K)(w+s)\right]\sin\left[(\pi/K)(w+s-j2K')\right]}\times\frac{\sin\left[(\pi/K)(w-s+j2K')\right]}{\sin\left[(\pi/K)(w+s+j2K')\right]},\qquad(18)$$

yields the three chains of poles and zeros shown in Fig. 5, and by the electrostatic potential analogy it can be seen that the equation:

$$V_g+j\phi_g=\ln\left|g(w)\right|+j\arg g(w)+M,\qquad(19)$$

for values of w within the shaded region of Fig. 5 will give a very accurate approximation of the complex potential field in quadrant II when the filaments are present but the plates are grounded. In (19) V_g is the scalar potential, ϕ_g is the flux, and M is an arbitrary complex constant which determines the potential and flux zero references.

Breaking the sine functions of (18) into their real and imaginary parts, the flux at the surface of the grounded

[10] This very useful technique for approximating elliptic functions by use of trigonometric or hyperbolic functions was first introduced to this author by Mr. D. K. Weaver, Stanford Research Inst., Menlo Park, Calif.

plate at side E of quadrant II (Fig. 3) is found to be:

$$\phi_g(v) = -1\{2\tan^{-1}[-\tanh(v\pi/K)\operatorname{ctn}(s\pi/K)] + 2\tan^{-1}[-\tanh(v-2K')\pi/K\operatorname{ctn}(s\pi/K)] + 2\tan^{-1}[-\tanh(v+2K')\pi/K\operatorname{ctn}(s\pi/K)] + \text{Im } M\}. \quad (20)$$

For simplicity, the constant (Im M) is evaluated so $\phi_g=0$, and the minus-one multiplier is introduced so $\phi_g(v)$ will be positive in the region from $v=0$ to $v=K'$.

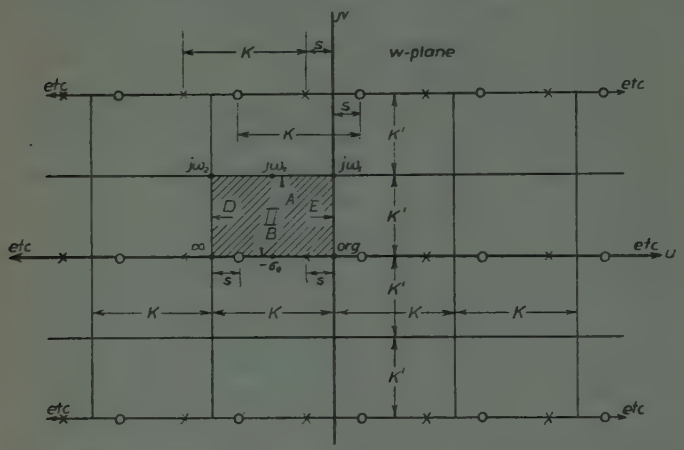

Fig. 5—Part of the array of poles and zeros of a "simulating function" used in the solution of an RC filter example.

If the ground connections are removed from the plates in Fig. 3 and if additional positive and negative charge is deposited on the stop- and pass-band plates respectively, then the total flux at the surface of the pass-band plate on side E of quadrant II will be given by the equation:

$$\phi_t(v) = \phi_g(v) + \tau v, \quad (21)$$

where τ is a constant. To evaluate τ recall that in this case the pass-band plate in Fig. 1 carries four units of negative charge and hence terminates a total of 8π lines of flux coming from the four quadrants. Thus the part of the plate bordering on quadrant II terminates 2π lines of flux. Then in the w-plane, since $\phi_t(0)=0$,

$$\phi_t(K') = \phi_g(K') + \tau K' = 2\pi, \quad (22)$$

and τ can be evaluated.

Using the single-charge quantization procedure described,[1] filaments of negative charge (or zeros) are established where $\phi_t(v)$ equals $\pi/2$ and $3\pi/2$. Since the $H(p)$ function in the p-plane will have even mirror symmetry with respect to the σ and $j\omega$ axes and odd geometric symmetry with respect to the circle of radius ω_0, we need only map to the p-plane the filaments associated with the right half of quadrant II. We can then easily find the locations of all of the poles and zeros of the $H(p)$ function by virtue of the electrostatic potential analogy and the symmetries.

Predetermination of Attenuation Ratios

Generally the fundamental design specifications which are significant in the synthesis of low-pass filter transfer functions such as those discussed are the bandwidth ratio ω_1/ω_2,[11] the allowable ripple amplitude in the pass band, and the attenuation ratio between pass and stop bands. The designer is at the outset faced with the question of how many poles and zeros will be required in order to give a transfer function which will meet the specifications. Let us see how this problem can be dealt with in our low-pass examples. The same techniques can be adapted to most any case.

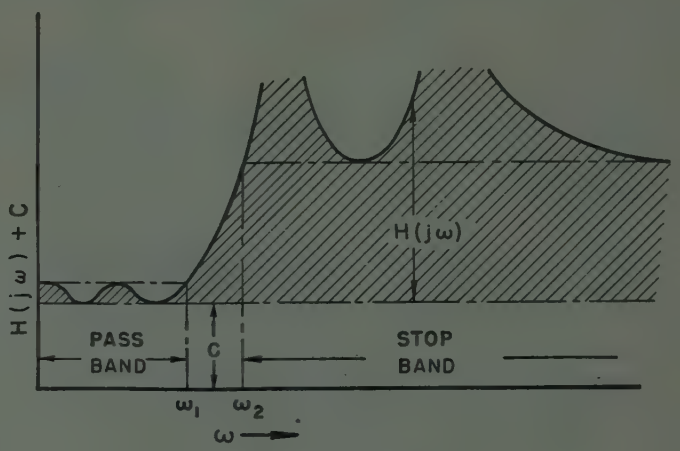

Fig. 6—The function $H(p)+C$ for $p=j\omega$.

Fig. 6 shows the function $H(p)+C$ when $p=j\omega$ for our four-pole LC filter being designed by the double-charge quantization procedure. It was noted[1] that the magnitude of the completed filter transfer function for steady-state frequencies $p=j\omega$ will in this case be:

$$|T(j\omega)| = \sqrt{H(j\omega)+C}. \quad (23)$$

Let us assume that our design specifications are given in the form of the bandwidth ratio ω_1/ω_2, the pass-band ripple ratio:

$$\rho = \frac{\text{max. amplitude in pass band}}{\text{min. amplitude in pass band}} = \sqrt{\frac{H(j\omega_1)+C}{C}}, \quad (24)$$

and the attenuation ratio:

$$\gamma = \frac{\text{min. amplitude in stop band}}{\text{min. amplitude in pass band}} = \sqrt{\frac{H(j\omega_2)+C}{C}}. \quad (25)$$

The constant C can be eliminated from (24) and (25) to give:

$$\nu = \frac{H(j\omega_2)}{H(j\omega_1)} = \frac{\gamma^2-1}{\rho^2-1}. \quad (26)$$

[11] The actual values of ω_1 and ω_2 need not be considered during synthesis since if the bandwidth ratio is correct, the scale can always be adjusted to meet the requirements of the application. During the synthesis it is convenient to let $\sqrt{\omega_1\omega_2}=\omega_0=1$.

In this manner our initial design problem becomes the problem of designing an $H(p)$ function having a bandwidth ratio ω_1/ω_2 and an amplitude ratio which will satisfy (26). If a single-charge quantization procedure is used,[12] (26) becomes:

$$\nu = \frac{H_x(j\omega_2)}{H_x(j\omega_1)} = \frac{\gamma - 1}{\rho - 1}. \tag{27}$$

When the synthesis of $H(p)$ is begun, ω_1/ω_2 is used to fix the elliptic function modulus, and ν is used to determine the number of poles and zeros which will then be required. It is easiest to determine the number of poles and zeros required by calculations in the w-plane. This is possible because, for example, a function $H'(w)$ having the infinite array of poles and zeros shown in Fig. 4 (with an appropriate constant multiplier) is related to the $H(p)$ function by:

$$H'(w) = H(A \text{ tn } (w, k)) = H(p). \tag{28}$$

Thus $H(j\omega_1)$ and $H(j\omega_2)$ can be determined by evaluating $H'(w)$ at w-plane points which are mappings of $j\omega_1$ and $j\omega_2$.

An array of double poles and zeros such as is shown in Fig. 4 can be generated exactly by use of the elliptic function $dn(w, k)$ squared. However, it is simpler to use an approximation. Note that the function cosh (w) consists of an infinite set of zeros located at intervals of pi along the $w=jv$ axis and an infinite order pole located in an essential singularity at $w=\infty$. Therefore a chain of double zeros such as appears along the line $u=0$ in Fig. 4 and a chain of double poles such as appears along the line $u=-K$ can be generated by the function:

$$\left[\frac{\cosh (n\pi w/2K')}{\cosh [n\pi(w+K)/2K']}\right]^2, \tag{29}$$

where n is an even number which designates the number of double poles and zeros in the $H(p)$ function. The function (29) approximates $H'(w)$ within a limited region, so by use of (29) we obtain:

$$\nu = \frac{H(j\omega_2)}{H(j\omega_1)} = \frac{H'(-K+jK')}{H'(jK')} \approx [\cosh (n\pi K/2K')]^4. \tag{30}$$

For cases where n is an odd number an equation analogous to (29) is constructed from hyperbolic sine functions and computation of ν yields (30), so (30) holds for n either odd or even. If a single-charge quantization procedure is used:

$$\nu \approx [\cosh (n\pi K/2K')]^2. \tag{31}$$

Knowing K, K', and ν, the number of poles and zeros required is easily determined by either (30) or (31) whichever is appropriate.

The reader may wonder how accurate (30) and (31) are. A sample $H(p)$ function having $\omega_1/\omega_2=0.7660$ and six simple poles and six simple zeros has $\nu=1{,}500$. For this example (31) yields about 1,505. Equations (30) and (31) will always be a little on the optimistic side, but their accuracy increases with either an increase in n or a decrease in ω_1/ω_2.

In the case of RC filter design things are a bit more complicated. More than one constant may be used when manipulating the $H(p)$ function; hence, equations such as (27) are only approximate though probably sufficiently close for most cases. The ratio $\nu=H(j\omega_2)/H(j\omega_1)$ can be determined by approximations similar to (30) and (31), but in this case the designer must also be careful to define the real-axis poles and zeros of $H(p)$ so that there will be a maximum number of saddle points on the real axis. The author found that these matters are easily taken care of by setting up part of $H'(w)$ in analog form on a rectangular sheet of Teledeltos paper[13] which represents one quadrant of a w-plane quasi-cell. Since the borders of each quadrant of the quasi-cells are lines of even mirror symmetry, the edges of the sheet are left open-circuited. Constant-current electrodes (corresponding to poles and zeros) placed on the paper cause a voltage field to be set up which is proportional to $\ln |H'(w)|$.[14] In this manner the number of poles and zeros required is easily determined experimentally, and the requirement that there be a maximum number of saddle points on the real axis of the $H(p)$ function resolves into experimentally adjusting the electrodes on the sheet so that the potential field on the edge which maps to the p-plane σ axis will have a maximum number of ripples of magnitude. If the accuracy required is not too high, the function $H'(w)$ may be completely determined by use of the analog, so it is then unnecessary to compute a solution for the potential problem.[15]

Mappings for Other Problems

With the aid of simulating function techniques such as were used in the RC filter example, a wide variety of low-pass and high-pass filter and amplifier problems can be solved by use of the elliptic-tangent function mapping. In many cases satisfactory band-pass or band-stop functions can be obtained from a low- or high-pass function by use of an additional mapping. For example, by mapping the poles and zeros of a low-pass filter function $T(p)$ to a new plane by use of the mapping:

$$\frac{p}{\delta} = \frac{p'}{\omega_0'} + \frac{\omega_0'}{p'}, \tag{32}$$

[12] In this case the right sides of (23), (24), and (25) will not have square roots, but the right side of (23) will require a magnitude sign.

[13] Conducting paper used in facsimile machines by Western Union Co.

[14] R. E. Scott, "Network synthesis by the use of potential analogs," Proc. I.R.E., vol. 40, pp. 970–973; August, 1952.

[15] G. L. Matthaei, "A General Method for Synthesis of Filter Transfer Functions as Applied to L-C and R-C Filter Examples," Tech. Report No. 39, Elec. Research Lab., Stanford University; August 21, 1951. (Also dissertation for the Ph.D. degree, Stanford University; October, 1951.)

a band-pass transfer function $T'(p')$ can be constructed. In (32) p' is the new complex frequency variable,

$$\delta = \frac{\omega_1 \omega_0' \omega_b'}{\omega_b'^2 - \omega_0'^2} \qquad \omega_b' > \omega_0', \tag{33}$$

and

$$\omega_0' = \sqrt{\omega_a' \omega_b'}, \tag{34}$$

where ω_1 is the pass-band edge for $T(p)$, and ω_a' and ω_b' are to be the pass-band edges of $T'(p')$. Labor can sometimes be saved by use of the fact that when $T'(p')$ is constructed in this manner it will necessarily have even geometric symmetry with respect to the circle of radius ω_0' about the p'-plane origin and even mirror symmetry with respect to the real axis.

For many problems other mappings will be more desirable than the elliptic-tangent mapping. All of the mappings of trigonometric, hyperbolic, Jacobian elliptic, and some hyper-elliptic functions have value for the solution of various different synthesis problems. Further discussion of the use of other mappings is presented, as previously described by the author.[15]

Acknowledgments

The author wishes to acknowledge many helpful suggestions received from Prof. D. F. Tuttle, Jr., of Stanford University, during the course of this research. This research was sponsored by the Office of Naval Research under contract N6-ONR-251. The topics dealt with in this sequel and in the previous paper, "Filter transfer function synthesis," are presented more fully in the report, "A General Method for Synthesis of Filter Transfer Functions as Applied to L-C and R-C Filter Examples."[15]

Complex Magnetic Permeability of Spherical Particles*

JAMES R. WAIT†

Summary—**The effective complex magnetic permeability of an array of spherical conducting permeable particles is computed. Curves are presented which illustrate the dependence of the conductivity, permeability and radius of the particle and the frequency.**

Introduction

MAGNETIC MATERIALS are used in many aspects of communication. Cores made up of a very fine powder or dust of ferromagnetic particles, with an insulating binder, are used in high-Q rf coils. It is known that the eddy-current losses are the most important and these are reduced by using small particles. Cores of dust-iron particles have also been used for low frequency loop antennas to improve their sensitivity. At microwave frequencies the magnetic properties of an artificial medium composed of an array of highly conducting metal particles are often utilized to attain a low effective magnetic permeability.

It is therefore considered desirable to discuss in a general way the magnetic properties of an array of conducting permeable spherical shaped particles embedded in a dielectric medium. Although the electromagnetic response of a sphere to a plane wave has been studied by many,[1] little effort has been expended in preparing convenient charts or curves that show the nature of the combined effect of conductivity and permeability of the particles.

* Decimal classification: R282.3. Original manuscript received by the Institute, February 13, 1953.

† Radio Physics Laboratory, Defense Research Board, Ottawa, Canada.

[1] J. A. Stratton, "Electromagnetic Theory," p. 563, McGraw-Hill Book Co., New York, N. Y.; 1941.

In this paper the theory of a single permeable conducting particle is outlined. Using this result, the effective complex permeability of an array of such particles is computed and a set of convenient curves is presented. The MKS system of units is used throughout and the fields vary with time as exp $(j\omega t)$.

Outline of Solution

It is convenient to consider first a single spherical particle of radius a, conductivity σ, dielectric constant ϵ, and magnetic permeability μ imbedded in an infinite and homogeneous dielectric medium of electrical constants ϵ_0 and μ_0. A uniform alternating magnetic field $\vec{H}_0$ is now applied to the sphere. The angular frequency ω is sufficiently low so that the dimensions of the sphere are small compared to the wavelength in the dielectric. If this condition is satisfied the secondary magnetic fields outside the sphere are expressible in terms of the equivalent magnetic dipole that is induced in the sphere. This dipole moment $\vec{M}$ is in the same direction as the applied field $\vec{H}_0$ and is in general a complex quantity.

The resultant field $\vec{H}$ is then

$$\vec{H} = \vec{H}_0 - \text{grad } \Phi, \tag{1}$$

where Φ is the magnetic potential of the induced dipole and is given by

$$\Phi = \frac{\vec{M} \cdot \vec{R}}{R^3}, \tag{2}$$

where $\vec{R}$ is the vector of magnitude R directed to the point of observation from the center of the sphere.

The expression for the dipole moment, neglecting any hysteresis effects, was given previously in a convenient form by the author.[2]

$$\vec{M} = -\vec{H}_0(p + jq)v, \tag{3}$$

where the real quantities p and q are given by

$$p + jq = -\frac{3}{2}\left[\frac{2\mu(\sinh\alpha - \alpha\cosh\alpha) + \mu_0(\sinh\alpha - \alpha\cosh\alpha + \alpha^2\sinh\alpha)}{\mu(\sinh\alpha - \alpha\cosh\alpha) - \mu_0(\sinh\alpha - \alpha\cosh\alpha + \alpha^2\sinh\alpha)}\right] \tag{4}$$

and where

$$\alpha = (j\sigma\mu\omega - \epsilon\mu\omega^2)^{1/2}a$$

and

$$v = 4\pi a^3/3. \tag{5}$$

Now if there are N such spherical particles per unit volume arranged in a cubic lattice the dipole moment m per unit volume per unit applied field is

$$m = -V(p + jq), \tag{6}$$

where $V = Nv$ is the volume of the spherical particles. The Clausius-Mossotti relation of dielectric theory[3] can now be used directly to obtain an expression for the effective complex permeability μ_e of the array of spherical particles, so that

$$\mu_e = \mu_0\left(1 + \frac{m}{1 - m/3}\right), \tag{7}$$

where μ_0 is the magnetic permeability of the matrix or binding medium. As in the completely analogous dielectric counterpart, this relation is valid not only for a cubic lattice, but also for any regular distribution of the particles that gives rise to macroscopic magnetic properties that are isotropic. It is also required that the separation of the particles be much less than a wavelength.

The effective permeability μ_e can be written in terms of a real and imaginary part as

$$\mu_e = \mu_e' - j\mu_e'' \tag{8}$$

where

$$\frac{\mu_e'}{\mu_0} = \frac{(3 + pV)(3 - 2pV) - 2q^2V^2}{(3 + pV)^2 + q^2V^2} \tag{9}$$

and

$$\frac{\mu_e''}{\mu_0} = \frac{9qV}{(3 + pV)^2 + q^2V^2}. \tag{10}$$

[2] J. R. Wait, "A conducting sphere in a time varying magnetic field," *Geophys.*, vol. 16, p. 666; October, 1951.

[3] H. Frohlich, "Theory of Dielectrics," p. 169, Oxford University Press, London, England; 1949.

For small packing of the spherical particles such that $V \ll 1$ these formulas simplify to

$$\frac{\mu_e'}{\mu_0} \cong 1 - pV, \tag{11}$$

and

$$\frac{\mu_e''}{\mu_0} \cong qV. \tag{12}$$

Discussion of Result

The quantities p and q which are functions of the conductivity, permeability, dielectric constant, and particle radius are given by (4) in terms of the hyperbolic functions with a complex argument α, for which tables are available.[4]

For applications to iron dust cores, and even for microwave lenses the conduction current in the particle is also much greater than the displacement current, that is

$$\sigma \gg \epsilon\omega$$

and therefore

$$\alpha \cong j^{1/2}A = (1 + j)A2^{-1/2}$$

where $A = (\sigma\mu\omega)^{1/2}a$. The quantities p and q are plotted as a function of A which can be called the relative radius, in Figs. 1 and 2. A wide range of values of the relative permeability, $K = \mu/\mu_0$, of the particle are chosen, and they are indicated on the curves.

It is apparent that when the relative radius A is much less than unity the conduction or eddy-current losses are very small and the magnetic flux penetrates to the center of the particles. Under these conditions the quantity p approaches its maximum negative value p_m and q becomes very small. The effective permeability then approaches its maximum value $\mu_e^{\max}$ given by

$$\mu_e^{\max} = \mu_e\Big]_{A=0} = \mu_0\left[1 - \frac{Vp_m}{1 + Vp_m/3}\right], \tag{13}$$

where

$$p_m = -3\left[\frac{\mu - \mu_0}{\mu + 2\mu_0}\right]. \tag{14}$$

or more concisely

$$\mu_e^{\max} = \mu_0\left[\frac{(\mu + 2\mu_0) + 2V(\mu - \mu_0)}{(\mu + 2\mu_0) - V(\mu - \mu_0)}\right]. \tag{15}$$

[4] A. E. Kennelly, "Tables of Complex Hyperbolic and Circular Functions," Harvard University Press, Cambridge, Mass.; 1927.

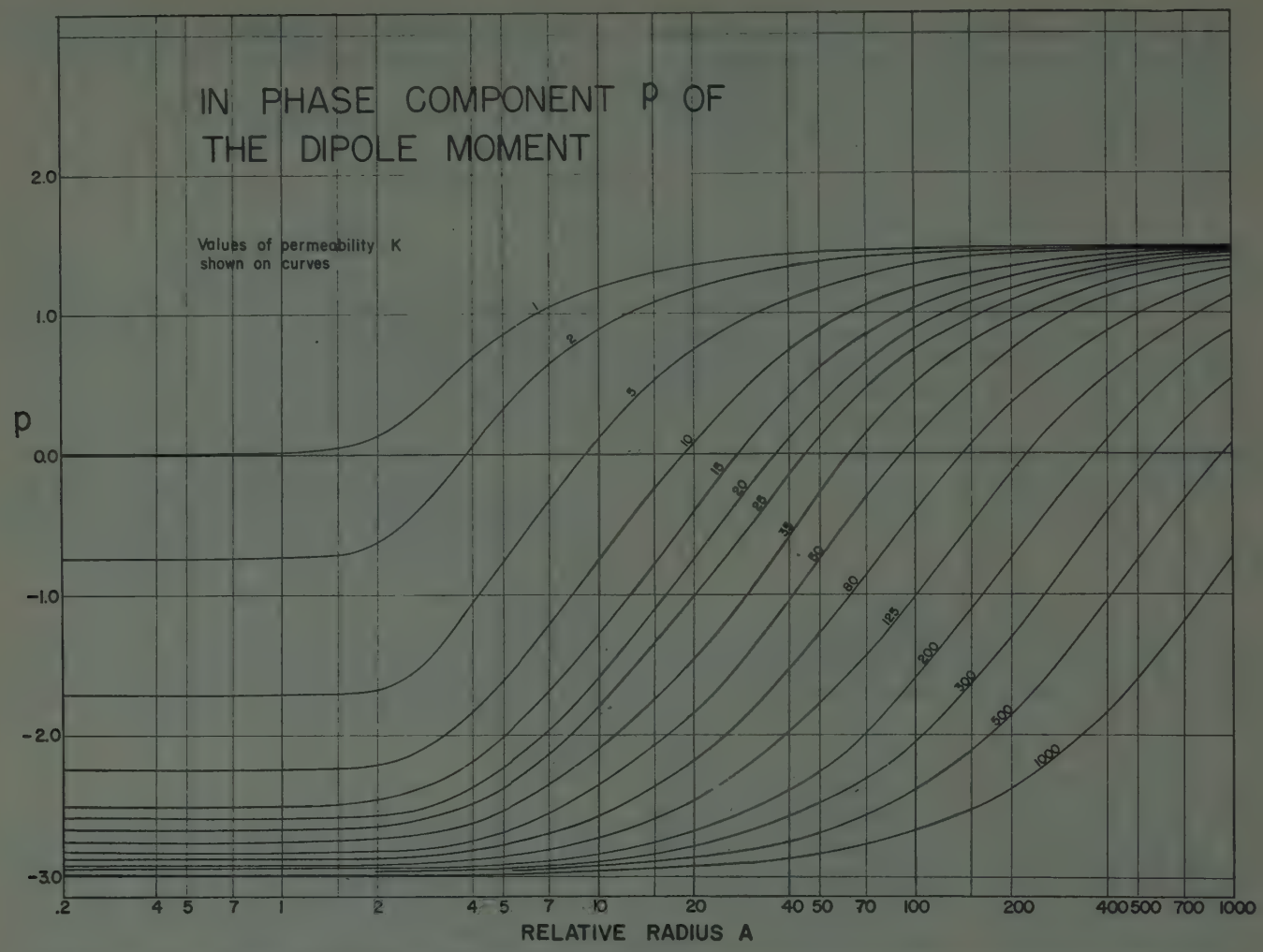

Fig. 1—The "in phase" component of the induced magnetic dipole of a conducting permeable sphere in an alternating magnetic field.

This equation is identical to the dielectric counterpart where the effective dielectric constant ϵ_e is given by (15) and the permeabilities μ and μ_0 are replaced by the respective dielectric constants ϵ and ϵ_0. Eckhart[5] has given charts for this quantity to facilitate the calculation of the dielectric constant of such mixtures. His charts can also be used for the magnetic case so long as the eddy-current losses are small, corresponding to the case $A \ll 1$.

A large effective permeability, of course, is a desirable characteristic for core materials, and if $\mu \gg \mu_0$ and V is not too near unity, then

$$\mu_e = \mu_0 \left(\frac{1 + 2V}{1 - V} \right), \tag{16}$$

which can be considerably greater than μ_0. If V is close to unity and μ is not too large then,

$$\mu_e \cong \mu.$$

For truly spherical particles this latter situation is never realized although for very tight packing of slightly non-spherical particles it is a good approximation.

When the relative radius A approaches the value of unity, the eddy currents become appreciable. These currents are out of phase with the applied field for intermediate values of A. For this reason the effective permeability of the array has a finite imaginary part. At very large values of A the flux does not penetrate the particle to any appreciable extent and the induced currents are largely on the surface. These currents are in anti-phase with the exciting field. The quantity p approaches its maximum positive value p_{0m} and q again becomes very small. The effective permeability then approaches its minimum value $\mu_e^{\min}$ given by

$$\mu_e^{\min} = \mu_e \Big]_{A=\infty} = \mu_0 \left[1 - \frac{V p_{0m}}{1 + V p_{0m}/3} \right]. \tag{17}$$

where

$$p_{0m} = 3/2$$

[5] G. Eckhart, "A dielectric constant of mixtures," *Zeits. für ange. Phys.*, vol. 4, p. 134; April, 1952.

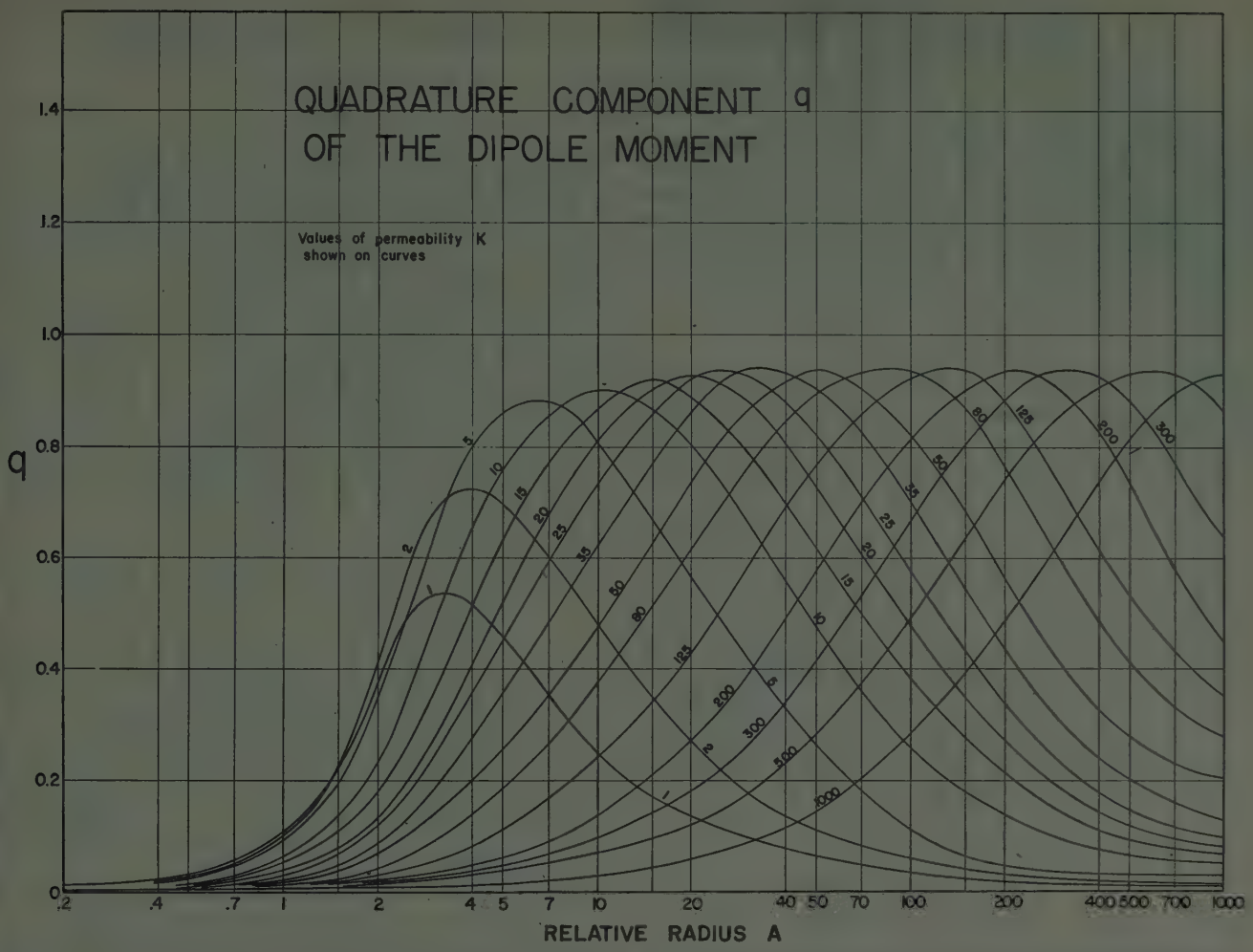

Fig. 2—The "quadrature" component of the induced magnetic dipole of a conducting permeable sphere in an alternating magnetic field.

or

$$\mu_e^{\min} = 2\mu_0\left[\frac{1-V}{2+V}\right]. \qquad (18)$$

Under these conditions the effective permeability is less than the permeability of the medium between the particles. This is often a desirable characteristic for microwave lenses.

Acknowledgment

The valuable assistance received from Mr. M. C Keating in preparing the curves is greatly appreciated.

CORRECTION

The following error in the paper, "RLC Lattice Networks," by Louis Weinberg, which appeared on pages 1139–1144, of the September, 1953 issue of the Proceedings of the I.R.E., has been brought to the attention of the editors by the author:

Page 1142, column two, sentence commencing on line eleven, should read

"Such cases are characteristic by the fact that the even function Re $[P(j\omega)]$ has all its zeros at ω equal to zero or infinity."

A Method of Band-Pass Amplifier Alignment*

J. J. HUPERT†, SENIOR MEMBER, IRE, AND A. M. RESLOCK†

Summary—**A method of alignment of band-pass amplifiers is discussed based on the oscilloscopic display of second order harmonic distortion as a function of the carrier frequency departure from the pass-band center. This method of alignment is thought particularly effective for band-pass amplifiers requiring high degree of linearity of transfer phase versus frequency function, such as for example, low-distortion FM intermediate frequency amplifiers.**

Introduction

IT IS GENERALLY KNOWN that in linear band-pass pulse amplifiers and amplitude-limited FM amplifiers linearity of transfer phase variation with frequency is required for the absence of nonlinear distortion.

Thus, the display on the oscilloscope of the amplitude function alone does not give the observer any quantitative idea as to the performance of the investigated circuit. In fact, for a given number of natural modes of the circuit, the maximally flat amplitude response, does not represent the best condition of adjustment from the point of view of distortion of transient and FM signals. It can be proved[1] that second harmonic distortion of the modulation frequency of an FM signal passing through a network can be expressed as

$$|D_2| \doteq \tfrac{1}{2}\omega_a \Delta\Omega \left|\frac{d^2\phi}{d\omega^2}\right|_{\omega=\Omega} \qquad (1)$$

where

$|D_2|$ = absolute value of the second harmonic distortion.

$\omega_a/2\pi$ = modulation frequency.

$\Delta\Omega/2\pi$ = frequency deviation.

$\left|\frac{d^2\phi}{d\omega^2}\right|_{\omega=\Omega}$ = absolute value of the second derivative of the transfer phase versus frequency function at the carrier frequency (or first deriative of the differential time delay $d\phi/d\omega$.

The above formula is valid for small $\Delta\Omega$ and for conditions of quasi-stationary operation. The phase-frequency curve and its derivatives may be computed from the frequencies and attenuations of the natural modes of the network.[1]

The authors have attempted to design a system of oscilloscopic presentation of the interstage alignment displaying the second harmonic distortion of an FM signal passing through the tested network on one axis and the carrier departure on the other. As a consequence of (1), such a display presents quantitatively the data concerning delay slope (or phase curve curvature) value in the region of frequencies of interest. Since the audio-frequency harmonic measuring apparatus is rather easily constructed, this proves an experimentally more practical method than that of displaying the transfer phase or delay. Furthermore, the quality requirements in modern FM transmission are such that significant distortions are introduced by phase characteristic curvatures which certainly could not be discerned by an oscilloscopic observation of the phase-frequency plot.

Experimental Verification of the Performance of Interstages as Compared with Theoretically Computed Data

Values of $|D_2|$ were measured for constant $\omega_a/2\pi$ (modulation frequency) and $\Delta\Omega/2\pi$ (frequency deviation) and the results plotted as a function of the carrier frequency around the center of the pass band for several typical interstages. The following precautions have to be taken in order to safeguard correct conditions of the measurements:

(*a*) The phase of the outgoing IF voltage should be formed in a stage of the chain prior to limiting.

(*b*) There should be no noticeable regeneration in the amplifier chain.

(*c*) The loading of the interstages tested should be linear (not dependent on the value of the RF or IF level).

(*d*) The contribution of the discriminator to the measured distortion should be negligible even at frequencies deviating from the crossover frequency by a value comparable to the half-bandwidth of the selective network under test.

(*e*) The distortion introduced by the network under test should predominate in the test circuit.

Fig. 1 represents the block diagram of the test circuit. The sensitivity of the RC-type amplifier is adequate to safeguard the saturation at levels available from the signal generator. The distortion introduced by elements of the demodulating circuit is insignificant. Also, the distortion introduced by the discriminator does not depend significantly on the frequency of the modulation.

On the other hand, the proportionality of the distortion data shown in Figs. 2, 3, 4, and 5 to the modulation frequency has been firmly established. Figs. 2, 3, 4, and 5 show the experimental data obtained in comparison to the theoretically computed curves. The theoretical data were obtained using

* Decimal classification: R363.12. Original manuscript received by the Institute, December 24, 1952; revised manuscript received May 19, 1953.

† A. R. F. Products, Inc., River Forest, Ill.

[1] J. J. Hupert, "A method of evaluation of the quasi-stationary distortion of FM signals in tuned interstages," *Proc. NEC* (Chicago), 1952.

$$|D_2| \doteq \frac{\omega_a \Delta\Omega}{\omega_0^2 \alpha_1^2} \left| \sum_{r=1}^{r=m} \frac{1}{\sigma_r^2} \frac{d^2}{dv_r^2} \arctan (v_r - v_{rr}) \right| \quad (2)$$

where

$\omega_a/2\pi$ = modulation frequency.
$\Delta\Omega/2\pi$ = frequency deviation.
$\omega_0/2\pi$ = frequency of the center of the pass band.
$\alpha_1 = 1/2Q_1$ = fractional attenuation associated with natural mode 1.
r = running subscript varying between 1 and the total number of natural modes of the system m.
$v_r = \Delta\omega/\omega_0\alpha_r$ normalized frequency variable.
$\Delta\omega = \Omega - \omega_0$ = difference between the angular frequencies of the carrier and the band pass center (treated as a variable).
$\sigma_r = \alpha_r/\alpha_1$.
v_{rr} = frequency of the natural mode r expressed in units of normalized frequency variable v_r.

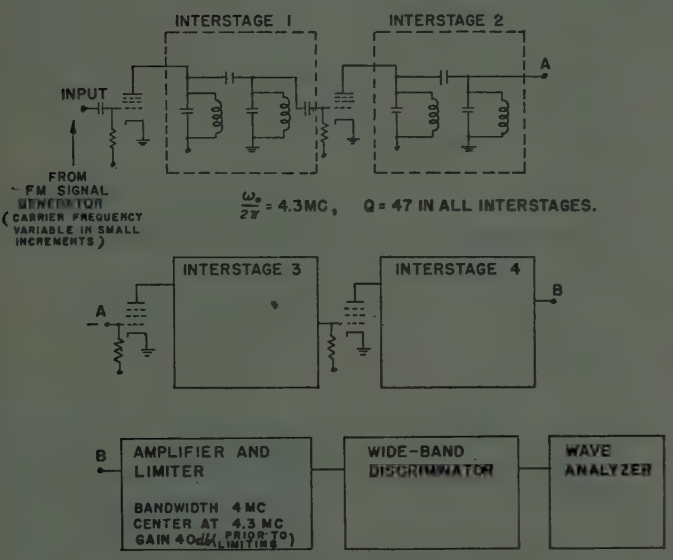

Fig. 1—Experimental circuit for the measurement of second harmonic distortion versus carrier frequency in four double-tuned interstages connected in cascade.

The formula (2) is quoted here without proof, which is given elsewhere.[1] It becomes greatly simplified in the case of a double-tuned interstage, since in that case $m=2$ and $\sigma_r=1$ for both circuits having the same Q. It can be proved that in this case $v_{11}=+kQ$ and $v_{22}=-kQ$, where k is the coupling coefficient and the Q value applied to each circuit of the double-tuned interstage individually.

For N identical double-tuned stages (2) takes the form

$$|D_2| \doteq \frac{1}{2} \frac{\omega_a \Delta\Omega N}{\omega_0^2 \alpha^2} \left| \frac{d^2}{dv^2} [\arctan (v - kQ) + \arctan (v + kQ)] \right| \quad (3)$$

where

$$v = v_1 = v_2 = 2(Q/\omega_0)\Delta\omega.$$

Figs. 2, 3, 4 and 5 show the comparison of theoretical computations with the experimental results. $|D_2|_T$ is the value calculated from (3) and (4) and plotted against $\Delta\omega$ treated as an independent variable, while $|D_2|_E$ is the result of measurements. The following data apply to the plots shown in these figures. In all figures

$$\omega_a/2\pi = 5 \text{ kc.}$$
$$\Delta\Omega/2\pi = 20 \text{ kc.}$$
$$\omega_0/2\pi = 4.3 \text{ mc.}$$
$$Q = 47.$$
$$\alpha = \frac{1}{2Q} = 0.0106.$$
$$v = 2Q\Delta\omega/\omega_0$$
$$\Delta\omega/2\pi = \frac{v(\omega_0/2\pi)}{2Q} = 45.7v \text{ (in kilocycles).}$$

The kQ data in Figs. 2, 3, 4 and 5 in individual interstages are

Fig. 2: $kQ=1$ in all four interstages.
Fig. 3: $kQ=0.6$ in all four interstages.
Fig. 4: $kQ=1.5$ in all four interstages.
Fig. 5: $kQ=0.6$ in two interstages.
$kQ=1.5$ in the other two interstages.

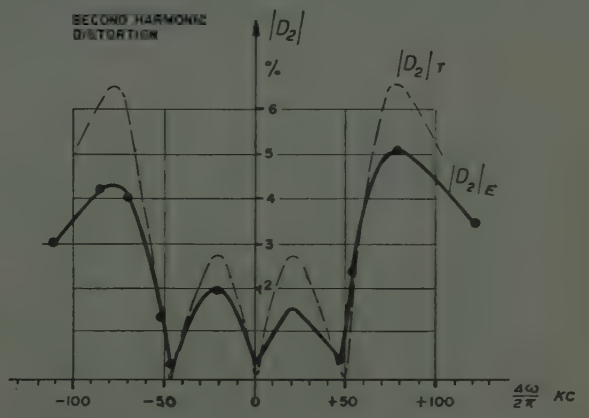

Fig. 2—Theoretical and experimental data. Four interstages of $kQ=1$ connected in cascade.

Since in the alternative of Fig. 5 there are two pairs of identical stages connected in cascade we have in this particular case

$$|D_2| \doteq \frac{\omega_a \Delta\Omega}{\omega_0^2 \alpha^2} \left| \frac{d^2}{dv^2} [\arctan (v - 1.5) + \arctan (v + 1.5) + \arctan (v - 0.6) + \arctan (v + 0.6)] \right|. \quad (4)$$

Fig. 2 depicts the case of four maximally flat (in amplitude) interstages. Fig. 3 represents the case of four stages maximally flat in delay. The reader will notice that in this case not only $|D_2|$, a value proportional to the first derivative of the delay, vanishes at the origin but that $d|D_2|/d\omega$ vanishes as well—which fact is a criterion of the maximal delay flatness. The conventionally used oscilloscopic alignment method showing the amplitude transfer versus frequency is not capable of showing the condition of maximum flatness of delay.

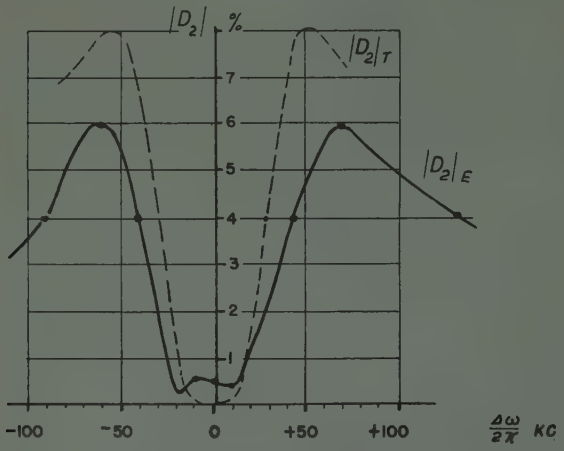

Fig. 3—Theoretical and experimental data. Four interstages of $kQ=0.6$ connected in cascade.

In all figures showing the results of the experiments there is a general agreement of expected shape and of positions of expected maxima and minima of distortion.

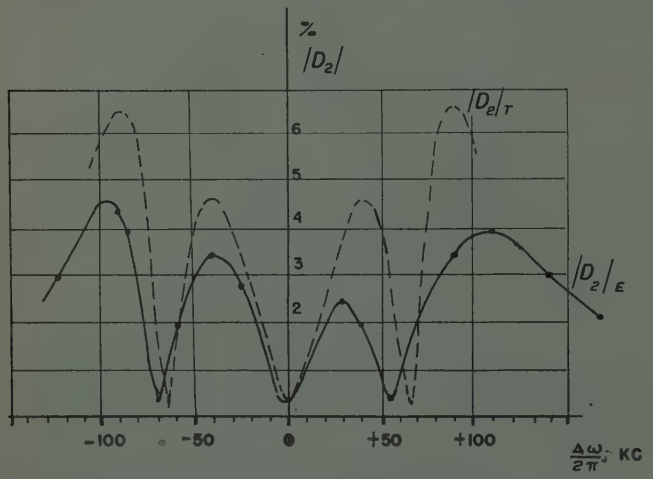

Fig. 4—Theoretical and experimental data. Four interstages of $kQ=1.5$ connected in cascade.

Discrepancies observed are due mainly to the neglected effect of terms containing higher order derivatives of the phase function and to inaccuracies of tuning of individual interstages by the bandwidth adjustment method. There is also some error resulting from the fact that the assumption of the quasi-stationary conditions applies only as an approximation.

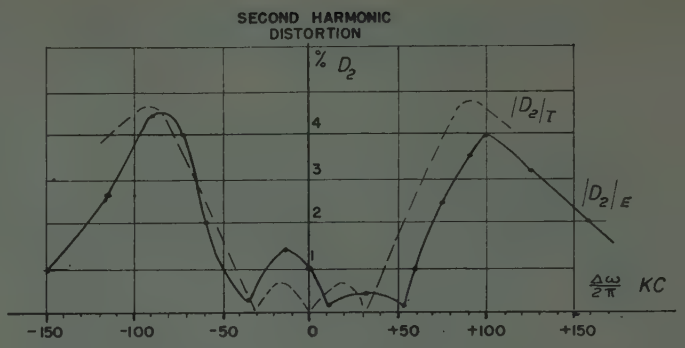

Fig. 5—Theoretical and experimental data. Two interstages of $kQ=0.6$ and two interstages of $kQ=1.5$ connected in cascade.

Apparatus for Oscilloscopic Display of Second Harmonic Distortion (Delay Derivative) as Function of Frequency

The block diagram and basic components of the instrument will be discussed shortly. Fig. 6 shows the block diagram of the apparatus used in preliminary experiments.

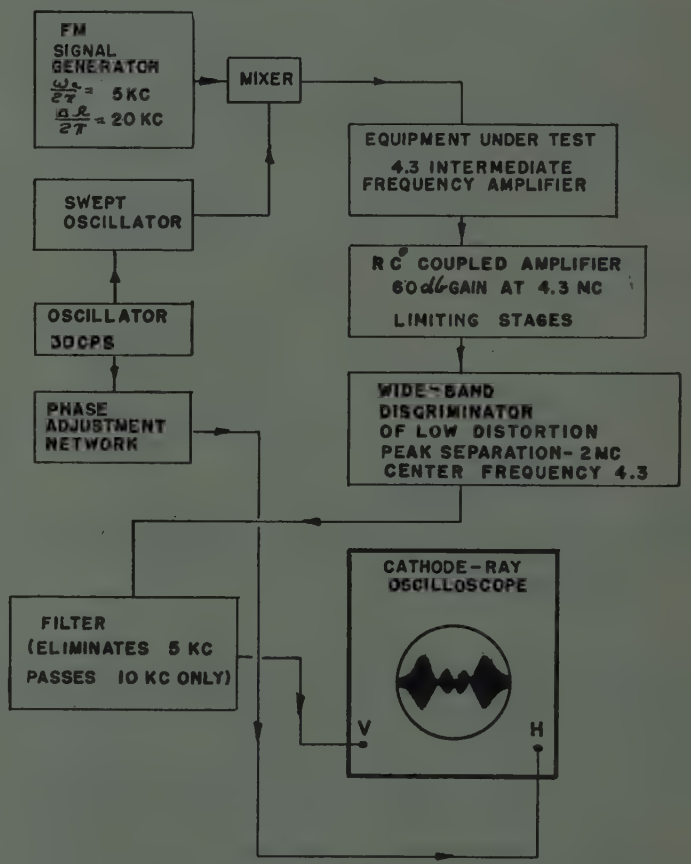

Fig. 6—Apparatus for oscilloscopic presentation of the second harmonic distortion as a function of $\Delta\omega$-block diagram. ($\Delta\omega/2\pi$ = carrier departure from the pass band center.)

The signal of intermediate frequency 4.3 mc is formed by mixing the outputs of FM signal generator (modulation frequency 5 kc) and swept frequency oscillator

(sweeping rate approximately 30 cps), and then applied to the tested network in the form of a signal simultaneously modulated in frequency and swept at a lower frequency rate. The limiter and discriminator circuits remain as described previously. The second harmonic voltage of the demodulated signal is applied to the vertical plates of the cathode-ray oscilloscope. The 10 kc filter should be adjusted to avoid excessive ringing as a consequence of fast changing levels and, at the same time, provide selectivity adequate for suppression of both fundamental and third harmonic voltage.

The attenuation of the filter for 5 kc signals is of the order of 60 db. Oscilloscopic displays obtained for various adjustments of the intermediate-frequency amplifier under test agree well with curves obtained using step-by-step method. Fig. 7 shows the oscillogram taken for four interstages of $kQ=1$ (slightly misaligned).

In conclusion it can be stated that the method of displaying second harmonic distortion or (in another scale) delay derivative versus frequency, provides more distinctive means of recognizing the conditions of network alignment than the conventional magnitude versus frequency display. The authors feel it may provide a useful means of aligning amplifiers intended for the reproduction of FM or transient signals.

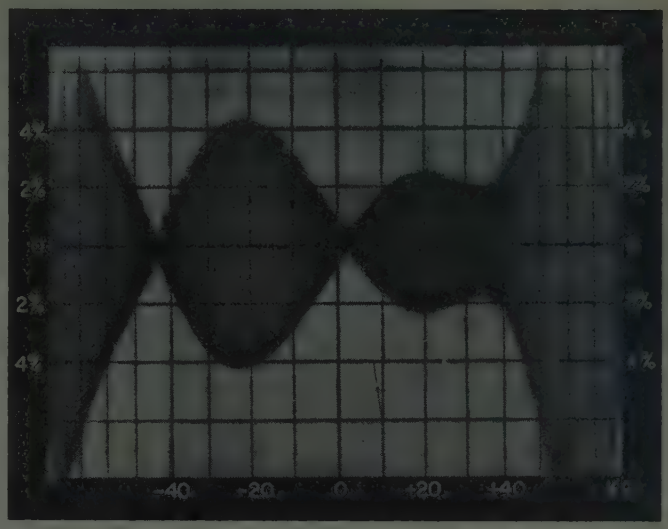

Fig. 7—Typical oscilloscopic presentation.

Acknowledgments

Acknowledgment is due to Arthur H. Maciszewski who, in earlier discussions with one of the authors, contributed to some of the ideas described here, and to Stanley Torode for suggesting a few useful refinements in the experimental circuits.

Excitation Coefficients and Beamwidths of Tschebyscheff Arrays*

ROBERT J. STEGEN†

Summary—**In this paper, exact expressions are obtained for the excitation coefficients of a Tschebyscheff array by equating the array space factor to a Fourier series whose coefficients are readily calculated.**

A set of curves is presented showing half-power beam width versus antenna length for various side-lobe levels. An approximate though very accurate expression for the half-power beamwidth is derived.

Introduction

DOLPH[1] SUGGESTED that a Tschebyscheff polynomial could be made to coincide with the polynomial representing an antenna pattern. He then proved rigorously that the resulting pattern would yield a minimum beamwidth when the side-lobe levels are fixed and a minimum side-lobe level when the beamwidth is specified. He derived the expressions for the currents of the Tschebyscheff arrays as

$$I_q = \frac{1}{A_{2q-1}{}^{2q-1}}\left\{A_{2q-1}{}^{2N-1}Z_0{}^{2q-1} - \sum_{k=q+1}^{N} I_k A_{2q-1}{}^{2k-1}\right\} \quad (1)$$

for $2N$ elements and

$$I_q = \frac{1}{A_{2q}{}^{2q}}\left\{A_{2q}{}^{2N}Z_0{}^{2q} - \sum_{k=q+1}^{N} I_k A_{2q}{}^{2k}\right\} \quad (2)$$

for $2N+1$ elements where

$$A_{2m}{}^{2n} = (-1)^{n-m}\sum_{p=n-m}^{n}\binom{p}{p-n+m}\binom{2n}{2p}, \quad (3)$$

$$Z_0 = \tfrac{1}{2}\left\{[r+\sqrt{r^2-1}]^{1/M} + [r-\sqrt{r^2-1}]^{1/M}\right\}, \quad (4)$$

$$T_M(Z_0) = r = \text{the main beam to side-lobe voltage ratio,} \quad (5)$$

M = one less than the number of elements in the array,

$$T_M(Z) = \cos\,(M \text{ arc cos } Z), \quad |Z| \leqq 1, \quad (6)$$

$$T_M(Z) = \cosh\,(M \text{ arc cosh } Z), \quad |Z| \geqq 1, \quad (7)$$

and

$$T_M(Z) = \tfrac{1}{2}\left[(Z+\sqrt{Z^2-1})^M + (Z-\sqrt{Z^2-1})^M\right], \text{ all } Z. \quad (8)$$

* Decimal classification: R125.1/R325.11. Original manuscript received by the Institute, February 16, 1953; revised manuscript received June 1, 1953.

† Member, Technical Staff, Hughes Research and Development Laboratories, Culver City, Calif.

[1] C. L. Dolph, "A current distribution which optimizes the relationship between beamwidth and side-lobe level," PROC. I.R.E., vol. 34, pp. 335–348; June 1946.

By clever algebraic manipulation, Barbiere[2] was able to obtain expressions for the currents which were much easier to handle than those of Dolph. The Barbiere current expressions are

$$I_k = \sum_{q=k}^{N} (-1)^{N-q} Z_0^{2q-1} \frac{(2N-1)(q+N-2)!}{(q-k)!(q+k-1)!(N-q)!} \quad (9)$$

for $2N$ elements and

$$I_k = \sum_{q=k}^{N} (-1)^{N-q} Z_0^{2q} \frac{(2N)(q+N-1)!}{(q-k)!(q+k)!(N-q)!} \quad (10)$$

for $2N+1$ elements.
In addition Barbiere also proved that

$$Z_0 = \cosh\left(\frac{1}{M} \operatorname{arc\,cosh} r\right) \quad (11)$$

which is much easier to evaluate than (4) by either using tables or appropriate series expansions. These expressions of Barbiere are a big improvement over those of Dolph; however, they have one serious drawback. This is the factor $(-1)^{N-q}$, in (9) and (10), which results in the currents being the difference of two large and almost equal numbers. For example, take the calculation of I_1 in a 24 element array designed to have -40 db side-lobe level. $Z_0 = 1.02665$ and I_1 then becomes $I_1 = 93{,}040{,}583.6338 - 93{,}040{,}569.0594 = 14.5744$. Six significant figures are lost in this calculation. It was necessary to keep Z_0^n accurate to 12 significant figures to obtain this result, i.e., Z_0 was assumed to be $Z_0 = 1.02665000000$. As the number of elements in the array becomes larger, the number of significant figures required increases.

The use of Dolph's or Barbiere's expressions for calculating the current distributions of Tschebyscheff arrays requires a tremendous amount of calculations for an array having a large number of elements. It is also possible to determine the excitation coefficients of the Tschebyscheff array by equating the array space factor to a Fourier series whose coefficients are readily calculated. This leads to expressions for the currents which are somewhat more amendable to calculations.

The Tschebyscheff-Fourier Coefficients

The space factor of a Tschebyscheff array is given by[3]

$$T_{2N}(Z) = \sum_{m=0}^{N} I_m \cos(2mu) \quad (2N+1 \text{ elements}) \quad (12)$$

and

$$T_{2N-1}(Z) = \sum_{m=0}^{N-1} I_{m+1} \cos(2m+1)u \quad (2N \text{ elements}) \quad (13)$$

where

I_m = the excitation coefficient of the mth element on each side of the array center-line,

$$Z = Z_0 \cos u \quad (14)$$

$$u = \frac{\pi d}{\lambda} \sin\theta \quad (15)$$

and Z_0 is defined by (4) or (7).

The excitation coefficients, I_m, are real and symmetrical about the array center because the power pattern is symmetrical and the space factor is real.

Whittaker and Robinson[4] and Sokolnikoff[5] present a method of finding a sum

$$F(x) = \sum_{m=0}^{r} (a_m \cos mx + b_m \sin mx) \quad (16)$$

which furnishes the best possible representation of a function $u(x)$ when we are given that $u(x)$ takes the values $u_0, u_1, u_2, u_3, \cdots u_{n-1}$ when x takes the values $0, 2\pi/n, 4\pi/n, \cdots 2(n-1)\pi/n$, respectively, where $n \geqq 2r+1$. The coefficients are evaluated by use of the following equations

$$a_0 = \frac{1}{n} \sum_{k=0}^{n-1} u_k, \quad (17)$$

$$a_m = \frac{2}{n} \sum_{k=0}^{n-1} u_k \cos \frac{2k\pi m}{n}, \quad (18)$$

and

$$b_m = \frac{2}{n} \sum_{k=0}^{n-1} u_k \sin \frac{2k\pi m}{n}. \quad (19)$$

The excitation coefficients of the Tschebyscheff array are easily determined by equating the Tschebyscheff polynomial to (16) and solving for the I_m in terms of the a_m and b_m coefficients. The space factor for the Tschebyscheff array of $2N+1$ elements, (12) may be equated to the Fourier series (16) by setting $2u = x$ and $N = r$. Then

$$I_m = a_m \quad m = 0, 1, 2, \cdots, N, \quad (20)$$

$$b_m = 0, \quad (21)$$

and

$$n = 2r + 1 = 2N + 1. \quad (22)$$

Z_0 may be calculated from (4) or (11).

The values of $u(x)$ are obtained from

$$u(x) = T_{2N}(Z) = T_{2N}(Z_0 \cos u) = T_{2N}\left(Z_0 \cos \frac{x}{2}\right) \quad (23)$$

at the $2N+1$ values of x, namely,

$$x = \frac{2\pi}{2N+1} s, \quad s = 0, 1, 2, \cdots, 2N. \quad (24)$$

$T_{2N}(Z)$ may be computed using the appropriate closed forms (6), (7), or (8).

The expressions for the excitation coefficients of the Tschebyscheff linear array then become

[2] D. Barbiere, "A method for calculating the current distribution of Tschebyscheff arrays," Proc. I.R.E., vol. 40, pp. 78–82; January, 1952.
[3] C. L. Dolph, "Discussion on a current distribution," Proc. I.R.E., vol. 35, pp. 489–492; May, 1947.
[4] E. T. Whittaker and G. Robinson, "The Calculus of Observation," D. Van Nostrand Company, New York, N. Y., pp. 260–267; 1924.
[5] I. S. and E. S. Sokolnikoff, "Higher Mathematics for Engineers and Physicists," McGraw-Hill Book Co., Inc., New York, N. Y., pp. 545–550; 1941.

$$I_0 = \frac{1}{2N+1}\sum_{s=0}^{2N} u_s(x) \tag{25}$$

$$= \frac{1}{2N+1}\left[u_0 + \sum_{s=1}^{N} u_s + \sum_{s=N+1}^{2N} u_s\right] \tag{26}$$

and

$$I_m = \frac{2}{2N+1}\sum_{s=0}^{2N} u_s \cos\frac{2s\pi m}{2N+1} \tag{27}$$

$$= \frac{2}{2N+1}\left[u_0 + \sum_{s=1}^{N} u_s \cos\frac{2s\pi m}{2N+1} + \sum_{s=N+1}^{2N} u_s \cos\frac{2s\pi m}{2N+1}\right]. \tag{28}$$

The $2N+1-k$ term of

$$\sum_{s=N+1}^{2N} T_{2N}\left(Z_0 \cos\frac{s\pi}{2N+1}\right)\cos\frac{s2\pi m}{2N+1} \tag{29}$$

is

$$T_{2N}\left[Z_0 \cos\frac{\pi(2N+1-k)}{2N+1}\right]\cos\frac{2(2N+1-k)\pi m}{2N+1} \tag{30}$$

$$= T_{2N}\left[-Z_0 \cos\frac{\pi k}{2N+1}\right]\cos\frac{2k\pi m}{2N+1} \tag{31}$$

and, since $T_{2N}(Z) = T_{2N}(-Z)$, this $2N+1-k$ term becomes the same as the kth term of

$$\sum_{s=1}^{N} T_{2N}\left(Z_0 \cos\frac{s\pi}{2N+1}\right)\cos\frac{s2\pi m}{2N+1}. \tag{32}$$

Since there is this asymmetrical term by term correspondence, the two summations are equal. The expressions for the excitation coefficients become

$$I_0 = \frac{1}{2N+1}\left[r + 2\sum_{s=1}^{N} T_{2N}\left(Z_0 \cos\frac{s\pi}{2N+1}\right)\right] \tag{33}$$

and

$$I_m = \frac{2}{2N+1}\left[r + 2\sum_{s=1}^{N} T_{2N}\left(Z_0 \cos\frac{s\pi}{2N+1}\right)\cos\frac{2s\pi m}{2N+1}\right] \tag{34}$$

where

$$m = 1, 2, 3, \cdots, N.$$

A similar procedure for a Tschebyscheff linear array of an even number ($2N$) of elements results in the follow expressions for the excitation coefficients:

$$I_{m+1} = \frac{1}{N}\left[r + 2\sum_{s=1}^{N-1} T_{2N-1}\left(Z_0 \cos\frac{s\pi}{2N}\right)\cos\frac{s\pi(2m+1)}{2N}\right] \tag{35}$$

where

$$m = 0, 1, 2, \cdots, N-1.$$

The excitation coefficients of a 144-element array having -40 db side-lobe level were calculated using (35). The values of I_{72} and I_{71} obtained from (35) were exactly the same as those calculated from (1) or (9). This was used as a check for errors in the calculations of $T_{2N-1}(Z_0 \cos s\pi/2N)$.[6]

The Half-Power Beamwidth

The beamwidth of a Tschebyscheff array may readily be calculated using (5) and (7). The maximum amplitude of the main beam is

$$T_M(Z_0) = r = \cosh(M \operatorname{arc\,cosh} Z_0) \tag{36}$$

or

$$Z_0 = \cosh\left(\frac{1}{M}\operatorname{arc\,cosh} r\right). \tag{37}$$

At the half-power points

$$T_M(Z_1) = \frac{r}{\sqrt{2}} \tag{38}$$

or

$$Z_1 = \cosh\left(\frac{1}{M}\operatorname{arc\,cosh}\frac{r}{\sqrt{2}}\right). \tag{39}$$

where

$$Z_1 = Z_0 \cos u_1 \tag{40}$$

$$u_1 = \frac{\pi d}{\lambda}(\sin\theta_1 - \sin\hat{\theta}) \tag{41}$$

$\hat{\theta}$ = the angle of the main beam from broadside

and

d = the element spacing.

Half-power beamwidth for broadside beam ($\hat{\theta} = 0°$) is

$$\theta_{HP} = 2\theta_1, \tag{42}$$

and is shown in Fig. 1 for a spacing

$$d = \tfrac{3}{4}\lambda. \tag{43}$$

The spacing of the elements has only a minor effect on the beamwidth. For other than broadside beams, i.e.,

[6] Method of determining excitation coefficients suggested by C. L. Dolph, "Discussion on a current distribution," Proc. I.R.E., pp. 489–492; May, 1947. Expressions (33), (34), (35), were obtained by Mrs. Wilma Bottaccini and Dr. N. H. Enenstein (unpublished work).

$\theta \neq 0°$, (41) may be used to obtain values θ_1^+ and θ_1^- which correspond to the positive and negative values of u_1, respectively. The half-power beamwidth is then

$$\theta_{HP} = \theta_1^+ - \theta_1^-. \tag{44}$$

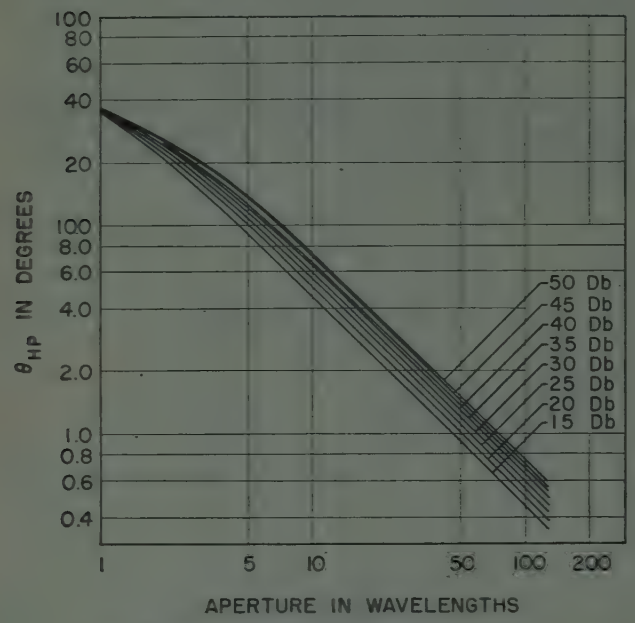

Fig. 1—Beamwidth of a Tschebyscheff array.

An approximate expression for the broadside half-power beamwidth may be obtained, which is quite accurate for the smaller beamwidths, by letting

$$\cos u_1 = 1 - \frac{u_1^2}{2}, \tag{45}$$

$$\cosh v = 1 + \frac{v^2}{2}, \tag{46}$$

$$\operatorname{arc\,cosh} r = \log 2r - \frac{1}{4r^2}, \tag{47}$$

and

$$l = Md = \text{the length of the array.} \tag{48}$$

By direct substitution the final expression becomes

$$\sin \frac{\theta_{HP}}{2} = \frac{1}{\pi l/\lambda} \sqrt{\frac{3}{4} \log_e^2 2 + 2 \log_e 2 \log_e r + \frac{\log_e r}{2r^2}}. \tag{49}$$

For

$$\theta_{HP} < 12°$$

$$\theta_{HP} = \frac{0.636}{l/\lambda} \sqrt{0.360 + 0.693 \log_e r + \frac{\log_e r}{2r^2}} \tag{50}$$

$$= \frac{A}{l/\lambda} \tag{51}$$

where A depends on the side-lobe level r. Some values are listed below.

r (db)	A (degrees)
−20	51.1
−25	56.0
−30	60.6
−35	65.0
−40	68.7

These may be compared with the value $\theta_{HP} = 50.9/l/\lambda$ for a uniform array.

Contributors to Proceedings of the I.R.E.

For a photograph and biography of MARVIN CHODOROW, see page 163 of the January, 1953 issue of the PROCEEDINGS OF THE I.R.E.

❖

Kenneth W. Goff was born in Salem, West Virginia, in 1928. He received the B.S. degree in electrical engineering from West Virginia University in 1950. After graduation, Mr. Goff joined the Staff of the M.I.T. Acoustics Laboratory and entered the M.I.T. Graduate School. He received his M.S. degree in electrical engineering from M.I.T. in 1952, and is now working toward his D.Sc. degree. His work in the M.I.T. Acoustics Laboratory has been in the field of Acoustical Instrumentation with particular attention given the application of correlation techniques to the localization of sound sources.

KENNETH W. GOFF

Mr. Goff is a member of Eta Kappa Nu, Tau Beta Pi and Sigma Xi.

❖

John N. Hines, (S'47–A'50) was born in Tientsin, China, on March 9, 1920. He received the B.S. degree in electrical engineering from the University of Connecticut in 1943 and entered the Armed Forces as a Radio Officer in the Signal Corps until the fall of 1946. Mr. Hines then enrolled in the graduate school of the Ohio State University where he was awarded the M.Sc. degree in electrical engineering in 1949. He is presently employed as a research associate at the Antenna Laboratory there, working on the problems of traveling-wave slot antennas. He is also a member of the technical school staff of Franklin University, Columbus, Ohio.

JOHN N. HINES

Mr. Hines is a member of the AIEE.

❖

Julius J. Hupert (SM'48) was born on May 6, 1910, in Tarnopol, Poland. He received the M.S. (El. Eng.) degree from the Polytechnic Institute of Warsaw, Poland, in 1933 and the Ph.D. degree from Northwestern University in 1951.

J. J. HUPERT

Dr. Hupert's considerable experience in research and development in the field of communications was acquired as head of the Transmitter Department,

Bureau of Research of the State Tele- and Radio Establishment in Warsaw before the outbreak of World War II, and as temporary Senior Scientific Officer (Naval Service assignment) at the British Admiralty Signal Establishment during World War II.

Dr. Hupert has also been active in the teaching field as lecturer (radio transmitter design) at the Polish University College in London (1943–1947) and, after his arrival to U.S.A., in 1947, as a member of the faculty of the Physics Department of De Paul University in Chicago, where he conducts graduate courses and thesis work in electronics.

Since 1947, Dr. Hupert has also been associated with A.R.F. Products, Inc., River Forest, Ill., as consulting engineer and project engineer on research and development projects, mostly in the field of electronic instrumentation. He now holds the position of Director of Research of A.R.F. Products, Inc.

Dr. Hupert is a member of the American Institute of Physics and of Sigma Xi.

❖

Rudolf Kompfner (F'50) was born in Vienna, Austria, on May 16, 1909. He attended the Realschule and Technische Hochschule in Vienna, and was graduated from the faculty of architecture in 1933. In 1934, he went to England to continue his studies in architecture privately, and became the director of a building firm in 1937. He has devoted much of his spare time to the study of television, radio, and physics.

Rudolf Kompfner

Mr. Kompfner entered the Admiralty Service in 1941 as temporary experimental officer, beginning in the physics department at Birmingham University. In 1944 he became associated with the Clarendon Laboratory at Oxford University, England. Since 1952, he has been at the Bell Telephone Laboratories, Murray Hill, N. J., working on microwave tubes.

❖

For a photograph and biography of George L. Matthaei, see page 400 of the March, 1953 issue of the Proceedings of the I.R.E.

❖

Thomas A. Pendleton (A'52) was born in Philadelphia, Pennsylvania, on March 31, 1930. He received the B.E.E. degree from Rensselaer Polytechnic Institute in 1952. As a graduate fellow in electrical engineering at the University of Maryland, he received the M.S. degree in 1953.

T. A. Pendleton

Since 1952, Mr. Pendleton has been engaged in work on primary standards of frequency and time for the High-Frequency Standards Section, Central Radio Propagation Laboratory, National Bureau of Standards, Washington, D.C.

Mr. Pendleton is a member of Tau Beta Pi, and an associate member of Sigma Xi.

❖

Alfred M. Reslock was born in Sioux City, Iowa, in 1925, and received the B.S. degree from Tri-State College of Engineering, Angola, Indiana, in 1947.

A. M. Reslock

At that time Mr. Reslock joined Motorola, Inc. as an assistant engineer in the Communications Department and was chiefly concerned with the design of mobile communications receivers.

In 1950, Mr. Reslock joined the engineering staff of A.R.F. Products, Inc., River Forest, Ill. as an electrical engineer. He has done much work of a practical nature on intermediate frequency amplifier design, particularly from the standpoint of design for low distortion of FM signals.

❖

D. K. Ritchie was born in Newtonville, Ontario, Canada, on December 28, 1925. In 1948 he received the B.A.Sc. degree in Engineering Physics from the University of Toronto.

D. K. Ritchie

Mr. Ritchie spent one year at the National Research Council at Ottawa where he was employed as a Junior Research Officer. In 1950 he returned to the University of Toronto for post-graduate work and obtained the degree of M.A. in 1951.

Since that time Mr. Ritchie has been employed as an engineer group leader in the Research Department of Ferranti Electric Ltd., Toronto, where he is carrying out work on data handling systems involving both analogue and digital techniques.

❖

V. H. Rumsey (SM'50) was born in 1919, in Devizes, England. He graduated from Cambridge in 1941 with an honors degree with distinction in Part III of mathematical tripos. In the United Kingdom civil service, he was a third-class assistant in 1941, a junior scientific officer in 1942, and a scientific officer in 1943 at TRE, Great Malvern, England. From 1943 to 1945 he was the head of the antenna section of the Combined Research Group at the Naval Research Laboratories in Washington, D. C. As a senior scientific officer in the United Kingdom civil service from 1945 to 1948, he worked as a theoretical physicist at the Canadian atomic energy project. Since 1948, Mr. Rumsey has been supervisor of the Antenna Laboratory at Ohio State University.

V. H. Rumsey

Mr. Rumsey is a member of the IRE Committee on Antennas and Waveguides, chairman of the Antenna Instrumentation Subpanel of the Research Development Board panel on antennas and propagation and a member of the URSI #1 Commission on Radio Standards and Measurements.

❖

Herbert J. Scott (A'19–M'42–SM'43) was born in Baltimore, Maryland, on February 12, 1897. He received the B.Sc. degree in electrical engineering in 1927 and the E.E. degree in 1933 from the University of Washington. From 1915 to 1923 he was a radio operator for the American Marconi Company and the Radio Corporation of America; from 1927 to 1934 he was a member of the technical staff of the Bell Telephone Laboratories engaged in radio research and development. In 1934 he was appointed assistant professor of electrical engineering at the University of California, associate professor 1941. From 1942 to 1947 he served as a commander, U. S. Navy, in the design branch, electronics division, Bureau of Ships, Navy Department. In 1947 Professor Scott resumed his teaching duties at the University of California. He is a member of Tau Beta Pi, Sigma Xi, and Eta Kappa Nu.

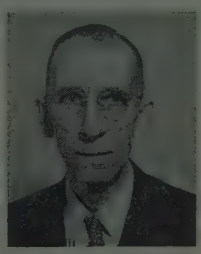

Herbert J. Scott

❖

Robert J. Stegen was born in Peru, Illinois, on February 24, 1921. He received the B.S. degree in E. E. from the University of Illinois in 1942 and attended the California Institute of Technology that summer. From 1942 to 1946 he was an officer in the U. S. Naval Reserve. Following his discharge, he became a staff member and graduate student at the Electrical Engineering Research Laboratory, University of Illinois, and received the M.S. degree in E. E. in 1947. While at the University of Illinois, he was engaged in research at the higher microwave frequencies.

R. J. Stegen

In 1947 to 1949, Mr. Stegen was employed by Convair (Consolidated Vultee Aircraft Corporation), San Diego, Calif., as an electronic engineer doing research and development work on airplane, missile, and radar antennas. Since 1949 he has become a member of the Hughes Research and Development Laboratories.

Mr. Stegen is a registered professional engineer in electrical engineering of California and a member of Eta Kappa Nu.

Ping King Tien (S'49–A'51) was born in Checkiang, China, on August 2, 1919. He received the B.S. degree in electrical engineering from the National Central University of China in 1942, and the M.S. and Ph.D. degrees from Stanford University in 1948 and 1951 respectively.

PING KING TIEN

From 1942 to 1947, Dr. Tien was an engineer at the Tien-Sun Industrial Company, Shanghai, China. He was research assistant from 1949 to 1951 and research associate from 1951 to 1952 at Stanford University. In 1952, he joined the Bell Telephone Laboratories as a member of the technical staff and has been concerned with microwave tube research.

Dr. Tien is a member of Sigma Xi.

❖

Arthur F. Van Dyck (Charter Member 1912—F'25) was born in Stuyvesant Falls, N. Y., May 20, 1891. He received the degree of Ph.B. in E.E. from Yale University in 1911.

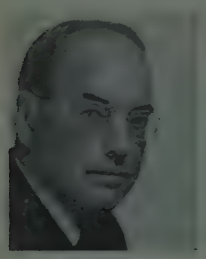

A. F. VAN DYCK

Mr. Van Dyck started in radio as an amateur in 1906, continued as commercial operator at sea during college summers, and except for three years as instructor in E.E. at Carnegie Institute of Technology, and two years in high voltage research at Westinghouse, has been in radio continuously ever since.

Mr. Van Dyck has done research with the Fessenden Co. at Brant Rock and with RCA, New York; design and production with Marconi, General Electric, and RCA, Camden; with the U. S. Navy in both World Wars. From 1930 to 1943 he was Manager of the Industry Service Laboratory of RCA, and is now Staff Assistant to the Vice President and Technical Director of RCA.

Mr. Van Dyck was an observer at the Bikini atom bomb tests and is Vice Chairman of the New York Committee on Atomic Information. He is a Past-President of IRE (1942) and Captain USNR (Retired).

For a photograph and biography of DR. JAMES R. WAIT, see page 1254 of the October 1952 issue of the PROCEEDINGS OF THE I.R.E.

❖

Carlton H. Walter (S'48–A'51) was born on July 22, 1924, in Willard, Ohio. After completing high school, Mr. Walter joined the Army, serving one year at the University of Chicago in an Army Air Forces Training Program and two years as a radar technician. On his discharge in February 1946. He enrolled at the Ohio State University, obtaining the B.E.E. degree in June 1948, and the M.S. degree in Physics in 1951. Since 1948, Mr. Walter has been employed as a research associate at the Ohio State University Research Foundation's Antenna Laboratory where his work has been primarily concerned with flush mounted antennas.

C. H. WALTER

Mr. Walter is a member of Tau Beta Pi, Eta Kappa Nu and Sigma Pi Sigma.

❖

For a photograph and biography of LOUIS WEINBERG, see page 1192 of the September, 1953 issue of the PROCEEDINGS OF THE I.R.E.

❖

H. William Welch, Jr., (A'47) was born in Beardstown, Ill., on October 21, 1920. He received the B.A. degree in physics and was elected to Phi Beta Kappa at DePauw University in 1942. After a summer with the Eastman Kodak Company test laboratories, he spent a year at the University of Wisconsin in graduate study, research, and teaching. In 1943 he went to the Harvard University Radio Research Laboratory as a research associate, where he became involved in magnetron research and development. After spending the first six months of 1946 as a part-time instructor of physics at Purdue University he went to the University of Michigan Engineering Research Institute as a research physicist. In this position he was concerned with problems of microwave-tube electronics in the Department of Electrical Engineering Electron Tube Laboratory. He is presently project engineer of the Electronic Defense Group, also in the Electrical Engineering Dept.

H. WILLIAM WELCH

Dr. Welch received the M.S. degree in physics at the University of Michigan in 1948 and the Ph.D. degree in electrical engineering in 1952. He is a member of Sigma Xi and the American Physical Society.

❖

Neal T. Williams was born March 16, 1921, in East Orange, N. J. From 1942 to 1944 he served as draftsman, production engineer and finally supervisor of engineering on 10 cm. magnetrons and klystrons at the Fairmont, W. Va., plant of the Westinghouse Electric Corp. From 1944 until the end of the war he was engaged as a research associate on the Columbia Radiation Laboratory development program concerned with 1.25 cm and 6 mm magnetrons.

NEAL T. WILLIAMS

In 1945 he returned to undergraduate school, receiving the A.B. in physics in 1948 from Cornell University. At this time he rejoined the staff of the Columbia Radiation Laboratory to continue earlier work on metal-ceramic vacuum seals and short wavelength magnetrons. In 1949 Mr. Williams became associated with the Electronic Tube Division of the Westinghouse Electric Corp., Bloomfield, N. J., as a development engineer on TR, ATR, and pre-TR tubes. In 1951 he became a member of the technical staff of the Bell Telephone Laboratories, Murray Hill, N. J. where he worked on the backward wave oscillator and amplifier. He joined the L. L. Constantin and Co., Lodi, N. J., in 1952, as chief engineer on metal to glass vacuum seals. At present, he is associated with the Edison Laboratory of T. A. Edison, Inc., West Orange, N. J., as a research engineer on fire detection systems.

Mr. Williams is a member of the American Physical Society.

Institute News and Radio Notes

W. L. Everitt Receives IRE Medal of Honor

Dr. William L. Everitt, renowned radio authority and Dean of the College of Engineering, University of Illinois, has been named the recipient of the Institute of Radio Engineers Medal of Honor for 1954, the highest annual technical award of the radio engineering profession. The award was made "for his distinguished career as author, educator, and scientist; for his contributions in establishing electronics and communications as a major branch of electrical engineering; for his unselfish service to his country; for his leadership in the affairs of the Institute of Radio Engineers."

Dr. Everitt is a Fellow, Director and Past President of the Institute of Radio Engineers.

The presentation of the Medal of Honor will be made during the annual banquet at the Waldorf-Astoria Hotel, New York, N. Y., on March 24, 1954 during the Institute's National Convention.

Calendar of COMING EVENTS

Conference on Radio Meteorology, University of Texas, Austin, November 9–12

Fourth Annual Meeting of the IRE Professional Group on Vehicular Communications, Hotel Somerset, Boston, Mass., November 12–13

IRE Kansas City Section Annual Electronics Conference, Hotel President, Kansas City, Mo., November 13 and 14

Joint IRE-AIEE 6th Annual Conference on Electronic Instrumentation in Medicine and Nucleonics, New York City, November 19–20

IRE PGME Symposium on Electronic Plethysmography, University of Buffalo Medical School Auditorium, Buffalo, N. Y., December 10–11.

IRE-IAS-ION-RTCA Conference on Electronics in Aviation, Astor Hotel, New York City, January 27.

1954 Sixth Southwestern IRE Conference and Electronics Show, Tulsa, Okla., February 4–6

1954 IRE National Convention, Waldorf Astoria Hotel and Kingsbridge Armory, New York, N. Y., March 22–25

Society of Motion Picture & TV Engineers, 75th Annual Convention, Hotel Statler, Washington, D. C., May 3–7

IRE-AIEE-IAS-ISA National Telemetering Conference, Morrison Hotel, Chicago, Ill., May 24–26

1953 Student Branch Awards

The annual IRE Student Branch Awards for 1953, as well as the name of the Student Branch in which the student winner was enrolled and the local Section giving the award are listed below. This is the second year that these awards have been made by the IRE Sections under a plan established in 1952 by the IRE Board of Directors.

Student Branch	*Student Branch Award Winner*	*Section*
University of Akron (Joint Branch)	Vincent J. DiCaudo	Akron
University of Arkansas	Clarence R. Alls	Kansas City
University of British Columbia (Joint Branch)	Harold Palmer	Vancouver
Polytechnic Institute of Brooklyn (Joint Branch)	Kenneth C. Kelly	New York
Carnegie Institute of Technology (Joint Branch)	William M. Kaufman	Pittsburgh
Clarkson College of Technology	Harold R. Ward	Syracuse
Columbia University (Joint Branch)	Lewis L. Haring	New York
Cooper Union (Joint Branch)	Israel Kalish	New York
Cornell University (Joint Branch)	Lester F. Eastman	Syracuse
University of Dayton	Donald A. Bange	Dayton
University of Detroit (Joint Branch)	Jerome T. Lienhard	Detroit
Illinois Institute of Technology	Charles M. Knop	Chicago
University of Illinois (Joint Branch)	John L. Muerle	Chicago
Johns Hopkins University (Joint Branch)	Francis J. Witt	Baltimore
University of Kansas (Joint Branch)	Melvin Spry	Kansas City
Kansas State College	Bruce W. Bell	Kansas City
Louisiana State University (Joint Branch)	Luong Van Be	Dallas-Ft. Worth
University of Louisville	Raymond F. Irby	Louisville
Manhattan College (Joint Branch)	Alfred E. Diebold	New York
Michigan State College (Joint Branch)	Lawrence M. Scholten	Detroit
University of Michigan (Joint Branch)	Michael E. Mitchell	Detroit
Missouri School of Mines & Metallurgy (Joint Branch)	Charles C. Poe	St. Louis
Newark College of Engineering	Ernest A. Preuss	New York
College of the City of New York	Norman Nesenoff	New York
New York University (Joint Branch)	A. W. Charmatz	New York
Northwestern University (Joint Branch)	Reinhold F. Nylander	Chicago
University of Notre Dame (Joint Branch)	Edward R. Byrne	Chicago
Pennsylvania State College (Joint Branch)	Richard A. Santilli	Emporium
University of Pittsburgh	Donald K. Bauerschmidt	Pittsburgh
Pratt Institute	Robert C. Wagner	New York
Princeton University (Joint Branch)	Thomas C. Henneberger, Jr.	Princeton
Rensselaer Polytechnic Institute (Joint Branch)	Herbert L. Thal, Jr.	Schenectady
Rutgers University (Joint Branch)	Arthur W. Crooke	Princeton
Seattle University	Arthur J. Burgh	Seattle
Southern Methodist University (Joint Branch)	Carl M. Schwalm	Dallas-Ft. Worth
University of Syracuse (Joint Branch)	Paul Dodge	Syracuse
University of Toronto (Joint Branch)	David E. Noble	Toronto
Tulane University (Joint Branch)	Frank X. Remond	Dallas-Ft. Worth
Utah State Agricultural College	Alvin G. Laird	Salt Lake City
University of Utah (Joint Branch)	Ferril A. Losee	Salt Lake City
University of Washington (Joint Branch)	Charles R. Bryant	Seattle
Wayne University (Joint Branch)	Clifford S. Winters	Detroit

Professional Group News

Ultrasonics Engineering

The Professional Group on Ultrasonics Engineering conducted a panel on ultrasonics at the National Electronics Conference, held in Chicago at the Hotel Sherman on September 28–30.

The following papers were presented: "A Non-contact Microdisplacement Meter," by H. M. Sharaf; "Ultrasonics and Medicine," by J. F. Herrick; "Ultrasonics and Industry," by O. Mattiat; "Characteristics of Ultrasonic Delay Lines Using Quartz and Barium Titanate Ceramic Transducers," by J. E. May, Jr.; and "A Temperature Controlled Ultrasonic Solid Acoustic Delay Line," by E. S. Pennell.

Mr. Morris Kenny of the Naval Ordnance Laboratory, White Oak, Maryland, has been appointed the new Secretary of the IRE Professional Group on Ultrasonics Engineering.

Vehicular Communications

The Fourth Annual Meeting of the Professional Group on Vehicular Communications will be held November 12 and 13, at the Hotel Somerset, Boston, Mass.

The theme of this meeting will be design, planning, and operation of mobile communication systems. Several papers have been offered. For example, RCA and Oklahoma Natural Gas Co. have offered a paper on "Integration of Microwave and Mobile Systems"; George Doddrill of REA has offered a paper on "Radio Systems for Rural Power Companies"; F.C.C. has offered a paper on "Railroad Communication Companies"; New England Telephone & Telegraph has offered a paper on "Maintenance Problems of Mobile Equipment"; Bill Claypoole of U.S.D.A. has offered a paper on "Systems, Designs and Operations for Forestry"; Philadelphia Electric has offered a paper on "Planning and Engineering Mobile Communication Systems"; and Motorola, Inc. has offered a paper on "Portable Communication Systems."

The Executive Committee of the IRE has recently approved the establishment of the Boston Chapter of the Professional Group on Vehicular Communications. Robert Lewis and S. M. Wolf will act as Interim Chairman and Secretary, respectively.

Medical Electronics

The Sixth Annual Conference on Electronic Instrumentation and Nucleonics in Medicine, sponsored jointly by the IRE Professional Group on Medical Electronics and the American Institute of Electrical Engineers, will be held on November 19 and 20 at the Hotel New Yorker, New York, N. Y.

On Thursday, November 19, papers will be given on the following subjects: "Multichannel Electromyography-Instrumentation and Application," John F. Davis, Allan Memorial Institute, McGill University, Montreal Canada; "A Stimulus Monitor—Its Use in Electrophysiology," Hal C. Becker, Tulane University; "Application of Positron Emitting Isotopes to the Localization of Brain Tumors," G. L. Brownell, Massachusetts General Hospital, Boston, Mass.; The "Application of Ultra-Sonic Mechanical Waves to the Visualization of Normal Soft Tissue Structures and Disease Processes, Including Cancer," Douglas H. Howry, Veterans Administration, Fort Logan, Colo.; "Isodose Plotting Instrument for X-Rays," John S. Laughlin, Memorial Center, New York, N. Y.; "The X-Ray Microscope," S. P. Newberry, General Electric Company.

The Thursday evening session will be devoted to the discussion of the application of motion-picture technique to the field of fluorgraphy, which has produced the new field of "cinefluorgraphy" providing the diagnostician with a new tool capable of recording the dynamics of the bone structure and various organs of the body. Sydney A. Weinberg of the University of Rochester will conduct a semi-popular type of session on the subject. He will discuss the three-dimensional techniques in use at his institution and will moderate a panel discussion on cinefluorgraphy. Material will be introduced on the new image brightness intensifiers and their impact on the field. Motion pictures will be included describing the work of the Westinghouse Electric Corp. in the field of image intensification. There will be an opportunity for audience participation in the session since it is anticipated that many will have questions for the panel to answer in this stimulating new field.

Papers to be heard at the morning session, Friday, November 20, are "A Method for the Exact Determination of Volume Concentration and Non-conducting Particles in Conducting Solvent," Herman P. Schwan and Theodore P. Bothwell, Moore School of Electrical Engineering, University of Pennsylvania; "An Instrument for Rapid Dependable Determination of Freezing Point Depression," Robert L. Bowman, National Institute of Health, Bethesda, Md.; "Blood Serum Analysis by a Quantitative Paper Electrophoresis Apparatus," E. L. Durrum and S. R. Gilford, Army Medical Center and National Bureau of Standards, Washington, D. C.; "An Electrical Method for Determining Action Spectra of CO-Inhibited Respiration," L. R. Caster and Britton Chance, Johnson Foundation for Medical Physics, Philadelphia, Pa.; "An Infra-red Analyzer for Continuous Respiratory CO_2 Analysis," Max D. Liston, Liston Becker Co., Stamford, Conn. At the afternoon session, papers will be heard on: "Physiological Effects of Condenser Discharge with Application to Tissue Stimulation and Ventricular Defibrillation," R. S. Mackay, University of California at Berkeley; "A Dynamic Heart-Body Simulator," E. Frank, Moore School of Electrical Engineering, University of Pennsylvania; "Application of Analogue Computer Techniques to Biological Problems," E. P. Radford, Harvard University; "A Method of Determination of Dispersion of Ultrasonic Velocity in Liquids," Edwin L. Carstensen, Moore School of Electrical Engineering, University of Pennsylvania.

The Group will also sponsor, with the Medical and Electrical Engineering Schools of the University of Buffalo, a symposium on electronic plethysmography, to be held in the auditorium of the new University of Buffalo Medical School, December 10 and 11. The keynote speaker will be Dr. Jan Nyboer, of Dartmouth College. The Buffalo-Niagara Chapter, under the chairmanship of Wilson Greatbatch, is handling local arrangements. A complete program will appear in the December issue.

Meteorological Factors in Radio-Wave Propagation

The Physical Society of England has available copies of the proceedings of a joint conference by the Royal Meteorological Society and the Physical Society held at the Royal Institution in London on April 8, 1946.

Twenty papers on the subject of "Meteorological Factors in Radio-Wave Propagation" were read at the conference and are included in the report.

Reports may be secured by writing to the following address: The Physical Society, 1 Lowther Gardens, Prince Consort Rd., London, S.W. 7, England, for 24 shillings, inclusive of postage, or 15 shillings each for orders of 12 or more.

SPECIAL PROCEEDINGS ISSUE ON COLOR TELEVISION

A special and greatly expanded issue of the Proceedings devoted exclusively to the subject of Color Television will be published in January 1954. The issue will contain several hundred pages of important contributions including the technical monographs of the National Television System Committee, reports of various NTSC panels and officials, and papers presenting the latest developments in this timely subject.

Single copies of the January 1954 issue may be purchased at $3.00 per copy. IRE members may purchase one extra copy at $1.25. Public libraries, colleges, and subscription agencies may order copies at the special rate of $2.40. For copies shipped outside of the United States and Canada, there is an additional charge of $0.25 for mailing. You are urged to send your order in promptly with your remittance to the Institute of Radio Engineers, 1 East 79th Street, New York 21, N. Y.

The second Color Television issue combined with the first Color Television issue published in October 1951 will form a complete bibliography of major historical importance. Copies of the first Color Television issue are still available at the following prices: $1.00 for IRE members; $2.25 for nonmembers.

IRE People

John L. Drew (M'45), electrical engineer in the Engineering and Technical Division of the War Department, Washington, D. C., passed away this past winter.

Born in Pennsylvania on June 12, 1888, Mr. Drew received the B.S. degree in electrical engineering from Villanova College in 1911. He also held a Certificate in the Elements of Radio Engineering from George Washington University received in 1942.

Mr. Drew was a student engineer with the Philadelphia Electric Co. and the General Electric Co. in Lynn and Pittsfield, Mass., from 1911 to 1917. He was an associate engineer in the design, manufacturing and application of electrical machinery when he joined the U. S. Corps of Engineers in 1917, serving until 1920 in the operation of searchlights for anti-aircraft defense.

From 1920 to 1927 Mr. Drew was associated with the Gray & Davis Corporation and the American Bosch Magneto Corporation as a research and experimental engineer working on the design, manufacturing and application of automotive, starting, lighting, and ignition equipment.

Following these associations Mr. Drew did sales promotion until 1939. After a two-year illness he joined the Office of the Chief Signal Officer in the War Department, supervising research and development of radio communication equipment. In 1945 he transferred to the Engineering and Technical Division as an electrical engineer.

❖

John Ruze (S'39–A'40–M'46) has been appointed director of the Gabriel Laboratories, Needham Heights, Mass.

JOHN RUZE

Since 1946 Dr. Ruze has been with the Air Force Cambridge Research Center, specializing in microwave optics. He had been assistant chief of the Antenna Laboratory; more recently he was with the Radar Laboratory.

Dr. Ruze was born in New York City on May 24, 1916. He received the B.S. degree in electrical engineering from the College of the City of New York in 1938, the M.S. from Columbia University in 1940, and the Sc.D. from Massachusetts Institute of Technology in 1952.

Previous to joining the Air Force Cambridge Research Center, from 1940 to 1946 Dr. Ruze was with the Signal Corps Engineering Laboratories, where he headed the antenna design section of the Evans Signal Laboratory after 1942. Here he directed the development and design of radar and IF antenna systems.

❖

Elliot Mehrbach (M'44) has been appointed chief engineer of the Maryland Electronic Manufacturing Corp. of College Park, Md.

E. MEHRBACH

Previously, Mr. Mehrbach had been with Allen B DuMont Labs., Inc. since 1950 as project engineer in charge of the transmitter section in the Research Division, where he was responsible for much of the uhf television transmitter development, including a commercial 5KW transmitter and a low power experimental station now operating as KE2XDR in New York City.

Mr. Mehrbach was born in New York City in 1916. He received the B.S. degree in electrical engineering from the Newark College of Engineering in 1938.

From 1938 to 1942 Mr. Mehrbach was a radio engineer for Federal Telegraph Co., Newark, N. J., where he worked on the design and development of air navigation aids and miscellaneous transmitting equipment. He then joined the J. H. Bunnel and Co., where he later became assistant chief radio engineer. He was a project engineer with Radio Receptor Co. and the Curtiss Wright Co. before going to the DuMont Labs.

Mr. Mehrbach is a member of Tau Beta Pi.

❖

John H. Howard (SM'50), senior research engineer with Burroughs Corporation, Philadelphia, has been elected chairman of the Joint Computors Committee of the AIEE, IRE and Association for Computing Machinery; also chairman of the Professional Group on Electronic Computers.

Before joining Burroughs Mr. Howard had his own consulting firm. During 1949 he was a senior project engineer on a special study project with Sperry Gyroscope Co.

Mr. Howard was born on November 14, 1913, in Topeka, Kan. He received the B.S. degree in electrical engineering from Kansas State College in 1935 and the M.S. in electrical engineering from Massachusetts Institute of Technology in 1939. From 1935 to 1942 he was a staff member of the electrical engineering department of MIT, working on cinema integraph, development of a rapid selector, and in charge of a NDRC project. He then became a special consultant on Navy development and operational work. Until 1946 he was on active duty with the Navy, and received the Legion of Merit.

From 1946 to 1948 Mr. Howard, as one of the founding members, was director of development of the Engineering Research Associates, St. Paul, Minn.

John E. Gorham (A'42–M'46–SM'49), chief of the Thermionics Branch of the Signal Corps Engineering Laboratories, Fort Monmouth, N. J., died recently.

As chief of the Evans Signal Laboratory Dr. Gorham was responsible for the planning and directing of research, design, development, construction, standardization, and qualification testing of electron tubes and solid-state devices for the Department of the Army, and of the Air Force.

Dr. Gorham was born on November 11, 1911, in Moline, Ill. He received the B.S. and M.S. degrees from Iowa State College in 1933 and 1934. He received his Ph.D. from Columbia University in 1938, having been a teaching assistant in the physics department since 1934.

In 1939 and 1940, Dr. Gorham was associated with Hawley Products Co. of St. Charles, Ill., as a loudspeaker design engineer, with Belmont Radio Co. of Chicago, Ill., where he was concerned with the designing, setting up and maintenance of production test equipment for home receivers, and the Continental X-Ray Corp. of Chicago, where he designed high-voltage industrial X-ray equipment, including transformers and switching gear.

In 1940 Dr. Gorham joined the U. S. Signal Corps Engineering Laboratories as an associate physicist in the Engineering Branch, serving as chief of the circuit subsection, where he developed modulator circuits to test developmental uhf transmitting tubes. In 1942 he became chief of the special components subsection, being responsible for radar development of modulators, transmitters, and indicator circuits. He then became chief of the vacuum tube development section of the Thermionics Branch, where he was responsible for all vacuum tube development work for the Signal Corps, before attaining his position as chief of the Branch.

Dr. Gorham was the author of many technical papers and held a number of patents dealing primarily with electron tubes. He served on many military and professional committees dealing with electron tubes and solid-state devices.

Dr. Gorham was a member of the Advisory Council for the Electrical Engineering Department of Princeton University, Delta Upsilon, Sigma Xi, Phi Kappa Phi, Pi Mu Epsilon, Delta Sigma, and the Armed Forces Communications Association.

Books

The Science of Color by the Committee on Colorimetry of the Optical Society of America

Published (1953) by Thomas Y. Crowell Company, 432 Fourth Ave., New York 16, N. Y. 340 pages+23-page index+xii pages+22-page references. 102 figures. 25 color plates+40 tables. 6¾×9¾. $7.

The Committee consists of L. A. Jones and R. M. Evans, Eastman Kodak Co.; E. Q. Adams, Cleveland, Ohio; B. R. Bellamy, Munsell Color Co.; Charles Bittinger, Washington, D. C.; E. C. Crittenden, National Bureau of Standards; C. Z. Draves, General Dyestuffs Corp.; J. W. Forest and F. W. Jobe, Bausch & Lomb Optical Co.; C. E. Foss, Princeton, N. J.; H. P. Gage, Corning, N. Y.; K. S. Gibson and D. B. Judd, National Bureau of Standards; I. H. Godlove, General Aniline & Film Corp.; A. C. Hardy, Massachusetts Institute of Technology; E. M. Lowry, D. L. Macadam, and S. M. Newhall, Eastman Kodak Co.; M. Luckiesh, General Electric Co.; Dorothy Nickerson, U. S. Department of Agriculture; Brian O'Brien, University of Rochester; M. R. Paul, Eagle-Picher Co.; L. L. Sloan, Johns Hopkins University.

In 1921 the Colorimetry Committee of the Optical Society of America prepared a report outlining the state of the art in color measurement and presenting tables, charts, and other data useful in that field. This report achieved considerable success and ten years later steps were taken to bring it up to date. Various causes delayed the project but some tentative chapters were published separately as papers in 1943–45. The present volume is the final outcome of this revision.

The work is designed to appeal to a wide audience, ranging from artists and students to manufacturers, engineers and scientists, and to serve as an authoritative and up-to-date source of information, and data. Its publication is particularly timely for the engineer engaged in color television, whose responsibilities and interests require an understanding of scientific color evaluation and measurement.

In order to sustain the interest of this wide audience, the successive chapters have been planned to be of graduated difficulty. The early chapters are simple and elementary, and the later ones become more technical and are particularly compiled for specialists. The scope runs from historical background on the appreciation of color, through a discussion of the physiology of vision and an analysis of the concepts involved in measurements of light and color, and closes with quantitative data on methods and equipment of colorimetry.

This great range of subject matter requires a nice selection of topics. Much thought has apparently been put into it, and in the resulting choice the various classes of readers each can find substantial fare not only in their own but in surrounding fields.

As an example, the engineer will find his principal interest in the second half of the book. However, his habits of considering phenomena definitely and objectively will be tempered by the background on the many and varied sensory effects which change color perceptions according to ambient conditions, and on the difference among surfaces, aperture, volume, and other modes of appearance of color. Only somewhat more remote to him are the treatments on esthetic and emotional responses to color, the nature of color blindness, and the nature of the nerve transmission of visual responses.

Criticism could perhaps be offered that the early chapters tend to labor "pet" topics and are marred by an unduly verbose style.

The second half contains many useful tables on color data compiled at various times. It is unfortunate that it was not feasible to keep those involving color temperature up-to-date with revisions in the constants of Planck's law. Thus the wary user of these tables must constantly regard the listed temperature as only normal, subject to a correction which must be made each time to obtain consistency with the present standards adopted in 1948.

Pierre Mertz
Bell Telephone Laboratories
New York, N. Y.

Synchros Self-Synchronous Devices and Electrical Servo Mechanisms by Leonard R. Crow

Published (1953) by the Scientific Book Publishing Co., Vincennes, Ind. 222 pages+X pages. 163 figures. 5½×8½. $4.20.

Leonard R. Crow is an educational specialist and director of research and development of the Universal Scientific Company.

The first purpose of the author, as expressed in the preface, is to present the basic principles of all types of self-synchronous devices and their methods of application in control systems. In this aim he has been quite successful, and the book contains very good descriptions of the various self-synchronous devices and their operating principles.

A second objective was to "cover all the important ideas and concepts that are essential to complete understanding of self-synchronous control systems." In this the author has been less successful, as indeed, such an ambitious objective would have been impossible of fulfillment in this small volume. As an example, the important problem of stabilization of closed-loop control systems is covered by a few sentences regarding "anti-hunt" devices.

Most of the material is descriptive with a minimum of analysis. It is presented on the trade school level and was obviously intended for use in technical schools of the Armed Forces. This book is new and will undoubtedly serve a useful purpose in helping technicians understand the principles of widely used self-synchronous devices. The descriptive material is quite complete on the various types of remote control and indicating devices commercially available and widely used.

W. C. Tinus
Bell Telephone Laboratories
Whippany, N. J.

Professional Groups

	Chairman
Airborne Electronics	K. C. Black Polytechnics Res. and Devel. Co. Brooklyn, N. Y.
Antennas and Propagation	P. S. Carter RCA Labs Rocky Point, L. I., N. Y.
Audio	Marvin Camras Armour Research Foundation Chicago, Ill.
Broadcast and Television Receivers	D. D. Israel 111 8 Ave., New York, N. Y.
Broadcast Transmission Systems	Lewis Winner 52 Vanderbilt Ave., New York, N. Y.
Circuit Theory	C. H. Page National Bureau of Standards Washington, D. C.
Communications Systems	Col. John Hessel Signal Corps Eng. Labs Fort Monmouth, N. J.
Component Parts	Floyd A. Paul Northrop Aircraft, Inc. Hawthorne, Calif.
Electronic Devices	L. S. Nergaard RCA Labs, Princeton 5, N. J.
Electronic Computers	John H. Howard Burroughs Adding Machine Co. Philadelphia, Pa.
Engineering Management	Gen. T. C. Rives General Electric Co., Syracuse, N. Y.
Industrial Electronics	Eugene Mittlemann 549 W. Washington Blvd., Chicago, Ill.
Information Theory	Dr. William G. Tuller Melpar, Inc., 452 Swann Ave. Alexandria, Va.
Instrumentation	I. G. Easton General Radio Co. Cambridge, Mass.
Medical Electronics	L. H. Montgomery, Jr. Vanderbilt U., Nashville, Tenn.
Microwave Theory and Techniques	Andre G. Clavier Federal Telecomm. Labs. Inc. Nutley, N. J.
Nuclear Science	L. V. Berkner 350 5th Ave. New York, N. Y.
Quality Control	Leon Bass General Elec. Co. Schenectady, N. Y.
Radio Telemetry and Remote Control	M. V. Kiebert, Jr. 463 Boulevard Hasbrouck Heights, N. J.
Ultrasonics Engineering	A. L. Lane Naval Ordnance Labs White Oak, Md.
Vehicular Communications	W. A. Shipman Columbia Gas. Sys. Ser. Corp. 120 E. 41 St., N. Y. 17, N. Y.

Sections*

Chairman		Secretary
R. M. Byrne 316 Melbourne Ave. Akron, Ohio	AKRON (4)	H. L. Flowers 2029—19 St. Cuyahoga Falls, Ohio
L. E. French 107 Washington St. SE Albuquerque, N. M.	ALBUQUERQUE-LOS ALAMOS (7)	R. K. Moore 2808 Mesa Linda Dr. NE Albuquerque, N. M.
S. R. Smith 278-12 St. N.E. Atlanta, Ga.	ATLANTA (6)	D. L. Finn School of Elec. Eng. Georgia Inst. of Tech. Atlanta, Ga.
G. R. White Bendix Radio Div. Towson 4, Md.	BALTIMORE (3)	C. F. Miller Johns Hopkins U. 105 Md. Hall Baltimore, Md.
L. B. Cherry 1418 Central Dr. Beaumont, Tex.	BEAUMONT-PORT ARTHUR (6)	C. B. Trevey 2555 Pierce St. Beaumont, Tex.
C. F. Maylott 41 River St. Sidney, N. Y.	BINGHAMTON (4)	Edward Klinko 27 Linden St. Binghamton, N. Y.
Beverly Dudley Technology Review Mass. Inst. Technology Cambridge, Mass.	BOSTON (1)	H. A. Dorschug Radio Station WEEI 182 Tremont St. Boston 12, Mass.
Luis M. Malvarez Commandant Franco 390 Olivos—FCGBM Buenos Aires, Arg.	BUENOS AIRES	Alejandro Rojo Transradio International San Martin 379 Buenos Aires, Arg.
R. R. Thalner 254 Rano St. Buffalo, N. Y.	BUFFALO-NIAGARA (4)	D. P. Welch 859 Highland Ave. Buffalo 23, N. Y.
R. M. Mitchell 357 Garden Dr., S.E. Cedar Rapids, Iowa	CEDAR RAPIDS (5)	G. W. March 424 Liberty Dr. Cedar Rapids, Iowa
A. R. Beach Loueridge Circle E. Eau Gallie, Fla.	CENTRAL FLORIDA (6)	Hans Scharla-Nielsen Radiation Inc. P.O. Dr. Q Melbourne, Fla.
A. A. Gerlach 4020 Overhill Ave. Chicago 34, Ill.	CHICAGO (5)	W. E. Berkey Westinghouse Electric Merchandise Mart Plaza Chicago 54, Ill.
W. B. Shirk 6342 Hamilton Ave. Cincinnati 24, Ohio	CINCINNATI (5)	W. W. Gulden 3272 Daytona Ave. Cincinnati 11, Ohio
S. J. Begun 3405 Perkins Ave. Cleveland 14, Ohio	CLEVELAND (4)	W. A. Howard National Broadcasting Co. 815 Superior Ave. Cleveland, Ohio
C. B. Sloan 568 Arden Rd. Columbus 2, Ohio	COLUMBUS (4)	P. I. Pressel 599 Northridge Rd. Columbus 14, Ohio
Eric Vaughan 657 Stafford Ave. Bristol, Conn.	CONNECTICUT VALLEY (1)	P. F. Ordung Dunham Lab. Yale Univ. New Haven, Conn.
J. K. Godbey Magnolia Petroleum Co. Field Research Lab. Box 900 Dallas, Tex.	DALLAS-FORT WORTH (6)	M. W. Bullock 6805 Northwood Rd. Dallas, Tex.
A. H. Petit 444 E. Peach Orchard Ave. Dayton, Ohio	DAYTON (5)	M. A. McLennan 304 Schenck Ave. Dayton, Ohio
E. H. Forsman 3609 East 34 Ave. Denver, Colo.	DENVER (5)	P. H. Wright 1010 S. Franklin St. Denver, Colo.
W. L. Cassell Iowa State College Ames, Iowa	DES MOINES-AMES (5)	R. E. Price 1706 Franklin Ave. Des Moines, Iowa
F. W. Chapman 1756 Graefield Rd. Birmingham, Mich.	DETROIT (4)	N. D. Saigeon 1544 Grant Lincoln Park, Mich.
H. F. Dart 923 Farnham St. Elmira, N. Y.	ELMIRA-CORNING (2)	E. M. Guyer Corning Glass Works Corning, N. Y.
Lt. Col. W. B. Sell A.F.F. Bd. No. 4 Fort Bliss, Tex.	EL PASO (7)	Harold Hopp 2404 Copper St. El Paso, Tex.
R. E. Neuber 130 Willonwood Center Emporium, Pa.	EMPORIUM (4)	E. H. Boden Box 14 Emporium, Pa.
B. H. Baldridge R.R. 12 Kratzville Rd. Evansville, Ind.	EVANSVILLE-OWENSBORO (5)	E. C. Gregory 1120 S.E. First St. Evansville, Ind.
L. F. Mayle The Magnavox Co. Fort Wayne, Ind.	FORT WAYNE (5)	Clifford Hardwick 2905 Chestnut St. Fort Wayne, Ind.
John Lucyk 77 Park Row S. Hamilton, Ont., Canada	HAMILTON (8)	A. L. Fromanger 79 Park Row Ave. N Hamilton, Ont., Canada
I. G. Mercer Box 1380 KHON Honolulu, T. H.	TERRITORY OF HAWAII (7)	M. S. Vittum Box 43 Honolulu, T. H.
K. O. Heintz 202 Humble Blvd. Houston, Tex.	HOUSTON (6)	E. W. Helken, Trans Tex. Airways Municipal Airport Houston, Tex.
H. R. Wolff 5135 E. North St. Indianapolis, Ind.	INDIANAPOLIS (5)	J. T. Watson 1304 N. Delaware St. Indianapolis, Ind.
R. E. Lee 205A Entwistle St. China Lake, Calif.	INYOKERN (7)	J. C. Keyes 704-A Kearsarge China Lake, Calif.
J. H. Van Horn Telecom, Inc. 1019 Admiral Blvd. Kansas City, Mo.	KANSAS CITY (5)	Mrs. G. L. Curtis Radio Industries, Inc. 1307 Central Ave. Kansas City, Kan.
W. F. Stewart 1219 Skyline Dr. N. Little Rock, Ark.	LITTLE ROCK (5)	J. E. Wylie 2701 N. Pierce Little Rock, Ark.
G. A. Robitaille 19 McKinnon Pl. London, Ont. Canada	LONDON, ONTARO (8)	J. D. B. Moore 27 McClary Ave. London, Ont., Canada
Vincent Learned 2 Prescott St. Garden City, L. I., N. Y.	LONG ISLAND (II)	J. F. Bisby 160 Old Country Rd. Mineola, L. I., N. Y.
E. F. King 3171 Federal Ave. Los Angeles 34, Calif.	LOS ANGELES (7)	W. E. Peterson 4016 Via Cardelina, Palos Verdes Estates, Calif.
M. I. Schwalbe Veterans Admin. Hosp. Louisville 2, Ky.	LOUISVILLE (5)	G. W. Yunk 2236 Kaelin Ave. Louisville 2, Ky.
Prof. F. B. Lucas 5340 Davis Rd., S.W. South Miami 43, Fla.	MIAMI (6)	C. E. Rogers 717 Santander Ave. Coral Gables 34, Fla.
H. J. Zwarra 722 N. Bdwy., Rm. 1103 Milwaukee, Wis.	MILWAUKEE (5)	Alex Paalu 1334 N. 29 St. Milwaukee, Wis.
D. A. Anderson 159 Sunnyside Ave. Lakeside Montreal 33, Que.	MONTREAL, QUEBEC (8)	Sydney Bonneville Beaver Hall Hill Montreal, P. Q., Canada
S. S. Shamis 11 Stanley Rd. West Orange, N. J.	NEW YORK (2)	A. C. Beck Box 107 Red Bank, N. J.
Prof. R. R. Wright Dept. Elec. Eng. Va. Polytechnic Inst. Blacksburg, Va.	NORTH CAROLINA-VIRGINIA (3)	B. C. Dickerson 1716 Broadfield Rd. Norfolk 3, Va.
C. W. Mueller Box 1082, c/o CAA Oklahoma City, Okla.	OKLAHOMA CITY (6)	F. T. Pickens, III 1333 Chestnut Dr. Oklahoma City, Okla.
V. H. Wight 1411 Nemaha St. Lincoln 2, Neb.	OMAHA-LINCOLN (5)	M. L. McGowan 5544 Mason St. Omaha 4, Neb.
J. A. Loutit 674 Melbourne Ave. Ottawa, Ont., Canada	OTTAWA, ONTARIO (8)	D. V. Carroll Box 527 Ottawa, Ont., Canada
J. G. Brainerd Moore School, U. of Penn Philadelphia 4, Pa.	PHILADELPHIA (3)	C. R. Kraus 1835 Arch St. Philadelphia 3, Pa.

* Numerals in parenthesis following Section designate Region number.

Sections

Chairman		Secretary
A. M. Creighton, Jr. 2201 E. Osborn Rd. Phoenix, Ariz.	PHOENIX (7)	W. R. Saxon Neely Enterprises 32 W. Jefferson St. Phoenix, Ariz.
J. H. Greenwood 530 Carleton Ho. WCAE Pittsburgh, Pa.	PITTSBURGH (4)	K. A. Taylor Bell Tele. Co. of Pa. 416 Seventh Ave. Pittsburgh, Pa.
G. C. Ellison, Jr. 11310 S.E. Market St. Portland, Ore.	PORTLAND (7)	R. W. Schmidt 1235 S.W. Freeman St. Portland, Ore.
J. S. Donal, Jr. RCA Labs. Princeton, N. J.	PRINCETON (3)	G. S. Sziklai Box 3 Princeton, N. J.
Allan Holstrom 551 Spencer Rd. Rochester, N. Y	ROCHESTER (4)	W. F. Bellor 186 Dorsey Rd. Rochester, N. Y.
H. C. Slater 1945 Bidwell Way Sacramento, Calif.	SACRAMENTO (7)	R. C. Bennett 2239 Marconi Ave. Sacramento, Calif.
E. F. O'Hare 8325 Delcrest Dr. University City 24, Mo.	ST. LOUIS (5)	F. A. Fillmore 5758 Itaska St. St. Louis, Mo.
Clayton Clark 710 N. First East St. Logan, Utah	SALT LAKE CITY (7)	J. S. Hooper 1936 Hubbard Ave. Salt Lake City 5, Utah
John Ohman 207 Windsor San Antonio, Tex.	SAN ANTONIO (6)	Paul Tarrodaychik 215 Christine Dr. San Antonio, Tex.
C. R. Moe 4669 E. Talmadge Dr. San Diego, Calif.	SAN DIEGO (7)	F. X. Byrnes 1759 Beryl St. San Diego, Calif.
J. R. Whinnery U. of Cal. EE. Dept. Berkeley, Calif.	SAN FRANCISCO (7)	A. J. Morris 812-11 Ave. Redwood City, Calif.
D. E. Norgaard 1908 Townsend Rd. Schenectady, N. Y.	SCHENECTADY (2)	R. L. Smith Station WRGB Schenectady, N. Y.
L. A. Traub 2816—31 Ave., N. Seattle, Wash.	SEATTLE (7)	G. K. Barger 1229 9 Ave., W. Seattle, Wash.
Richard F. Shea 225 Twin Hills Drive Syracuse, N. Y.	SYRACUSE (4)	Major A. Johnson 162 Lincoln Ave. Syracuse, N. Y.
R. G. Larson 2647 Scottwood Ave. Toledo, Ohio	TOLEDO (4)	R. E. Weeber 3141 Westchester Toledo, Ohio
J. R. Bain 169 Kipling Ave. S. P. O. 54 Toronto, Ont., Canada	TORONTO, ONTARIO (8)	E. L. Palin 2139 Bayview Ave. Toronto, Ont., Canada
C. E. Day Geophysical Research Corp. 2607 N. Boston Pl. Tulsa, Okla.	TULSA (6)	C. S. Dunn 1926 S. Knoxville Tulsa, Okla.
O. W. Muckenhirn EE Dept., U. of Minn. Minneapolis, Minn.	TWIN CITIES (5)	N. B. Coil 1664 Thomas Ave. Saint Paul 4, Minn.
D. D. Carpenter 1689 W. 29 Ave. Vancouver, B. C., Canada	VANCOUVER (8)	J. E. Breeze 5591 Toronto Rd. Vancouver, B. C., Canada
H. P. Meisinger Hull & Old Courthouse Rds. Rt. 3, Vienna, Va.	WASHINGTON (3)	H. I. Metz Dept. of Commerce, CAA Room 2094, T-4 Bldg. Washington, D. C.
R. C. Lepley R.D. 2 Williamsport, Pa.	WILLIAMSPORT (4)	W. H. Bresee 818 Park Ave. Williamsport, Pa.
John Greenaway 403 Tinniswood St. Winnipeg, Canada	WINNIPEG (8)	R. M. Simister 179 Renfrew St. Winnipeg, Canada

Subsections

Chairman		Secretary
R. F. Lee 2704-31 St. Lubbock, Tex.	AMARILLO-LUBBOCK (6) (Dallas-Ft. Worth)	C. M. McKinney 3102 Oakmont Austin, Tex.
R. V. Higdon 1030 S. Atherton St. State College, Pa.	CENTRE COUNTY (4) (Emporium)	W. L. Baker 1184 Oneida St. State College, Pa.
F. G. McCoy Rt. 4, Box 452-J Charleston, S. C.	CHARLESTON (6) (Atlanta)	C. B. Lax Sergeant Jasper Apts. Charleston, S. C.
W. W. Salisbury 910 Mountain View Dr. Lafayette, Calif.	EAST BAY (7) (Los Angeles)	J. M. Rosenberg 1134 Norwood Ave. Oakland 10, Calif.
Allen Davidson 3422 Argyle Ave. Erie, Pa.	ERIE (4) (Buffalo-Niagara Subsection)	
J. R. Haeger 1107 Times Bldg. Huntsville, Ala.	HUNTSVILLE (6) (Atlanta)	C. O. Brock 220 W. Rhett Ave. Huntsville, Ala.
C. R. Burrows 116 Mitchell St. Ithaca, N. Y.	ITHACA (4) (Syracuse Subsection)	Benjamin Nichols Franklin Hall, Cornell U. Ithaca, N. Y.
G. F. Brett 326 E. Orange St. Lancaster, Pa.	LANCASTER (3) (Philadelphia)	M. B. Lemeshka RCA, New Holland Ave. Conestoga, Pa.
D. M. Saling 2 Baker St. Poughkeepsie, N. Y.	MID-HUDSON (2) (New York)	E. A. Keller Red Oaks Mill Rd. R.D. 2 Poughkeepsie, N. Y.
O. D. Perkins Signal Corps Eng. Labs. Fort Monmouth, N. J.	MONMOUTH (2) (New York)	Edward Massell Box 433 Locust, N. J.
G. P. McCouch Aircraft Radio Corp. Boonton, N. J.	NORTHERN N. J. (2) (New York)	W. R. Thurston 923 Warren Parkway Teaneck, N. J.
W. M. Kidwell 1516 Laurel Ave. Pomona, Calif.	ORANGE BELT (7) (Los Angeles)	Eli Blutman 6814 Glacier Dr. Riverside, Calif.
H. M. Stearns 990 Varian St. San Carlos, Calif.	PALO ALTO (7) (San Francisco)	W. W. Harman Elec. Research Lab. Stanford U. Stanford, Calif.
J. H. Vogelman 404 W. Cedar St. Rome, N. Y.	ROME (4) (Syracuse Subsection)	Fred Moskowitz 1014 N. Madison St. Rome, N. Y.
George Weiler 1429 E. Monroe South Bend, Ind.	SOUTH BEND (5) (Chicago)	A. R. O'Neil WSBT-WSBT-TV South Bend, Ind.
Capt. L. A. Yarbrough 3001 USAFIT Wright-Patterson Air Force Base, Ohio	USAFIT	Lt. Col. R. D. Sather Box 3344 USAFIT Wright-Patterson Air Force Base, Ohio
P. A. Bunyar 1328 N. Lorraine Wichita, Kan.	WICHITA (Kansas City)	H. O. Byers 333 Laura Ave. Wichita, Kan.

Abstracts and References

Compiled by the Radio Research Organization of the Department of Scientific and Industrial Research, London, England, and Published by Arrangement with that Department and the *Wireless Engineer*, London, England

NOTE: The Institute of Radio Engineers does not have available copies of the publications mentioned in these pages, nor does it have reprints of the articles abstracted. Correspondence regarding these articles and requests for their procurement should be addressed to the individual publications, not to the IRE.

Acoustics and Audio Frequencies..... 1683
Antennas and Transmission Lines..... 1684
Circuits and Circuit Elements..... 1685
General Physics..... 1687
Geophysical and Extraterrestrial Phenomena..... 1688
Location and Aids to Navigation..... 1689
Materials and Subsidiary Techniques.. 1689
Mathematics..... 1691
Measurements and Test Gear..... 1692
Other Applications of Radio and Electronics..... 1693
Propagation of Waves..... 1693
Reception..... 1694
Stations and Communication Systems.. 1694
Subsidiary Apparatus..... 1694
Television and Phototelegraphy..... 1694
Transmission..... 1695
Tubes and Thermionics..... 1695
Miscellaneous..... 1696

The number in heavy type at the upper left of each Abstract is its Universal Decimal Classification number and is not to be confused with the Decimal Classification used by the United States National Bureau of Standards. The number in heavy type at the top right is the serial number of the Abstract. DC numbers marked with a dagger (†) must be regarded as provisional.

The index to the Abstracts and References published in the PROC. I.R.E., from February, 1952 through January, 1953, is published by the *Wireless Engineer* and may be purchased for $0.68 (including postage) from the Institute of Radio Engineers, 1 East 79th St., New York 21, N. Y. As supplies are limited, the publishers ask us to stress the need for early application for copies. Included with the Index is a selected list of journals scanned for abstracting, with publishers' addresses

ACOUSTICS AND AUDIO FREQUENCIES

534:061.3 2855

Trends in Electro-acoustics—(*Wireless World*, vol. 59, pp. 352–354; Aug., 1953.) Report of the proceedings at the International Electro-acoustics Congress held in the Netherlands, June, 1953. The subjects covered were (*a*) sound recording, (*b*) public-address systems, (*c*) acoustic measurements, (*d*) hearing aids and audiometers, (*e*) electro-acoustics in ultrasonics, (*f*) electro-acoustics applied to musical instruments, (*g*) sound insulation of light-weight structures.

534.01 2856

Response of Linear Time-Dependent Systems to Random Inputs—D. B. Duncan. (*Jour. Appl. Phys.*, vol. 24, pp. 609–611; May, 1953.)

534.21 2857

On a Variational Principle in Acoustics—O. K. Mawardi. (*Acustica*, vol. 3, pp. 187–191; 1953.) A generalized theory is presented for the propagation of sound waves in a tube of rectangular cross section with staggered openings in thin partitions placed at periodic intervals. A variational principle is applied to determine the wave-propagation constant for the labyrinth, and the phase velocity and attenuation for the simpler type of waves propagated are evaluated.

534.213.4–14 2858

Propagation of Acoustic Waves in a Liquid-Filled Cylindrical Hole surrounded by an Elastic Solid—N. V. Somers. (*Jour. Appl. Phys.*, vol. 24, pp. 515–521; May, 1953.) The theory of propagation in systems in which discontinuities in the physical parameters occur along coaxial cylindrical surfaces is developed for an annular impulsive source. The field problem is solved for a basic model consisting of a cylindrical liquid column surrounded by an elastic solid.

534.22:534.321.9–14 2859

A New Precision Method for the Measurement of Ultrasonic Velocities in Liquids—B. R. Ras and K. S. Rao—(*Nature* [London], vol. 171, pp. 1077–1078; June 13, 1953.) Description of a simple method based on diffraction effects in a resonant liquid column. It is suitable only for transparent liquids and cannot be used at very high frequencies. Results obtained at frequencies in the range 1–3 mc are quoted for water and some organic liquids.

534.231 2860

Remarks on the Concept of Acoustic Energy—A. Schoch. (*Acustica*, vol. 3, pp. 181–184; 1953.) The conventional expressions for acoustic energy are shown to have characteristic properties which justify their use in acoustics. See also 2194 of August (Markham).

534.24+[538.566:535.3 2861

The Scattering of Waves at an Uneven Surface—Brekhovskikh. (*See* 2968.)

534.24+[538.566:535.3 2862

Scattering of Waves by a Statistically Irregular Surface—M. A. Isakovich. (*See* 2969.)

534.321.9:534.23 2863

Transmission of Ultrasonic Waves through a Plane Plate made of Viscoelastic Material Immersed in a Liquid Medium—Y. Torikai. (*Jour. Phys. Soc.* [Japan], vol. 8, pp. 234–242; March/April, 1953.) Formulas relative to transmission through a nonabsorptive plate in a liquid medium are quoted and the corresponding formulas for the case of an absorptive plate are derived. The expression for the ratio of the incident and transmitted energy is of the same form as for the nonabsorptive plate, but the propagation constants are complex quantities. When the absorption coefficient of the plate is appreciable, a simple approximate formula can be applied which gives results in good agreement with experiment.

534.321.9–14 2864

Demodulation of Ultrasonic Waves in Liquids—K. Altenburg and S. Kästner. (*Ann. Phys.* [Lpz.], vol. 11, pp. 161–165; Nov. 20, 1952.) The relations between the ultrasonic-wave energy density, lf sound amplitude and the depth of modulation, for a modulated ultrasonic wave, are investigated theoretically and experimentally. In water, the lf amplitude increases linearly with the depth of modulation and is also proportional to the energy density of the carrier wave. The second harmonic of the lf sound is proportional to the square of the depth of modulation. The experimental method may be used to determine the energy density of ultrasonic waves of intensity $\geqq 0.25$ μbar.

534.522.1 2865

The Application of the Phase Method in Visualizing Ultrasonic Waves—Y. Torikai and K. Negishi. (*Jour. Phys. Soc.* [Japan], vol. 8, pp. 119–124; Jan./Feb., 1953.) Theory of the phase microscope is extended to the visualization of ultrasonic waves and confirmed experimentally. Comparison is made with the schlieren method.

534.614+534.64 2866

The Properties of Water-Filled Tubes for Acoustic Impedance and Velocity Measurements.—W. Kuhl. (*Akust. Beihefte*, no. 1, pp. 111–123; 1953.)

534.64 2867

The Practical Representation of Standing Waves in an Acoustic Impedance Tube—W. K. R. Lippert. (*Acustica*, vol. 3, pp. 153–160; 1953.) The pressure/distance envelope function is considered for highly reflecting to normally absorbing samples and for highly absorbing samples. Measurement of the SWR is described, and the detection of disturbances of the equipment, by comparison of envelope curves derived from theory with those obtained by experiment, is illustrated by examples. A definition of the resolving power of an impedance tube is proposed and discussed.

534.641 2868

Acoustic-Impedance Measurement by the Transmission-Characteristic Method—A. F. B. Nickson and R. W. Muncey. (*Acustica*, vol. 3, pp. 192–198; 1953.) The transmission-characteristic method used by Harris (3577 of 1945) is applied to the determination of acoustic impedance of materials at various frequencies and angles of incidence. The most suitable dimensions are determined for the reverberation chambers used, and their construction is described. Allowances can be made for the impedance of the bare walls, so that for comparison measurements over a range of frequencies, wooden boxes lined with sheet metal are satisfactory.

534.75 2869

Contribution to a Scientific Theory of Single-Channel Transmission of Sound: Part 3—P. Burkowitz. (*Funk u. Ton*, vol. 7, pp. 241–249; May, 1953.) Data required in measurement and calculation of sound intensity and transit time are considered. Reverberation effects are discussed in relation to the theory. Part 2: 1890 of July.

534.75:534.322.1 2870
The Influence of Nonlinear Distortions on the Audibility of Frequency Vibrator—E. Zwicker and W. Spindler. (*Akust. Beihefte*, no. 1, pp. 100–104; 1953.) Investigations were carried out on musical intervals with FM in the range 0.8–6.0 cps, the loudness level at the receiving headphones being adjusted over a 2:1 range and nonlinear distortion introduced. The more consonant the musical interval, the sooner additional beats appear when the applied distortion is increased. This effect is partly due to the nonlinearity of the characteristic of the ear.

534.839 2871
The Measurement of the Attenuation of Impact Sound Sinusoidal Excitation—T. Lange. (*Acustica*, vol. 3, pp. 161–168; 1953. In German.) Sinusoidal excitation, instead of the standard hammer impact, is used to determine the attenuation of sound by ceilings. The two methods are compared.

534.843 2872
The Effect of Wall Shape on the Decay of Sound in an Enclosure—J. W. Head. (*Acustica*, vol. 3, pp. 174–180; 1953.) The method of Feshbach (4026 of 1944) is applied to determine the effect of regularly spaced symmetrical projections on the natural frequencies and normal modes of a two-dimensional room. An explanation is given of the superior subjective properties of rooms with rectangular coffering, as shown experimentally by Somerville and Ward (14 of 1952).

621.395.623.7:534.62 2873
Direct Measurement of the Efficiency of Loudspeakers by Use of a Reverberation Room—H. C. Hardy, H. H. Hall and L. G. Ramer. (*Proc. NEC* [Chicago], vol. 8, pp. 99–107; 1952.) A relatively simple method is described for integrating the power output from a loudspeaker excited by a warble tone in a large reverberation room. Typical measurement results are presented and correlated with results calculated from free-field measurements.

621.395.623.7:681.142 2874
An Analogue for Use in Loudspeaker Design—J. J. Baruch and H. G. Lang. (*See* 3050.)

621.395.625.2 2875
The Calibration of Disc Recordings by Light-Pattern Measurements—P. E. Axon and W. K. E. Geddes. (*Proc. IEE*, part III, vol. 100, pp. 217–227; July, 1953.) Analysis of the light-pattern formation suggests that more accurate results are obtained if the light pattern is observed in the focal plane instead of on the disk surface. In the apparatus developed, the pattern width is measured as the distance between centers of twin images after they have been adjusted to lie edge to edge. Other simplifications enable calibration accuracy to be attained with compact equipment involving relatively inexpensive optical items. Experimental results confirm theoretical expectations.

621.395.625.3 2876
Interference Effects in Magnetic Recording Heads—A. H. Mankin. (*Proc. NEC* [Chicago], vol. 8, pp. 108–112; 1952.)

621.395.625.3.001.4 2877
Noise Test for Magnetic Recording Media—R. C. Curtis. (*Electronics*, vol. 26, pp. 216–222; July, 1953.) Dc bias current sufficient to saturate the medium to be tested is supplied from a filtered dc source through a resistance high compared with that of the head. Variations of voltage across the head are fed, after amplification, to a tube voltmeter. This measures total noise. With a suitable filter or harmonic wave analyzer inserted the noise contribution in various parts of the spectrum can be measured. Typical test curves are shown and discussed.

ANTENNAS AND TRANSMISSION LINES

621.315.212 2878
Noise-Free Instrument Cable—(*Commun. Eng.*, vol. 13, pp. 22, 39; March/April, 1953.) Spurious electrical signals caused by mechanical shock and vibration arise in instrument cables due to the separation of static charges at the surfaces of the dielectric. Covering the inner and outer surfaces of the dielectric by a well-bonded conductive coating suppresses these unwanted signals. Details of laboratory procedure for making short lengths of noise-free cable are given. See also *Electronic Eng.*, vol. 25, p. 293; July, 1952.

621.392.029.63/.64 2879
The Use of Short Transmission Lines in Ultra-High Frequency Techniques—P. Rohan. (*See* 2917.)

621.392.21:512.831 2880
Synthesis of Uniform Transmission Line—D. W. C. Shen. (*Electronic Eng.*, vol. 25, pp. 287–289; July, 1953.) The application of matrix theory to network synthesis is illustrated. The uniform line is treated as an infinite number of quadripole networks and the limiting values of the associated matrixes are evaluated.

621.392.26 2881
Attenuation and Surface Roughness of Electroplated Waveguides—F. A. Benson. (*Proc. IEE*, part III, vol. 100, pp. 213–216; July, 1953.) Examination of the surfaces of copper- and silver-plated waveguides shows that the plated surfaces are generally rougher than and bear no relation to the original drawn-tube surface. After 19 weeks' exposure of waveguides to weathering, the attenuation at 9.375 kmc showed increases of up to 22%.

621.392.26 2882
Field in a Rectangular Waveguide with Conducting Membrane—H. L. Knudsen. (*Onde élect.*, vol. 33, pp. 217–234; April, 1953.) General theory is given of the field in a waveguide divided into several homogeneous sections by longitudinal conducting membranes parallel to one of the walls. The only possible waves in such waveguides are the longitudinal H and E types. Calculation of the components of these waves involves the solution of a transcendental equation whose roots are, in general, complex. A detailed study is made of the TE_{mo} waves in a rectangular waveguide with a single membrane. The dependence of the types of wave on the position of the membrane, the resistance per unit of surface, and the frequency, is shown by a curve in the complex plane for each type of wave. From these curves the attenuation and phase constants and the field configuration for the different types of wave can easily be found. Such calculations are made for typical cases. With suitable choice of the position of the membrane and of its unit-surface resistance, a value of the attenuation or phase can be obtained, for a given type of wave, that is fairly independent of frequency over a wide band. Theory of attenuators in which the conducting membrane does not extend from one waveguide wall to the opposite one is being developed.

621.392.26 2883
Electromagnetic Propagation through Waveguides of Rhombic Cross-Section—W. B. Swift and T. J. Higgins. (*Proc. NEC* [Chicago], vol. 8, pp. 274–283; 1952.) Analysis is presented for waveguides of rhombic cross section which permits determination of the effects produced in rectangular waveguides by deformation. The frequency of the lowest possible mode is calculated for waveguides (*a*) with sides of equal width, (*b*) with sides of width $2a$ and a, the smaller angle of the cross-section ranging from 60° to 90°. 36 references.

621.392.26 2884
The Theory of a Waveguide containing a Spiral, Partly Filled with a Dielectric—V. P. Shestopalov. (*Zh. Tekh. Fiz.*, vol. 22, pp. 414–425; March, 1952.) Mathematical theory is developed which enables determination to be made of the structure of the field in the waveguide, the phase velocity and dispersion, the energy flow inside and outside the spiral and in the dielectric, and the losses in the spiral and in the waveguide wall. The advantages and disadvantages of this type of waveguide are enumerated.

621.392.26 2885
Duo-Dielectric Coaxial Waveguide—R. E. Beam and D. A. Dobson. (*Proc. NEC* [Chicago], vol. 8, pp. 301–312; 1952.) Analysis is presented for a cylindrical waveguide with coaxial polystyrene rod. The guide wavelength is determined and curves are given showing its variation with frequency for the E_{00}, E_{01}, H_{01} and HE_{11} modes. Representative field-distribution curves are also given for the various modes. The characteristic impedance for the principal and E_{00} is determined. This mode has an axial component of electric field which vanishes at zero frequency. At high frequencies the field is concentrated mainly within the polystyrene rod and the radius of the outer conductor has little effect on the propagation in the waveguide.

621.392.26 2886
Cut-Off Frequency for Circular Waveguides containing Two Coaxial Dielectrics—R. D. Teasdale and G. N. Crawford. (*Proc. NEC* [Chicago], vol. 8, pp. 296–300; 1952.) A conditional equation is derived for a cylindrical waveguide with a coaxial dielectric rod. The solution of this equation determines the cut-frequency of the structure in the TM_{01} mode. A graphical method of solving the equation is described and curves are given which show how the cut-off frequency of the composite waveguide compares with that of the same waveguide without the dielectric rod.

621.392.26 2887
Electromagnetic Transients in Waveguides—G. I. Cohn. (*Proc. NEC* [Chicago], vol. 8, pp. 284–295; 1952.) Transient effects in cylindrical waveguides with arbitrary driving functions are determined in terms of Fourier integrals, the form of which gives some information on the general characteristics of the propagation of transients in waveguides. The Fourier integral is put into a form suitable for computation and a solution is obtained for the case of an applied sine-wave voltage with a unit-step-function envelope.

621.396.26:538.614 2888
Modes in Waveguides containing Ferrites—M. L. Kales. (*Jour. Appl. Phys.*, vol. 24, pp. 604–608; May, 1953.) Formal solutions are obtained of the equations for wave propagation in waveguides of circular section containing a ferrite material, and with an axial magnetic field. TE, TM, and TEM modes are shown to be nonexistent. Variation of the relative phase of the two circularly polarized wave components with distance along the waveguide is demonstrated, corresponding to the Faraday effect. Similar results have been obtained by Suhl and Walker (2710 of 1952).

621.392.26:538.614 2889
The Faraday Rotation of Waves in a Circular Waveguide—H. Gamo. (*Jour. Phys. Soc.* [Japan], vol. 8, pp. 176–182; March/April, 1953.) Exact solutions for the magnetic rotation of waves in a circular waveguide of infinite length are obtained, the rotational terms in both magnetization and electric polarization being considered. The effect of the applied field is to produce two partial waves, with right-hand and left-hand circular polarization, which are neither pure TE nor TM modes, but reduce to these for zero field. Curves showing the fre-

quency dependence of the propagation constants for both partial waves are given for the quasi-TE_{11} and quasi-TM_{11} modes for particular values of the coefficients of the rotational terms. The dependence of the cut-off frequencies on these coefficients is determined. For TM modes, the cut-off frequencies of both partial waves are identical.

621.392.26:538.614 2890

Experiments on the Faraday Rotation of Guided Waves—A. A. T. M. van Trier. (*Appl. Sci. Res. B*, vol. 3, pp. 142–144; 1953.) A cylindrical waveguide, with a Ni-ferrite rod mounted axially and a movable plunger sliding on the rod, was used to determine the Faraday rotation at 24 kmc. The two resonance lengths for each magnitude of the axial magnetic field were measured and the specific rotation calculated.

621.392.26(083.75) 2891

Rigid-Waveguide Specifications—(*Commun. Eng.*, vol. 13, p. 32; May/June, 1953.) A table and graphs show the frequency range, attenuation, dimensions and maximum power-handling capacity of American standard sizes of rigid waveguide.

621.392.26.016.3 2892

High-Powered Microwave Dummy Loads—T. N. Anderson. (*Tele-Tech.*, vol. 12, pp. 92–94, 164; May, 1953.) The development of a series of dry dummy loads for waveguides is described The loads are designed for operation, without auxiliary cooling, at 2-kw average power dissipation at frequencies in the range 2.6–12.4 kmc.

621.396.67 2893

An Experimental Investigation on Models of Aerials with Passive Directors—D. M. Visokovski. (*Zh. Tekh. Fiz.*, vol. 22, pp. 1477–1482; Sept., 1952. German translation, *Nachr Tech.*, vol. 3, pp. 59–62; Feb., 1953.) Measurements are reported on reduced-scale models of systems comprising a radiating dipole with a somewhat longer reflector and several shorter directors. The radiation patterns obtained differ considerably from those published by Uda and Yagi and reproduced in many textbooks. The discrepancy is attributed to the unsuitability of their methods. The influence of the number of directors on the antenna gain and beam width is discussed.

621.396.67 2894

The Absorption Gain and Back-Scattering Cross-Section of the Cylindrical Antenna—S. K. Dike and D. D. King. (PROC. I.R.E., vol. 41, pp. 926–934; Aug., 1953.) Discussion on 2716 of 1952.

621.396.67:621.396.828 2895

New Antenna Fittings reduce P-Static Interference—C. de Vore. (*Tele-Tech*, vol. 12, pp. 77–79. 143; May, 1953.) Illustrated description of insulated antenna fittings, developed at the Naval Research Laboratory, which reduce precipitation interference.

621.396.67.029.64 2896

Recent Investigations on U.H.F. Dielectric Aerials—H. Aberdam. (*Électronique* [Paris], no. 77, pp. 27–34; April, 1953.) The design and performance of various dielectric antennas are discussed and compared, including an omnidirectional type described by Ducot (*La Recherche Aéronautique*, May/June, 1949), which takes the form of a thin disk with central aperture. Compared with a biconical antenna this has the advantage of reduced size. It is particularly useful for frequencies of the order of 10 kmc, whereas the type described by Mueller (1205 of 1952) is preferred for use at 25 kmc.

621.396.676:621.396.933 2897

FM Altimeter Slot Radiators—L. E. Raburn. (*Tele-Tech.*, pp. 73–75, 180; April, 1953.) The use of single-slot and double-slot radiators, in conjunction with a 440 mc FM altimeter (1863 of 1946), is described and the best location and type of radiator for conventional aircraft are indicated. An outline of the method of measurement of feed-through between the transmitter and receiver is given, and radiation patterns of dipole single-slot and double-slot radiators are shown.

621.396.677 2898

Free-Space Radiation Impedance of Rhombic Antenna—J. G. Chaney. (*Jour. Appl. Phys.*, vol. 24, pp. 536–540; May, 1953.) The expression for the driving-point impedance of a generalized electric circuit is partially integrated, and the physical significance of certain terms is discussed in connection with their application to antenna problems. Assuming an unattenuated traveling wave as a first approximation to the current along a terminated rhombic or V antenna, a formula is derived for the free-space radiation impedance of each. The resistive component of the impedance of the rhombic antenna is in agreement with the radiation resistance given by Lewin.

621.396.677 2899

Radiation Field of a Conical Helix—J. S. Chatterjee. (*Jour. Appl. Phys.*, vol. 24, pp. 550–559; May, 1953.) If a conical helix is used instead of a cylindrical helix, the axial mode of radiation can be maintained over a much wider band of frequencies. The radiation pattern of a conical helix (base diameter 60 cm, linear taper to 20 cm at top in 10 turns, height 112 cm, ground plane 100 cm in diameter) was studied experimentally. The axial mode of radiation was maintained from 150 to 450 mc. The bandwidth can be increased by increasing the number of turns. Radiation diagrams are given for various feed arrangements.

621.396.677 2900

U.H.F.-TV Radiators using Slot Arrays—R. J. Stegen. (*Electronics*, vol. 26, pp. 152–155; July, 1953.) Slot arrays consisting of longitudinal slots offset from the center line of the broad face of a waveguide are considered. Graphs, scale-model results and typical azimuth patterns indicate methods of design and range of application. The advantages include simplicity of feed arrangements, low cost, low transmission-line power loss, improved aperture efficiency and ease in obtaining shaped vertical-plane patterns.

621.396.677 2901

Experimental Investigation and Calculation of End-fire Aerial Arrays—D. M. Visokovski. (*Compt. Rend. Acad. Sci.* [URSS], vol. 89, pp. 41–44; March 1, 1953. In Russian.) A short account of an investigation of the dependence of the radiation characteristics on the number of radiator dipoles and on the length of the director elements.

621.396.677.537.226 2902

The Properties of Artificial Dielectrics Comprising Arrays of Conducting Elements—M. M. Z. Kharadly and W. Jackson. (*Proc. IEE*, part III, vol. 100, pp. 199–212; July, 1953.) Analysis is made of the effective permittivity of rectangular arrays of perfectly conducting elements of simple geometric shapes, such as circular-section rods, thin strips, spheres and disks, and results of experimental investigations at 1 kc are given. Representation of the elements as simple dipoles is inadequate at high concentration; higher-order multipole interaction between them must be taken into account. In cases where this interaction can be evaluated, experimental and theoretical permittivity values are in close agreement over the whole range of concentrations investigated. The same method was applied in calculations of the dielectric properties of a cubical array of imperfectly conducting spheres. Agreement with experiment is good except where the conducting elements occupy more than about 20% of the total volume.

621.396.677:621.392.26 2903

Waveguide Arrays with Symmetrical Conductance Functions—H. D. Griffiths. (*Canad. Jour. Phys.*, vol. 31, pp. 520–528; May, 1953.) Formulas for the efficiency and for the radiation pattern of nonresonant slotted-waveguide arrays are derived and methods are described for calculating the patterns from the asymmetrical near-field distributions produced by symmetrical arrays. Experimental results for two arrays with squint angles of 1.75° and 5.25° are shown graphically and are in satisfactory agreement with theory.

621.396.677.012.12:621.317.755 2904

Aerial Radiation Patterns. Apparatus for Cathode-Ray-Tube Display— T. T. Ling. (*See* 3069.)

621.396.677.5 2905

Radiation Resistance of a Small Circular Loop in the presence of a Conducting Ground—J. R. Wait. (*Jour. Appl. Phys.*, vol. 24, pp. 646–649; May, 1953.) The total power flow from an oscillating vertical magnetic dipole above a flat homogeneous conducting earth is evaluated. The result is used to derive an expression for the radiation resistance of a small horizontal wire loop. For the case of earth with finite conductivity, the radiation resistance is very great when the height of the loop is a small fraction of λ.

621.396.677.6 2906

Null Characteristics of the Rotating Adcock Antenna System—J. G. Holbrook. (*Jour. Appl. Phys.*, vol. 24, pp 530–532; May, 1953.) Mathematical analysis indicates that the optimum spacing of the dipoles for the most clearly defined nonmultiple nulls approaches the value of the shortest wavelength for which the system is designed, whereas the usual practice is to adopt a $\lambda/2$ spacing.

CIRCUITS AND CIRCUIT ELEMENTS

621.3.011.21:517.75 2907

Geometrical Transformation of Impedance Diagrams—H. Briner and W. Graffunder. (*Helv. Phys. Acta*, vol. 25, pp. 487–488; Sept. 15, 1952. In German.) Note on the use of graphical methods and of Riemann's number sphere in impedance calculations.

621.3.018.41 2908

The Concept of Instantaneous Frequency—P. Poincelot. (*Onde élect.*, vol. 33, pp. 214–216; April, 1953.) Discussion shows that this concept can properly be applied to the cases of demodulation by a linear discriminator and FM of a self-oscillator by variation of a parameter of the circuit, but its use in other cases, such as calculation of the harmonic distortion of a simple tuned circuit, leads to erroneous results. This is demonstrated by rigorous calculation of the distortion introduced by an *LGC* circuit in the anode circuit of a pentode amplifying stage.

621.314.3† 2909

Theory of the Magnetic Amplifier with Free Magnetization—L. Kühn. (*Frequenz.* vol. 7, pp. 89–94; April, 1953.)

621.314.3† 2910

Comparison of Methods of Analysis of Magnetic Amplifiers—L. A. Finzi and G. F. Pittman, Jr. (*Proc. NEC* [Chicago], vol. 8, pp. 144–157; 1952.)

621.314.3† 2911

Types of Magnetic Amplifiers—Survey—J. G. Miles. (*Trans. Amer. IEE*, vol. 71, part I, pp. 229–238; 1952.) A scheme for classifying magnetic amplifiers under three main headings, with subdivisions by number and letter, is proposed and discussed.

621.314.3† 2912

The Figure of Merit of Magnetic Amplifiers—J. T. Carleton and W. F. Horton. (*Trans. Amer. IEE*, vol. 71, part I, pp. 239–244; 1952.)

621.316.54.512 2913

Sketch for an Algebra of Switchable Networks—J. Shekel. (PROC. I.R.E., vol. 41, pp. 913–921; Aug., 1953.) A combination of complex-number and Boolean algebra is outlined which can be applied in the analysis and synthesis of networks containing switches.

621.318.572:621.314.7 2914

A Method of Designing Transistor Trigger Circuits—F. C. Williams and G. B. B. Chaplin. (*Proc. IEE*, vol. 100, part III, pp. 228–244; July, 1953. Discussion, pp. 245–248.) A fairly general technique was developed after the war for designing circuits that would operate with tubes having characteristics which varied within fairly wide tolerances, without component adjustments being necessary when tubes were changed. A similar technique is outlined for point-contact transistors; this is based on tube-circuit technique, and particularly on the analogy between the characteristics of transistors and pentodes. Basic pulse circuits considered include 2-state devices, timing circuits, counters and relaxation oscillators. Their application in digital computers is reviewed in detail.

621.319.4 2915

Nonlinear Condensers—B. G. Lewis. (*Radio & Telev. News. Radio-Electronic Eng. Sec.*, vol. 49, pp. 3–5, 25; May, 1953.) The properties and applications of high-permittivity materials containing TiO_2 are discussed, with particular reference to the dependence of the dielectric constant on temperature and on the voltage applied. Applications of the variation of capacitance with the dc bias voltage in a modulator and in a capacitor-type amplifier is described.

621.319.4:621.315.612.4 2916

The Nonlinearity of Titanate Capacitors—M. Kornetzki. (*Frequenz*, vol. 7, pp. 121–127; May, 1953.) Ferroelectric and ferromagnetic materials are compared and expressions for the "specific nonlinearity" are derived for both. These expressions give the hysteresis loss/cm³ referred to unity circular frequency and a reactive power of 1W/cm³. The specific nonlinearities of (*a*) (Ba, Sr)TiO_3 material with a dielectric constant of 2000 and (*b*) (Mn, Zn) ferrite with an initial permeability of 1100 are of the same order of magnitude.

621.392.029.63/.64 2917

The Use of Short Transmission Lines in Ultra-High-Frequency Techniques—P. Rohan. (*Philips Tech. Commun.* [Australia], no. 1, pp. 3–12; 1953.) Lines of length $<\lambda$ are considered; their uses as inductances, capacitances and resonant circuits are reviewed. Numerical examples are given. Applications as filters and impedance transformers are described.

621.392.21.011.21 2918

New H.F. Proximity-Effect Formula—A. C. Sim. (*Wireless Engr.*, vol. 30, pp. 204–207; Aug., 1953.) Arnold's results (1017 of 1947) are somewhat complex. A new asymptotic formula was therefore developed which is valid whenever the proximity effect is so great that the resistance of the pair of parallel conductors is more than doubled. A combination of the Maxwell-equation and integral-equation approaches is used in deriving the new impedance formula, which is rigorous and very simple.

621.392.5+621.396.615 2919

The Equivalent *Q* of *RC* Networks—D. A. H. Brown. (*Electronic Eng.*, vol. 25, pp. 294–298; July, 1953.) The effective *Q* factor of a *RC* phase-shift network is defined as one half the rate of change of phase with frequency at the operating point. For networks commonly used as frequency-determining elements the effective *Q* value is about unity, but a capacitance type of bridged-T network may have a *Q* value of 10.

621.392.5 2920

Design of Low-Frequency Constant-Time-Delay Lines—C. M. Wallis. (*Trans. Amer. IEE*, vol. 71, part I, pp. 135–140; 1952.) Full paper. See 1603 of June.

621.392.5:534.321.9 2921

Ultrasonic Delay Lines—(*Electronics*, vol. 26, pp. 210, 216; July, 1953.) Survey of the characteristics and operation of delay lines using fused-quartz or glass rods with quartz-crystal transducers.

621.392.5.029.64 2922

A New Non-reciprocal Waveguide Medium using Ferrites—E. H. Turner. (PROC. I.R.E., vol. 41, p. 937; Aug., 1953.) A narrow ferrite strip is attached along the wall of a circular-section waveguide and subjected to a transverse magnetic field. A difference in phase constant exists for the two directions of transmission along the guide. For suitable ferrite dimensions, a nonreciprocal rotation of the plane of polarization of an em wave takes place. A more complete theoretical explanation is to be published. The case of an axial ferrite rod with an applied axial field has been considered by Hogan (1233 of 1952).

621.392.52 2923

Semifinite-Terminated Electric Wave Filters—S. S. L. Chang. (*Trans. Amer. IEE*, vol. 71, part I, pp. 149–156; 1952.) Intended for use either as channel filters or to work between a finite resistance at one end and a very high or very low impedance at the other. Two design methods are presented, one based on the equivalent image-parameter filter, the other on Norton and Darlington's insertion-loss procedure. The minimum ratio of terminating resistances lies between 5 and 50 for most applications.

621.392.52 2924

A New Approach to Optimum Filtering—E. W. Pike. (*Proc. NEC* [Chicago], vol. 8, pp. 407–418; 1952.) In filter problems, if enough is known about the signal and the noise to describe them accurately by their power spectra, conventional methods based on Wiener's original method will provide the most effective filters. An alternative procedure for computing optimum filters, based on description of the signal in terms of a partial sum of orthogonal functions, is presented. This will specify good filters with far less labor than is necessary in the Wiener method, and it has a wider range of practical application. A table of summation-orthogonal analogues of the Laguerre functions, which are useful in this procedure, is appended.

621.392.52 2925

Synthesis of a Dynamically Variable Electronic Filter—J. G. Truxal and J. N. Warfield. (*Proc. NEC* [Chicago], vol. 8, pp. 419–426; 1952.) The principles of network synthesis are applied to the design of a variable-bandwidth filter with an upper cut-off frequency which can be varied dynamically over the frequency range 1–10 kc. The bandwidth variation is automatically controlled by voltages applied to the control grids of pentodes, slight changes occurring in selectivity and midband gain.

621.396.6 2926

Printed and Potted Electronic Circuits—G. W. A. Dummer and D. L. Johnston. (*Proc. IEE*, vol. 100, part III, pp. 177–186; July, 1953. Discussion, pp. 187–191.) Survey and assessment of production techniques, and description of some applications.

621.396.611(083.72)(47) 2927

Russian Circuit Notations—G. F. Schultz. (PROC. I.R.E., vol. 41, p. 936; Aug., 1953.) The methods adopted for indicating the values of resistors and capacitors on Russian circuit diagrams are explained.

621.396.611.1 2928

A Relation between Susceptance Slope and Selectivity for Oscillator Design—W. A. Edson and R. D. Teasdale. (*Proc. NEC* [Chicago], vol. 8, pp. 427–434; 1952.) Two quantities, (*a*) the slope of the susceptance curve, computed at an antiresonance frequency, (*b*) the dimensionless selectivity factor *Q*, are significant in specifying the performance of oscillatory circuits. The relation between the two quantities for practical resonant circuits is discussed and general conclusions are drawn relating to resonant-circuit design. These conclusions are applied to the comparison of the Clapp and Colpitts types of oscillator and to the study of the equivalent circuit of a quartz crystal operating near resonance.

621.396.611.1 2929

Subharmonics in a Series Nonlinear Circuit as Influenced by Initial Capacitor Charge—W. J. McKune and M. F. Brust. (*Trans. Amer. IEE*, vol. 71, part I, pp. 200–205; 1952.)

621.396.611.1 2930

Note on "The Response of an *LCR* Circuit"—S. V. Soanes. (PROC. I.R.E., vol. 41, p. 935; Aug., 1953.) Comment on 3041 of 1952 (Marique).

621.396.611.3:621.392.26 2931

The Transvar Directional Coupler—K. Tomiyasu and S. B. Cohn (PROC. I.R.E., vol. 41, pp. 922–926; Aug., 1953.) The coupling element consists of n closely spaced identical apertures, separated by $(n-1)$ grid wires, in the common narrow wall between two waveguides. By changing the relative longitudinal position of the two waveguides, the number of exposed apertures, and hence the effective coupling length, can be changed. Power transfer is variable between 0 and 100%. Maximum power transfer is available at one frequency only, and hence bandwidth depends on the tolerable decrease in power transfer. Two models, with $n=22$, and differing only in grid-wire diameter, having maximum power transfer at about 9 and 10 kmc respectively. Agreement between theory and performance is close.

621.396.611.4 2932

External Influences on the Circuit Properties of U.H.F. Resonators—G. Megla. (*Nachr-Tech.*, vol. 2, pp. 323–336; Nov., 1952.) The *Q* of a cavity resonator depends not only on its physical dimensions and the material of which it is made, but also on the surface finish. The influence of the material and its finish on the fundamental damping and resonance resistance is investigated for resonators of various types. An examination is made of the degree of roughness permissible, with reference to standard specifications on surface finishes. Effects due to variations of atmospheric temperature, pressure and humidity, and methods of eliminating these effects, are also discussed.

621.396.611.4 2933

Interaction of Modes in a Microwave Cavity Resonator—S. K. Chatterjee. (*Jour. Indian Inst. Sci.*, sect. B, vol. 35, pp. 59–69; April, 1952.) The minimum energy differences between the desired and undesired modes in a 9-kmc cylindrical resonator are calculated by considering the em field inside the resonator as due to an infinite number of harmonic oscillators. Expressions for the mutual energy and the coefficient of coupling between the companion modes $TE_{0,1}$ and $TM_{1,1}$ are derived. The significance of the total energy of a microwave cavity resonator is discussed.

621.396.615 2934

Power Spectrum of a Nonlinear Oscillator perturbed by Noise—A. Blaquière. (*Ann.*

Radiotech., vol. 8, pp. 153–179; April, 1953.) Analysis of the effect of background noise in producing amplitude fluctuations. If the steady state of an oscillator is disturbed, recovery takes place exponentially with a time constant τ which is the principal factor affecting the noise-power spectrum. Simple relations between τ and the circuit parameters are derived which show that for minimum noise power oscillations of large amplitude should be used, without introducing too many harmonics, and the phase of the feedback should vary only slowly with frequency. See also 968 of April and back references.

621.396.615 2935

Two RC Oscillator Circuits—H. L. Armstrong. (*Electronics*, vol. 26, pp. 234–238; July, 1953.) Cathode-coupled and transitron types of *RC* oscillator are described which operate at frequencies of about 400 kc and 20 kc respectively.

621.396.615 2936

Low-Power Blocking Oscillators—J. R. Clark. (*Proc. NEC* [Chicago], vol. 8, pp. 231–235; 1952.) Information of use in final adjustment of blocking oscillators, particularly as regards requirements for short rise-times and narrow pulses, is reviewed. A linearized equivalent circuit is used to derive an explicit expression for pulse duration which gives results in agreement with experiment, particularly when the grid coupling capacitor is small.

621.396.615:621-526 2937

Use of Servo Techniques in the Design of Amplitude-Stabilized Oscillators—A. W. Dickson. (*Proc. NEC* [Chicago], vol. 8, pp. 166–176; 1952.) Expressions for the oscillation amplitude in terms of the stabilizing-signal voltage are derived and the amplitude-stabilizing system is discussed as a negative-feedback loop. Experimental and theoretical results for a high-Q oscillator are compared.

621.396.615:621.314.7 2938

F.M. Transistor Oscillator—H. H. Wieder and N. Cass. (*Electronics*, vol. 26, pp. 198–202; July, 1953.) A titanate capacitor is coupled to the resonant-circuit inductor of the transistor oscillator, the transformation ratio being chosen at will. Varying the potential applied to this capacitor alters its effective capacitance and hence the resonance frequency. A polarization potential is applied from a Zamboni pile to keep the capacitance variations within the linear range. A 2.5-mc oscillator constructed used a CK722 junction transistor and had a power output of 1 mw when supplied from a 30-v battery. The titanate capacitor consisted of two series-connected 100-pF units. A 3.5-mc oscillator using a Type-1698 point-contact transistor gave similar results. Some form of afc is desirable in view of the temperature variations of the components.

621.396.615:621.316.722.1 2939

An Oscillator with Constant Output Voltage—L. Ensing and H. J. J. van Eyndhoven. (*Philips Tech. Rev.*, vol. 14, pp. 304–312; April, 1953.) The theory and design of an output-voltage stabilizer circuit are given. By a suitable choice of the values of two resistors and of the constant reference voltage, the oscillator output voltage is made virtually independent of tube characteristics and circuit impedance. An application to the calibration of tube voltmeters is described.

621.396.615:621.316.729 2940

Mechanism of the Synchronization of *LC* Oscillators—J. van Slooten. (*Philips Tech. Rev.*, vol. 14, pp. 292–298; April, 1953.) The pulling effect on the phase and frequency of an *LC* oscillator due to interference is considered. The phase change is calculated for the case of a single interfering pulse, a series of equidistant pulses, and a sinusoidal voltage. Interfering pulses occurring at an oscillator voltage peak affect the amplitude, those occurring at zero voltage cause a change in phase only. These phase changes are permanent. A differential equation, relating oscillator-voltage phase deviation, time, peak oscillator voltage and the magnitude of the interference current, is solved and the conditions for synchronism are obtained.

621.396.615:621.396.611.21 2941

Some Aspects of Mixer-Crystal Performance—P. D. Strum. (Proc. I.R.E., vol. 41, pp. 875–889; Aug., 1953.) A method of calculating conversion loss and conductances of a crystal mixer is presented, and their dependence on terminations at the image frequency and at the sum frequency is considered. Experimental data from various sources support the calculations. Graphs showing (*a*) excess crystal noise versus output frequency, and (*b*) mixer noise temperature versus crystal noise temperature for varying conversion loss, are derived and applied, together with the conversion-loss data, to practical calculations of optimum mixer configuration and optimum if. Two examples are worked out. Experimental confirmation of results was obtained.

621.396.615.142.2:621.316.726.078 2942

Automatic Frequency Control of High-Power Klystrons—R. F. Denton, T. A. Wilson and A. R. Margolin. (*Proc. NEC* [Chicago], vol. 8, pp. 56–63; 1952.) A method of control is described in which a cavity resonator and two microwave crystals are used as a standing-wave discriminator in a system for automatic frequency search and lock for a pulsed klystron oscillator. Frequency stability to within 1 part in 10^4 is achieved.

621.396.615.142.2:621.396.822 2943

Length of Coherent Microwaves Generated by an Electronic Oscillator—K. Shimoda. (*Jour. Phys. Soc.* [Japan], vol. 8, pp. 131–132; Jan./Feb., 1953.) Investigation of the noise associated with the generation of oscillations, of frequency 8 kmc, by a reflex klystron showed a bandwidth of about 3 kc. This is attributed to fluctuation of the electron beam.

621.396.615.17 2944

The Square-Wave Generator—E. Piepgras. (*Funk u. Ton*, vol. 7, pp. 230–240; May, 1953.) The circuit of a multivibrator type of generator with stabilized input is shown and a complete analysis based on the characteristics of the double triode, Type ECC40, is given.

621.396.615.17 2945

A Reliable Locked-Oscillator Pulse Timer—P. G. Sulzer. (*Tele.-Tech*, vol. 12, pp. 68–69; 173; April, 1953.) Description, with complete circuit diagram and method of adjustment, of a highly stable locked-oscillator pulse timer providing pulses with recurrence frequency 25/seconds from a 100-kc input. The frequency divider has previously been described (944 of 1952). The unit has an over-all phase stability to within $\sim 0.1\mu s$ per volt of line-voltage change.

621.396.615.17 2946

An Analogue Reciprocal-Function Unit for Use with Pulsed Signals—P. A. V. Thomas. (*Electronic Eng.*, vol. 25, pp. 302–304; July, 1953.) A monostable multivibrator operates so that the width of the pulse generated is approximately inversely proportional to the peak voltage of an input pulse. The pulse-width variation is converted to a corresponding amplitude variation of sawtooth output pulses by means of a constant-velocity timebase circuit.

621.396.645:621.313.2 2947

Calculations for a Power Amplifier for [driving] a D.C. Motor—J. Zakheim. (*Onde Elect.*, vol. 33, pp. 235–239; April, 1953.) Analysis of a symmetrical class-A amplifier supplying energy to a motor connected in the cathode circuit of the output stage. See also 687 of March.

621.396.645.029.3 2948

High-Power Audio Amplifiers—L. F. Deise and H. J. Morrison. (*Proc. NEC* [Chicago], vol. 8, pp. 81–88; 1952.) Recent applications for af power up to 10kw include vibration work, servomechanism studies, pulsed service, and variable-frequency power sources, all of which require response, distortion and noise-level characteristics similar to those for broadcasting service. In high-power amplifiers with class-B push-pull output, the output transformer is the largest and most expensive item in the equipment and may weigh some hundreds of pounds. A new equivalent circuit is used in the design of such transformers. Harmonic distortion caused by the transformer is analyzed and methods of improving the performance of class-B amplifiers are described. A few details are given of a 5/10-kw amplifier with a response curve flat to within 1 db from 10 cps to 30 kc.

621.396.645.029.62/.63 2949

General Design Considerations of a Cavity-Type Power Amplifier—W. S. Elliott. (*Proc. NEC* [Chicago], vol. 8, pp. 64–72; 1952.) Details are given of the construction of a single-stage amplifier using a Type-2C39A triode tube. Constant-current curves for class-C grounded-grid operation were used to determine the operating parameters of the triode. A 3-stage amplifier using Type-2C39A and Type-5893 triodes is described, with performance details.

621.396.645.3.029.424 2950

A Simple Low-Frequency Amplifier—J. R. Beattie and G. K. T. Conn. (*Electronic Eng.*, vol. 25, pp. 299–301; July, 1953.) Description of a tuned-amplifier circuit for the range 1–3 cps, incorporating a damped phase-shift oscillator with independent control of resonance frequency and Q-factor.

621.396.822:621.3.014.1.025 2951

Differential Law for the Intensities of Electrical Fluctuations, and Influence of Skin Effect—M. A. Leontovich and S. M. Rytov. (*Zh. Eksp. Teor. Fiz.*, vol. 23, pp. 246–252; 1952.) An investigation is made of the form of the correlation function of the external field which expresses the thermal electrical fluctuations in a conductor, and of the "differential law" on which Nyquist's integral formula (1) is based.

621.396.822:[621.316.86+621.314.63 2952

On the Temperature Dependence of Contact Noise—Y. Inuishi. (*Jour. Phys. Soc.* [Japan], vol. 8, p. 128; Jan./Feb., 1953.) Results of noise measurements on Se and Cu_2O rectifiers and on carbon resistors over different temperature ranges between $-40°$ and 130°C are shown graphically.

GENERAL PHYSICS

534.01 2953

Subharmonic Oscillations in Nonlinear Systems—C. Hayashi. (*Jour. Appl. Phys.*, vol. 24, pp. 521–529; May, 1953.) The order of the subharmonics in systems with nonlinear restoring force is closely related to the form of the nonlinearity. A detailed analysis is presented for the subharmonic oscillation of order $\frac{1}{3}$, for the cases in which the nonlinearity is expressed by a cubic or a quintic function. Stability is discussed by means of the criterion previously given (2361 of August).

535.12:535.31 2954

Step-By-Step Transition from Wave Optics to Ray Optics in Inhomogeneous Absorbing Media: Part 1—Equations for Wave Normal, Refractive Index and Polarization—K. Suchy. (*Ann. Phys.* [Lpz.], vol. 11, pp. 113–130; Nov. 20, 1952.) The transition is made by successive approximations. Each approximation is consid-

ered from the physical point of view and the physical significance of the equations derived is considered.

537.37 2955
Luminescent Layers and Films with Polyvinyl Alcohol as Protective Colloid and Binder—F. Eckart. (*Ann. Phys.* [Lpz.], vol. 11, pp. 169–174; Nov. 20, 1952.)

535.37:537.228:621.32 2956
Electroluminescence—Electrical and Optical Properties—J. F. Waymouth, C. W. Jerome and W. C. Gungle. (*Sylvania Technologist*, vol. 5, pp. 54–59; July, 1952.) Electro-optical measurements are reported on electroluminescent lamps operating on the principle described by Payne et al (1341 of 1951), and fundamental properties of electroluminescent phosphors are studied.

537.12 2957
Method for Measurement of the Charge of Fast Electrons—R. Fleischmann and R. Kollath. (*Z. Phys.*, vol. 134, pp. 526–529; April 17, 1953.) A method is outlined for determining whether the variation of m/e with the electron velocity depends entirely on m.

537.12 2958
Measurement of Charge on Electrons in Motion—R. Kollath and D. Menzel. (*Z. Phys.*, vol. 134, pp. 530–539; April 17, 1953.) No variation in the electron charge was detected in the range 2.5–30 keV. The method used was that outlined by Fleischmann and Kollath (*See* 2957 above).

537.525.5:621.327.43:538.561 2959
Oscillatory Phenomena of Arc in Hot-Cathode Discharge Tube: Part 1—Experimental (Characteristics of Oscillation)—H. Yosimoto. (*Jour. Phys. Soc.* [Japan], vol. 8, pp. 59–68; Jan./Feb., 1953.)

537.525.5:621.327.43:538.561 2960
Oscillatory Phenomena of Arc in Hot-Cathode Discharge Tube: Part 2—Theoretical (Mechanism of Oscillation)—H. Yosimoto. (*Jour. Phys. Soc.* [Japan], vol. 8, pp. 69–76; Jan./Feb., 1953.)

537.533:537.525.92 2961
Space-Charge Spread of Reflected Electron Beams studied by a Photographic Method—J. T. Wallmark. (*Jour. Appl. Phys.*, vol. 24, pp. 590–597; May, 1953.)

537.533.7:537.241:530.145.61 2962
The Self-Charge Spreading of a Focused Electron Beam—H. Grümm. (*Ann. Phys.* [Lpz.], vol. 11, pp. 131–144; Nov. 29, 1952.) Simple formulas, derived from wave-mechanical considerations, are obtained for the upper limits of the self-charge effects, i.e., spreading of beam, and displacements of image plane and Fraunhofer plane.

537.582 2963
Energy Distribution of Thermo-electrons in Electron-Beam Devices—H. Boersch. (*Naturwissenschaften*, vol. 40, pp. 267–268; May, 1953.) Experiments are described which show that the energy distribution of the thermo-electrons in oscillograph tubes, electron microscopes, etc., is not of the Maxwell type. The deviations from the Maxwell distribution, particularly in the low-energy range, are attributed to reciprocal dynamic effects.

538.114 2964
On the Theory of the Ising Model of Ferromagnetism—G. F. Newell and E. W. Montroll. (*Rev. Mod. Phys.*, vol. 25, pp. 353–389; April, 1953.)

538.122+537.212 2965
The Two-dimensional Magnetic or Electric Field above and below an Infinite Corrugated Sheet—N. H. Langton and N. Davy. (*Brit. Jour. Appl. Phys.*, vol. 4, pp. 134–137; May, 1953.)

538.311 2966
A Conducting Permeable Sphere in the presence of a Coil carrying an Oscillating Current—J. R. Wait. (*Canad. Jour. Phys.*, vol. 31, pp. 670–678; May, 1953.) The secondary magnetic fields due to the sphere are calculated for frequencies <500 cps.

538.311 2967
Current Element near the Edge of a Conducting Half-Plane—R. F. Harrington. (*Jour. Appl. Phys.*, vol. 24, pp. 547–550; May, 1953.) "The two-dimensional problem of the Maxwellian field from a line source of current adjacent to a conducting half-plane is treated by a transform method of solution. Expressions in the form of contour integrals are given for the current induced in the conductor and for the radiated field."

538.566:535.3]+534.24 2968
The Scattering of Waves at an Uneven Surface—L. M. Brekhovskihk. (*Zh. Eksp. Teor. Fiz.*, vol. 23, pp. 275–304; 1952.) An approximate method is proposed for calculating the field of acoustic and electromagnetic waves scattered by an uneven surface, the irregularities being large in comparison with the wavelength. Particular cases considered include that of sinusoidal corrugations.

538.566:535.3]+534.24 2969
Scattering of Waves by a Statistically Irregular Surface—M. A. Isakovich. (*Zh. Eksp. Teor. Fiz.*, vol. 23, pp. 305–314; 1952.) A method is proposed for calculating the field of plane waves scattered by a perfectly reflecting, statistically irregular surface, the irregularities being large in comparison with the wavelength. The method can be used for acoustic as well as electromagnetic waves.

538.566:537.562 2970
Quenching of Afterglow in Gaseous Discharge Plasmas by Low-Power Microwaves—L. Goldstein, J. M. Anderson and G. L. Clark. (*Phys. Rev.*, vol. 90, pp. 486–487; May 1, 1953.) Continuation of work noted in 2637 of September. Results are reported for neon of the effect on the plasma decay of applying microwave pulses at various time intervals after the production of the plasma. The state of decay was determined by observing the afterglow by means of photocells, and displaying the amplified photocurrent on an oscilloscope. Decrease of light intensity observed during the application of the pulse is most probably due to reduction of the recombination rate. Differences in the traces observed at pressures of 20 mm Hg and 1 mm Hg are discussed. The effect may be useful for detecting em energy.

GEOPHYSCIAL AND EXTRA-TERRESTRIAL PHENOMENA

523.72:621.396.822 2971
On Some Features of Noise Storms—T. Hatanaka and F. Moriyama. (*Rep. Ionosphere Res.* [Japan], vol. 6, pp. 99–109; June, 1952.) Discussion of solar RF emission of abnormally high intensity on meter wavelengths. The radiation is circularly polarized, may last for several hours, and is often associated with sudden bursts of nonpolarized radiation. The association of such noise storms with large and magnetically active sunspots is considered.

550.384 2972
Time Variation of the Earth's Magnetic Field at the Time of Bay Disturbance—Y. Kato and J. Ossaka. (*Rep. Ionosphere Res.* [Japan], vol. 6, pp. 37–41; March, 1952.)

550.385 2973
Distribution of S.C.* of Magnetic Storms—T. Nagata. (*Rep. Ionosphere Res.* [Japan], vol. 6, pp. 13–30; March, 1952.) The abbreviation S.C.* is used to denote the reverse impulse preceding a sudden commencement. The distribution with respect to local time and latitude was examined from records obtained at five U.S. stations during a period of $3\frac{1}{2}$ years, and also from world-wide records of individual geomagnetic storms. The reverse impulses appear chiefly in the afternoon, with a maximum at about 1600 local time. The pulse magnitude, as well as its ratio to the succeeding main pulse, increases markedly with geomagnetic latitude.

550.385 2974
The Recurrence Tendency of Magnetic Storms—M. Ota. (*Rep. Ionosphere Res.* [Japan] vol. 6, pp. 212–214; Dec., 1952.) Data relative to 196 storms observed at Aso Magnetic Observatory during the period Sept., 1949–Aug., 1952 are analyzed. 23 storms showed no recurrence tendency. The rest are divided into 33 groups, each containing several storms recurring at intervals of about 27 days.

550.385:523.755 2975
Correlation of Magnetic M-Storms with the Monochromatic Corona—R. Müller. (*Observatory*, vol. 73, pp. 75–77; April, 1953.) Results obtained at Wendelstein show that a maximum of geomagnetic activity is observed 3.7 days before the central-meridian passage of a region of high coronal activity, or 3.1 days after the appearance of bright coronal emission at the east solar limb. Similar characteristics are found for the minimum epochs. The relation apparently holds good only when no visible or significant sunspot phenomena exist.

550.385+551.594.5]:621.396.9 2976
Radio Echoes observed during Aurorae and Terrestrial Magnetic Storms, using 35- and 74-Mc/s Waves Simultaneously—L. Harang and B. Landmark. (*Nature* [London], vol. 171, pp. 1017–1018; June 6, 1953.) A report of observations at Tromsö, near the auroral zone, and at Kjeller, near Oslo. The two pulse transmitters at each station had common pulse modulators, so that the shape and energy of the pulses could be made identical. The peak pulse power was 25 kw and repetition frequency 50/seconds. Echoes on 35 mc appeared regularly at Tromsö during auroral displays and in a number of cases also on 74 mc. Study of the results led to the conclusion that the echoes were not due to direct scatter from the ionosphere, but could be explained by reflection of backwards scatter from land or sea via the E_s layer, the ionization of which increases greatly during auroras and geomagnetic storms. In all cases, the echoes on 35 mc showed a smaller range than those on 74 mc, the difference in range usually exceeding 100 km. Differences between the echo patterns on the two frequencies are noted. A full account of the observations will be given in *Jour. Atmos. Terr. Phys.*

550.385(98) 2977
Constitution of Polar Magnetic Storms—T. Nagata and N. Fukushima. (*Rep. Ionosphere Res.* [Japan], vol. 6, pp. 85–97; June, 1952.) Analysis of data obtained in the International Polar Year indicates that polar magnetic storms consist of a number of elementary disturbances which occur successively. The equivalent current system corresponding to these disturbances can be represented approximately by that due to an electric dipole located in the auroral zone.

550.385(98) 2978
Constitution of Polar Magnetic Storms—N. Fukushima. (*Rep. Ionosphere Res.* [Japan], vol. 6, pp. 185–193; Dec., 1952.) An examination of world-wide data relative to the polar magnetic storm on April 30, 1933, confirms the conclusions noted *in* 2977 above.

551.510.534:551.524.7 2979
Annual Variation of Reduced Density and Mean Temperature of Atmospheric Ozone in

Afghanistan—A. Khalek. (*Compt Rend. Acad. Sci.* [Paris], vol. 236, pp. 2424–2426; June 22, 1953.)

551.510.535+523.71 2980

Abbreviated Codes of European Ursigrams: Part 2—(URSI *Inform. Bull.*, no. 78, pp. 16–37; March/April, 1953.) The codes here given are: (*a*) Data on Monochromatic Intensity of the Solar Corona, "CORON" code; (*b*) Data on E_s Critical Frequency (fE_s), "ESFRE" code; (*c*) Data on F_2 Critical Frequency (f_0F_2) "FODEU" code for f_0F_2 hourly values, "SYMBO" code for descriptive symbols for the values given; (*d*) Terrestrial Magnetism, "MAGNE" code; (*e*) Ionospheric-Disturbance Warning, "PERTU" code, (*f*) Radio Solar-Emission Observatories, "SOLER" code. Part 1: 2650 of September.

551.510.535+523.71 2981

European Ursigrams—(*URSI Inform.Bull.*, no. 78, p. 16; March/April, 1953.) Correction to 2650 of September.

551.510.535 2982

Some Characteristics of Ionospheric Storms—T. Obayashi. (*Rep. Ionosphere Res.* [Japan], vol. 6, pp. 79–84; June, 1952.) Analysis of data for the F_2 region. The frequency of occurrence of disturbances in this region is closely related to its seasonal height, being greater in summer than in winter.

551.510.535 2983

Classification of F_2-Layer Storms with Respect to their World-Wide Distribution and Characteristics: Part 1—H. Uyeda and Y. Arima. (*Rep. Ionosphere Res.* [Japan], vol. 6, pp. 1–12; March, 1952.) Analysis of available data shows that there is no correlation between F_2-layer storms and sunspot activity, but close correlation with geomagnetic storms. A classification of these storms with respect to their distribution over the geomagnetic latitudes is suggested, based on layer-height or critical-frequency charactertics.

551.510.535 2984

On World-Wide Distributions of f_0F_2—Y. Aono. (*Rep. Ionosphere Res.* [Japan], vol. 6, pp. 69–78; June, 1952.) Hourly values of f_0F_2 observed at 40 stations, distributed all over the world, during the period May 8–11, 1948, are analyzed, contour lines being used to indicate places with common critical frequencies. Diagrams are also given showing (*a*) the distribution of the difference between f_0F_2 and its monthly mean value at 0700 and 0800 on May 9, 1948, (*b*) the distribution of f_0F_2 for noon local time on the same date, (*c*) the latitude distription of f_0F_2 for noon local time on longitudes 135°E and 75°W.

551.510.535 2985

On the Cause for Unnatural Distribution of Occurrence of fE_s and $f_{min}F$—H. Uyeda, K. Miya and T. Kobayashi. (*Rep. Ionosphere Res.* [Japan], vol. 6, pp. 179–183; Dec., 1952.) Observations carried out at Kokubunji indicate a correlation between receiver interference and the frequency of occurrence of fE_s and $f_{min}F$.

551.510.535:550.384.4 2986

A Relation between F_2-Layer Disturbance and Geomagnetic Condition—F. Fukushima and T. Hayasi. (*Rep. Ionosphere Res.* [Japan], vol. 6, pp. 133–136; Sept., 1952.) A correlation is found between the daily mean value of the electron density of the F_2 layer and the storminess of the geomagnetic field. The F_2-layer electron density appears to decrease in local summer and increase in local winter in the middle-latitude regions of both the northern and southern hemispheres.

551.510.535:550.385 2987

Characteristics of Ionospheric Disturbances during Severe Magnetic Storms—K. Miya and N. Wakai. (*Rep. Ionosphere Res.* [Japan], vol. 6, pp. 137–146; Sept., 1952.) Analysis of world-wide data from 40 ionosphere stations for the period May 8–11, 1948, including two geomagnetic storms with sudden commencements (sc), shows that an inospheric disturbance coincident with a sc in a region of high geomagnetic latitude spreads down to lower latitudes. In high latitudes the disturbances travel at a high velocity, which is about 300 km/hr in the vicinity of Japan. The intensity of the disturbance decreases with latitude. The connection between the time of occurrence of a sc and disturbance of radio communication is briefly discussed.

551.510.535:551.594 2988

Studies on Ionospheric Storms—H. Uyeda. (*Rep. Ionosphere Res.* [Japan], vol. 6, pp. 169–177; Dec., 1952.) A definite relation is found between the types of storm discussed by Appleton and Piggott (891 of 1950) and the seasons in which they occur. The development of ionospheric storms is discussed in some detail. The need for further world-wide ionospheric investigations, particularly in high latitudes and at intervals less than an hour, is stressed.

551.510.535:621.3.087.4 2989

Modern Ionosphere Sounding Equipment of the Netherlands P.T.T.—P. L. M. van Berkel. (*Tijdschr. ned. Radiogenoot.*, vol. 18, pp. 149–165; May, 1953. In English.) Full description, with block diagram, of a 1-kw pulse equipment for the range 1–20 mc. Pulse duration is adjustable from 50 to 100 μs; repetition frequency is 50/seconds. A complete frequency sweep can be made in either 10 or 20 seconds. Two cr tubes in parallel provide monitoring and photographic facilities.

551.510.535:621.396.11 2990

C.C.I.R.—U.R.S.I. Cooperation. Exchange of Information for Forecasts and Warnings—(*See* 3092.)

551.510.535(98):537.56:550.385 2991

Anomalous Ionization in the Upper Atmosphere over the Auroral Zone during Magnetic Storms—M. Sugiura, M. Tazima and T. Nagata. (*Rep. Ionosphere Res.* [Japan], vol. 6, pp. 147–154; Sept., 1952.) The depth of penetration of and the rate of ionization by protons of extraterrestrial origin are estimated. An explanation is given of the rapid variations of the geomagnetic field in and near the auroral zone.

LOCATION AND AIDS TO NAVIGATION

621.396.9 2992

Magnetic Modulators for Pulsed Radar—W. S. Melville. (*B.T.-H. Activ.*, vol., 23 pp. 169–173; Nov./Dec., 1952.) The use of magnetic materials with rectangular B/H characteristics for the generation of pulses is described. The principles of polarization and cascade discharge are outlined and the operation of a marine radar modulator is described. Constructional features of magnetic switches, termed pulsectors, are mentioned. Magnetic and electronic modulators are compared, the principal advantages of the former being low radiated interference, instantaneous operation and the facility with which high-power pulses can be generated.

621.396.9:551.508.11 2993

Pulse Observations of Wind by Radio "Echosonde" without Responder—J. Lugeon. (*Compt. Rend. Acad. Sci.*, [Paris], vol. 236, pp. 2426–2428; June 22, 1953.) A description is given of a method in which the radiosonde oscillator, quiescent in the intervals between its pulse transmissions, is triggered by a pulse from the ground station. The distance between ground station and radiosonde is found by the usual radar method.

621.396.9:551.578.1 2994

Vertical Recording of Rain by Radar—S. K. H. Forsgren and O. F. Perers. (*Chalmers Tek. Hogsk. Handl.*, no. 107; 19 pp. 1951.) Reprint 681 of 1952.

621.396.93 2995

Radio Rescue Beacon—(*Wireless World*, vol. 59, pp. 381–382; Aug., 1953.) Short description of a small battery-operated transmitter, with a RF pulse power of about 16 w, designed for attachment to an airman's life-saving jacket. Known as "Sarah" (Search And Rescue And Homing) the apparatus, when brought into action, continues to transmit omnidirectional pulse signals for about 20 hours. One version of the equipment also provides for two-way speech communication over a limited distance.

621.396.93 2996

Radio Navigational Aids—A. van Weel. (*Tijdschr. ned. Radiogenoot.*, vol. 18, pp. 129–148; May, 1953.) Survey of the basic principles and characteristics of (*a*) nondirectional beacons and radio compass, (*b*) radio range, (*c*) instrument landing system, (*d*) directional beacons, (*e*) distance-measuring equipment, (*f*) loran and decca systems.

621.396.932/.933].2 2997

Radio Direction Finding. Influence of Buried Conductors on Bearings—F. Horner. (*Wireless Eng.*, vol. 30, pp. 187–191; Aug., 1953.) "The currents induced, at low frequencies, in a buried cable in good contact with the ground may greatly exceed those in a similar cable insulated from the ground. These currents may lead to large errors in a loop direction finder, even when the length of the cable is a small fraction of the wavelength. The errors are likely to be small if the direction finder is near one end of the cable. Formulas are derived for the currents induced in a buried conductor and these lead to calculated errors in reasonable agreement with measured errors, at a frequency of 10 kc. The results show that the effect of burying a cable in soil of good conductivity is to increase errors at low frequencies and to reduce errors at high frequencies. The transition frequency depends on the length of the cable and is, for example, about 300 kc for a cable 200 meters long. Adcock direction finders are less liable to errors due to cables, but there is some risk of errors if a cable is laid in close proximity to an antenna feeder."

621.396.933 2998

Continuous-Indicating Loran Navigator—R. B. Williams, Jr. (*Electronics*, vol. 26, pp. 166–169; July, 1953.) A 12-tube unit is added to the standard Sperry Mark-2 indicator to synchronize it with the received signals, maintain correct pulse amplitude as shown on the cr tube screen and maintain pulse superposition in height and time. Details are given of the circuits provided for agc, automatic amplitude-balance control, pulse-amplitude sampling with time-sharing relay, afc, automatic time-difference control and pulse-position detection. The time-sharing relay is an em servo-type switch. One unit gives continuous indication of one line of position of the aircraft. Two units synchronized on separate pairs of stations give continuous indication of exact position.

MATERIALS AND SUBSIDIARY TECHNIQUES

53.087.3:537.311.33 2999

A Micromanipulator for Electrical Investigations of Semiconducting Materials—A. Kelen. (*Appl. Sci. Res. B*, vol. 3, pp. 125–128; 1953.) The construction is described of a simple instrument for the accurate location of 1–5 point contacts.

531.788.7 3000

A Cylindrical Magnetron Ionisation Gauge

—A. H. Beck and A. D. Brisbane. (*Vacuum*, vol. 2, pp. 137–146; April, 1952.) The gauge is essentially a diode with an axial magnetic field, its cylindrical structure distinguishing it from the Penning-type gauge. Its working range is 10^{-4}–10^{-3} mm Hg and when used in a bridge type of leak detector its sensitivity is of the same order as that of the mass spectrometer.

531.788.7 3001

Degassable Penning Gauge—A. Bobenrieth. (*Le Vide*, vol. 8, pp. 1302–1304; March, 1953.) Description of a gauge whose electrodes can be degassed by the Joule effect, AF heating not being required.

535.215+537.323]:546.36.863 3002

Some Experimental Studies of the Conductivity and Thermo-electromotive Force of Cs_3Sb Photo-Cathodes—T. Sakata. (*Jour. Phys. Soc.* [Japan], vol. 8, pp. 125–126; Jan./Feb., 1953.) Experimental results are shown graphically. The thermo-emf ranges from 1.1 mV/deg at 268° to 0.3 mV/deg at 343° K. The resistivity is given by the formula $\rho=\rho_0 \exp(\epsilon/kT)$, where T is the absolute temperature and ϵ is about 0.2–0.3, *p*-type conductivity being indicated.

535.215.1:621.396.822 3003

Noise Measurements on Thin-Lead-Sulphide Photoelectric Layers—F. Eckart. (*Ann. Phys.* [Lpz.], vol. 11, pp. 166–168; Nov. 20, 1952.) Electrical noise measurements were made on PbS layers treated with oxygen. The absolute value of noise input is proportional to the cell current for both thermal and photoelectric excitation. The dark current and mean noise input are proportional to the es field strength. The mean life of the charge carries is estimated to lie between 1.3×10^{-3} and 3.7×10^{-5} seconds.

535.215.2 3004

Photoelectric Emission and Energy Structure of Cs_3Sb—H. Miyazawa. (*Jour. Phys. Soc.* [Japan], vol. 8, pp. 169–175; March/April, 1953.) Spectral distributions of the emission and energy distributions of the photoelectrons were determined for Cs_3Sb at room temperature, 195°K and 90°K. A possible energy structure is discussed.

535.371+535.377+535.215.1]:546.47–13 3005

Photodielectric Effect, Ferroelectricity and Thermoluminescence in Zinc Oxide under Ultraviolet Irradiation—J. Roux. (*Compt. Rend. Acad. Sci.*, [Paris], vol. 236, pp. 2492–2494; June 29, 1953.) The sample of ZnO considered had a greenish fluorescence under ultraviolet irradiation, was thermoluminescent but not phosphorescent, and had a marked photodielectric effect (permittivity variation) affected by the intensity of an applied es field and also by infrared light during and after the excitation. The material is ferroelectric under excitation at room temperature.

535.377 3006

The Characteristics of a Class of Sulphate-Base Phosphors—M. A. Konstantinova-Shlezinger, N. A. Gorbacheva and E. I. Panasyuk. (*Zh. Eksp. Teor. Fiz.*, vol. 23, pp. 588–592; 1952.) Attenuation and thermal luminescence curves are plotted for $PbSO_4$-Sm with different fluxes, and also thermal luminescence curves for $CdSO_4$ activated with Mn, Pb and Mn-Pb and for $PbSO_4$ with the double activator Sm-Ce.

537.226 3007

The Properties of Very Small Ferroelectric Particles—M. Anliker, W. Känzig and M. Peter. (*Helv. Phys. Acta*, vol. 25, pp. 474–475; Sept. 15, 1952. In German.) Preliminary report of investigations of anomalies in the ferroelectric state about the Curie point.

537.226:537.533.8 3008

The Secondary Emission from Dielectrics under Single-Impulse Conditions—A. R. Shul'man and V. L. Makedonski. (*Zh. Tekh. Fiz.*, vol. 22, pp. 1540–1542; 1952.) The coefficient of secondary emission σ varies with time owing to changes taking place in the surface layer of the target. To eliminate these effects in measurements of σ, single pulses may be used. A circuit was developed by the aid of which it is possible to measure the σ of dielectrics with constant primary current, with periodic impulses. The main requirements of this circuit are discussed and a block diagram is given.

537.226:546.431.824–31 3009

The Dielectric Properties and Optical Anomalies of $BaTiO_3$ Single Crystals—I. N. Belyaev, N. S. Novosil'tsev, E. G. Fesenko and A. L. Khodakov. (*Zh. Eksp. Teor. Fiz.*, vol. 23, pp. 211–216; 1952.) Three groups of $BaTiO_3$ crystals were investigated, of which two were grown from a solution and one was obtained by reaction between $BaCo_3$ and Na_2TiO_3. The temperature and frequency dependence of permittivity and loss angle were studied.

537.226:546.431.824–31 3010

The Effect of Deviations from the Stoichiometric Composition on the Properties of $BaTiO_3$ Ceramics in Strong Fields—N. S. Novosil'tsev, A. L. Khodakov and M. S. Shul'man. (*Zh. Eksp. Teor. Fiz.*, vol. 23, pp. 336–339; 1952.) An experimental investigation shows that even slight deviations from the stoichiometric composition (from 1.024 to 0.940) seriously affect the dielectric properties of $BaTiO_3$. The dependence of permittivity and loss angle on the composition was investigated at mains frequency and several anomalies in strong fields were observed.

537.226:546.431.824–31 3011

Theory of the Dielectric Properties of Barium Titanate in Stationary Fields—A. E. Glauberman and A. F. Lubchenko. (*Zh. Eksp. Teor. Fiz.*, vol. 23, pp. 188–198, 1952.) Approximate calculations are made of the effective field in $BaTiO_3$ and of its permittivity below the Curie point. The calculations are based on the concept of the existence of a covalent bond between the Ti ion and one of the oxygen ions, taking account of the lattice structure. Theory is developed for the qualitative determination of the temperature dependence of permittivity for temperatures below the Curie point, and a method is indicated for calculating the dependence of permittivity on the intensity of the external field and also the dependence of spontaneous polarization on temperature.

537.226.33:546.431.824–31 3012

Hysteresis Loops of Ceramic Barium Titanate at Higher Frequencies: Part 1—K. Kambe, I. Nakada and H. Takahasi. (*Jour. Phys. Soc.* [Japan], vol. 8, pp. 9–14; Jan./Feb., 1953.) Report of observations, using pulse voltages, of polarization hysteresis loops at frequencies up to 3 mc and temperatures from room temperature up to 150°C.

537.226.33:546.431.824–31 3013

Hysteresis Loops of Ceramic Barium Titanate at Higher Frequencies: Part 2—K. Kambe. (*Jour. Phys. Soc.* [Japan], vol. 8, pp. 15–20; Jan./Feb., 1953.) Investigations show that with pulse voltage the shape of the hysteresis loops corresponds to the initial shape on applying direct voltage. The loop shape is almost independent of pulse width and shape and varies only slightly in the range 10–100 kc.

537.228.1:534.213 3014

On the Theory of Sound-Wave Propagation in Piezoelectric Crystals—R. Meier and K. Schuster. (*Ann. Phys.* [Lpz.], vol. 11, pp. 397–406; Feb. 10, 1953.) Formal treatment of the propagation of plane acoustic waves, taking account of electromechanical reactions. Calculations are made of the velocity of propagation and oscillation directions in quartz, $LSH(Li_2SO_4H_2O)$ and ADP crystals.

537.311.33 3015

Theory of Thermal Rectification: Part 1—Thermal Rectification Effect—K. B. Tolpygo and I. M. Tsidil'kovski. (*Zh. Tekh. Fiz.*, vol. 22, pp. 1442–1454; Sept., 1952.) A theoretical discussion of the effect discovered and investigated by Amirkhanov *et al.* (*Bull. Acad. Sci. URSS, sér. phys.*, vol. 5, p. 447; 1941.) The voltage/current characteristic is derived for a homogeneous semiconductor with no resistances at the electrodes but with a temperature gradient in the direction of the electric field. See also 2552 and 2602 of 1946 (Amirkhanov).

537.311.33 3016

Electronic Conductivity of Anthracene Single Crystals—H. Mette and H. Pick. (*Z. Phys.*, vol. 134, pp. 566–575; April 17, 1953.) The preparation of pure anthracene crystals is described. Measurements in the range 85–190°C established an exponential dependence of the conductivity on the temperature. The results show that the crystals are semiconductors.

537.311.33 3017

Cyclotron Resonances, Magnetoresistance, and Brillouin Zones in Semiconductors—W. Shockley. (*Phys. Rev.*, vol. 90, p. 491; May 1, 1953.)

537.311.33:538.632 3018

The Adiabatic Hall Effect in Semiconductors—V. A. Johnson and F. M. Shipley. (*Phys. Rev.*, vol. 90, pp. 523–529; May 15, 1953.) The relative difference between the adiabatic and isothermal Hall coefficients is calculated for the following cases:—(*a*) "classical" impurity semiconductor; (*b*) degenerate impurity semiconductor; (*c*) "classical" semiconductor at high temperature. For the thermal and electrical conductivities characteristic of Si and Ge, the relative differences are of the order of 1% or less. Tables are presented from which the relative difference may be calculated for any semiconductor of known electrical conductivity, thermal conductivity, and variation of carrier density with temperature.

537.311.33:[546.863.221+546.873.221 3019

Electrical Properties of Sb_2S_3 and Bi_2S_3—G. Galkin, G. Dolgikh and V. Yurkov. (*Zh. Tekh. Fiz.*, vol. 22, pp. 1533–1539; 1952.) The temperature dependence of electrical conductivity of Sb_2S_3 and Bi_2S_3 samples was investigated. The value and sign of the temperature coefficients of sulphides as well as of the thermo-emf of the metal/semiconductor couple depend essentially on the heat treatment of the samples and on the temperature range under investigation. The results obtained are discussed from the standpoint of the band theory of semiconductors.

537.311.33:621.314.7 3020

Impurity Diffusion and Space-Charge Layers in "Fused-Impurity" *p-n* Junctions—J. S. Saby and W. C. Dunlap, Jr. (*Phys. Rev.*, vol. 90, pp. 630–632; May 15, 1953.) Diffusion calculations for various impurities, heating times and temperatures show that diffusion for even a few seconds at very moderate temperatures results in the introduction of more than 2×10^{12} atoms per cm^2 in the case of the common donors or acceptors. Diffusion of this order ensures the location of the space-charge layer entirely within the base material.

537.311.33:621.314.7 3021

Transistors: Theory and Application: Part 5—Point-Contact Transistor Operation—A. Coblenz and H. L. Owens. (*Electronics*, vol. 26, pp. 158–163; July, 1953.) A simple but detailed analysis of current theory of operation.

537.311.33:621.396.822 3022

Boundary-Layer Noise in Semiconductors—W. M. Buttler. (*Ann. Phys.* [Lpz.], vol. 11, pp. 362–367; Jan. 16, 1953.) Starting from Gisolf's formula for current fluctuations (667 of 1950) and considering mean-square field strength, an expression is derived which gives the total noise figure, taking account of both boundary-layer noise and noise originating within the semiconductor.

537.311.33:621.396.822 3023

Boundary-Layer Noise in CdS Single Crystals—W. M. Buttler. (*Ann. Phys.* [Lpz.], vol. 11, pp. 368–376; Jan. 16, 1953.) The expression derived *in* 3022 above forms the basis of a new theory of boundary-layer noise, which is the greater the less the length of the semiconductor. Experiments to determine the dependence of noise on the applied voltage are described. Results indicate that in CdS the noise originates predominantly in the boundary layer.

538.221 3024

Determination of the Coercive Force of Nonuniformly Magnetized Specimens—A. I. Bulanova, M. N. Mikhnevich and V. B. Perets. (*Zh. Tekh. Fiz.*, vol. 22, pp. 1325–1333; Aug., 1952.) Results are given of an experimental and theoretical investigation of the errors which arise in the determination of coercive force in specimens of complex configuration and magnetically anisotropic structure.

538.221 3025

Ferromagnetism and Order in Nickel/Manganese Alloys—G. R. Piercy and E. R. Morgan. (*Canad. Jour. Phys.*, vol. 31, pp. 529–536; May, 1953.)

538.221 3026

Theoretical Considerations on the Effect of Ellipsoidal Inclosures, of Dimensions Small compared with the Thickness of the Bloch Wall, on the Ferromagnetic Coercive Force—E. Schwabe. (*Ann. Phys.* [Lpz.], vol 11, pp. 99–112; Nov. 20, 1952.)

538.221 3027

The Structure of the Ferromagnetic State in a Fe and some Fe Alloys—G. Heber. (*Ann. Phys.* [Lpz.], vol. 11, pp. 155–160; Nov. 20, 1952.)

538.221:538.652 3028

On the Theory of Magnetostriction and of Other Even Effects in Strong Magnetic Fields—G. P. D'yakov. (*Zh. Eksp. Teor. Fiz.*, vol. 23, pp. 525–531; 1952.) A mathematical theory is developed for multicrystal ferromagnetic materials. Formulas are derived for calculating even effects in non-textural materials, and the following conclusions are made: (1) the law of the approach of even effects to saturation relates all the main characteristics of a ferromagnetic material to one another; (2) on the basis of this law it is possible, from measurements of magnetostriction in multicrystal samples, to determine all the main constants of ferromagnetic materials; (3) from the experimental variation of magnetostriction when approaching saturation it is possible to determine the constant of the magnetic energy anisotropy and its sign. The relations obtained are generalized to cover the case when elastic stresses are present in the material, and the following two limiting cases are considered: (*a*) when stresses are nonuniform, (*b*) when stresses are uniform and coincide with the direction of the magnetic field.

538.221:621.396.822 3029

The Space Correlation of Noise of Cyclical Magnetic Reversals—A. A. Grachev. (*Compt. Rend. Acad. Sci.* [URSS], vol. 85, pp. 741–744; Aug. 1, 1952. In Russian.) Investigations on permalloy wires.

538.221:669.15.782-194 3030

Grain-Oriented Iron-Silicon Alloys—G. H. Cole. (*Elect. Eng.*, vol. 72, pp. 411–416; May, 1953.) Chemical compositions and graphs of the magnetic properties of typical alloys are given. The maximum permeability is obtained when the orientation is in the direction of rolling, parallel to the applied field. This gives also the condition for minimum power losses. Applications of such materials are noted.

539.234:537.311.31 3031

Experimental Study of the Electrical Conductivity of Very Thin Metal Films obtained by Thermal Evaporation—N. Mostovetch. (*Ann. Phys.* [Paris], vol. 8, pp. 61–125; Jan./Feb., 1953.) Full report and discussion of results of investigations on various metal films of thickness <100 Å deposited on glass, quartz and mica. Results obtained show (*a*) that the action of absorbed gases causes a decrease in resistance, (*b*) exponential variation of resistance with temperature, (*c*) a linear relation between log R and $F^{1/2}$ where R is resistance and F is the intensity of an applied electric field of between 1 and 50 V/cm. See also 376, 1634 (Mostovetch and Duhautois), and 2192 (Mostovetch *et al.*), of 1952.

539.234:546.289 3032

Evaporation of Germanium Films from a Carbon Crucible—K. Lehovec, J. Rosen, A. MacDonald and J. Broder. (*Jour. Appl. Phys.*, vol. 24, pp. 513–514; May, 1953.) Equipment for evaporation of Ge in vacuo at various measurable rates is described. The activation energy of evaporation is 3.5 eV, a value in close agreement with data recently published by Searcy.

546.28+546.289 3033

The Solubility of Silicon and Germanium in Gallium and Indium—P. H. Keck and J. Broder. (*Phys. Rev.*, vol. 90, pp. 521–522; May 15, 1953.) Solubility values for the temperature range of interest in preparing junction transistors are presented in graphs. Si crystals of fair purity have been obtained by slow cooling of saturated solutions.

546.831:621.385.032.461 3034

Quality Estimation for Powdered Zirconium for use in Valve Manufacture—H. Figour and H. Bonnell. (*Le Vide*, vol. 8, pp. 1305–1306; March, 1953.) A simple method of evaporation in vacuo is suggested for rapid determination of the quality of Zr intended as getter material.

548.7:[546.723-31+546.711.241 3035

The Antiferromagnetic Structure Deformations in CoO and MnTe—S. Greenwald. (*Acta cryst., Camb.*, vol. 6, part 5, pp. 396–398; May 10, 1953.)

548.7:546.76.86 3036

Crystal Structure and Antiferromagnetism of CrSb—B. T. M. Willis. (*Acta cryst., Camb.*, vol. 6, part 5, pp. 425–426; May 10, 1953.)

621.315.615.9 3037

Some Fluorinated Liquid Dielectrics—N. M. Bashara. (*Elec. Eng.*, vol. 72, p. 424; May, 1953.) Digest only. The remarkable properties of fluorocarbon materials, including stability at high temperatures, high dielectric strength, low power factor, non-inflammability, etc., make them suitable for many electrical applications.

621.318.2.042.15 3038

Micropowder Magnets—(*Elect. Jour.*, vol. 150, pp. 1645–1646; May 8, 1953.) Short account of the properties of permanent magnets now manufactured in England. Coercive forces approaching 1000 oersted can be obtained with pure iron power, the best results being obtained with a particle size between 0.01 and 0.1μ. The best micropowder available includes 30% Co and has an energy factor equivalent to that of alnico, but its density of about 4.5 gm/cm^3 gives it a great advantage over cobalt steel or similar alloys. Similar accounts in *Engineering* [London], vol. 175, pp. 682–684; May 29, 1953, and *Engineering* [London], vol. 195, pp. 740–741; May 22, 1953.

621.318.23 3039

Optimum Design of Permanent Magnets—H. K. Ziegler. (*Elec. Eng.*, vol. 72, p. 443; May, 1953.) Digest only. Discussion of the use of the average value of the slope of minor loops of the B/H demagnetization curve, in the region of the maximum energy product, for optimum magnet design. Design curves are given for Alnico V, VI and XII.

621.383.4:546.817.221 3040

Effect of Oxygen on Conductivity and Photoconductivity of Lead-Sulphide Photoresistors—S. M. Rivkin and L. N. Malakhov. (*Compt. Rend. Acad. Sci.* [URSS], vol. 85, pp. 765–768; Aug. 1, 1952. In Russian.) The variation of conductivity with the degassing time at temperatures in the range 32.5–63°C was investigated. The characteristics of PbS photoresistors are apparently determined solely by the effect of oxygen on the properties of the interstitial layer surrounding the grains of PbS. See also 702 of 1952 (Ehrenberg and Hirsch).

MATHEMATICS

517.63 3041

A Contribution to the Clear Interpretation of the Laplace Transformation—H. F. Schwenkhagen. (*Elektroiech. Z., Edn A*, vol. 74, pp. 133–136; March 1, 1953.) Discussion of analytical methods and the connection between Fourier and Laplace transforms.

681.142 3042

Linear-to-Logarithmic Voltage Converter—R. C. Howard, C. J. Savant and R. S. Neiswander. (*Electronics*, vol. 26, pp. 156–157; July, 1953.) For use with analogue computers. The logarithmic output is obtained by adjustment of anode voltage and anode and cathode resistors in a triode circuit with a large grid resistor and a much smaller input-to-cathode resistor. A cathode-follower stage cancels the offset voltage and also isolates the converter from the actual output. Logarithmic bases and output voltages obtainable with various types of tube are listed. The logarithm base can be adjusted, after conversion, by changing the gain.

681.142 3043

The Analog Computer—D. H. Pickens. (*Prod. Eng.*, vol. 24, pp. 176–185; May, 1953.) Description of the different types of element used in analogue computers, and their combination for the solution of specific problems.

681.142 3044

Analog Computer for the Roots of Algebraic Equations—L. Löfgren. (Proc. I.R.E., vol. 41, pp. 907–913; Aug., 1953.)

681.142 3045

DINA, a Digital Analyzer for Laplace, Poisson, Diffusion, and Wave Equations—C. Leondes and M. Rubinoff. (*Trans. Amer. IEE*, vol. 71, part I, pp. 303–308; 1952. Discussion, pp. 308–309.)

681.142 3046

Basic Features of a Programme for a Chess-playing Computer—G. Schliebs. (*Funk u. Ton*, vol. 7, pp. 257–265; May, 1953.)

681.142:519.272.119 3047

Simple Computer Automatically plots Correlation Functions—A. H. Schooley. (*Tele-Tech*, vol. 12, pp. 71–73, 158; May, 1953.) An analogue computer for use in evaluating the autocorrelation and cross correlation functions of time functions is described. Loops of 35-mm film, cut to the shape of the time functions, are

moved by two sprockets at a uniform speed. Slide-wire resistors are operated by levers resting against the cut edges of the films; the resistor outputs are passed via a *RC* filter to the amplifier and paper-strip recorder.

681.142:621.314.3† 3048
The Single-Core Magnetic Amplifier as a Computer Element—R. A. Ramey. (*Trans. Amer. IEE*, vol. 71, part I, pp. 442–446; 1952).

681.142:621.315.612.4 3049
Ferroelectric Materials as Storage Elements for Digital Computers and Switching Systems—J. R. Anderson. (*Trans. Amer. IEE*, vol. 71, part I, pp. 395–401; 1952.)

681.142:621.395.623.7 3050
An Analogue for Use in Loudspeaker Design—J. J. Baruch and H. C. Lang. (*Proc. NEC* [Chicago], vol. 8, pp. 89–93; 1952. *Trans. IRE*, vol. AU-1, pp. 8–13; Jan./Feb., 1953.) Description of a computer designed to facilitate analysis of loudspeaker performance as a function of frequency.

MEASUREMENTS AND TEST GEAR

621.3.018.41(083.74):[621.314.7 +621.396.611.21 3051
Precision Transistor Oscillator—P. G. Sulzer. (*Radio & Telev. News, Radio-Electronic Eng. Sec.*, vol. 49, pp. 18, 29; May, 1953.) See 2064 of July.

621.3.087.4:551.510.535 3052
A 16-kW Panoramic Ionospheric Recorder—R. Lindquist. (*Chalmers Tek. Högsk. Handl.*, no. 109, 41 pp.; 1951.) Reprint. See 1425 of 1951.

621.314.7.001.4 3053
Methods and Equipment for Transistor Testing—B. J. O'Neill and A. Gutterman. (*Electronics*, vol. 26, pp. 172–175; July, 1953.) Description of cro equipment for tracing characteristics, and of an accessory circuit for reforming defective units.

621.317.3:538.632 3054
On the Geometrical Arrangement in Hall Effect Measurements—V. Frank. (*Appl. Sci. Res. B*, vol. 3, pp. 129–140; 1953.) The short-circuiting effect of the current electrodes in Hall-effect measurements is discussed for the case of an arbitrary geometrical arrangement. For singly connected geometries the correction to be applied is a universal function of a single parameter characteristic of the geometry. This parameter can be determined experimentally. The theory was verified experimentally for a particular geometry by measurements on copper.

621.317.3:621.396.822](083.74) 3055
Standards on Electron Devices: Methods of Measuring Noise—(Proc. I.R.E., vol. 41, pp. 890–896; Aug., 1953.) Standard 53 IRE 7S1.

621.317.331.028.3 3056
Measurement of Multimegohm Resistors—A. H. Scott. (*Jour. Res. Nat. Bur. Stand.*, vol. 50, pp. 147–152; March, 1953.) Measurements made by a null method using an electrometer are described. A variable air-dielectric capacitor supplies the charge flowing through the resistor on test. The potential is maintained constant by decreasing capacitance at the correct rate. Protracted measurements on resistors in the range 10^8–10^{11} Ω show that the most stable resistors available are subject to fluctuations of 0.5–1.0% and are generally sensitive to voltage change. For a shorter account, see *Tech. News Bull. Nat. Bur. Stand.*, vol. 37, pp. 90–92; June, 1953.

621.317.335 3057
Use of Classical Circuits for the Measurement of Dielectric Constants and Losses at Frequencies between 80 c/s and 40 Mc/s—R. Dalbert. (*Rev. gén. Élect.*, vol. 62, pp. 237–246; May, 1953.) Analysis is made of three methods using known bridge arrangements in which the required determination is effected by obtaining a balance. The accuracy of these methods is evaluated, and the influence of parasitic circuit elements on the validity of the approximations introduced is studied.

621.317.336:621.315.212 3058
More on the Sweep-Frequency Response of RG/6U Cable—D. A. Alsberg. (Proc. I.R.E., vol. 41, p. 936; Aug., 1953.) Comment on 3168 of 1952 (Blackband).

621.317.35:621.3.018.783 3059
The Rigorous Basis of an Intermodulation Method of Nonlinear-Distortion Measurement—H. Söding. (*Frequenz*, vol. 7, pp. 127–133; May, 1953.) The mathematical representation of the intermodulation factor of an amplifier having a characteristic of order n is considered. The measurement circuit used is shown schematically and the method of exact determination of the intermodulation factor from two voltage readings is established. See also 2734 (Bloch), 2735 (Maxwell), 2736 (Roys), and 2737 (Scott), of September.

621.317.4:538.221 3060
Measuring Methods for some Properties of Ferroxcube Materials—C. M. van der Burgt, M. Gevers and H. P. J. Wijn. (*Philips Tech. Rev.*, vol. 14, pp. 245–256; March, 1953.) For measurement of permeability and losses in weak fields a resonance method is applied using (*a*) lumped circuit elements for the frequency range 50 kc–10 mc, (*b*) a coaxial line for the range 5 mc–3 kmc. Sources of error and limitations of the methods are discussed. In strong fields, determination of the magnetization curve replaces permeability measurement. For measurement of losses, a calorimetric or coaxial-line method may be used according to flux density and operating frequency. Distortion is measured by a selective voltmeter or, at frequencies below about 2 kc, may be determined from the hysteresis resistance. See also 2823 of 1952 (Went and Gorter).

621.317.41 3061
Apparatus for Bulk Tests on Sheet Iron—E. Wettstein. (*Helv. Phys. Acta*, vol. 25, pp. 488–490; Sept. 15, 1952. In German.) Outline description of equipment for rapid measurement of permeability and thickness.

621.317.444:621.396.645.35:621.317.755 3062
An Integrating Amplifier for the Oscillographic Recording of Magnetic Flux—S. Ekelöf, L. Bengtson, G. Kihlberg and P. Leithammel. (*Chalmers Tek. Högsk. Handl.*, no. 120, 23 pp., 1951.) Reprint. See 2276 of 1952.

621.317.7:621.396.61/.62 3063
Test Equipment for the TD-2—A. S. May. (*Bell Lab. Rec.*, vol. 31, pp. 187–193; May, 1953.) Illustrated descriptions are given of (*a*) transmitter/receiver testing equipment used at all the stations of this radio relay system; this includes if (70 mc±25 mc) and RF (3.7–4.2 kmc) variable-frequency generators, signal-power meters and oscilloscope, (b) equipment for terminal stations only, including oscilloscope, FM test set and linearity test set.

621.317.72 3064
An Isolating Potential Comparator—T. M. Dauphinee. (*Canad. Jour. Phys.*, vol. 31, pp. 577–591; May, 1953.) A double-pole double-throw chopper, with a capacitor connected between the vibrating contacts, is used with a galvanometer or electronic amplifier to indicate the inequality between two emf's such as those of two thermocouples. There is no net current flow between the circuits. Theory of the method is given and applications are suggested.

621.317.73.012.11 3065
Automatic Smith-Chart Plotter—K. S. Packard. (*Tele-Tech*, vol. 12, pp. 65–67, 183; April, 1953.) An outline description of the Impedance Plotter is given. This instrument is designed to cover 100–400 mc in two ranges, either range being swept at 2 cps. The measured impedance/frequency curve is traced out on a cr screen with a Smith-chart overlay.

621.317.75:621.392.26 3066
A Direct-reading Standing-Wave Indicator—A. C. Grace and J. A. Lane. (*Jour. Sci. Instr.*, vol. 30, pp. 168–179; May, 1953.) A waveguide squeeze-section (Montgomery, 2865 of 1948, is used together with a cro to give an instantaneous indication of changes in SWR at wavelengths of the order of 1 cm. One side of the squeeze-section is fixed, while the other is given a small transverse displacement by means of a cam driven at about 10 rps. The test signal, modulated at 10 kc, is obtained from a reflex klystron giving about 20 mw and is detected by a Type-VX-4042 crystal. Load matching to within about 2% can be achieved.

621.317.755 3067
A Direct-Reading Oscilloscope for 100-kV Pulses—R. C. Hergenrother and H. G. Rudenberg. (Proc. I.R.E., vol. 41, pp. 896–901; Aug., 1953.) Description of the design, construction and performance of a unit using es deflection, and responding to pulses of duration of a fraction of a μsec.

621.317.755:531.765 3068
A Recurrent-Sweep Chronograph—H. Moss. (*Electronic Eng.*, vol. 25, pp. 282–286; July, 1953.) The operation and circuit details of a counter-type chronograph designed for ballistics measurements are described. Timing signals are displayed on a cro so that confusion with spurious noise signals is avoided. In the form of clipped pulses they are traced on a 10-line raster on which a 10-line time scale is superimposed. Line-sweep and frame-sweep generators are controlled by a 1-kc tuning fork operating through decade frequency dividers. The maximum period measurable is 10^5 μs; time resolution, ±15 μs.

621.317.755:621.396.677.012.12 3069
Aerial Radiation Patterns. Apparatus for Cathode-Ray-Tube Display—T. T. Ling. (*Wireless Eng.*, vol. 30, pp. 192–195; Aug., 1953.) The receiving antenna under investigation is mounted on a turntable rotatable at 1 to 30 rpm. The RF power picked up by the antenna from a pulsed magnetron transmitter (3.2 cm λ) is converted to a sine wave whose amplitude is proportional to the power of the received signal. The sine wave is applied to the primary of a magslip, geared to the turntable, via a cathode follower. The outputs from the two mutually perpendicular secondaries, after amplification, are fed to the x and y coils of a cro with long-persistence screen. As the turntable rotates, a luminous area is swept out on the screen, the contour representing the antenna polar diagram. With suitable blanking arrangements, the contour only is obtained. Typical radiation patterns are illustrated.

621.396.611.21.029.45/.51 3070
The Sunbury Portable Frequency Standard for 100 c/s to 100 kc/s—A. H. Morser. (*Electronic Eng.*, vol. 25, pp. 290–293; July, 1953.) Description, with complete circuit details, of a tone source designed for calibrating electronic tachometers. It provides an output >25V rms and accurate to within 0.1% at 100, 10, 1 or 0.1 kc, derived from a vacuum-mounted 100-kc quartz crystal. Frequency division is effected by regenerative modulation.

621.396.619.13:621.317.755 3071
A Method for Establishing the Modulation Index of Periodic F.M. Signals—A. H. Phillips and M. Cooperstein. (*Sylvania Technologist*,

vol. 6, pp. 31–34; April, 1953.) The case of modulation by a single sinusoidal voltage is considered. By means of a mixing process the original FM signal is used to derive a new FM signal whose carrier frequency is less than the FM excursion, so that over certain parts of the modulation cycle the instantaneous frequency is "negative," corresponding to a negative rate of change of phase. The output from the mixer, after passing through a low-pass filter, is displayed on an oscilloscope, and the modulation index is deduced from the observed number of oscillations between the points of stationary phase. The use of high-order side-frequency components for rapid interpretation of large modulation indexes is demonstrated.

OTHER APPLICATIONS OF RADIO AND ELECTRONICS

534.522.1:539.3 3072

Ultrasonic Waves measure the Elastic Properties of Polymers—G. W. Willard. (*Bell Lab. Rec.*, vol. 31, pp. 173–179; May, 1953.) Ultrasonic light-diffraction apparatus operating on the principle previously described (3754 of 1947) is used to measure the velocity of ultrasonic waves in the polymer; the elastic constants of the material can then be determined.

535.82:621.397.611.2 3073

Flying-Spot Microscope—F. Roberts, J. Z. Young and D. Causley. (*Electronics*, vol. 26, pp. 137–139; July, 1953.) See 1733 of 1951 (Young and Roberts). Other applications of this microscope are briefly mentioned.

537.533:535.417 3074

Electron Beam Interferometer—L. Marton, J. A. Simpson and J. A. Suddeth. (*Phys. Rev.*, vol. 90, pp. 490–491; May 1, 1953.) A practical form of the instrument discussed previously (Marton, 2562 of 1952) uses a three-crystal beam-splitting device.

621.316.7:681.142 3075

Analysis of Control Systems involving Digital Computers—W. K. Linvill and J. M. Salzer. (PROC. I.R.E., vol. 41, pp. 901–906; Aug., 1953.)

621.384.611/.612 3076

The Synchrocyclotron at Amsterdam: Part 4—Details of Construction and Ancillary Equipment—F. A. Heyn and J. J. Burgerjon. (*Philips Tech. Rev.*, vol. 14, pp. 263–279; March, 1953.) Part 3: 223 of 1952 (Heyn). Please note change in UDC numbers for particle accelerators.

621.384.622.2 3077

Axial Motion of Electrons in a Linear Accelerator with $\beta=1$—J. Swihart and E. Akeley. (*Jour. Appl. Phys.*, vol. 24, pp. 640–643; May, 1953.)

621.384.622.2 3078

Study and Development of a Standing-Wave Linear Accelerator for Electrons—A. Sarazin. (*Ann. Radioélect.*, vol. 8, pp. 134–152 and 228–263; April/July, 1953.) Theoretical and experimental investigations relating to an accelerator giving 1.2-Mev electrons.

621.384.622.2:537.291 3079

Effect of Variation of the Amplitude of the Accelerating Field on the Motion of Ions in Linear Accelerators—M. Y. Bernard. (*Compt. Rend. Acad. Sci.* [Paris], vol. 236, pp. 2226–2228; June 8, 1953.)

621.385.833 3080

A Method of Observing Selected Areas in Electron and Optical Microscopes—J. F. Nankivell. (*Brit. Jour. Appl. Phys.*, vol. 4, pp. 141–143; May, 1953.) Brief description of simple apparatus for positioning plastic replicas as desired on electron-microscope specimen grids, to enable direct comparison to be made of electron- and photo-micrographs.

621.385.833 3081

Aberrations of Electronic Images of Irregular Emissive Cathodes—F. Bertein. (*Jour. Phys. Radium*, vol. 14, pp. 235–240; April, 1953.) Investigation of the astigmatism, field curvature and distortion resulting from surface irregularity. The astigmatism can appreciably reduce the resolution.

621.385.833 3082

The Field Emitter: Fabrication, Electron Microscopy, and Electric-Field Calculations—W. P. Dyke, J. K. Trolan, W. W. Dolan and G. Barnes. (*Jour. Appl. Phys.*, vol. 24, pp. 570–576; May, 1953.)

621.385.833 3083

Practical Calculation of the Third-Order Aberrations of Centred Electronoptical Systems—M. Barbier. (*Ann. Radioélect.*, vol. 8, pp. 111–133; April, 1953.)

621.385.833+621.392.5].001.362 3084

Representation of Optical or Electronic Lenses by Quadripoles consisting of Pure Resistances—F. Bertein. (*Compt. Rend. Acad. Sci.* [Paris], vol. 236, pp. 2494–2496; June 29, 1953.) The equivalence is established for certain types of lens.

621.387.42 3085

Low-Voltage Counter Tubes—P. Kunze and G. Schulz. (*Ann. Phys.* [Lpz.], vol. 11, pp. 225–238; Jan. 16, 1953.) Discussion of design requirements and report of experimental investigations on tubes with Ne, He, Ar and Hg-vapor filling.

621.387.424 3086

The Functioning of Geiger-Müller Self-Quenching Counters—D. Blanc. (*Jour. Phys. Radium*, vol. 14, pp. 260–269; April, 1953.) Review of theory of operation, different types, and applications. 152 references.

621.387.424 3087

Geiger-Müller Counters with External Cathode and Pure Methyl-Alcohol Filling, for Intense Radiation—D. Blanc. (*Jour. Phys. Radium*, vol. 14, pp. 271–272; April, 1953.) A counter of this type, 8-cm long and 2-cm diameter, with vapor pressure of 2 cm Hg, has a threshold voltage of 1.3 kv, a plateau of 500 v with a slope of 2% per 100 v, and a counting rate of 20,000/min. It can deal with radiation much more intense than counters with usual fillings.

621.387.424 3088

The Photoelectric Sensitivity of Self-Quenching Geiger Counters with Glass Envelope and External Cathode—H. Schwarz. (*Z. Phys.*, vol. 134, pp. 540–545; April 17, 1953.)

621.387.424 3089

The Maze Counter—A. Aron. (*Z. Phys.*, vol. 134, pp. 622–641; April 17, 1953.) Investigation of the characteristics of G-M counters with glass envelope and external cathode.

PROPAGATION OF WAVES

621.396.11 3090

Radiocommunication on Frequencies exceeding Predicted Values—E. V. Appleton and W. J. G. Beynon. (*Proc. IEE*, vol. 100, part III, pp. 192–198; July, 1953.) Communication data for BBC transmissions during 1943 at frequencies around 20 mc showing cases of satisfactory reception of frequencies higher by 1–6 mc than the predicted muf are analyzed. A high proportion of the apparent anomalies occurring during the winter and equinoctial months can be explained in terms of reflection from the normal E region and of variability of F_2 normal-incidence critical frequency. The remainder can be attributed to reflections from the abnormal-E layer. Analysis of Japanese 30-mc data for the years 1935–1939 leads to similar conclusions.

621.396.11:535.42 3091

Some V.H.F. Experiments upon the Diffraction Effect of Hills—G. C. Rider. (*Marconi Rev.*, vol. 16, pp. 96–106; 2nd quarter, 1953.) Experiments at 160.2 mc on propagation over steep hills show that the signal increase obtained when passive repeater antennas are used may be satisfactorily predicted by the method normally used for calculating the field in the shadow of a knife edge. Passive repeaters are expected to be most useful in the uhf band. For prediction of field strength across a valley, when transmitter and/or receiver are close to the hill, the spherical diffraction treatment gives results in closer agreement with experiment than the knife-edge method. A preliminary survey of the polarization and direction of arrival of radio waves at receiver positions round the hill was also made.

621.396.11:551.510.535 3092

C.C.I.R.-U.R.S.I. Co-operation. Exchange of Information for Forecasts and Warnings—(*URSI Inform. Bull.*, no. 78, pp. 42–54; March/April, 1953.) Report on the steps taken in the U.S.A. The current codes used by the C.R.P.L. for forecasts and cosmic data are given in an appendix.

621.396.11:551.510.535 3093

Some Calculations of Ray Paths in the Ionosphere—S. K. H. Forsgren. (*Chalmers Tek. Högsk. Handl.*, no. 104, 23 pp.; 1951.) Reprint. See 782 of 1952.

621.396.11:551.510.535(98) 3094

Polar Blackouts Recorded at the Kiruna Observatory—R. Lindquist. (*Chalmers Tek. Högsk. Handl.*, no. 103, 25 pp.; 1951.) Reprint. See 783 of 1952.

621.396.11:621.317.353.3† 3095

The Theory of the Interaction of Radio Waves in the Ionosphere—I. M. Vilenski. (*Zh. Eksp. Teor. Fiz.*, vol. 22, pp. 544–561; May, 1952.) An elementary theory of the Luxemburg effect was given by Bailey (1934 Abstracts, p. 606). In a subsequent paper by Ginzburg, a kinetic theory of the phenomenon was presented in which collisions between electrons and ions were taken into account. These two papers, however, considered only the depth and phase of the cross modulation of the waves which had passed through the "disturbed" region, and the hf terms of the interaction were neglected. A more detailed investigation, taking account of all terms, is here given. In addition to cross modulation, "side" waves of combination frequencies are found to appear. Formulas are derived for determining the amplitudes of the "side" waves, and the effect of collisions between electrons and ions is considered for various cases.

621.396.11.029.53 3096

The Influence of the Ionosphere on Medium-Wave Broadcasting—G. J. Phillips. (*BBC Quart.*, vol. 8, pp. 40–54; Spring, 1953.) A general summarized description of the ionosphere and its characteristic effects, with particular reference to those affecting mf broadcasting. Reduction of fading achieved by use of mast radiators designed to minimize the sky wave may be limited by the diffuseness of reflection from the ionosphere. Quantitative measurements of the angular scatter on reflection by the ionosphere are being made at medium frequencies.

621.396.11.029.64 3097

Microwave Propagation in the Optical Range—O. F. Perers, B. K. E. Stjernberg and S. K. H. Forsgren. (*Chalmers Tek. Högsk. Handl.*, no. 108, 20 pp.; 1951.) Reprint. See 789 of 1952.

621.396.812.3 3098

On the Frequency of the Scintillation Fading of Microwaves—O. Tukizi. (*Jour. Phys. Soc.* [Japan], vol. 8, pp. 130–131;

Jan./Feb., 1953.) Experimental results are reported which appear to support the theoretical prediction of proportionality between the scintillation-fading frequency and the mean wind speed over the propagation path.

RECEPTION

621.396.621 3099

Counter-Circuit Multiplex Receiver—A. R. Vallarino, H. A. Snow and C. Greenwald. (*Electronics*, vol. 26, pp. 178–181; July, 1952.) In a FM multiplex subcarrier system, a RF receiver demodulates the RF signal and passes the resulting FM 1-mc subcarrier to a second receiver for demodulation. The subcarrier receiver described involves no alignment problems and introduces only 0.2% distortion over the modulation frequency band 250 cps=150 kc. Details are given of the 6-stage limiter using cathode-coupled clippers, and of the counter-discriminator circuit. Output voltage is a linear function of input frequency.

621.396.722:551.594.6 3100

Existing and Planned Spherics Stations—(*URSI Inform. Bull.*, no. 78, pp. 38–41; March/April, 1953.) The geographical position, the frequency of operation and type of equipment of 52 stations are tabulated.

STATIONS AND COMMUNICATION SYSTEMS

621.39.001.11 3101

Information Theory—P. M. Woodward. (*Brit. Jour. Appl. Phys.*, vol. 4, pp. 129–133; May, 1953.) An introduction to the early work of Hartley and the newer statistical theory developed by Shannon.

621.396.1:621.396.931 3102

Channel Spacings at 152 to 174 Mc/s—H. E. Strauss. (*Commun. Eng.*, vol. 13, pp. 17–21, 48; March/April, 1953.) Mobile-radio tests were made on frequencies around 160 mc, using channel spacings of 60, 30 and 20 kc. Tests covered range, adjacent-channel interference and intermodulation. A system having 30-kc channel spacing and ±7.5-kc modulation deviation was 4 or 5 db more sensitive to noise than the system with 60-kc channel spacing. A system with 20-kc channel spacing and ±5-kc modulation deviation was 8 db more sensitive to noise than that with 60-kc spacing and had 15% less range.

621.396.41.018.424 3103

Bandwidth of Multiplex Channels—J. S. Smith. (*Commun. Eng.*, vol. 13, pp. 22–23, 43; May/June, 1953.) Discussion of factors involved in the relation of channel response speed to the subcarrier bandwidth.

621.396.619.13:621.3.018.78 3104

The Distortion Introduced by Frequency Modulation of an Oscillator by a Perfect Reactance Valve—P. S. Brandon. (*Marconi Rev.*, vol. 16, pp. 88–95; 2nd quarter, 1953.) Assuming no distortion present when the instantaneous angular frequency is given by $1/(LC)^{1/2}$, analysis shows that a change in the inductance or capacitance of the oscillatory circuit introduces a form of amplitude modulation which in turn causes an unwanted change in frequency. Approximate expressions for the fundamental and second harmonic of this form of distortion are developed in terms of modulation depth, angular frequency of modulation, mean oscillator frequency and deviation.

621.396.619.16 3105

Consequences of the Amplitude Spectrum [transformation] in Pulse Technology—H. Kleinwächter and H. Weiss. (*Funk u. Ton*, vol. 7, pp. 221–229; May, 1953.) A general expression relating pulse duration and bandwidth required for transmission of square-wave pulse trains is derived by Fourier analysis. The bandwidth for which the signal/noise ratio is a maximum and the mean power required for pam transmission are calculated.

621.396.619.16 3106

Pulse-Code Modulation Systems—A. J. Oxford. (Proc. I.R.E., vol. 41, pp. 859–865; Aug., 1953.) Principles of pcm systems are reviewed and two modulator systems are considered in detail. In one system, the incoming signal sample charges a capacitor, which is then "examined" successively by 5 pulses, each of 30-μs duration, a charge of logarithmically decreasing amplitude being added to or subtracted from the capacitor before the arrival of the next pulse. This provides a five-digit code for transmission. In a simplified system, the residual charge on the capacitor is amplified after each pulse, so that a fixed amount of charge can be added to or subtracted from the capacitor. Demodulation and synchronization arrangements are also dealt with.

621.396.65 3107

A New Multiplex Microwave System—N. B. Tharp. (*Commun. Eng.*, vol. 13, pp. 31–34, 46; March/April, 1953.) Types FR and FJ equipments operating together at about 1.9 kmc can provide 30 two-way voice-frequency channels. The Type-FR equipment comprises transmitter-receiver, oscillator-modulator, afc, power-supply, service-channel and test-meter units. The Type-FJ equipment is the multiplexing unit.

621.396.65 3108

Microwave Developments Overseas—V. J. Nexon. (*Commun. Eng.*, vol. 13, pp. 19–21, 46; May/June, 1953.) A survey of the vhf and uhf radio link systems used in 16 countries in Europe, North Africa and the Near East, and in Australia.

621.396.65:621.396.41 3109

Multichannel Radio Link between Mestre and Trieste—L. Bernardi. (*Poste e Telecomunicazioni*, vol. 6, pp. 159–167; April, 1953. A description is given of the equipment used for this link, which operates in the frequency band 1.3–1.6 kmc and has a relay station at Clauzetto, the lengths of the two sections being respectively 98 and 92 km. Parabolic antennas are used at all three stations, the antenna power being 2.1 W. Performance curves for the whole system are given.

621.396.65:621.396.41.029.64 3110

A Multichannel Microwave Relay System—R. D. Boadle. (Proc. I.R.E. [Australia], vol. 14, pp. 80–89; April, 1953.) Description of the development in Australia of equipment based on an American design (Lerlach, 3283 of 1947, and back references).

SUBSIDIARY APPARATUS

621-526 3111

The Application of Nonlinear Techniques to Servomechanisms—K. C. Mathews and R. C. Boe. (*Proc. NEC* [Chicago], vol. 8, pp. 10–21; 1952.

621-526 3112

The Transient Response of a Single-Point Nonlinear Servomechanism—K. N. Burns. (*Proc. NEC* [Chicago], vol. 8, pp. 22–30; 1952.)

621-526 3113

Servo-System Comparators—M. Cooperstein. (*Proc. NEC* [Chicago], vol. 8, pp. 31–36; 1952.)

621-526:621.314.3† 3114

Compensation of a Magnetic-Amplifier Servo System—H. H. Woodson and C. V. Thrower. (*Proc. NEC* [Chicago], vol. 8, pp. 158–165; 1952.

621-526:621.392.5.076.12 3115

Synthesis of Compensation Networks for Carrier-Frequency Servomechanisms—R. S. Carlson and J. G. Truxal. (*Proc. NEC* [Chicago], vol. 8, pp. 37–49; 1952.)

621.3.013.783 3116

Screening of Test Rooms and Instruments from Electromagnetic Fields—J. Deutsch and O. Zinke. (*Frequenz*, vol. 7, pp. 94–101; April, 1953.) Screens made of wire mesh, metal foil and sheet, and of materials with a high permittivity or permeability are considered and expressions are given for the attenuation of incident em waves. Experimental curves for sheet and mesh screens are given. The construction of a large screened room is described and the attenuation of magnetic fields in this room (>70 db for frequencies from 200 kc to 500 mc) is compared with that of other rooms. A novel type of honeycomb wire-mesh-strip window screen is described.

621.352.32 3117

Reactivating the Dry Cell—R. W. Hallows. (*Wireless World*, vol. 59, pp. 344–347; Aug., 1953.) Discussion of the effect on cell life of repeated passage of current in the reverse direction.

TELEVISION AND PHOTOTELEGRAPHY

621.397.24/.26 3118

The Television Transmission of the English Coronation Ceremonies—A. W. M. Paling. (*Tijdschr. ned. Radiogenoot.*, vol. 18, pp. 167–174; May, 1953.) An illustrated description of the radio-link system and line-standard converter devised to transmit pictures of the Coronation ceremonies to Western Europe.

621.397.335:621–526].001.11 3119

Servomechanism Theory applied to A.F.C. Circuit Design—G. D. Doland. (*Tele-Tech*, vol. 12, pp. 95–97. 155; May, 1953.)

621.397.5 3120

Television Study Centre—M. Boella. (*Ricerca Sci.*, vol. 23, pp. 799–802; May, 1953.) A survey of activities up to the end of 1952. Of the investigations undertaken during these first few years, the most important are the choice of the Italian television standard and the construction of a scanning unit.

621.397.5:519.272 3121

An Application of Autocorrelation Theory to the Video Signal of Television—M. B. Ritterman. (*Sylvania Technologist*, vol. 5, pp. 70–75; July, 1952.) Autocorrelation theory is used to analyze the power-density spectrum of a video signal. Statistical parameters representing motion and complexity in the picture are introduced. The problem is simplified by considering a signal representing only blacks and whites, but extension of the conclusions to cover intermediate greys is justified by reference to the work of Kretzmer (2904 of 1952).

621.397.5:519.272 3122

Application of Autocorrelation Theory to the Video Signal of Television—M. B. Ritterman. (*Proc. NEC* [Chicago], vol. 8, pp. 201–207; 1952.) The power-density spectrum of the television video signal is derived, certain assumptions being made about the autocorrelation function.

621.397.5:535.623 3123

Colorimetry in Color Television—F. J. Bingley. (Proc. I.R.E., vol. 41, pp. 838–851; Aug., 1953.) Relations between colorimetric quantities and the electrical signals into which they are encoded for transmission are considered. The specific type of video signal envisaged comprises a monochrome component together with a color carrier, though the colorimetric equations derived apply to any type of system.

621.397.5:535.623 3124

The National Television Systems Committee Color Television Transmission: Part 2—R. M. Bowie and D. C. Livingston. (*Sylvania Technologist*, vol. 5, pp. 36–40; April, 1952.) A

mathematical treatment is given of the method of vestigial-sideband modulation of the color sub-carriers described in part 1 (Bowie and Tyson, 2343 of 1952), and the question of color phase alternation is considered quantitatively.

621.397.5:778.5 3125

Reversible Process for Recording on and Electronic Reproduction from Cinematograph Films—P. Mandel. (*Onde élect.*, vol. 33, pp. 206–213; April, 1953.) Description, with discussion of the performance and limitations, of the flying-spot method, which can be used either to derive television pictures from cinematograph films or, conversely, to record such pictures on films.

621.397.61 3126

Television Transmitter at Wenvoe, Glamorganshire—(*Engineering* [London], vol. 174, pp. 249–250; Aug. 22, 1952.) Description of medium-power equipment in operation pending installation of high-power transmitters.

621.397.61:656.134 3127

Mobile Television Transmitters—E. W. Hayes. (*Wireless World*, vol. 59, pp. 372–375; Aug., 1953.) A description is given of the BBC mobile transmitters which provided a television service for NE England, Northern Ireland, and the Brighton area much more quickly than would have been possible if permanent stations had to be constructed. The equipment, of a rugged type, is installed in a trailer 17 ft by 7 ft by 7 ft high. Duplicate vision transmitters, with peak-white output power ~500 w are provided; the duplicate sound transmitters have a maximum carrier power of 200 w. The frequency of the vision signals is adjustable over the whole range of the present broadcasting band (41–68 mc). The antennas used near Newcastle-on-Tyne and near Belfast were of the batwing type mounted on 250-feet lattice masts. The station on the downs near Brighton receives its vision signals direct from Alexandra Palace, using a Yagi Antenna. The transmitters feed a vertically polarized dipole fitted with a reflector and mounted on a 70-ft mast. The Belfast station obtains its vision programme by direct reception of the Kirk o' Shotts transmissions until a permanent program link with Britain can be provided.

621.397.611.2 3128

A Camera Tube with Photoconductive Layer: the Conductron—B. Bartels and M. Munsch. (*Le Vide*, vol. 8, pp. 1320–1325; March, 1953.) Description of the characteristics of the conductron in its present stage of development, with an indication of possible improvements. At present the internal photoelectric inertia is about 0.1 seconds, which should be reduced below 0.04 seconds if the tube is to be used for ordinary television. See also 1498 of 1951 (Veith).

621.397.62:535.623 3129

Theory of Synchronous Demodulator as used in N.T.S.C. Color Television Receiver—D. C. Livingston. (*Sylvania Technologist*, vol. 5, pp. 60–63; July, 1952.) The operation of the synchronous demodulator [see also McGregor, 253 of January) is analyzed, and possible distortion effects are studied. These may result from rectification of the color subcarrier or from incomplete exclusion of the luminance signal. The analysis indicates that each of these may produce perceptible distortion. *See* also 3124 above.

621.397.62:535.623 3130

A 42-Tube Compatible Color Television Receiver—K. E. Farr. (*Proc. NEC* [Chicago], vol. 8, pp. 208–217; 1952.) See 1501 of May.

621.397.62:535.623 3131

The PDF [post-deflection-focusing] Chromatron—a Single- or Multi-gun Tricolor Cathode-Ray Tube—R. Dressler. (Proc. I.R.E., vol. 41, pp. 851–858; Aug., 1953.) Red, green and blue phosphor strips, 15-mil wide, are deposited on the image plate and are backed with Al. Directly behind the image plate is a grid of parallel wires with one set of wires behind the red and another set behind the blue strips. The cr tube cone is made in two sections to permit insertion of the color structure after the front plate has been sealed on. Varying the potential difference between the two sets of wires directs the beam on to one of the sets of colored strips. A focusing and accelerating potential is applied between the wire grid and the Al coating. Color distortion due to nonlinear sweeps or misalignment of gun position is absent. Analysis of operation is given, and a three-gun version is also described. The tube will operate with existing color-television transmission systems.

621.397.621.2:621.385.832 3132

A Steel Picture-Tube for Television Reception—J. de Gier, T. Hagenberg, H. J. Meerkamp van Embden, J. A. M. Smelt and O. L. van Steenis. (*Philips Tech. Rev.*, vol. 14, pp. 281–291; April, 1953.) The development of steel cr tubes and of the lead-free "iron-glass" screen is described.

621.397.645 3133

Video Amplifiers for Optimum Transient Response—W. K. Squires and H. L. Newman. *Proc. NEC* [Chicago], vol. 8, pp. 218–230; 1952.) From Laplace-transform analysis of typical video coupling networks, relations among the various parameters resulting in optimum transient response are derived. A design procedure, based on these relations and on figures of merit for the tubes used, is presented which is applicable to both triode and pentode amplifiers. Examination of response curves and tests of actual circuits show that the triode amplifier is definitely superior to the pentode amplifier when attainment of maximum voltage is the major criterion. In addition, the triode has certain advantages as regards the signal /noise ratio of the synchronizing signal.

621.397.743 3134

Television Coverage of the National Political Conventions—R. W. Ralston and B. D. Wickline. (*Elec. Eng.*, vol. 72, pp. 383–389; May, 1953.) Detailed description of the wire and microwave links used for the 1952 Chicago Conventions.

TRANSMISSION

621.396.61.029.53/.55 3135

400-Watt H.F. Channellized Transmitter Type HC. 100—P. W. Jinkings. (*Marconi Rev.*, vol. 16, pp. 69–87; 2nd quarter, 1953.) Six editions of this self-contained equipment, which is suitable for use in the tropics, cover the range 1.6–27.5 mc.

TUBES AND THERMIONICS

621.314.632:546.482.21 3136

Cadmium Sulfide as a Crystal Rectifier—G. Strull. (*Proc. NEC* [Chicago], vol. 8, pp. 510–521; 1952.) Tests on CdS crystals produced for X-ray detection showed they were *n*-type semiconductors with both rectification and photoelectric properties. The optimum operating voltage for rectification is 6–8 v, but the range of voltage extends from 0.1 v to 40 v. The current at any given voltage can be varied by changing the intensity of illumination. The best performance is obtained with single crystals mounted so that the field is down the length of the crystal. The resistance of a typical crystal is ~100 kΩ with 6 v applied in the forward direction and an illumination intensity of 30 lumens/ft^2.

621.383.2 3137

On the Fatigue of Ag-Cs Photoelectric Tubes—G. Kuwabara. (*Jour. Phys. Soc.* [Japan], vol. 8, pp. 229–233; March/April, 1953.)

621.383.2 3138

The Appearance of an Alternating Component in the Photocurrent of Photocells under Strong Illumination—L. A. Vainshtein and L. P. Malyavkin. (*Zh. Tekh. Fiz.*, vol. 22, pp. 1315–1317; Aug., 1952.) It has been observed that when an Sb-Cs photocell is illuminated by a powerful source of light an af component appears in the photocurrent, sometimes together with a hf component of the order of several megacycles per second. Experiments are described and oscillograms are shown. It is suggested that these oscillations appear in the space charge, and that the presence of gas is necessary for this. In the case of vacuum cells, gas is apparently liberated as a result of the partial destruction of the photolayer by intense illumination.

621.383.27 3139

On the Development of Secondary-Electron Multipliers—F. Eckart. (*Ann. Phys.* [Lpz.], vol. 11, pp. 181–202; Jan. 16, 1953.) The secondary-emission properties of various materials and metal-based emissive layers are tabulated and the sensitivities of different photocathodes are noted. Different designs of multiplier are described and their noise and dark-current characteristics are discussed. The marked decrease in dark current of Ag-Cs_2O multipliers of mesh type is achieved by increasing the insulation path between the individual electrodes. 83 references.

621.383.4 3140

Action of a Stream of Electrons on the Current Sensitivity of Photocells—B. P. Angelov, E. M. Lobanov and S. V. Starodubtsev. (*Compt. Rend. Acad. Sci.* [URSS], vol. 85, pp. 733–735; Aug. 1, 1952. In Russian.) A report of an investigation of the dependence of the current in the external circuit of Se and Ag_2S photocells on the energy (800–20000 eV) and intensity of the primary electron stream.

621.383.4 3141

Tentative Interpretation of the Laws governing the Characteristics of Photocells—G. Blet. (*Jour. Phys. Radium*, pp. 241–250; April, 1953.) Analysis of the action of the blocking layer in a photocell enables a scheme to be developed which permits qualitative and quantitative verification of observations relating to the laws connecting illumination, voltage and current. Formulas derived give results in good agreement with experiment and permit calculation of the quantum output of a photocell.

621.383.4:535.33-1 3142

The Application of Lead Selenide Photoconductive Cells to Infra-Red Spectroscopy—V. Roberts and A. S. Young. (*Jour. Sci. Instr.*, vol. 30, pp. 199–200; June, 1953.)

621.385.012.6 3143

Investigation of the Fine Structure of Valve Characteristics—H. Schneider. (*Nachr Tech.*, vol. 3, pp. 274–279; June, 1953.) An electric current can be expressed in terms of a Taylor series with electric potential as the independent variable. If the differential coefficients are known, the series can be evaluated. Two methods of evaluating the differential coefficients, illustrated by considering the I_a/V_g characteristic of a triode, are shown in detail and the experimental determination of the coefficients is described.

621.385.029.6:621.396.615.142.2 3144

Equations for the Oscillations in Uniform Electron Beams—Yu A. Katsman. (*Zh. Tekh. Fiz.*, vol. 22, pp. 1467–1476; Sept., 1952.) The electrodynamic processes taking place in klystrons are discussed.

621.385.029.63/.64:621.396.822 3145

Noise Measurements on a Traveling-Wave Tube—B. N. Agdur and C. G. L. Åsdal. (*Chalmers Tek. Högsk. Handl.*, no. 106, 9 pp; 1951.) Reprint. See 1152 of 1952.

621.385.029.64/.65 3146
Experimental Observation of Double-Stream Amplification—B. N. Agdur. (*Chalmers Tek. Högsk. Handl.*, no. 105, 13 pp; 1951.) Reprint. See 1154 of 1952.

621.385.029.64 3147
The Resistive-Wall Amplifiers—C. K. Birdsall, G. R. Brewer and A. V. Haeff. (PROC. I.R.E., vol. 41, pp. 865–875; Aug., 1953.) In the resistive-wall amplifier, the gain is obtained through interaction between the electron-stream charge and the wall charge induced by the stream. Increasing bunching of the electrons takes place and hence wave amplification results. In contrast with the traveling-wave tube, there is no interaction between the highly-damped circuit wave and the stream. Although some energy is dissipated in wall loss, there is a finite rate of growth for all stream currents. Theory is confirmed by experiments performed at 1–4 kmc on streams passed through glass tubes coated with tin oxide as the resistive material. Helixes or resonant cavities were used as input and output coupling circuits. Gain and bandwidth are comparable to those of low-power traveling-wave tubes. The resistive-wall amplifier is relatively insensitive to changes in circuit parameters or operating voltages, and there is no tendency to self-oscillation, in view of the high isolation between input and output. Amplifiers of this type with honeycomb or sandwich structure are expected to give better performance.

621.385.032.213.2 3148
Metal Capillary Cathodes—H. Katz. (*Jour. Appl. Phys.*, vol. 24, pp. 597–603; May, 1953.) The operating conditions of cathodes basically similar to the L cathode Lemmens et al, (773 of 1951), are discussed, and descriptions are given of five variants with working temperatures ranging from 1500° to 850°C and pulsed emission from 3 to 5 A/cm². A low working temperature is advantageous, as surface evaporation is reduced. The best cathode is that with lowest evaporation and highest migration speed of the substance used for reducing the work function of the tungsten emitting surface. Substances other than tungsten, which may be better as regards low evaporation and high migration speed, may not maintain their porosity at the operating temperatures, but porous tungsten may serve as a base for surface layers with better properties. A considerable increase of emission was obtained from areas around marks made on a cathode surface with an ordinary pencil.

621.385.032.216:621.317.336 3149
Cathode-Interface Impedance and Its Measurement—H. M. Wagner. (*Proc. NEC [Chicago]*, vol. 8, pp. 553–561; 1952.) In tubes with oxide-coated cathodes, failure is sometimes due to the formation of an interface impedance layer between the coating and its metal base. This type of failure occurs more frequently when tubes are operating in circuits involving periods of anode-current cut-off [see Waymouth, 1526 of 1951]. The effect of interface impedance is approximately equivalent to the insertion of a resistor shunted by a capacitor in the cathode lead. The effect is studied for various pulse waveforms and a method for determining the value of the impedance in any particular tube is described which makes use of rectangular voltage pulses. The measurement of low values of impedance is made possible by use of a difference amplifier; this produces an output signal that represents the difference between the voltage across the load of the tube under test and a variable fraction of the input-pulse voltage.

621.385.032.216:621.396.822 3150
Temperature Dependence of Low-Frequency Fluctuations in Thermionic Emitters—T. B. Tomlinson. (*Jour. Appl. Phys.*, vol. 24, pp. 611–615; May, 1953.) A method is described for measuring the temperature variation of the flicker effect in diodes with oxide-coated cathodes. The results show that in most tubes the fluctuations of emission are minimum for a cathode temperature near 1000°K. Two separate effects appear to be involved, one with a rising and the other with a falling temperature characteristic. Various theories of the effect are discussed; none is found completely satisfactory. See also 281 of January.

621.385.032.216.1:546.841.4–31 3151
Measurements relating to the Filament of Directly Heated Thoria Cathodes—G. Mesnard. (*Le Vide*, vol. 8, pp. 1326–1331; March, 1953.) The variations of heating current in the tungsten wire carrying the thoria coating, and of the wire resistance and applied power, are shown graphically as a function of temperature to indicate the effect of various heat treatments of the cathodes. The effect of the thickness of the thoria coating, and its relation to the spectral emissivity in the red region and to the thermionic emission, are also discussed. See also 2506, 2507, and 2508 of August.

621.385.032.216.2 3152
Double Activators in Oxide-Cathode Base Alloys—A. Eisenstein, H. John and J. H. Affleck. (*Jour. Appl. Phys.*, vol. 24, pp. 631–632; May, 1953.) The existence of Si as a minor impurity in a W-Ni cathode base metal with 4.7% W was found to result in the formation, towards the end of a 6000-hour life test, of a high-resistance Ba_2SiO_4 interface compound, the Si replacing W in the Ba_3WO_6 interface layer formed at first. Similar reactions between Ti, Al and other interface compounds were examined.

621.385.24 3153
Squirrel-Cage Filament Structures—A. M. Hardie. (*Wireless Eng.*, vol. 30, pp. 196–204; Aug, 1953.) "The solution of problems of space-charge-limited current flow is discussed with particular reference to the squirrel-cage filament structure commonly employed in high-power tubes. Experiments are described which were made to determine the solid-cathode diameter equivalent to squirrel-cage structures containing an even number of wires up to 16. An example is given of the large error caused in the estimation of tube characteristics by an optimistic assumption of cathode diameter."

621.387 3154
Arc Drop and Deionization Time in Inert-Gas Thyratrons—S. Pakswer and R. Meyer. (*Jour. Appl. Phys.*, vol. 24, pp. 501–509; May, 1953.)

621.387:621.316.722 3155
Variations in the Characteristics of Some Corona-Stabilizer Tubes—F. A. Benson and J. P. Smith. (*Jour. Sci. Instr.*, vol. 30, pp. 192–194; June, 1953.) Measurements made on six 500-v tubes are reported. The effects of ambient-temperature changes and of excess current are noted. An indication is given of the drift of running voltage to be expected during the first 1200 hours of life. The properties of the tubes when operated with reversed polarity are discussed.

621.387:621.395 3156
New Thyratrons for Telephone-Circuit Engineering: Part 1—Introduction—K. L. Rau. (*Frequenz*, vol. 7, pp. 134–139; May, 1953.) Static characteristics of the simple, coincidence and anticoincidence types of thyratron are discussed and the effects of grid resistance, grid-cathode spacing and gas pressure are shown graphically. The operation of these thyratrons is compared with that of relays.

621.396.615.141.1 3157
Motion of Electrons in Retarding-Field Tubes under Optimum Receiving Conditions—M. Hirashima. (*Jour. Phys. Soc.* [Japan], vol. 8, pp. 182–193; March/April, 1953.) Measurements are described of the anode-current distribution in a tube with tungsten-filament cathode, spinal grid, mesh anode, and a collecting electrode, arranged coaxially. The energy distribution of electrons flowing into the mesh anode was also determined. A signal of frequency near 550 mc, modulated at 1 kc, was applied to grid and anode via a Lecher-line system.

621.396.615.141.2 3158
Theory of the Multisegment Magnetron—L. E. Bakhrakh. (*Zh. Tekh. Fiz.*, vol. 22, pp. 1008–1015; June, 1952.) The phase focusing of an electron beam passing consecutively through a number of phase lenses is investigated and the results obtained are used for explaining the maintenance of oscillations in a multisegment magnetron.

621.396.615.142.2 3159
Experimental Investigation of the Oscillation Mode and Bunching Efficiency of a Reflex Klystron—M. de Bennetot. (*Ann. Radioélect.*, vol. 8, pp. 103–110; April, 1953.) The method of determining the oscillation mode, previously described by Hamilton (3570 of 1948), is illustrated. From a law of similitude in electron optics which takes account of space charge, two relations are deduced which show how the phase of the modulated current varies with slight change of (*a*) the accelerating voltage, (*b*) the reflector voltage. These relations enable the bunching efficiency to be determined. Results of measurements on a Type-KR331 klystron are shown graphically. Both the oscillation mode and the bunching efficiency must be known if a satisfactory explanation of the operation of the reflex klystron is to be given, and since the combination of curved reflector, space charge and drift space is not very amenable to mathematical treatment, experimental determination of the bunching efficiency is particularly useful for obtaining design data.

621.396.615.142.2 3160
A Coupled-Resonator Reflex Klystron—E. D. Reed. (*Bell Sys. Tech. Jour.*, vol. 32, pp. 715–766; May, 1953.) Output-power/repeller-voltage and frequency/repeller-voltage characteristics suitable for various applications of variable-frequency oscillators are obtained by means of a reflex klystron having two coupled resonators instead of the usual single resonator. The theory of the system is developed and an experimental tube and circuit are described. The characteristics can be adjusted to suit a particular use by varying the coupling between the resonators and the ratio of their Q values. This advantage is gained at the expense of using greater power to supply the losses in the second resonator.

621.396.615.142.2:621.384.622.1 3161
High-Power Klystron Amplifier—J. Jasberg. (*Electronics*, vol. 26, pp. 244–248; July, 1953.) Description of a gridless three-cavity klystron with oxide-coated indirectly-heated cathode, designed for the 100-MeV linear electron accelerator at Stanford University. Beam spreading is prevented by focusing coils surrounding the cavities. Pulses of 2-μs duration at a repetition frequency of 60/seconds are used, and peak output power is 17 mw at 10.5-cm wavelength.

MISCELLANEOUS

53.08:061.4 3162
Industrial Instrumentation—(*Elec. Rev. [London]*, vol. 153, pp. 3–13; July 3, 1953.) A survey of instruments exhibited at the British Instrument Industries Exhibition at Olympia, London, June 30–July 11, 1953.

621.39:061.4 3163
20th National Radio Exhibition—(*Wireless World*, vol. 59, pp. 397–406; Sept., 1953.) Classified guide to the principal exhibits.

Having the RIGHT CONNECTIONS *is a big help!*

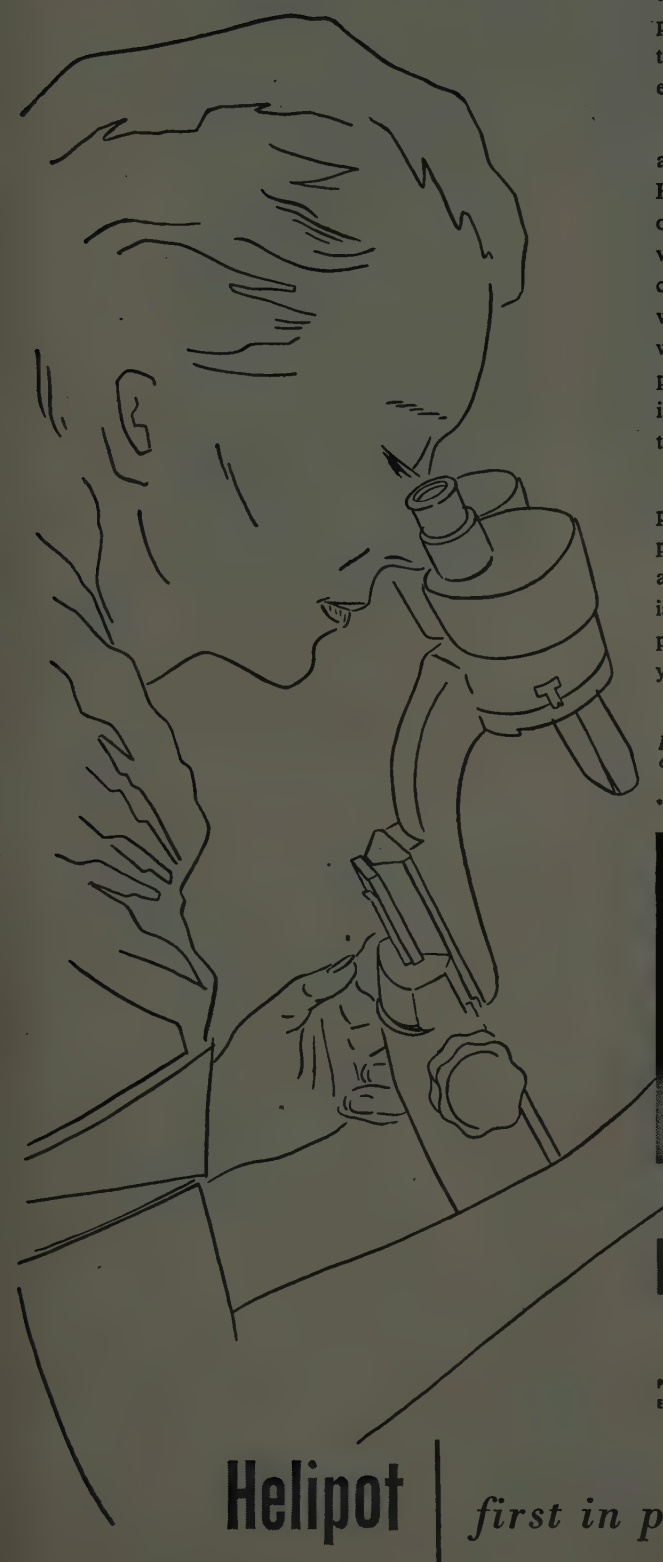

Helipot* ... first in precision potentiometers ... makes sure that, in *every* Helipot, you do have the right connections. No pressure-type connections are used in *any* Helipot. Tap connections are spot-welded by a Helipot-developed process, and other electrical connections are soldered ... they all *stay put!*

The spot welding process is a particularly interesting one ... and more important, it offers a very real advantage to users of Helipot precision potentiometers. Skilled workers, using binocular microscopes, employ a new technique in spot welding the very fine electrical connections. This technique assures that tap connections are attached to a single turn *only* of the resistance wire, rather than to several adjacent turns as is usually the case with the conventional method. Thus the high resolution, so important to the proper functioning of a precision potentiometer, is not reduced, and none of the wire turns adjacent to the one tapped are shorted out.

The spot welding process offers the further advantage of providing the strongest possible type of connections ... vibration proof, shock proof, corrosion proof, unaffected by temperature and humidity changes. And to cap the climax, the new process is efficient and economical ... another example of the Helipot policy offering the lowest price consistent with the high quality you expect in Helipot products.

For information about Helipot's complete line of precision potentiometers, call your nearest Helipot representative or write direct!

*T.M. Reg. U.S. Pat. Off.

WRITE FOR YOUR COPY!

Your copy of the HELIPOT Condensed Catalog describing every model of HELIPOT Precision Potentiometers and Duodials is now ready. Please write for it on your company letterhead.

Write for Data File #212-1106

Helipot *corporation*

a division of **BECKMAN INSTRUMENTS, INC.**
SOUTH PASADENA, CALIFORNIA

PLANTS AT SOUTH PASADENA, CALIFORNIA & MOUNTAINSIDE, NEW JERSEY
ENGINEERING REPRESENTATIVES IN PRINCIPAL CITIES

Helipot | *first in precision potentiometers*

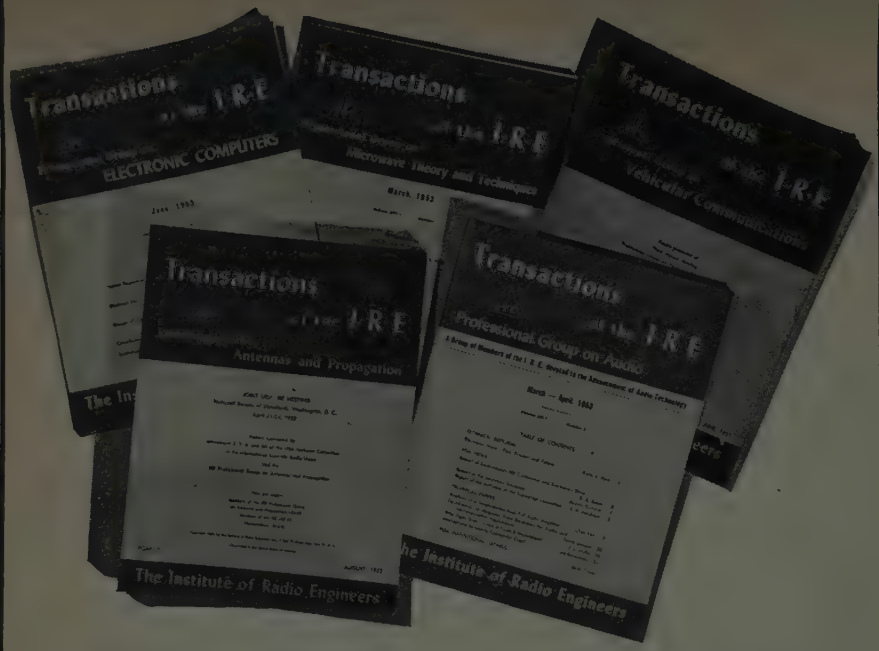

At least one of your interests is now served by one of IRE's 21 Professional Groups

Each group publishes its own specialized papers in its *Transactions*, some annually, and some bi-monthly. The larger groups have organized local Chapters, and they also sponsor technical sessions at IRE Conventions.

Airborne Electronics (G 11)	Fee $2
Antennas and Propagation (G 3)	Fee $4
Audio (G 1)	Fee $2
Broadcast & Television Receivers (G 8)	Fee $2
Broadcast Transmission Systems (G 2)	Fee $2
Circuit Theory (G 4)	Fee $2
Communication Systems (G 19)	Fee $2
Component Parts (G 21)	Fee to be set
Electron Devices (G 15)	Fee $2
Electronic Computers (G 16)	Fee $2
Engineering Management (G 14)	Fee $1
Industrial Electronics (G 13)	Fee $2
Information Theory (G 12)	Fee $2
Instrumentation (G 9)	Fee $1
Medical Electronics (G 19)	Fee $1
Microwave Theory and Techniques (G 17)	Fee $2
Nuclear Science (G 5)	Fee to be set
Quality Control (G 7)	Fee $2
Radio Telemetry & Remote Control (G 10)	Fee $1
Ultrasonics Engineering (G 20)	Fee to be set
Vehicular Communications (G 6)	Fee $2

IRE Professional Groups are only open to those who are already members of the IRE. Copies of Professional Group Transactions are available to non-members at three times the cost-price to group members.

The Institute of Radio Engineers
1 East 79th Street, New York 21, N.Y.

USE THIS COUPON

PG 11 53

Miss Emily Sirjane
IRE—1 East 79th St.
New York 21, N.Y.

Please enroll me for these IRE Professional Groups

..... $.....
..... $.....

Name .....
Address .....
Place .....

Please enclose remittance with this order.

Professional Group on Antennas and Propagation

Although the subject of antennas and radio wave propagation is as old as radio itself, it nevertheless offers the engineer of today problems as new and as challenging as the youngest branch of the radio-electronic field. The continual development of new forms of communications, detection, and navigation systems and of equipment capable of operating at higher and higher frequencies brings with it a constant need for new approaches to antenna design and propagation theory.

It is not surprising that the IRE Professional Group on Antennas and Propagation was one of the first Groups to be formed. For here was a field that, while highly specialized, was at the same time a prolific contributor to progress in the radio art. There was an urgent need for an organization specialized in technical scope and yet able to provide sufficient outlets for disseminating these many technical contributions among workers in the field.

Since its formation in February 1949, the Group's efforts to develop these outlets have met with conspicuous success. It annually co-sponsors two meetings with URSI and sponsors sessions at the National and Western Conventions of the IRE.

Perhaps of even greater significance is the Group technical publication, *Transactions,* which during its first year contained over 600 pages of valuable and otherwise unavailable material. The *Transactions* is now issued quarterly, and is already regarded as the principal publication in its field.

Group membership has now swelled to 1200. As a result, local Chapters have sprung up in Los Angeles and Chicago, with additional Chapters under formation in New York, San Diego, and San Francisco.

Thus the Group, through meetings and publications, has been able to provide the engineer with the specialized technical information he wants and needs.

W. R. G. Baker

Professional Group Chairman

Now...The Most Compact and Only Complete VOR System

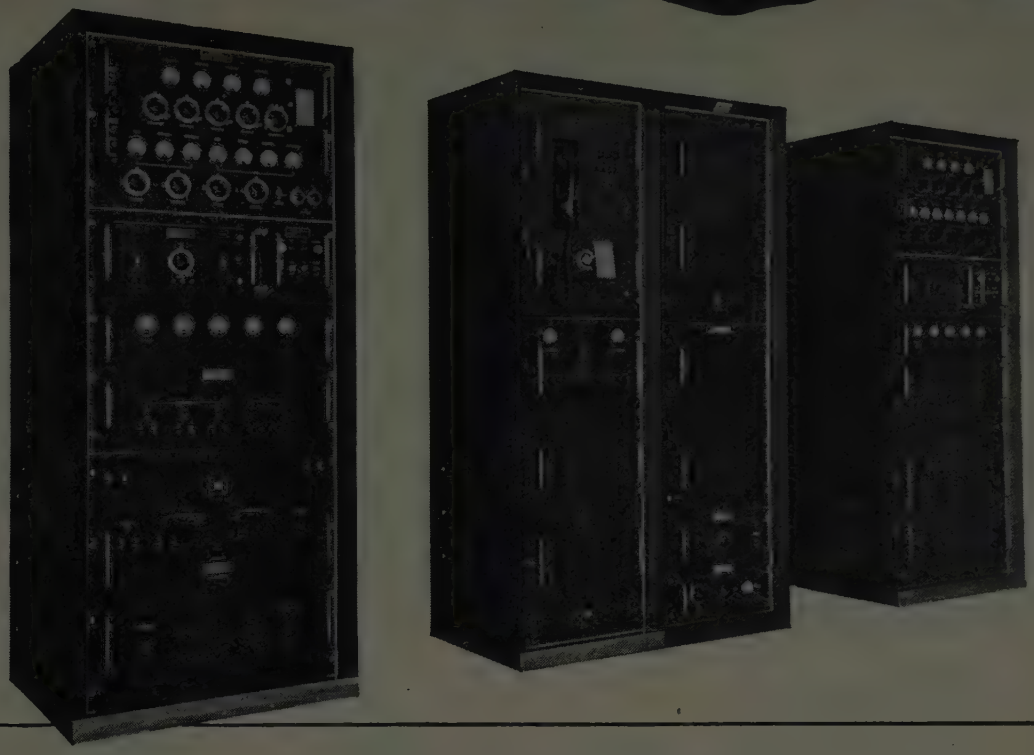

Another Lavoie First

Lavoie, and only Lavoie, manufactures a complete VOR System for short range aircraft navigation. By its use, accurate course, bearing and position are easily determined.

As perfected by Lavoie Laboratories, Inc., two fields are radiated by the system. One rotates at 30 revolutions per second; the other carries a reference 30 cycle signal in all directions. Only one small control panel in the control tower console, plus an extremely compact amplifier monitor are all that are required for complete, efficient transmitter control. The transmitter itself may be located up to 30 miles from the tower. All control functions, including voice modulation from the tower, are handled by one telephone pair.

Built to military standards of ruggedness and precision, the Lavoie VHF Omni Range system may be used with maximum efficiency in any part of the world. A mobile unit is also available.

We shall be glad to give you complete details on this unique, compact, thoroughly reliable Omnidirectional Radio Range System.

SPECIFICATIONS:

Frequency Range: 112 to 118 megacycles

Frequency Control: Crystal accuracy 0.001%; crystal frequency 12.4444 to 13.1MC.

Power Output 200 watts; power in sidebands 25 watts.

Modulation: Speech 30% AM; Identification Code, 10% AM at 1020 cycles; Reference Signal, 10 KC subcarrier at 30%; frequency modulated ±480 cycles at 30 cycle rate. Equipment is capable of 85% modulation.

Power Requirements: 230 volts, 60 cycles single phase, maximum demand 6 kilowatts, normal demand 4 kilowatts, power factor approx. 85%.

Total Weight: 2250 pounds less antenna equipment.

U H F

Lavoie Laboratories, Inc.

MORGANVILLE, NEW JERSEY

Designers and Manufacturers of Electronic Equipment

50 WATTS OF R-F "BOTTLED UP"!

M. O. P. A.
6C4 OSC.
829-B AMPLIFIER

POWER
TO DRIVE AN
ANTENNA

160 db

MICROVOLTS
TO MEASURE
RECEIVER
SENSITIVITY

ROLLIN

MODEL 20
POWER TYPE
STANDARD SIGNAL GENERATOR

- 10 WATTS MAXIMUM R-F OUTPUT—LOW IMPEDANCE.
- 160 DB RANGE OF ATTENUATION—15.0 VOLTS TO 0.10 UV.
- CURRENT OUTPUT UP TO 1.0 AMPERES.
- MASTER OSCILLATOR—TUNED POWER AMPLIFIER CIRCUIT.
- 8 BAND SPREAD TUNING RANGES—85 Kc TO 40.0 Mc.
- DIAL CALIBRATED AT INTERVALS OF 1% IN FREQUENCY.
- LEAKAGE FIELDS LESS THAN .1 UV/METER.

Write for details

ROLLIN

THE ROLLIN COMPANY
2010 LINCOLN AVENUE • PASADENA 3, CALIF.

Industrial Engineering Notes*

RETMA Activities

Election of Chairmen of the Radio-Television Industry Committee and the Electronics Industry Committee and approval by the Board of Directors of an EIC request for a paid general manager for electronics highlighted three days of RETMA meetings, Sept. 15–17, at the Biltmore Hotel, New York City. Max F. Balcom, past President and a Director of the Association, was elected Chairman of the Radio-Television Industry Committee, while Director F. R. Lack was elected Chairman of the Electronics Industry Committee. Board Chairman Robert C. Sprague, who had been Acting Chairman of the RTIC, asked that he be relieved of this chairmanship so that he could maintain his impartiality between the two committees as Chairman of the Board. Responding to a unanimous request of the EIC, supported by Board Chairman Sprague, the Board of Directors authorized President Glen McDaniel and EIC Chairman Lack to employ a general manager and staff, if necessary, who will devote full time to serving the interests of electronic manufacturers in RETMA. . . . **Four new RETMA Directors and an Executive Committee of the Tube Division were elected at Division meetings during the three-day conference.** Fred W. Wilson, Capehart-Farnsworth Corp., was elected a Director for the Set Division, while Russel E. Cramer, Jr., Radio Condenser Co., L. S. Racine, Chicago Standard Transformer Corp., and W. Myron Owen, Aerovox Corp., were elected Directors by the Parts Division Executive Committee. . . . **Joseph J. Peterson, who was recently appointed regional manager of the West Coast office of the RETMA Engineering Department, this week opened his office in the Ambassador Hotel.** Mr. Peterson's duties will include those of acting as a liaison between RETMA headquarters in Washington and Association members on the West Coast. He will also promote the affiliation with RETMA of non-member electronic manufacturers in that area.

Federal Personnel

Col. Thew J. Ice, Jr., USAF, Director of the Armed Services Electro Standards Agency, Fort Monmouth, N. J., has been transferred to Wright-Patterson Air Force Base, Dayton, Ohio. In his new post, Col. Ice will be Chief of the Operations and Development Division. The new Director of ASESA is Col. Glenn S. Meader, USA, formerly Deputy Commanding Officer of the Signal Corps Supply Agency, Philadelphia. . . . **Assistant Secretary of the Federal Communications Commission, William P. Massing, is now Acting Secretary, pending the selection of a permanent Secretary to succeed T. J. Slowie who resigned recently after 16 years of service with the Commission.**

(Continued on page 86A)

* The data on which these Notes are based were selected by permission from *Industry Reports*, issues of August 14, 21, and 28, and September 4, 11, and 18, published by the Radio-Electronics-Television Manufacturers Association, whose helpfulness is gratefully acknowledged.

BNC

CONNECTORS BY KINGS

The B N C Connectors shown are small, lightweight Connectors designed for use with small cables such as RG-58/u, RG-59/u and RG-71/u. Widely used for video and aircraft test equipment, they are recommended for frequencies as high as 3000 M.C., where impedance matching is important. The B N C series is used successfully in the region of microwave frequencies.

Whether your connector requirements call for the B N C series, N series, the new C series or special adaptations of standard connectors, you can rely on Kings. Our staff of highly specialized engineers invite your inquiries.

KINGS Electronics CO., INC.

40 MARBLEDALE ROAD, TUCKAHOE, N. Y.

IN CANADA: ATLAS RADIO CORP., LTD., TORONTO

teflon*

. . . and We Can Deliver!

EXTRUDED
MOLDED **ROD and TUBE**

Small Machined Parts! Sheets!

Heavy demand has put many TEFLON fabricators in a "back ordered" condition. The effect — stymied or crippled production on your end.

At FLEXROCK we have licked this problem. New TEFLON producing equipment has been added. We have substantially increased capacity. We can't take on all things just yet. But soon we will be ready to "throw the book at you" with a complete range of TEFLON services. RIGHT NOW we are set to ship you TEFLON Rod and Tube, extruded or molded, Sheets, and small parts — no matter how intricate — machined from Rod and Tube. We can promise good delivery — yes, FAST DELIVERY . . . with closest possible tolerances on your small parts. Tell us your needs — we will be happy to quote delivery and price.

*DuPont trade-mark for tetrafluoroethylene resin

for teflon it's
FLEXROCK
PHILADELPHIA 4, PA.

SEND US YOUR "SPECS"
LET US QUOTE

FLEXROCK COMPANY, 3608-A Filbert St., Phila. 4, Pa.

☐ *We are enclosing sample, specs, and quantity for our TEFLON requirements. Please furnish quotation.*
☐ *Please send us your TEFLON Bulletin including stock list.*

Name .....
Company .....
Address .....
City ..... *Zone* ..... *State* .....

Industrial Engineering Notes

(Continued from page 84A)

TELEVISION

The American Radio Relay League has requested the co-operation of the television receiver industry and the Federal Communications Commission in alleviating a new problem of television interference arising in sets converted for the UHF bands by means of channel strips. The League contends that the dual-conversion strip system, while an ingenious expedient, fails to meet the engineering principles laid down by FCC as necessary to provide an interference-free service in the UHF bands. Such "converted" receivers become susceptible to interference from innumerable other services in the general region 108–174 meg., ARRL said. The League notes that in more than half of the UHF TV channels there is considerable possibility of interference from amateurs properly operating in their 144 meg. band. ARRL, in a letter to TV manufacturers, asks that if they use such a conversion system in their receivers they take necessary steps to service the problem where it arises. In another letter, to FCC, the League requests that the Commission's field organization make it perfectly plain both to the public and to industry where the fault lies in cases of interference from this source. The League's view is that the amateur service will not "go through another difficult period, again not of its own making, carrying the burden of public misunderstanding and abuse which arises solely because of the inadequacy of television receiving apparatus." . . . **The Federal Communications Commission this week granted construction permits to nine television stations, including the second such grant for a station in Puerto Rico, and issued special temporary authorizations to six outlets, bringing to 127 the total number of STAs.** The total number of CPs as of mid-August stands at 440, including 20 non-commercial educational stations. . . . **Four UHF grantees have petitioned the Federal Communications Commission to develop regulations, rules and standards for a subscription television service "at an early date" and to designate a system or systems to be used.** The petition backs up the one submitted to the FCC in February of last year by the Zenith Radio Corp., Chicago, asking the Commission to authorize this type of service. The petition was submitted by Home News Publishing Co., New Brunswick, N. J., holder of a permit for WDHN, Channel 47; Pennsylvania Broadcasting Co., grantee for WIP-TV Channel 29, Philadelphia; Stamford-Norwalk Television Corp., Channel 27, Stamford, Conn., and Connecticut Radio Foundation, Inc., grantee of WELI-TV, Channel 59, New Haven, Conn. The firms stated that subscription TV is important to UHF as a means of programming the stations so as to provide revenues, enabling a UHF station to compete, quality-wise, with network programs, and thus greatly speed the conversion of UHF sets in VHF areas. The

(Continued on page 88A)

FIRST WITH THE FINEST IN . . .

- **CATHODE-RAY OSCILLOGRAPHY**

  Instrument Division,
  760 Bloomfield Ave., Clifton, N.J.

- **CATHODE-RAY TUBES AND COMPONENTS**

  Cathode-ray Tube Division,
  750 Bloomfield Ave., Clifton, N.J.

- **TELEVISION TRANSMITTING EQUIPMENT**

  Television Transmitter Division,
  1500 Main Ave., Clifton, N.J.

DU MONT

ALLEN B. DU MONT LABORATORIES, INC.

Measurements Corporation
MODEL 78

STANDARD SIGNAL GENERATORS

FREQUENCY RANGE: Choice of two bands; frequency ratio of each band 1.8 to 1 within range of 10 Mc. to 250 Mc. Special single band instruments also available up to 420 Mc.

OUTPUT VOLTAGE: Continuously variable from 1 to 100,000 microvolts.

MODULATION: AM, fixed at 30%.

POWER SUPPLY: 117 v., 50/60 cycles.

MEASUREMENTS CORPORATION
BOONTON NEW JERSEY

FAIRCHILD precision potentiometers
FAIRCHILD TYPE 756 precision potentiometer
FAIRCHILD TYPE P-746 precision plug-in potentiometers
FAIRCHILD precision linear potentiometers TYPES 747 and 749
FAIRCHILD TYPE 736 precision potentiometer
FAIRCHILD TYPE 746 precision potentiometer

how to select...

PRECISION POTENTIOMETERS

New specification file is valuable guide for design engineers

Here's help for you in the selection of precision potentiometers. Fairchild Camera and Instrument Corporation has prepared detailed specification sheets on each potentiometer model in its extensive line. In each of these you'll find outline drawings and electrical and mechanical specifications to help you select the proper type potentiometer. While your requirements may not precisely pattern these specifications, adequate data is furnished for your initial decision.

For your copy of this useful specification file, write to Potentiometer Division, Fairchild Camera and Instrument Corporation, 225 Park Ave., Hicksville, Long Island, N. Y., Department 140-42H.

FAIRCHILD
PRECISION POTENTIOMETERS

STANDARD

Radio Interference and Field Intensity

MEASURING EQUIPMENT

Complete Frequency Coverage—14kc to 1000 mc!

VLF

14kc to 250kc
Commercial Equivalent of AN/URM-6B.
Very low frequencies.

HF

150kc to 25mc
Commercial Equivalent of AN/PRM-1A.
Self-contained batteries. A.C. supply optional. Includes standard broadcast band, radio range, WWV, and communications frequencies.

VHF

15mc to 400mc
Commercial Equivalent of TS-587/U.
Frequency range includes FM and TV Bands.

UHF

375mc to 1000mc
Commercial Equivalent of AN/URM-17.
Frequency range includes Citizens Band and UHF color TV Band.

These instruments comply with test equipment requirements of such radio interference specifications as MIL-I-6181, MIL-I-16910, PRO-MIL-STD-225, ASA C63.2, 16E4, AN-I-24a, AN-I-42, AN-I-27a, MIL-I-6722 and others.

STODDART AIRCRAFT RADIO Co., Inc.

6644-C Santa Monica Blvd., Hollywood 38, California • Hollywood 4-9294

Industrial Engineering Notes

(Continued from page 86A)

petitioners concluded by stating that the economic problem facing UHF broadcasters in areas now receiving television from VHF stations "should be of grave concern" to the FCC since it raises "a substantial question" as to whether a fully competitive system using the UHF system, as envisaged by the FCC, can be achieved without a satisfactory solution to the problem.

Materials

The Interior Department has announced the discovery of possible new sources of germanium in the ashes of certain domestic coals. In a technical report on the discovery, the Interior Department said evidence indicates the germanium and many other trace elements are concentrated in that part of the coal which once was trunk and branches of woody plants, with highest germanium concentration occuring in thin beds, isolated coalified logs and pieces of woody coal in clayey sediments.

Aeronautical

The Radio Technical Commission for Aeronautics has announced that it has initiated an investigation of possible interference by ultra high frequency television with distance measuring and other aviation devices in the UHF band. RTCA established a committee, SC-68, which is to determine whether UHF television transmitters or receivers will interfere with the operation of aeronautical distance measuring devices and other systems and, if such problem exists, it is to make recommendations on corrective actions to be taken to minimize the interference.

Technical

The Eisenhower Administration, according to Defense Department officials, has given top priority for development by the armed forces of a new type of audible radar which may greatly increase this country's defenses against a surprise atomic attack, and at the same time lead to a completely automatic warning net that would eliminate the necessity of having thousands of men and women attend the present radar screens. This new audio or "Doppler" radar would give out a "ping" sound when a plane is detected, thus eliminating the present necessity of constant scanning. It also has tremendous advantage over present radar equipment in that it reportedly can determine the number and types of aircraft approaching. It is said to be so accurate it can determine the number of propellers on a bomber. . . . **An experimental wrist radio, dubbed the "Dick Tracy," which is able to pick up broadcasts within a range of 40 miles has been developed by the Signal Corps as a means of further exploring the possibilities of miniaturization.** The radio, weighing less than three ounces, was developed at the Army Signal Corps Engi-

(Continued on page 90A)

for high permeability applications

now—the first time available . . .

PERFORMANCE GUARANTEED

TAPE WOUND CORES

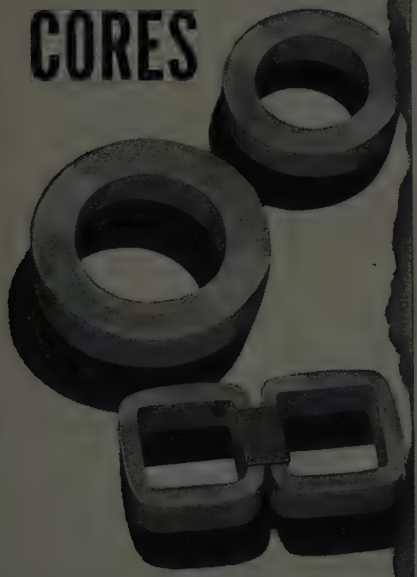

ONLY MAGNETICS, INC.

offers Performance-Guaranteed Tape Wound Cores. Guaranteed performance to specifications means truly economical production of high permeability magnetic devices in your plant . . . and controlled buying by your purchasing department. If you haven't investigated Performance-Guaranteed Tape Wound Cores, why not let us send you the complete story?

FACTORY CORE MATCHING

For applications in which closely matched characteristics are required, save time and money by using the Magnetics, Inc. factory core matching service.

free engineering design service for high permeability magnetic applications

Magnetics, Inc. engineering is second to none in the field of high permeability magnetics. Services are free to customers.

Write for full information

MAGNETICS, inc.

Specializing in High Permeability Magnetics

Dept. I-2 BUTLER, PA.

HERMEFLEX*

Cut-away view of HERMEFLEX* approximately twice actual size.

. . . TRANSMITS ROTARY MOTION THROUGH A METAL-TO-METAL SEAL

Through the ingenious application of a toggle and metal bellows, the HERMEFLEX provides a positive metal-to-metal seal of shaft rotation through a wall of solid metal. Employing no gaskets nor sliding seals this device is a compact, unitized seal essential to the control of hermetically sealed instruments, electronic devices and high vacuum apparatus.

At present the HERMEFLEX is produced in two standard diameters—1-inch and ½-inch. These units are designed for the manual control of shaft rotation in pressure differentials up to 1 atmosphere. Your inquiries for HERMEFLEX developments to meet different duty cycles, special environmental conditions or other unusual problems, are cordially invited.

Bulletin will be sent upon request.

**PATENTED U. S. Patent Office. Trade name copyrighted.*

KEARFOTT COMPONENTS INCLUDE:

Gyros, Servo Motors, Synchros, Servo and Magnetic Amplifiers, Tachometer Generators, Hermetic Rotary Seals, Aircraft Navigational Systems, and other high accuracy mechanical, electrical and electronic components.

Kearfott

SINCE 1917

CREATIVE ENGINEERING PRODUCTION ACHIEVEMENT

KEARFOTT COMPANY, INC., 1150 McBride Ave., Little Falls, N. J.
Midwest Office: 188 W. Randolph St., Chicago 1, Illinois
West Coast Office: 253 N. Vinedo Ave., Pasadena, Calif.
A General Precision Equipment Corporation Subsidiary

the most economical way to FOCUS a TV tube

the original Focomag

CUTS RECEIVER COSTS BY ELIMINATING CENTERING AND FOCUSING RHEOSTATS. Also lowers cost of power transformer. Perfectly focuses 27", 21" and all smaller tubes having magnetic deflection. Highly efficient ring magnet uses only 4 oz. Alnico P. M.

NO HARMFUL EXTERNAL FIELD. Ring magnet is completely enclosed by the external shunt (an original Heppner design). This prevents the leakage field from having any magnetic effect on other components. Uniform field produced by ring magnet.

FLEXIBLE NYLON ADJUSTING SHAFT ELIMINATES BREAKAGE.
Picture-positioning lever. You specify mounting arrangement.

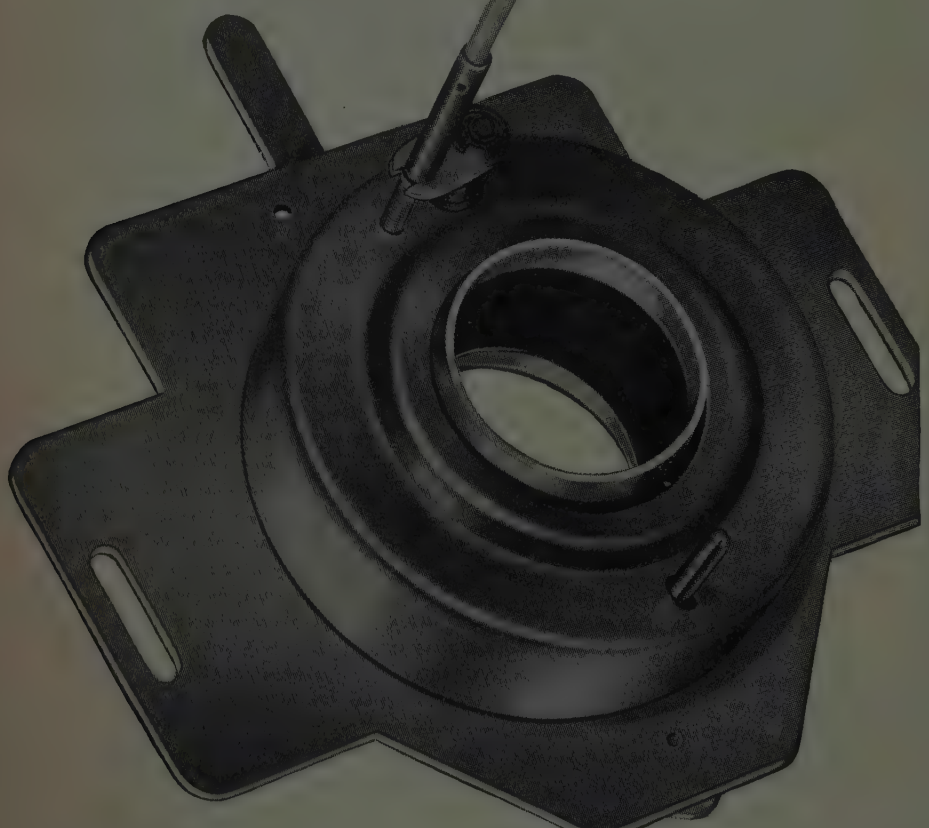

Write today for information on lowering your set costs with this FOCOMAG.

HEPPNER
MANUFACTURING COMPANY
Round Lake, Illinois (50 Miles Northwest of Chicago)
Phone: 5-2101
SPECIALISTS IN ELECTRO-MAGNETIC DEVICES

Representatives:
John J. Kopple
60 E. 42nd St., New York 17, N. Y.
James C. Muggleworth
506 Richey Ave., W. Collingswood, N. J.
Ralph Haffey
R. R. 1, U. S. 27, Coldwater Rd.,
Ft. Wayne 3, Indiana
Irv. M. Cochrane Co.
408 So. Alvarado St., Los Angeles, Calif.

Industrial Engineering Notes

(Continued from page 88A)

neering Laboratories, Fort Monmouth, N. J., and it is worn on the wrist in the same manner as a watch. The miniature receiving set is contained in a plexiglass case two inches long, one inch wide, and nearly an inch thick. Its small size is made possible through replacement of the conventional vacuum tube with five tiny germanium transistors and other miniature components. The set is powered by a mercury battery little larger than the tip of a pencil, and the "wiring" in the chassis is made up of printed circuits produced by an etching process. A short antenna wire and a cord connecting the radio with the hearing-aid-type of receiver worn on an ear are concealed in the user's sleeve. A miniature switch is pushed to turn the radio on, and a knob on the face of the set is employed to select stations or frequency. Operating on a tuning range of 1,000 to 1,500 kc or approximately one-half the standard broadcast band, broadcasts reportedly have been picked up clearly at Fort Monmouth from New York, an airline distance of about 40 miles from the Laboratories. . . . **Since modern electronic computers have been handicapped by the inability of the memory to attain speeds matching practical arithmetic units, the National Bureau of Standards has announced the development of an information storage device utilizing diodes and capacitors as the basic storage unit.** Developed by A. W. Holt of the NBS electronic computers laboratory, a recently completed prototype memory unit based on this idea appears to be faster than any other system. The diode-capacitor memory, which can be designed to present in excess of 100,000 randomly located 50-digit words per second to the computer, attains a speed corresponding to that of the arithmetic unit, with a resulting decrease in machine computation time for mathematical problems. Dubbed the Williams cathode-ray tube storage system, its acoustic memory has a random access rate of up to 60,000 words per second. In contrast, the Bureau of Standards Eastern Automatic Computer's acoustic memory has a random access of 6,000 words per second. Information on this development will be reported in the NBS Technical News Bulletin. Further details of the diode-capacitor memory are contained in a report given by A. W. Holt, "Proceedings of the Association for Computing Machinery," Toronto meeting, September, 1953. . . . **A number of research papers and studies in the electronics field, recently published by the Office of Technical Services, Department of Commerce, are included in its September issue of the "Bibliography of Technical Reports."** Of interest to the electronics industry, all of which can be purchased from the Photoduplication Section, Library of Congress, Washington 25, D. C., for the reported price, are the following: "Electromagnetic Wave Propagation on Helical Conductors," PB 109631, microfilm, $5; photo-

(Continued on page 94A)

G. E. WILL HAVE THEM FOR YOU!

TRI-COLOR PICTURE TUBES
Aluminized glass, in the needed sizes

***New* receiving tubes to improve color-TV circuit efficiency and economy, such as:**

SYNCHRONOUS DETECTOR

HIGH-VOLTAGE REGULATOR

TRIPLE DIODE

HIGH-CURRENT FULL-WAVE RECTIFIER

HIGH-VOLTAGE RECTIFIER

HIGH-CURRENT DAMPING DIODE

THE first color-TV sets will be expensive to build. For one thing, their large tube complements will be made up of types not designed for color-circuit applications.

From the start, designers and builders will strive to cut color-chassis costs, in order to bring down receiver prices and profit from the wider market these reductions will create.

G-E tube designers already are working toward that end! At left are some of the tubes in development. Each will help give you one, or both, of these benefits: (1) a more efficient, simpler color circuit, (2) fewer tube sockets to be filled.

Make the most of tomorrow's massive opportunity in color TV by planning ahead for lower set prices! Get in touch *now* with your G-E tube commercial engineer!

Phone, wire, or write the General Electric tube engineer nearest you!

CHICAGO
R. E. BERRY
C. J. BIVER
H. W. A. CHALBERG
■
Tube Department
General Electric Company
3800 North Milwaukee Ave.
Chicago 41, Ill.
●
Phone: SPring 7-1600

CLIFTON, N. J.
W. E. CRONBURG
W. R. RATE
F. W. TIETSWORTH
●
Tube Department
General Electric Company
200 Main Avenue
Clifton, N. J.
●
Phone: GRegory 3-6387

LOS ANGELES
R. R. W. LACY
■
Tube Department
General Electric Company
11840 West Olympic Blvd.
Los Angeles, Calif.
●
Phone: BRadshaw 2-8566
or ARizona 9-7765

GENERAL ELECTRIC

The HHB Engineering Representative..

IS READY TO SERVE YOU..ANYWHERE IN THE U.S.A.

offering ELECTRONIC COMPONENTS AND PARTS..MADE BY THE WELL-KNOWN HHB CRAFTSMEN

AN Types

RF Types

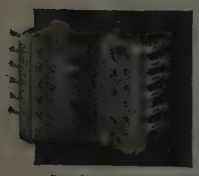

Rack and Panel

Cable Assemblies

Now! . . . experienced HHB Engineering Representatives will call to serve you . . . where, and when, you are in need of a reliable source of electronic components, and parts. They offer the complete facilities of HHB including research, design, engineering, as well as manufacturing of quality products.

The HHB staff is eager to work with engineering departments on standard requirements, and special components parts problems. Over the years HHB has consistently surpassed the rigid specifications of America's leading users of connectors, cable assemblies, and many types of miscellaneous electronic parts.

Wherever you are . . . we invite your inquiries.

H. H. BUGGIE Inc.

TOLEDO 4, OHIO

Skilled in Electronic Component Parts RESEARCH • DESIGN ENGINEERING MANUFACTURING

Sales Engineers in All Principal Cities

Industrial Engineering Notes

(Continued from page 90A)

stat, $16.25. "Electromagnetic Waves in Iris-loaded Waveguides," PB 109973, microfilm, $1.75; photostat, $2.50. "High-frequency Electrical Breakdown of Gases," PB 109632, microfilm, $1.75; photostat, $2.50, "Factors Affecting Speech Intelligibility in Aircraft Control Towers," PB 109606, microfilm, $2; photostat, $3.75. . . . **The National Bureau of Standards announced the issuance of three new publications containing information of interest to the electronics industry, all obtainable from the Government Printing Office, Washington 25, D. C. for the reported price.** "Reference Data for Orienting Quartz Plants by X-Ray Diffraction," NBS Circular 543, 15 cents. "Table of Dielectric Constants and Electric Diploe Moments of Substances in the Gaseous State," NBS Circular 537, 20 cents. "Electrodeposition Research," NBS Circular 529, $1.50.

Mobilization

The role of electronics not only in defense but in civilian needs, was highlighted recently as two new applications were reported. An electronic "eye," known as a transmissometer, and which "peers" down airport runways and reports changes in visibility to control tower operators for relay to pilots, is now being used at the Washington National Airport, according to an announcement by F. B. Lee, Administrator of Civil Aeronautics, Department of Commerce. It is the first such installation for operational use, he said, and it is used by the tower when visibility along the instrument runway gets down to one and one-half miles. The transmissometer is an "all-Commerce" device, having been developed by the National Bureau of Standards; designed, purchased and installed by the Weather Bureau, and used by the Civil Aeronautics Administration—all branches of the Department of Commerce. At the Navy Bureau of Aeronautics an eight-ton electronic computer, believed to be one of the largest in the world, has been recently installed. The memory unit alone weighs 4,500 pounds and is capable of performing a multiplication or division in 15 thousandths of a second, which is 20 times faster than the blink of a human eye. The computer will undergo rigid testing for the next fews weeks until it is certain that all "bugs" have been eliminated. When this is completed, periodic aircraft logistics, for example, will be computed on the machine at a great saving in time and money to the Navy. . . . **Defense Secretary Charles Wilson has a special committee looking into the armed services programs for the development and production of guided missiles, it has been recently reported.** The new group is headed by Trevor Gardner, Special Assistant to Air Force Secretary Talbott for Research and Development. The Committee has been in existence several weeks reviewing the missile activities of the various services and inspecting production plants. On the committee, along with Mr. Gardner, are two

(Continued on page 96A)

Top Service

IS ASSURED WHEN YOU ORDER YOUR

RAYTHEON TUBES

and JUNCTION TYPE

TRANSISTORS

FROM

DALIS

Metropolitan New York's Foremost Electronic Distributor

Immediate Delivery From Stock

Seal of HLD Service

PHONE: ALgonquin 5-3000
WRITE or **WIRE:** Dept. IND
TELETYPE: N. Y. 1-2482

H. L. DALIS INC.

WHOLESALE DISTRIBUTORS
ELECTRONIC EQUIPMENT

175 VARICK ST., NEW YORK 14

SERVING THE TRADE FOR OVER A QUARTER CENTURY

PLUG IN THE VERTICAL-AMPLIFIER CHARACTERISTICS YOU NEED

...with this new Tektronix Oscilloscope

No need to switch oscilloscopes when your requirements change. An extremely wide range of work is now handled by one oscilloscope—the Tektronix Type 535—with its moderately-priced plug-in units.

Wide-band Plug-in Preamplifier. Bandpass dc to 10 mc, risetime 0.035 μsec, calibrated sensitivity to 0.05 v/cm, two signal inputs with more than 60 db isolation. Type 53A Wide-band Plug-in Unit—$85

High-gain Plug-in Preamplifier. 1 millivolt/cm sensitivity dc to 250 kc with bandpass increasing to dc to 750 kc at 50 mv/cm sensitivity and lower, differential input. Type 53D High-gain Plug-in Unit—$145

Dual-trace Plug-in Preamplifier. Two identical amplifier channels, dc to 8.5 mc, 0.04 μsec risetime, calibrated sensitivity to 0.05 v/cm, triggered or 100 kc switching, polarity reversal switches. Type 53C Dual-trace Plug-in Unit—$275

The use of plug-in preamplifiers providing this wide range of facilities is made possible by the broad basic specifications of the Type 535.

600,000,000 to 1 Time-base Range—0.02 μsec/cm to 12 sec/cm.
10 KV Accelerating Potential—Brighter display at low repetition rates.
New Flexible Sweep Delay—Accurate, jitter-free, 5 μsec to 20,000 μsec.

Type 535 Oscilloscope—$1300 plus price of desired plug-in unit
Prices f.o.b. Portland, Oregon

Please write for complete specifications

TEKTRONIX

Tektronix, Inc.

P.O. Box 831B • Portland 7, Oregon • Cable: TEKTRONIX

... Complete line of Microwave Components from magnetron to antenna ...
designed and produced by experts—

WAVEGUIDE SWITCH
A complete line; compact, rugged, suitable for military usage; VSWR less than 1.10; crosstalk greater than 50 Db; operation 24 v. DC, 110 v. AC; may be specially designed to meet switching problems.

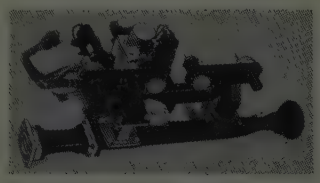

MIXER DUPLEXER
Precision-built to closest tolerances; completely tested. Designed to meet your basic requirements, or produced from your blueprints.

DUMMY LOADS
Designed for military field operation; built to meet all standard military vibrations and shock requirements. Capable of operating at extremely high average powers.

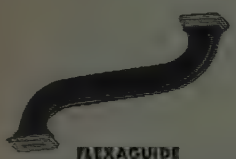

FLEXAGUIDE
Pressure-tight; rugged enough to meet roughest requirements; VSWR less than 1.10; attenuation equal to brass rigid guide.

COUPLERS
Complete series for all waveguide sizes. Flange combination, and waveguide or coaxial outputs. Designed to meet your particular problems.

For RIGID Waveguide Specify
GUIDELINE
Rigid Bends • Twists • Tapers • Crystal Mixers • Duplexers
Flanges • Magic Tees • Directional Couplers • Dummy Loads
Waveguide Switches • Coax Adaptors • Precision Castings
Waveguide Transformers • Quick Disconnect Clamps

For FLEXIBLE Waveguide Specify
FLEXAGUIDE
Army and Navy Standard Waveguides
Flexible Twists • Bends • Tapers
Straight Sections • All Lengths and Sizes

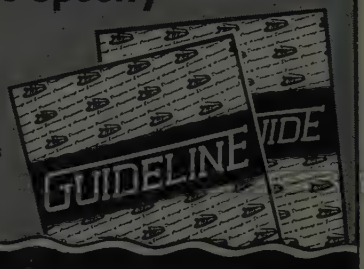

Write for Catalogs

Airtron inc.
Linden, New Jersey

BRANCH OFFICES
DAYTON CHICAGO LOS ANGELES DALLAS
KANSAS CITY SEATTLE ALBUQUERQUE

Industrial Engineering Notes

(Continued from page 94A)

former members of the extinct Research and Development Board, plus representatives of the three armed services. The objective of the group is to "review the whole guided missile program, to avoid duplications and save money, resources and manpower." The committee is a part of Secretary Wilson's program to standardize guided missiles among the services. The Air Force and Navy are conducting duplicate work on air to air and air to ground missiles, while the Navy and the Army are developing surface to air missiles, according to information received this week. Defense Department officials pointed out that a final report on the findings of the Committee seems remote at this time.

Research

Commerce Secretary Sinclair Weeks announced recently that Dr. Allen V. Astin will be retained as Director of the National Bureau of Standards and that the Bureau will operate under the immediate supervision of Assistant Secretary of Commerce for Administration James C. Worthy. The Bureau formerly was under the supervision of Craig Shaeffer, Assistant Secretary for Domestic Affairs. In the announcement, Mr. Weeks listed the Bureau's problems as: (1) serious lack of balance in the Bureau's programs; (2) imperfections in the system of evaluating commercial products; and (3) inadequacies of organization and administrative control. Retaining Dr. Astin as the Bureau's Director was approved unanimously by the Kelly Evaluation Committee, headed by Dr. M. M. J. Kelly, President of Bell Telephone Laboratories, which was assigned the job of studying the Bureau's organization and programs. "All the changes in the National Bureau of Standards, to take place in the near future, including those recommended by the Kelly Committee, are positive improvements in the Bureau," Mr. Weeks said. "They correct conditions which in many cases considerably antedate Dr. Astin's period as Director and for which he cannot be held responsible." . . . **Technological developments of importance to the electronics industry are reviewed in the August issue of "Bibliography of Technical Reports," released by the Office of Technical Services, Department of Commerce.** Featured in the issue are summaries of governmental research reports now available to the public on the prevention and correction of deterioration of electronic and other equipment due to moisture and fungi; radio transmission of hand-written messages; a new system of testing junction triode transistors; a unified theory of reciprocity calibration of electro-mechanical transducers; a series of reports on atmospheric direction finding and ranging plus a score of other significant electronics research reports. The following reports all can be obtained from the Library of Congress, Photoduplication Section, Washington 25, D. C., for the reported prices:

(Continued on page 100A)

KEEP YOU FLYING . . . SAFELY!

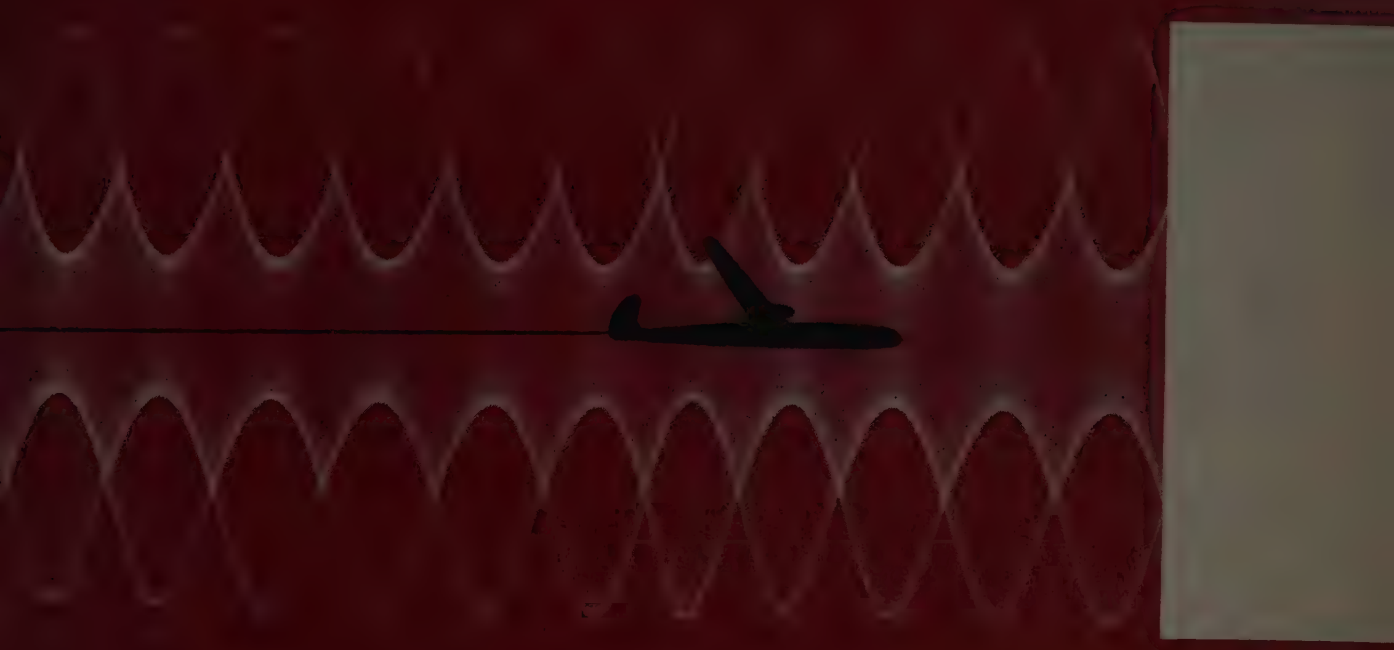

Type 482 TVOR • Type 483 VOR
Terminal VHF
Omni-Range Unit
Low cost answer to improved safety and regularity of operation under adverse weather conditions

Type 99
Multi-Frequency
Transmitter
Provides any combination up to four R.F. channels for operation 125-525 kc/s, 2-20 mc/s, 400 watts, and 118-152 mc/s, 250 watts

Whoever you are, wherever you fly—the signals from Wilcox equipment will help you get where you're going and help you land . . . *safely.*

What's more, Wilcox equipment has been helping scheduled, non-scheduled, government airlines—here and abroad—fly safely for more than 21 years.

So, this suggestion—if you need communication or navigation equipment . . . contact Wilcox *first.*

wilcox
ELECTRIC COMPANY, INC.
Fourteenth and Chestnut
Kansas City 27, Missouri, U.S.A.

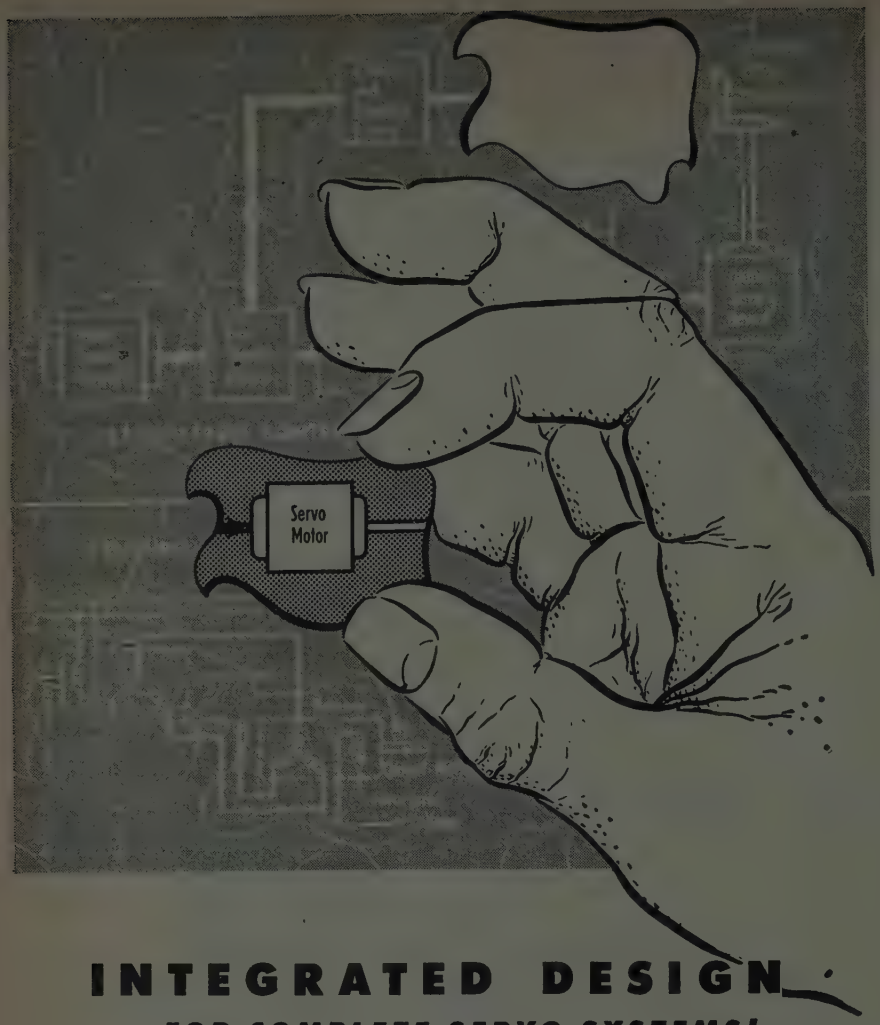

INTEGRATED DESIGN

...FOR COMPLETE SERVO SYSTEMS!

Like pieces in a jig-saw puzzle, all components in a Transicoil servo system are designed to fit each other . . . coordinating to form the complete picture. Systems made by piecing together unmatched components usually spoil the picture by limiting the final efficiency of the entire system.

But if building your own system seems desirable, you'll find that individual Transicoil components offer the best performance in the job each is required to do. Built to your exact specifications, ready for immediate application, their ability to fit into the picture of your system is limited only by the restrictions you place upon them.

Details covering Transicoil Servo Systems, or components are available upon request to . . .

TRANSICOIL

CORPORATION 107 GRANDSTREET NEW YORK 13, N.Y.

Industrial Engineering Notes

(Continued from page 96A)

"Design Notes on Distributed Amplifiers," (PB 109633), microfilm, $2; photostat, $3.75. "Electric Pencil: Performance Over Radio Circuits," (PB 108811), microfilm, $1.25; photostat, $1.25. "Evaluation of CEE (German) Obtained by Naval Technical Mission to Europe," (PB 109272), microfilm, $3.50; photostat, $10. "Field Comparison of Modulation Methods for Facsimile Communication Over Ionospheric Radio Circuits," (PB 109470), microfilm, $4.50; photostat, $13.75. "Optic-Axes and Critical Coupling in the Ionosphere," (PB 109627), microfilm, $2.00; photostat, $3.75. "Outline of a Theory of Semantic Information," (PB 109609), microfilm, $2.75; photostat, $7.50. "X-Band Frequency Measuring System," (PB 109568), microfilm, $1.75; photostat, $2.50.

Patents

The Patent Office announced recently that Westinghouse Electric Corp. has made available for free, unrestricted use by the public through dedication 231 patents, including a number in the electronics field. Patents dedicated to the public, it was pointed out, may be used by anyone without obtaining licenses or the payment of royalties. Lists of the patents, as well as a pamphlet listing 609 patents previously dedicated to the public for free, unrestricted use, may be obtained without charge upon request from the Patent Register, U. S. Patent Office, Washington 25, D. C. . . . **The Atomic Energy Commission recently released 28 additional patents, including nine in the electronics field.** Non-exclusive royalty-free licenses on the listed patents will be granted by the Commission as part of its program to make non-secret technological information available for use by industry. Applicants for licenses should apply to the Chief, Patent Branch, Office of the General Counsel, U. S. Atomic Energy Commission, Washington 25, D. C., identifying the subject matter by patent number and title. The following nine patents of interest to the electronics industry were released: Stabilized Pulse Circuit, 2,632,103; Torque Compensated Galvanometer, 2,640,866; Point Electron Source, 2,640,950; Radio-Frequency Oscillator, 2,642,531; Voltage Supply Regulator, 2,643,360; Magnetic Flux Direction Determining Apparatus, 2,644,922; Electric Integrator, 2,646,925; and Ultra-Wide Band Amplifier Tube, 2,647,175.

Federal Communications Commission Actions

The Federal Communications Commission last Friday issued a Notice of Proposed Rule Making looking toward assigning new UHF TV channels to 35 cities in 16 states. . . . Dr. W. R. G. Baker, Chairman of the National Television System Committee and General Electric Co.

(Continued on page 104A)

Type U70, 3/4" diameter *miniaturized* variable composition resistor with special printed circuit terminals. Wattage rating: .3 watt for resistances through 10,000 ohms, .2 watt with 350 volts maximum across end terminals for resistances over 10,000 ohms.

Type U45, 15/16" diameter, variable composition resistor with blade-type printed circuit terminals. Wattage rating: 1/2 watt for resistances through 10,000 ohms, 1/3 watt for resistances over 10,000 ohms through 100,000 ohms and 1/4 watt with 500 volts maximum across end terminals for resistances over 100,000 ohms.

Type GC-U45, 15/16" diameter, variable composition resistor with blade-type printed circuit terminals same as U45 except with attached SPST, 3 ampere, 125 volt "GC" type switch. Also available with type "WF", DPST, 3 ampere, 125 volt switch. (Variable resistor type WF-U45.)

CTS

CHICAGO TELEPHONE SUPPLY
Corporation

ELKHART • INDIANA

REPRESENTATIVES

Henry E. Sanders, McClatchy Bldg.
69th & Market St., Upper Darby, Penna.
Phone: Flanders 2-4420

W. S. Harmon Company, 1638 So. La Cienega Blvd.
Los Angeles 35, California • Phone: Bradshaw 2-3321

John A. Green Company, 6815 Oriole Drive
Dallas 9, Texas

IN CANADA

C. C. Meredith & Co., Ltd., Streetsville, Ontario

SOUTH AMERICA

Jose Luis Pontet
Buenos Aires, Argentina • Montevideo, Uruguay
Rio de Janeiro, Brazil • Sao Paulo, Brazil

OTHER EXPORT

Sylvan Ginsbury
8 West 40th Street, New York 18, N. Y.

Specialists in Precision Mass Production of Variable Resistors

Burton Browne advertising

Just Off the Press

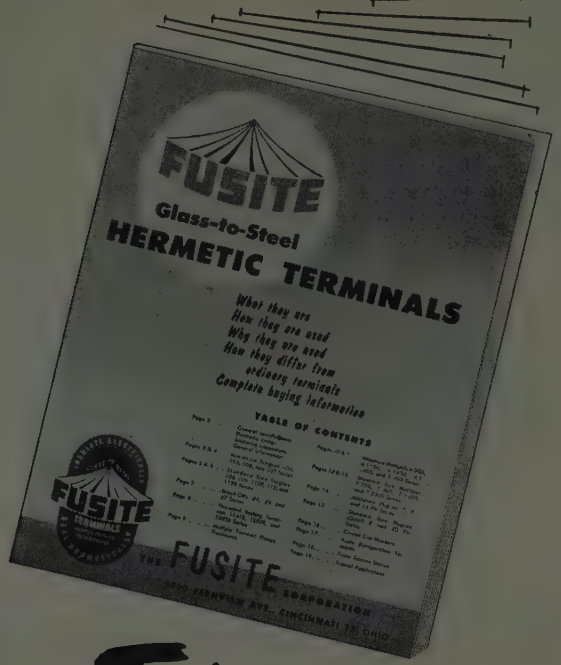

Send Today for your FREE copy of the New 20 page Fusite Catalog

Your information on glass-to-steel hermetic terminals is not up-to-date until you have seen this new Fusite catalog. Many brand-new types of terminals and many new variations are now available in this most famous line. Write today for your copy, Dept. B-3.

INSULATE ELECTRICALLY · GLASS TO METAL · FUSITE TERMINALS · PROTECT PRODUCT PERFORMANCE · SEAL HERMETICALLY

THE FUSITE CORPORATION

6000 FERNVIEW AVE., CINCINNATI 13, OHIO

Industrial Engineering Notes

(Continued from page 100A)

Vice President, recently presented over 52 pounds of technical documents to FCC Chairman Rosel H. Hyde in support of the NTSC request for adoption of its proposed standards for compatible color television. As the deadline for filing initial comments in the proceedings passed, statements were submitted by six additional organizations. Although none directly opposed FCC adoption of the proposed NTSC signal specifications, several pointed out the economic implications of the introduction of color television, and questioned whether receivers would be "cheap enough in price to be available to the great mass of the American purchasing public." Dr. Baker answered a number of questions about color television for the press and said that the first sets probably would have a 14-inch screen and be priced at between $750 and $800. From a year to 18 months after production starts, he said, the screen size probably will jump to 21 inches in response to public demand and as the industry overcomes technological problems. The color tube, as has been pointed out before, is still the basic problem, Dr. Baker said, and when that is licked, set production will be ready to go. He estimated that between 50,000 and 75,000 color tubes will be produced in the next year with production at four or five times that rate in the second year. About 1.5 million color tubes will be produced in the third year, he estimated. Dr. Baker said that pilot lines already are producing color tubes and pointed out that 12 manufacturers built receivers for use in the NTSC program. He estimated that color television for the mass buying public probably is three or four years away and cited the development of the black-and-white television industry. When production gets started, he said, the industry will produce color sets at prices acceptable to the public. . . . **The FCC recently finalized its Notice of Proposed Rule Making of May, 13, listing specific dates for changing from old to new frequencies by ship and coast stations using maritime mobile radiotelephone frequencies in the band 4,100-18,000 kc. in the Great Lakes area, and amended Parts 7 and 8 of its maritime rules accordingly.** The Commission also finalized earlier rule making amended Section 9.312(e) of its aeronautical rules, effective Oct. 1, to make the frequency 8364 kc available for assignment to lifeboats, liferafts and other survival craft for search and rescue communications with stations of the maritime mobile service. . . . **Through the end of August, the FCC approved special temporary authorizations for 148 stations to start operating, including three education outlets.** Listed below are all stations which received STAs from the lifting of the "freeze" to the end of August:

EDUCATIONAL

State and City	*Permittee*	*Channel*
Houston, Texas	U. of Houston, Houston Indep. School District	8
Los Angeles, Calif.	U. of Southern Calif.	28
St. Louis, Mo.	St. Louis Ed. Tele. Comm.	9

(Continued on page 106A)

RMC DISCAPS®

APPROVED AND USED BY LEADING MANUFACTURERS

"Heavy Duty" By-Pass *DISCAPS*

TYPE B

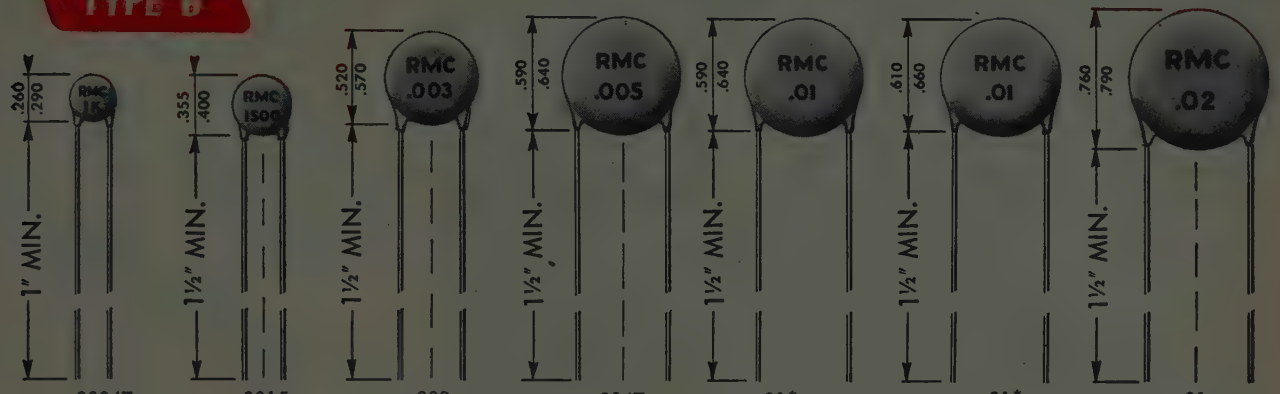

.00047	.0015	.003	.0047	.01*	.01*	.01
.00068	.002	.004*	.005	±20%	.02*	.02
.0008	2x.001	.005*	2x.002	.02*		2x.004
.001		2x.0015		+80%−20%		
		2x.002*				

*Rated 600 V.D.C.W. Flash test 1200 V.D.C.

SPECIFICATIONS

TYPE B BY-PASS SERIES—GUARANTEED MINIMUM VALUE

POWER FACTOR: 1.5% Max. @ 1 KC (initial)
POWER FACTOR: 2.5% Max. @ 1 KC (after humidity)
WORKING VOLTAGE: 1000 V.D.C.
TEST VOLTAGE (FLASH): 2000 V.D.C.
LEADS: No. 22 tinned copper (.026 dia.)
INSULATION: Durez phenolic—vacuum waxed
INITIAL LEAKAGE RESISTANCE: Guaranteed higher than 7500 megohms
AFTER HUMIDITY LEAKAGE RESISTANCE: Guaranteed higher than 1000 megohms

HIGH VOLTAGE DISCAPS—*Designed for Deflection Yokes*

NOW AVAILABLE IN ANY CAPACITY BETWEEN 15 MMF AND 240 MMF

SPECIFICATIONS

POWER FACTOR: .1% Max. @ 1 M C (initial)
POWER FACTOR: 2.5% Max. @ 1 M C, after humidity
WORKING VOLTAGE: 2000, 3000, 4000, 5000 V.D.C.
TEST VOLTAGE: 4000, 6000, 8000, 10,000 V.D.C.
LEADS: No. 22 tinned copper (.026 dia.)
INSULATION: Durez phenolic—vacuum waxed
INITIAL RESISTANCE: Guaranteed higher than 7500 megohms
AFTER HUMIDITY LEAKAGE RESISTANCE: Guaranteed higher than 1000 megohms
AVAILABLE TOLERANCE: ±5% ±10% ±20%

SEND FOR SAMPLES AND TECHNICAL DATA

DISCAP CERAMIC CONDENSERS

RMC

RADIO MATERIALS CORPORATION

GENERAL OFFICE: 3325 N. California Ave., Chicago 18, Ill.

FACTORIES AT CHICAGO, ILL. AND ATTICA, IND.

DISTRIBUTORS: Contact Jobber Sales Co., 146 Broadway, Paterson 1, N. J.

Fine Aluminum Wire
To meet the growing demand from producers of lightweight, high-frequency Galvanometer movements, we have expanded our facilities designed to process Wire of 2S Aluminum . . . This wire can be supplied in diameters ranging from approximately .001 inch through .005 inch . . . Anodized with an exceptionally thin and flexible dielectric coating
Also available: wires of aluminum alloys enameled as small as .001 inch diameter, to meet rigid specifications of resistance, size and straightness
Write for Latest List of Products
SIGMUND COHN CORP.

NEW MODEL 202C

WIDE-BAND CHAIN AMPLIFIER

EXTENDED LOW FREQUENCY RESPONSE
1 kc - 210 mc

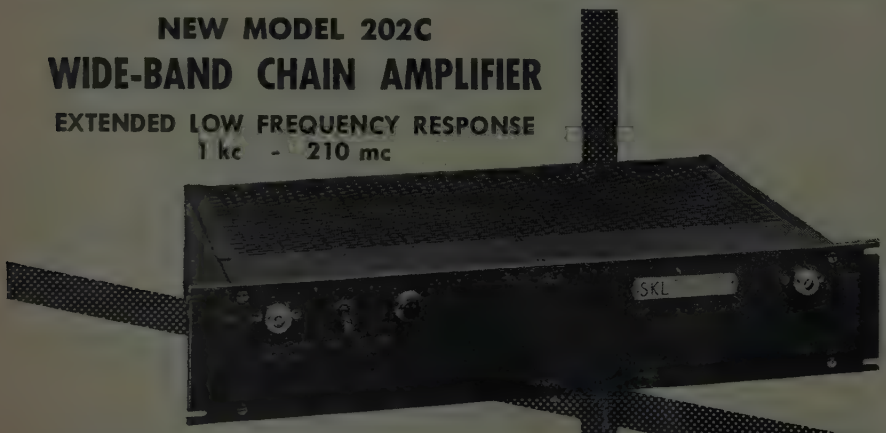

Extended bandwidth, stable gain, and linear phase shift make the new SKL Model 202C Wide-Band Chain Amplifier ideal for the accurate amplification of pulses and transients. The flat frequency response curve of the Model 202C Wide-Band Chain Amplifier permits cascading of a number of stages. Thus, low-level broad band voltages such as pulses, transients, and television signals can be amplified to useful levels. The Model 202C Wide-Band Chain Amplifier finds application in oscillography, radar, nuclear and television research.

For further information write for Bulletin 202P-4

SPECIFICATIONS

- RISE TIME .0026 μsec
- VOLTAGE GAIN 20 db
- BANDWIDTH 1 kc - 210 mc
- IMPEDANCE 200 ohms
- REGULATED POWER SUPPLY

SKL SPENCER-KENNEDY LABORATORIES, INC.
186 MASSACHUSETTS AVE., CAMBRIDGE 39, MASS.

Industrial Engineering Notes

(Continued from page 104A)

State and City	*Permittee*	*Channel*
	COMMERCIAL	
Denver, Colo.	Eugene P. O'Fallon, Inc.	2
Portland, Ore.	Empire Coil Co., Inc.	27
Denver, Colo.	Colorado Television Corp.	9
Lubbock, Texas	Texas Telecasting, Inc.	13
Honolulu, T.H.	Radio Honolulu, Ltd.	11
Roanoke, Va.	Shenandoah Life Stations, Inc.	10
Austin, Texas	Texas Broadcasting Corp.	7
Honolulu, T. H.	Hawaiian Broadcasting System, Ltd.	9
Tucson, Ariz.	Old Pueblo Broadcasting Co.	13
El Paso, Texas	Roderick Broadcasting Corp.	4
Youngstown, Ohio	The Vindicator Printing Co.	73
Colorado Springs, Colo.	TV Colorado, Inc.	11
Atlantic City, N. J.	Neptune Broadcasting Corp.	46
South Bend, Ind.	South Bend Tribune	34
Spokane, Wash.	KHQ, Inc.	6
Mobile, Ala.	Pape Broadcasting Co., Inc.	10
Spring Garden, Pa.	Susquehanna Broadcasting Co.	43
Mobile, Ala.	Pursley Broadcasting Service	48
Wilkes-Barre, Pa.	Louis G. Baltimore	28
Youngstown, Ohio	WKBN Broadcasting Corp.	27
El Paso, Texas	Tri-State Broadcasting Co., Corp.	9
Jackson, Miss.	Miss. Publishers Corp.	25
Altoona, Pa.	Goble Broadcasting Co.	10
Bangor, Me.	Community Telecasting Service	5
Peoria, Ill.	Robert S. Kerr—West Central Bdcstg. Co.	43
Roanoke, Va.	Radio Roanoke, Inc.	27
Spokane, Wash.	Symons Broadcasting Co.	4
Lynchburg, Va.	Lynchburg Broadcasting Corp.	13
New Britain, Conn.	New Britain Broadcasting Corp.	30
Lincoln, Neb.	Cornhusker Radio & TV Corp.	12
Reading, Pa.	Eastern Radio Corp.	61
Wichita Falls,	Wichtex Radio & TV Co.	3
Tacoma, Wash.	Tribune Publishing Co.	11
Lawton, Okla.	Okla. Quality Bdcstg. Corp.	7
Wichita Falls, Texas	Wichita Falls TV, Inc.	6
Springfield, Mo.	Independent Broadcasting Co.	10
Bridgeport, Conn.	Southern Conn. & L. I. TV Co., Inc.	43
Sioux City, Iowa	Cowles Broadcasting Corp.	9
Green Bay, Wis.	Norbertine Fathers	2
Agawam, (Springfield) Mass.	Springfield TV Broadcasting Corp.	61
Amarillo, Texas	Plains Radio Broadcasting Co.	4
Little Rock, Ark.	Little Rock Telecasters, Inc.	17
Pueblo, Colo.	Pueblo Radio Co., Inc.	3
Galveston, Texas	Gulf Television Co.	11
Ft. Lauderdale, Fla.	Gore Publishing Co.	23
Harrisburg, Pa.	WHP, Inc.	55
Minot, N. Dak.	North Dakota Broadcasting Co.	13
Amarillo, Texas.	Amarillo Broadcasting Co.	10
New Castle, Pa.	WKST, Inc.	45
Montgomery, Ala.	Capitol Broadcasting Co.	20
Springfield, Mass.	The Hampden-Hampshire Corp.	55
Reading, Pa.	Hawley Broadcasting Corp.	33

(Continued on page 108A)

ALPHA's

CEN-TRI-CORE

"ENERGIZED"

ROSIN-FILLED

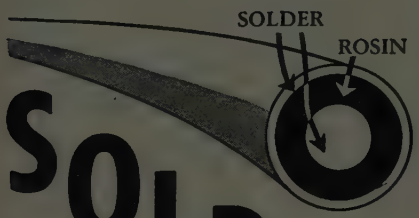

SOLDER

Now Available For

PRINTED CIRCUIT SOLDERING

This solder provides improved electrical conductivity, with melting point below the tin-lead eutectic.

Special alloys for all types of PRINTED CIRCUITS.

Solder also available in bar form for dipping, with Alpha's PRINTED CIRCUIT FLUXES.

Approved by leading manufacturers of PRINTED CIRCUITS.

for further information write . . .

FASTER MELTING · POSITIVE FLUXING

ALPHA METALS, INC.
61 WATER ST., JERSEY CITY 4, N. J.

Specialists IN SOLDER
For Over Fifty Years

THE *Dependable*

BALLANTINE MODEL 300

Famous for

SENSITIVITY
▪
ACCURACY
•
STABILITY

VOLTAGE RANGE	.001v to 100v
FREQUENCY RANGE	10 cps to 150 kc
ACCURACY	2% ENTIRE RANGE
INPUT IMPEDANCE	½ meg shunted by 30 uuf

- Stability insured by the exclusive use of wire-wound resistors in the attenuator and feedback network.
- Same accuracy of reading at *ALL* points on the logarithmic voltage scale and linear decibel scale.
- Only ONE voltage scale to read with decade range switching.
- No "turn-over" discrepancy on unsymmetrical waves.
- Accessories available to extend the range to 20 uv and to 10 kv.
- Provides 70 DB amplifier flat within 1 DB from 10 cps to 150 kc.

Write for further details of this and other Ballantine voltmeters and accessories

BALLANTINE LABORATORIES, INC.

102 Fanny Road, Boonton, N.J.

NEW "PARAFORMED" PAPER TUBES

MAKE YOUR COIL WINDING
EASIER! FASTER! BETTER!

SPIRAL WOUND
NOT DIE FORMED

- No sharp outside edges to cut wire
- Has full rigidity and physical strength
- Permits winding coils to closer tolerances
- No need for wedges to tighten wire
- Allows faster stacking of wound coils

ANY SIZE—SQUARE OR RECTANGULAR

Entirely new technique in tube making developed and perfected by PARAMOUNT now for the first time solves many coil winding problems, *yet costs you no more!* Hi-Dielectric. Hi-Strength. Kraft, Fish Paper, Acetate, Red Rope or any combination wound on automatic machines. Produced from stock arbors or special sizes engineered for you.

Write on Company letterhead for Stock Arbor List of over 2000 sizes

PARAMOUNT PAPER TUBE CORP.

617 LAFAYETTE STREET, FORT WAYNE 2, INDIANA

Manufacturers of Paper Tubing for the Electrical Industry Since 1931

ANOTHER BETTER TOOL...

for the ELECTRONIC ENGINEER and the RESEARCH SCIENTIST

A versatile instrument for research involving high repitition rates

MODEL B-2
PULSE GENERATOR

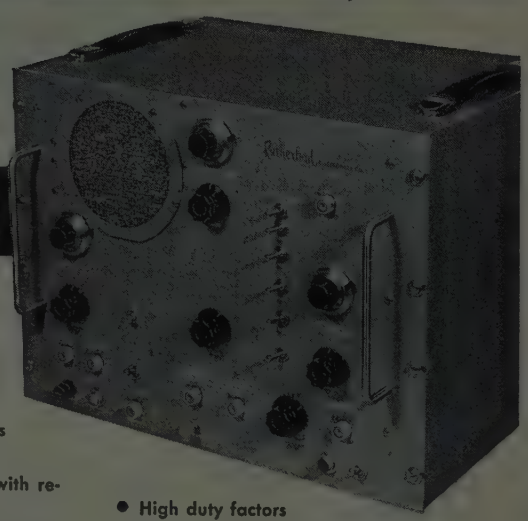

PULSE WIDTH: variable in 4 ranges from .2μs to 1,000μs

PULSE RISE TIME: .02 μs

PULSE AMPLITUDE: $\pm$ 80 volts open circuit

INTERNAL IMPEDANCE: 93 ohms

INTERNAL DELAYS: variable in 5 ranges from 0 to 10,000 μs with respect to synchronizing pulse

INTERNAL REPETITION RATES: variable in 4 ranges from 10 cycles at 100 KC

SYNCHRONIZING PULSES: 5—independently available at separate output jacks

- High duty factors
- Can be triggered externally and for single pulse operation
- Calibrating potentiometers are provided for each range

Write for complete data: our Bulletin I-B-2

Rutherford ELECTRONICS CO. 3707 S. ROBERTSON BLVD. CULVER CITY, CALIFORNIA

Industrial Engineering Notes

(Continued from page 106A)

State and City	*Permittee*	*Channel*
Lima, Ohio	WLOK, Inc.	73
Baton Rouge, La.	Modern Broadcasting Co. of Baton Rouge, Inc.	28
Ann Arbor, Mich.	Washtenau Broadcasting Co.	20
Rockford, Ill.	Winnebago Television Corp.	39
Columbia, S. C.	Radio Columbia	25
Saginaw, Mich.	Lake Huron Broadcasting Co.	57
Mesa, Ariz.	Harkins Broadcasting Co.	12
Bellingham, Wash.	KVOS, Inc.	12
Bethlehem, Pa.	Associated Broadcasters, Inc.	51
Lubbock, Texas	Bryant Radio & TV Stations Inc.	11
Battle Creek, Mich.	Booth Radio & TV Stations Inc.	64
Zanesville, Ohio	Orville Littick, (Southern Ohio TV System)	50
Muncie, Ind.	Tri-City Radio Corp.	49
Sioux Falls, S. Dak.	Midcontinent Broadcasting Co.	11
San Luis Obispo, Calif.	Christena M. Jacobson & Leslie H. Hacker (Valley Electric Co.)	6
Rochester, Minn.	Southern Minn. Broadcasting Co.	10
Peoria, Ill.	Hilltop Broadcasting Co.	19
Elmira, N. Y.	John S. Booth (Elmira TV)	24
St. Petersburg, Fla.	City of St. Petersburg, Fla.	38
Fresno, Calif.	McClatchy Broadcasting Co.	24
Lincoln, Neb.	Cornbelt Broadcasting Co.	10
Fargo, N. Dak.	WDAY, Inc.	6
Kansas City, Mo.	Empire Coil Co., Inc.	25
Scranton, Pa.	Scranton Broadcasters, Inc.	22
Duluth, Minn.	Great Plains Television Properties of Minn., Inc.	38
Akron, Ohio	Summit Radio Corp.	49
Lafayette, Ind.	WFAM, Inc.	59
Tucson, Ariz.	Arizona Broadcasting Co.	4
Nampa, Ohio	Frank E. Hurt & Son, Inc.	6
Roswell, N. Mex.	John A. Barnett	6
Charleston, S. C.	WCSC, Inc.	5
Harrisburg, Pa.	Harrisburg Broadcasters, Inc.	71
Pueblo, Colo.	Star Broadcasting Co., Inc.	5
Oshkosh, Wis.	Wm. F. Johns, Jr. (Oshkosh Broadcasting Co.)	48
Hutchinson, Kans.	Hutchinson TV, Inc.	12
Asheville, N. C.	Radio Station WISE, Inc.	62
San Angelo, Texas	Westex Television Co.	8
Madison, Wis.	Bartell Television Corp.	33
Madison, Wis.	Monona Broadcasting Corp.	27
Milwaukee, Wis.	Midwest Broadcasting Co.	25
Raleigh, N. C.	Sir Walter Television Co.	28
Rome, Ga.	WROM-TV, Inc.	9
Boise, Idaho	KIDO, Inc.	7
Las Vegas, Nev.	Las Vegas TV, Inc.	8
Butte, Mont.	Cooper Broadcasting Co.	4
Pittsburgh, Pa.	Agnes J. Reeves Greer	53
Easton, Pa.	Easton Publishing Co.	57
Yakima, Wash.	Cascade Broadcasting Co., Inc.	29
Fort Smith, Ark.	Southwestern Publishing Co.	22
Belleville, Ill.	Signal Hill Telecasting Corp.	54
Austin, Minn.	Minnesota-Iowa Television Co.	6
Santa Barbara, Calif.	Santa Barbara Broadcasting and Telecasting Corp.	2
Waterbury, Conn	WATR, Inc.	53
Lansing, Mich.	Lansing Broadcasting Co.	54

(Continued on page 114A)

ONLY THE LFE 401 OSCILLOSCOPE

Offers all these Important Features

HIGH SENSITIVITY AND WIDE FREQUENCY RESPONSE OF Y-AXIS AMPLIFIER

The vertical amplifier of the 401 provides uniform frequency response and high sensitivity from D-C. Coupled with a sensitivity of 15 Mv./cm peak to peak at *both D-C* and A-C is a response characteristic which is 3 db. down at 10 Mc. and 12 db. at 20 Mc. Alignment of the amplifier is for best transient response, resulting in no overshoot for pulses of short duration and fast rise time. An example of the wide band response of the amplifier is shown in the accompanying photographs.

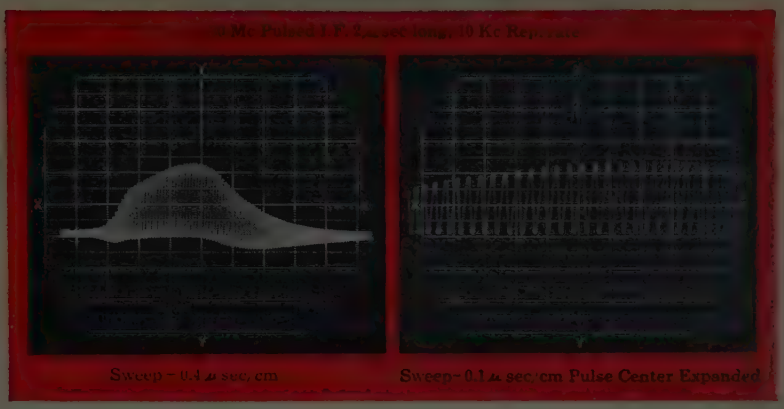

Sweep – 0.4 μ sec/cm

Sweep – 0.1 μ sec/cm Pulse Center Expanded

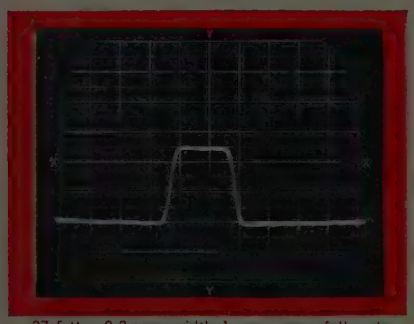

37.5 Mv., 0.2 μ sec width, 1 μ sec sweep full scale

75 Mv., 0.2 μ sec width, 1 μ sec sweep full scale

LINEARITY OF VERTICAL DEFLECTION The vertical amplifier provides up to 2.5 inches positive or negative uni-polar deflection without serious compression; at 3 inches, the compression is approximately 15%. The accompanying photographs illustrate transient response and linearity of deflection.

SWEEP DELAY The accurately calibrated delay of the 401 provides means for measuring pulse widths, time intervals between pulses, accurately calibrating sweeps and other useful applications wherein accurate time measurements are required.

The absolute value of delay is accurate to within 1% of the full scale calibration. The incremental accuracy is good to within 0.1% of full scale calibration.

SPECIFICATIONS

Y-Axis

Deflection Sens.—15 Mv./cm, p-p
Frequency Response—DC to 10 Mc
Transient Response—Rise Time (10%-90%) 0.035 μ sec
Signal Delay—0.25 μ sec
Input line terminations—52, 72 or 93 ohms, or no termination
Input Imp.—Direct—1 megohm, 30 μ μ f
Probe—10 megohms, 10 μ μ f

X-Axis

Sweep Range—0.01 sec/cm to 0.1 μ sec/cm
Delay Sweep Range—5-5000 μ sec in three adjustable ranges.
Triggers—Internal or External, + and −, trigger generator, or 60 cycles, undelayed or delayed triggers may be used.
Built-in trigger generator with repetition rate from 500-5000 cps.

General

Low Capacity probe
Functionally colored control knobs
Folding stand for better viewing
Adjustable scale lighting
Facilities for mounting cameras

PRICE: $895.00

Additional Features:

TRIGGER GENERATOR with variable repetition rate from 500 to 5000 cps.

POSITIVE & NEGATIVE UNDELAYED TRIGGERS and a **POSITIVE DELAYED TRIGGER** are externally available.

An **INPUT TERMINATION SWITCH** for terminating transmission lines at the oscilloscope.

A **FOLDING STAND** for convenient viewing.

FUNCTIONALLY COLORED KNOBS for easier location of controls.

Designed and built *for* electronic engineers, the 401, with its high gain and wide band characteristics, and its versatility, satisfies the ever-increasing requirements of the rapidly growing electronics industry for the ideal medium priced oscilloscope.

Write for Complete Information.

LABORATORY for ELECTRONICS, INC.
75-4 PITTS STREET • BOSTON 14, MASS.

PRECISION ELECTRONIC EQUIPMENT • OSCILLOSCOPES • MAGNETOMETERS • COMPUTERS • MICROWAVE OSCILLATORS • MERCURY DELAY LINES

There's More to a Good Filter Than Meets the Eye!

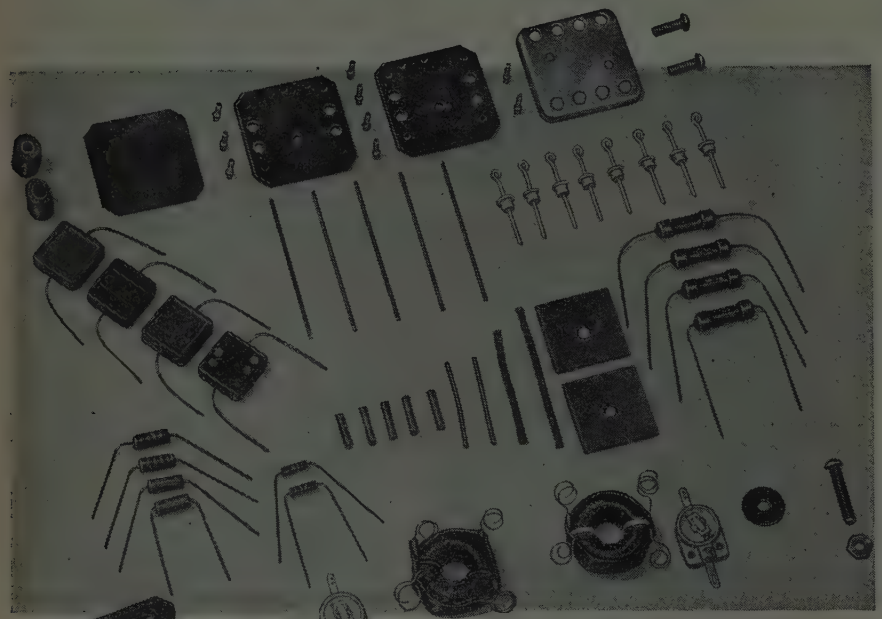

All of these 66 parts are from a single B&W Toroidal-coil type discriminator only 1¾" square by 3½" long exclusive of terminals!

Throughout, the job is one calling for precision components plus a wealth of engineering "know how" in producing and assembling them for maximum performance and effectiveness.

Like all other B & W Special Components, the one illustrated here was designed and produced for a specific application—in this instance a critical military use.

FILTERS

In addition to "tailor-made" discriminators, B & W offers a complete line of performance-proved filters including high-pass, low-pass, band-pass and band suppression types.

TOROIDS

B & W Toroidal Coils of various styles and sizes are available in a wide range of inductance values in open, shielded, potted and hermetically sealed types.

B&W Barker & Williamson, Inc.

237 Fairfield Ave., Upper Darby, Pa.

Industrial Engineering Notes

(Continued from page 108A)

State and City	Permittee	Channel
Buffalo, N. Y.	Buffalo-Niagara Television Corp.	59
Greenville, S. C.	Greenville Television Corp.	22
Kansas City, Mo.	WHB Broadcasting Co.	9
Kansas City, Mo.	Midland Broadcasting Co	9
Tacoma, Wash.	KMO, Inc.	13
Medford, Ore.	Southern Oregon Broadcasting Co.	5
Salem, Ore.	Lawrence A. Harvey	24
Hampton, Va.	Peninsula Broadcasting Corp.	15
Portland, Ore.	Mount Hood Radio & TV Broadcasting Corp.	6
Evansville, Inc.	Premier Television, Inc.	62
Decatur, Ill.	Prairie Television Co.	17
Billings, Mont.	The Montana Network	2
San Diego, Calif.	Airfan Radio Corp., Ltd.	10
Monroe, La.	Delta Television, Inc.	43
Texarkana, Texas	KCMC, Inc.	6
Scranton, Pa.	Appalachian Co.	73
Buffalo, N. Y.	WBUF-TV, Inc.	17
Bakersfield, Calif.	Bakersfield Broadcasting Co.	29
Columbus, Ga.	Television Columbus	28
Butte, Mont.	Television Montana	6
Pittsburgh, Pa.	Telecasting Co. of Pittsburgh	16
Salinas, Calif.	Salinas Broadcasting Corp.	8
Monterey, Calif.	The Monterey Radio-Television Co.	8
Chambersburg, Pa.	Chambersburg Broadcasting Co.	46
Albuquerque, N. M.	New Mexico Broadcasting Co.	13
Quincy, Ill.	Quincy Broadcasting Co.	10
Macon, Ga.	Macon Television Co.	47
Hannibal, Mo.	Lee Broadcasting, Inc.	7
Wichita, Kans.	KEDD, Inc.	16
Tyler, Texas	Jacob A. Newborn, Jr.	19
Columbia, S. C.	Palmetto Radio Corp.	67
Minneapolis, Minn.	Minnesota Television Public Corp.	11
Abilene, Texas	The Reporter Broadcasting Co.	9
St. Louis, Mo	Broadcast House, Inc.	36
Memphis, Tenn.	Harding College	13
Portland, Me.	The Portland Telecasting Corp.	53
Fresno, Calif.	O'Neill Broadcasting Co.	47
St. Paul, Minn.	WMIN Broadcasting Co.	11
Johnson City, Tenn.	WJHL, Inc.	11
Chico, Calif.	Golden Empire Broadcasting Co.	12

Reports From Chapters

Information Theory

The Albuquerque-Los Alamos Chapter of the Professional Group on **Information Theory** met on September 9 at Mitchell Hall, University of New Mexico, under the chairmanship of B. L. Basore. Mr. Basore also presented a paper, "A Review of Information Theory Fundamentals," which reviewed some important aspects of information theory presented at a series of meetings during the previous season. Subjects touched upon were the derivation of the unit of information in terms of prob-

(Continued on page 118A)

IRE's 21 Professional Groups

Communications Systems

Radio and wire telephone, telegraph and facsimile in marine, aeronautical, radio-relay, coaxial cable and fixed station services.

Col. John Hessel, Chairman, Signal Corps Engineering Laboratories, Fort Monmouth, N.J.

Fee $2. *Vol. CS-1, No. 1

Electronic Component Parts

The characteristics, limitations, applications, development, performance and reliability of component parts.

Mr. Floyd A. Paul, Chairman, Supervisor, Electronic Reliability Sec., Dept. 3230, Northrop Aircraft, Inc., Hawthorne, Calif.

Fee not yet established.

Electron Devices

Electron devices, including particularly electron tubes and solid state devices.

Dr. Leon S. Nergaard, Chairman, RCA Laboratories, Princeton, N.J.

Fee $2. Transactions *1, *2 and *3

Electronic Computers

Design and operation of electronic computers.

Mr. John H. Howard, Chairman, Burroughs Corp., 511 North Broad Street, Philadelphia 23, Pa.

Fee $2. Transactions 1, 2, and *Vol. EC-2, No. 2

Engineering Management

Engineering management and administration as applied to technical, industrial and educational activities in the field of electronics.

Gen. Tom C. Rives, U.S.A. (Ret'd.), Chairman, General Electric Company, Electronics Park, Syracuse, N.Y.

Fee $1. *Convention Report

Industrial Electronics

Electronics pertaining to control, treatment and measurement, specifically in industrial processes.

Dr. Eugene Mittelmann, Chairman, Consulting Engineer, 549 W. Washington Blvd., Chicago 6, Ill.

Fee $2. *Convention Report

Information Theory

Information theory and its application in radio circuitry and systems.

Dr. William G. Tuller, Chairman, Melpar, Inc., 452 Swann Ave., Alexandria, Va.

Fee $2. Transaction 1.

Instrumentation

Measurements and instrumentation utilizing electronic techniques.

Mr. Ivan G. Easton, Chairman, General Radio Co., 275 Massachusetts Ave., Cambridge 39, Mass.

Fee $1. Transactions 1, *2. *Convention Report

Medical Electronics

The application of electronics engineering to the problems of the medical profession.

Mr. L. H. Montgomery, Jr., Chairman, 612 Craighead Street, Nashville, Tenn.

Fee $1. *Convention Report

Microwave Theory and Techniques

Microwave theory, microwave circuitry and techniques, microwave measurements and the generation and amplification of microwaves.

Mr. Andre G. Clavier, Chairman, Federal Telecommunication Laboratories, 500 Washington Ave., Nutley, N.J.

Fee $2. *Vol. MTT-1, #1

Nuclear Science

Application of electronic techniques and devices to the nuclear field.

Dr. Lloyd V. Berkner, Assoc. Universities, Inc., 350 5th Ave., New York 1, N.Y.

No fee established yet.

Quality Control

Techniques of determining and controlling the quality of electronic parts and equipment during their manufacture.

Mr. Leon Bass, Chairman, General Electric Co., Electronics Div., Syracuse, N.Y.

Fee $2. Transactions *1, *2

Radio Telemetry and Remote Control

The control of devices and the measurement and recording of data from a remote point by radio.

Mr. Martin V. Kiebert, Jr., Chairman, 463 Boulevard, Hasbrouck Heights, N.J.

Fee $1. *Convention Report

Vehicular Communications

Communications problems in the field of land and mobile radio services, such as public safety, public utilities, railroads, commercial land transportation, etc.

Mr. W. A. Shipman, Chairman, Columbia Gas Sys. Ser. Corp., 120 East 41 Street, New York 17, N.Y.

Ultrasonics Engineering

Ultrasonic measurements and communications, including underwater sound, ultrasonic delay lines, and various chemical and industrial ultrasonic devices.

Mr. A. L. Lane, Chairman, 706 Chillum Road, Apt. 101, Hyattsville, Md.

No fee established yet.

ENGINEERS 1 East 79th Street, New York 21, N. Y.

Saratoga Industries

STAR PERFORMANCE AS MANUFACTURERS OF TRANSFORMERS, REACTORS, FILTERS, TOROIDAL COILS FOR THE ELECTRONICS INDUSTRY

Now in its ninth year of operation, Saratoga Industries, Inc. has built a solid reputation for the manufacture of precision windings. Approved for in-plant testing under MIL-T-27, Saratoga Industries, Inc. is also prepared to handle all types of commercial production. Saratoga engineers invite your inquiry to help solve your problems relating to reactors, transformers, filters and windings of all types.

SARATOGA INDUSTRIES, INC. SARATOGA SPRINGS, N. Y.

PROFESSIONAL GROUP MEETINGS

(Continued from page 114A)

ability, and the analysis of a simplified hypothetical data transmission system to yield an expression for average information transmitted in the presence of noise in terms of message probabilities. This expression was further simplified to the familiar form of entropy.

Audio

The Philadelphia Chapter of the Professional Group on **Audio** held its annual organization meeting at the Bell Telephone Building. Murlan S. Corrington, RCA Victor Corp., was elected chairman; William G. Chaney, Bell Telephone Co. of Pa., vice-president, and William P. West, Leeds and Lathrop Co., secretary. An interesting series of meetings has been planned for the coming year. Tentative meeting dates are as follows: October 22, November 19, February 18, March 18, and April 22.

Engineering Management

The Los Angeles Chapter of the Professional Group on **Engineering Management** met on July 22 at the IAS Building, Los Angeles, Calif., under the chairmanship of T. W. Jarmie. Robert Loomis, Computer Research Corp., presented a paper entitled "Administrative Com-

(Continued on page 120A)

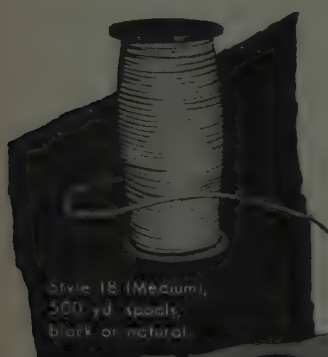

for lacings that stay put!

GUDELACE

BRAIDED NYLON LACING TAPE*

A New and Revolutionary Type of Lacing

- Saves time, saves money, greatly reduces the number of rejects
- Won't "bite through" insulation
- Won't cut wiremen's fingers or cause dermatitis
- Ties easier, ties tighter and cuts down on slipping of knots

Let GUDELACE answer your lacing problems.

Write for FREE samples and prices.

*Patent Pending.

GUDEBROD BROS. SILK CO., INC.
Electronics Division Dept. D
Main Office: 12 South 12th Street, Philadelphia 7, Pa.
225 West 34th Street, New York 1, N.Y.

PHAZOR Pat. Pend. NULL METER MODEL 100A

$229.50 F.O.B. New York, N. Y.

A phase sensitive null detector wherein noise and harmonic voltages are effectively eliminated.

- For use in conjunction with bridge and potentiometer circuits.
- Simplified and precise zeroing of synchro devices.
- Allows separate adjustment of phase and magnitude in null circuits.
- Eliminates the necessity for filters.

SPECIFICATIONS

Input Impedance
High Gain—2 megohms shunted by 30 mmfd.
Low Gain—2.5 megohms shunted by 15 mmfd.
Sensitivity—5 millivolts off-scale deflection
Frequency Range—
30-10,000 cps (higher ranges available)
Selectivity—40 db. down on all noise & harmonics
Reference Input Power—10 milliwatts
Maximum Input Voltage—125 volts RMS
Peak Input Voltage—400 volts
Power Supply—105-125 volts, 60 cps, 25 watts
Dimensions—Hgt. 9 in., Width 15 in., Depth 8 in.
Weight—25 pounds

INDUSTRIAL TEST EQUIPMENT CO.
55 EAST 11th ST., N. Y. 3 - Tel. GR. 3-4686

ATR AUTO RADIO VIBRATORS

Have Ceramic Stack Spacers

A COMPLETE LINE OF VIBRATORS

Designed for Use In Standard Vibrator-Operated Auto Radio Receivers. Built with Precision Construction, featuring Ceramic Stack Spacers for Longer Lasting Life. Backed by more than 22 years of experience in Vibrator Design, Development, and Manufacturing.

Free

"A" Battery Eliminators, DC-AC Inverters, Auto Radio Vibrators

ATR

✓ NEW MODELS ✓ NEW DESIGNS ✓ NEW LITERATURE

See your jobber or write factory

AMERICAN TELEVISION & RADIO CO.

Quality Products Since 1931

SAINT PAUL 1, MINNESOTA—U. S. A.

D.C. to 5-MEGACYCLE SCOPE

model OA-16

for MEASUREMENTS OVER WIDE RANGES

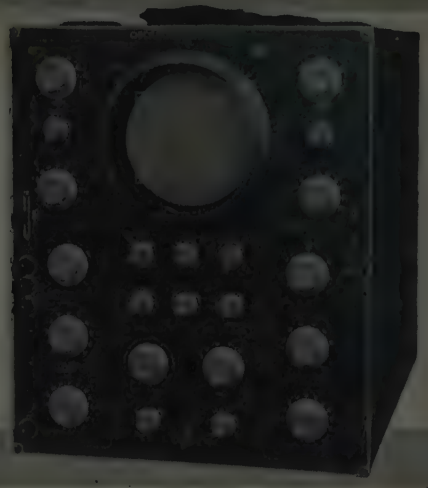

Self-contained... Calibrated...

D.C. "BUCK-OUT" VOLTAGE

permits HIGH GAIN examination of small D.C. level shifts and hard-to-see A.C. COMPONENTS

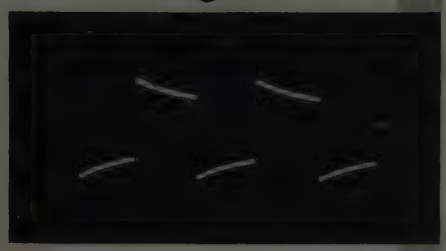

The above photograph shows a 5-volt peak-to-peak signal at a D.C. level of 400 volts. By bucking out the 400-volt component, high gain can be used to give a large image for detailed study. With such a presentation, a D.C. level shift of as little as 0.25% is readily observable.

- **5X sweep expansion**
- **Trace position stability**
- **Broadband X axis amplifier**
- **Accurate X and Y axis calibrations**
- **Triggered or recurrent sweeps**

MODEL OA-16 OSCILLOSYNCHROSCOPE

$745.00

f.o.b. Winchester

Write for detailed literature

SPECIFICATIONS

- Vertical amplifier — D.C. to 5 megacycles — .08 μsec rise time — sensitivity 50 millivolts peak-to-peak/inch — signal delay line.
- D.C. "buckout" voltage up to 600 volts depending on vertical attenuator setting.
- Triggered or recurrent sweeps — 10 seconds total sweep time to 0.4 microseconds per centimeter.
- 5X sweep expansion.
- Horizontal amplifier — D.C. to 1 megacycle — sensitivity 120 millivolts peak-to-peak/inch.
- Regulated plate and heater supplies for best trace stability.
- Flat-faced 5" cathode-ray tube. Deflection plates brought out for direct connections.
- Vertical deflection calibration accuracy 5%. Sweep calibration accuracy 10%.
- Blower cooling.
- Edgelighted rule screen.

BL BROWNING Laboratories, Inc. Winchester, Mass. ENGINEERED FOR ENGINEERS

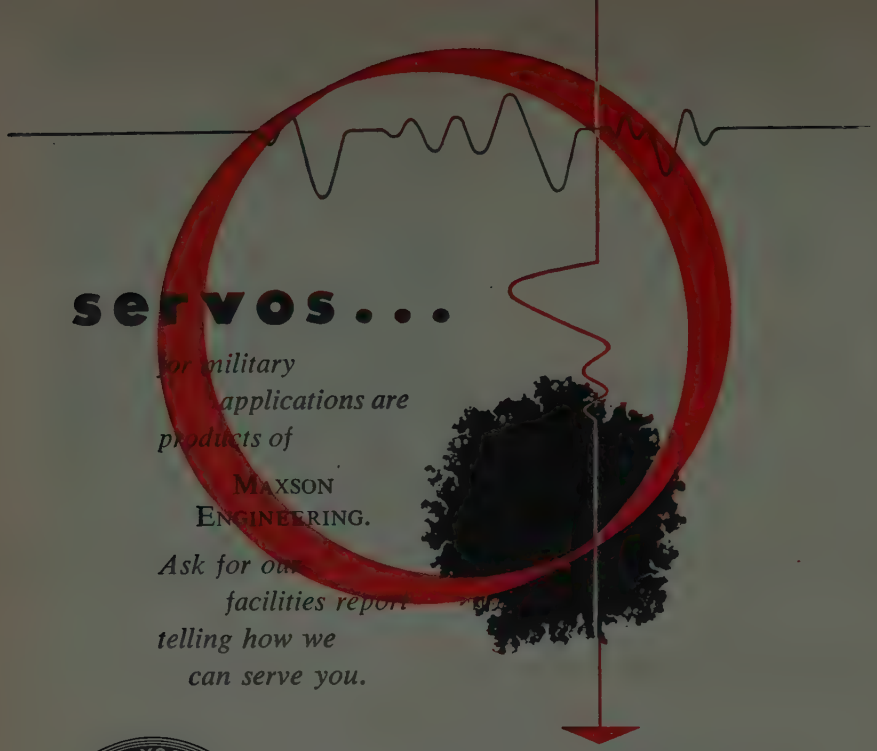

servos . . .

for military applications are products of

MAXSON ENGINEERING.

Ask for our facilities report telling how we can serve you.

THE W. L. MAXSON CORPORATION

460 West 34th Street, New York 1, New York

Plants at Long Island City, N. Y. and Old Forge, Pennsylvania

IT'S

HARVEY

FOR PROMPT

"OFF-THE-SHELF" DELIVERY

Whether it's equipment, components or other electronic requirements, you will always find them in Harvey's extensive stocks, ready for immediate delivery to you anywhere.

WRITE PHONE or WIRE

Harvey's twenty-five years of service to the industry are your assurance of understanding 'know-how' and complete dependability.

hrc

HARVEY

RADIO COMPANY, INC.

103 West 43rd St., New York 36, N. Y.

Telephone JUdson 2-1500

PROFESSIONAL GROUP MEETINGS

(Continued from page 118A)

munications in an Engineering Department." In his paper, Mr. Loomis discussed various aspects of project versus functional organization, giving numerous analogies and examples. He stated that military eras were characterized by line organization in the Civil War, by the establishment of functional groups in World War I, and by the innovation of task-force operation in World War II. Task-force operation proved that a man could have more than one boss, provided that their fields of authority did not overlap or conflict. Military methods have had major effects upon business organization. Mr. Loomis recommended that the task force principle be applied in an engineering department by establishing functional departments having major hiring, firing, and technical responsibilities, and by establishing a project head for each project who would have sole authority over delegates appointed by functional heads with respect to time, place, and sequence of work. The project engineer could discharge a man from his project task force, but not from the company. Mr. Loomis would like to see engineering departments challenge purchasing, personnel, hiring, budget allocation, and accounting operations which are not in accordance with the needs and circumstances of engineering. He concluded by saying that engineers have a responsibility to make themselves articulate about their specialties.

SECTION MEETINGS

BALTIMORE

"Motors for High-Accuracy Servo Systems," by Robert Brown, Kearfott Company, Inc.; September 9, 1953.

BEAUMONT-PORT ARTHUR

"Long Distance Dialing including Transistor Applications," by J. T. Mathews, Southwestern Bell Telephone Co.; Houston, Texas.

BINGHAMTON

"The Daystrom Story," by Harold Bechtol, Daystrom Instrument Corp.; September 14, 1953.

BUFFALO-NIAGARA

"U.H.F. in Buffalo," by S. Grossman, WBUF-TV, Chautaugua Broadcasting Corp.; and "U.H.F. Transmitters," by P. Tissot, Dumont Laboratories, Inc.; September 16, 1953.

DAYTON

"Limitations of Transistors," by Leo E. Dwork, Raytheon Manufacturing; September 10, 1953.

DENVER

"Our Expanding Technology," by Dr. J. W. McRae, President, IRE; brief talk on activities in the Colorado Engineering Council by T. G. Morrissey; September 14, 1953.

(Continued on page 122A)

Resistors
Rheostats
TRU-OHM PRODUCTS
General Sales Office:
2800 N. Milwaukee Avenue, Chicago 18, Ill.
Write for FREE Engineering Catalog NOW!

the Waterman HIGH GAIN INDUSTRIAL POCKETSCOPE®

MODEL S-14-A

Size:
12" x 5¾" x 7"
12¾ Pounds

ANOTHER EXAMPLE OF Waterman PIONEERING . . .

The HIGH GAIN POCKETSCOPE, model S-14-A, is an outstanding achievement in the field of oscilloscopes. The high vertical and horizontal sensitivities of 10 and 15 millivolts rms/inch respectively; frequency responses within —2 db from DC to 200 KC; non-frequency discriminating attenuators and gain controls; plus individual calibration voltages are but a few of the heretofore unobtainable characteristics of DC coupled oscilloscopes. The sweep is operated in either a repetitive or trigger mode over a range from 0.5 cycles to beyond 50 KC with synchronization polarity optional. All this and portability too! The incredibly small size and light weight of the S-14-A now permits "on-the-spot" use of the oscilloscope in all industrial, medical, and communications fields. Its rugged construction assures "laboratory performance" regardless of environment.

WATERMAN PRODUCTS CO., INC.

PHILADELPHIA 25, PA.

CABLE ADDRESS: POKETSCOPE

MEMO... *Write for details today!*

WATERMAN PRODUCTS INCLUDE

S-4-A	SAR	PULSESCOPE®
S-5-A	LAB	PULSESCOPE
S-11-A	INDUSTRIAL	POCKETSCOPE
S-12-B	JANized	RAKSCOPE®
S-14-B	HIGH GAIN	POCKETSCOPE
S-15-A	TWIN TUBE	POCKETSCOPE

Also RAYONIC® Cathode Ray Tubes and Other Associated Equipment

WATERMAN PRODUCTS

SECTION MEETINGS

(Continued from page 120A)

EVANSVILLE-OWENSBORO

"An On-Channel Television Booster Station," by L. E. Rawls, WSM-Inc.; September 9, 1953.

LOUISVILLE

"Microwaves in TV Broadcasting," by A. C. Shelton, WSM-TV; demonstration of mobile equipment by Paul Kinchloe, WSM-TV; September 10, 1953.

NEW YORK

"A New P-N-P Alloy Junction Transistor for R.F. Amplification," by C. W. Mueller and J. I. Pankove, RCA Labs.; "An Experimental Transistor Personal Broadcast Receiver," by L. E. Barton, RCA Labs.; September 16, 1953.

OKLAHOMA CITY

"Our Expanding Technology," by Dr. J. W. McRae, President, IRE; September 15, 1953.

PITTSBURGH

Tour through the studios and transmitter of new UHF Television Station WENS (The Telecasting Co. of Pittsburgh) and the nearby Troy Hill microwave relay tower of the American Telephone & Telegraph Co.; September 14, 1953.

PORTLAND

"What Does Current Standardization Mean to You," by P. K. McElroy, General Radio Company; August 24, 1953.

"History of Magnetic Tape Recordings," by W. A. Morrison, Reeves—Soundcraft Corporation; "Design and Use of Dage Industrial and Broadcast Television Cameras," by F. D. Meadows, Dage Electronics Corporation; August 25, 1953.

"Our Expanding Technology," by Dr. J. W McRae, President, IRE; September 10, 1953.

WASHINGTON, D. C.

"Measuring Tube Performance at U.H.F.," by J. W. Rush, General Electric Company; September 14, 1953.

SUBSECTIONS

HUNTSVILLE

Installation of officers; July 24, 1953.

"Introduction to TV Receiving Antennas," by William Neal, Neal Electronic Co., Inc.; August 18, 1953.

"Old Mother Nature and Reliability," by Prof. Walter R. Jones, Faculty, Cornell University; September 10, 1953.

NORTHERN NEW JERSEY

"A Transistor Feedback Amplifier for Carrier Frequencies," by J. C. Lozier and D. D. Cherry, Bell Telephone Labs.; "Automatic Gain Control of Junction Transistor Amplifiers," by F. H. Blecher, Bell Telephone Labs.; September 9, 1953.

ROME

"Automatic Factory," by Walter Hausz, General Electric Company; September 14, 1953.

STUDENT BRANCH MEETINGS

DREXEL INSTITUTE OF TECHNOLOGY, IRE-AIEE BRANCH

"Stability of Electric Power Systems," by W. Brown, Philadelphia Electric Company; August 6, 1953.

(Continued on page 124A)

Potter & Brumfield

STANDARD RELAYS

offer you **4** *important advantages*

PROVEN DESIGN

P & B's 20 years' experience in relay design is your assurance of long, trouble-free performance.

LOWER COST

These relays are already tooled. Mass production economies are passed on to you.

FAST DELIVERY

Orders for standard relays can be filled from stock or with a minimum of delay.

DISTRIBUTOR SALES

Popular types available through P & B Distributors located in all principal cities.

MORE THAN 110 P & B STANDARD RELAY STRUCTURES FOR EVERY ELECTRICAL AND ELECTRONIC APPLICATION

General Purpose	Telephone
Power	Motor Starting
Multiple Contact	Photo Flash
Multiple Leaf	Control
Latching	Sensitive
Plate Circuit	Miniature
Impulse	Shock Proof

Write for new master catalog describing our wide line of basic relay structures, housings and enclosures. Samples, quotations and recommendations promptly furnished on special problems.

POTTER & BRUMFIELD

PRINCETON, INDIANA

Export: 13 E. 40th Street, New York, New York

Sales Engineers in Principal U. S. and Canadian Cities

now...TEFLON* with Certified performance

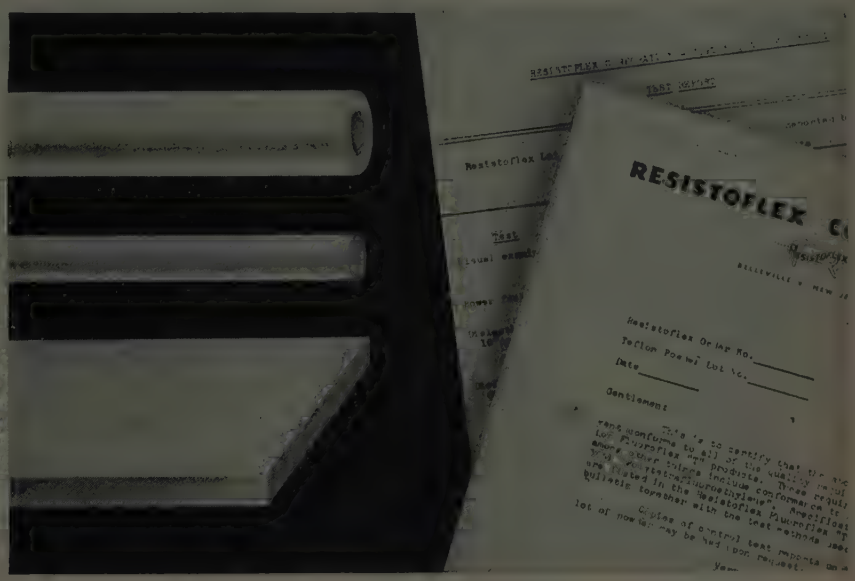

Conformance to specifications assured in **FLUOROFLEX®-T** *rod, sheet, tube*

Resistoflex will certify each shipment of "electrical grade" Fluoroflex-T products on six vital physical and electrical properties. Qualification tests are performed on all incoming Teflon powder to determine whether it will yield rods, tubes and sheets which are in conformance with specification AMS-3651 "Polytetrafluoroethylene." Processing under a quality control and inspection system approved by the USAF under MIL-Q-5923 specification maintains the identity of each lot of material through all stages of manufacture — from virgin powder to finished product.

An affidavit accompanies each shipment attesting to its conformance with AMS-3651. Certified test reports of the actual properties of any shipment will be furnished whenever they are requested.

Be *sure* of optimum performance in Teflon by specifying electrical grade Fluoroflex-T. Remember, too—Fluoroflex-T products are non-porous and stress-relieved. This means better dimensional stability, less costly machining and fewer rejects. For more details, write or phone...

**DuPont trade mark for its tetrafluoroethylene resin.*
®Resistoflex trade mark for products from fluorocarbon resins.

RESISTOFLEX *corporation*

Belleville 9, N. J.

TAKE NO CHANCES WITH VITAL EQUIPMENT... *Specify*

SERIES 6918 or 6924

RACKS by PAR-METAL

18½" or 24" DEEP, for 19" WIDE PANELS

- *Panel Spaces:* 61¼", 70", or 77" high.
- Finished in Prime Coat, Black Wrinkle, Grey Lacquer, Grey Wrinkle.
- Series 6918 or 6924 Racks may be used in "rows" or "gangs," as corner trims are removable from *front* of cabinet.
- Standard shelves and roller trucks are manufactured by us for use with these Racks.

THESE RACKS ARE MODERATELY PRICED and AVAILABLE FOR SHIPMENT FROM STOCK

Planning an electronic product? Consult Par-Metal for

RACKS • CABINETS CHASSIS • PANELS

Our P-6924 Rack as used by Gai-Tronics, Inc., Reading, Pa.

Remember, Par-Metal equipment is made by electronic specialists, not just a sheet metal shop.

Made by Electronic Specialists!

PAR-METAL
PRODUCTS CORPORATION
32-62 — 49th ST., LONG ISLAND CITY 3, N. Y.
Tel.: AStoria 8-8905
Export Dept.: Rocke International Corp.
13 East 40 Street, New York 16, N. Y.

WRITE FOR CATALOG!

NET-11 AGASTAT

NEW!

TWO STEP
AGASTAT
Trademark
TIME DELAY RELAYS

Single units for applications requiring a sequence of time delay relay periods—such as sequential starting of motors—or an adjustable momentary impulse, as in operating air valves of air cylinders on indexing machines. Time delay range of from 0.1 seconds to 10 or more minutes, with a secondary delay period up to 15 seconds. Compact, lightweight pneumatically timed units, low in cost and remarkably versatile.

Write for specifications—and ask our application engineers for help with your timing problem. Address Dept. A7-117.

AGA DIVISION — ELASTIC STOP NUT CORPORATION OF AMERICA
1027 Newark Avenue, Elizabeth, New Jersey
Pioneers in pneumatic timing

Student Branch Meetings

(Continued from page 122A)

Missouri School of Mines & Metallurgy, IRE-AIEE Branch

General meeting; September 17, 1953.

South Dakota School of Mines & Technology, IRE Branch

General meeting; September 17, 1953.

The following transfers and admissions were approved to be effective as of November 1, 1953.

Transfer to Senior Member

Arnold, D. C., 394—25 St., S.E., Cedar Rapids, Iowa
Bixby, H. O., Bailey Island, Me.
Bolt, R. H., Acoustics Laboratory, Massachusetts Institute of Technology, 77 Massachusetts Ave., Cambridge 39, Mass.
Carson, H. E., 1804 E. 30 St., Indianapolis 18, Ind.
Cone, D. I., 1257 Martin Ave., Palo Alto, Calif.
Disenhaus, N., 1207 Radnor Pl., Falls Church, Va.
Fowler, C. J., 7806 Beech La., Wyndmoor, Pa.
Hornberg, K. O., 1013 S. Tejon, Colorado Springs, Colo.
Hyland, L. A., 1104 Fisher Bldg., Detroit 2, Mich.
Karakash, J. J., Lehigh University, Bethlehem, Pa.
Mathis, H. F., Electrical Engineering Department, University of Oklahoma, Norman, Okla.
McGee, K., 811 N. Van Buren St., Marion, Ill.
Misra, R. P., Philco Corp., Church Rd., Lansdale, Pa.
Mohr, M. E., Hughes Aircraft Co., Culver City, Calif.
Rife, W. E., 6762 Rings Rd., Amlin, Ohio
Ruiter, J. H., Jr., 16 Braemore Rd., Upper Montclair, N. J.
Schrot, E. H., 2640 Burling St., Chicago 14, Ill.
Tucker, E. A., 821 Catalina Blvd., San Diego 6, Calif.
Wallace, R. P., Mycalex Corporation of America, Clifton Blvd., Clifton, N. J.
Wolin, S., 7825 Gilbert St., Philadelphia 19, Pa.
Zenr, N. J., 1538 Bradford Ave., St. Louis 14, Mo.

Admission to Senior Member

Assadourian, F., 333 Third Ave., New York 10, N. Y.
Bailin, L. L., Hughes Aircraft Co., Culver City, Calif.
Berline, S. D., 45 Rue de l'Etang, Mareil, Marly (S&O), France
Chun, M. E., 203 E. Quill Dr., San Antonio, Tex.
Eachus, J. J., 2802 Wisconsin Ave., N.W., Washington 7, D. C.
Engstrom, H. T., 507—18 St., S., Arlington 2, Va.
Fossum, D. E., 1815 Ross Pl., S.E., Albuquerque, N. Mex.
Gehlke, D. A., 10639 Johanna Ave., Sunland, Calif.
Grillo, J., 4755 White Plains Rd., New York 70, N. Y.
Harry, H. E., 517 Austin Ave., Barrington, N. J.
Kidd, M. C., 5-3, RCA Victor Division, Camden 2, N. J.
Lynch, E. E., 31 Strathmore Rd., Wakefield, Mass.
Peters, J. F., Harvestehuderweg 7, (24a) Hamburg 13, Germany
Sattinger, I. J., 410 Keech Ave., Ann Arbor, Mich.
Simon, J. C., 151 Rue de Grenelle, Paris 7, France
Sherr, S., 32 Beaumont Cir., Tuckahoe 7, N. Y.
Underhill, B. B., 707 Lees La., Collingswood, N. J.

(Continued on page 126A)

NEW! ....ADDITIONAL FREQUENCY RANGE FOR GYRALINE....
....D-92 AUDIO DRIVER FOR GYRALINE.....

Gyraline*

THE MICROWAVE AMPLITUDE MODULATOR

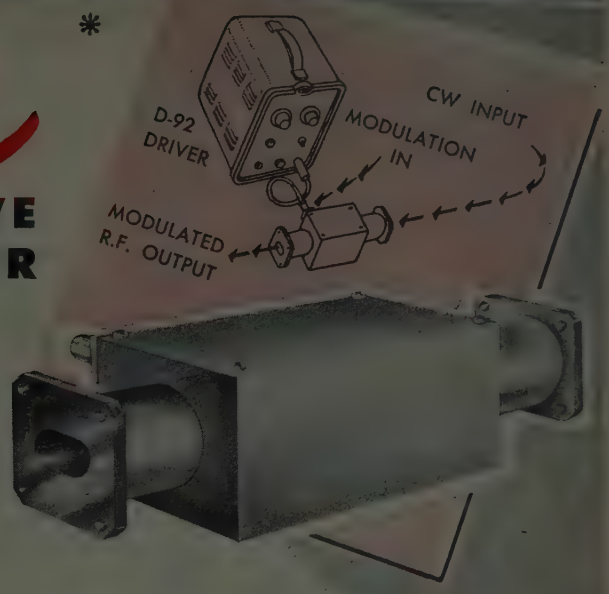

Gyraline . . . a new ferromagnetic resonance device which operates as a continuously variable microwave attenuator controlled by an applied magnetic field. Amplitude modulation of a CW microwave signal is readily obtained by varying the magnitude of the magnetic field by means of an external modulating source.

- **Eliminates FM and double moding with CW Klystron operation.**
- **Permits detection and amplification at audio frequencies.**
- **Makes possible single oscillator heterodyning.**
- **A continuously variable, electronically-controlled, microwave attenuator.**
- **Used as a level set attenuator merely by varying percent modulation. (Controlled by gain knob on D-92 driver.)**

TYPICAL CHARACTERISTICS

FREQUENCY RANGE:
MODEL 920: 8500-9900 mcs. . . .
MODEL 1000: 9600-11,200 mcs. . .

WAVE GUIDE SIZE: ½" x 1" x 6.1" . . . . . .

INSERTION LOSS: Less than 1 decibel . . . . . .

MODULATION FREQUENCY: Up to 3000 c.p.s. . .

VOLTAGE STANDING WAVE RATIO:
1.4 to 1. (or less) . . . . . .

POWER HANDLING CAPABILITIES:
Maximum continuous microwave power dissipation, 2 watts . . . . .

COIL IMPEDANCE:
Nominal coil impedance at 1000 cps: 500 or 2000 ohms (either). . . . . .

*Previously announced as "Moduline".

D-92 Driver

The D-92 driver provides a flexible and convenient source of audio power for operating the Gyraline. Circuit consists of an audio oscillator having sine wave output which is tunable over a frequency range of 800 to 1200 cps. This oscillator drives an 8 watt resistance coupled amplifier with output impedances to match Gyraline input. Frequency response is essentially flat to 3000 cps. The gain of this unit is sufficient to drive the Gyraline to greater than 90% modulation.

OUTPUT: 22V, 110 ma. (into 500 ohm load) at 1000 cps.
INPUT REQUIREMENTS: 0.9 Volts. (for above output level.)
INPUT IMPEDANCE: 500,000 ohms. (approx.)
POWER REQUIREMENTS: 115V, 50/60 cycles, 110 watts.
OVERALL DIMENSIONS: 11½" high, 7½" wide, 9½" deep.
WEIGHT: 16 pounds. (approx.)

WRITE FOR DESCRIPTIVE LITERATURE

CASCADE RESEARCH
CORPORATION
53 VICTORY LANE, LOS GATOS, CALIF.

Also: UNILINE....the undirectional transmission line

In "Lavite" Ferrites —you specify —we justify!

For example:

—consider the "Lavite" F7B FERRITE MATERIAL, another product of Steward's private research and development, which has set a standard for antenna rods. It offers sufficiently low losses in the broadcast frequency range, permeability of relatively high value and excellent temperature stability — "must" characteristics for that application. Yet, this is only one of many property combinations of our ferrite materials, which provide the desirable basic advantages of high saturation, higher permeabilities, high Q and FM frequencies, low temperature coefficient, etc. "Lavite" Ferrites may well reduce the size and weight of your components, and materially reduce production costs of these parts as well. Send me your specifications and let me get in a huddle with our engineers—no obligation.

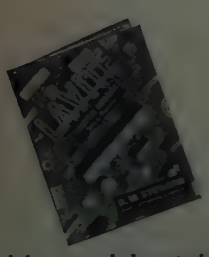

Ask for general characteristic data on all "Lavite" Technical Ceramics — ("Lavite" steatite, "Lavite" Titanates, "Lavite" Ferrites, and others).

D. M. STEWARD MFG. COMPANY

3605 Jerome Avenue Chattanooga 1, Tennessee

Sales Offices in Principal Cities

(Continued from page 124A)

Walker, A. P., Engineering Department, NARTB, 1771 N St., N.W., Washington 6, D. C.
Wege, H. R., Radar Engineering Section, Bldg. 53A-1, RCA Victor Division, Camden 2, N. J.
Werner, R. L., RCA Bldg., 30 Rockefeller Pl., New York 20, N. Y.

Transfer to Member

Carlsten, E. E., Office of the Chief of Naval Operations, Navy Department, Washington 25, D. C.
Chamberlain, I. J., 4300 Witherbee Dr., Lincoln 8, Neb.
Chanes, H., 161 Spring La., Paramus, N. J.
Eklund, M. H., 3534 Anderson Ave., S.E., Albuquerque, N. Mex.
Fox, B., 268 E. Durard Rd., Philadelphia 19, Pa.
Harmatz, H. J., 64-10—110 St., Forest Hills, L. I., N. Y.
Jones, E. D., 3rd AACS I&M Sqdn., APO 862, c/o Postmaster, New York, N. Y.
Kaluger, M. M., 616 N. Huntington Ave., Monterey Park, Calif.
Kuck, B. M., 2530 Ritchie Ave., Cincinnati 8, Ohio
Lagomarsini, G. C., 231 W. Olive St., Burbank, Calif.
Little, S., 3189 S. Stafford St., Arlington 6, Va.
McDowell, A. P., Jr., 6921 N. 19 St., Philadelphia 26, Pa.
McNally, W. P., c/o W. L. Maxson, 460 W. 34 St., New York 1, N. Y.
McNamara, J. E., 601 S. Crocker St., Sulphur, La.
Price, M., 206, Granville Ct., Grafton Rd., Yeoville, Johannesburg, South Africa

(Continued on page 128A)

SQUARE PULSE GENERATOR

MODEL 300

for the

MILLIMICROSECOND to MICROSECOND RANGE

New Basic Test Instruments for NUCLEAR, RADAR, TV, UHF, and other fields in which FAST PULSE CIRCUITS are employed. Three or more pulse outputs are available in Model 300.

SPECIFICATIONS

PULSE SHAPE: square pulse
RISE TIME: .001 μsec. from 10% to 90% amplitude
PULSE WIDTH: .001 μsec to several μsec., selectable.
PULSE AMPLITUDE: From 100 volts to .006 volts in one db steps
OUTPUT IMP: Matched to any impedance for standard coax lines
POWER INPUT: 105-125 V, 60 cy.
SIZE: 17-1/2" x 19" x 10-3/16"
Catalog RP-11 on request

EPIC ELECTRICAL & PHYSICAL INSTRUMENT CORP.
42-19 27th Street, L.I.C. 1, N. Y.

A TRUE ELECTROSTATIC VOLTMETER

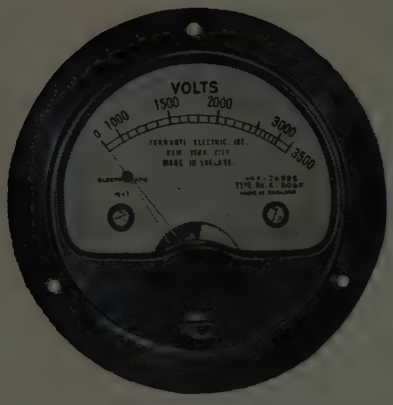

This instrument permits voltage readings on AC or DC circuits of very high resistance. The only current drawn is the very small leakage current and a very low capacitance current on AC circuits. Very useful for the many high voltage—low current circuits employed in nuclear research. Available with full scale voltages ranging between 300 and 3500 volts. Special laboratory instrument available with full scale reading of 150 volts. Full scale capacitance ranges from 8 mmfds for the 3500 volt model to 100 mmfds for the 150 volt instrument. Magnetic damping. 2½" dial. Write for complete specifications.

FERRANTI

FERRANTI ELECTRIC, INC.
30 Rockefeller Plaza • New York 20, N. Y.
FERRANTI, LTD., Hollinwood, England
FERRANTI ELECTRIC, LTD., Toronto, Canada

EBY 7 PIN MINIATURE UHF SOCKETS

A high quality, high performance socket that has been thoroughly tested and meets all requirements of UHF-TV application.

The Eby UHF Socket is made to standard 7 pin miniature dimensions and is available in mica-filled phenolic.

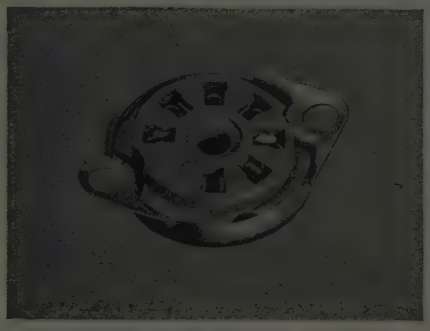

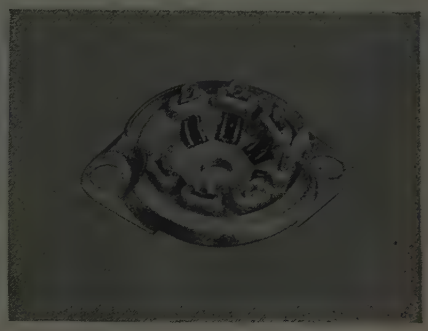

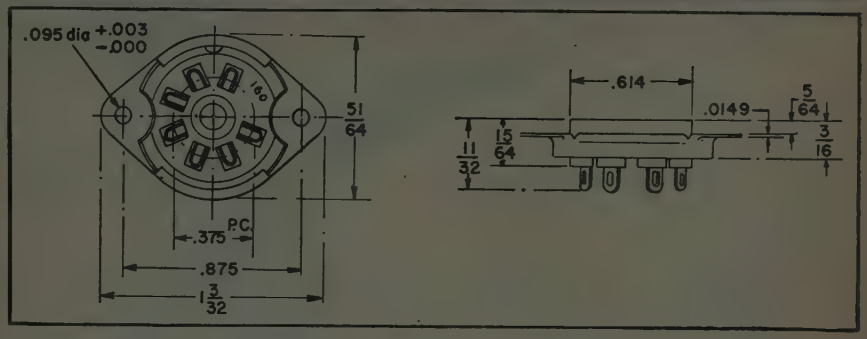

three types of mounting—on 7/8" centers

(1)—STANDARD SADDLE
(2)—SPLIT SADDLE
(3)—WELL-TYPE

peak performance contacts

- **LOWEST CAPACITANCE AND INDUCTANCE**
- **MINIMUM CONTACT DIMENSIONS**
- **EXCELLENT CONTACT LIFE CHARACTERISTICS**

This new UHF socket is another example of Eby Leadership for the Electronics Industry.

Write for complete details

HUGH H. EBY INC.

4702 Stenton Ave., Phila. 44, Pa.

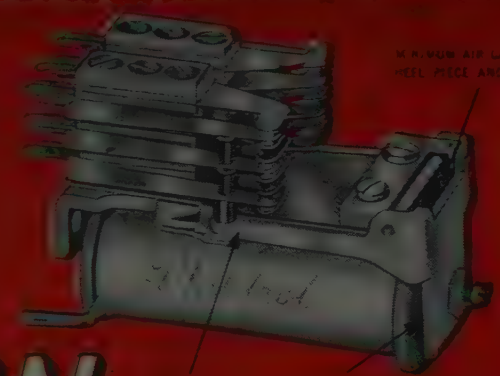

NEW

6QA Phil-trol RELAY

Adds Sales Appeal and Top Performance to Your Products

The new Phil-Trol 6QA Relay has found wide acceptance in a variety of products because of its extreme compactness, capacity and exceptional sensitivity.

The 6QA is only 2 9/16" long, yet it provides large cubic area for winding (maximum 20,000 ohm coil). Armature ratio and electro magnetic features assure high sensitivity.

Phil-Trol 6QA performance equals that of larger telephone type relays. Its construction makes possible mounting and wiring from under the chassis, using less space and saving assembly time and costs.

For added convenience, the Phil-Trol 6QA Relay is available with a plug-in adaptation for use in panels and annunciator racks.

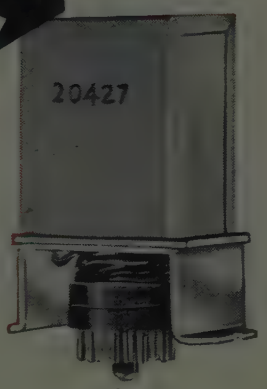

PLUG-IN—
DUST COVERED
TYPE 6QA—(Quick Acting)

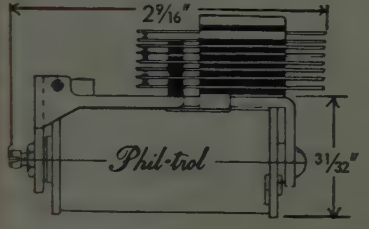

2 MOUNTING HOLES
No. 6-32 N.C. THREADS

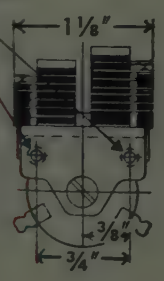

Phil-trol

IS THE REGISTERED TRADE MARK OF
PHILLIPS CONTROL CORP., JOLIET, ILLINOIS
OFFICES IN ALL PRINCIPAL CITIES

PHILLIPS CONTROL CORP., DEPT. PI, JOLIET, ILLINOIS
Please send me a free copy of the new Phil-Trol Relay and Actuator Catalog.

Name _____ Title _____
Company _____
Address _____
City _____ Zone _____ State _____

MEMBERSHIP

(Continued from page 120A)

Silberman, R. T., 4635 Edgeware, San Diego, Calif.
Skeist, S. M., 7101 Shore Rd., Brooklyn 9, N. Y.
Stoklas, F. P., 3512 E. Flower St., Phoenix, Ariz.
Taylor, J. J., 8242 Appelton Dr., University City 14, Mo.
Vittum, M. S., Box 881, Honolulu, T. H.
Wells, A. F., 4500 Barclay, Montreal 26, Que., Canada

Admission to Member

Albin, A. L., 922 E. 55 St., Chicago, Ill.
Brenton, G. P., 512 Cherry, Galion, Ohio
Brown, L., 247-A Haddon Hills, Haddonfield, N. J.
Carnes, F. W., U.S.S. Juneau CLAA119, Fleet Post Office, New York, N. Y.
Graham, R. H., 1528 Marshall St., Houston 6, Tex.
Jennings, H. K., Box 1663, Los Alamos, N. Mex.
Kelley, H. A., 1400 Fairfield Dr., El Paso, Tex.
Mageoch, N. H., Daystrom Instrument, Archbald, Pa.
McNary, B. D., 1051 Ringwood Ave., Pompton Lakes, N. J.
Meyer, S., 4415 Spruce St., Philadelphia 4, Pa.
Nomura, K., 44 Takaban-cho, Meguro-ku, Tokyo, Japan
Plummer, R. T., 355 S. Irving Ave., Tucson, Ariz.
Pollard, W. H., Radio Station WBHP, Huntsville, Ala.
Renwick, E. B., Jr., 19 Harriman Ave., Denville, N. J.
Robinson, B. R., 4 St. Osmund's Close, Salisbury, Wilts., England
Scullin, C. H., Box 56, Breesport, N. Y.
Sloan, R. R., 80-49—90 Ave., Woodhaven 21, L. I., N. Y.
Stewart, R. A., International Business Machines Corp., Plant 2, Poughkeepsie, N. Y.
Stork, J. E., 9356 Santa Monica Blvd., Beverly Hills, Calif.
Strumwasser, E., 314 N. Bowling Green Way, Los Angeles 49, Calif.
Thresher, W. E., 3229 Wonderview Dr., Dayton 4, Ohio
Thun, R. J., 11 rue du Donjon, Brunoy (S&O), France
Valliant, J. G., 1432 S. Burlington St., Los Angeles, Calif.

The following elections to Associate have been approved and are effective as of October 1, 1953:

Adams, E. C., 2315 Scott St., Des Plaines, Ill.
Alexander, W. A., 555 S. Hudson, Tulsa, Okla.
Allen, K. J., c/o Douglas Aircraft Co., White Sands Proving Grounds, Las Cruces, N. M.
Argyle, B. E., 341 Larchmont Rd., Elmira, N. Y.
Armstrong, D. T., 221 Angelique St., Weehawken, N. J.
Austein, E. E., 38 Monroe St., New York 2, N. Y.
Belsky, M. L., ET3, 419-10-62, Navy No. 230, Box 10, 3rd Div., c/o PM, Seattle, Wash.
Berger, A., 5634 Florence Ave., Philadelphia, Pa.
Bird, R., 3 Factory Tech. Division, British Tabulating Machine Co., Letchmouth, Herts., England
Bloodworth, G. M., 602 N. Bloodworth St., Raleigh, N. C.
Bolt, C. A., Jr., 103 Sycamore Rd., Linthicum Heights, Md.
Brown, L. J., 4607 Ridgeway Dr., Los Alamos, N. M.
Bushong, J. G., 4616 E. Montecito Ave., Phoenix, Ariz.
Carmichael, R. L., Highland Ave., Stanhope, N. J.
Casciato, L., 39 Pendrith St., Toronto, Ont., Canada
Caserta, J. N., 385 S. Division St., Buffalo 4, N. Y.
Cerra, M. B., Campanario 815, Havana, Cuba

(Continued on page 143A)

News—New Products

These manufacturers have invited PROCEEDINGS readers to write for literature and further technical information. Please mention your I.R.E. affiliation.

(Continued from page 45A)

Beam Power Amplifier

Tube Dept., Radio Corp. of America, Harrison, N. J., is now producing the 12AQ5, a beam power amplifier of the 7-pin miniature type intended primarily for use in the output amplifier of automobile radio receivers operating from a 12-volt storage battery. Within its maximum ratings, the 12AQ5 is the performance equivalent of the larger glass-octal type 12V6-GT.

The application of directed electron beam principles in the design of the 12AQ5 makes it capable of producing relatively high power output with high power sensitivity. For example, a single 12AQ5 operated with a plate and screen voltage of 250 volts can deliver a maximum-signal power output of 4.5 watts with a peak driving voltage of only about 12 volts. These features together with the relatively low plate-current drain make the 12AQ5 suitable for use in the output stage of automobile receivers.

(Continued on page 154A)

ENGINEERS

Electronics, television and radio design engineers—this established electronics manufacturer, located in the beautiful Finger Lakes region of Western New York, requires men with design experience. Permanent positions available for senior and junior men with EE degree or equivalent experience.

Moderate size of company offers excellent opportunities for advancement. Fine community with good homes, schools, and outstanding cultural opportunities.

Write to

Chief Electronics Engineer
Stromberg-Carlson Company
Rochester 3, New York

electronic frequency changers

250VA and 1000VA capacity

60~ to 60~ or 60~ to 400~

accuracy to ±0.01%

- *accurate control of frequency*
- *accurate control of voltage*
- *good wave shape*
- *portable*
- *no special wiring or installation*

SPECIFICATIONS

Model	FCD250	FCD1000	FC1000
Input voltage	95-130VAC, 1ø, 50-60~	208 or 230VAC, 1ø, 50-60~	208 or 230VAC 1ø, 50-60~
Output voltage	115VAC, 1ø, adjustable between 110-120 volts		
Output frequency	400~, adjustable ±10%	400~, adjustable ±10%	60~, adjustable between 45 and 65
Output voltage regulation	±1.0%	±1.0%	±1.0%
Output frequency regulation	±1.0% in standard models; ±0.01% with auxiliary frequency standard (output frequency is fixed when using frequency standard)		
Capacity	250VA	1000VA	1000VA
Load range	0.1 to full load		
Distortion	5% maximum		
P. F. range	Down to 0.7 F		
Time constant	0.25 seconds		
Envelope modulation	2% maximum		

These industrial and laboratory frequency changers resulted from contracts for precision inverters. They should prove useful for testing components or complete instruments that must operate over variable frequency conditions. They can also be used as sources for precision 60~ or 400~ for timing applications, or used with servo and/or gyro motors in design work.

Sorensen electronic frequency changers are also being used with field equipment such as geophysical vans, where motor generator set frequency control is often inadequate. Another use will be for checking equipment designed for 50~ (foreign) usage; conversely, the same instrument can be used to convert 50~ line to 60~ source.

Electronic frequency changers of other ratings are now in design. We shall be happy to send further information, or to correspond with you concerning your individual requirements. Address Sorensen & Co., Inc., 375 Fairfield Avenue, Stamford, Conn. In Europe, write directly to Sorensen A.G., Gartenstrasse 26, Zurich 2, Switzerland.

SORENSEN

375 FAIRFIELD AVENUE, STAMFORD, CONN.

The Van Nostrand Series in Electronics and Communications

MICROWAVE THEORY AND TECHNIQUES

By Herbert J. Reich, Herbert L. Krauss, Philip F. Ordung, and John G. Skalnik

This comprehensive treatment of present-day microwave theory and techniques covers the entire microwave field—defined as extending upward from 300-400 megacycles per second, and applying to devices operating at frequencies at which distributed-element circuits are generally used. Features of special interest are the emphasis upon underlying physical principles, as in the treatment of the operation of microwave amplifiers and oscillators, the many hundreds of clarifying illustrations, and the extensive selection of exemplifying problems, laboratory experiments and bibliographical references.

914 Pages $12.50

MEASUREMENTS AT CENTIMETER WAVELENGTH

By Donald D. King

This book on the principles, methods, and laboratory techniques of measurement in the V.H.F. and microwave regions, emphasizes the importance in this work of transmission-line theory, and achieves a unified presentation relating the practical formulas to basic line equations. There are complete schematic diagrams of the experimental equipment for each type of measurement. Graphs and line charts illustrate the various methods, and antenna measurements are covered most thoroughly, including material on surface currents.

330 Pages $5.50

FUNDAMENTALS OF RADIO COMMUNICATIONS

By Abraham Sheingold

A comprehensive and clearly-written account of both the principles and techniques of present-day radio-communication systems. From basic principles this book develops a broad treatment of the operational features of a-m and f-m sound-communication systems: television, and facsimile, frequency-sharing and time-sharing multiplex systems; loran, radar and other aids to navigation. The important characteristics of the components and circuits used in such equipment are fully explained. The description and analysis of each circuit shows its capabilities and limitations when used in the radio-system applications. Basic circuits are analyzed in a detailed, quantitative fashion by algebraic and trigonometric methods. Examples, numerous references, and more than 300 illustrative figures add materially to the clarity and thorough coverage of this important new work.

442 Pages $5.25

free-examination copy

D. VAN NOSTRAND CO., INC.
250 Fourth Ave., New York 3, N.Y.

Please send me for 10-day free examination the book or books I have checked below. After ten days I will either return the book or books and owe nothing, or I will send you the full purchase price plus postage.

☐ Microwave Theory and Techniques $12.50
☐ Measurements at Centimeter Wavelength $5.50
☐ Fundamentals of Radio Communications $5.25

Name .....
Address .....
City ..... *Zone* .... *State* .....

SAVE! (If you enclose full purchase price with this coupon, we will pay the postage. Same return privilege if not entirely satisfied.)

Microwave Assemblies, Radar Components, and Precision Instruments . . . manufactured to your Blueprints and Specifications.

N.R.K. MFG. & ENGINEERING CO.
4601 WEST ADDISON STREET • CHICAGO 41, ILL. • SPring 7-2970

2400 to 10,200 Mc FREQUENCY METER

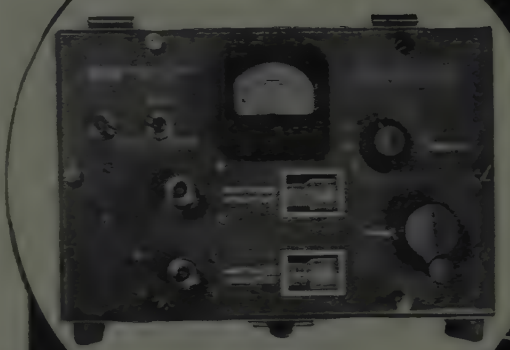

NARDA
Model 802

COVER: Unit is equipped with detachable cover—not shown.

For additional information regarding this unit, send for bulletin #1053.

SPECIFICATIONS

- FREQUENCY RANGE: 2400 - 10,200 Megacycles
- ACCURACY: ±0.2%
- SENSITIVITY: 10 milliwatts to 5 watts
- RESONANCE INDICATOR: 50 microamp movement
- TEMPERATURE COEFFICIENT: 15 parts per million per °C.

The NARDA Line INCLUDES:

Hi-Power Impedance meters • 12.4 to 18.0 Kmc Frequency meter • Microwave mixers, detectors, and test equipment • Waveguide Bends and Components • Pulsed R-F Signal generators • Microwave Engineering.

Custom built Microwave and Electronic Test Equipment

NARDA — NARDA RESEARCH & DEVELOPMENT ASSOCIATES INCORPORATED
68 MAIN STREET — MINEOLA, NEW YORK
Subsidiary of PEERLESS INSTRUMENT CO., INC. — GARDEN CITY 3-3570

MEMBERSHIP

(Continued from page 128A)

Chapelle, W. E., 9260 Sheldon Rd., Plymouth, Mich.
Chatfield, B. H., Box 646, Bridgehampton, L. I., N. Y.
Corey, S. A., Bendix Radio Division, Department 70, Bendix Aviation, Baltimore 4, Md.
Cunningham, R. W., 2510 E. Michigan St., Indianapolis 1, Ind.
Dias, G. C., Bush Radio Ltd., Power Rd., Chiswick, London, England
Dickens, W. D., 2828 Roselawn Ave., Baltimore, Md.
Dock, S. J., Jr., 217 Mt. Joy St., Mt. Joy, Pa.
Duay, T. M., 2067 Stanley Hills Dr., Hollywood 46, Calif.
Ehrlich, S. L., 110 Berkley St., Waltham 54, Mass.
Elvidge, R. E., Canadian Westinghouse Co., Plant 2, Dept. WA, Aberdeen Ave., Hamilton, Ont., Canada
Epstein, S., 964 Tiffany St., New York 59, N. Y.
Farkas, J., 21-10—35 Rd., Long Island City, N. Y.
Francis, J. P., 2125 Sunset Plaza Dr., Los Angeles 46, Calif.
Freeman, E. F., 2802 W. Fourth Ave., Vancouver, B. C., Canada
Gates, A. F., 2811 N. Howard St., Baltimore, Md.
Gaumann, T., Karl Staufferstr 1, Zurich, Switzerland
Gieseler, W. L., 7908—15 Ave., Apt. 102, Hyattsville, Md.
Gotcher, A. W., 7715 S.E. Salmon St., Portland 16, Ore.
Grisamore, N. T., 209 Whitmoor Terr., Silver Spring, Md.
Habermann, R., Jr., General Electric Co., Schenectady, N. Y.
Hamilton, H. A., 1615 Filion St., Ville St. Laurent, Que., Canada
Hawes, R. C., 771 Oakglade Dr., Monrovia, Calif.
Heacock, R. J., 252 S. 61 St., Philadelphia 39, Pa.
Heavner, W. S., Rome Air Development Center, Griffiss AFB, Rome, N. Y.
Hebert, J. D., c/o Carter Residence, Knobside, W. Clifton Rd., Bristol, Tenn.
Helenek, A. R., 210 Fuss St., Dunellen, N. J.
Helms, M. E., 3 Nassau Blvd., Garden City, L. I., N. Y.
Helperin, J., 112 Via Palermo, Newport Beach, Calif.
Hollsworth, D. M., 1100 W. 81 Pl., Los Angeles, Calif.
Hubbard, C. L. R., 1217 Delence St., Toledo 5, Ohio
Ilner, J. J., 932 McKimmon Rd., Fayetteville, N. C.
Jickling, R. M., Division 14-8, National Bureau of Standards, Washington, D. C.
Joiner, E. R., RCA Service Co., Inc., Government Service Division, Essex & Ellis Sts., Gloucester, N. J.
Jones, J. W., 738 Park Lane Rd., Swarthmore, Pa.
Kearns, W. P., 252 Washington Ave., Nutley, N. J.
Kling, W. R., 9230 E. Hecla St., Temple City, Calif.
Knopow, H. S., 201 W. Mall, Milwaukee 11, Wis.
Kovach, L. D., 8925 McConnell Ave., Los Angeles, Calif.
Lawson, H. C., Springwood Village, Apt. G-2, Hyde Park, N. Y.
Lucas, G. W., 840 Lakeside Pl., Chicago, Ill.
Mahler, J. H., 3rd AACS I & M Sq., Pepperrell AFB, St. John's, Newfoundland
Manteck, P. A., 420 Longfellow, N.W., Washington 11, D. C.
Mavromatis, A., Box 961, Grand Central Station, New York, N. Y.
Mazur, E. F., 7670 Brecksville Rd., Cleveland 9, Ohio
McAllister, M. W., Jr., 15915 McGill, Covina, Calif.

(Continued on page 144A)

Now a NEW "Pencil Point" SOLDERING TOOL

FOR SMALL OR MINIATURE WORK

IDEAL Thermo-Tip

INSTANT HEAT—
PINPOINT ACCURACY!
NOTHING TO HOLD
BUT AN ELECTRODE
"PENCIL"

Tips Screw In to Fit the Job
DOUBLE METALLIC
DOUBLE CARBON
Other Tips Available

Pencil-Thin
FOR EASIER, FASTER SOLDERING OF:

- Electronic Circuits and Parts
- Aircraft Connectors
- Pin Type Plugs
- Wire-to-Wire
- Terminals
- Radio and TV Chassis
- Instruments
- Printed Circuits

Here is an all-new production tool expressly designed to make small and miniature soldering simpler and surer than ever before. It is so fast that some joints can now be soldered in less than 1 second! . . . so much lighter and easier to handle than soldering irons or guns that a woman can use it all day long without fatigue! Check this unique combination of features against your job requirements:

GETS INTO SMALL, TIGHT SPOTS because of smaller electrode pencil.

NO HEAT DAMAGE—instant resistance heating makes sound joints before resistors, condensers, printed circuits, terminal fibre, etc., can be damaged. Pinpoints the heat!

NO "COLD FLOW JOINTS"—resistance principle *requires* that metal be heated before the solder will flow. Tap switch adjust heat as needed.
SAFE—soldering pencil uses harmless (6v) voltage and high amperage from separate step-down transformer.

LESS FIRE HAZARD—electrodes are hot only when in use.

LESS REPLACEMENT COST—only low cost electrodes to buy.

TIPS FOR EVERY SMALL JOB —2 sizes of double carbon, single carbon with ground clamp, double metallic. May also BE USED AS SOLDERING IRON —two sizes of chisel tip irons.

SOLD THROUGH LEADING DISTRIBUTORS

IDEAL INDUSTRIES, Inc.
3313 Park Avenue, Sycamore, Illinois

Please send catalog data on NEW IDEAL THERMO-TIP.

NAME.....
COMPANY.....
CITY.....ZONE....STATE.....
ADDRESS.....

MAIL FOR FURTHER DATA

In large scale production NOW!

American Electronic

Model 140
SYNCHRO GENERATORS

Model 141
SYNCHRO CONTROL TRANSFORMERS

A pair with an established reputation.
The heart of modern two-speed systems.

AVAILABLE FOR IMMEDIATE DELIVERY!

Size 15
UNIVERSAL-FREQUENCY PRECISION RESOLVER.
Minimum noise, highest accuracy. Basic to all trigonometric operations.

Size 15
UNIVERSAL-FREQUENCY PRECISION POTENTIOMETER
Continuous rotation, induction type. Accuracy comparable to resolver.

Model 171
SERVO COMPUTING TACHOMETER
Companion to Model 172 Servomotor. Superior linearity and signal-to-noise ratio

READY FOR FALL DELIVERY:

Sizes 11 and 23 Induction Resolvers and Potentiometers · Sizes 11 and 15 Servo Control Motors and Computing Tachometers · Model 293 Brushless Potentiometers.

Model 172
SERVO CONTROL MOTORS
"Standard" in many modern computers and controls. Thousands in use

FEATURES

- Maximum accuracy, signal-to-noise ratio, range of linear operation.
- Minimum noise, size and friction.
- Total magnetic shielding.
- Internal winding or external network compensation.
- High temperature resistant models.
- Corrosion and fungus resistant.
- Complete line of "packaged" compensating isolation driver-amplifiers.
- Reliable delivery commitments.

American Electronic Mfg., Inc.
9583 W. Jefferson Blvd., Culver City, Calif.

MAKING TRANSFORMERS IS OUR BUSINESS

• For more than 35 years Acme Electric transformers have become components of all types of electrical and electronic equipment. The vast technical experience accumulated during this time is now available to west coast manufacturers through our Los Angeles branch.

ACME ELECTRIC CORPORATION
MAIN PLANT: 4411 Water Street • Cuba, N. Y.
West Coast Engineering Laboratories: 1375 W. Jefferson Blvd. • Los Angeles, Calif.
In Canada: ACME ELECTRIC CORP. LTD. • 50 North Line Rd. • Toronto, Ont.

Acme ACME Electric
TRANSFORMERS

MEMBERSHIP

(Continued from page 143A)

McEver, W. L., 527 S. Canoler St., Decatur, Ga.
McMillan, S. H., 1037 Packard Rd., Ann Arbor, Mich.
McNeill, T. J., 1611 Pontiac Ave., E. Cleveland 12, Ohio
Metts, L. W., 620 W. Second St., Washington, N. C.
Micheli, A., Jr., 45 Windermere Ave., Lansdowne, Pa.
Miller, G. L., Sandia Trailer Park, Rt. 5, Box 293, Albuquerque, N. M.
Moreno, M., 703 Eaton St., Key West, Fla.
Morrison, S. C., 9537 W. Olympic Blvd., Beverly Hills, Calif.
Nambudiripad, M. N., House 236, Kottapuram, Trichur, S. India
Nye, J. W., Oak St., Cheverly Gardens, Landover, Md.
Obolensky, G., Dept. Plant Science, University of Alberta, Edmonton, Alta., Canada
Ohman, B. V., 110-43—64 Ave., Forest Hills 75, L. I., N. Y.
Osborn, R. F., 310 W. Liberty St., Louisville 7, Ky.
Peirce, R. W., 273 Sources Rd., Strathmore, Town of Dorval, Que., Canada
Persons, L. D., 1506 N. Van Ness, Apt. 1, Santa Ana, Calif.
Rea, R. C., 3606-D Parkwood Dr., Greensboro, N. C.
Rees, B. A., 5522 Linda Rosa, La Jolla, Calif.
Robbins, S., 409 Wisler, Davison, Mich.
Roberts, A. J., 40 Chestnut St., Monroe, Mich.
Roberts, L. E., Jr., 1809½ Frederica, Owensboro, Ky.
Rolfe, F. R., 75-50 Bell Blvd., Bayside, L. I., N. Y.
Salzberg, E., 101 Ewing Dr., Stoughton, Mass.
Schrader, R. H., General Electric Co., 1405 Locust St., Philadelphia, Pa.
Sichelstiel, B. A., 3807 Fleetwood Ave., Baltimore 6, Md.
Silvestre, H., 2133 E. Third St., Dayton, Ohio
Sims, R. C., 691 W. Ferry, Detroit, Mich.
Smith, P. E., 3524 Anderson Ave., S.E., Albuquerque, N. M.
Stanton, G. L., 2827 Trent St., Winston-Salem, N. C.
Starkey, D. J., 14409 E. La Forge St., Whittier, Calif.
Stoutenburg, D. V., 18 S. Central Ave., Fairborn, Ohio
Sturm, N., 265 Park Ave., Park Ridge, N. J.
Sundaram, V., Dy. Director, Ministry of Communications, New Delhi, India
Swanson, J. P., 515—15 Ave., Menlo Park, Calif.
Tarot, A., 1603 W. 135 St., Gardenia, Calif.
Tasch, A., 3727 St., Cleveland, Ohio
Traub, R. A., 118 Cloverland Dr., Rochester 10, N. Y.
Tuerck, W., Jr., 182 Bellmore St., Floral Park, L. I., N. Y.
Tunsey, F. P., Jr., 29 Hellenington Rd., Nutley, N. J.
Van Jepmond, H. K., 1615 Washington St., Evanston, Ill.
Varga, J., R.D. 2, Box 103-A, Lancaster, Pa.
Warner, D. P., 1314—16 St., N.W., Washington 6, D. C.
Wegstein, J. H., 3421—34 Pl., N.W., Washington, D. C.
Wells, P. E., 2705—13 St., N.E., Washington 18, D. C.
Wentworth, H. B., 2721 Ordway St., N.W., Washington, D. C.
Wickersham, P. D., Lake of the Forest, Rural Station, Bonner Springs, Kans.
Yarbrough, L. E., 4936 Kendall Dr., New Orleans, La.
Zeps, H., 1215 W. Sycamore St., Kokomo, Ind.

STOCK INSULATORS...for virtually every electronic application!

Samples available on request

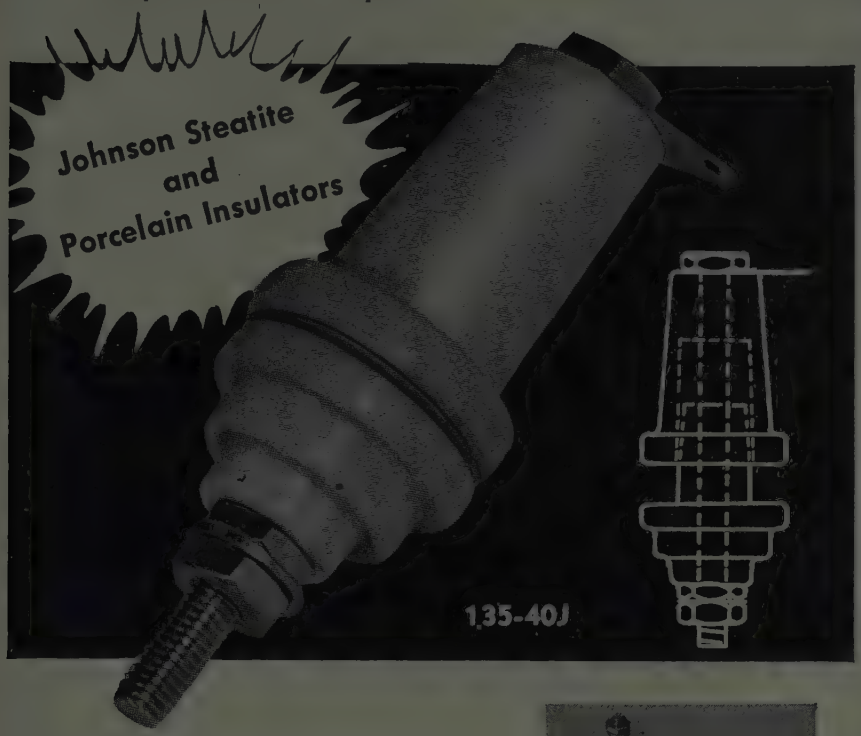

- Low loss factor and moisture absorption
- Highly fracture resistant
- Maximum voltage breakdown ratings
- Heavily nickel plated brass hardware

JOHNSON low-loss Steatite and procelain insulators are rugged . . . performance proved throughout the years. Highly fracture resistant, dense molded and glazed for low moisture absorption. Available with DC-200 impregnation. Stable performance under adverse operating conditions. Extended creepage paths develop maximum voltage breakdown ratings, heavy integral mounting bases withstand heavy compression loads and considerable lateral stress. Equipped with hardware and cushion washers—feed-thru types available with jacks for accommodation of standard banana plug. For complete information on the standard JOHNSON insulators shown here, or types custom-built to specification, call or write today.

Items from catalog 973. For detailed information on JOHNSON'S complete selection of insulators, write for your copy of General Products Catalog 973.

E. F. JOHNSON COMPANY

CAPACITORS, INDUCTORS, SOCKETS, INSULATORS, PLUGS, JACKS, BRASS, AND PILOT LIGHTS

204 SECOND AVENUE SOUTHWEST • WASECA, MINNESOTA

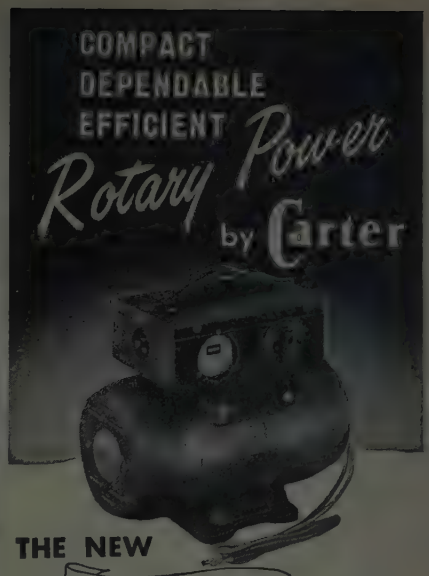

THE NEW

Custom

DC-AC CONVERTER

These latest of all Carter DC to AC Converters are specially engineered for professional and commercial applications requiring a high capacity source of 60 cycle AC from a DC power supply. Operates from storage batteries, or from DC line voltage. Three "Custom" models, delivering 300, 400, or 500 watts 115 or 220 V. AC. Wide range of input voltage, 12, 24, 32, 64, 110 or 230 V. DC. Unequalled capacity for operating professional recording, sound movie equipment and large screen TV receivers. Available with or without manual frequency control feature.

MAIL COUPON FOR CATALOG

Carter Rotary Power Supplies are made in a wide variety of types and capacities for communications, laboratory and industrial applications. Used in aircraft, marine, and mobile radio, geophysical instruments, ignition, timing, etc. MAIL COUPON NOW for complete Dynamotor and Converter Catalogs, with specifications and performance charts on the complete line.

Carter MOTOR CO.
2645 N. Maplewood Ave.
Chicago 47

Carter Motor Co.
2645 N. Maplewood Ave., Chicago 47

Please send new catalogs containing complete information on Carter "Custom" Converters and other Rotary Power Supplies.

Name_____

Address_____

City_____ State_____

CLOSE-TOLERANCE CONSTRUCTION PLUS...

QUALITY CONTROL... brings you the best in paper tubes

PRECISION

PAPER TUBES

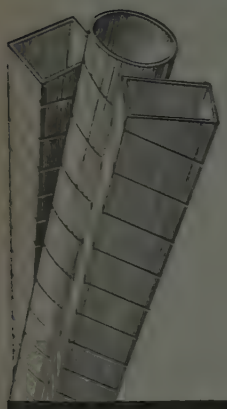

Made of the finest dielectric kraft, fish paper, acetate, combinations or phenol impregnated materials, PRECISION Paper Tubes are die formed under heat and pressure. Uniformity, strength, and light weight are assured. High manufacturing standards and rigid testing result in maximum insulation, heat dissipation, and moisture resistant characteristics.

Available in any shape, length, I.D. or O.D. Finished to your exact specifications.

SEND TODAY FOR FREE SAMPLE AND REQUEST NEW ARBOR LIST OF OVER 2000 SIZES.

PRECISION PAPER TUBE CO.

2051 W. CHARLESTON ST. CHICAGO 47, ILL.

Plant No. Two, 79 Chapel St., Hartford, Conn.—Also Mfrs. of Precision Coil Bobbins

FREQUENCY STANDARDS

MICROMETER HEADS

JOB TESTED!

- Precision Built
- Positive Resetting
- Automatic Compensation for Spindle Wear
- Positive Spindle Lock
- Anodized Finish

FIELD CHECKED!

AVAILABLE IN SEVERAL MODELS —WRITE FOR LITERATURE

This new precision instrument affords the highest degree of accuracy in reading. Elimination of backlash assures positive resetting in either direction of rotation and automatically compensates for wear of spindle and nut thread. Calibrations are large, legible, easy to read. Features include temperature compensation construction, thimble stop to prevent thread jamming and a positive spindle lock. The instrument is easily reset for calibrated instruments.

Frequency Standards

General Offices: ASBURY PARK, NEW JERSEY

PLANTS AT NEW SPRINGFIELD AND ASBURY PARK, N. J.

Telephone:
ASBURY PARK 1-1718

Positions Wanted

(Continued from page 152A)

ENGINEER

B.E.E. Manhattan College 1952. 1 years experience instructor (lab. & lecture). Electronic and radio Manhattan College. Age 26, single. Desirous of obtaining employment in industry research or development. Metropolitan area only. Box 701 W.

PATENT ATTORNEY

B.S.E.E., Member IRE, State and Federal Boards, age 33. Experienced in preparation and prosecution of patent applications, including electronics; excellent knowledge foreign languages. Desires to relocate in New York City, full or part time. Box 702 W.

News—New Products

These manufacturers have invited PROCEEDINGS readers to write for literature and further technical information. Please mention your I.R.E. affiliation.

(Continued from page 141A)

Rectifier for Magnetic Devices

A small, compact and inexpensive single phase bridge rectifier, Type DO3575, has been developed by **International Rectifier Corp.**, El Segundo, Calif., for the operation of magnetic devices such as relays, solenoids and electric counters.

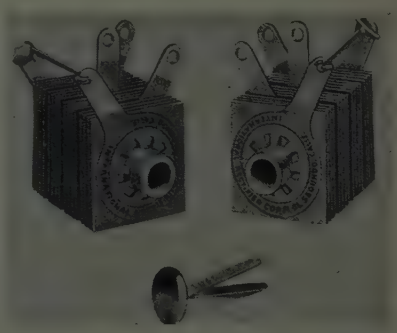

The unit is designed for use directly from 117 volt ac systems and is rated to deliver an output of 9 watts at 90 volts dc, continuous duty. With the addition of a 3 μf or larger filter capacitor, the rectifier will deliver 117 volts dc for operation of devices normally designed for this voltage. The magnetic device, therefore, can be used in conjunction with this rectifier to operate directly from the conventional 117 volt ac line. The rectifier measures 11/16 $\times$11/16$\times$1$\frac{1}{4}$ inches mounting dimension and the terminals extend $\frac{3}{4}$ inch above the plates, making a maximum total space requirement of 11/16$\times$11/16$\times$1$\frac{1}{4}$ inches.

The use of the Type D-3575 selenium rectifier reduces the iron core losses and the undesirable hum common with ac magnetic devices. Shock and vibration characteristics are also materially improved. Moreover, the burning of delicate contacts is eliminated when the device is converted to dc operation by the use of the Type DO3575.

(Continued on page 156A)

Improve Tube Performance with WESGO "AL-300" ALUMINA INSULATORS

- 97% Al_2O_3 content
- Vacuum tight—extraordinary strength
- Low loss factor — High Te value
- Non "gassing" — no poisoning of emitters
- High strength at all temperatures up to 1500°C.
- Can be supplied in most any shape to extremely close tolerances

Our Engineering Department will gladly answer all inquiries relative to your particular problems

WESTERN GOLD & PLATINUM WORKS
Ceramic Division
589 BRYANT STREET
SAN FRANCISCO, CALIF.

TIC nography of INSTRUMENTS

Measurement of

- Impedance
- Inductance
- Capacitance
- Resistance
- Dissipation Factor (D)
- Storage Coefficient (Q)
- Plot Impedance Functions

310A Z-Angle Meter

The type 310A Z-Angle Meter measures impedance directly in polar coordinates as an impedance magnitude in ohms and phase angle in degrees: $Z\angle\theta$

Impedance Range: .5 to 100,000 ohms, covered by a single dial and a four position range switch.

Accuracy: ± 1%

Frequency Range: 30 cycles to 20 kc. for impedances below 5000 ohms, measurements can be made up to 40 kc. For frequencies from 100 kc. to 2 mc., write for specifications for the type 311A-RF Z-Angle Meter.

Phase Angle Range: 0° to 90° Direct reading on panel meter. Meter is also Calibrated in D and Q.

Phase Angle Accuracy: Within 2° of meter indication.

Internal Oscillator: 60 cycles and 400 cycles. Terminals are provided for an external, variable frequency signal generator for measurements at other frequencies.

In the field, the laboratory, the production test floor or the class room, the extreme accuracy and the simplicity of operation has proved the type 310A Z-Angle Meter to be a superb and reliable instrument.

Write now for more detailed information.

ENGINEERING REPRESENTATIVES

Chicago, Ill.—UPtown 8-1141
Cleveland, Ohio—PRospect 1-6171
Waltham, Mass.—WAltham 5-6900
Rochester, N.Y.—Monroe 3143
Dayton, Ohio—Michigan 8721
Arnprior, Ont., Can.—Arnprior 400
Hollywood, Cal.—HOllywood 9-6305
Dallas, Texas—DIxon 9918
Roseland, New Jersey—Caldwell 6-4545
Wyncote, Pa.—Ogontz 8805
Silver Spring, Md.—Sligo 7-550

TECHNOLOGY INSTRUMENT CORP.

535 Main Street · Acton, Massachusetts · Tel. ACton 3-7711

now...
RESINITE brings you the HIGHEST RESISTIVITY of any RESINATED PRODUCT

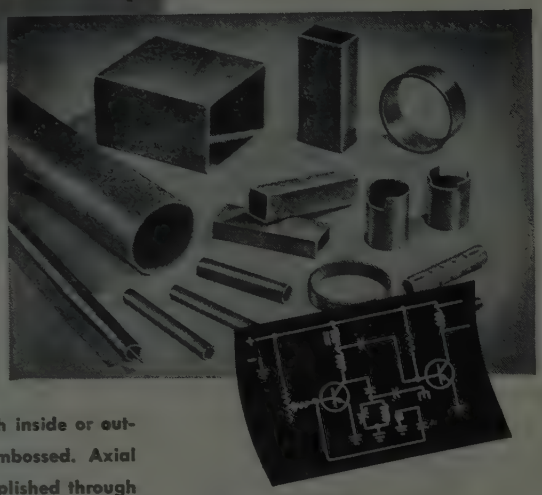

Resinite Coil Forms are laboratory tested and field proven. Their operating characteristics—volume resistivity . . . power factor . . . thermal properties . . . low moisture absorption . . . and resistance to voltage breakdown — represent a new achievement in basic components for electronic application.

Resinite Coil Forms are available with inside or outside threads, slotted, punched or embossed. Axial pressure in excess of 25 lbs. is accomplished through a special three-row threaded design. Torque can be controlled to + or —1 in. oz.

RESINITE 8104: for coil forms requiring very high dielectric properties under extreme humidity.

RESINITE "AC": for applications requiring very high dielectric strength. ELECTROLYTIC CORROSION IS IMPOSSIBLE.

RESINITE 104: for stapling, severe forming, fabricating.

Send today for full details and technical information.

RESINITE CORPORATION
DIVISION OF PRECISION PAPER TUBE
2035G W. Charleston St., Chicago 47, Ill.
79 Chapel St., Hartford, Conn.

Saratoga Industries

STAR PERFORMANCE AS MANUFACTURERS OF TRANSFORMERS, REACTORS, FILTERS, TOROIDAL COILS FOR THE ELECTRONICS INDUSTRY

Now in its ninth year of operation, Saratoga Industries, Inc. has built a solid reputation for the manufacture of precision windings. Approved for in-plant testing under MIL-T-27, Saratoga Industries, Inc. is also prepared to handle all types of commercial production. Saratoga engineers invite your inquiry to help solve your problems relating to reactors, transformers, filters and windings of all types.

SARATOGA INDUSTRIES, INC. SARATOGA SPRINGS, N. Y.

News—New Products

These manufacturers have invited PROCEEDINGS readers to write for literature and further technical information. Please mention your I.R.E. affiliation.

(Continued from page 154A)

Test Equipment Catalog

A new 12-page electric test equipment catalog has just been completed and is now being offered by **Industrial Instruments, Inc.**, 89 Commerce Rd., Cedar Grove, N. J. The new catalog is designated as Catalog No. 19A.

A large selection of electric test instruments for both laboratory and production applications are listed along with full specifications on each. In addition to the instruments, necessary accessories and test jigs are listed and described.

Transistor Bulletins

Electronic Research Associates, Inc., P.O. Box 29, Caldwell, N. J., offers a new bulletin on available types of transistors, with supplementary data.

Also available is a bulletin on the Model TT-11 Transistor Tester. Information is also available on the Model CC-60 Constant Current Converter and the Model 110 Transistor Power Supply.

Stabilized Crystal

A new stabilized crystal, the JK G-12, has just been introduced by the **James Knights Co.**, Sandwich, Ill. Specially designed to handle applications in the 500 to 1500 kc range, the new unit provides ultra-stable frequency control for applications such as frequency standards, timing and counting circuits, broadcast equipment, and frequency monitors.

Electrodes are deposited directly on the quartz plate which is shockmounted in an evacuated glass envelope. Crystal may be designed for a minimum temperature coefficient from 0°C to 50°C or for temperature controlled operation at 60°C with a JKO7E-115V Oven.

The new JK Stabilized G-12 is $2\frac{3}{4}$ inches in height above chassis, maximum diameter of octal base, $1\frac{3}{4}$ inches. The use of the evacuated glass envelope assures freedom from contamination, and greater shock resistance.

(Continued on page 158A)

GOLD BONDED
Germanium Diodes

. . . designed for
Superior Service

The smallest, most efficient and economical diodes commercially available, Transistor Products germanium diodes offer superior advantages in many applications.

All TP diodes have uniform characteristics and low shunt capacity; specific types meet highest forward current requirements and have a minimum voltage drop.

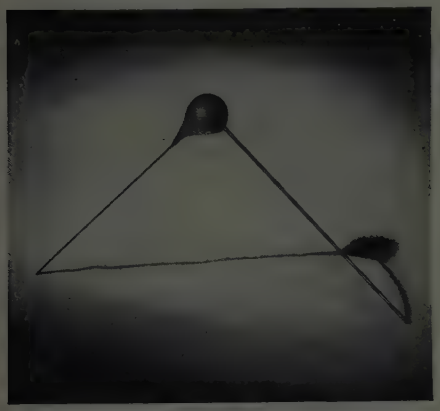

Transistor Products germanium diodes give dependable performance because they are designed and assembled for maximum mechanical strength. These diodes have the gold electrically bonded to the germanium — creating a welded alloy which meets shock resistance requirements. Only 3/16" in diameter, they are compact and ideal for sub-miniature assembly. TP germanium diodes also have tinned copper leads which permit easier soldering in production lines.

For data sheets and complete information on Transistor Products diodes, transistors and transistor test set, write Dept. P11.

TP

TRANSISTOR PRODUCTS, INC.
SNOW AND UNION STREETS, BOSTON 35, MASSACHUSETTS
AN OPERATING UNIT OF
CLEVITE CORPORATION

INTRICATE SHAPES with tolerances often as close as ±.005 *without Grinding or Finishing!*

The costly headaches and limitations of loose tolerances—which have vexed the engineer with variations of 1/32" in permanent magnet design—have been virtually eliminated by Thomas & Skinner, specialists in magnetics for more than half a century.

Now your engineers can specify the intricate casting shapes—with sharply defined relief—which in the past have been too difficult or too expensive to produce. Through radically new techniques, Thomas & Skinner permanent magnets are cast with such close precision that little or no grinding and finishing is required for dimensional accuracy.

Call in a Thomas & Skinner engineer—let him work with your own development specialists—learn how your permanent magnet problems of close tolerances and intricate designs may be solved by the new Thomas & Skinner technique—now! Write today—ask for the new Thomas & Skinner Permanent Magnet Bulletin, No. 151.

THOMAS & SKINNER Steel Products Company
1120 East 23rd Street · Indianapolis, Indiana

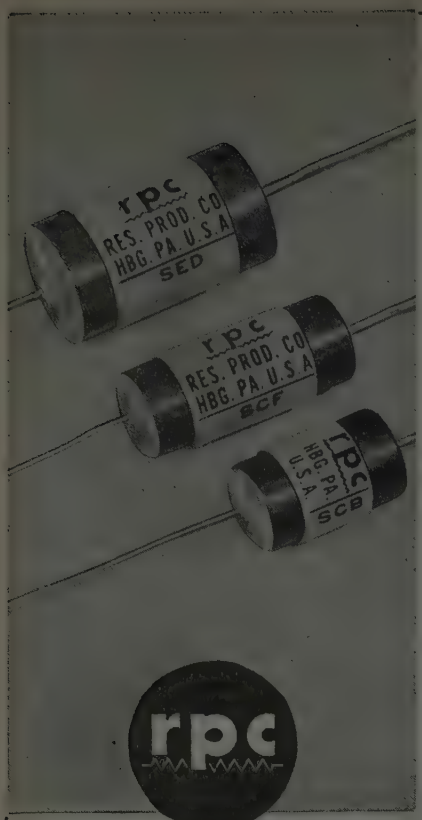

MINIATURE

HERMETICALLY SEALED PRECISION WIRE WOUND

Where the utmost in permanence and stability are required, Type S has proven successful. Unaffected by extreme temperature cycling, aircraft altitude or salt water immersion.

Wound on steatite forms, solder sealed into steatite jackets. Vacuum tested. Long leakage path. Can be wired into circuit. Self supporting. Low coefficient alloys used.

Standard resistance tolerance 1%, ½% and ¼% also available. Write for complete information and engineering data.

Type	Dimensions		Jan-R-93	Power Rating		Resistance	
	Len.	Diam.		Jan.	Comml.	Min. ohm	Max. meg
SCB	9/16	11/32	——	—	watts ¼	2.0	0.15
SCF	13/16	11/32	RB51A	¼ watts	½	1.0	0.40
SED	13/16	15/32	RB51A	¼ watts	½	0.5	1.0

rpc

RESISTANCE PRODUCTS CO.

714 RACE ST. HARRISBURG, PENNA.

IF IT'S NEW . . . IF IT'S NEWS . . . IT'S FROM ELCO

News indeed, is Elco Corporation's new transistor socket, point contact and junction type. The transistor is now emerging as a tremendous new tool for practical everyday electronics; and Elco, with a deep background of experience in transistor socket development for laboratory use, now offers these same highly-refined sockets in mass production for commercial applications. And, as with all Elco products, the use of Elco transistor sockets offers many advantages previously unavailable.

New contact design automatically centers the transistor pins in position, eliminating strain on the transistor body. Positive contact retention assures excellent circuit performance. Insulator construction affords adaption for printed circuitry, a decided extra advantage; and creates a longer creepage path between contacts. Mounting retainer securely locks body of socket to chassis and is self-adjusting to any variation in chassis thickness from .015" to .062". The retainer is of heat-treated steel cadmium plated; the insulator of low-loss mica filled phenolic. Elco also offers many other new sub-miniature, miniature and printed circuit types. Complete details are yours upon request, as is full information about Elco's quality line of sockets, shields, and sensational new Varicon connectors.

For Catalog Sheets, Call GArfield 6-6620 or Write ELCO Corp., 190 W. Glenwood, Phila. 40, Pa.

News—New Products

These manufacturers have invited PROCEEDINGS readers to write for literature and further technical information. Please mention your I.R.E. affiliation.

(Continued from page 156A)

Synchro Transmitters and Control Transformers

Synchro transmitters and control transformers with maximum error limits of 7 minutes are available in production quantities from the **Kearfott Company, Inc.**, 1150 McBridge Ave., Little Falls, N. J.

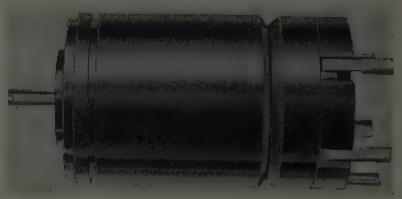

The components are 1.062 inches in diameter and 1 23/32 inches long, models for either 26 volt or 115 volt 400 cps excitation can be obtained. By virtue of their unique integral construction, these units assure performance under extreme conditions of humidity, temperature, altitude and vibration.

Kearfott also offers a complete line of servo motors, synchros, tachometer generators, and gyros for airborne control and industrial servo systems.

Interval Timer

A new enclosed electronic timer that is particularly well-suited for dependable industrial and laboratory services, that require timed intervals, time delay periods or other programming, has been announced by **G. C. Wilson & Co.**, 2 N. Passaic Ave., Chatham, N. J.

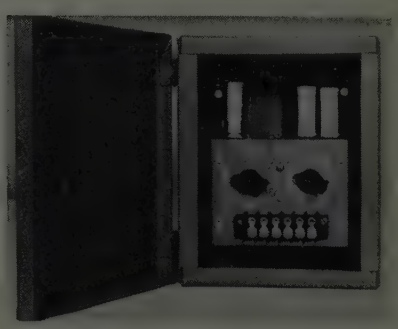

Type 60 MC timer was designed to provide operation by foot switch, push button, pressure switch, or any other momentary or sustained contact closing device. Accurate setting of the time interval is obtained by fine and coarse controls. Timing intervals are unaffected by variations in line voltage or line frequency.

The unit is supplied in gray wrinkle finished steel box, 9×7×4½ inches, with hinged cover and knockouts. It may be operated from any 105–125 volt, 50–60 cps line and consumes eight watts. Time intervals provide range from 1/10 second to 60 seconds. Its single pole, double throw relay has 10 ampere contacts.

(Continued on page 163A)

MYCALEX
GLASS-BONDED MICA
WITHSTANDS ADVERSE COMBINATIONS

MYCALEX glass-bonded mica will withstand more — much more — of *combined* high temperature, radiation effects, thermal shock, high voltage, high frequency, mechanical stresses and high altitude than traditional electrical design calculation tables say that *any* insulation can stand.

It is the high "across the board" average that causes engineers to call Mycalex glass-bonded mica "the world's most nearly perfect insulation."

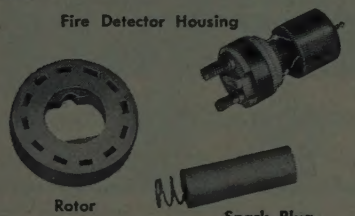

YES, bad conditions can "gang" Mycalex glass-bonded mica, or they can attack it one at a time. Mycalex glass-bonded mica, the only Ceramoplastic, will endure them no matter how they come.

Write for the whole story.

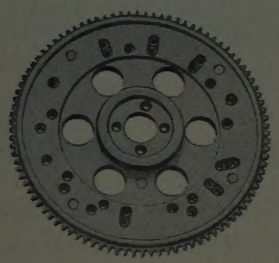

Insulated gear illustrates breakage resistance under wide temperature changes, even with large inserts.

SINCE 1919 MYCALEX THE INSULATOR ®

MYCALEX CORPORATION of AMERICA
World's Largest Manufacturer of Glass-bonded Mica Products
Executive Offices: 30 Rockefeller Plaza, New York 20, N.Y.
GENERAL OFFICES AND PLANT
111 CLIFTON BOULEVARD, CLIFTON, N. J.

News—New Products

These manufacturers have invited PROCEEDINGS readers to write for literature and further technical information. Please mention your I.R.E. affiliation.

(Continued from page 158A)

Correction Notice

Sub-Miniature Blower

Sanders Associates, Inc., Nashua, N. H., announces production of the "Minicube" subminiature blower. This 1 inch cube, which weighs 1 ounce, includes the motor and blower housing and delivers 3 cubic feet of air per minute. It is designed for circulation of air and the cooling of electronic parts and equipment.

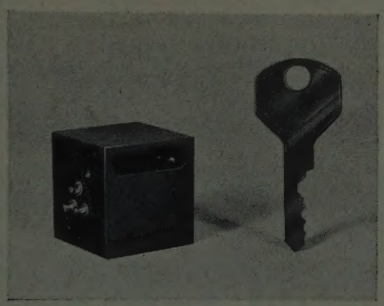

The unit can be mounted next to a component for spot cooling or anywhere else for general circulation of air. The rating of a component, such as a power resistor, can be increased by properly attaching a blower directly to the component. The "Minicube" can be used in hermetically sealed equipment for heat transfer to or from the case. Mounted on the inside the blower affords efficient heat transfer to the case. Mounted on the outside it can be used to remove heat from the case. The manufacturer claims the "Minicube" can replace large external blowers for cooling klystrons and magnetrons.

Standard models are available for operation over a temperature range of −55°C to +125°C, with an expected life of 1,000 hours. Other models are also available for extremely wide temperature ranges. The "Minicube" utilizes an integral hysteresis-type synchronous motor turning at a speed of 24,000 rpm. Motors can be supplied for either 6.3 v, 3 watt, or 26 v, 4 watt, 400 cps operation. The motor is normally two-phase, but can be operated from a three-phase source or a single-phase source with a phase shifting capacitor.

(Continued on page 165A)

30,000 IRE MEMBERS USE THE IRE DIRECTORY

YOU CAN'T do THAT with MYCALEX
GLASS-BONDED MICA

YOU CAN'T use Mycalex glass-bonded mica as a hammer head to drive a nail.

BUT it is used in one installation because it is the only high temperature insulation that will stand the abuse that mechanics give it when installing the equipment.

YOU CAN'T use Mycalex glass-bonded mica as a crucible over a Bunsen flame.

BUT you can solder and re-solder the hardware or inserts molded into, or fastened to, this material. It withstands assembly line abuse.

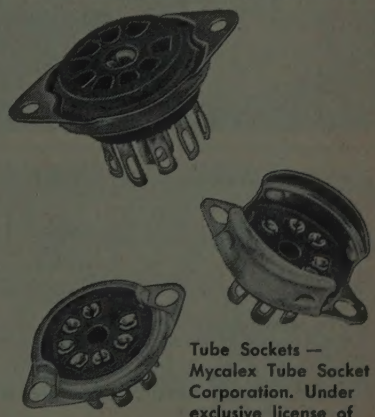

Tube Sockets — Mycalex Tube Socket Corporation. Under exclusive license of Mycalex Corporation of America

THE LIMITATIONS AND ABILITIES of Mycalex glass-bonded mica have been carefully studied. Here is a major engineering material that you can specify with confidence. The very stability of Mycalex glass-bonded mica guarantees that its properties will be true, constant and enduring. Write for the full story.

SINCE 1919 MYCALEX THE INSULATOR ®

MYCALEX CORPORATION of AMERICA
World's Largest Manufacturer of Glass-bonded Mica Products
Executive Offices: 30 Rockefeller Plaza, New York 20, N.Y.
GENERAL OFFICES AND PLANT
111 CLIFTON BOULEVARD, CLIFTON, N. J.

FOR
FREQUENCY
Stability
IN
Mobile
EQUIPMENT . . . .

make sure your crystals are made by Standard Piezo.

For years, our Crystals have been standard as original equipment with leading manufacturers and for replacement purposes by large operators of mobile equipment.

Precise, accurate, Standard Piezo Crystals are available for *ALL* types of mobile communication equipment.

Request catalog R for complete details.

Standard Piezo COMPANY
CARLISLE, PENNSYLVANIA

Star Performers

EPCO "QUALITY-PLUS"

TRANSFORMERS

For Industrial and Electronic Equipment

DESIGNED TO COMMERCIAL & MILITARY SPECIFICATIONS (MIL-T-27 and AN-E-19). ALSO CLASS A, B, H, AND MINIATURES.

Sample, Short and Long Runs. Let us quote on your specifications. No obligation.

Delivery as promised!

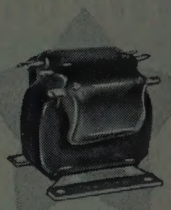

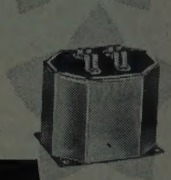

EPCO
PRODUCTS, INC.
2500 ATLANTIC AVE.
BROOKLYN 7, N. Y.

RADIO-RESEARCH INSTRUMENT CO.

CRYSTAL MOUNT. Holds any IN23 type xtal. 1" x ½" guide std coax output, UG40 flg input. $19.50

DIRECTIONAL COUPLER. Uni. dir. 20db, type "N" output, UG39flg. to UG40chk. JAN type CG-176/AP. $39.50

WAVEGUIDE. Std RG-52/U sharp internal corners. Any lgth up to 12 ft. $1.45 per ft.

3 CM. "X" Band

BEND 90 DEGREE. E or H plane. Std radius. UG39cvr to UG40chk. Silver plated. $10.50

TWIST 90 DEGREE. UG39 to UG40. Silver plated. $7.50

FLEXIBLE SECTION. Apx 6". UG39 flgs. $14.50

TR-ATR SECTION. Duplexer assy w/UG-39 to UG40 run, iris cplg, cplg to 1B24 type TR tube, ATR cavity 724 type compl. w/tuning slugs. SO-3 Radar component. $12.50

ROTARY JOINT. UG40 choke to choke. w/mounting plate for easy installation. 360 deg. rotary coupling for lab or high speed scanner. $14.50

Accessories

PARABOLIC REFLECTOR. 4ft. dia. RCA high gain dish $84.50
SELSYN 2J1Q1. 57.5V-57.5V 400cy w/connector $11.25
VARIA. COND. 4 gang. 7 to 144 mmf/sect. Ball brg. shaft. $3.25
PATCHING CABLE. Male type "N" ea. end 3ft. $2.50
COUNTER DIAL Veeder Root 4 digit. Mech. drive $.75
BATHTUB COND. 2x.1mfd 600V side term. CD. Ten for $1.75
CAPACITOR NETWORK 2x.36-mfd 800 VAC 3 for $1.10
MINIATURE IF 455kc $1.85

Antenna Drives

COMPLETE. 12rpm clockwise. rotation, 115V 60 cy GE motor, incl sine potentiometer & bearing indicator. $137.50

GEAR-MOTOR ASSY. Gear speed 95.5, gear ratio 9 to 1, motor speed 860, shunt wd. 6 amp, volts, 250A-125F cont duty. $64.50 each

MOTOR DRIVE ASSY. 115VDC motor 1/20hp, 1725 rpm. Gear box 172 rpm, 11 in. lbs. torque, cpld to 9 in. step down gear. $35.00

Pulse Components

KS-9643 Miniature, perm. core. Z ratio 1:1:1. $5.00
145EWP AND 132AWP low volt pulse xtmr. $5.00 each
D168983 Network 125 ohm, herm sld. $3.50
LV PULSE 50-4000kc, 120-2350 ohms, perm core $6.50
PULSE CONN. UG180/type rubber insert, male chassis mt. w/12" cable D166389 $2.00
UG36/type male cable mt. $5.00
UG38/type female w/mtg flg. air to oil $5.50

F-28/APN-19 FILTER CAVITY. 2700-2900mc. Max 1.5db loss at ctr. freq over band, 3db at 15 mc band ends. Meets full JAN spec. Gov't source insp. available. Fully calibrated to above spec. $42.50 each. Uncalibrated. guaranteed $28.50

ECHO BOX. TS-207/UP, 2700-2900mc, micro adj. $64.50
PICKUP DIPOLE in lucite ball, type "N" output 3" o.a. $3.75

UG53, UG54, UG65/66 flanges, RG48 rt. angle bends "E", available.

10 CM. "S" Band

COAXIAL MIXER. Xtal detector assy designed for beacon rcvrs. Trombone tuned input. "N" fittings. 2 types available-feed thru or take off to xtal. $17.50
LIGHTHOUSE CAVITY. For 2C40 tube. Tuneable 2700-2900mcs w/suitable adj of grid cylinders. Can be freq. modulated. $25.00
2C40 tube. JAN. $11.25
1N21B crystal $3.25
DOALL MIXER assy. pick-up loop, xtal mt. $5.50

STANDARD-REFERENCE CAVITY. 2650-3050mc. Invar tuning center conductor of ¾ wave-lgth. 50 ohm coax "N" input output conn. 1mc./sec. stability. Loaded Q betwn 650 and 3000 w/xmsn loss .5 to 5 db adjustable. Unloaded Q apx 6000. Concentric xmsn type resonator. Tuning mech. lock. $28.50
CRYSTAL MOUNT. ⅜" std coax. "N" fittings. Holds any 1N21 type xtal. Incl. impedance match tuner. $17.50
FEEDBACK DIPOLE ⅞" coax. for parabola. 11¾" o.a. $14.50

All material guaranteed surplus. Immediate delivery. Budget prices

Large stock **400 cycle transformers** available. Write us.

Immediate delivery — Telephone: JUdson 6 4691 — Immediate delivery
550 FIFTH AVENUE, NEW YORK, N.Y.

Measurements Corporation
MODEL 79-B

PULSE GENERATOR

REPETITION RATE: 60 to 100,000 pulses per second.

PULSE WIDTH: Continuously variable from 0.5 to 40 microseconds.

RISE TIME: Approx. 0.25 microseconds.

OUTPUT VOLTAGE: 150 volts (peak) positive.

POWER SUPPLY: 117 volts, 50/60 cycles.

MEASUREMENTS CORPORATION
BOONTON NEW JERSEY

News—New Products

These manufacturers have invited PROCEEDINGS readers to write for literature and further technical information. Please mention your I.R.E. affiliation.

(Continued from page 163A)

Tube Base Plugs

Vector Electronic Co., 8352 San Fernando Rd., Los Angeles 65, Calif., has three new plugs which fit the 7 and 9 pin miniature sockets and the 8 pin loctal socket, respectively.

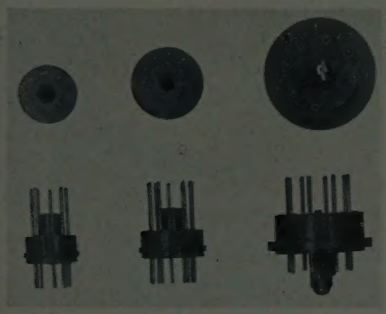

Bodies are mica filled phenolic and may be mounted by means of a center screw or by a retainer ring. These plugs are suitable for small plug-in units, potted circuits or tube adaptation uses. Round cans to slip over the plugs are available.

Packaged Bridge Comparator

Sanders Associates, Inc., Nashua, N. H., announces production of their packaged bridge comparator. This is a well-balanced, hermetically sealed unit for phase and amplitude comparison. It is a full-wave bridge comparator that can be used as a modulator, rectifier, switch, or chopper.

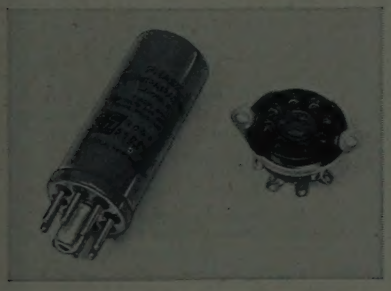

It consists of two complete bridges with appropriate switching resistors, and has a frequency range of 0 to 5,000 cps. It has a conversion efficiency of 85 per cent. The dynamic range is 46 db with fixed reference amplitude and 60 db with variable reference. The linearity over this range is 1 per cent of full scale. Because there are no moving parts the comparator is mechanically secure against shock, acceleration and vibration. It is a plug-in unit with standard octal mounting and is mechanically interchangeable with mechanical choppers and electronic tube comparators. It is 3 inches long, 1 inch in diameter and weighs 2 ounces. The operating temperature range is −55° C to +85° C. Maximum signal voltage is 60 volts RMS; maximum reference voltage is 120 volts RMS, with a dc output of ±50 volts when used as a comparator.

ONLY THE **Servoscope**®

HAS ALL THESE FEATURES

applicable to both AC carrier and DC servo systems

built-in low frequency sine wave generator for obtaining frequency response of DC servo systems

built-in electronic sweep with no sweep potentiometer to wear out and require replacement

dynamic frequency control range of 200 to 1

SERVOSCOPE is a versatile, time-saving test instrument for use in the development of all types of Servo-mechanisms and Process Controls.

SC105A

Write for bulletin giving complete specifications

SERVO CORPORATION OF AMERICA
NEW HYDE PARK, NEW YORK

Why LAMBDA laboratory power supplies are among the most FREQUENTLY RECOMMENDED

RACK MODEL 28
Standard rack mounting.
Panel size 5¼" x 19".
Weight 16 lbs.

SPECIFICATIONS:

Input: 105-125 Volts AC, 50-60 cycles, 120 watts.

DC Output: Continuously variable from 200 to 325 Volts DC regulated from 0 to 100 ma max. Either postive or negative side of supply may be grounded.

DC Voltage Regulation: Output constant to better than 1% for loads from zero to full load and line voltage variations from 105 to 125 volts.

Noise and Ripple Output: Less than 10 millivolts rms for above ratings.

AC Output: 6.3 Volts AC at 3A unregulated.

ALSO AVAILABLE NOW: Model 28-M, with voltmeter and milliammeter.

Lambda power supplies are made by engineers who pioneered in this field and have continued to specialize in it. Used by many of the country's leading laboratories, Lambda units are recommended by them for value, versatility and dependable performance. Models for many purposes. Conservatively rated, constructed for long, trouble-free service, priced moderately. Fully guaranteed.

LAMBDA
ELECTRONICS CORP.
103-02 NORTHERN BOULEVARD
CORONA 68, NEW YORK

SEND FOR NEW CATALOG. Comprehensive, authoritative, up-to-the-minute. An important addition to your power supply reference library.

INDEX AND DISPLAY ADVERTISERS

Meetings with Exhibits 2A
News and New Products 20A
Industrial Engineering Notes 84A
Professional Group Meetings 114A
Section Meetings 120A
Membership 124A
Positions Open 132A
Positions Wanted by Armed Forces Veterans 138A

DISPLAY ADVERTISERS

A'G'A Div. Elastic Stop Nut Corp. of America 124A
Acme Electric Corp. 144A
Aerovox Hi-Q Corp. ..... 24A & 25A
Air Marine Motors, Inc. 53A
Airborne Instruments Laboratory, Inc. 39A
Aircraft Radio Corp. 3A
Airtron, Inc. 96A
Alden Products Co. 64A
Alfax Paper & Engineering Co. 115A
Allen-Bradley Co. 66A
Allied Radio Corp. 97A
Alpha Metals, Inc. 107A
American Electronic Labs., Inc. 111A
American Electronic Mfg. Inc. 144A
American Lava Corp. 109A
American Phenolic Corp. ..... Facing 64A & 65A
American Television & Radio Co. 119A
Ampex Electric Corp. 11A
Andrew Corp. 6A
Arnold Engineering Co. 22A
Audio Products Corp. 23A

Ballantine Laboratories, Inc. 107A
Barber Laboratories, Alfred W. 145A
Barker & Williamson, Inc. 114A
Bell Aircraft Corp. 136A
Bell Telephone Laboratories 4A
Bell Telephone Laboratories, Inc. (Empl.) 132A
Bendix Aviation Corp. (Eclipse-Pioneer) 97A
Bendix Aviation Corp. (York Div.) 140A
Blaw-Knox Co. 67A
Bliley Electric Co. 79A
Blonder-Tongue Labs., Inc. 140A
Bodnar Industries, Inc. 146A

Brand & Co., William 145A
Browning Laboratories, Inc. 119A
Brush Electronics Co. (Magnetic Equip.) 74A
Buggie and Company, H. H. 94A
Burroughs Corp. 33A
Bussmann Mfg. Co. 7A

Cambridge Thermionic Corp. 10A
Cannon Electric Co. 111A
Capehart-Farnsworth Corp. 140A
Cargo Packers, Inc. 146A
Carter Motor Co. 153A
Cascade Research 125A
Centralab (Div. Globe Union) 19A
Chicago Telephone Supply Co. ..... 102A & 103A
Cleveland Container Co. 15A
Cohn Corp., Sigmund 106A
Collins Radio Co. 31A
Communications Equipment Co. 160A
Conrad & Moser 68A
Consolidated Vultee Aircraft Corp. (Convair) 137A
Constantin & Co., L. L. 46A
Content, Edward J. 145A
Cornell Aeronautical Laboratory, Inc. 132A
Cornell-Dubilier Electric Corp. ..... Cov. III
Corning Glass Works 5A
Crosby Laboratories 145A
Custom Gear Co. 146A

Dalis Inc., H. L. 95A
Dalmo-Victor, Inc. 50A
Daven Company 21A
Delco Radio (Div. Gen. Motors Corp.) 130A
Dialight Corp. 58A
DuMont Labs., Inc., Allen B. (Instr.) 87A
Dynamic Electronics-N.Y., Inc. 145A

Eby Inc., Hugh H. 127A
Eitel-McCullough, Inc. 54A
Elco Corp. 158A
Eldico of New York, Inc. 145A
Electrical Industries 41A
Electrical & Physical Instrument Corp. 126A
Electro-Metric Instrument Co. 145A
Electro Motive Mfg. Co., Inc. 27A
Electro-Search 145A
Electronic Engineering Co. of Calif. 139A
Electronic Research Associates, Inc. 147A
Electronic Transformer Co. 8A
Elk Electronic Labs., Inc. 147A
Engineering Associates 166A
Epco Products, Inc. 164A
Erie Resistor Corp. 57A

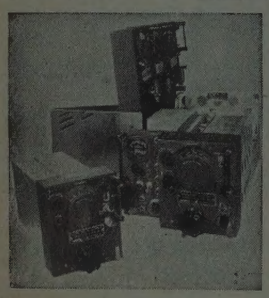

AN/APR-4 LABORATORY RECEIVERS

Complete with all five Tuning Units, covering the range 38 to 4,000 Mc.; wideband discone and other antennas, wavetraps, mobile accessories, 100 page technical manual, etc. Versatile, accurate, compact—the aristocrat of lab receivers in this range. Write for data sheet and quotations.

We have a large variety of other hard-to-get equipment, including microwave, aircraft, communications, radar; and laboratory electronics of all kinds. Quality standards maintained. Get our quotations!

We will buy any Electronic Material at top prices. SCHOOLS —unload your dusty surplus for cash or credit.

ENGINEERING ASSOCIATES

434 PATTERSON ROAD — DAYTON 9, OHIO

LOOK IT UP!

30,000 IRE members now have and use the IRE DIRECTORY

- It lists 2550 firms and their products
- It is a Directory of 30,000 Members
- Ten Product and Service Indexes organize over 500 product groups.

PRECISION

SERIES ES-500A

HIGH SENSITIVITY—WIDE RANGE

5" OSCILLOSCOPE

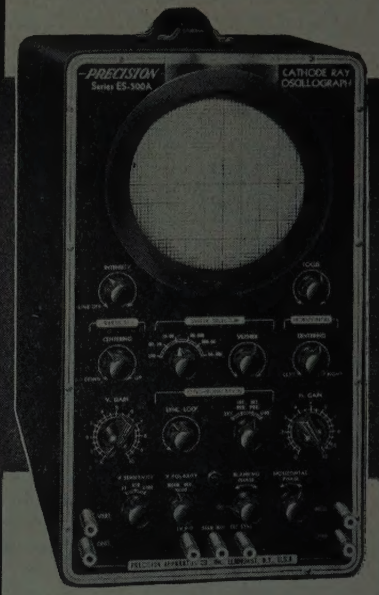

PUSH-PULL 'V' and 'H' AMPLIFIERS

20mv. per inch 'V' Sensitivity

1 Volt P-P Internal Calibrator

★ **Regulated, Push-Pull Vertical Amplifier:** .02v. per inch sensitivity. 10 cycles to 1 MC response. 2 Megs. and 22 mmf. input.
★ **1 Volt Peak to Peak, Regulated, Built-in Voltage Calibrator.**
★ **Compensated Vert. Input Step Attenuator.**
★ **'V' Phase-Reversing Switch.**
★ **Push-Pull Horizontal Amplifier:** .15v. per inch deflection sensitivity. 10 cycles to 1 MC response at full gain. ½ Meg. and 20 mmf. input.
★ **Internal Linear Sweep:** 10 cyc. to 30 KC.
★ **Controlled, 4-Way Synch. Selection:** Internal Pos., Internal Neg., External and Line.
★ **'Z' Axis Modulation Input.**
★ **Internal, Phasable 60 Cyc. Beam Blanking.**
★ **Sinusoidal Sweep Phasing Control.**
★ **All 4 Horizontal and Vertical Plate Connections Directly Accessible at Rear.**
★ **Four-Way Lab-Type Input Terminals.**
★ **Light Shield and Mask, removable and rotatable.**
★ **Fully Licensed under W.E. Co. patents.**

SERIES ES-500A: In louvered, black ripple, heavy gauge steel case. 8¼" x 14½" x 18". **Net Price $173.70**

SERIES SP-5

Oscilloscope Test Probe Set

for

WAVEFORM ANALYSIS, TROUBLE-SHOOTING, SIGNAL TRACING AND ALIGNMENT

(with Series ES-500 and ES-500A)

Set includes shielded Master Cable and four different, detachable probe heads:

1. **High Impedance—Low Capacity Probe**
2. **Signal-Tracing—Crystal Probe**
3. **Resistive—Isolating Probe**
4. **Shielded—Direct Probe**

★ **In vinyl-plastic carrying case.** **Net Price $23.50**

PRECISION APPARATUS COMPANY, INC.

92-27 HORACE HARDING BLVD., ELMHURST 73, N. Y.

Export Division: 458 Broadway, New York 13, U.S.A. • Cables — Morhanex

In Canada: Atlas Radio Corp., Ltd., 560 King Street, W., Toronto 2B